

Heterologous Biosynthesis of 2-Methyl-6-geranylgeranyl Benzoquinone and δ -Tocotrienol in Recombinant *Escherichia coli* Strains

Von der Fakultät Energie-, Verfahrens- und Biotechnik der Universität Stuttgart zur Erlangung der Würde eines Doktors der Naturwissenschaften (Dr. rer. nat) genehmigte Abhandlung

vorgelegt von
Shashank Ghanegaonkar
aus **Kolhapur, INDIEN**

Hauptberichter: Prof. Dr. G. A. Sprenger

Mitberichter: Prof. Dr. V. Urlacher

Tag der mündlichen Prüfung: 04. Feb. 2013

Institut für Mikrobiologie der Universität Stuttgart, 2013

Die experimentellen Arbeiten für die vorliegende Abhandlung wurden unter der Leitung von Prof. G. A. Sprenger am Institut für Mikrobiologie der Universität Stuttgart (von Jan. 2006 – Sept. 2009) durchgeführt.

Table of Contents

Abbreviations	7
Abstract	10
Zusammenfassung	13

CHAPTER 1 – Introduction

1.1. Vitamin E and its chemical structure.....	18
1.2. Natural food sources of Vitamin E	19
1.3. Biological and Chemical Synthesis of Vitamin E.....	21
1.4. Significance of Vitamin E compounds in animals and humans.....	31
1.5. Proposed pathway for δ -Tocochromanol biosynthesis in recombinant	33
<i>E. coli</i>	
1.6. Glucose and Glycerol Uptake Mechanism in <i>E. coli</i>	39
1.7. Extraction & Chemical Synthesis and of 2-Methyl-6-geranylgeranyl-	46
benzoquinol (MGGBQ)	
1.8. Aim of the work	48

CHAPTER 2 – Material and Methods

2.1. Materials

2.1.1. Chemicals and enzymes	50
2.1.2. Bacterial strains, plasmids and primers	52

2.2. Methods

2.2.1. Microbiological methods.....	62
2.2.2. Molecular biological methods	68
2.2.3. Biochemical Methods	69
2.2.4. Analytical methods.....	73
2.2.5. Other Methods.....	76

CHAPTER 3 – Results

A) Microbial Synthesis of δ -Tocotrienol using *E. coli* strain possessing plasmid carrying heterologous genes

3.1. *In-vivo* biosynthesis of homogentisate (HGA) in recombinant *E. coli*

3.1.1. Overexpression of <i>p</i> -hydroxyphenylpyruvate dioxygenase	82
--	----

	(Hpd) from <i>Pseudomonas putida</i> in <i>E. coli</i> DH5 α / pCAS2JF	
3.1.2.	HGA production in shaking flask (100 RPM) in <i>E. coli</i> BW25113 lacZ ⁺ / pCAS2JF	84
3.2.	<i>In-vivo</i> biosynthesis of Geranylgeranylpyrophosphate (GGPP) in recombinant <i>E. coli</i>	
3.2.1.	Overexpression of geranylgeranylpyrophosphate synthase (<i>crtE</i>) from <i>Pantoea ananatis</i> in <i>E. coli</i> DH5 α / pCAS30	89
3.2.2.	GGPP production in bioreactor in <i>E. coli</i> LJ110 / pCAS30	90
3.3.	<i>Attempts for in-vivo</i> biosynthesis of Phytylpyrophosphate (PPP) in recombinant <i>E. coli</i>	
3.3.1.	Overexpression of membrane bound Ggh from <i>Synechocystis</i> PCC6803 in recombinant <i>E. coli</i>	94
3.3.2.	Shaking flask cultivation of <i>E. coli</i> DH5 α / pCAS11 and PPP analysis using GC-MS	96
3.4.	<i>In-vivo</i> biosynthesis of δ-Tocochromanol precursors (MGGBQ and / or MPBQ) in recombinant <i>E. coli</i>	
3.4.1.	Overexpression of Homogentisate Phytyl transferase (<i>hpt</i>) from <i>Synechocystis PCC6803</i> in pCAS7	98
3.4.2.	HPLC Analysis and LC-MS characterization of δ -tocochromanol precursor compounds produced in <i>E. coli</i> DH5 α / pCAS29	103
3.4.3.	Quantification of MGGBQ produced in recombinant <i>E. coli</i> carrying plasmid pCAS29	106
3.4.4.	MGGBQ production in Infors bioreactor	107
3.5.	Enzymatic <i>In-vitro</i> synthesis of δ-Tocotrienol	
3.5.1.	Overexpression and His-Tag purification of tocopherol cyclase (<i>Cyc-At</i>) from <i>Arabidopsis thaliana</i> in pQE31- <i>vte1</i> in recombinant <i>E. coli</i>	114
3.5.2.	<i>In-vitro</i> assay of His- <i>Cyc-At</i> fusion proteins and purified MGGBQ	116
3.6.	<i>In-vivo</i> biosynthesis of δ-Tocotrienol in Recombinant <i>E. coli</i>	
3.6.1.	Overexpression of tocopherol cyclase (<i>Cyc-At</i>) from <i>Arabidopsis</i> <i>thaliana</i> in <i>E. coli</i> DH5 α / pCAS50	119
3.6.2.	HPLC and LC-MS Analysis of δ -Tocotrienol Produced in <i>in-vivo</i> in <i>E. coli</i> DH5 α / pCAS47	119
3.6.3.	Characterization of extracted product from <i>E. coli</i> DH5 α /pCAS47 by LC-MS114	122

B) Microbial Synthesis of δ -Tocotrienol using *E. coli* strain carrying chromosomal inserted heterologous genes

3.7. *In-vivo* biosynthesis of HGA in recombinant *E. coli*

- 3.7.1. Construction of *E. coli* CS1 strain129
- 3.7.2. HGA Biosynthesis in *E. coli* CS1 in Shaking Flask Cultivation.....132

3.8. *In-vivo* biosynthesis of GGPP in recombinant *E. coli*

- 3.8.1. Construction of *E. coli* CS2 strain.....135
- 3.8.2. GGPP Production in Bioreactor in *E. coli* CS2.1136

3.9. Biosynthesis of MGGBQ in recombinant *E. coli*

- 3.9.1. Construction of *E. coli* CS3, *E. coli* CS4, *E. coli* CS5 &138
E. coli CS6 strains
- 3.9.2. MGGBQ biosynthesis in Infors bioreactor in *E. coli* CS6144
- 3.9.3. Characterisation of MGGBQ using LC-MS149
- 3.9.4. Elucidation of the chemical structure of MGGBQ by NMR149

3.10. Biosynthesis of δ -tocotrienol in a chromosomal integrated *E. coli* strain

- 3.10.1. Construction of *E. coli* CS7 strain151
- 3.10.2. δ -Tocotrienol Biosynthesis in Bioreactor in *E. coli* CS7155

3.11. Increased MGGBQ in Recombinant *E. coli* Strains

- 3.11.1. Construction of *E. coli* CS8 and biosynthesis of MGGBQ in bioreactor.....165
- 3.11.2. Construction of *E. coli* CS10 and biosynthesis of MGGBQ in Infors bioreactor.....175

3.12. Increased δ -Tocotrienol production in recombinant chromosomal integrated strain *E. coli* CS9 strain

- 3.12.1. Construction of *E. coli* CS9 strain182
- 3.12.2 δ -Tocotrienol Biosynthesis in *E. coli* CS9 in Bioreactor184

3.13. Study to increase the conversion of MGGBQ to δ -tocotrienol in *E. coli* strains

- 3.13.1. Effect of inducer concentration on δ -tocotrienol and protein expression level187
- 3.13.2. New plasmid constructs carrying *cyc-At* gene in multi-copy vectors191
and co-expression in *E. coli* CS6 and / or *E. coli* CS8 strains
- 3.13.3. Purification of GST-Cyc_{At} fusion protein200
- 3.13.4. Comparison of His- and GST- fusion protein i.e. His-Cyc_{At} and 201
GST-Cyc_{At} in *in-vitro* enzymatic reaction with MGGBQ

3.14. Attempts to produce MPBQ using new reductase and transferase.....	203
enzymes	

CHAPTER 4 – Discussion

4.1. Hpd over-expression and HGA biosynthesis	211
4.2. CrtE over-expression and GGPP biosynthesis	214
4.3. MGGBQ biosynthesis	216
4.3.1. Purification of MGGBQ and analysis of its chemical structure by NMR	219
4.3.2. Improved MGGBQ yield as a result of increased precursor	220
4.3.3. Instability of MGGBQ _{reduced}	222
4.4. Ggh activity and its influence on PPP, MPBQ and δ -Tocopherol	222
Biosynthesis in this study	
4.4.1. Over-expression of Ggh-Syn in recombinant <i>E. coli</i>	223
4.4.2. Possible reasons for no conversion of GGPP to PPP	223
4.4.3. δ -Tocopherol biosynthesis	227
4.5. δ -Tocotrienol Biosynthesis	
4.5.1. Over-expression of <i>Cyc-At</i> in recombinant <i>E. coli</i>	227
4.5.2. Heterologous biosynthesis of δ -Tocotrienol recombinant <i>E. coli</i>	228
4.5.3. Cyclization reaction in recombinant <i>E. coli</i> - a bottleneck?	230
4.6. CONCLUSION	231
4.7. OUTLOOK	233
APPENDIX	235
ACKNOWLEDGEMENTS	247
REFERENCES	249

Abbreviations

Amp100	Ampicillin 100 µg/l
bp	Base pairs
CBB	Coomassie brilliant blue
CDW	Cell Dry Weight
DNA	Deoxyribonucleic acid
DMAPP	Dimethyl allyl pyrophosphate
dNTP	Deoxynucleoside triphosphate
DTT	Dithiothreitol
Da	Dalton
EDTA	Ethylenediamine tetraacetic acid
E4P	Erythrose-4-phosphate
FLP	Flippase recombination enzyme
FRT	Flippase Recognition Target
Fru-1,6-BP	Fructose-1,6-Bisphosphat
Fig.	Figure
FPP	Farnesyl pyrophosphate
GGPP	Geranylgeranylpyrophosphate
HPLC	High performance liquid chromatography
HMBC	Heteronuclear multiple-bond correlation spectroscopy
HSQC	Heteronuclear Single Quantum Coherence
HGA	Homogentisic acid
IPTG	Isopropyl-β-D- thiogalactopyranoside
IPP	Isopentenyl pyrophosphate
kDa	Kilo Dalton
LB	Luria Broth
LB+Glycerol	Luria Broth with 5 g/l Glycerol
LC-MS	Liquid Chromatography – Mass Spectrometry
l	Liter
MM	Mineral/Minimal Medium
MM-Glucose	Mineral/Minimal Medium with Glucose
MM-Glucose-Amp100	Mineral/Minimal Medium with Glucose with 100 µg/l Ampicillin
MM-Glycerol-Amp100	Mineral/Minimal Medium with Glycerol with 100 µg/l Ampicillin

mAU*min	milli-ampere units * minutes
min	minutes
m/z	mass/charge ratio
μ	growth rate in h^{-1}
MGGBQ	2-methyl-6-geranygeranylbenzoquinol
MPBQ	2-methyl-6-phytylbenzoquinol
M_w	Molecular weight
MGGBQ yield = $\mu\text{g/g CDW}$	microgram of MGGBQ produced in 1 gram of cell dry Weight
MGGBQ conc. = $\mu\text{g/l}$	microgram of MGGBQ produced over 1 liter of cultivation broth
MGGBQ _{reduced}	MGGBQ in reduced form i.e. 2-methyl-6-geranygeranylbenzoquinol
MGGBQ _{oxidised}	MGGBQ in oxidised form i.e. 2-methyl-6-geranygeranylbenzoquinone
MM	Minimal Medium
mmol	millimole
μg	microgram
mg	milligram
$\mu\text{g/l}$	microgram per liter
NAD(H)	Nicotinamide adenine dinucleotide
NADP(H)	Nicotinamide adenine dinucleotide phosphate
nm	nanometer
Ni	Nickel
NMR	Nuclear magnetic resonance
NTA	Nitrilotriacetic acid
OD _{600nm}	Optical Density at 600nm
p-HPP	<i>p</i> -hydroxyphenyl pyruvate
P_i	Inorganic phosphate
PPP	Phytylpyrophosphate
PCR	Polymerase chain reaction
ROESY	Rotating frame Overhauser Effect Spectroscopy
Pwo	Pyrococcus woesei
RBS	Ribosome binding site
R_f	mobility factor
SDS-PAGE	Sodium dodecyl sulfate polyacrylamide gel electrophoresis

S.D	Standard Deviation
Taq	Thermus aquaticus Polymerase
UV	Ultraviolet
WT	Wild type
w.r.t	with respect to
δ	Delta
β	Beta
γ	Gamma
α	Alpha

Abstract

Vitamin E is a group of lipid soluble compounds, consisting of 4 forms (δ , β , γ , α) of tocopherols and tocotrienols, each. In nature, all 8 vitamin E compounds are exclusively synthesized by photosynthetic organisms (green plants, some cyanobacteria and some algae), with the exception of recently reported tocopherol synthesis in a non-photosynthetic eukaryote, *Plasmodium falciparum*. Out of the 8 forms of Vitamin E compounds, α -tocopherol is ubiquitously found in photosynthetic organisms, while δ -tocotrienol is a rare form. Unlike α -tocopherol, δ -tocotrienol is being discussed for its possible unique biological functions in humans and animals like anti-cancer effects, neuroprotective and hypocholesterolemic effects apart from its antioxidant activity. Humans and animals cannot produce any of the Vitamin E compounds, and hence, they form an essential dietary component.

Chemical synthesis of δ -tocotrienol (analogue to that found in nature, i.e. single stereoisomer), requires a series of asymmetric synthetic reactions, that usually results in low yields. Even though, all the δ -tocotrienol found in nature is in its active form, its presence in low amounts (e.g. 15.2 μg of δ -tocotrienol per gram of fresh weight of palm fruit) makes the extraction process less economical feasible compared to the chemical synthesis route. Additionally, finding a suitable solvent for extraction of δ -tocotrienol from natural food sources is difficult as it should be environmental friendly and economical for the process technology. Molecular biologists and plant breeding scientists are making efforts to increase the biosynthesis of vitamin E compounds in photosynthetic organism itself. Increasing the vitamin E yield, by approx. 50-100 times in natural sources may result the extraction technology to be more economical than chemical synthesis process. In the current work, a new approach for the biosynthesis of active stereoisomer of δ -tocotrienol and its precursor, 2-methyl-6-geranylgeranyl benzoquinol (MGGBQ) in recombinant non-photosynthetic *Escherichia coli* (*E. coli*) strain, has been investigated. δ -tocotrienols consists of a polar aromatic head group linked to a lipophilic hydrocarbon tail. Wild type *E. coli* is able to provide the two donor groups, for the biosynthesis of δ -tocotrienol i.e. in form of *p*-hydroxyphenyl pyruvate (*p*-HPP), produced via shikimate pathway and in form of farnesyl pyrophosphate (FPP) and isopentenyl pyrophosphate (IPP) produced via the 1-deoxy-D-xylulose-5-phosphate (DXP) pathway.

To realise the heterologous biosynthesis of δ -tocotrienol in recombinant *E. coli*, four additional genes, encoding for *p*-hydroxyphenyl-pyruvate dioxygenase (Hpd) from *Pseudomonas putida*, geranylgeranylpyrophosphate synthase (CrtE) from *Pantoea ananatis*, homogentisate phytyltransferase (Hpt-Syn) from *Synechocystis* sp. PCC6803, and tocopherol cyclase (*Cyc-At*) from *Arabidopsis thaliana*, were successfully cloned and over-expressed in recombinant *E. coli* encoded within one expression plasmid. The plasmid-encoded strains produced homogentisic acid (HGA) and/or geranylgeranyl pyrophosphate (GGPP) and/or MGGBQ, and/or δ -tocotrienol when tested for *in-vivo* activity in complex medium.

In order to scale up any fermentation process from laboratory/pilot scale to commercial/industrial scale, the heterologous genes should be stable (segregational and structural), during fermentation. Recombinant strains encoded with plasmid(s) have a risk for segregational instability during fermentation, resulting in loss of productivity and hence the plant capacity. Use of antibiotics in the fermentation medium for cultivation of plasmid-encoded strains, increases the operating cost of the whole process and is undesired in food related products. To solve the problem of segregational instability and to reduce the cost of antibiotic during fermentation, homologous recombination techniques were used in the current study to construct plasmid-free recombinant *E. coli* strains, which could produce

MGGBQ and δ -tocotrienol, without affecting the production level compared to plasmid-encoded *E. coli* strains. Rare sugar degradation loci in *E. coli* BW25113 *lacZ*⁺, were replaced by gene expression cassettes using a simple, reliable chromosomal integration, and screening method, based on λ -red mediated recombination techniques. Usually, for production of recombinant proteins, a plasmid-encoded system with low, medium or high copy plasmids is suitable. For production of a certain metabolite in complex pathway like δ -tocotrienol, use of a single copy of pathway gene may be advantageous.

The homologous recombination method used in this study, allows easy screening of clones on MacConkey agar plates supplemented with appropriate sugar(s), and most importantly, allows elimination of the antibiotic resistance cassette by transient expression of flippase (FLP) recombinase. This study focuses on comparing the levels of δ -tocotrienol pathway metabolites HGA, GGPP, MGGBQ and δ -tocotrienol, in plasmid-free and plasmid-encoded *E. coli* strains in bioreactor cultivation in minimal medium using glucose/glycerol as sole carbon and in energy source. In this study, plasmid-free strains refer to, a single copy of foreign gene(s) and fermentation being carried out without addition of antibiotics while, plasmid-encoded *E. coli* strains refers to, several copies of foreign gene(s) and fermentation being carried in presence of antibiotics.

The *hpd* expression cassette was integrated in the fucose locus of *E. coli* BW25113 *lacZ*⁺ strain, to obtain a plasmid-free *E. coli* CS1 strain (*E. coli* BW25113 *fuclP::P_{tac}-hpd*). The product HGA is a water soluble compound and was detected in supernatant samples of plasmid-free *E. coli* CS1 and plasmid-encoded *E. coli* BW25113/pCAS2JF strain, by HPLC method. Plasmid-encoded *E. coli* BW25113/pCAS2JF strain produced 1.6 times more HGA than plasmid-free *E. coli* CS1 strain in glucose medium (i.e. $1213 \pm 45 \mu\text{g/l}$ vs. $750 \pm 34 \mu\text{g/l}$). While in glycerol medium, plasmid free strain produced more HGA than plasmid-encoded strain ($870 \pm 69 \mu\text{g/l}$ vs. $530 \pm 43 \mu\text{g/l}$). HGA compound readily oxidises under the cultivation conditions (used in this study) and further polymerises to produce ochronotic pigment. Due to this effect, plasmid-free and plasmid-encoded culture supernatant samples turned dark brown at the end of respective cultivations.

The *crtE* expression cassette was integrated in maltose locus of *E. coli* LJ110 strain to obtain a plasmid-free *E. coli* CS2.1 strain. Isoprenoid precursors, FPP & GGPP, are lipophilic and had to be extracted from cells. In this study, a simple, sensitive and non-radioactive based GC-MS method was used to quantify the FPP and GGPP produced in *E. coli* strains. GGPP production in plasmid-free *E. coli* CS2.1 strain showed a robust GGPP production in terms of yield i.e. nmol of GGPP per gram of cell dry weight (nmol/g CDW). GGPP yield in plasmid-free *E. coli* CS2.1 strain was higher than in plasmid-encoded *E. coli* LJ110/pCAS30 strain i.e. $310 \pm 19 \text{ nmol/g CDW}$ and $249 \pm 14 \text{ nmol/g CDW}$, respectively.

HGA and GGPP produced in both, plasmid-free and plasmid-encoded strains have to undergo a decarboxylation and prenylation reaction to form MGGBQ. This reaction is catalysed by Hpt-Syn. Chromosomal integration of *hpt-Syn* expression cassette in a plasmid-free strain capable of producing HGA and GGPP resulted in a new plasmid-free *E. coli* CS6 strain. MGGBQ, due to its carbohydrate side chain is lipophilic, and has to be extracted from cells. MGGBQ yields achieved in plasmid-free *E. coli* CS6 strain were $604 \pm 24 \mu\text{g/g CDW}$ vs. $325 \pm 13 \mu\text{g/g CDW}$, and $669 \pm 31 \mu\text{g/g CDW}$ vs. $554 \pm 29 \mu\text{g/g CDW}$ than that produced in plasmid-encoded *E. coli* BW25113/pCAS29 strain in glucose and glycerol containing medium, respectively. One reason for the lower MGGBQ yield in plasmid-encoded *E. coli* strains is the lower segregational stability i.e. at the end of fermentation, approx. 50 % and approx. 40 % of cells had lost the plasmids, in medium containing glucose and glycerol respectively. Similar to HGA, MGGBQ is also an unstable compound. MGGBQ is oxidised to form 2-methyl-6-geranylgeranylbenzoquinone (MGGBQ_{oxidised}). Similar to HGA the MGGBQ_{oxidised} may undergo a polymerisation reaction to produce brown pigment. Plasmid-free and plasmid-encoded cell pellet samples (after centrifugation) collected during

the last 12 hours of fermentation were partially brown in colour. Mass Spectroscopy (MS) analysis of MGGBQ revealed a mass of 396 and 394 Da, which corresponded to the calculated mass of MGGBQ (reduced form) and MGGBQ_{oxidised}, respectively. MGGBQ produced in plasmid-free *E. coli* CS6 strain was enriched and the proposed chemical structure was elucidated by nuclear magnetic resonance (NMR) spectroscopy.

Tocopherol cyclase (Cyc) enzyme, catalyzes the ring closing reaction on the aromatic head at C1 position of MGGBQ (common single precursor to all tocotrienol compounds) to produce δ -tocotrienol. Integration of *cyc-At* expression cassette in *E. coli* CS6 strain resulted in a new plasmid-free *E. coli* CS7 strain. Plasmid-free *E. coli* CS7 strain successfully produced higher MGGBQ than produced in plasmid-encoded strain *E. coli* BW25113/pCAS47, in glucose and glycerol medium respectively i.e. $1581 \pm 82 \mu\text{g/g CDW}$ vs. $940 \pm 32 \mu\text{g/g CDW}$ and $1026 \pm 23 \mu\text{g/g CDW}$ vs. $346 \pm 13 \mu\text{g/g CDW}$. Unexpectedly, the conversion of high level of MGGBQ into δ -tocotrienol, in case of plasmid-free strain was lower, compared to that in plasmid-encoded strain. *E. coli* BW25113/pCAS47 strain produced approx. 2.5 times and 1.5 times higher δ -tocotrienol, compared to plasmid-free *E. coli* CS7 strain in glucose & glycerol medium i.e. $9.4 \pm 0.9 \mu\text{g/g CDW}$ vs. $3.7 \pm 0.1 \mu\text{g/g CDW}$ and $5.4 \pm 0.2 \mu\text{g/g CDW}$ and $3.6 \pm 0.2 \mu\text{g/g CDW}$, respectively. In both cases (plasmid-free and plasmid-coded *E. coli* strains), the low δ -tocotrienol yields may be due to lower expression level of eukaryotic protein (*Cyc-At*) or its lower activity during *in-vivo* δ -tocotrienol biosynthesis. Another possible reason for conversion of MGGBQ into δ -tocotrienol may be the inaccessibility of *Cyc-At* proteins to the aromatic head group MGGBQ.

To study the tocopherol cyclase activity, tocopherol cyclase (*Cyc-At*) protein were overexpressed in a His-tagged and a GST-tagged form in recombinant *E. coli* and purified. GST-tagged *Cyc-At* proteins showed higher enzyme activity compared to His-tagged *Cyc-At* i.e. $60.2 \text{ nmol/mg protein/h}$ and $39.4 \text{ nmol/mg protein/h}$, respectively. Results of the *in-vitro* enzymatic reactions and the *in-vivo* δ -tocotrienol biosynthesis could not be resolved yet.

To increase the product yield ($\mu\text{g/g CDW}$), it is important to increase the carbon flux entering the shikimate and DXP pathway, especially when a simple sugar is used as sole carbon and energy source. Carbon flux in the direction of DXP pathway was increased, by enhancing the expression level of the rate limiting *E. coli* enzymes, by integrating the *Idi* (isopentenyl diphosphate isomerase) expression cassette in ribose loci, and by enhancing the expression level of another rate limiting *E. coli* enzyme, *Dxs* (1-deoxy-D-xylulose-5-phosphate synthase) by promoter exchange in the chromosome, to obtain *E. coli* CS8 and *E. coli* CS10 strains, respectively. As a result of that, MGGBQ yield increased by 1.4 and 2.4 times in *E. coli* CS8 and *E. coli* CS10 compared to that produced in *E. coli* CS6. Despite 1.4 times increase in MGGBQ by the increased formation of isoprenoid precursor, yield of δ -tocotrienol did not increase.

In the current work, the shikimic acid pathway is not limiting, while the DXP pathway is. It is shown in this study that the single copy gene (i.e. plasmid-free system) offers an optimal product yield as it reduces the metabolic burden which is otherwise exerted in case if a plasmid (i.e. plasmid-encoded system carrying several copies of genes per cell) is used. Construction of plasmid-free system as shown in this study ensures the segregational stability of heterologous genes, unlike in plasmid-coded systems. Simple and efficient recombination methods followed in this work, to construct a heterologous host system in *E. coli*, has a potential in investigating more such complex natural product biosynthesis studies.

Zusammenfassung

Vitamin E stellt eine Gruppe von fettlöslichen Verbindungen, bestehend aus jeweils vier Formen (δ , β , γ , α) der Tocopherole und Tocotrienole, dar. In der Natur werden „Vitamin-E-Verbindungen“ ausschließlich von Pflanzen und anderen photosynthetisch aktiven Organismen (z.B. Cyanobakterien, einigen Algen) synthetisiert, mit der einzigen Ausnahme einer kürzlich entdeckten Tocopherol-Synthese in einem nicht-photosynthetisch aktiven Eukaryoten dem Malaria-Erreger *Plasmodium falciparum*. Von den insgesamt acht Vitamin E-Formen kann α -Tocopherol ubiquitär in photosynthetischen Organismen nachgewiesen werden, während δ -Tocotrienol eine seltene Form darstellt. Im Gegensatz zu α -Tocopherol, welches die höchste Antioxidationsaktivität der Vitamin E Verbindungen aufweist, wird δ -Tocotrienol als Wirkstoff in der Prävention und Behandlung von Krankheiten wie Arteriosklerose, Alzheimer, Parkinson oder Krebs diskutiert. Menschen und Tiere können Vitamin-E-Verbindungen nicht selbst produzieren und müssen diese Substanzen somit durch die Nahrung aufnehmen.

Die chemische Synthese von natürlichem δ -Tocotrienol hat den Nachteil, dass ein racemisches Gemisch aus acht Isoformen entsteht, die in ihrer Vitamin-E-Aktivität variieren. Mehrere komplexe, asymmetrische synthetische Reaktionen sind nötig, um die natürlichen δ -Tocotrienol-Isomere herzustellen. Diese Synthese ist jedoch nur mit niedrigen Ausbeuten durchführbar. Alternativ dazu können geringe Mengen (ca. 15 μ g δ -Tocotrienol je Gramm frischer Palmölfrüchte) von δ -Tocotrienol aus Pflanzen mittels Extraktion gewonnen werden. Aufgrund der geringen Konzentration steht die Extraktion der chemischen Synthese in puncto Wirtschaftlichkeit deutlich nach. Die erfolgreiche Suche nach einem - aus prozesstechnischer Sicht - umweltfreundlichen und wirtschaftlich sinnvollen Lösungsmittel ist für diese Extraktion essentiell, jedoch bis lang nicht ausreichend untersucht. Die Biotechnologie könnte mittels *Metabolic Engineering* einen wichtigen Betrag leisten, um den weltweit stetig steigenden Bedarf an δ -Tocotrienol zu decken. Molekularbiologen und Pflanzenzüchter bemühen sich die Biosynthese von Vitamin-E-Verbindungen in photosynthetisch aktiven Organismen zu erhöhen. Verglichen mit der chemischen Synthese müsste jedoch die δ -Tocotrienol Ausbeute in rekombinanten Pflanzen um das ca. 50-100 fache erhöht werden, um ein wirtschaftliches Extraktionsverfahren zu ermöglichen.

In der vorliegenden Arbeit wurde ein neuer Ansatz für die Biosynthese des aktiven δ -Tocotrienol-Stereoisomers und seiner Vorstufe 2-Methyl-6-geranylgeranyl-benzoquinol (MGGBQ) - mittels eines nicht-photosynthetisch aktiven, rekombinanten Stammes von *Escherichia coli* (*E. coli*) - untersucht. δ -Tocotrienol besteht aus einer fettlöslichen, ungesättigten Kohlenwasserstoffkette verbunden mit einer polaren, aromatischen Gruppe. Der Wildtypstamm von *E. coli* kann beide Donorgruppen, sowohl in Form von *p*-Hydroxyphenylpyruvat (*p*-HPP) über den Shikimatweg, als auch in Form von Farnesylpyrophosphat (FPP) und Isopentenyl Pyrophosphat (IPP) über den 1-Desoxy-D-Xylulose-5-phosphat (DXP)-Weg, produzieren.

Um die Bildung von δ -Tocotrienol in *E. coli* zu realisieren, müssen vier Biosyntheseschritte, ausgehend von FPP und *p*-HPP, in *E. coli* etabliert werden. Hierzu wurden die Gene für die Hydroxyphenyl-Pyruvat-Dioxygenase (Hpd) aus *Pseudomonas putida*, die Geranylgeranylpyrophosphate Synthase (CrtE) aus *Pantoea ananatis*, die Homogentisat-Phytyltransferase (Hpt-Syn) aus *Synechocystis sp.* PCC6803 und die Tocopherol-Cyclase (Cyc-At) aus *Arabidopsis thaliana* mit Hilfe eines Expressionsvektors ausgeprägt. Die plasmid-kodierten Stämme produzierten während des *in-vivo* Aktivitätstests in komplexem Nährmedium Homogentisinsäure (HGA), und/oder Geranylgeranylpyrophosphat (GGPP) und/oder MGGBQ und/oder δ -Tocotrienol.

Um einen stabilen und skalierbaren Produktionsprozess für den kommerziellen/industriellen Maßstab zu entwickeln, ist ein Stamm mit einer stabilen Expressionsleistung über die gesamte Fermentationszeit notwendig. Gängige *E. coli* Expressionsplasmide erweisen sich als instabil bei der Segregation und es besteht die Gefahr, dass während des Produktionsprozesses Schwankungen in der Expressions- bzw. Produktionsleistung entstehen. Ein Plasmidverlust während der Fermentation würde zum Verlust der heterologen Biosynthesegene führen und somit zu einer Verringerung der Produktivität. Für den Erhalt von plasmid-basierten Expressionssystemen ist daher die Verwendung von Antibiotika notwendig. Der Einsatz von Antibiotika ist ein großer Kostenfaktor und zudem in der Lebensmittelindustrie unerwünscht. Um das Problem der Plasmidinstabilität zu lösen und auf Antibiotika während der Fermentation zu verzichten, wurden in dieser Arbeit mittels homologer Rekombinationstechniken, plasmid-freie Stämme erzeugt, die δ -Tocotrienol und MGGBQ produzieren.

Dazu wurden Expressionskassetten mit den Genen *hpd*, *crtE*, *hpt-Syn* und *cyc-At* erzeugt, die mittels des λ -Red-Rekombinase-Systems in die Loci der Zucker-Abbaugene für L-Fucose, Maltose, Lactose und D-Xylose ins Chromosom integriert wurden. Der durch die Integration bedingte Verlust der Zucker-Abbaugene ermöglicht ein effizientes Screening des Rekombinationsereignisses mit Hilfe von MacConkey Indikator-Platten. Durch die transiente Expression einer Flippase (FLP)-Rekombinase konnten die Markergene entfernt werden. Die so erzeugten plasmid-freien und plasmid-tragenden Stämmen wurden in Minimalmedium mit Glukose oder Glycerin als einziger Kohlenstoff- und Energiequellen kultiviert und die jeweiligen Ausbeuten an HGA, GGPP, MGGBQ und δ -Tocotrienol ermittelt und miteinander verglichen.

Die *hpd*-Expressionskassette wurde in den L-Fucose-Locus des *E. coli* BW25113lacZ⁺ Stammes integriert und somit der Stamm *E. coli* CS1 erzeugt. Homogentisinsäure ist eine wasserlösliche Verbindung, die mittels HPLC in den Überständen der Kulturen nachgewiesen wurde. Mit Glukose als Kohlenstoffquelle produzierte der plasmid-tragende Stamm (*E. coli* BW25113/pCAS2JF) 1,6 – fach mehr HGA als der *E. coli* CS1 Stamm mit der chromosomalen Integration des *hpd* Gens ($1213 \pm 45 \mu\text{g/l}$ gegenüber $750 \pm 34 \mu\text{g/l}$). Während in Glycerin-Medium, der plasmid-freie Stamm *E. coli* CS1 ca. 1,2 - fach mehr HGA produzierte als der plasmid-tragende Stamm *E. coli* BW25113/pCAS2JF ($870 \pm 69 \mu\text{g} / \text{l}$ vs $530 \pm 43 \mu\text{g} / \text{l}$).

In den Maltose-Locus von *E. coli* LJ110 wurde die *crtE*-Expressionskassette integriert und somit der plasmid-freie Stamm *E. coli* CS2.1 erzeugt. Die Isoprenoidvorstufen FPP & GGPP, sind lipophil und mussten aus den Zellen extrahiert werden. Zur Quantifizierung der FPP und GGPP Produktion in den *E. coli*-Stämmen wurde in dieser Arbeit eine einfache, sensitive und nicht-radioaktive GC-MS-Methode verwendet. Die GGPP-Produktion im plasmid-freien *E. coli* Stamm CS2.1 zeigte eine stabile GGPP-Produktion bezüglich der Ausbeute angegeben in nMolen GGPP pro Gramm Zelltrockengewicht (nmol / g CDW). Die GGPP Ausbeute bei dem plasmid-freien *E. coli*-Stamm CS2.1 war höher als bei dem plasmid-tragenden *E. coli*-Stamm LJ110/pCAS30 (d.h. $310 \pm 19 \text{ nmol} / \text{g CDW}$ bzw. $249 \pm 14 \text{ nmol} / \text{g CDW}$).

Durch eine Decarboxylierungs und Prenylierungs-Reaktion zwischen HGA und GGPP wird MGGBQ gebildet. Diese Umsetzung wird durch das Enzym *Hpt-Syn* katalysiert. Durch die chromosomale Integration der *hpt-Syn*-Expressionskassette in einen Stamm, in dem die Gene für die Produktion von HGA und GGPP bereits integriert worden waren, wurde der Stamm *E. coli* CS6 erzeugt. Aufgrund der Prenyl- Seitenkette ist MGGBQ lipophil und muss zum Nachweis aus den Zellen extrahiert werden. Die MGGBQ-Ausbeuten im plasmid-freien Stamm *E. coli* CS6 unter Verwendung von Glucose als Kohlenstoffquelle betragen $604 \pm 24 \mu\text{g} / \text{g CDW}$ verglichen mit $325 \pm 13 \mu\text{g} / \text{g CDW}$ im plasmid-tragenden Expressionssystem. Mit Glycerin als Kohlenstoffquelle erreichte der plasmid-freie Stamm MGGBQ-Ausbeuten von $669 \pm 31 \mu\text{g} / \text{g CDW}$ verglichen mit $554 \pm 29 \mu\text{g} / \text{g CDW}$ im plasmid-tragenden *E. coli*

BW25113/pCAS29 Stamm. Ein Grund für geringe MGGBQ-Ausbeute im plasmid-tragenden Expressionsystem ist die niedrigere segregationale Stabilität. Am Ende der jeweiligen Fermentationen enthielten ca. 50% (Glucose als Kohlenstoffquelle) bzw. ca. 40% (Glycerin als Kohlenstoffquelle) der Zellen keine Plasmide mehr. Wie HGA ist auch MGGBQ eine leicht zu oxidierende Verbindung. MGGBQ oxidiert zu 2-Methyl-6-geranylgeranylbenzochinon (MGGBQ_{oxidiert}). So wird, wie im Fall des HGA, auch MGGBQ_{oxidiert} durch eine Polymerisationsreaktion in ein braunes Pigment umgesetzt. Im Zellsedimentet der Fermentationsproben (in den letzten 12 Fermentationsstunden) konnten in den plasmid-tragenden und in den plasmid-freien Stämmen braun Farbe nachgewiesen werden.

MGGBQ, das mit Hilfe des *E. coli* CS6 Stamm gebildet worden war, wurde aus den Zellen isoliert und die chemische Struktur wurde durch Kernspinresonanz (NMR)-Spektroskopie aufgeklärt.

Die Tocopherol-Cyclase katalysiert die Ringschlussreaktion an der C1-Position des aromatischen Rings des MGGBQ (gemeinsame Vorstufe aller Tocotrienol-Verbindungen) zur Bildung von δ -Tocotrienol. Durch die chromosomale Integration der *cyc-At* Expressionskassette in den D-Xylose Locus des *E. coli* CS6 Stammes wurde der Stamm *E. coli* CS7 erzeugt. Der plasmid-freie Stamm *E. coli* CS7 produziert mehr MGGBQ als der plasmid-tragende Stamm *E. coli* BW25113/pCAS47. Im Glucose Medium wurden im *E. coli* CS7 Stamm Ausbeuten von $1581 \pm 82 \mu\text{g} / \text{g CDW}$ erreicht. Der plasmid-tragende Stamm produzierte dagegen $940 \pm 32 \mu\text{g} / \text{g CDW}$. Unter Verwendung von Glycerin als Kohlenstoffquelle konnten Ausbeuten von $1026 \pm 23 \mu\text{g} / \text{g CDW}$ im Stamm *E. coli* CS7 und $346 \pm 13 \mu\text{g} / \text{g CDW}$ im plasmid-tragenden *E. coli* erzielt werden. Die Umwandlung dieser MGGBQ-Mengen zu δ -Tocotrienol durch die rekombinante Tocopherol-Cyclase war im plasmid-freien Stamm geringer im Vergleich zum plasmid-tragenden Stamm. Somit konnten im *E. coli* BW25113/pCAS47 Stamm ca. 2,5-fach mehr Tocotrienol im Vergleich zum plasmid-freien *E. coli*-Stamm nachgewiesen werden. (Glukose als Kohlenstoffquelle: $9,4 \pm 0,9 \mu\text{g} / \text{g CDW}$ beim plasmid-freien Stamm und $3,7 \pm 0,1 \mu\text{g} / \text{g CDW}$ beim plasmid-tragenden Stamm; Glycerin als Kohlenstoffquelle: $5,4 \pm 0,2 \mu\text{g} / \text{g CDW}$ beim plasmid-freien Stamm verglichen mit $3,6 \pm 0,2 \mu\text{g} / \text{g CDW}$ beim plasmid-tragenden Stamm.

Diese Beobachtung könnte durch ein niedriges Expressionsniveau des eukaryotischen *Cyc-At* Proteins oder durch eine niedrigere Aktivität der rekombinanten *Cyc-At* im Stamm *E. coli* CS7 erklärt werden. Eine weitere Ursache für die niedrige Umwandlung von MGGBQ könnte die Unzugänglichkeit des Kohlenstoffatoms an der 1'-Position des aromatischen Rings des MGGBQ sein. Um die Aktivität der Tocopherol-Cyclase (*Cyc-At*) zu untersuchen, wurde das Enzym mit verschiedenen *Tags* (plasmid-kodiert) versehen (Histidin (*His-Tag*) bzw. Glutathion-S-Transferase (GST)-markiert), in *E. coli* exprimiert und mittels Affinitätschromatographie gereinigt. Das so gewonnene *Cyc-At*-Protein wurde unter Verwendung von gereinigtem MGGBQ als Substrat (MGGBQ-Cyclodextrin-Komplex) in einem *in-vitro* Enzymtest untersucht. Das GST-markierte *Cyc-At*-Enzym zeigte eine höhere Enzymaktivität im Vergleich zum *His*-markierten *Cyc-At* ($60,2 \text{ nmol} / \text{mg Protein} / \text{h}$ und $39,4 \text{ nmol} / \text{mg Protein} / \text{h}$).

Um die MGGBQ-Ausbeute zu erhöhen, ist es wichtig den Kohlenstofffluss in diesem Reaktionsweg zu erhöhen, insbesondere, wenn einfache Zucker wie Glucose als einzige Kohlenstoff- und Energiequelle verwendet werden. In *E. coli* stellen die durch *Dxs* (1-Desoxy-D-xylulose-5-Phosphat-Synthase) und *Idi* (Isoprenyldiphosphat-Isomerase) katalysierten Reaktionen die wichtigsten limitieren Schritte in der Isoprenoidsynthese dar. Um die Expression der entsprechenden Gene und somit den Kohlenstofffluss in Richtung der FPP-Bildung zu erhöhen, wurde zum einen eine zusätzliche *idi* Expressionskassette chromosomal in den D-Ribose-Locus des Stammes *E. coli* CS6 integriert (*E. coli* CS8), zum anderen wurde durch einen Promotoraustausch im Chromosom von *E. coli* CS8 die Expression des nativen *dxs* Gens verstärkt. Dadurch wurde der Stamm *E. coli* CS10 erzeugt.

Die so erzeugten Stämme *E. coli* CS8 und *E. coli* CS10 zeigten 1,8 - und 2,4 - fach höhere MGGBQ-Ausbeuten im Vergleich zum *E. coli* CS6 Stamm. Jedoch führte die 1,8 - fache Erhöhung in der MGGBQ-Ausbeute zu keinem signifikanten Anstieg in der δ -Tocotrienol-Ausbeute zum Beispiel im Vergleich mit dem *E. coli* CS9 Stamm (Cyc-At-Expressionkassette im Stamm *E. coli* CS8).

In der vorliegenden Arbeit wurde für die Biosynthese von MGGBQ und δ -Tocotrienol in *E. coli* nachgewiesen, dass der Shikimisäure-Weg nicht limitierend ist, während dies für den DXP-Weg der Fall ist. Es wurde erfolgreich gezeigt, dass ein niedriges Niveau der heterologen Expression, bedingt durch die chromosomale Integration mit einer einzigen Kopie des Gens (plasmid-freie Stämme), ausreichend für eine effiziente heterologe *in-vivo*-Biosynthese von komplexen Naturstoffen wie dem lipophile MGGBQ und dem Tocotrienol ist. Durch die stabile Insertion der heterologen Gene ins Chromosom wird, im Gegensatz zur Verwendung von Plasmidvektoren, eine zuverlässige Weitergabe der Gene an die Tochterzellen gewährleistet. Die in dieser Arbeit erhaltenen Ergebnisse und molekularbiologische Rekombinationsmethoden zur Erzeugung heterologer *E. coli* Produktionsstämme bilden eine gute Ausgangsbasis um mittels biotechnologischer Methoden ähnlich bedeutende Naturstoffe herzustellen und vielleicht zukünftig dem Markt in ausreichenden Mengen zur Verfügung zu stellen.

Some of the results mentioned in this chapter (Chapter 3 – Results) have been partially published in articles in following journals:

1) C. Albermann*, S. Ghanegaonkar*, K. Lemuth, T. Vallon, M. Reuss, W. Armbruster, G. Sprenger, *Biosynthesis of Vitamin E Compound δ -Tocotrienol in Recombinant Escherichia coli Cells*, *Chembiochem.* **2008**, 9, 2524-2533

2) T. Vallon*, S. Ghanegaonkar*, O. Vielhauer, A. Müller, C. Albermann, G. Sprenger, M. Reuss, K. Lemuth. *Quantitative analysis of isoprenoid diphosphate intermediates in recombinant and wild type Escherichia coli strains.* *Applied Microbiology and Biotechnology*, **2008**, 81, 175-182

3) S. Ghanegaonkar*, J. Conrad, G. Sprenger, U. Beifuss, C. Albermann*. *Towards the in vivo production of tocotrienol compounds: engineering of a plasmid free Escherichia coli strain for the heterologous synthesis of 2-methyl-6-geranylgeranyl benzoquinone.* *Journal of Biotechnology*, **2012**. (Manuscript submitted on April 3, 2012. Manuscript re-submitted on June 12, 2012, after incorporating reviewer's comments. Current status at the time of submission of the doctoral thesis: "In review").

* authors contributed equally to the manuscript

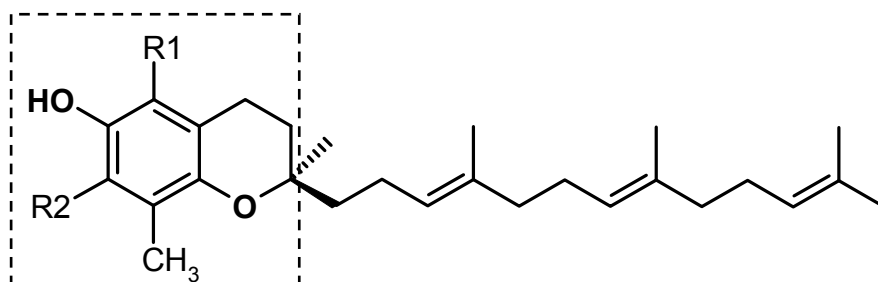
Chapter 1 - Introduction

1.1. Vitamin E and its chemical structure

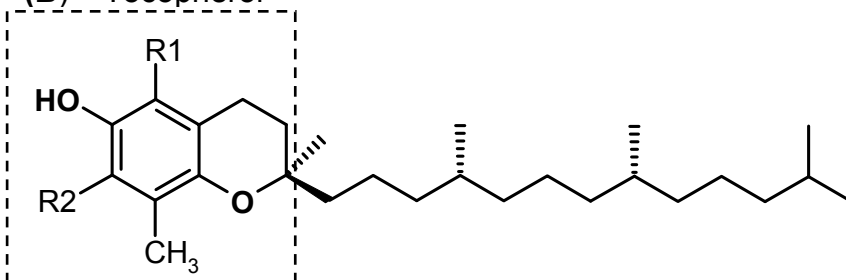
Vitamin E is synthesized exclusively by photosynthetic organisms e.g. green plants, green algae, cyanobacteria e.g. *Synechocystis* PCC6803 (DellaPenna and Pogson 2006). Recently, tocopherol biosynthesis was detected in a malaria parasite *Plasmodium falciparum*, a non-photosynthetic eukaryote (Sussmann 2011). Vitamin E comprises of lipid soluble antioxidants, which have a potential to protect the photosynthetic organisms against reactive oxygen species (Azzi 2007).

Vitamin E is a generic term, which is composed of 2 derivatives called Tocochromanols, i.e. Tocotrienols and Tocopherols as shown in figure 1.1 A & B (Brigelius-Flohé and Traber 1999). Tocochromanols consist of a polar chromanol ring and a non-polar isoprenoid side chain (C16 molecule) but differ, in the degree of saturation in the phytyl side chain. Tocotrienol consists of three unsaturated double bonds (*trans*) while, the tocopherols consist of a fully saturated side chain. (Kamal-Eldin and Appelquist 1996).

(A) Tocotrienol



(B) Tocopherol



(C)

	α :	β :	γ :	δ :
R1	CH ₃	CH ₃	H	H
R2	CH ₃	H	CH ₃	H

Figure 1.1: Chemical structure of Vitamin E compounds (A) Tocotrienol (B) Tocopherol i.e. the two tocochromanol compounds. (C) Site and position of methylation of the 2 tocochromanol compounds (Sen. et.al. 2007). The box with dotted line shows the chromanol ring.

Further, the two tocopherol compounds are composed of 4 forms each, i.e. α , β , γ , and δ , which, differ in the site and degree of methylation (see Figure 1.1 C) (Sen et. al. 2007). Tocopherols are characterised by, a saturated phytyl side chain with three chiral centers (1', 4' and 8' positions) with the naturally occurring tocopherols having R-configuration at all the 3 positions while, the tocotrienols consisting of double bonds on the isoprenoid side chain at 3', 7' and 11' (Schneider 2005). Common among both the respective forms, is the same substitution pattern on the chromanol ring (Schneider 2005).

In green plants all forms of tocopherols are synthesized in plastids (Austin et. al. 2006). The isoprenoid precursors for the tocopherols are derived via two ways; one, from the 2C-Methyl-D-Erythritol 4-Phosphate pathway (MEP) pathway (also called as 1-Deoxy-D-xylulose 5-phosphate (DXP) pathway or also called as non-mevalonate pathway) and secondly, via the Mevalonate pathway (Lange et. al. 2000). The aromatic precursor for the tocopherols, are derived from the shikimate pathway (DellaPenna 2005).

1.2. Natural food sources of Vitamin E

Vitamin E is known as essential component of human and animal diet (Della Penna et.al. 2006). As humans and animals are unable to synthesize their own Vitamin E compounds, their primary source comes from food and supplements (Chen et. al. 2006). The amounts of Vitamin E compounds in different food ingredients are shown in table 1.1, 1.2 and 1.3.

Table 1.1: Tocopherol and Tocotrienol content in different selected fruits and vegetables (Chun et. al. 2006)

Fruits and Vegetables	Tocopherol [$\mu\text{g/g}$ FW]				Tocotrienol [$\mu\text{g/g}$ FW]			
	α	β	γ	δ	α	β	γ	δ
Red Apples	3.8	N.D	0.4	0.1	N.D	N.D	0.00	0.00
Avocados from Florida	26.6	0.8	3.9	N.D	N.D	N.D	0.00	0.00
Kiwi	13.1	N.D	0.3	N.D	N.D	1.1	0.00	0.00
Oranges	2.5	N.D	N.D	N.D	N.D	N.D	0.00	0.00
Raw Broccoli	14.4	Trace	3.1	N.D	Trace	N.D	0.00	0.00
Raw Carrots	8.6	Trace	N.D	N.D	N.D	N.D	0.00	0.00
Iceberg Lettuce	2.2	N.D	1.1	N.D	N.D	N.D	0.00	0.00
Raw Spinach	19.6	N.D	2.1	N.D	N.D	N.D	0.00	0.00
Raw Tomatoes	5.3	Trace	1.4	Trace	Trace	N.D	0.00	0.00

FW is Fresh Weight (or Edible weight)

N.D: Not detectable

These values have a standard deviation between 1 to 20 %.

A detailed list, with 55 fruits and 144 vegetables (processed, raw) was compiled by Eitenmiller & Lee 2004. The amount of Vitamin E compounds in fruits and vegetables is influenced by the species, variety, maturity and the growing conditions (Chun et.al. 2006). A

few fruits and vegetables were selected and are shown in table 1.1. α -tocopherol was the Vitamin E found in almost all the fruits and vegetables. In some cases β - and γ tocopherols were also detected but in trace amounts (below 1 $\mu\text{g/g}$ FW).

Traces of δ -tocopherols were found only in apples and raw tomatoes. On the other hand, traces of α - & β -tocotrienol were detected (if any), while no γ - and δ -tocotrienols were detected in the fruits and vegetables shown in table 1.1. This shows that, in general, all forms of tocotrienols and δ -tocopherols are very rare forms of Vitamin E. If the vegetables are processed, the tomato paste and blanched frozen spinach consists of 47 and 40 $\mu\text{g/g}$ edible weights, respectively (Chen et. al. 2006).

Table 1.2: Vitamin E content in different selected grains

Type of Fresh Grain	Tocopherol [$\mu\text{g/g}$ FW]				Tocotrienol [$\mu\text{g/g}$ FW]			
	α	β	γ	δ	α	β	γ	δ
Barley	2	4	0.3	1	11	3	2	0
Rice, White	1	0	1	Trace	Trace	0	2	0
Wheat	14	7	0	0	5	33	0	0
Corn (fresh, yellow)	0.6	0	4	0	2	0	4	0

FW is Fresh Weight of grains

Values calculated in $\mu\text{g/g}$ Seed based on Slover et. al. 1971

Table 1.3: Vitamin E content in different selected vegetable oils

Type of Oil	Tocopherol [$\mu\text{g/g}$ Oil]				Tocotrienol [$\mu\text{g/g}$ Oil]			
	α	β	γ	δ	α	β	γ	δ
Palm Oil	256	0	316	70	143	32	286	69
Peanut Oil	130	0	214	21	0	0	0	0
Rapeseed Oil	184	0	380	12	0	0	0	0
Sunflower Oil	487	0	51	8	0	0	0	0
Wheat Germ Oil	1330	710	260	271	26	181	0	0

Values calculated in $\mu\text{g/g}$ Seed based on Slover et. al. 1971

Out of all the natural food sources, the richest natural sources are vegetable oils, nuts and whole grains, when considered per g of oil. Wheat germ oil is the single richest widely available source known till date (Souci et. al. 1989).

In the past, tocopherols have been found in plant seeds, leaves, roots, fruits, stems, hypocotyls and cotyledons of higher plants (Horvath 2006) but tocopherol content and composition is very heterogeneous (S. Munne-Bosch 2002). On the other hand tocotrienols are not widely found in plants as compared to tocopherols (also seen from tables 1.1, 1.2 & 1.3). Tocotrienols are relatively less widespread in plants when compared with tocopherols with significant levels of tocotrienols being found in the photosynthetic tissues in monocot seeds (Horvath 2006; Cahoon et.al. 2003).

α -tocopherol (IUPAC name: (2R)-2,5,7,8-teramethyl-2-[(4R,8R)-4,8,12-trimethyltridecyl]-3,4-dihydrochromen-6-ol)) is the widely found form out of the 8 forms of natural Vitamin E. α -tocopherol also shows the highest biological activity as it is preferentially retained in large quantities and transported to human body components (Ching et. al. 2001). When compared, α -tocotrienol has one third activity while γ -tocopherol only one tenth when compared to α -tocopherol (Kamal Eldin 1996).

1.3. Biological and Chemical Synthesis of Vitamin E

In this section, Vitamin E synthesis pathways (i.e. natural and synthetic) are described. Vitamin E biosynthetic pathway has been well studied in model photosynthetic organisms i.e. higher plants (*Arabidopsis thaliana*) or cyanobacteria (*Synechocystis* PCC6803).

1.3.1. Vitamin E biosynthesis in higher plants and cyanobacteria

Tocopherols are found ubiquitously in plant tissues, especially in leaves and seeds, roots, fruits, stems of many dicotyledons of higher plants (Kamal-Eldin and Appelqrist 1996). Tocotrienols are usually concentrated in seeds, the germ and other oil containing fraction. Tocopherols and Tocotrienols are synthesized in plants via the same biosynthesis pathway.

In plants, the head group of tocopherols is derived from the shikimic acid pathway. Refer to figure 1.2. The *p*-hydroxyphenylpyruvate dioxygenase (Hpd) enzyme which catalyses this conversion of *p*-hydroxyphenylpyruvate (*p*-HPP) into homogentisic acid (HGA) is localised to the cytosol (Dörmann et. al. 2007). In case, if *Arabidopsis thaliana*, HGA is also used as precursor for tocopherol as well as for plastoquinol biosynthesis. Phytol pyrophosphate (PPP) is the side chain donor for the tocopherol synthesis. Homogentisate phytoltransferase (Hpt) catalyses the reaction between HGA and PPP, to synthesize, 2-methyl-6-phytylbenzoquinol (MPBQ). MPBQ is the common precursor for all forms of tocopherols. Genes encoding Hpt were isolated from *Arabidopsis thaliana* (At2g18950) (Collakova and DellaPenna 2001) and from cyanobacteria (Savidge et. al. 2002). All plants carry the *hpt* genes. Monocotyledons species contain an additional gene which encodes for homogentisate geranylgeranyl transferase (HggT). This HggT has substrate specificity towards GGPP (Cahoon et. al. 2003). HggT catalyses the condensation reaction between geranylgeranyl pyrophosphate (GGPP), and HGA, to synthesize 2-methyl-6-geranylgeranyl benzoquinol (MGGBQ), which is the precursor for all forms of tocotrienols. Barley, a monocot species possesses *hggT* gene, and hence produces twice the amount of tocotrienols compared to tocopherols (refer to table 1.2). In plants, plastoquinol, are also produced along with Vitamin E compounds. Homogentisate solanesyltransferase (Hst) catalyses the

condensation of a C45 compound solanyl diphosphate, and HGA to produce 2-methyl-6-solaneyl-benzoquinol (MSBQ). Methylation of MSBQ is catalysed by MPBQ methyltransferase (MPBQ-MT) to produce plastoquinol. In tocopherol pathway, the same MPBQ-MT catalyses the methylation at C3 position of MPBQ to produce 2,3-dimethyl-5-phytyl-benzoquinone (DMPBQ). Methylation reaction occurs only in presence of a methyl donor S-adenosyl-methionine (SAM) (van Eenennamm et. al. 2003). Tocopherol cyclase (Cyc) closes the second ring of DMPBQ to synthesize γ -tocopherol. Methylation at C5 position produces α -Tocopherol. This reaction is catalysed by γ -tocopherol methyltransferase (γ -TMT) which requires a methyl donor SAM (Shintani and DellaPenna 1998).

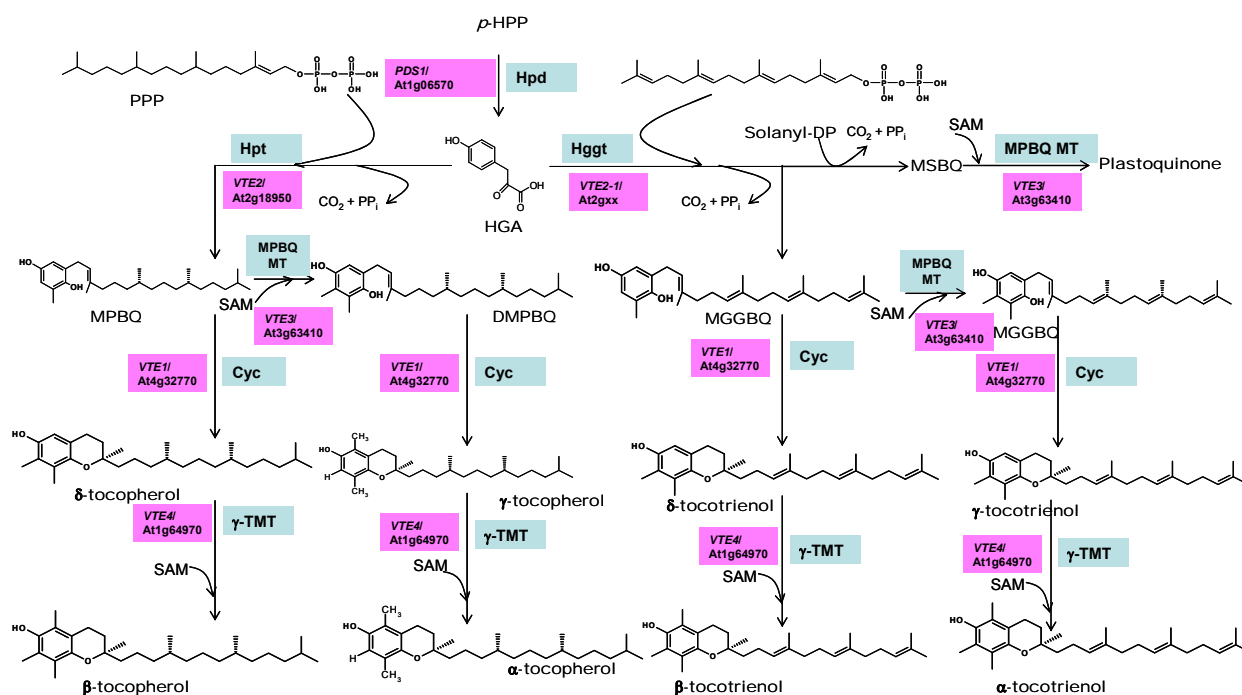


Figure 1.2 (Rippert et. al. 2004): Vitamin E and Plastoquinone biosynthesis in plants. *p*-HPP is *p*-hydroxyphenylpyruvate; Hpd is *p*-hydroxyphenylpyruvate dioxygenase; HGA is homogentisic acid; PPP is phytyl pyrophosphate; Hpt is Homogentisate phytyl transferase; MPBQ is 2-methyl-6-phytyl-benzoquinol; Ppi is Pyrophosphate; MPBQ-MT is MPBQ methyltransferase; DMPBQ is 2,3-dimethyl-5-phytyl-benzoquinone SAM is S-adenosyl-methionine; γ -TMT is γ -Tocopherol methyltransferase; GGPP is geranylgeranylphosphate; MGGBQ is 2-methyl-6-geranylgeranylbenzoquinol; DMGGBQ is 2,3-dimethyl-5-geranylgeranyl-benzoquinone.

The same above mentioned Cyc enzyme, catalyses the ring closing reaction on MPBQ, to produce δ -Tocopherol. Methylation at C6 position of the chromonal ring converts δ -Tocopherol into β -Tocopherol. This reaction needs SAM as methyl donor and is catalysed by the same γ -TMT which converts γ -Tocopherol into α -Tocopherol. Similarly, the same enzymes i.e. MPBQ-MT catalyse the methylation of MGGBQ to DMGGBQ, the Cyc further catalyses the ring closing reaction on 2,3-dimethyl-5-geranylgeranyl-benzoquinone (DMGGBQ) to produce γ -Tocotrienol (Porfirova et. al. 2002). Same enzyme γ -TMT

methylates the γ -Tocotrienol at C6 position to produce α -Tocotrienol. The same enzyme Cyc, closes the second ring of MGGBQ to produce δ -Tocotrienol and further methylation of δ -Tocotrienol produces β -Tocotrienol.

Table 1.3: Tocochromanol contents in wild type *Arabidopsis thaliana* seeds

	δ	β	γ	α	Source
Tocopherol [ng/mg seed]	4.03	n.d	354.9	7.4	Shintani & DellaPenna 1998
Tocopherol [ng/mg seed]	5.25	0	273	27.5	Sattler et. al. 2004

n.d: not detected

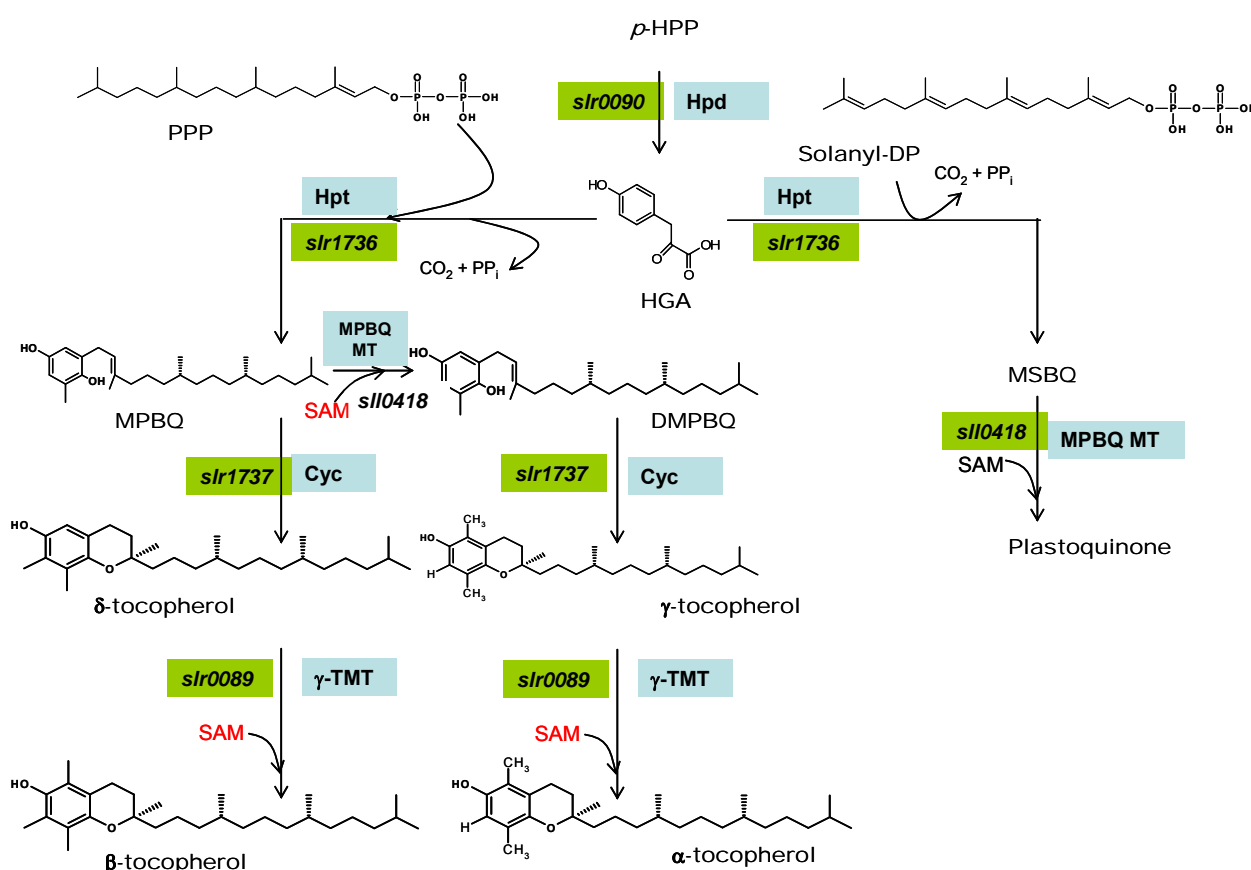


Figure 1.3 (Collakova et. al. 2001): Vitamin E and Plastoquinone biosynthesis in cyanobacteria e.g. *Synechocystis* PCC6803. *p*-HPP is *p*-hydroxyphenylpyruvate; *slr0090* gene encoding for *p*-hydroxyphenylpyruvate dioxygenase (Hpd); HGA is homogentisate; PPP is phytol pyrophosphate; *slr1736* gene encoding for Homogentisate phytol transferase enzyme (Hpt); MPBQ is 2-methyl-6-phytyl-benzoquinol; *slI0418* gene encoding for MPBQ methyltransferase enzyme (MPBQ MT); Ppi is Pyrophosphate; *slI0418* gene encoding for MPBQ methyltransferase enzyme (MPBQ-MT); DMPBQ is 2,3-dimethyl-5-phytyl-benzoquinone; S-adenosyl-methionine (SAM) is the co-factor which donates the methyl-group during methylation reactions; *slr0089* gene encoding for γ -Tocopherol methyltransferase enzyme (γ -TMT); GGPP is geranylgeranylphosphate. *slr1737* gene encoding for tocopherol cyclase enzyme (Cyc).

Table 1.4: Tocochromanols contents in wild type *Synechocystis PCC6803*

	δ	β	γ	α	Source
Tocopherol [ng/mg CDW]	251 \pm 15	22 \pm 0.3	22 \pm 0.3	170 \pm 9	Scheldz et. al. 2001
Tocopherol [ng/mg CDW]	75 \pm 40				Qi et. al. 2005
Tocotrienol [ng/mg CDW]	n.d	n.d	n.d	n.d	Scheldz et. al. 2001
Tocotrienol [ng/mg CDW]	n.d	n.d	n.d	n.d	Collakova et. al. 2001

CDW: Cell Dry Weight; n.d: not detected

Wild type *Synechocystis PCC6803* consists of less than 2 % of the total tocochromanols, with no δ -Tocotrienol in the extracts. Overexpression of hpd-At (p-hydroxyphenylpyruvate dioxygenase, from *Arabidopsis thaliana*) in transgenic *Synechocystis PCC6803*, increased the tocotrienols by 10-20 % of total tocochromanols (Karunandaa et.al. 2005).

1.3.2. Extraction of Vitamin E compounds from natural sources

Vitamin E is extracted from higher plant seeds in the form of vegetable oils with further purification and concentration steps (Ogbonna 2009). Approx. 10 % of total Vitamin E is produced via extraction from natural food sources. Extracted Vitamin E is enriched and the different homologues are further purified e.g. from soybean deodorizer distillates. Vitamin E content in many food sources are relatively low (max. 2.8 g/kg of wheat germ oil) with further lower levels of active forms of vitamin E i.e. α -tocopherol (0.257 g/kg of wheat germ oil). As seen from table 1.1, 1.2 and 1.3 the amount of total Vitamin E in food is relatively low (especially tocotrienol) when compared to the amount recommended as daily diet by FDA to show beneficial effects from regular diet. Processing of 1000 kg of crude palm oil is needed to obtain 1 kg of commercial vitamin E product Tocomin® 50% (Carotech, NJ) (Khanna et.al. 2005). For example one has to consume atleast 60 g of wheat germ oil, 100 to 200 g of palm oil or rice bran oil or 1.5 to 4 kg of wheat germ, barley or oat daily if one has intake the FDA recommended amount of Vitamin E uptake (Sen. et. al. 2007). These amounts are too high, and unhealthy, to be consumed by a normal human being. Hence dietary supplements of Vitamin E were recommended by different health organisations (Sen. et. al. 2007). Negative effects of Vitamin E are discussed in section 1.4.

1.3.3. Vitamin E biosynthesis in other photosynthetic organisms

Table 1.5: Tocopherol contents in different algae and cyanobacteria (Azzi and Stocket 2000).

Since no tocotrienols are produced in these micro-organisms they are not shown in the table below,

Micro-organism	Tocopherol [$\mu\text{g/g}$ CDW]			
	δ	β	γ	α
<i>Chlorella</i> (green algae)	7.6			
<i>Stichococcus bacillaris</i> (green algae)	134.2			
<i>Dunaliella salina</i> (green algae)	63.8			
<i>Cladophora stichotoma</i> (green algae)	0.7			
<i>Macrocystis intergrifolia</i> (brown algae)	12.2			
<i>Fucus distichus</i> (brown algae)	11.1			
<i>Anabaena variabilis</i> (cyanobacteria)	213.5			

For the first time, it was revealed that tocopherol was produced in a non-photosynthetic malarial parasite *Plasmodium falciparum* (Sussmann 2011). Shikimic acid and DXP pathway were reported to be functional in the Vitamin E biosynthesis pathway. Information regarding the genes, responsible for the other reactions in Vitamin E biosynthesis is not yet completed studied.

1.3.4. Chemical synthesis of Vitamin E

a) Chemical synthesis of α -tocopherol

Vitamin E compounds were chemically synthesized in as early as 1930's (Karrer 1938). Chemical synthesis of α -Tocopherol has been shown in figure 1.4. First commercial synthesis of all racemic α -tocopherol was carried out via chemical synthesis using racemic Isophytol and Trimethylhydroquinone (TMHQ) by F.Hoffmann-La Roche in 1950 (Buss 2008). The two reactants react well in presence of Lewis/Bronsted acids, e.g. HCl/ZnCl₂ or BF₃ or AlCl₃ dissolved in solvents. Chemically synthesized α -tocopherol is an equimolar racemic mixture of 8 stereoisomers (figure Appendix A 1-1). Out of these eight stereoisomers, 2R, 4'R,8'R- α -tocopherol (i.e. R-R-R- α -tocopherol) form has the highest Vitamin E activity. Natural R-R-R- α -tocopherol is 1.5 times more biologically more active than the chemically synthesized R-R-R- α -tocopherol (Valentin & Qi 2005).

Out of the 8 natural forms of Vitamin E, α -tocopherol has the highest Vitamin E activity (determined by the fetal resorption-gestation tests in rats).

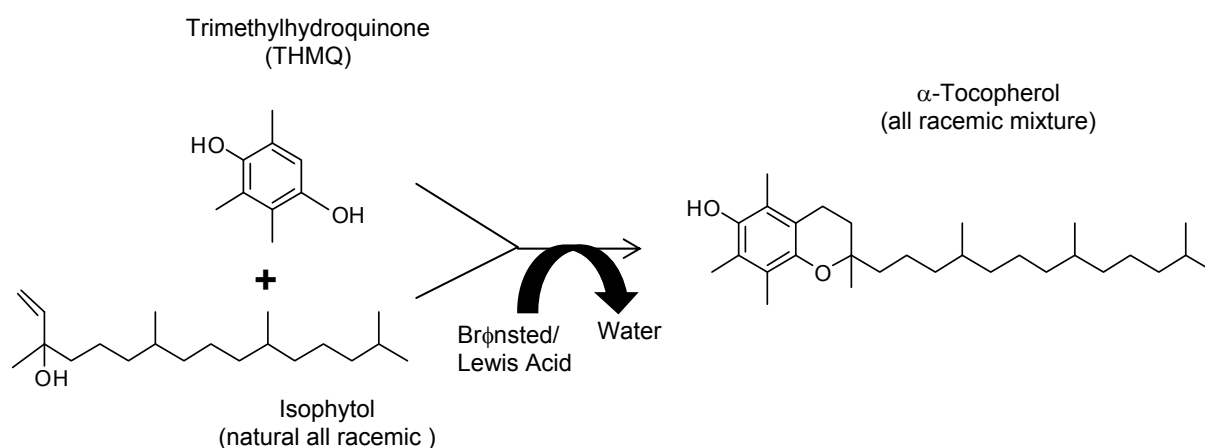


Figure 1.4: First chemical Synthesis of all racemic α -Tocopherol (reaction according to Karrer et. al. 1938)

Years of advances in stereoselective synthesis, and after many efforts, RRR- α -Tocopherol and SRR- α -Tocopherol was successfully synthesized (Mayer et.al. 1963). First, the synthesis of the chromanol building block and the second building block C15 compound was obtained by degradation of natural 2E, 7R, 11R phytol. The two building blocks undergo a two step reaction to form stereoisomer RRR- α -tocopherol.

In 2008, Lui, Chougnnet and Woggon, showed the shortest route for the chemical synthesis of RRR- α -Tocopherol. An organocatalyst was used to synthesis the chroman building block. This group concluded that this method can be useful in synthesizing other members of Vitamin E family and natural compounds with chiral centers.

Recently, Gomory et. al. 2011, achieved a higher yield of 89 % during chemical synthesis of R-R-R- α -tocopherol. Cyclocondensation of Isophytol and Trimethylhydroquinone (TMHQ) at reduced pressure was carried out in presence of water as solvent and ZnCl₂ as catalyst.

b) Chemical synthesis of δ -Tocotrienols

Limited availability of tocotrienols in natural sources (seen from Table 1.1-1.5), and its difficult isolation/extraction method forced synthetic chemists to start synthesizing tocotrienols using the available raw material.

First attempt to synthesize, δ -tocotrienol (and other forms α, γ, β), by reacting geranylgeranyl bromide and Trimethyl-hydroquinone (TMHQ), in presence of benzol (as solvent) and Zinc chloride (Karrer and Rentschler 1944). It was unable to perform the cyclisation (at the correct position) to tocotrienols. Later, several attempts were made to synthesize δ -tocotrienol and α -tocotrienol, which resulted in racemic mixtures (approx. 50:50 mixture of R to S enantiomers (at the C2 position) (Schudel et.al.1963). Hence, the critical task for the chemical synthesis of δ -tocotrienol (and for α, γ, β) had been, to set the chirality at position 2 (of the chromanol ring) and ring-closure, to obtain chromanol compound. Attempts to solve this problem was made using, kinetic resolution, enzymatic resolution asymmetric/stereoselective synthesis (Chenevert et.al. 2006; Scott et. al.1976). Many tocotrienol synthesis studies were published between 1970 and 2007 (Mayer et.al. 1967; Kabbe and Heitzer 1978). Reaction yields were improved compared to the previous processes, but they all failed to produce enantiomerically pure natural tocotrienols (Couladouros et. al. 2007).

Scott et.al. 1976 was successful in synthesizing a natural form of tocotrienol. This was synthesized using Trimethyl-hydroquinone (TMHQ) and a natural enantiomer 2,5,7,8-tetramethyl-6-hydroxychroman-2-acetic acid .

In order to commercialize a process, raw materials should be available in large quantities. Most of the raw materials available are not cheap, and chemical synthesis methods which uses it, usually ends up producing racemic mixture. Assymmetric/stereoselective synthesis is able to synthesize natural tocotrienols, but it includes numerous chemical reactions in

synthesizing raw material (intermediates). This increases the processing cost and hence makes the commercialization, difficult.

The new convenient chemical route towards synthesis of natural δ -tocotrienols (and other forms α , γ , β), was published by Couladouros et. al. 2007. According to Couladourous et.al. 2007, there method overcomes all of the above mentioned obstacles in commercialising the chemical synthesis, as it uses relatively less expensive raw material which is available in large quantities (all relative to existing raw materials), have short synthetic steps and isomerization during chemical manipulations was avoided (e.g. modifying δ -tocotrienol to α or γ -tocotrienols)

In first step, the building block “chromanmethanol” for tocotrienol synthesis was produced (scheme can be seen in appendix figure A1-3 (a) – (c). This step uses a cheap raw material i.e. quinones or hydroquinones, whichever is available. Acylation of hydroquinone with benzoyl chloride, results in a 1:4 mixture of di- Methylhydroquinone Dibenzoate to 2-Methylhydroquinone-4-Monobenzoate. Via series of critical reactions consisting of condensation of phenols to esters and further resolving the racemic mixture to obtain 2,8-Dimethyl-6-hydroxychroman-2-methanol i.e. DHCM (reaction scheme can be seen in appendix figure A1-2(a)). In the next step, the racemic mixture of DHCM obtained in first step was purified using enzymatic resolution. Racemic mixture of DHCM, hyflosupercell-supported PS-30 lipase, succinic anhydride, and *tert*-butyl methyl ether was stirred at room temperature for 5 h. After addition of ethyl acetate, acetone, it was extracted several times with aqueous sodium bicarbonate. Phase separation, acidification and extraction with ethyl acetate resulted succinate salt and pure (S) – DHCM with enantiomeric excess of approx. 96-97 % was achieved. In the last step, farnesol was converted into farnesyl sulfone. In a series of 3 reactions, δ -tocotrienol was synthesized. Similarly, the other forms of tocotrienols i.e. β , γ , α forms could also be produced by this method explained in Couladouros et.al. 2007).

c) Global commercial production of Vitamin E

In 1999, world wide production of vitamin E was in the range of 25,000 tons/year (Wilke et.al. 1999). For example, in-case of tocopherols, it was 80 % synthetic R/S- α -tocopherol and 20 % natural R-R-R- α -tocopherol (Wilke 1999, Netscher 1996). Due to its increasing importance in health nutrition, the global demand is on the rise and hence production of Vitamin E is increasing year after year. In 2001, BASF became the largest producer of Vitamin E by doubling its production capacity to reach 20,000 tons/year (Nutraingredients/

Mar.2001). In 2004, DSM Nutritional Product became the largest Vitamin E producer by increasing the production capacity to 25,000 tons/year. (Nutraingredients / 2004).

In the 1970's, Vitamin E synthesis in China was below 5 metric tonnes per year (MT/year), and below 500 MT/year in 1980's. In 1990's and 2000's the production reached almost 10000 MT/year and one of the reasons were the Chinese producers Zhejiang Medicine Co. Ltd. Xinchang Pharmaceutical Factory and Zhejiang NHU Co. Ltd. (Xinchang Synthetic Chemical Factory) along with dozens of other companies in China which included Southwest Synthetic Pharmaceutical Co. Ltd., Roche-Sunve (Shanghai) Vitamin Co. Ltd., BASF (Shenyang) Vitamin Co. Ltd. China has emerged as an important Vitamin E producer in world in the last decade. It is estimated that approximately 40 % of global Vitamin E is produced in China (PN Newswire, 9 May 2011, Production, Market and Benchmarking of Synthetic Vitamin E in China).

Approximately, 70 % of the world production is consumed for animal nutrition, with majority of the remaining 30 % for different cosmetic applications. Only, a small portion is used for human nutrition (Nutraingredients/Nov.2010). Almost all of the synthetic Vitamin E sold, is in the form its acetate form (Valentin & Qi 2005).

Access to recent commercial data is difficult, needs special registration to professional portals like ICIS pricing etc.

d) Advantages and Disadvantages of natural and synthetic Vitamin E production process

Disadvantage of chemical synthesis of Vitamin E is that the end product is a racemic mixture of 8 stereoisomers. On the contrary, the Vitamin E compounds extracted from natural sources (Drotleff et. al. 1999) e.g. α -tocopherol obtained from vegetable oil occurs in single stereoisomer where the 3 chiral centers have R-configuration (2R, 4'R, 8'R which is also called RRR- α -tocopherol) (Hoppe et. al. 2000). Process for chemical synthesis of tocopherols (Patent 2004, EP1095001) or tocotrienols (Couladouros, E.A et.al. 2004) include numerous steps, and hence more complicated as compared to extraction of Vitamin E from natural sources.

Many of these reaction steps are too complex to be performed on large scale application. Additionally, they have limited space-time yield, produces large amounts of waste material. Due to these reasons, no economic industrial process exists till date which synthesizes exclusively only the stereoisomer pure RRR- α -tocopherol.

One disadvantage of the extraction of Vitamin E from natural sources is its low yields due to lower contents in food sources.

1.3.5. Recommended Daily Allowance of Vitamin E

The Recommended Daily Allowance (RDA) in 1989, for Vitamin E was 8 mg tocopherol for adult women and 10 mg tocopherol for adult men. Within the last 2 decades, different function of Vitamin E in humans resulted in increasing the daily recommended intake to 15 mg of tocopherol for adult men and women (DellaPenna 2005).

1 I.U for Vitamin E is the biological equivalent of about 0.667mg R-R-R- α -tocopherol of 1 mg of R/S- α -tocopherol acetate

1.3.6. Commercial Price of Vitamin E

Often chemically synthesized α -tocopherol (i.e. racemic) is commercially represented as synthetic vitamin E. Vitamin E produced via natural sources cost around 20 USD/kg and mainly used for human applications, while cost of chemically synthesized Vitamin E is approx. 11 US \$/kg and is used in animal feed (Ogbonna 2009). The price for Vitamin E i.e. 93-98 % Oil was approx. 24-30 US \$/kg in 1998. As a result of increased production capacity between 1998 to 2002, the Vitamin E price dropped down to 8-12 US\$/kg in 2001-2002 (China Chemicals Market Research <http://www.cnchemicals.com>). No current prices for Vitamin E were available.

Until 2008-2009, Vitamin E market was dominated with synthetic tocopherols, while tocotrienols had a very small share. Since then tocotrienols has been termed as the next generation of Vitamin E (Nutraingredients/Nov.2010) while it represented approx. 10 % of the total market of US \$ 350 to 400 million. The biggest tocotrienol supplier in 2010 was Carotech from Malaysia with American River Nutrition, MA, USA, extracting tocotrienols from annatto (roots) (i.e. *Bixa orellana* L.) (Tan 2005). The estimated market for tocotrienols is still in its early stage at 50 metric t/a compared to that of tocopherols (Nutraingredients / Nov. 2010). The estimated price for tocotrienols is approx. 4 to 5 times that of tocopherol. In June 2011, Davos Life Science, Singapore, started supplying natural tocotrienols including δ -tocotrienols extracted from palm oils into Japanese and Korean market (Nutraingredients / Jun. 2011). Natural vitamin E compounds are commercially extracted from vegetable oils. Approximately, 0.5 to 2.8 g of vitamin E is extracted from 1 kg of oil depending on its source (Sundram et. al. 1992). In order to make the biological synthesis competitive with the chemical synthesis, the yield has to be increased to 2.0 kg vitamin E per kg of oil (Wilke 1999), i.e. 0.44 kg vitamin E/ kg of palm fruits, which is a real challenge. This could not be confirmed, as the basis data for the cost of raw materials via chemical synthesis route were

not available for economic calculations. Hence, many groups (Caretto et. al. 2004; Cahoon et. al. 2003; Van Eenennaam et. al. 2003; Karunanandaa et. al. 2005) are working to improve the vitamin E content in oil seeds itself by molecular breeding. Tocopherols are found in abundance among Vitamin E compounds, with α -tocopherol having the highest Vitamin E activity. Tocotrienol family possesses different biological functions compared to the tocopherols, but unfortunately they are found in small quantities in nature (Sen et. al. 2010).

In order to meet the increased demand of Vitamin E for human health and feed utility, it is important to increase the Vitamin E content in plants (Savidge et.al. 2002). Many research groups and companies around the world are working on increasing the Vitamin E levels in food sources itself i.e. through plant engineering (Cahoon 2007, Lee et. al. 2007) in order to meet the demand in human consumption or by producing them via chemical synthesis. Natural α -tocopherol level was increased by 70 to 100 % using sunflower cell cultures during *in-vitro* production system (Caretto et. al. 2004). Overexpression of *p*-hydroxyphenylpyruvate dioxygenase (Hpd) enzyme encoded by *hpd* gene from Barley into Tobacco plant elevated the vitamin E content 2 fold in leaves and 1.5 fold in seeds (Falk et. al. 2005). Similarly, expression of Hggt (homogentisic acid geranylgeranyl transferase) from Barley into Corn increased the vitamin E level by 6 fold and Hggt (from Barley) into corn increased the vitamin E level by 15 fold (Cahoon et. al. 2003). Vitamin E levels were increased by 18 % and 28 %, by expressing *Cyc* from *Arabidopsis thaliana* in Canola was shown by Kumar et. al. 2005.

1.4. Significance of Vitamin E compounds in animals and humans

Vitamin E family is a group of lipid soluble, radical chain breaking antioxidants (Schneider 2005). Vitamin E compounds cannot be produced by humans and animals and hence, these are considered to be an important dietary component (Schneider 2005). Vitamin E was discovered by Evans and Bishop in 1922, as a micronutrient, essential for the reproduction in rats (Azzi and Stocker 2000).

Molecular complexes in human body like DNA, proteins, lipids, carbohydrates can be easily targeted by the reactive oxygen free radicals (Atkinson et. al. 2008). Some studies have shown that the antioxidant activity of Vitamin E has the ability to prevent some chronic diseases, especially those, which have an oxidative stress aspect related to it like, cardiovascular diseases, cancer, atherosclerosis etc. (Azzi and Stocker 2000). Some clinical studies have shown that Vitamin E deficiency in humans may lead to neurodegenerative disease like Parkinson's and Alzheimer's (Sano et. al. 1997), then cardiovascular diseases such as atherosclerosis (Das et. al. 2007). During *in-vitro* tests, it

was proved that tocotrienols and δ -tocopherol inhibits proliferation of breast cancer cells (Wu. et. al. 1999).

Vitamin E Antioxidant like Vitamin E (for e.g. found in vegetable oil) is considered to be the most potent chain breaking antioxidant within cell membrane (Brigelius-Flohe´2006). The abundance of α -tocopherol in natural sources, its ability to be retained in human body after its uptake and its antioxidant activity motivated the scientific community to carry basic and clinical research on this molecule (Sen et. al. 2007). Due to its significance much work was done on tocopherols, specifically α -tocopherol, which resulted in less research on the other potentially significant molecules like Tocotrienols.

The present study focuses on δ -tocochromanols i.e. δ -tocopherols and δ -tocotrienol biosynthesis in recombinant *E. coli*. Hence, data specific to δ -tocochromanol is discussed in this study. δ -tocochromanols are rare forms of vitamin E found in food sources (see table 1.2, 1.3, 1.4), less research study and interest was given to δ -tocotrienols and δ -tocopherols. δ -Tocochromanols content is only 12 % in palm oil and 5 % in wheat germ. In case of wheat germ no δ -tocotrienol was detected. δ -tocotrienol is a rare form and shows significant activity which is different from that of widely available α -tocopherol.

Based on the result of clinical studies, it is being discussed that tocotrienols may act as molecular targets in therapeutic applications like apoptotic regulators (In silico simulations and *in-vitro* binding studies; Comitato et.al. 2009), cytokines, adhesion molecules (Patel et.al. 2011), receptors (*in-vitro* studies; Zhou et.al. 2004) & neuroprotective mechanism (*in-vitro* studies; Khanna et.al. 2007) etc. Feeding chicken and rats with food rich in tocotrienol extract reduced the cholesterol synthesis by suppressing the HMG-CoA reductase activity (Pearce et al., 1992 and 1994). Pigs which had hypercholesterol level when fed with food rich of tocotrienol fraction, showed approx. 44 % reduction in total serum cholesterol and approx. 60 % reduction in LDL cholesterol (Qureshi et.al. 1996). Out of the 4 isomeric forms of tocotrienols, one study concluded that δ - and then γ -tocotrienol has the highest ability to reduce cholesterol (no data) (Aggarwal et. al. 2010), while another *in-vivo* clinical study with rabbits showed that γ -tocotrienol and α -tocotrienol had the highest ability to reduce ischemia in hypercholesterolemic hearts (i.e. 50 % and 39 % reduction in cholesterol resp.) (Das et. al. 2012). These specific examples show that the function of tocotrienols in humans is an ongoing research topic and still many results of studies have to be yet consolidated by scientific community. Despite of evidence on health benefits of tocotrienols in humans and animals some mechanism (e.g. selective estrogen receptor modulators, apoptosis etc.) and

are still unclear (Zhou et.al. 2004; Patel. et. al. 2011). More studies and investigation with tocotrienols is needed to determine its efficacy and safety (Patel et. al. 2011).

The bioavailability and bioequivalence of different forms of vitamin E differ. Higher level (150 µg/g tissue) of α-tocopherol is found in adipose tissue and in adrenal glands (132 µg/g tissue). Similarly, higher level of α-tocopherol was found in other human organs such as the heart/liver (40 µg/g tissue) and kidneys (7 µg/g tissue) (Buss 2008). Of the eight vitamin E family members only α-tocopherol (and to a much lesser extent γ-tocopherol) is retained in significant amounts in human body. The RRR-α-tocopherol (i.e. natural) is the active form and hence shows higher bioavailability in human body as compared to the commercially available racemic α-tocopherol (chemical synthesized) (Brigelius-Flohé et. al. 2002).

The extent of most of the benefits of Vitamin E on human health is still a debated issue. Most of these health benefits were the results of clinical trials with large study populations (between 2000 and 32400 patients/participants) (Klein et.al. 2001; Klein 2004; Schneider 2005). Some reports showed that, in large randomized preclinical trials, Vitamin E in combination with Selenium reduced the risk of prostate cancer (Klein et.al. 2001). Another report published in 2005 consisted analysis and review of 19 clinical trials which included 135,967 participants/patients. This study concluded that high dosage of Vitamin E supplements (for humans, in excess of 400 International Units (IU) for at least 1 year), increased the risk of all cause deaths ((Miller et. al. 2005). This study couldn't confirm benefits and risks of low Vitamin E dosages. There are studies published (Lonn et. al. 2005; Traber 2006) by scientists which are not convinced with the reports and results of positive results in clinical and intervention trials, and doubt that the dietary supplementation of vitamin E has health benefits as being portrayed.

1.5. Proposed pathway for δ-Tocochromanol biosynthesis in recombinant *E. coli*

The tocochromanol biosynthesis pathway, was first elucidated using radioactive-labelled carbon-10 (C₁₀) i.e. IPP and carbon-15 (C₁₅) i.e. GGPP, PPP compounds in 1971 (Threlfall et. al 1971 and Soll and Schultz 1979). New advanced genomic based methods and genetic analysis were established. Especially in the past decade these methods and tools have enabled researchers to study key enzymes involved in tocochromanol biosynthesis pathway. Tocochromanol biosynthetic pathway has been well studied in *Arabidopsis thaliana* and *Synechocystis sp. PCC6803* using mutants and transgenic approach (DellaPenna 2005).

Tocochromanol pathway enzymes from *Arabidopsis* (DellaPenna 2005, 2006, Porfirova 2002), *Synechocystis* (Shintani 2002, Scheldz 2001, Cheng 2003, Maeda 2007), were successfully over-expressed in *E. coli* and studied for their respective enzyme activities.

Tocochromanol non-specific pathway enzymes, Hpd from *Pseudomonas putida* (Arias-Barrau et.al. 2004), and CrtE from *Erwinia urevedora* (Misawa et.al. 1990) were also over-expressed in *E. coli* and studied for respective enzyme activities. The necessary tocochromanol biosynthesis genes are absent in wild type *E. coli* and hence, are not able to produce any tocochromanol compounds.

Hence, the initial objective was to show that δ -tocochromanol compounds i.e. δ -tocotrienol and δ -tocopherol can be produced in a non-photosynthetic microorganism like *E. coli* K-12 cells (recombinant). *Escherichia coli* (*E. coli*) is a gram negative, rod shaped bacterium and belongs to the group of Enterobacteria. Due to the combination of several advantages *Escherichia coli* has to offer, it was the preferred choice for heterologous biosynthesis of tocochromanol compounds. Firstly, the complete genome sequences of several *E. coli* K-12 strains are available (Blattner et.al. 1997; Hayashi et. al. 2006). Genome sequence of *E. coli* K-12 MG1655, accelerated the metabolic engineering studies involving *E. coli* strains. In many examples, it has been successfully shown that *E. coli* can be a good host for heterologous synthesis of natural products like polyketides, isoprenoids, alkanoids, flavanoids (Watts et.al. 2005). The genetic data of many *E. coli* strains is well characterised and the tools for gene cloning and expression in *E. coli* are well developed, and hence it is being widely used as laboratory workhorse for genetic modification (Durfee et.al. 2008). Advantages of *E. coli* as host strain during experimental phase, is the higher cell growth rate, growth on simple and inexpensive sugars, and the relative ease for genetic manipulation it offers. Secondly, the breakthrough method developed by Datsenko and Wanner in 2000, which allowed simple and efficient method for gene deletion and insertion of a linear DNA possible in *E. coli*. Before this method, the assembly of different chromosomal modifications were realized by P1-phage transduction (Miller 1972) and relatively complicated method for the elimination of the chloramphenicol resistance gene was conducted as described in Cherepanov and Wackernagel 1995. Since 2000, this method enabled molecular biologists to accurately target the multiple genes for deletion, and later eliminate the antibiotic resistance marker, if required. The result of using this recombination method would result in construction of a stable strain, which is one of the aims of this study. Thirdly, tocochromanol biosynthesis requires one aromatic and one isoprenoid precursor.

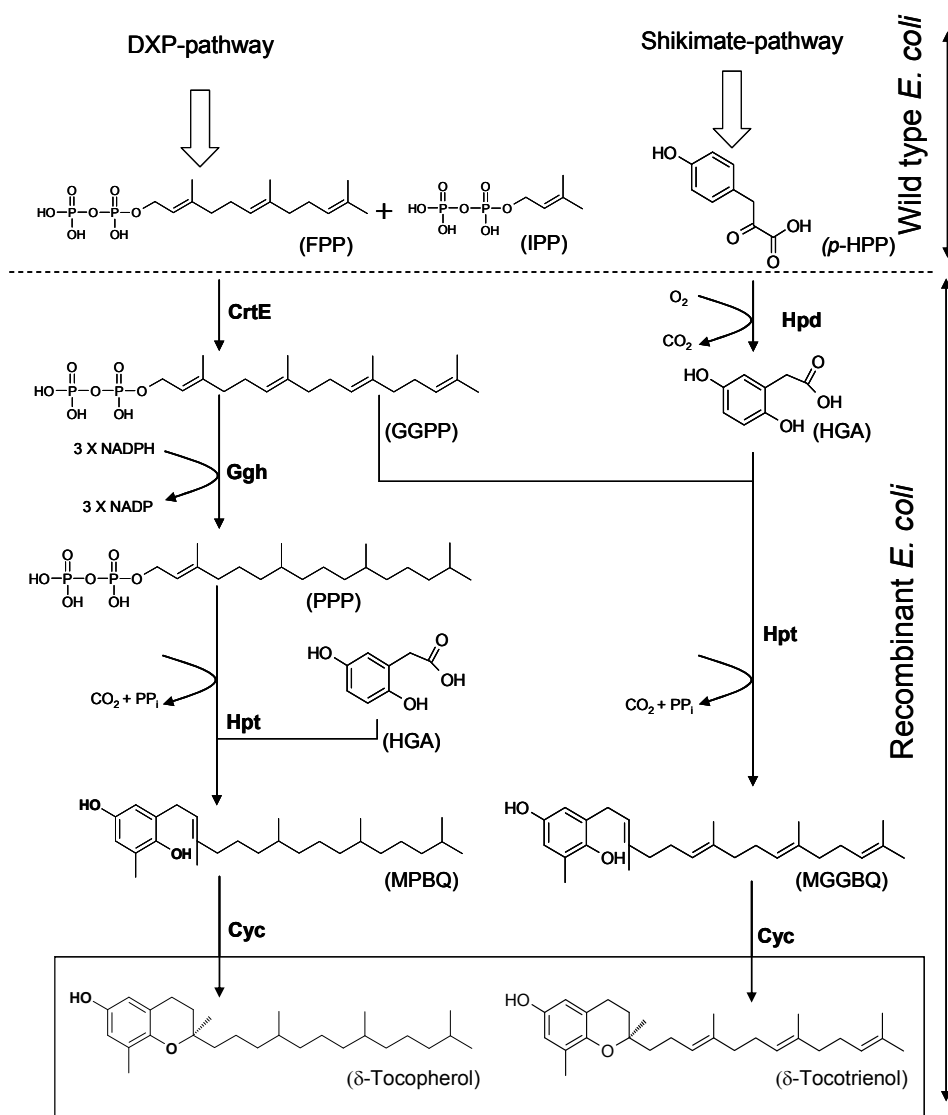


Figure 1.5: Proposed Pathway for Vitamin E (δ -Tocochromanol) biosynthesis in recombinant *E. coli*. Glucose or Glycerol is used as sole carbon and energy source to MGGBQ (tocotrienol precursor). The upper part of the dotted horizontal line indicates that the shikimate pathway and DXP pathway already exist in wild type *E. coli*. Block arrows indicates that some enzymatic steps in the shikimate and DXP pathway are not shown here. Enzymes are shown in bold letters. Pathway intermediates are denoted as *p*-HPP (*p*-hydroxyphenyl-pyruvate), HGA (homogentisic acid), FPP (farnesyl-pyrophosphate), IPP (Isopentenyl-pyrophosphate), GGPP (Geranylgeranyl-pyrophosphate), MPBQ (2-methyl-6-phytyl-benzoquinol), and MGGBQ (2-Methyl-6-geranylgeranyl-benzoquinol). Enzymes catalyzing these reactions are shown in 3 letters with first letter capital. Hpd (*p*-Hydroxy-phenylpyruvate dioxygenase); CrtE (Geranylgeranyl pyrophosphate synthase); Ggh (Geranylgeranyl reductase); Hpt (Homogentisate phytyl transferase); Cyc (Tocopherol cyclase). Figure modified from Albermann et. al. 2008.

Wild type *Escherichia coli* K-12, is able to produce *p*-HPP (via shikimic acid pathway) and IPP/FPP (DXP pathway) precursors (Bongaerts et. al. 2001; Rohmer 1993 and Sprenger et.al. 1997) This provided the best platform for heterologous biosynthesis of natural compounds like Vitamin E using *E. coli* as host strain.

To show whether *E. coli* can produce tocochromanol compounds, it had to be genetically modified using metabolic engineering methods. A proposed pathway for δ -tocochromanol biosynthesis in recombinant *E. coli* K-12 is shown in figure 1.5 (Albermann et.al. 2008) Wild type *E. coli* K12 can produce *p*-HPP via shikimate pathway (figure 1.2) (Bongaerts et. al. 2001). It can also produce FPP and IPP via DXP pathway (Hunter 2007). To produce HGA from *p*-HPP in recombinant *E. coli* K-12, Hpd has to be overexpressed which then can catalyse the oxidation decarboxylation reaction. To produce GGPP and PPP in recombinant *E. coli* K-12, CrtE and Ggh has to be overexpressed which could catalyse the condensation addition and reduction reaction, respectively. Overexpression of Hpt in recombinant *E. coli* K-12 producing HGA, GGPP/PPP would catalyse prenylation of HGA to produce MGGBQ/MPBQ respectively. Further expression of tocopherol cyclase (Cyc) in recombinant *E. coli* strain producing MGGBQ or MPBQ would catalyse its cyclization reaction to produce δ -tocotrienol or δ -tocopherol respectively (Albermann et.al. 2008). The individual steps are described in the following sections below.

1.5.1. *p*-Hydroxyphenylpyruvate dioxygenase (Hpd)

A single copy of a gene encoding the Hpd enzyme was identified from different species like i.e. bacteria *Streptomyces avermitilis*26 (Fritze et. al. 2004), *Shewanella colwelliana*, *Pseudomonas putida* (Brownlee et. al. 2004, Nelson et. al. 2002, Gunsior et. al. 2004), fungi, *Coccidioides immitis*, plants i.e. *Zea mays*, *Arabidopsis thaliana*, Barley (Fritze et. al. 2004) and mammals (Moran 2005). Hpd overexpressed from *Pseudomonas putida* was also shown to be functionally active producing HGA *in-vivo* in recombinant *E. coli* (Moran 2004). Hpd enzyme was expressed as a soluble protein and found to be a homodimer in eukaryotes and homotetramers in prokaryotes (Gunsior et. al. 2004). Hpd is a member of α -keto acid dependent dioxygenases family that requires Fe(II) and an α -keto acid (mostly α -ketoglutarate) to oxygenate the organic substrate. It incorporates both oxygen atoms of molecular oxygen into a single substrate one oxygen atom going into the carboxylate group and another oxygen atom into the 2-hydroxyl group (figure 1.2 and figure 3.1 (Johnson-Winters et. al. 2003). Hpd catalyzes the first committed step in the synthesis of vitamin E in *Synechocystis* sp. PCC6803 (Dähnhardt et. al. 2002) and *Arabidopsis thaliana* (Norris et. al. 1998). In the last decade, protein crystal structures of Hpd from *Pseudomonas fluorescens*

(Serre et. al. 1999), *Zea mays* (Fritze et. al. 2004), *Arabidopsis thaliana* (Yang et. al. 2004), and *Streptomyces avermitilis* (Brownlee et. al. 2004) have been solved.

1.5.2. Geranylgeranyl pyrophosphate synthase (CrtE)

CrtE enzyme (E.C. 2.5.1.29) is able to catalyse the condensation reaction of FPP (C₁₅) and IPP (C₅) molecules to produce GGPP (C₂₀) (Misawa et. al. 1990). CrtE is a key enzyme also called as branch enzyme (Takaya et. al. 2003) which belongs to a large family of enzymes called prenyltransferases involved in biosynthesis of terpenoids or isoprenoids (S.K. Oh et. al. 2000). This class of prenyltransferases catalyzes chain elongation of allylic pyrophosphate substrates using consecutive condensation reactions with the C₅ molecule IPP. This result in linear polymers with defined chain lengths like different isoprenoid compounds C₂₀, C₂₅, C₃₀, C₄₀ etc. (Lee et. al. 2005). Isoprenoids belong to a large group of over 23,000 distinct compounds serving different functions in bacteria, archea and eukaryotes (Liang et. al. 2002). Some of the examples of isoprenoid molecules are sterols, carotenoids, dolichols, ubiquinone etc. Genes encoding CrtE have been isolated from carotenogenic and non-carotenogenic bacteria, plants, fungi and animal tissues. The gene encoding CrtE enzyme was first found when the complete carotenoid biosynthesis cluster (*crt* genes) from *Pantoea ananatis* (formerly known as *Erwinia uredovora*) were elucidated (Misawa et. al. 1990). Size of CrtE protein from *Pantoea ananatis* is 32.6 kDa and it does not require any cofactors for condensation reactions (<http://www.uniprot.org>). The two existing natural pathways to produce the isoprenoid precursor building block (IPP) are the mevalonate pathway and non-mevalonate pathway (or DXPP or MEP pathway) (Lange et. al. 2000; Hunter 2007). *crtE* gene encoding CrtE enzyme from *Erwinia uredovora* (now called as *Pantoea ananatis*) had been expressed in recombinant *E. coli*, purified and is well characterized with respect to the reaction kinetics study (Wiedemann et. al. 1993).

1.5.3. Geranylgeranyl reductase (Ggh)

Ggh is a multifunctional enzyme involved in catalyzing the sequential reduction of geranylgeranyl pyrophosphate into phytyl pyrophosphate or geranylgeranyl-chlorophyll *a* into phytyl-chlorophyll *a* in photosynthetic organisms (Keller et. al. 1998). This reaction requires NADPH as hydrogen donor for reduction. Three of the four double bonds in the GGPP molecule are reduced and hence 3 moles of NADPH are required as cofactor (Keller et. al. 1998). The gene *chlP* (ORF *sll1091*) encoding Ggh enzyme from *Synechocystis* sp. PCC6803 (named as Ggh-Syn throughout this study) had been inactivated (Shpilyov et. al. 2005). The resulting mutant accumulated geranylgeranyl-chlorophyll-*a* instead of phytylated-chlorophyll-*a* and small amounts of α -tocotrienol instead of α -tocopherol (Shpilyov et. al. 2005). Ggh-Syn was found as thylakoid membrane protein in *Synechocystis* sp. PCC6803

during the proteomic studies (Srivastava et. al. 2005). *ggh* gene encoding Ggh enzyme from *Arabidopsis thaliana* has been expressed in *E. coli* and the sequential reduction reaction was studied during *in-vitro* reaction assay with radioactive GGPP (Keller et. al. 1998). The enzyme structure of Ggh from any organism is not known to this date.

1.5.4. Homogentisate phytyl transferase (Hpt)

Hpt is a key enzyme involved in catalysing the condensation reaction between the aromatic polar head group (i.e. HGA) and the lipophilic prenyl chain i.e. GGPP and/or PPP to produce MGGBQ and/or MPBQ respectively (Collakova & DellaPenna 2003). During this enzymatic step one molecule of carbon dioxide and one molecule of water are released. A deletion mutant study in *Synechocystis* sp. PCC6803 found out that *slr1736* gene encoded Hpt (Schledz et. al. 2001). *hpt* genes encoding Hpt enzymes from *Synechocystis* sp. PCC6803 and *Arabidopsis thaliana* were identified based on the DNA sequence similarity to chlorophyll synthases. These chlorophyll synthases are also involved in prenylation reactions taking PPP as substrate to produce phylloquinones i.e. vitamin K1 (Collakova and DellaPenna 2001). Biosynthesis of tocopherols and plastoquinones takes place in the chloroplasts of plants. Condensation of HGA with PDP (phytyl diphosphate) or SDP (solanesyl diphosphate) yielded MPBQ or DMPQ (2-dimethyl-plastoquinol) respectively. These were intermediates in tocopherol and plastoquinone formation, respectively (Soll et. al. 1980). It was later found that two different homogentisate phytyl transferases exist in *Arabidopsis thaliana*, one which has substrate specificity towards GGPP (At2g18950) and another which shows substrate specificity towards PPP (At3g11950). Both Hpt's were expressed in *E. coli* as recombinant proteins and characterized with respect to enzyme kinetics (Sadre. et. al. 2006). Hpt enzyme from *Arabidopsis thaliana* and *Synechocystis* sp. PCC6803 when expressed in recombinant *E. coli* was found as membrane bound (Albermann et. al.2008). Enzyme structure of Hpt from any organism is not known till date.

1.5.5. Tocopherol cyclase (Cyc)

Cyc catalyzes the key step in the biosynthesis of the chromanol substructure of the vitamin E family (Kumar et. al. 2005). The cyclization of MGGBQ to δ -tocotrienol, MPBQ to δ -tocopherol, DMGGBQ to γ -tocotrienol and DMPBQ to γ -tocopherol is catalyzed by single tocopherol cyclase enzyme in *Arabidopsis thaliana* (Stocker et.al. 1996, Porfirova et.al. 2002). Conversion of DMPBQ (2,3-dimethyl-6-phytyl-benzoquinone) to γ -tocopherol is an acid promoted cyclization and takes place in two steps (Fig. 1.6). In order to synthesize the oxygen containing heterocyclic ring, the ring closure proceeds by *Si* protonation of the double bond of DMPBQ followed by a attack of the phenolic oxygen atom to trap the intermediate carbocation (Stocker et al., 1994). It is assumed that pre-ionization of the phenol to a

phenolate occurs in the enzyme binding pocket to favour double bond protonation, thereby resulting *de facto* in a single step process without an actual carbocation intermediate. In any case, the enantioselectivity of the enzyme catalyzed cyclization implies that the enzyme induces and immobilizes a single enantiomeric conformation of the substrate during the reaction (Manetsch et al., 2004). Studies on substrate specificity revealed that Cyc recognizes three main features namely, the OH group at C1 of the hydroquinone, the E-configuration of the double bond, and the length of the lipophilic side chain (Stocker et al., 1993, 1996). Tocopherol cyclase protein from *Arabidopsis thaliana* consists of a functional transit peptide (+FTP) is abbreviated as (Cyc_{+FTP}-At). Once (Cyc_{+FTP}-At) proteins are transported to the chloroplast of *Arabidopsis thaliana* the transit / signal peptide is cleaved. This Cyclase protein is abbreviated as (Cyc-At) in this study. The Cyc-At proteins without functional transit peptide gives a molecular size of 47 kDa (Porfirova et.al 2002). Tocopherol Cyclase enzyme from *Arabidopsis thaliana* and maize was purified by Kumar et.al. 2005. No cofactors are needed for cyclisation reaction. Till date no structure of subunit protein of Cyclase has been published.

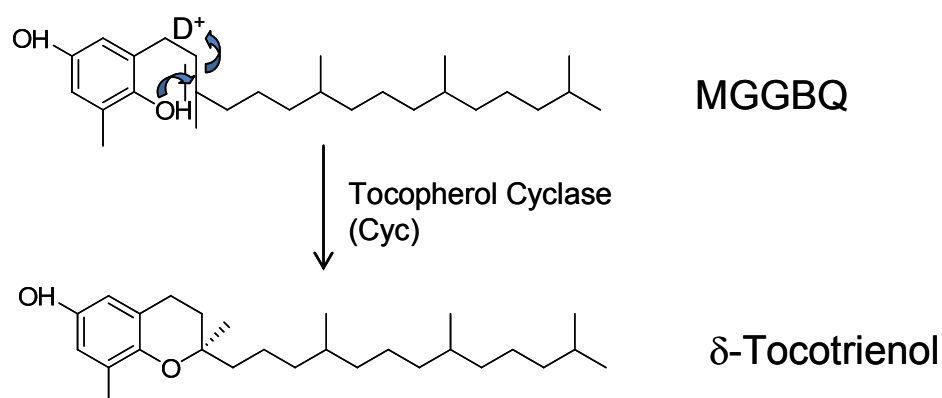


Figure 1.6: The chromanol head ring formation δ -tocotrienol from 2-methyl-6-geranylgeranyl-4-hydroxy-1,4-benzoquinol catalyzed by tocopherol cyclase. The same enzyme was shown to convert 2,3-dimethyl-6-phytyl-1,4-hydroquinol to γ -tocopherol by Stocker et.al. 1993.

1.6. Glucose and Glycerol Uptake Mechanism in *E. coli*

One aim of this study is to use glucose or glycerol as sole carbon and energy sources in minimal medium for the biosynthesis of tocochromanols in recombinant *E. coli*. Glucose is one the preferred carbon source for *E. coli*, as it grows faster than in most of the other carbon sources (Götz and Goebel 2010) and can be constantly supplied in large quantities for industrial scale fermentations throughout the year. The first step in glucose degradation (when glucose is used as sole carbon and energy source during cultivation) is phosphorylation carried out by PEP (phosphoenolpyruvate) dependent phosphotransferase system (PTS) using translocation transport mechanisms and produces G-6-P (glucose-6-

phosphate) (Postma 1993). In animals, glucokinase (isoenzyme of hexokinase) carries the phosphorylation of glucose to produce G-6-P. As shown in figure 1.7, one pathway in which G-6-P can further get converted to GA3P (in many enzymatic steps), is the Glycolysis pathway (or also called as Embden-Meyerhof pathway) (highlighted in pink). GA3P is further converted into PEP in 4 enzymatic steps (not shown here). PEP is converted to Pyruvate, and oxaloacetate. Oxaloacetate along with Acetyl-CoA (formed from Pyruvate) enters the Tricarboxylic acid cycle. An alternative to Glycolysis pathway is the pentose phosphate pathway (PPP) where G-6-P can be further converted to E4P & GA3P via oxidative & non-oxidative PPP pathways (highlighted in blue and green respectively in figure 1.4). This GA3P can re-enter the Glycolysis pathway (shown by centered line). When *E. coli* is grown in glucose medium, the Entner-Doudoroff Pathway is not active (Wang 1958) and hence as a result G-6-P can be either utilized via PPP or Glycolysis pathway.

In this study, glycerol would be used (for δ -tocochromanol production in recombinant *E. coli* strains) as an alternative to glucose as the sole carbon and energy source in minimal medium. In such a case glycerol has to undergo a few reactions to produce the intermediate glyceraldehyde 3-phosphate before it can enter the glycolysis pathway. Glycerol uptake in bacteria is via simple diffusion or is mediated by the glycerol diffusion facilitator, an integral membrane protein catalyzing the rapid equilibration of concentration gradients of glycerol across the cytoplasmic membrane (Heller et. al. 1980; Voegelé et. al.1993). Intracellular glycerol is converted to glycerol-3-Phosphate (Glycerol-3-P) by the enzyme glycerol kinase that uses ATP as phosphoryl donor (Lin 1976). Further this glycerol-3-P can be further metabolized to dihydroxyacetone phosphate (DHAP) by either of two membrane-bound enzymes glycerol-3-P dehydrogenase (G-3-PD) depending on the growth conditions. Under aerobic conditions, a homodimeric aerobic G-3-PD (encoded by the *gldD* gene) is produced (Weiner 1974). Under anaerobic conditions, a different glycerol-3-P dehydrogenase (tri-heteromeric protein, encoded by *gldACB* operon) is preferentially expressed (Schryvers and Weiner 1981).

The aromatic precursor for the production of δ -tocochromanol intermediates (MGGBQ and MPBQ, see figure 1.5) which are produced by wild type *E. coli* is the *p*-HPP is produced via shikimate pathway (1.3.1) and the isoprenoid precursors IPP and FPP are produced via DXP pathway (1.3.2) (Baba et.al. 1985).

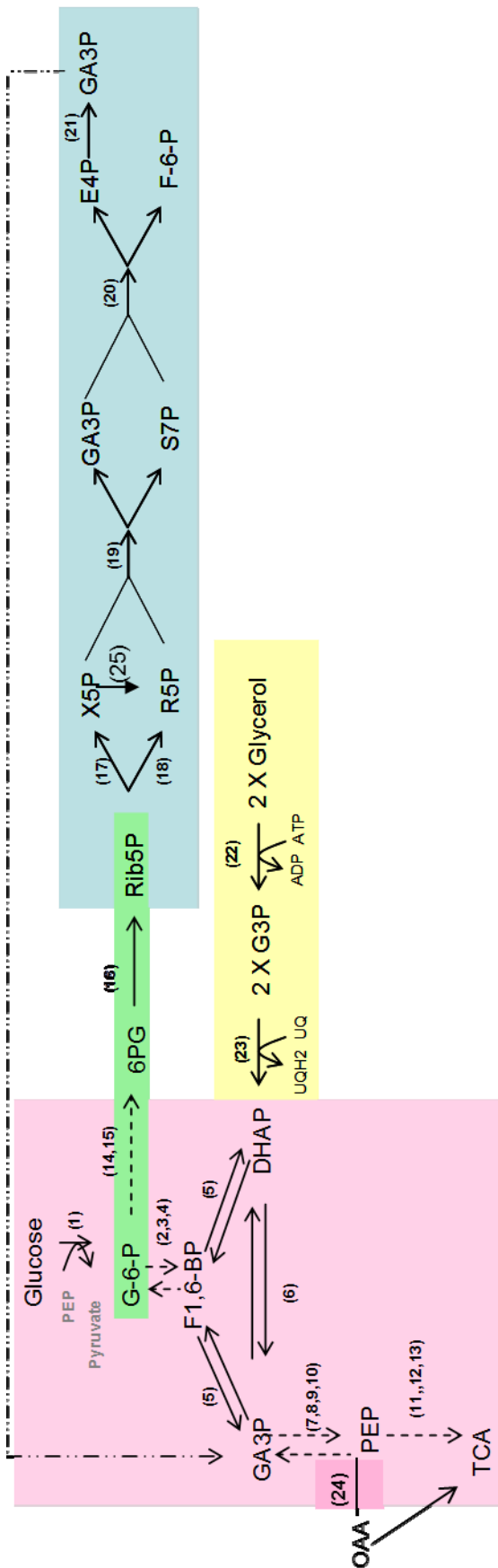


Figure 1.7: Scheme showing the glucose metabolism pathway. In pink colour box, is the Glycolysis pathway; green colour box is the oxidative pentose pathway. Dotted arrows represents, more than one enzymatic reactions; centered dotted line represents the possibility of two pathways connecting each other. G-6-P is Glucose-6-phosphate; F1,6-BP is Fructose-1,6-bisphosphate; GA3P is Glyceraldehyde-3-phosphate; PEP is Phosphoenolpyruvate; TCA is Tricarboxylic acid cycle; 6PG is 6-phosphogluconate; Rib5P is Ribulose-5-phosphate; X5P is Xylulose-5-phosphate; R5P is Ribose-5-phosphate; S7 is Sedoheptulose-7-phosphate; E4P is Erythrose-4-phosphate; F-6-P is Fructose-6-phosphate; OAA is Oxalacetate; (1) Phospho-transferase system; (2) Phospho-gluco-isomerase; (3) Fructose-1,6-bisphosphatase; (4) 6-phosphofruktokinase; (5) Fructose-bis-phosphate aldolase; (6) Triosephosphate isomerase; (7) Glycerol aldehyde-3-Phosphate-dehydrogenase; (8) Phosphoglycerol kinase; (9) Phosphoglycerol mutase; (10) Enolase; (11) Pyruvate kinase; (13) Phosphopyruvatecarboxylase; (14) Glucose-6-Phosphate dehydrogenase; (15) Phosphogluconolactonase; (16) Phosphogluconate dehydratase; (17) Ribulose phosphate-3-epimerase; (18) Ribulose phosphate isomerase; (19) Transketolase; (20) Transaldolase; (22) Glycerol kinase; (23) Glycerol-3-Phosphate dehydrogenase; (24) phosphoenolpyruvatecarboxylase; (25) Transketolase;

1.6.1. Shikimate pathway in wild type *E. coli* K-12

Biosynthesis of three aromatic amino acids (namely L-phenylalanine, L-tryptophan and L-tyrosine) in *Escherichia coli* takes place via general aromatic amino acid pathway or shikimate pathway (Pittard et. al. 1996). First step in the pathway is the condensation of Phosphoenolpyruvate (PEP) derived from glycolysis and Erythrose-4-phosphate (E4P) derived from pentose phosphate pathway (Pittard et. al.1996).

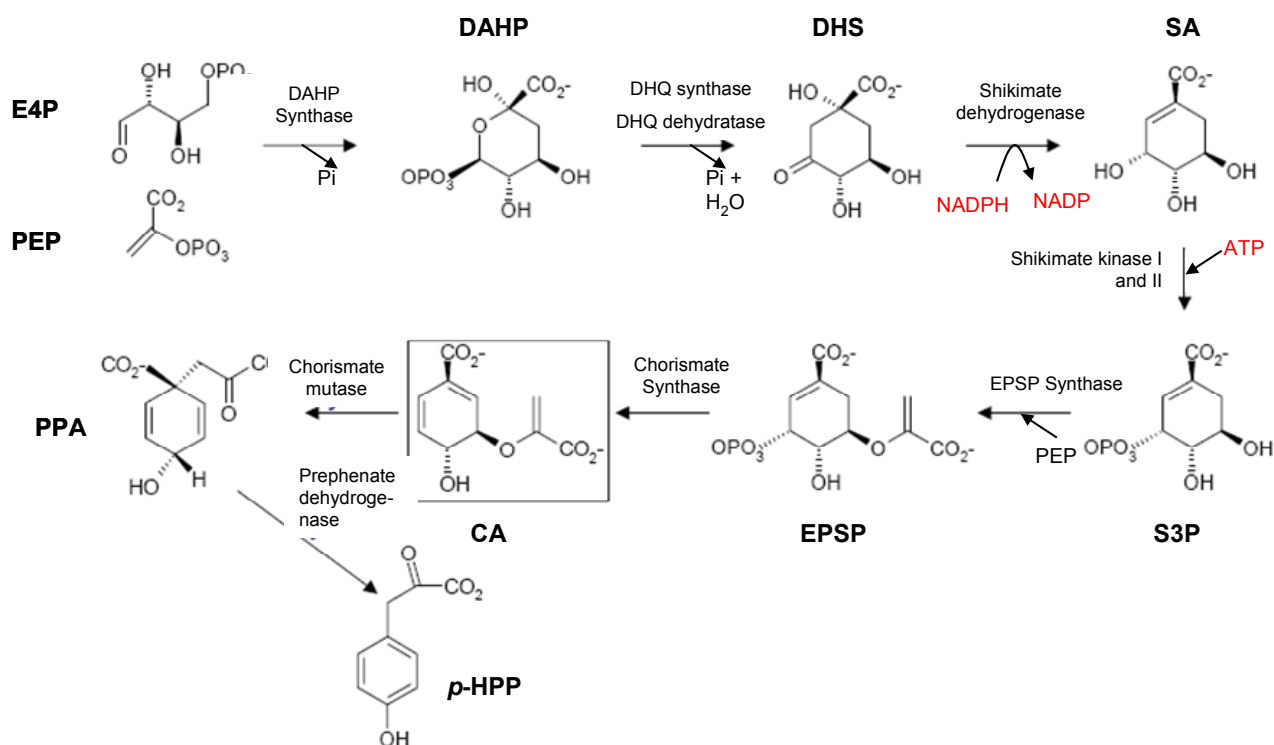


Figure 1.8 (Sprenger 2006): Scheme showing the general aromatic amino acid up to chorismic acid and extended further to 4-HPP in wild type *E. coli* K12 type strain. PEP from glycolysis pathway (section 1.6) and E4P from pentose phosphate pathway (section 1.6) are the precursors. Abbreviations are as follows: PEP (phosphoenolpyruvate); E4P (erythrose 4-phosphate); DAHP (3-deoxy-D-arabinoheptulosonate 7-phosphate); DHS (dehydroshikimate); SA (shikimate); S3P (shikimate 3-phosphate); EPSP (5-EP-S-3-P5-enolpyruvoylshikimate 3-phosphate); CA (chorismate); PPA: Prephenic Acid; 4-HPP (*p*-hydroxyphenylpyruvate)

In *E. coli*, DAHP synthase (EC 2.5.1.54) (three isoenzymes encoded by *aroF*, *aroG* and *aroH* genes) catalyses the condensation reaction between 1 molecule of PEP and 1 molecule of E4P to form DAHP releasing a phosphate group (from PEP) as inorganic phosphate (Krämer et. al. 2003). Refer to figure 1.8. These three isoenzymes in *E. coli* are regulated by feedback inhibition by the three terminal products (Sprenger 2007). Based on the ¹³C NMR studies it was shown that DAHP synthase is the most important enzyme as far as the carbon flux is concerned as this reaction controls the carbon flux going into this pathway (Ogino 1982). The AroG represents 80% of the total DAHP synthase activity (Tribe et. al. 1976).

Dehydroquinate synthase (encoded by *aroB* gene) converts DAHP into DHQ (step not shown in figure 1.8) and DHQ dehydratase (encoded by *aroD* gene) converts DHQ into DHS by removing a water molecule (Krämer et.al.2003). Shikimic dehydrogenase encoded by *aroE* gene reduces DHS to shikimic acid in presence of co-factor NADPH. Two isoenzymes of shikimate kinase encoded by genes *aroK* and *aroL* catalyse the formation of shikimic acid from S3P. Based on level of intermediates accumulated the rate limiting enzymes in shikimic acid pathway are the *aroB*, and *aroL* (Dell and Frost 1993). In the next step EPSP is formed with one mole of PEP catalysed by EPSP synthase (EC 2.5.1.19) encoded by *aroA*. The last step in this pathway is the formation of chorismate compound from EPSP by chorismate synthase (EC 4.2.3.5) encoded by *aroC* gene.

In *Escherichia coli* chorismic acid serves as a common substrate and hence the central branch point for the biosynthesis of individual aromatic amino acids (Gibson 1964). If chorismate is converted into prephenate (catalysed by chorismate mutase) L-phenylalanine and L-tyrosine are produced from it. L-tryptophan is produced when chorismate is converted into anthranilate (Sprenger 2006).

1.6.2. MEP or DXP pathway in wild type *E. coli* K-12

IPP and DMAPP are the universal C₅ building blocks for the production of isoprenoids. Isoprenoids being a large family of more than 35000 distinct compounds like dolichols, sterols, ubiquinone, triterpenes etc. (Hunter 2007). In plants, carotenoids are produced using IPP as a common metabolic precursor which is produced via the known mevalonate pathway (Lange et. al. 2000). In mid 1990's studies showed that a second pathway apart from mevalonate pathway exists in some species of eubacteria (Rohmer 1993) and in green algae (Schwender 1996) and plants, which were able to produce IPP.

The first step in the 1-Deoxy-D-xylulose-5-phosphate (DXP) pathway (shown in figure 1.9) starts with the condensation of pyruvate and glyceraldehyde 3-phosphate to produce DXP catalysed by 1-deoxy-D-xylulose 5-phosphate synthase (Dxs) making use of thiamine pyrophosphate as cofactor (Sprenger et. al. 1997, Lois et. al. 1998). This gene was cloned from various higher plants (Lichtenhalter 1999) and *Escherichia coli* (Sprenger et.al. 1997) and *Streptomyces* strains ((a) Kuzuyama 2000). The formed DXP is converted into MEP catalysed by an enzyme called 1-Deoxy-D-xylulose 5-phosphate reductoisomerase (encoded by *dxr*). It is an NADPH dependent class B dehydrogenase ((b) Kuzuyama 1998). Further MEP is converted into 2C-methyl-D-erythritol 2,4-cyclodiphosphate in 3 enzymatic steps catalyzed by enzymes 4-Diphosphocytidyl-2C-methyl-D-erythritol Cytidyltransferase (encoded by *IspD*) 4-Diphosphocytidyl-2C-methyl-D-erythritol kinase (encoded by *IspE*), 2C-

methyl-D-erythritol 2,4-cyclodiphosphate Synthase (encoded by *IspF*) ((c) Kuzuyama 2000). The 2C-methyl-D-erythritol 2,4-cyclodiphosphate synthesized is converted into IPP catalysed by enzymes 1-Hydroxy-2-methyl-2-(*E*)-butenyl-4-diphosphate Synthase (encoded by *IspG*) and 4-Hydroxy-3-methyl-2-(*E*)-butenyl-4-diphosphate Reductase (encoded by *IspH*) (Hunter 2007). The IPP isomerase (encoded by *idi* gene) isomerises the carbon carbon double bonds of IPP to form DMAPP (Kuzuyama 2002). Finally, FPP synthase encoded by *ispA* catalyses the sequential elongation of C₅ (DMAPP) with two molecules of C₅ (IPP) to produce C₁₅ (FPP) compound.

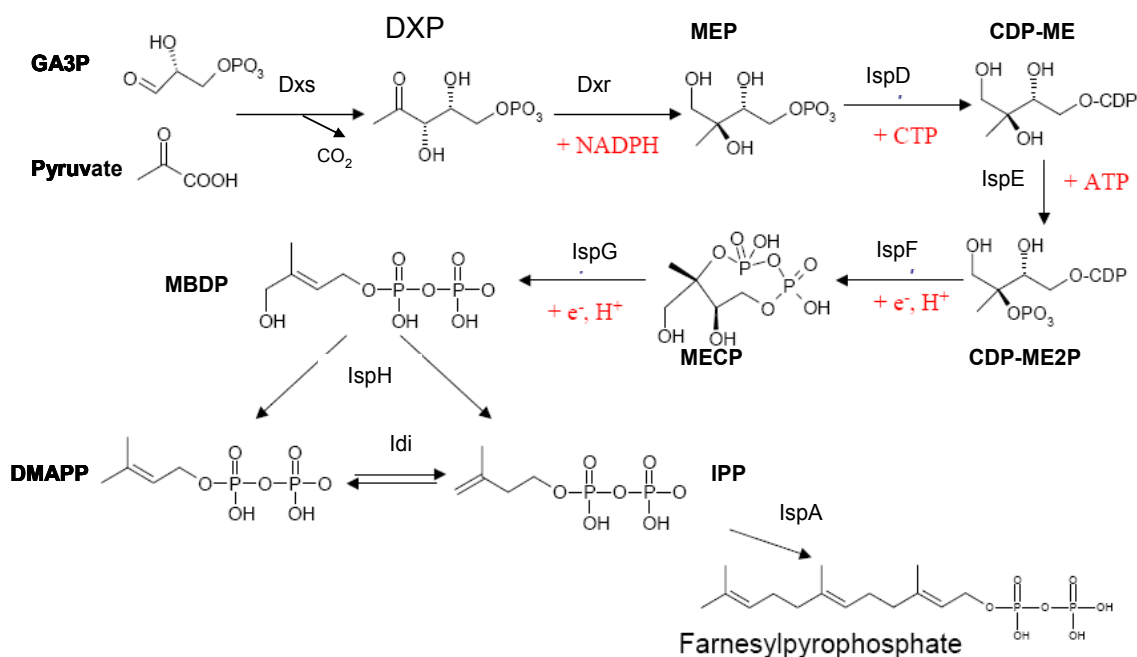


Figure 1.9: MEP or DXP pathway or Non-mevalonate pathway in wild type *E. coli* K12. Abbreviations of substrate, intermediate and products: GA3P is D-Glyceraldehyde 3-phosphate; PYR is Pyruvate; DXP is 1-Deoxy-D-Xylulose 5-Phosphate; MEP is 2C-Methyl-D-Erythritol 4-Phosphate; CDP-ME is 4-diphosphocytidyl-2C-methyl-D-erythritol; CDP-ME2P is 4-diphosphocytidyl-2C-methyl-D-erythritol-2-phosphate; MECP is 2C-methyl-D-erythritol-2,4-cyclo-diphosphate; MBDP is 4-hydroxy-3-methyl-2-(*E*)-butenyl-4-diphosphate; DMAPP is Dimethylallyldiphosphate; IPP is Isopentenyl pyrophosphate; Abbreviations of the enzymes catalysing these reactions: Dxs is DOXP synthase; Dxr is DOXP reductoisomerase; IspD is CDP-ME cytidyltransferase; Isp E is CDP-ME kinase; IspF is MECP synthase; IspG is MBDP Synthase; IspH is HMBDP reductase; Idi is IPP isomerise; IspA is FPP synthase (Hunter 2007)

1.6.3. Mevalonate Pathway

Mevalonate pathway for the biosynthesis of the universal terpenoid precursors, IPP (isopentenyl pyrophosphate) and DMAPP (dimethylallyl diphosphate) was well studied till 1998. Mevalonate independent pathway for the biosynthesis of IPP and DMAPP was detected in plants and eubacteria in 1999 (Rohmer & Rohmer 1999; Lichtenhalter 1999).

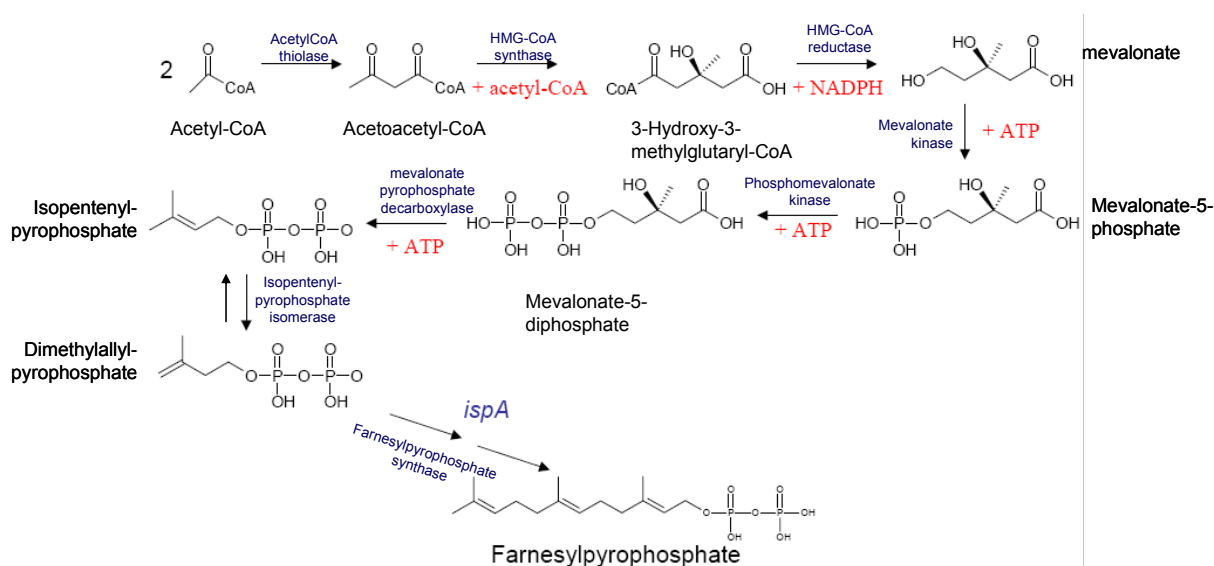


Figure 1.10: Scheme showing mevalonate pathway in *Escherichia coli*. In blue colour is the name of enzyme catalysing individual step, and in red colour is the co-factor required for each step.

Acetoacetyl-CoA is formed via condensation of 2 moles of Acetyl Co-A, catalysed by Acetyl-CoA thiolase enzyme. 3-hydroxy-3-methylglutaryl-CoA (HmG-CoA) synthase, catalyses the condensation reaction between acetoacetyl-CoA and AcetylCo-A, to form HMG-CoA (Rohmer 1999). Please refer to figure 1.10. Further the HMG-CoA is reduced to mevalonate in presence of cofactor NADPH. This reduction is catalysed by HMG-Co-A reductase, which is a rate limiting step in cholesterol (Rodwell et. al. 2000). Mevalonate is subsequently converted into carbon-5 compound Isopentenyl pyrophosphate (IPP) in three steps including phosphorylation and decarboxylation. IPP isomerase isomerises the IPP to form DMAPP (Rohmer 1999). Sequential elongation of 1 mole of DMAPP with 2 moles of IPP produces FPP compound. This reaction is catalysed by FPP synthase (encoded by *ispA*).

1.7. Extraction & Chemical Synthesis and of 2-Methyl-6-geranylgeranylbenzoquinol (MGGBQ)

MGGBQ in oxidized form i.e. MGGBQ_(oxidized) and MGGBQ in its reduced form i.e. MGGBQ_(reduced), were isolated as light yellow and colourless oil respectively, from a tropical brown alga *Stygodium zonale* (Lamouroux) Papenfuss as an intermediate, while extracting Ichthyotoxic and Cytotoxic metabolites (Gerwick and Fenical 1981). Fresh *Stygodium zonale* was extracted with chloroform/methanol several times. Extract obtained, was fractionated by silica gel column chromatography, and finally each fraction was purified by silica gel preparative high performance liquid chromatography (HPLC). MGGBQ_(oxidized) and MGGBQ_(reduced) fractions present in complete extract was approx. 2 % each. MGGBQ_(oxidized) and MGGBQ_(reduced) were characterised and structure were confirmed using Infrared Spectra and ¹H NMR and ¹³C NMR spectrum.

MGGBQ_(oxidized) and MGGBQ_(reduced) were also detected in extract samples of marine brown alga *Halidrys siliquosa* as intermediate metabolite, during an antifouling activity study of Meroditerpenoids (Culioli et.al. 2008).

Chemical Synthesis of MGGBQ

MGGBQ_(reduced) and MGGBQ_(oxidized) were chemically synthesized via the following steps (Begley et.al. 1990). For details of each step, please refer to appendix A1-2 (a) – (c).

Step 1:

In this step (Figure 1.11a), alkylbromination of (E,E,E)-geranylgeraniol (GGol) was carried out with phosphorus tribromide (PBr₃), in presence of Tetrahydrofuran (THF) solvent to produce (E,E,E)-geranylgeranyl bromide (i.e. GGBr). The yield of this reaction, carried out at -10 °C, for 15 minutes was 93 %. PBr₃ is toxic and reacts violently with water and alcohols. During the reaction it gives away HBr, which is corrosive.

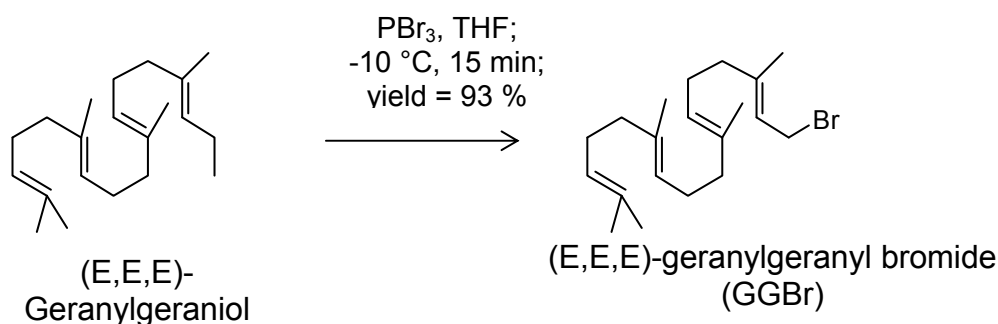
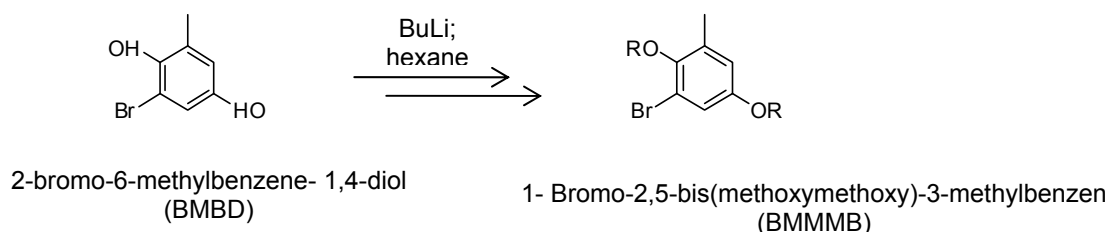


Figure 1.11a: First step in chemical synthesis of MGGBQ_(reduced) & MGGBQ_(oxidized).

Step 2:

In this step, 2-bromo-6-methylbenzene-1,4-diol (BMBD) was converted into 1-Bromo-2,5-bis(methoxymethoxy)-3-methylbenzen (BMMMM) within 2 reaction steps, and further processed in 6 purification steps. The yield of Step 2 was 81 %.



BuLi: butyl lithium

Figure 1.11b: Second step in chemical synthesis of *MGGBQ* (reduced) & *MGGBQ* (oxidized).

Step 3:

Product of step 2, i.e. BMMMM was converted into 2,5-Bis(methoxymethoxy)-1-methyl-3-[(E,E,E)-3,7,11,15-tetramethylhexadeca-2,6,10,14-tetraenyl]benzene (MMMTMHDTB) within 3 reaction steps. This was processed further in 4 purification steps to obtain pale straw coloured oil i.e. MMMTMHDTB.

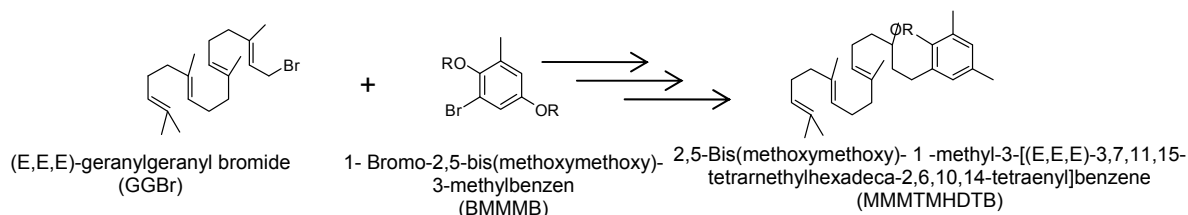


Figure 1.11c: Third step in chemical synthesis of *MGGBQ* (reduced) & *MGGBQ* (oxidized).

Step 4:

Product of third step i.e. MMMTMHDTB, was reacted with hydrogen chloride gas to produce, *MGGBQ* in reduced form i.e. *MGGBQ* (reduced). This was further processed in 5 purification steps.

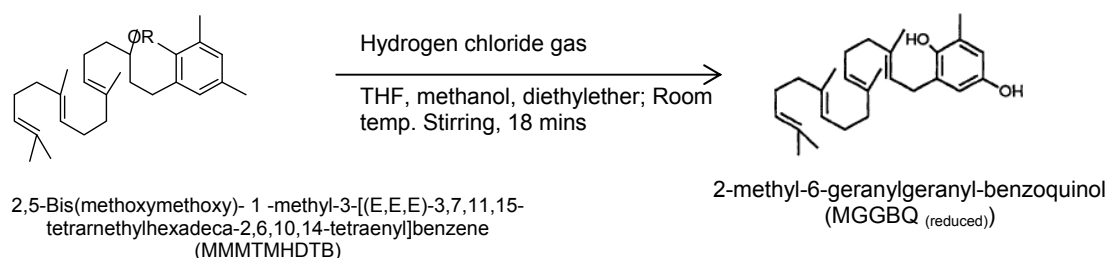


Figure 1.11d: Fourth step in chemical synthesis of *MGGBQ* (reduced) & *MGGBQ* (oxidized).

Step 5:

Air was continuously bubbled through MGGBQ (reduced) solution in dichloromethane, which was stirred at room temperature for 24 h. After evaporation and drying, yellow/orange oil was obtained, which was further purified via chromatography on silica gel. The eluent obtained was MGGBQ oxidized. The yield of this reaction (from MGGBQ (reduced) to MGGBQ (oxidized)) was 16 %.

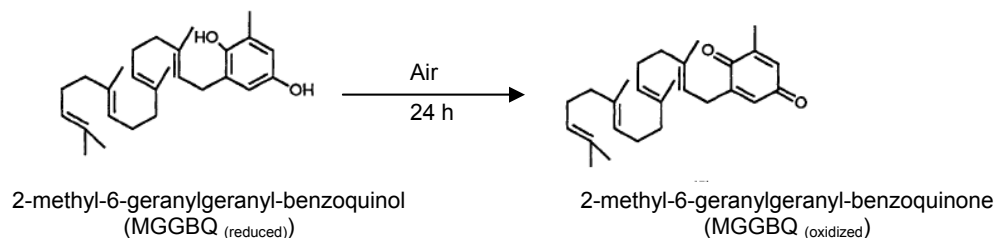


Figure 1.11e: Fifth step in chemical synthesis of MGGBQ (oxidized).

Hence, in total of 7 or 8 reaction steps and 19 or 24 purification/operations, geranylgeraniol & 2-bromo-6-methylbenzene-1,4-diol were converted to MGGBQ (reduced) and MGGBQ (oxidized), respectively.

1.8. Aim of the work

In section 1.2 and 1.3 different sources of Vitamin E and production methods were discussed. Each method has its own advantages and disadvantages. Synthetic chemists are making efforts to optimise the long complicated chemical synthesis route by increasing yield of every intermediate involved in chemical synthesis route (Couladouros et.al. 2007; Liu et. al. 2008; Buss 2008; Gömöry et.al. 2011). Chemists are synthesizing novel catalysts, nanocomposites which can achieve higher yields, trying new solvents, medium etc. Biologist, molecular biologists, plant breeding scientists (Shintani and Della Penna 1998; van Eenennaam et.al. 2003; Qi et.al. 2005; Karunanandaa et.al. 2005); are working to improve the vitamin E content in the plant source itself through plant breeding or studying the biosynthetic pathway by making use of model photosynthetic organisms. Process Engineers are involved in efficient and economical scale-up of the biological and chemical process. Companies and researchers are working to reduce the production cost by using simple, inexpensive raw materials, minimizing the number of production and purification steps, to obtain pure stereoisomer of one homologue (e.g. RRR- α -tocopherol).

This study uses a relatively new approach in solving this scientific problem. Besides chemical synthesis or extraction from natural sources, a promising alternative is the use of a model micro-organism *Escherichia coli* (*E. coli*) to produce Vitamin E compounds. *E. coli* was preferred over *Synechocystis* PCC6803, because of its fast growth on simple carbon

sources in fermenter. Different experiments i.e. cloning, protein expression, cultivation could be performed relatively faster and easier with *E. coli* compared to cyanobacteria. It is a challenge to use *E. coli* for producing a Vitamin E compounds which are exclusively synthesized by photosynthetic organisms. The reasons for selection of *E. coli* as host strain are mentioned in section 1.5. In past *E. coli* has been used to produce complex natural compounds like carotenoids, ubiquinones etc. (Watts et.al. 2005). Here, one of the compounds of δ -tocochromanol (δ -tocopherol) has 3 chiral centers in the saturated phytyl isoprenoid side chain.

Genes responsible for producing δ -Tocotrienol and δ -Tocopherol in any Vitamin E natural organism are not clustered (*ggh*, *hpt*, *cyc*), hence each individual gene would be cloned separately into an expression vector. Genes that are not specific to δ -tocochromonal biosynthesis e.g. *hpd*, and *crtE* would also be cloned separately into an expression vector. Then, an artificial cluster would be constructed by combining all the necessary genes into an expression vector. Stepwise, each biosynthetic reaction in the pathway would be studied until the whole pathway is functional.

To scale-up the vitamin E production to large industrial fermenters and keep it economical, the Vitamin E producing recombinant *E. coli* strain should be robust during fermentation over longer cultivation times. Homologous recombination techniques would be used to construct a segregational stable strain which is free of antibiotic resistance marker. The rare sugar degradation gene loci in *E. coli* chromosome were used as the integration sites for expression cassettes carrying foreign genes. Finally, the plasmid free, δ -tocochromanol producing recombinant *E. coli* strains, would be tested in fermenter, with use of mineral medium and simple carbon source like glucose or glycerol as the sole carbon and energy source.

CHAPTER 2 – Material and Methods

2.1. Materials

2.1.1. Chemicals and enzymes

Luria Broth (LB) media components:	Carl Roth GmbH & Co. KG (Karlsruhe).
Minimal media components:	Carl Roth GmbH & Co. KG (Karlsruhe).
Agar-Base:	Carl Roth GmbH & Co. KG (Karlsruhe).
MacConkey Agar-Base:	Becton Dickinson GmbH (Heidelberg)
60 % (w/v) Glycerol:	Merck KgaA (Darmstadt)

Standards for HPLC, LC-MS:

Homogentisic acid (> 99.5 % purity, HPLC):	Fluka
δ -tocopherol (\geq 96 % purity, HPLC):	Sigma–Aldrich
δ -Tocotrienol (min. 97 % purity):	Davos Life Science Pte Ltd. (Singapore).

Standard for GC-MS (all analytical grade)

geraniol, farnesol, geranylgeraniol (GGOH):	Sigma–Aldrich (Steinheim, Germany)
eicosan, phytol:	Sigma–Aldrich (Steinheim, Germany)
geranyl diphosphate, farnesyl diphosphate:	Sigma–Aldrich (Steinheim, Germany)
geranylgeranyl pyrophosphate:	Sigma–Aldrich (Steinheim, Germany)
bis-tris-propane:	Sigma–Aldrich (Steinheim, Germany).
Phytyl diphosphate:	Biotrend Chemikalien (Cologne, Germany).

Sugars:

Glucose (\geq 90 % purity),	Sigma (Steinheim)
L-fucose, maltose (\geq 99 % purity):	Sigma (Steinheim).
lactose, L-ribose, L-xylose (\geq 99 % purity):	Sigma (Steinheim).
Antibiotics, IPTG:	Carl Roth (Karlsruhe).

Solvents:

All solvents were of analytical grade and were purchased from VWR International, Germany or Carl Roth GmbH & Co. KG (Karlsruhe).

Others:

Protein Standard: Biorad (München, Germany)
Methyl- β -cyclodextrin (98 % purity, TLC): Fluka, Germany.

Molecular Biology:

Synthesis of oligonucleotides (primers) - Biomers GmbH (Ulm, Germany)
Shrimp alkaline phosphatase (bovine intestinal mucosa)-Sigma-Aldrich (Steinheim, Germany)
Endonuclease restriction enzymes – NEB or MBI Fermentas (St. Leon Rot., Germany)
DNA polymerase (Taq, Pwo) – Genaxxon (Konstanz, Germany)
Takara Polymerase: Takara, Germany
DNA ligases – Genaxxon (Biberbach, Germany)
DNA sequencing - GATC Biotech GmbH (Konstanz, Germany).

Purification Kits:

All purification kits were used as per the recommended protocol by the supplier.

Plasmid Isolation: Performed with “Nucleospin Plasmid Kit” from, Machery-Nagel (Düren).

PCR purification Kit: Performed using the Qiagen Kit, Qiagen GmbH, (Hilden).

Purification of DNA from Agarose Gel: Performed using “QIAquick Gel Extraction Kit”, Qiagen GmbH (Hilden).

Histidine-tag affinity purification: Performed using column matrix Nickel-NTA Superflow, Qiagen (Hilden).

GST-Tagged affinity purification: Performed using GST-Tag purification kit from Macherey-Nagel (Dürren)

2.1.2. Bacterial strains, plasmids and primers

Table 2.1 Strains used in this work.

Strain	Relevant properties or genotype	Source
<i>E. coli</i> DH5 α	F ⁻ , ϕ 80d, <i>lacZ</i> Δ M15, <i>endA</i> 1, <i>recA</i> 1, <i>hsdR</i> 17(<i>r</i> _K ⁻ <i>m</i> _K ⁻), <i>supE</i> 44, <i>thi</i> -1, <i>gyrA</i> 96, <i>relA</i> 1, Δ (<i>lacZYA-argF</i>)U169	Hanahan, 1983
<i>E. coli</i> LJ110 (also known as W3110)	F ⁻ , lambda ⁻ , IN(<i>rrnD-rrnE</i>)1, <i>rph</i> ⁻¹	Zeppenfeld 2000; Bachmann, 1972
<i>E. coli</i> M15 [pREP4]	F ⁻ , <i>lacZ</i> Δ M15, <i>thi</i> -1, <i>lac</i> ⁻ , <i>mtf</i> ⁻ , <i>recA</i> ⁺ , Km ^R	Porfirova et.al. 2002 ; [a]
<i>E. coli</i> BW25113	<i>rrnB</i> _{T14} , Δ <i>lacZ</i> _{WJ16} , <i>hsdR</i> 514, Δ <i>araBAD</i> _{AH33} , Δ <i>rhaBAD</i> _{LD78}	Datsenko and Wanner (2000)
<i>E. coli</i> BW25113 <i>lacZ</i> ⁺	<i>rrnB</i> _{T14} , <i>hsdR</i> 514, Δ <i>araBAD</i> _{AH33} , Δ <i>rhaBAD</i> _{LD78}	Albermann et. al. 2010
<i>Pseudomonas putida</i> KT2440	type strain	DSMZ
<i>Synechocystis</i> sp. PCC 6803	type strain	[b]
<i>Arabidopsis thaliana</i>	type strain	[c]

[a] A kind gift from, Dr. Peter Dörmann

[b] A kind gift from Prof. Forchhammer, Universität-Tübingen, Germany

[c] cDNA insert of *hpt-At* from The Arabidopsis Information Resource (TAIR)

DSMZ: Deutsche Sammlung von Mikroorganismen und Zellkulturen

Table 2.2 List of plasmids used in this work for cloning in vector

Plasmids	Relevant properties or genotype	Source
pCAR16	β -carotene biosynthesis gene cluster from <i>Pantoea ananatis</i> in pUC19, Amp ^R	Misawa et. al. 1990
pJF119EH	cloning vector, tac-promoter, IPTG inducible, Amp ^R	Fürste et. al. 1986
pJF119 Δ N	cloning vector, RBS, tac-promoter, IPTG inducible, Amp ^R	Albermann et.al 2008
pAW229	cloning vector, RBS, rha-promoter, L-rhamnose inducible, Cm ^R	Wiese et. al. 2001

pKD46	L-arabinose inducible λ -Red recombinase, Amp ^R	Datsenko et. al. 2000
pUNI51	cloning vector, RBS, P _{T3} promoter, Km ^R	Kayoko et. al. 2003
pQE31	P _{T5} promoter/lac operator element, 6xHis-tag coding sequence, Amp ^R	Qiagen
pCP20	FLP ⁺ , λ cl857 ⁺ , λ p _R Rep ^{ts} , Amp ^R , Cm ^R	Cherepanov and Wackernagel (1995)
pGEX-TN*	alias pGEX4T2: P _{tac} , Ampr, ori _{pBR322} , <i>lacIq</i> , N-term GST-Tag with TEVcleavage site between the GST-Tag and the ORF (TEV recognition site: ENLY FQ↓G; size of the GST-Tag:234 aa, 27kDa) , NdeI cleavage siteinstead of a NcoI cleavage site	Schneider et.al. 2008
pQE31- <i>vte1</i>	Tocopherol-cyclase (<i>vte1</i>) from <i>Arabidopsis thaliana</i> in pQE31, IPTG inducible, Amp ^R	Porfirova et. al 2002
pCAS2JF	1.2 kb EcoRI/ BamHI -PCR-Fragment <i>hpd</i> in pJF119EH	Albermann et.al 2008
pCAS8	1.1 kb NdeI/ BamHI -PCR-Fragment <i>ggh</i> in pJF119ΔN	Albermann et.al 2008
pCAS10	<i>E. coli idi</i> gene, in pJF110ΔN, Amp ^R	Lemuth et. al. 2011
pCAS11	0.9 kb BglII/ BamHI -PCR-Fragment <i>crtE</i> in pCAS8	Albermann et.al 2008
pCAS12	1.0 kb BglII/ BamHI -PCR-Fragment <i>hpt-Syn</i> in pCAS11	Albermann et.al 2008
pCAS15	1.2 kb NdeI/ BamHI -PCR-Fragment <i>hpd</i> in pAW229	Albermann et.al 2008
pCAS18	1.2 kb BglII/ BamHI -PCR-Fragment <i>hpd</i> in pCAS11	Albermann et.al 2008
pCAS19	1.0 kb NdeI/ BamHI -PCR-Fragment <i>hpt-Syn</i> in pAW229	Albermann et.al 2008
pCAS23	1.0 kb NdeI/ BamHI -PCR-Fragment <i>hpt-Syn</i> in pJF119ΔN	Albermann et.al 2008
pCAS24	0.9 kb NdeI/ BamHI -PCR-Fragment <i>crtE</i> in pCAS23	Albermann et.al 2008
pCAS27	1.1 kb NdeI/ BamHI -PCR-Fragment <i>cyc-syn</i> in pAW229	Albermann et.al 2008
pCAS29	1.2 kb BglII/ BamHI -PCR-Fragment <i>hpt-Syn</i> in pCAS18	Albermann et.al 2008

pCAS30	0.9 kb NdeI/ BamHI -PCR-Fragment <i>crtE</i> in pJF119ΔN	Albermann et.al 2008
pCAS47	1.3 kb BglII -PCR-Fragment <i>cyc-At</i> in pCAS29	Albermann et.al 2008
pCAS7	0.9 kb NdeI/ BamHI <i>hpt-Syn</i> - PCR-Fragment in 5.4 kb NdeI/BamHI pJF119ΔN fragment	This study (Personal communication Dr. Albermann)
pCAS50	1.3 kb BglII digested <i>vte1-At</i> PCR fragment in BamHI digested pJF119ΔN fragment	This study (Personal Communication Dr. Albermann)
pJF119HE -dxs-C.glut	<i>dxs</i> gene from <i>Corynebacterium. glutamicum</i> in pJF119ΔN, AmpR	This study (Personal communication Dr. Trachtmann)
pJF119-idi	PCR amplified <i>Idi</i> digested with NdeI and BamHI ligated to NdeI/BamHI digested pJF119ΔN vector	Lemuth et.al. 2011
pJOE5559	<i>dxs</i> , <i>idi</i> and <i>ispA</i> genes from <i>Escherichia coli</i> in pAW229 vector	(Personal communication Dr. Altenbuchner)
pSGS7	1.23 kb EcoRI/ XbaI <i>hpt-At</i> fragment from <i>Arabidopsis thaliana</i> (pUNI51-cDNA <i>hpt-At</i>) in 5.4 kb EcoRI/XbaI pJF119ΔN fragment	This study
pGEX-Vte1	1.3 kb NdeI/ BamHI - PCR-Fragment <i>vte1</i> in pGEX-TN	This study

Table 2.3: List of plasmids used in this work for homologous recombination

Plasmids	Relevant properties or genotype	Source
pCAS2JF-FRT-CAT-FRT	1.1 kb HindIII / HindIII FRT-CAT-FRT fragment in 6.2 kb HindIII / HindIII pCAS2JF fragment	this study
pCAS30-FRT-CAT-FRT	1.1 kb HindIII / HindIII FRT-CAT-FRT fragment in 6.2 kb HindIII / HindIII pCAS30 fragment	Vallon et. al 2008
pCAS7-FRT-CAT-FRT	1.1 kb SphI / SphI FRT-CAT-FRT fragment in 6.0 kb SphI / SphI pCAS7.1 fragment	this study
pCAS50-FRT-CAT-FRT	1.1 kb HindIII / HindIII FRT-CAT-FRT fragment in 6.4 kb HindIII / HindIII pCAS50 fragment	this study
pCAS10-FRT-CAT-FRT	1.1 kb HindIII / HindIII FRT-CAT-FRT fragment in 5.8 kb HindIII / HindIII pCAS10 fragment	this study
pQE31-T5-FRT-cat-FRT	1.1 kb XhoI digested FRT-cat-FRT fragment in 3.46 kb XhoI digested pQE31 fragment	Lemuth et.al. 2011

Table 2.4 Primers used for homologous recombination of vitamin E biosynthesis genes in chromosome of *E. coli*

Primer No.	Primer Name	Primer Sequence	Primer Description
1	fucP - integr.	5'-TGC TGT GCT CAC TGT TTT TTC TTT GGG CGG TAG CCA ATA ACC TTA ACG ACA TTT TAT TA <u>TCA AGG CGC ACT CCC GTT CTG G</u> -3'	Used for integration of <i>hpd</i> in <i>fucI</i> and <i>fucP</i> locus.
2	fucI -integr	5'-CAG CAT GGA GGC GAG AGT GAT AAA GTC TGC GCC AAC GTG GCC GAT GGT CAG AAC CCC <u>CAG GGT TAT TGT CTC ATG AGC G</u> -3'	
3	malE - integr.	5'- AAG GTA AAC TGG TAA TCT GGA TTA ACG GCG ATA AAG GCT ATA ACG GTC TCG CTG <u>TCA AGG CGC ACT CCC GTT CTG G</u> - 3'	Used for integration of <i>crtE</i> in <i>malE</i> , <i>malF</i> and <i>malG</i> locus.
4	malG - integr.	5'- GAT CGG TAA TGC AGA CAT CAC GGC AGC GGC GGC AAA GTC ACC CCA CAG GTA GTT TT <u>CAG GGT TAT TGT CTC ATG AGC G</u> - 3'	
5	Δ <i>lacZYA</i> 2	5'-AAT TGC GGC CTA TAT GGA TGT TGG AAC CGT AAG AGA AAT AGA CAG GCG GTC <u>AGA CCG CTT CTG CGT TCT G</u> -3'	Used for integration of <i>hpt</i> in <i>lacZ</i> , <i>lacY</i> and <i>lacA</i> locus.
6	Δ <i>lacZYA</i> 3	5'-CCC CGC GCG TTG GCC GAT TCA TTA ATG CAG CTG GCA CGA CAG GTT TCC CGG <u>CGC CGA CAT CAT AAC GGT TC</u> -3'	
7	rbsD-integr	5'- ACC GTT CTT AAT TCT GAT ATT TCA TCG GTG ATC TCC CGT CTG GG ACA TAC CGA TA <u>TCA AGG CGC ACT CCC GTT CTG G</u> - 3'	Used for integration of <i>idi</i> in <i>rbsD</i> and <i>rbsK</i> locus.
8	rbsK-integr	5'- ATT CAC GCT AGC CCA TAC ACC ACG ACT TCC TAA AGT AAT CAG TAC AGT ACG GAT ACC <u>CAG GGT TAT TGT CTC ATG AGC G</u> - 3'	
9	P1-control-fucA	5'-GAA AAC ATA ACC GAT TAC GTG C -3'	Used for control PCR to verify the exact location of <i>hpd</i> expression cassette
10	P2-control- <i>hpd</i>	5'- CGT AGA ACC CGG CCC AGT AGG C-3'	
11	P3-control- <i>cat</i>	5'-CCG TCA CAG GTA GGC GCG CC - 3'	
12	P4-control-fucK	5'- CCC GGT AGC CGG AGC GAC CG - 3'	
13	P1-malG-screen	5'-CGTCAGGATGGCCTTCTGCTTAATTTG-3'	Vallon et. al
14	P2-control- <i>cat</i>	5'-CCGTCACAGGTAGGCGCGCC-3'	
15	P3-malK-screen	5'-GCTTTTCGTTACA7TTTGCAGCTGTACG-3'	Vallon et. al
16	4-control- <i>crtE</i>	5'-CCCGTTCTCCCTCCACGGGC-3'	

17	P1-control-lacZ	5`- GAA TGA GGG CAT CGT TCC CAC TGC GA – 3`	Used for control PCR to verify the exact location of <i>hpt-Syn</i> expression cassette
18	P2-control- <i>hpt</i>	5`- ACA GGG CCG CCA GCA GGG AAA AGC GC – 3`	
19	P1-control-kup	5`- GCG CGG CAA GCT GTA CTT GC – 3`	Used for control PCR to verify the exact location of <i>idi</i> expression cassette
20	P2-control- <i>idi</i>	5`- GTT AGT CCA CAC GCC AGG CC – 3`	
21	<i>xylA</i> -integr	5`-GACGAACTGGTGTGGTAAGCGTA TGGAAGAGCACTTGCCTTTGCCGCCT GCTCAAGGCGCACTCCCGTTCTGG– 3`	Used for integration of <i>cyc-At</i> in <i>xylA</i> and <i>xylB</i> locus.
22	<i>xylB</i> -integr	5`- ATTAAGCTGGGACATTGCTCAGGCCG GTTAATTTGCGGCCCAATCCAGACACCAG GGTTATTGTCTCATGAGCG – 3`	
23	T5- <i>dxs</i> -P1	5`-GGCATGAAGAAACACAAATGTCGCAGATTGAAAA CA TCA AGG CGC ACT CCC GTT CTG G – 3`	Used to amplify P _{T5} - <i>dxs</i> -FRT-cat-FRT fragment from plasmid pQE31-FRT-cat-FRT
24	T5- <i>dxs</i> -P2	5`-GTGACCAATGGGTTGATGGCTGGTTAC CAGGGTTATTGTCTCATGAGCG-3`	
25	Control- <i>dxs</i> -1	5`-ACAAGCTGGCTGAACAGTCACTCGAT-3`	Used for control PCR to verify the exact location of <i>dxs</i> expression cassette
26	Control- <i>dxs</i> -2	5`-AAGAGTAAAGCTTACCGGAAAG-3`	
27	P1-Control- <i>vte1-xyl</i>	5`-GGCTGGCCTGCAGCTTTTCC-3`	Used for control PCR to verify the exact location of <i>cyc-At</i> expression cassette
28	P2-Control- <i>vte1-xyl</i>	5`- ATTGCCCCACCTGCGGTGGC-3`	
29	P1-Control- <i>idi-rbs</i>	5`-GCGCGGCAAGCTGTACTTGC-3`	Used for control PCR to verify the exact location of <i>idi</i> expression cassette
30	P2-Control- <i>idi-rbs</i>	5` GTTAGTCCACACGCCAGGCC-3`	

The primers were obtained from biomers.net, Ulm, Germany. Reverse phase (cartridge) or HPLC quality of primers were used.

Table 2.5 List of chromosomally integrated strains constructed in this study

No.	Strain name	Strain Details	Genes integrated	Source
1.	<i>E. coli</i> CS1-cat	<i>E. coli</i> BW25113 <i>fuclP::P_{tac}-hpd-cat</i>	<i>hpd</i>	This study
2.	<i>E. coli</i> CS1	<i>E. coli</i> BW25113 <i>fuclP::P_{tac}-hpd</i>	<i>hpd</i>	This study
3.	<i>E. coli</i> CS2-cat	<i>E. coli</i> BW25113 <i>malEFG::P_{tac}-crtE-cat</i>	<i>crtE</i>	This study
4.	<i>E. coli</i> CS2	<i>E. coli</i> BW25113 <i>malEFG::P_{tac}-crtE-cat</i>	<i>crtE</i>	This study
5.	<i>E. coli</i> CS2.1-cat	<i>E. coli</i> LJ110 <i>malEFG::Ptac-crtE-cat</i>	<i>crtE</i>	This study
6.	<i>E. coli</i> CS2.1	<i>E. coli</i> LJ110 <i>malEFG::Ptac-crtE-cat</i>	<i>crtE</i>	This study
7.	<i>E. coli</i> CS2.2-cat	<i>E. coli</i> LJ110 <i>fuclP::Ptac-hpd-malEFG::Ptac-crtE-cat</i>	<i>hpd, crtE</i>	This study
8.	<i>E. coli</i> CS2.2	<i>E. coli</i> LJ110 <i>fuclP::Ptac-hpd-malEFG::Ptac-crtE-cat</i>	<i>hpd, crtE</i>	This study
9.	<i>E. coli</i> CS3-cat	<i>E. coli</i> BW25113 <i>lacZYA::Ptac-hpt-cat</i>	<i>hpt</i>	This study
10.	<i>E. coli</i> CS3	<i>E. coli</i> BW25113 <i>lacZYA::Ptac-hpt</i>	<i>hpt</i>	This study
11.	<i>E. coli</i> CS4-cat	<i>E. coli</i> BW25113 <i>lacZYA::Ptac-hpt-fuclP::Ptac-hpd-cat</i>	<i>hpt, hpd</i>	This study
12.	<i>E. coli</i> CS4	<i>E. coli</i> BW25113 <i>lacZYA::Ptac-hpt-fuclP::Ptac-hpd</i>	<i>hpt, hpd</i>	This study
13.	<i>E. coli</i> CS5-cat	<i>E. coli</i> BW25113 <i>lacZYA::Ptac-hpt-malEFG::Ptac-crtE-cat</i>	<i>hpt, crtE</i>	This study
14.	<i>E. coli</i> CS5	<i>E. coli</i> BW25113 <i>lacZYA::Ptac-hpt-malEFG::Ptac-crtE</i>	<i>hpt, crtE</i>	This study
15.	<i>E. coli</i> CS6-cat	<i>E. coli</i> BW25113 <i>lacZYA::Ptac-hpt-fuclP::Ptac-hpd-malEFG::Ptac-crtE-cat</i>	<i>hpt, hpd, crtE</i>	This study
16.	<i>E. coli</i> CS6	<i>E. coli</i> BW25113 <i>lacZYA::Ptac-hpt-fuclP::Ptac-hpd-malEFG::Ptac-crtE</i>	<i>hpt, hpd, crtE</i>	This study
17.	<i>E. coli</i> CS7-cat	<i>E. coli</i> BW25113 <i>lacZYA::Ptac-hpt-fuclP::Ptac-hpd-malEFG::Ptac-crtE-xylAB::Ptac-cyc-cat</i>	<i>hpt, hpd, crtE, cyc</i>	This study

18.	<i>E. coli</i> CS7	<i>E. coli</i> BW25113 <i>lacZYA::Ptac-hpt-fucIP::Ptac-hpd-malEFG::Ptac-crtE-xylAB::Ptac-cyc-At</i>	<i>hpt</i> , <i>hpd</i> , <i>crtE</i> , <i>cyc-At</i>	This study
19.	<i>E. coli</i> CS8-cat	<i>E. coli</i> BW25113 <i>lacZYA::Ptac-hpt-malEFG::Ptac-crtE-rbsDK::Ptac-idi-cat</i>	<i>hpt</i> , <i>hpd</i> , <i>crtE</i> , <i>idi</i>	This study
20.	<i>E. coli</i> CS8	<i>E. coli</i> BW25113 <i>lacZYA::Ptac-hpt-malEFG::Ptac-crtE-rbsDK::Ptac-idi</i>	<i>hpt</i> , <i>hpd</i> , <i>crtE</i> , <i>idi</i>	This study
21.	<i>E. coli</i> CS9-cat	<i>E. coli</i> BW25113 <i>lacZYA::P_{tac}-hpt-malEFG::P_{tac}-crtE-rbsDK::P_{tac}-idi-xylAB::P_{tac}-cyc-At-cat</i>	<i>hpt-Syn</i> , <i>hpd</i> , <i>crtE</i> , <i>idi</i> , <i>cyc-At</i>	This study
22.	<i>E. coli</i> CS9	<i>E. coli</i> BW25113 <i>lacZYA::P_{tac}-hpt-malEFG::P_{tac}-crtE-rbsDK::P_{tac}-idi-xylAB::P_{tac}-cyc-At</i>	<i>hpt-Syn</i> , <i>hpd</i> , <i>crtE</i> , <i>idi</i> , <i>cyc-At</i>	This study
23.	<i>E. coli</i> CS10-cat	<i>E. coli</i> BW25113 <i>lacZYA::Ptac-hpt-fucIP::Ptac-hpd-malEFG::Ptac-crtE-rbsDK::P_{tac}-idi- P_{T5}-dxs-cat</i>	<i>hpt-Syn</i> , <i>hpd</i> , <i>crtE</i> , <i>idi</i> , and IPTG inducible <i>dxs</i>	This study
24.	<i>E. coli</i> CS10	<i>E. coli</i> BW25113 <i>lacZYA::P_{tac}-hpt-fucIP:: P_{tac}-hpd-malEFG::P_{tac}-crtE-rbsDK::Ptac-idi-P_{T5}-dxs</i>	<i>hpt-Syn</i> , <i>hpd</i> , <i>crtE</i> , <i>idi</i> , and IPTG inducible <i>dxs</i>	This study

2.1.3. Cultivation media (Sambrook et. al.1989)

<u>LB medium:</u>	10 g/l Tryptone, 5 g/l Yeast Extract, 5 g/l NaCl; pH 7.0
<u>SOB medium:</u>	20 g/l Tryptone, 5 g/l Yeast Extract, 0.5 g/l NaCl, 0.2 g/l of KCl, Adjust pH at 7.0 with NaOH, Sterilize at 121 °C for 20 minutes. Before use, add 10 ml of 1M MgCl ₂ and 10 ml of 1 M MgSO ₄ * 7 H ₂ O to 1 L of sterilised medium.
SOC medium:	SOB medium supplemented with 20 mM Glucose (end concentration)
<u>LB Agar:</u>	LB medium with 15 g/l agar
<u>LB Agar + Amp100:</u>	LB Agar with 100 µg/ml ampicillin (end concentration in LB Agar)
<u>LB Agar + Cm25:</u>	LB Agar with 25 µg/ml chloramphenicol (end concentration in LB Agar)
<u>LB Agar + Km25:</u>	LB Agar with 25 µg/ml kanamycin (end concentration in LB Agar)
<u>LB-Glycerol medium:</u>	LB medium supplemented with 2 % (v/v) glycerol (end concentration in LB-Glycerol medium)
LB-Glycerol-Amp100:	LB-Glycerol supplemented with 100 µg/ml ampicillin (end concentration in LB-Glycerol medium)

Antibiotics concentrations: Ampicillin 100 µg/ml end concentration; Chloramphenicol 50 µg/ml end concentration; Kanamycin 25 µg/ml end concentration.

Minimal Medium(MM): According to Albermann et. al. 2008. KH_2PO_4 3 g/l, K_2HPO_4 12 g/l), $(\text{NH}_4)_2\text{SO}_4$ 5 g/l, $\text{MgSO}_4 \cdot 7\text{H}_2\text{O}$ 0.3 g/l, $\text{CaCl}_2 \cdot 2\text{H}_2\text{O}$ 0.015 g/l), NaCl (0.1 g/l), $\text{FeSO}_4 \cdot 7\text{H}_2\text{O}$ /sodium citrate (15 ml/l); from a solution of $\text{FeSO}_4 \cdot 7\text{H}_2\text{O}$ (7.5 g/l) and sodium citrate (100 g/l), thiamine, trace elements solution 1 ml (1000 X modified Pan et. al 1987)

MM with glucose: Above minimal medium with glucose (5 g/L)

MM with glycerol: Above minimal medium with glycerol (5 g/L)

Minimal Medium 2: According to Vallon et.al. 2008 Na_2SO_4 10 H_2O 2 g L^{-1} , $(\text{NH}_4)_2\text{SO}_4$ 2.68 g L^{-1} , NH_4Cl 1 g L^{-1} , K_2HPO_4 14.6 g L^{-1} , NaH_2PO_4 2 H_2O 4.02 g L^{-1} , glucose 8 g L^{-1} , MgSO_4 0.49 g L^{-1} , CaCl_2 0.04 g L^{-1} , thiamine 0.01 g L^{-1} , TES 3 mL L^{-1} (TES: FeCl_2 6 H_2O (16.67 g L^{-1}), ZnSO_4 7 H_2O (0.18 g L^{-1}), CuCl_2 2 H_2O (0.12 g L^{-1}), MnSO_4 1 H_2O (0.12 g L^{-1}), CoCl_2 6 H_2O (0.18 g L^{-1}), Na_2EDTA 2 H_2O (22.25 g L^{-1}))

2.6 Table of different buffers used in this study.

Buffer Name	Ingredients	Final concentration
Bradford reagent	Coomassie Brilliant Blue G 250, ethanol 96% (v/v), phosphoric acid 85% (v/v)	100 mg/l 50 ml/l 100 ml/l
DNA loading buffer	24%(w/v) urea, EDTA, sucrose, bromophenolblue)	24 % (w/v) 0.2%(w/v) 50%(w/v) 0.1%(w/v)
Coomassie staining solution	Coomassie Brilliant Blue G 250 methanol, acetic acid	0.2% (w/v) 30% (v/v) 10% (v/v)
Destaining solution	glacial acetic acid	20% (v/v)
SDS-PAGE electrophoresis buffer	Tris-HCl (pH 8.3), Glycine, SDS	25 mM 192 mM 0.1% (w/v)
TAE buffer	Tris-acetate pH 8.0, EDTA	40 mM 1 mM
PBS buffer - GST-tagged protein purification (Macherey Nagel)	Na ₂ HPO ₄ KH ₂ PO ₄ KCl NaCl Adjust pH to 7.3	10 mM 1.8 mM 2.7 mM 140 mM
Elution Buffer - GST-Tagged protein purification (Macherey-Nagel)	Tris base Glutathione Adjust pH to 8.0	50 mM 10 mM
TSS Buffer	PEG 8000 1 M MgCl ₂ DMSO MgSO ₄ * 7 H ₂ O LB medium Sterile filter through 0.22 µm filter & store at 4 °C	100 g 30 ml 50 ml 12.3 g Fill till 1 Liter

2.2. METHODS

2.2.1. Microbiological methods

2.2.1.1. Cultivation conditions in shaking flask

Whenever a new plasmid or chromosomal integrated strain was constructed, it was tested for protein expression. Once the respective protein(s) were detected, these plasmids or chromosomal integrated strains were studied further for cell growth curve and enzyme activity by analysing the intermediates and products (in-vivo biosynthesis).

Cultivations for studying protein expression:

Strains harbouring plasmids were freshly transformed, while chromosomal integrated strains were freshly streaked on LB agar plate. Strains harbouring plasmids were cultivated in LB medium with the appropriate antibiotics. Chromosomally integrated strains were cultivated in LB medium without any antibiotics. Pre-cultures were started from a single colony from fresh agar plate in 10 ml medium in 100 ml Erlenmeyer flask (without baffles). Main cultures were inoculated such that the starting OD_{600nm} of 0.05 was reached. Cultures were induced with 1 mM IPTG (end concentration) at OD_{600nm} of 0.8. Culture samples were taken at the time of induction and 6 h after induction, for SDS-PAGE analysis.

Cultivations for studying cell growth and enzyme activity:

The following method was followed for HGA, GGPP, MGGBQ, and δ -tocotrienol biosynthesis. After the strain possessing plasmid, or chromosomal integrated strain was able to express the desired protein, these strains were tested in a separate shaking flask experiment for cell growth curve and enzyme activity. Enzyme activity was studied by analysing its biosynthetic pathway intermediates and products. 10 ml of fresh LB-Glycerol (appropriate antibiotics for strain possessing plasmids, and no antibiotics for chromosomal integrated strain) was inoculated, and incubated overnight at 30 °C, at 100 RPM. 200 ml of same medium in which precultures were grown, in 1 L Erlenmeyer flask (without baffles), were inoculated with the overnight preculture (starting OD_{600nm} of 0.05). Main cultures were incubated at 30 °C, at 100 RPM. At OD_{600nm} of approx. 0.8, cultures were induced with 0.25 mM IPTG (end concentration). 1 ml culture sample was taken for OD measurement, and 2 X 25 ml culture sample were taken for analysis of product. HGA was analysed in the supernatant samples, while GGPP, MGGBQ and δ -tocotrienol were analysed by extracting the respective product from cell pellet.

At the start of this study, it was decided that *E. coli* LJ110 strain would be used as for production of δ -tocochromanols and its intermediates in fermenter and *E. coli* BW25113 *lacZ*⁺ as strain for homologous recombination experiments. After construction of *E. coli* CS6

strain, i.e. (*E. coli* BW25113 as host strain) After the fermentation experiments with GGPP with *E. coli* LJ110 strain was completed, it was observed during an shaking flask experiment that *E. coli* BW25113 *lacZ*⁺ strain can also be directly used for production in fermenter. After GGPP production experiments, production of HGA, MGGBQ and δ -tocotrienol were performed with *E. coli* BW25113 *lacZ*⁺ as host strain. This new strategy saved time and efforts of transducing the *E. coli* LJ110 recipient cell.

2.2.1.2. Cultivation conditions in bioreactor

a) MGGBQ and δ -Tocotrienol Production Experiments

Seed 1, was prepared in 10 ml MM-Glucose or MM-Glycerol (Amp100 added for strains carrying plasmids pCAS30, pCAS29 and pCAS47). A single colony from fresh agar plate (prepared a day before from glycerol stock culture) was inoculated and incubated at 30°C overnight. Seed 2 pre-culture was started by inoculated 150 ml fresh minimal medium 1, with glucose / glycerol, in 1 L Erlenmeyer flask. The starting OD_{600nm} of seed 2 adjusted to 0.05 and incubated at 30 °C, till the cultures reached the middle of exponential phase (approx. 12 to 16 h).

1.5 L of minimal medium 1, with glucose/glycerol in 3.6 L (total volume) Infors fermenter (Labfors® System, Infors AG, Switzerland) was inoculated with seed 2 cultures. The starting OD_{600nm} in main fermenter was adjusted to approx. 0.10-0.12. The vessel of the Infors fermenter was made of borosilicate glass with supporting structure, baffles and top of the glass vessel made up of stainless steel 316L. The Infors fermenter is a table fermenter with its own microprocessor system, and LCD display with control panel. The temperature of the cultures was controlled by circulating cooling water through the glass jacket. Cultivation was carried out at 30 °C. Cultivation parameters at start of fermentation were 200 RPM, 100 % saturated oxygen concentration in medium (pO₂), 60 l/min air flow rate, pH 7.0. Air supplied during aeration was first, sparged through water, and then through sterile filter before entering the fermenter broth. pH was maintained constant at 7.0, throughout the fermentation by automatic addition of 5 N KOH or 1 M H₃PO₄ whenever required. The pO₂ concentration was always kept above 30 % by controlling the stirrer speed (200 - 600 RPM). Batch fermentation was followed till the initial 5 g/L of glucose/glycerol was consumed. Fed batch fermentation process was started by feeding the 500 g/l of stock solution of glucose / glycerol to the growing cultures. Feeding rate was calculated such that the concentration of carbon source is limiting i.e. no overflow of glucose or glycerol occurs in medium. As nitrogen source, 200 g/L of ammonium sulphate stock was fed manually whenever the concentration ammonium concentration in fermentation broth dropped down below 0.5 g/L.

b) GGPP Production Experiments:

Batch fermentation strategy was followed during the cultivation of different bacterial strains (*E. coli* LJ110 wild-type, *E. coli* LJ110 / pCAS30 and *E. coli* CS2.1) during GGPP production. These cultivations were carried out at the Institute of Biochemical Engineering, Universität Stuttgart). 1.8 L of minimal medium 2 supplemented with glucose as the sole carbon and energy source was fed in a 3.7 L bioreactor KLF 2000 (Bioengineering AG, Wald, Switzerland). Additional ampicillin (100 mg/l) was added for cultivation of *E. coli* LJ110 / pCAS30 strain. Cultures were induced in exponential phase with 0.1 mM IPTG (final concentration). The process parameters maintained during cultivation were, dissolved oxygen concentration > 50% saturation, pH 7, pressure absolute $p = 1.3$ bar, temperature of 30°C. pH value was maintained constant by addition of either H₃PO₄ (20% v/v) or 2 M NaOH. Foaming was controlled by addition of Struktol J647 (Schill und Steinacker, Hamburg, Germany), whenever needed.

2.2.1.3. MacConkey Agar Test

This test was used for control or as screening test, after homologous recombination was completed. This was to verify, whether the gene expression cassette was integrated in the chromosome, in the desired sugar operon. Hence, clones obtained after transformation (for chromosomal integration of the expression cassette) were spread on 1.5 % (w/v) MacConkey agar plates supplemented with 1 % (w/v) of any one respective sugar (L-fucose or maltose or lactose or L-ribose, or L-xylose). Corresponding control strains were also streaked on the same plate. These plates were incubated at 37°C for 10 - 12 h. Clones which turned red were negative and hence discarded. Clones which remained pale/white were considered positive clones and further tested with control PCR.

2.2.1.4. Plasmid Stability Test

This test was carried out for samples from bioreactor cultivation of strains carrying plasmids to understand how many of the host *E. coli* cells during the course of cultivation in bioreactor had lost the antibiotic resistance plasmid. Cell density of the culture samples at different cultivation time points from bioreactor (only restricted to experiments where *E. coli* cells carried a plasmid) was adjusted to OD_{600 nm} of 1.0 (dilutions made in sterile minimal medium) and final volume of 1 ml. Serial dilutions were performed and 10⁻⁷ mixture was spread evenly on LB plates and LB + Amp 100 agar plates and incubated overnight at 37°C. Each dilution and its spreading on agar plates were performed twice for the same culture sample to calculate the standard deviation. Colony forming units (cfu's) were counted on both plates. If cfu's on both plates were equal in number then it meant that all the *E. coli* cells carried the

ampicillin resistance plasmid. Based on the cfu's, % of cells harbouring plasmids were calculated and plotted vs. time.

2.2.1.5. Preparation of competent cells

Electrocompetent cells for homologous recombination (Datsenko and Wanner 2000):

Fresh *E. coli* BW25113 *lacZ*⁺ strain carrying plasmid pKD46 was streaked on LB-Amp100 agar plate and incubated at 30 °C. Pre-culture was started by inoculating 5 ml of SOB medium supplemented with ampicillin (100 µg/ml) and arabinose (1 mM end concentration) with a single colony and incubated at 30 °C overnight. Main cultures were started by inoculating 25 ml of fresh medium (as used for pre-culture) using overnight pre-culture such that the starting OD_{600nm} of 0.05. The cultures were incubated at 30 °C till an OD_{600nm} of 0.6 was reached. Cultures were placed on ice for 30 minutes, centrifuged for 10 minutes at 2000 g at 4°C, washed with cold 10 % (w/v) glycerol. Washing was repeated 2 times, and cells were re-suspended in 0.5 ml of 10 % (w/v) glycerol (i.e. concentrated 50 fold) to obtain electro-competent cells for homologous recombination.

Chemically Competent Cells (Chung et.al. 1989):

Chemically competent *E. coli* cells were obtained by inoculating 5 ml of fresh LB medium in 50 ml Erlenmeyer flask and incubating at 37 °C overnight with a single colony. Main cultures were inoculated with overnight pre-culture in 20 ml LB medium in 200 mL Erlenmeyer flask with starting OD_{600nm} of 0.05 and incubated at 30 °C. Place the cultures on ice for 30 minutes, when they reach exponential phase, i.e. OD_{600nm} of 0.3-0.4. Centrifuge the cultures at 1000 g for 10 minutes at 4°C and the cell pellet was re-suspended with 500 µl TSS buffer and vigorously vortexed for 2 minutes and placed on ice. These chemically competent cells were not stored for further use. Whenever chemically competent cells were needed they were freshly prepared.

2.2.1.6. Transformation of cells

Electroporation for homologous recombination:

Electrocompetent cells (50 µl) were mixed with approx. 10 to 100 ng of PCR purified DpnI treated expression cassette fragment in a cooled 0.2 cm electroporation cuvette. This mixture was placed for 30 minutes and further electroporation was performed at 2.5 kV. Immediately 800 µl of SOC medium was added and the whole mixture was transferred into an sterile eppendorf reaction cup and incubated at 30 °C overnight (i.e. approx. 16 hours). 100 µl of this mixture was spread on one LB agar plate supplemented with respective antibiotics depending on the resistance marker the PCR fragment (expression cassette) carries. Such 8 agar plates were used to spread the complete mixture and incubated overnight at 30 °C.

Chemical Transformation:

Chemical competent cells (50 μ l) were mixed with the ligation mixture (overnight incubated at 16°C) and placed on ice for 30 minutes. The mixture was incubated in 42 °C water bath for 90 seconds and incubated again on ice for 2 minutes. 800 μ l of SOC medium was added and mixture was incubated at 37 °C for 45 minutes and later spread on 2 LB agar plates with or without antibiotics depending on the corresponding antibiotic resistance. LB agar plates were incubated at 37 °C overnight and clones obtained were tested in different ways depending upon the aim of the experiment.

2.2.1.7. Preparation of P1 lysate

Pre-culture of the donor *E. coli* strain (e.g. *E. coli* CS1-*cat*) was inoculated in 5 ml LB medium supplemented with 5 mM CaCl₂ and 0.2 % (w/v) glucose, 25 μ g/ml chloramphenicol and incubated overnight at 37 °C. Main cultures in same medium as pre-culture were inoculated with overnight pre-culture (10 ml medium in 100 ml Erlenmeyer flask without baffles) and incubated at 37°C. Simultaneously 0.6 % (w/v) agar in liquid form was kept ready in 42 °C water bath. After reaching an OD_{600 nm} of 0.6, 100 μ l of this culture was added 10.0 μ l P1 phages. This mixture of cells and P1 phages was added to 4 ml of 0.6 % (w/v) pre-warmed (37-38 °C) agar. This complete mixture was poured on LB agar plates supplemented with 5 mM CaCl₂ and 0.2 % (w/v) glucose and spread evenly. These plates were incubated overnight at 37°C. One such plate was prepared without P1 lysate as control to compare the cell lysis on plates with and without P1 lysate. 3 ml of LB medium was added to the overnight incubated agar plate and incubated at 4 °C for 1 h. The top layer i.e. 0.6 % (w/v) agar was scrapped off and filtered after centrifugation along with the LB medium through 0.2 μ m sterile filter and stored at 4 °C till use. The filtered P1 lysate is stored at 4 °C till transduction is performed.

2.2.1.8. Transduction

Pre - culture of recipient cells (e.g. *E. coli* LJ110, in case of integration of crtE expression cassette from *E. coli* CS2-*cat*) was grown in LB medium supplemented with 5 mM CaCl₂ and 0.2 % (w/v) glucose at 37°C overnight. 10 ml of fresh medium (same used for pre-culture) was inoculated with overnight pre-culture so that the starting OD_{600nm} is 0.05. After reaching an OD_{600 nm} of 0.6, 100 μ l of this recipient cell culture was added with different concentrations of P1 lysate suspension i.e. 0.5, 1.0, 2.0, 5.0 and 10.0 μ l and incubated exactly for 20 minutes at 37 °C on a heating block (without shaking). Then it was washed with 1 ml of LB medium supplemented (no vortex) which consisted of sodium pyrophosphate (125 μ M end concentration) (i.e. LB + sodium pyrophosphate) After washing, the mixture

was centrifuged at 11000 g for 1 minute, and re-suspended again in 1 ml medium (LB + sodium pyrophosphate) and incubated at 37°C for 1 h. Further it was centrifuged at 11000 g for 1 minute and re-suspended in 200 µl LB medium with sodium pyrophosphate, spread on LB chloramphenicol agar plates and incubated overnight at 37°C. Transductants after testing positive on MacConkey agar plates with respective sugar still carries residual phages and were therefore further cleaned for phage removal.

2.2.1.9. Single colony purification

To get rid of phages after successful transduction, every positive transductant was spread on LB / LB-Cm25 agar plate such that a single colony is obtained after incubation at 37°C overnight. Single colony from the overnight incubated agar plate was again spread on fresh LB agar plate and same procedure repeated in total for 3 times. Transductants free of phages were verified on LB agar plates (with or without resp. antibiotics) by observing the morphology of single colony by eyes if it lyses after overnight incubation at 37 °C. Single colonies that didn't have jagged edges were assumed to be free of phage.

2.2.1.10. Removal of chloramphenicol cassette

The chloramphenicol cassette (*cat*) had to be removed from the strain obtained after homologous recombination (e.g. *E. coli* CS1.1-*cat*). Same method as described in Datsenko and Wanner (2000) was used here. The strain from which the *cat* resistance cassette was to be removed (e.g. *E. coli* CS1.1-*cat*) was inoculated in LB medium supplemented with 5 mM CaCl₂, 0.2 % glucose, Cm 25 and incubated overnight at 30 °C. Main culture in same medium (10 ml) was inoculated and incubated till OD_{600 nm} of 0.6 was reached. This culture was placed on ice for 30 minutes and centrifuged at 3000 g for 10 minutes, washed with same volume of cold 100 mM CaCl₂ solution, vortexed, centrifuged. This was repeated once and re-suspended in 250 µl cold CaCl₂ solution. 5 µl of plasmid pCP20 was mixed with 50 µl of the freshly prepared above chemically competent cells and placed in ice for 30 minutes. Then the mixture was incubated at 42 °C for 90 sec and then incubated on ice for 2 minutes. 800 µl of SOC was added and mixture was incubated at 30 °C for 1 h. Mixture after 1 h was spread on LB Amp100 agar plates, incubated overnight at 30 °C. Transformants were spread on new LB agar plate, incubated for 4 h at 42 °C and then overnight at 37 °C. These transformants were tested on LB Cm25 and LB Amp100 agar plates to check for the removal of *cat* resistance cassette (e.g. *E. coli* CS1.1) and loss of pCP20 plasmid.

2.2.2. Molecular biological methods

2.2.2.1. Isolation and cloning of DNA

DNA Isolation:

Plasmid DNA was isolated and purified using either “QIAprep Spin Mini Kit” (Qiagen) or “Nucleospin Extract”(Macherey-Nagel GmbH & Co.KG, Düren) from overnight cultures.

Digestion:

Digestion of DNA was performed by incubation with restriction endonucleases in a suitable buffer and at an optimal temperature recommended by the respective enzyme company, New England Biolabs (NEB) or Fermentas MBI or according to Sambrook et. al. (1989).

Agarose Gel Electrophoresis:

DNA was separated using agarose gel electrophoresis in TAE buffer. DNA samples were mixed with 6x loading buffer and loaded on 1 % (w/v) agarose gel prepared by adding 1 µg/mL of ethidiumbromide. DNA was isolated from agarose gels using one of the above mentioned kits. DNA was visualized by excitation of fluorescence of the intercalated ethidium bromide under UV light. For documentation a gel documentation system with a CCD-camera was used.

Alkaline phosphatase treatment and Ligation:

Linear plasmid DNA or PCR products were de-phosphorylated using alkaline phosphatase. Ligation of DNA was performed with T4 DNA ligase or “Rapid DNA Ligation Kit” (Roche Applied Science) as recommended by the supplier.

2.2.2.2. Polymerase chain reaction (PCR)

Standard PCR procedure (Saiki et.al. 1985) was used for amplification of DNA fragments for molecular cloning and for homologous recombination. PCR was also used to verify the location of certain DNA fragment in plasmid construct or in a newly constructed chromosomally integrated strain. PCR reaction components are shown in table 2.7, were mixed in PCR tubes and placed on ice.

Table 2.7: PCR reaction components:

Component	Volume	Final Concentration
dNTP's (2.5 mM each)	4 µl	0.2 mM
PwoI buffer with Mg ²⁺ (10X)	5	1 X (1.5 mM Mg ²⁺)
DMSO	variable	0.1 µM
Forward primer 1	Variable	0.1 – 0.2 µM
Reverse primer 2	Variable	0.1 – 0.2 µM
DNA template	Variable	1 – 150 ng

PwoI Polymerase	0.2 – 0.5 μ l	0.5 – 2.5 U
Distilled water	Variable	
Total volume	50 μ l	

2.2.3. Biochemical Methods

2.2.3.1. Bradford Assay

Protein concentration was determined as according to the Bradford method (Bradford, 1976). 100 μ l of protein solutions was mixed with 900 μ l of Bradford reagent and incubated for 10 minutes at room temperature. Absorbance at 595 nm was measured against a blank containing 100 μ l of the protein buffer or water (if sample is diluted in water) in 900 μ l Bradford reagent. 1 μ g to 20 μ g bovine serum albumin (Sigma-Aldrich) was used as standard to obtain a calibration curve.

2.2.3.2. Over-expression of recombinant proteins in *E. coli*

5 ml of LB medium (with antibiotics in case of *E. coli* cells harboring plasmid) was inoculated with *E. coli* cells carrying plasmid or chromosomally integrated strains. These were incubated overnight at 30 °C in Erlenmeyer flasks at 100 RPM. Main cultures were started by inoculating 50 ml fresh medium (same as used for pre-culture) with overnight pre-culture so that the starting OD_{600nm} was 0.05. At OD_{600nm} of 0.8 cultures were induced with 1.0 mM IPTG. Culture samples taken (before induction and 6 h after induction) were centrifuged, and the cell pellet was stored at -20 °C.

2.2.3.3. Cell disruption and preparation of crude extracts

Cell pellet was suspended in 50 mM Tris-HCl buffer, pH 8.0. Cells were disrupted by using ultrasonic disintegrator (Heinemann, Germany). 3 cycles of disruption at 50 % amplitude for 15 seconds and cooling phase for 15 seconds were used. During disruption, the cell suspension was cooled in an ice bath. Cells and cell debris were removed by centrifugation at 10,000 g for 15 minutes at 4°C.

2.2.3.4. SDS-Polyacrylamide gel electrophoresis

Sodium dodecyl sulphate polyacrylamide gel electrophoresis (SDS-PAGE) method as described by Laemmli 1970 for analysis of protein molecular size or purity was used. SDS-PAGE gel consisted of stacking gel and separating gel (Sambrook et. al 1989). Protein samples to be loaded on gel were denatured by adding SDS loading buffer. Mixture was boiled in water for 5 minutes and centrifuged for 5 minutes at 10000 g. Each lane of the gel was loaded with 10 μ g of protein. In one lane 5 μ l of pre-stained broad range protein marker was loaded as reference. After running the gel in SDS-PAGE buffer (constant 200 V) till the

dye in loading buffer reached the bottom of the gel, the gel was stained in Coomassie brilliant blue R-250 for 1 h, with slow shaking. Finally the gel was destained in 20 % (v/v) acetic acid overnight.

2.2.3.5. Over-production and purification of His-Cyc-At fusion proteins

E. coli M15 cells harbouring repressor plasmid pREP4 (Qiagen, Hilden, Germany) was transformed with plasmid pVTE1 (pQE31 vector carrying *vte1* alias *cyc-At* from *Arabidopsis thaliana*). As control *E. coli* M15/pREP4 cells were transformed with plasmid pQE31 (control vector). The two resulting recombinant strains were cultivated each in 2 times 400 ml LB medium in presence of ampicillin (100 mg/l) and kanamycin (25 mg/l). Cultures were induced at an optical density (measured at 600 nm) with IPTG (final concentration 1 mM) and incubated at room temperature (22 °C) for another 12 hours. Cultures were then put on ice for 1 h and harvested at 2200 g for 15 min. Cells were suspended in lysis buffer, lysozyme (30 µg/ml) was added and incubated for 15 min on ice. Cells were sonicated using ultrasonic disintegrator for 6 times for 15 secs, with intermediate cooling on ice-water for 15 sec, and at 50 % amplitude. Further purification steps were carried out as described by Qiagen (Hilden, Germany) in Qiagen Expressionist 5th Edition in Protocol 9 for preparation of clear *E.coli* lysate under native conditions. His-tag purification was carried out as described in protocol 16. The flow through fraction, washed fraction and the eluted fraction were loaded on SDS-PAGE to check the protein purity.

2.2.3.6. Overproduction and Purification of GST-Cyc-At fusion proteins

E. coli BW25113/pGEX-*vte1* was cultivated in 2 Erlenmeyer flasks (2 L) with 400 ml of LB-Amp100 medium in each flask. Cultivation was carried out at room temperature (22 °C) and induced with 1 mM IPTG at approx. OD_{600nm} of 0.6-0.7. Cultures were incubated overnight for 10-12 hours after induction. Cultures were harvested at 2200 g for 15 minutes and cell pellet was stored at -20 °C till purification was performed.

User manual from Macherey Nagel “Protino Glutathione Agarose 4B” was used for purification of GST-Cyc-At proteins. Cell lysate was prepared by suspending each gram of wet cell (stored cell pellet) in 2.5 ml PBS buffer and vortexed and placed on ice. Lysozyme was added to a final concentration of 1 mg/ml. The suspension was stirred and incubated on ice for 30 minutes before cells were lysed using ultrasonic disintegrator. Sonication was performed on ice at 50 % amplitude for 15 secs with 15 secs cooling time. This was repeated 6 times and centrifuged at 10000g for 15 minutes at 4 °C. Cell debris was discarded and supernatant was transferred to fresh cooled tube. Protein purification was performed on batch process i.e. protocol 5.3 was strictly followed.

2.2.3.7. *In-vitro* enzymatic reaction for δ -tocotrienol biosynthesis (modified based on Kumar et. al. 2005)

In-vitro enzymatic reaction for δ -tocotrienol biosynthesis was performed with enriched His-Cyc-*At* fusion proteins with purified MGGBQ (MGGBQ-cyclodextrin complex substrate) to verify the cyclase activity of *Arabidopsis thaliana* (*cyc-At* gene in pQE31-Vte1) before cloning it into plasmid pCAS47. Different concentrations of His-Cyc-*At* fusion proteins were used.

Enriched His-Cyc-*At* protein was assayed for cyclase activity in a 1000 μ l reaction volume consisting of 200 mM potassium phosphate, pH 7.3, 4 mM dithiothreitol, 75 mM ascorbic acid, and approximately 9.5 μ M formulated MGGBQ-cyclodextrin substrate. Reactions were incubated at 30 °C. 200 μ l each sample was taken after 0 h, 0.5 h, 2.0 h, 11 h & 35 h. Reaction was stopped by the addition of 200 μ l ethanol. 200 μ l of hexane was added to extract the lipophilic compounds from the reaction mixture. The reaction mixture was separated in two phases; the upper organic phase was injected to HPLC for analysis of unreacted MGGBQ and product δ -tocotrienol. Same HPLC solvent system was used for analysis which was used for extraction & analysis of MGGBQ & δ -tocotrienol from *E. coli* cultures.

Finally, a comparison of GST-Cyc-*At* and His-Cyc-*At* fusion proteins was performed to study enzyme activity during *in-vitro* enzymatic reaction. This was performed with 10 μ g of protein each.

Table 2.8: Experimental conditions used during the *in-vitro* enzymatic reaction for biosynthesis of δ -tocotrienol. Five reactions with varying His-Cyc-*At* proteins with concentration ranging from 0 - 50 μ g / ml were used.

Cyc- <i>At</i> fusion Protein	μ g	0.0	0.1	1.0	10.0	50.0
His Cyc- <i>At</i> fusion Protein	Variable					
1 mM Ascorbic acid	75 mM	75 μ l	75 μ l	75 μ l	75 μ l	75 μ l
1 mM DTT	4 mM	4 μ l	4 μ l	4 μ l	4 μ l	4 μ l
Potassium phosphate (7.3 pH)	200 mM	200 μ l	200 μ l	200 μ l	200 μ l	200 μ l
Substrate-cyclodextrin complex	Approx. 9.5 mM	100 μ l	100 μ l	100 μ l	100 μ l	100 μ l
Water (balance)	Variable	Rest	Rest	Rest	Rest	Rest
Volume	TOTAL	1000 μ l	1000 μ l	1000 μ l	1000 μ l	1000 μ l

Table 2.9: *In-vitro* enzymatic assay to compare the His- and GST- tagged Cyc-At proteins for δ -tocotrienol biosynthesis

Cyc-At fusion Protein	μg	10.0	0	10.0	0
Cyc-At fusion Protein	Variable	40 μl	0	40 μl	0
1 mM Ascorbic acid	75 mM	75 μl	75 μl	75 μl	75 μl
1 mM DTT	4 mM	4 μl	4 μl	4 μl	4 μl
Potassium phosphate (7.3 pH)	200 mM	200 μl	200 μl	200 μl	200 μl
Substrate-cyclodextrin complex	Approx. 9.5 mM	100 μl	100 μl	100 μl	100 μl
Water (balance)	Variable	Rest	Rest	Rest	Rest
Buffer		-	40 μl ⁽¹⁾	-	40 μl ⁽²⁾
Volume	TOTAL	1000 μl	1000 μl	1000 μl	1000 μl

⁽¹⁾ His-Tag elution buffer

⁽²⁾ GST-Tag elution buffer

2.2.3.8. 2-D Gel Electrophoresis

2D gel electrophoresis is a very useful and widely used method for analysis of complex protein mixtures from cell lysate. This method separate proteins in two steps, in the first dimension via Isoelectric focusing i.e. proteins are separated based on their isoelectric point. In the second dimension proteins are further separated based on their molecular weight by SDS-PAGE (O'Farrell 1975). Two 1 L Erlenmeyer flasks with each 200 ml LB Glycerol fresh medium were inoculated once with overnight pre-culture of *E. coli* CS10 and second with overnight preculture of *E. coli* BW25113 (*lacZ*⁺) (as control strain). Cultures were incubated at 30 °C at 100 RPM. Cultures were induced at OD_{600nm} of 0.8 with 0.25 mM IPTG. 8 h after induction 2 X 50 ml of each culture was harvested (4500 RPM, 10 min, 4°C) to obtain a cell pellet. One part was used for sample preparation for 2 D gel electrophoresis and another for MGGBQ analysis. For sample preparation for 2 D gel electrophoresis cell pellet was washed twice with 5 ml wash buffer (40 mM Tris), re-suspended by vortexing. Twice washed cell pellet was re-suspended in 1 ml Lysis buffer (40 mM Tris, 8 M Urea, 4 % (v/v) CHAPS, freshly prepared 65 mM DTT) and sonicated (50% amplitude, 3 cycles of 30 seconds each of sonication and 30 seconds cooling) with cooling on ice. Sample after sonication was centrifuged at 14000 RPM for 30 min at 4°C and the supernatant was transferred in pre-cooled plastic reaction cups. Protein content in crude extract samples was determined by Bradford assay.

Rehydration buffer was added to 50 µg of crude extract sample (final volume of 340 µl) and incubated at room temperature for 1 h. The rehydration buffer was prepared using 7 M Urea, 2 M Thiourea, 2 % CHAPS, 0.002 % Bromophenol Blue, freshly prepared 10 mM DTT, and 2 % (v/v) pharmalyte with pH 3-10). After 1 h of incubation time, the 340 ml crude extract sample was pipetted in one lane of the swelling tray. Place the IPG stripes (7 cm long and pH 3 – 10 range) on the sample (avoid air bubbles between sample and stripes). Cover the stripes with mineral oil. Rehydration of IPG stripes is carried out for > 10 h (usually overnight). First dimension of Iso-electric focusing (IEF) was carried out using the following gradient mode: Step 1: 500 V; 10 mA; 5 W; 0.01 h. Step 2: 3500 V; 30 mA; 25 W; 1:30 h. Step 3: 3500 V; 30 mA; 25 W; 6:20 h. The second dimension i.e. SDS-PAGE was run at 120 V, temp. of approx. 4°C, for 10-12 hours and in SDS-Equilibrium Buffer (4 % (w/v) SDS, 50 mM Tris, 6 M Urea, 30 % (v/v) Glycerol, 0.002 % Bromophenol Blue, pH 8.8 (HCl)). The SDS-gels were scanned and protein spots were evaluated and analyzed by Delta 2D decodon software.

2.2.4. Analytical methods

2.2.4.1. High Performance Liquid Chromatography

Dionex HPLC Instrument, Germany, fitted with Chromeleon Software, Gina autosampler, P580 pumps, and a detector with a UV lamp.

RP18 Lichrospher100 (5 mm particle size) analytical column (250P4.6 mm, Merck, Darmstadt, Germany) attached to a guard column containing a matrix of the same material as the column.

Solvent A: Water with 0.1 % (v/v) trifluoroacetic acid (TFA)

Solvent B: Acetonitrile 0.1 % (v/v) TFA

HPLC Program for MGGBQ (reduced and oxidized) and δ -Tocotrienol analysis:

Equilibration conditions with flowrate of 0.8 ml/min at 30 % A / 70 % B; 0 to 10 min linear gradient from 30% A / 70 % B to 10 % A / 90 % B; 10 to 40 min linear gradient from 10% A / 90 % B to 0 % A / 100 % B; 40 to 70 min isocratic conditions 0 % A / 100 % B; 70 min to 71 min linear gradient from 0 % A / 100 % B to 30 % A / 70 % B; isocratic conditions to equilibrate the column at 30 % A / 70 % B from 71 min to 78 min. The retention time for HPLC peaks for compound 1 & 2 differ during the *in-vitro* analysis (figure 3.39) and *in-vivo* analysis (figure 3.42) because of different HPLC conditions and different solvents used for dissolving the samples. The *in-vitro* samples analyzed by HPLC were dissolved in hexane and the *in-vivo* samples were dissolved in acetonitrile.

HPLC Program for HGA analysis:

The following HPLC flow gradient was used: 0 to 5 min equilibration conditions at 100% A / 0% B; 5 to 30 min linear gradient from 100% A / 0% B to 70% A / 30% B; 30 to 31 min linear

gradient from 70% A / 30% B to 0% A / 100% B; 31 to 38 min isocratic conditions 0% A / 100% B; 38 min to 39 min linear gradient from 0% A / 100% B to 100% A / 0% B; isocratic conditions to equilibrate the column at 100% A / 0% B.

2.2.4.2. Enzymatic determination (Glycerol, acetate, ammonium)

Glycerol was determined by using an enzymatic kit from Boehringer Mannheim by measuring the UV absorption of NADH oxidized during the last reaction step. Supernatant samples from bioreactor cultivations (MM-Glycerol and MM-Glycerol-Amp100) were diluted 1:100 before analysing the glycerol concentration.

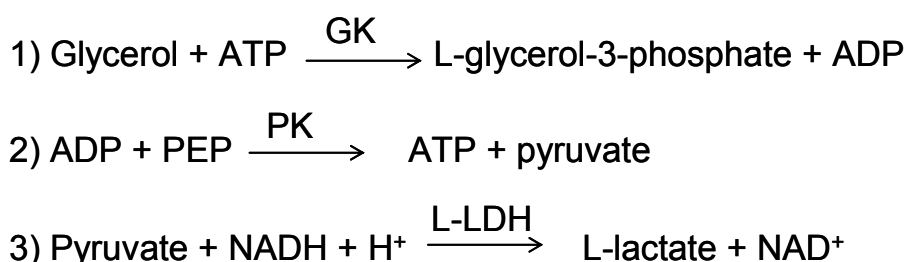


Figure 2.1: Enzymatic assay for analysis of glycerol. GK is Glycerol kinase; PK is Pyruvate kinase; L-LDH is L-lactate dehydrogenase; PEP is Phosphoenolpyruvate;

Acetic acid was determined by using an enzymatic kit from Boehringer Mannheim by UV measurement of formation of NADH released during the 3rd reaction (shown below) and is measured by increase in UV absorbance at 340 nm. Supernatant samples from bioreactor cultivation were diluted 1:20 to 1:100 in water before analysing the acetic acid concentrations.

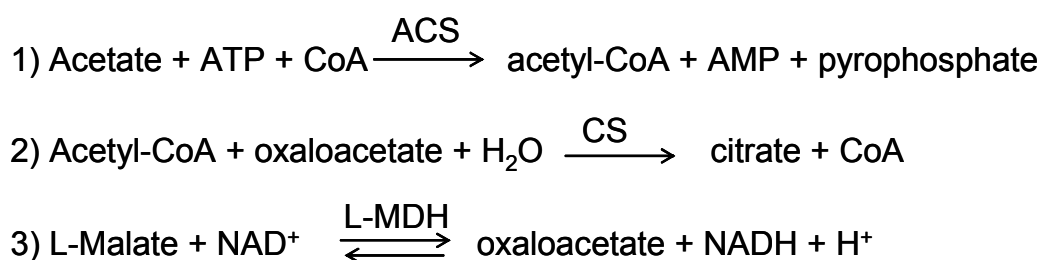


Figure 2.2: Enzymatic assay for analysis of acetic acid. ACS is acetyl-CoA synthetase; CoA is coenzyme; CS is citrate synthase; L-MDH is L-malate dehydrogenase.

Ammonium in medium was measured by using Spectroquant 1.14752.0001 kit from Merck KGaA, Darmstadt, Germany based on colorimetry of blue 2-2'-isopropyl-5.5'-methyl-indophenol. The supernatant samples from bioreactor cultivations were diluted 1:1000 to 1:5000 in water before determining the ammonium concentration in medium.

2.2.4.3. Glucose measurement

For a fast analysis of glucose concentration between 0.4 and 5 g/l was performed with blood sugar measuring kit “One touch ultra” from company Lifescan, Ortho-Clinical Diagnostics GmbH, Germany. This was useful in setting the correct glucose feeding rate during fed-batch cultivation. Glucose concentrations below 0.4 g/l were determined using an enzymatic kit, from R-Biopharm AG, Darmstadt, Germany).

2.2.4.4. Gas Chromatography-Mass Spectroscopy

Conversion of isoprenoid into corresponding alcohol was performed according to Song 2003 i.e. 0.1M Bis-Tris propane/HCl, pH 7, or 0.1M glycine/NaOH, pH 10.4. Hydrolysis was performed using alkaline phosphatase (between 0.28 and 0.56 U). Mixture incubated at 37 °C for 20 min and extracted with 0.3 ml hexane. Isoprenoid alcohol in the hexane layer was analysed by GC-MS. But this method didn't detect any isoprenoid (also when repeated with standard FPP and GGPP) (Personal communication Mr. Dipl. Ing. Tobias Vallon). This method from Song was used for extraction of FPP in yeast, *S. cerevisiae*. Hence, a new two phase extraction system was developed in order to shift the reaction equilibrium forward. Use of basic conditions (pH 9.8), 1M diethanolamine with 0.5 mM MgCl₂ as reaction buffer and alkaline phosphatase resulted in recovery of the di-phosphates of more than 90 % (Vallon et.al. 2008).

Samples for isoprenoid analysis (FPP, GGPP, and PPP) using GC-MS method were performed by Mr.Vallon, at the Institute of Biochemical Engineering, Universität Stuttgart, Stuttgart, Germany. Gas chromatography was performed on a PerkinElmer Autosystem XL (PerkinElmer, Walham, USA) with combined autosampling. The column (ZB-5 ms, 30 m×0.25 mm, df 0.25 µm, Phenomenex (Torrance, USA)) was directly connected to the mass spectrometer (TurboMass, Perkin-Elmer, Walham, USA). The GC–MS system was computer controlled (software TurboMass, Version 5.4 (PerkinElmer, Walham, USA)). The column was loaded splitless with 1 µL of the prepared sample. The flow rate of the helium carrier gas was set to 1.0 mL min⁻¹. Injector programs were 70 °C, 0.1 min; heating to 280 °C (120 °C min⁻¹); 280 °C, 15 min; and cooling to 70 °C (20 °C min⁻¹). Oven programs were 50 °C, 2.5 min; heating to 150 °C (30 °C min⁻¹); and heating to 300 °C (10 °C min⁻¹), 8 min. Retention times for farnesol - $t_d=10.3$ min, for geranylgeraniol - $t_d=15.0$ min, for internal standard (eicosane) - $t_d=13.3$ min, for geraniol— $t_d=6.85$ min, and for phytol - $t_d=14.27$. Quantification masses (m/z) —farnesol 93, eicosan (internal standard) 85, and geranylgeraniol 93.

2.2.4.5. Liquid Chromatography – Mass Spectroscopy (LC-MS)

LC-MS measurements were carried by Dr. Wolfgang Armbruster, Universität Hohenheim, Stuttgart, Germany. LC-MS was performed on an API-ES (Agilent 1100 Series, USA). Mass fragmentation spectra of the extracted samples and δ -tocotrienol standard were monitored over a mass range (m/z) of 200 to 800.

2.2.4.6. Nuclear Magnetic Resonance (NMR)

NMR measurements were performed by Dr. Jürgen Conrad, Universität Hohenheim, Stuttgart, Germany. NMR spectra for reduced MGGBQ structure were recorded in acetone- d_6 on a Varian Unity Inova 500 MHz spectrometer (Darmstadt, Germany). The ^1H and ^{13}C chemical shifts were referenced to residual solvent signals at δ_{H} 2.04 and δ_{C} 29.8 relative to TMS. ^1H , ^{13}C , ^1H , ROESY, LR-COSY, TOCSY, adiabatic broadband and band-selective gHSQC and gHMBC NMR spectra were recorded using CHEMPACK 4.0 pulse sequences.

2.2.5. Other Methods

2.2.5.1. MGGBQ extraction (Albermann et. al. 2008)

Cell pellet from 10 ml culture sample was re-suspended in 10 ml analytical grade acetone. The cell-acetone suspension was vigorously mixed on vortex for 2 minutes. After centrifugation for 15 minutes at 3000 g at room temperature the supernatant was transferred into a fresh falcon tube. Using a rotary vapour under vacuum all the acetone was removed until the falcon tube was dry. The dried rest in tube was re-suspended in 1 ml acetonitrile and vortexed for 1 minute.

2.2.5.2. MGGBQ purification

Purified and concentrated MGGBQ required for NMR analysis was isolated by adding 250 ml analytical grade acetone and 3 g of ascorbic acid in 52 g of wet cell pellet (*E. coli* CS6). After mixing and suspending the cells completely mixture was shaken for 30 minutes at room temperature. After centrifugation at 2200 g for 15 minutes at room temperature the acetone supernatant was concentrated using vacuum rotary evaporator. 4 ml of methanol was added to re-suspend the cell extract. The HPLC column was overloaded with concentrated sample extract in methanol (250 μl). Same HPLC system was used mentioned in section 2.2.4.1. This time the HPLC program used was different. Separation was carried under isocratic conditions of 100 % methanol (0.8 ml/min). HPLC peak with the highest peak area at retention time (8.5 min) was collected in a flask which already contained ascorbic acid (75 mM). This was repeated 10 times and all the eluted fractions (8.0 – 9.0 minutes) were pooled together and concentrated by vacuum rotary evaporator. Washed with 100 ml methanol

twice and concentrated using vacuum rotary evaporator. This concentrated sample was stored in -20 °C till NMR analysis.

2.2.5.3. Formulation of MGGBQ – methyl-β-cyclodextrin complex

50 µl of the above purified MGGBQ (eluted fraction from HPLC) in methanol (described above) was dried under nitrogen gas. Residue mixed in 1 ml 2.25 mM cyclodextrin which was prepared in 50 mM potassium phosphate buffer at pH 7.0 (Kumar et. al. 2005). This mixture was incubated at 40°C for 15 minutes on a shaker. Then 0.5 ml of 500 mM ascorbic acid & 50 mM potassium phosphate buffer, pH 7.0 was added. This mixture was incubated at 30 °C for 15 minutes with constant shaking. The substrate-cyclodextrin mixture was ready and aliquots of 100 µl each were stored at -20°C.

2.2.5.4. Calculation of MGGBQ coefficient

Since MGGBQ (either reduced or oxidized) standard was not commercially available, MGGBQ detection by HPLC was confirmed by characterization using LC-MS and NMR analysis. For the quantification of MGGBQ was done based on the *in-vitro* enzymatic reaction between purified MGGBQ (i.e. MGGBQ-methyl-β-cyclodextrin complex) and enriched His-tagged Cyc-At proteins (section 2.2.5.5). MGGBQ coefficient was calculated based on the stoichiometry of the *in-vitro* enzymatic reaction. 1 mole of MGGBQ resulting in 1 mole of δ-tocotrienol i.e. all the MGGBQ consumed during the reaction was converted into δ-tocotrienol. Amount of δ-tocotrienol produced during this reaction could be analyzed and quantified (based on quantification of δ-tocotrienol standard). Hence, the decrease in MGGBQ peak area (mAU*min) was related with the δ-tocotrienol produced in moles. Based on the assumption, one mole of δ-tocotrienol was produced from one mole of MGGBQ, the following correlation was obtained:

$$y = 7.8708 / x$$

Where, y = MGGBQ in µg

x = MGGBQ peak area in mAU*min (at 290 nm)

Hence, the calculated MGGBQ concentrations (i.e reduced and oxidized) in this study are approximate and should not be considered accurate. Since the same correlation was used for quantification of total MGGBQ levels produced by strains carrying multi-copy plasmids and chromosomal integrated strains the comparison between these two holds completely valid.

2.2.5.5. Calculation of coefficient to calculate oxidized MGGBQ to reduced MGGBQ

Double sample of 10 ml culture sample was harvested. First cell pellet was added with 10 ml acetone and the second with 10 ml acetone and ascorbic acid (75 mM final concentration). Both were vortexed for 2 minutes and centrifuged at 3000 g for 15 minutes at room temperature. Acetone was dried from the supernatant of both samples and re-suspended in 1 ml acetonitrile. 200 µl of the final sample in acetonitrile was analyzed by HPLC. HPLC analysis of the first sample (without ascorbic acid) resulted in reduced and oxidized peaks of MGGBQ whereas, second sample (with addition of ascorbic acid) showed only reduced MGGBQ peak with much higher peak area (in mAU*min) as compared to the first sample. Similar method was used using 2 ml, 5 ml, 20 ml and 50 ml of culture sample. Acetone volume used was always 1:1 with respect to culture volume. This experiment was performed 2 times and the average values were taken to calculate the correlation between oxidized and reduced MGGBQ. The following correlation was obtained:

$$y = x/5.064$$

Where, y = reduced MGGBQ in mAU*min (equivalent to that measured at 290 nm)

x = oxidized MGGBQ peak area in mAU*min (at 253 nm)

2.2.5.6. R_f method of calculation

The experimental determination of protein molecular mass was determined by SDS-PAGE and 2D. But to calculate the exact mass from the gel R_f (distance migrated by a each protein/total gel length) values for standard protein sizes in the protein marker were calculated. Then a graph was plotted between log(Mw) vs. R_f where Mw = molecular weight in Dalton. From this correlation sizes of each unknown protein band or spot were determined and compared with the expected sizes calculated from ExPASy proteomic server (www.expasy.org).

CHAPTER 3 – Results

To produce Vitamin E (δ -tocochromanol compounds), via the proposed Vitamin E biosynthetic pathway (shown in figure 1.2) in recombinant *E. coli* cells, several desired genes had to be cloned in an expression vector. In order to do that successfully, it was important to select a suitable expression vector, and the desired genes from a suitable donor organism(s). No synthetic genes were used for any cloning work in this study.

As, one of the main objectives of this study was, to show that δ -Tocochromanols and their pathway metabolites can be produced in recombinant *E. coli*, a multi-copy number plasmid was selected over medium or high copy number plasmid. In general, high copy number plasmids are used in over-production of recombinant proteins (Jones et. al. 2000). High copy number plasmids have a high gene dosage and lead to high expression levels. This high expression level imposes a metabolic burden and decreases the cell growth rate, also leading to a possible decrease in productivity (Friehs 2004). Protein overproduction not being the objective of this study, a multi-copy number vector pJF119EH (Fürste et. al. 1986) was selected as the cloning vector for the molecular biological work, to construct a plasmid carrying the necessary δ -tocochromanol producing genes. Second objective of this study, was to show the heterologous biosynthesis of δ -tocochromanol and its precursors using recombinant *Escherichia coli* strains. Wild type *E. coli* K12 is able to produce *p*-HPP via the shikimate pathway (Bongaerts et.al .2001). Via DXP pathway it is able to produce FPP in wild type *E. coli* K12 (Kuzuyama 2002). Additional genes to be cloned could be taken either from a single donor organism producing δ -tocotrienol compounds for e.g. *Arabidopsis thaliana* or from different sources. For heterologous biosynthesis of δ -tocochromanol in recombinant *E. coli*, heterologous genes (i.e. desired genes) from different donor organisms were chosen for molecular cloning (Albermann et. al. 2008). Details of these genes which were cloned in modified pJF119EH vector i.e. pJF119 Δ N are shown in table 3.1.

Arabidopsis thaliana and *Synechocystis* PCC6803 possess *hpd* and *crtE* genes. From the list of these genes *hpd* encoding *p*-hydroxyphenylpyruvate dioxygenase (Hpd) and *crtE* encoding geranylgeranylpyrophosphate synthase (CrtE) are not specific to Vitamin E biosynthesis. Hpd is involved in tyrosine catabolism (Bradley et. al. 1986) and CrtE is involved in carotenoid production (Misawa et. al. 1990).

Table 3.1: Details of genes encoding enzymes cloned into multi-copy vector pJF119 Δ N for δ -tocochromanol biosynthesis

Biosynthetic pathway gene	Gene/Locus /ORF	Organism	Encoded enzyme
<i>hpd</i>	<i>hpd</i>	<i>Pseudomonas putida</i> KT2440	<i>p</i> -Hydroxyphenyl-pyruvate dioxygenase
<i>crtE</i>	<i>crtE</i>	<i>Pantoea ananatis</i>	Geranylgeranyl pyrophosphate synthase
<i>ggh-Syn</i>	<i>chlP</i>	<i>Synechocystis</i> PCC6803	Geranylgeranyl reductase
<i>hpt-Syn</i>	<i>slr1736</i>	<i>Synechocystis</i> PCC6803	Homogentisate phytyl transferase
<i>cyc-At</i>	<i>At4g32770</i> alias <i>vte1</i>	<i>Arabidopsis thaliana</i>	Tocopherol cyclase
<i>cyc-Syn</i>	<i>slr1737</i>	<i>Synechocystis</i> PCC6803	Tocopherol cyclase

To start with, each single gene (*hpd*, *crtE*, *ggh-Syn*, *hpt-Syn*, *cyc-At*) was cloned into pJF119 Δ N to obtain 5 different plasmid constructs (no. 1 to 5 in table 3.2). Further, these genes were combined together in a single vector by constructing an artificial Vitamin E biosynthesis gene cluster. As a result, different plasmid constructs nr. 6 to 9 were obtained as shown in table 3.2. All the plasmids shown in table 3.2 were constructed by Dr. Christoph Albermann, Universität Stuttgart, Institute of Microbiology (Albermann et. al. 2008). These plasmids were kindly provided by Dr. C. Albermann for further experimental studies regarding protein overexpression and *in-vivo* production of δ -tocochromanols and its intermediates.

Table 3.2: List of plasmids used for biosynthesis of δ -tocochromanol

No.	Vector/ Plasmid name	Gene (Donor organism)	Gene order in respective plasmid
1	pCAS2JF	<i>hpd</i> (<i>Pseudomonas putida</i> KT2440)	Ptac <i>hpd</i>
2	pCAS30	<i>crtE</i> (<i>Pantoea ananatis</i>)	Ptac <i>crtE</i>
3	pCAS8	<i>ggh-Syn</i> (<i>Synechocystis</i> PCC6803)	Ptac → <i>ggh-Syn</i>
4	pCAS7	<i>hpt-Syn</i> (<i>Synechocystis</i> PCC6803)	Ptac → <i>hpt-Syn</i>
5	pCAS50	<i>cyc-At</i> (<i>Arabidopsis thaliana</i>)	Ptac → <i>cyc-At</i>
6	pCAS11	<i>crtE</i> (<i>Pantoea ananatis</i>) <i>ggh-Syn</i> (<i>Synechocystis</i> PCC6803)	Ptac → <i>ggh-Syn</i> → <i>crtE</i>
7	pCAS18	<i>hpd</i> (<i>Pseudomonas putida</i> KT2440) <i>crtE</i> (<i>Pantoea ananatis</i>) <i>ggh-Syn</i> (<i>Synechocystis</i> PCC6803)	Ptac → <i>ggh-Syn</i> → <i>crtE</i> → <i>hpd</i>
8	pCAS29	<i>hpd</i> (<i>Pseudomonas putida</i> KT2440) <i>crtE</i> (<i>Pantoea ananatis</i>) <i>ggh-Syn</i> (<i>Synechocystis</i> PCC6803) <i>hpt-Syn</i> (<i>Synechocystis</i> PCC6803)	Ptac → <i>ggh-Syn</i> → <i>crtE</i> → <i>hpd</i> → <i>hpt-Syn</i>
9	pCAS47	<i>hpd</i> (<i>Pseudomonas putida</i> KT2440) <i>crtE</i> (<i>Pantoea ananatis</i>) <i>ggh-Syn</i> (<i>Synechocystis</i> PCC6803) <i>hpt-Syn</i> (<i>Synechocystis</i> PCC6803) <i>cyc-At</i> (<i>Arabidopsis thaliana</i>)	Ptac → <i>ggh-Syn</i> → <i>crtE</i> → <i>hpd</i> → <i>hpt-Syn</i> → <i>cyc-At</i>

All plasmids were based on *pJF119 Δ N* vector with the resp. genes under the control of tac –promoter, IPTG inducible, and ampicillin resistance marker.

A) Microbial Synthesis of δ -Tocotrienol using *E. coli* strain possessing plasmid carrying heterologous genes

3.1. *In-vivo* biosynthesis of homogentisate in recombinant *E. coli*

3.1.1. Overexpression of *p*-hydroxyphenylpyruvate dioxygenase (Hpd) from *Pseudomonas putida* in *E. coli* DH5 α pCAS2JF

p-Hydroxyphenylpyruvate dioxygenase (Hpd) (E.C. 1.13.11.27) converts *p*-Hydroxyphenylpyruvate (*p*-HPP) via oxidative decarboxylation reaction into Homogentisic acid (HGA). It incorporates both atoms of molecular oxygen into a single substrate, one in the 2-hydroxyl and one in the carboxylate group as shown in figure 3.1. HGA is the aromatic precursor in the production of tocochromanol compounds.

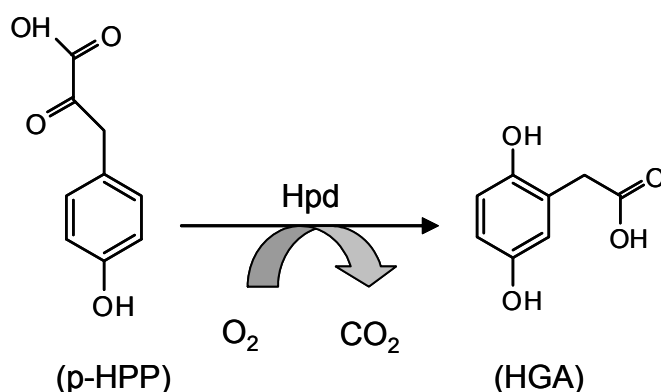


Figure 3.1: Reaction scheme showing HGA production. Hpd catalyses the conversion of *p*-HPP into HGA in presence of molecular dioxygen releasing CO₂ as by-product.

Wild type *E. coli* can produce *p*-HPP via the Shikimate pathway (see figure 1.8 in Chapter 1). Hence, the first step in order to produce HGA in recombinant *E. coli* is, to clone *hpd* gene in an expression vector and study the overexpression in *E. coli*. *Pseudomonas putida* KT2440 genome sequence was published in 2002 (Nelson et. al. 2002). *hpd* gene from *Pseudomonas putida* KT2440 had been successfully cloned and expressed in *E. coli* (Moran 2004). Hpd overexpressed from *Pseudomonas putida* was also shown to be functionally active, by producing HGA in *in-vivo* recombinant *E. coli* (Moran 2004). Plasmid pCAS2JF was obtained after cloning *hpd* from chromosomal DNA of *Pseudomonas putida* KT2440 (chapter 2, table 2.2).

To study the overexpression of Hpd in *E. coli*, *E. coli* DH5 α was transformed (chemical transformation) with plasmid pCAS2JF, and as control, it was transformed with an empty

vector pJF119 Δ N. Cultivation was carried out in shaking flask at 30°C, in Luria Broth supplemented with 100 μ g/ml of ampicillin i.e. LB - Amp100 medium. Cultures were induced with 1 mM IPTG (final conc.) at OD_{600nm} of 0.8. Samples tested on SDS-PAGE can be seen in figure 3.2. After IPTG induction, a strong additional protein band of apparent size of 38 kDa (calculated based on relative mobility (R_f) method) appeared in case of *E. coli* DH5 α / pCAS2JF sample (lane 1), which was absent in control (lane 3). No strong additional protein bands were seen in the same culture sample before IPTG induction, either in *E. coli* DH5 α /pCAS2JF (lane 2) neither in *E. coli* DH5 α /pJF119 Δ N (lane 4). Hpd protein (358 amino acid residues) from *Pseudomonas putida* KT2440 has a calculated molecular mass of 40.04 kDa (calculated using ExPASy Proteomic server). The size of the additional protein band (apparent size of 38 kDa) seen on SDS-PAGE (shown by arrow) is slightly smaller than the calculated mass of 40.04 kDa. This may be due to the fact that hydrophobic proteins tend to migrate faster than the hydrophilic proteins (Shirai et. al. 2008). Hpd being relatively hydrophobic (Rüetschi et.al 1992) migrates faster than the protein marker at 39.2 kDa. Hence, it can be concluded that the overexpressed protein in lane 1 corresponds to Hpd protein based on the molecular mass.

Table 3.3: Calculated properties of recombinant protein Hpd

Protein Name (Source)	Molecular size - M_w [kDa]	Isoelectric point - pI
Hpd (<i>Pseudomonas putida</i> KT2440)	40.04	5.07

M_w and pI values were calculated using the ExPASy proteomic server.

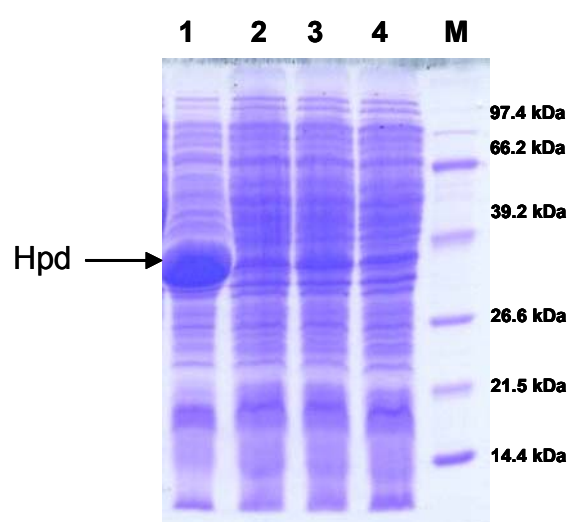


Figure 3.2: SDS-PAGE (12 %) analysis of Hpd overexpression in *E. coli* DH5 α /pCAS2JF. Shaking flask cultivation in LB-Amp100. The expected Hpd protein has molecular weight of 40.04 kDa. Strong protein band in lane 1 at approx. size of 38 kDa was seen. This band represents Hpd and is shown by arrow. Approx. 20 μ g of protein samples were loaded in each lane. The description of samples loaded in each lane are as below,

- 1 - *E. coli* DH5 α / pCAS2JF - 3 h after 1 mM IPTG
 - 2 - *E. coli* DH5 α /pCAS2JF - before IPTG
 - 3 - *E. coli* DH5 α / pJF119 Δ N - 3 h after 1 mM IPTG
 - 4 - *E. coli* DH5 α / pJF119 Δ N - before IPTG
- M - Protein Marker

3.1.2. HGA production in shaking flask (100 RPM) in *E. coli* BW25113 lacZ⁺/ pCAS2JF

After Hpd protein was overexpressed in *E. coli* DH5 α / pCAS2JF, Hpd activity was further studied. *E. coli* DH5 α / pCAS2JF was cultivated at 30 °C in shaking flask in LB medium supplemented with glycerol (2 % w/v) and 100 μ g/ml ampicillin i.e. LB-Glycerol-Amp100. As control strain *E. coli* DH5 α / pJF119 Δ N was cultivated. To check the activity of Hpd, cultures were induced with 1 mM IPTG (final conc.) at approx. OD_{600nm} of 0.8. Culture supernatant samples and cell pellets were analysed (section 2.2.4.1) for HGA production using HPLC method tested previously for HGA standard. HGA is water soluble and the experimental solubility can go up to 850 mg/ml (human metabolome database www.hmdb.ca). Culture supernatants were injected to the HPLC (HPLC method see section 2.2.4.1) for HGA analysis. Approximately 2 mM HGA was produced in *E. coli* DH5 α / pCAS2JF and no HGA was detected in the control strain *E. coli* DH5 α /pJF119 Δ N. Negligible amount of HGA (< 0.01 mM) was found in cell pellet of *E. coli* DH5 α / pCAS2JF and not detected in control (Albermann et. al. 2008). After induction, the *E. coli* DH5 α / pCAS2JF strain produced HGA as the major product in supernatant. After confirming that, *E. coli* DH5 α /pCAS2JF was able to produce HGA in shaking flask LB-Glycerol-Amp100, further cultivation was done in the production strain *E. coli* BW25113 lacZ⁺ as host strain. In the later stage, chromosomal integration of each individual gene was planned to be carried out in *E. coli* BW25113 lacZ⁺ strain. These chromosomal integrated strains (plasmid-free) would then be used as production strains. In order to compare the results of chromosomal integrated strain with strain carrying plasmid (plasmid-encoded), same host strain was essential. Hence, here for HGA production the host strain was changed from *E. coli* DH5 α to *E. coli* BW25113 lacZ⁺.

E. coli BW25113 lacZ⁺ / pCAS2JF and *E. coli* BW25113 lacZ⁺/ pJF119 Δ N were cultivated in shaking flask in minimal medium (section 2.1.3) with glucose or glycerol (5 g/l each) as sole carbon and energy source and 100 μ g/ml ampicillin. HPLC chromatogram for HGA analysis can be seen in figure 3.3, and the cultivation results of this experiment are shown in figure 3.4.

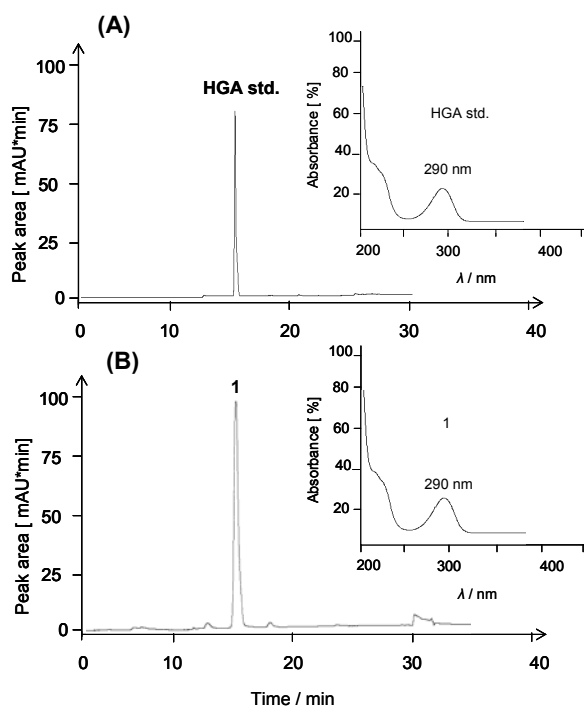


Figure 3.3: HPLC chromatogram showing HGA standard and HGA produced from *E. coli* BW25113/pCAS2JF.

(A) HGA standard. Single peak at retention time of 15.6 min with a UV spectrum (shown in inset) with an absorbance maximum at 290 nm.

(B) Supernatant sample from cultivation of *E. coli* BW25113 / pCAS2JF in MM with 27.8 mM glucose as carbon source. Major peak at 15.6 min (denoted by 1) was detected. This peak has a UV spectrum (shown in inset) with an absorbance maximum at 290 nm. Peak 1 was confirmed as HGA based on the identical retention time and maximum UV absorbance, at 290 nm.

Since the main aim in this sub-chapter was to produce high level of HGA and not to over-produce Hpd proteins, *E. coli* BW25113/pCAS2JF cultures were induced with 0.25 mM IPTG at OD_{600nm} between 0.7 and 0.8. HGA standard was analysed by HPLC which resulted in a major peak at retention time of 15.6 minutes seen in figure 3.3 A. This peak has a maximum UV absorption at 290 nm shown in the insets of the chromatogram. Analysis of supernatant samples from *E. coli* BW25113 / pCAS2JF in glucose and in glycerol resulted in a major peak at retention time of 15.6 min with a maximum UV absorption of 290 nm (seen in Fig. 3.3B). This was identical with the retention time and maximum UV absorption of the standard HGA. No HGA was detected in the control strain *E. coli* BW25113 / pJF119 Δ N. Cell growth, glucose and glycerol concentrations can be seen in figure 3.4 A and 3.4 B.

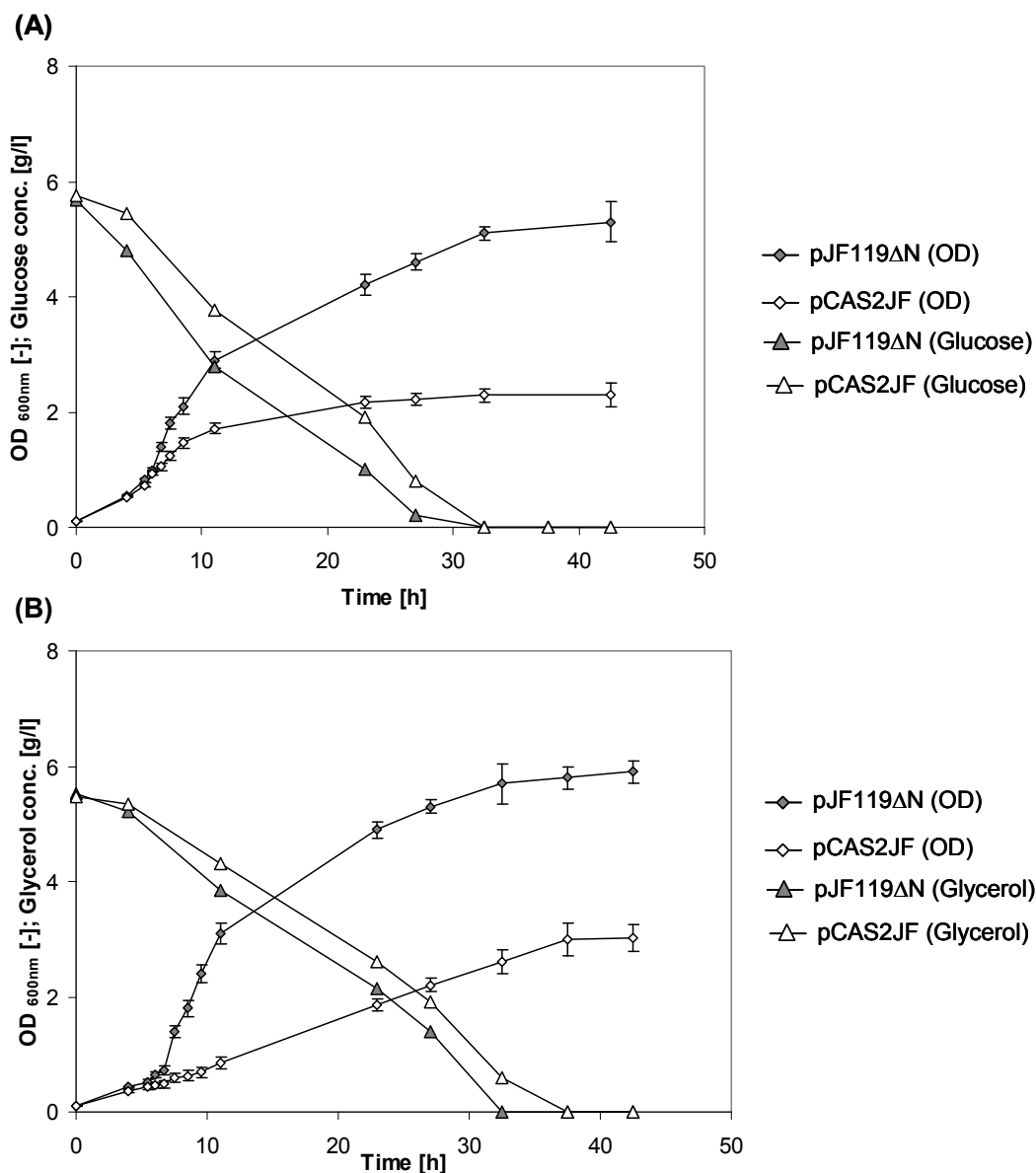


Figure 3.4: Cell growth curve and glucose/glycerol concentration in HGA production experiments. *E. coli* BW25113 strain was used as host strain carrying pJF119ΔN (control) or pCAS2JF. Cultivations were carried out at 30 °C in shaking flask in minimal medium with different carbon sources. Cultures were induced with 0.25 mM IPTG (final conc.) at OD_{600nm} of 0.8. (A) Shows cell density i.e. OD_{600nm} and glucose conc. (as carbon, energy source) as function of time. (B) Shows cell density i.e. OD_{600nm} and glycerol conc. (as carbon, energy source) as function of time.

Growth of *E. coli* BW25113 / pCAS2JF in MM-Glucose slowed after 11 h and ceased completely after 23 h (i.e. 19 h after induction). While growth in MM-Glycerol slowed down between 32 and 37 h and ceased completely after 37 h (i.e. 25 h after induction). In the control strain *E. coli* BW25113 / pJF119ΔN, cell growth continued after induction to reach OD_{600nm} of 4.2 and OD_{600nm} of 5.6, in glucose and glycerol respectively (Figure 3.4). HGA production in *E. coli* BW25113 / pCAS2JF in glucose started earlier (7 - 11 h) compared to that in glycerol (11-23 h). Approx. 80 % of the HGA was produced between 23-32 h HGA in

both cultivations. HGA levels decreased (after 32.5 h), probably due to oxidation of HGA as a result of prolonged incubation time. No *p*-HPP was detected in any of the supernatant samples in *E. coli* BW25113 / pCAS2JF in. On the other side, neither HGA, nor *p*-HPP was detected in the supernatant samples of the control strain, *E. coli* BW25113 / pJF119ΔN in glucose or in glycerol.

HGA can get easily oxidized and further polymerized to form brown ochronotic pigment (Gunsior *et.al.* 2004). Hence it was not possible to conclude the maximum HGA concentration which *E. coli* BW25113/pCAS2JF could produce in MM-Glucose and in MM-Glycerol. No HGA peak was detected in the control strain *E. coli* BW25113 / pJF119ΔN neither in MM-Glucose nor in MM-Glycerol. Finally, it can be concluded that HGA was produced using glucose or glycerol as sole carbon and energy sources, by using a low-copy number plasmid pCAS2JF in recombinant *E. coli* BW25113. Cell growth in HGA producing strains i.e. *E. coli* BW25113 / pCAS2JF (in MM-Glucose and MM-Glycerol) was impaired, when compared to the control strain. It could not be confirmed, whether the reason for the low OD_{600nm} in *E. coli* BW25113/pCAS2JF cultures was due to the toxicity of HGA, or the toxicity of oxidation product of HGA or the overexpressed Hpd proteins itself.

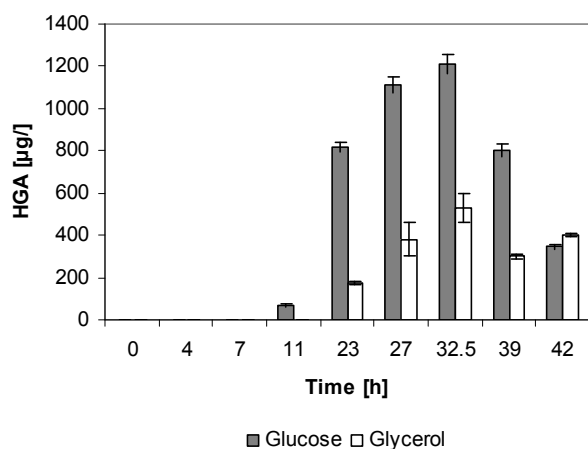


Figure 3.5A: HGA production in *E. coli* BW25113/pCAS2JF strain, in shaking flask in minimal medium with glucose (filled bars) and in minimal medium with glycerol (empty bars). No HGA was detected in the control strain *E. coli* BW25113/pJF119ΔN neither in glucose nor in glycerol as carbon source, and hence not shown in the figure.

E. coli BW25113 / pCAS2JF cultures started turning brown after 27h and 33 h respectively in Glucose and Glycerol containing medium. After centrifugation of culture samples (1 ml, 13000 RPM, 5 minutes), it was confirmed that the culture supernatant was brown in colour and cell pellet remained white/pale. Due to the brown colour of the culture supernatant, the cultures looked brown. Figure 3.5B shows the difference in supernatant colour in *E. coli* BW25113 / pCAS2JF and its control *E. coli* BW25113 / pJF119ΔN in MM-Glucose. *E. coli* BW25113 / pCAS2JF culture supernatant (in MM-Glucose and MM-Glycerol) turned dark brown after 42 h. On the other side, the respective control strains i.e. *E. coli* BW25113 /

pJF119 Δ N and *E. coli* BW25113 lacZ⁺ cultures didn't turn brown during the entire cultivation time of 42 h.

Brown colour is assumed to be due to the oxidation of HGA (accumulated in the medium) to benzoquinonacetate and further polymerisation to form ochronotic pigment which is brown coloured.

Since no direct correlation between the brown pigment and HGA was available or could be established, it was difficult to calculate the highest concentration of HGA produced in each recombinant *E. coli* strain used in this study. *E. coli* BW25113 / pCAS2JF cultures in MM-Glucose resulted in 1213 \pm 30 μ g/l is one of the highest quantifiable HGA concentration reported so far in literature. Possibly, even higher HGA levels could have been reached during cultivations, if HGA oxidation was avoided.

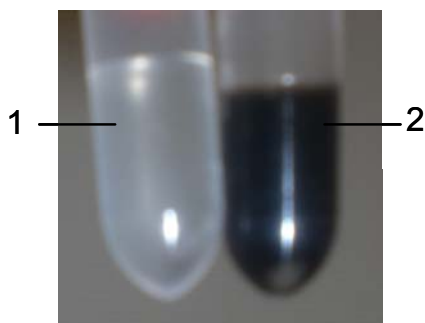


Figure 3.5B: Colour of culture supernatant after 39 h of cultivation. (1) *E. coli* BW25113/pJF119 Δ N supernatant after 42 h. (2) *E. coli* BW25113/pCAS2JF supernatant after 42 h. HGA oxidises and further polymerises to form brown ochronotic pigments (Gunsior et.al.2004). Similarly, HGA released in medium during HGA production in *E. coli* BW25113/pCAS2JF strain after prolonged cultivation (42 h, in shaking flasks at 30 °C in MM-Glucose medium) also probably oxidises and polymerises. This can be seen in right hand side of the figure marked by 2. The control strain where no HGA is detected, the colour of the culture supernatant stayed colourless, which is marked by 1.

3.2. *In-vivo* biosynthesis of Geranylgeranyl Pyrophosphate (GGPP) in recombinant *E. coli*

3.2.1. Overexpression of geranylgeranylpyrophosphate synthase (*crtE*) from *Pantoea ananatis* in *E. coli* DH5 α / pCAS30

The second step in the δ -Tocochromanol biosynthesis pathway, is to produce the isoprenoid precursor i.e. GGPP as prenyl donor for producing MGGBQ and/or MPBQ, the central precursor for all forms of tocotrienol and tocopherol compounds respectively. Wild type *E. coli* can produce FPP and IPP via DXP pathway, but not GGPP. *E. coli* can produce long chain polyprenyl diphosphates via sequential condensation reactions between IPP and FPP catalyzed by polyprenyl diphosphates (IspB and IspU) (Baba et. al. 1985). To produce high amounts of GGPP a gene encoding geranylgeranyl pyrophosphate synthase was cloned from *Pantoea ananatis* which could catalyze the reaction shown in Figure 3.6.

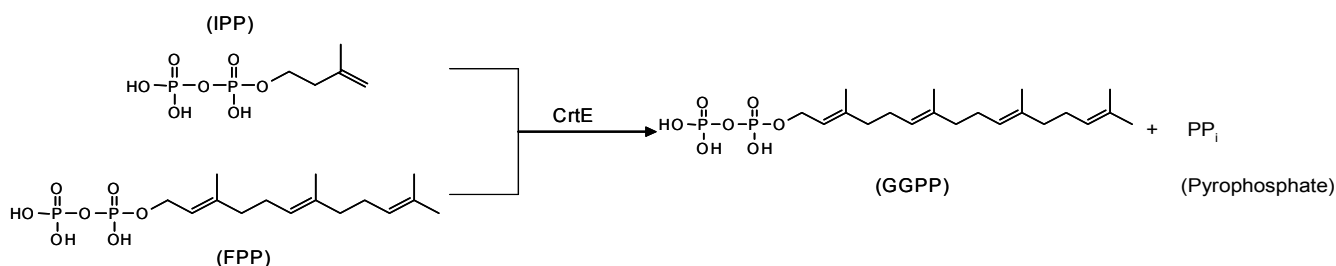


Figure 3.6: Scheme showing formation of GGPP. CrtE catalyzes the head to tail condensation reaction between carbon-15 (FPP) and carbon-5 (IPP) molecules. PP_i is the pyrophosphate released during formation of GGPP.

The plasmid obtained after cloning *crtE* in pJF119 Δ N was pCAS30 (chapter 2, table 2.2). Overexpression of CrtE in *E. coli* DH5 α / pCAS30 was tested on SDS-PAGE and can be seen in figure 3.7. As control *E. coli* DH5 α /pJF119 Δ N was used. CrtE protein has a calculated mass of 32.5 kDa (table 3.4). A strong protein band at approx. 31.8 kDa (R_f method) was observed in *E. coli* DH5 α / pCAS30 sample (3 h after induction in lane 4) which was absent in the control (lane 3). The molecular size of overexpressed protein (lane 4) is slightly smaller than the calculated mass. It was concluded, that the apparent size of the overexpressed protein in lane 4, is in accordance to the calculated mass of CrtE protein. No additional band at approx. 32 kDa was observed in *E. coli* DH5 α /pJF119 Δ N and *E. coli* DH5 α /pCAS30 before IPTG induction (lane 1 and 2 respectively).

Table 3.4: Calculated properties of recombinant protein

Protein Name (Source)	Molecular size - M_w [kDa]	Isoelectric point - pI
CrtE (<i>Pantoea ananatis</i>)	32.5	6.04

M_w and pI values were calculated using the ExPASy proteomic server.

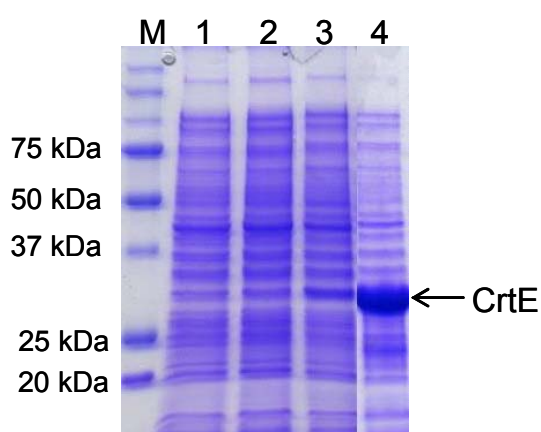


Figure 3.7: SDS-PAGE showing overexpression of CrtE protein. *E. coli* DH5 α /pCAS30 and *E. coli* DH5 α /pJF119 Δ N were cultivated in LB-Amp100 medium in shaking flask at 37 °C. Cultures induced at approx. OD_{600nm} of 0.8 with 0.25 mM IPTG
M: Protein marker
Lane 1: *E. coli* DH5 α / pJF119 Δ N (before IPTG)
Lane 2: *E. coli* DH5 α / pCAS30 (before IPTG)
Lane 3: *E. coli* DH5 α / pJF119 Δ N (3 h after IPTG)
Lane 4: *E. coli* DH5 α / pCAS30 (3 h after IPTG)
Strong protein band in lane 4 corresponded to the calculated size of CrtE protein.

3.2.2. GGPP production in bioreactor in *E. coli* LJ110 / pCAS30

Before studying the FPP and GGPP production levels in *E. coli* LJ110 / pCAS30 (in bioreactor in minimal medium 2 with glucose as sole carbon source), it was important to verify the activity of the overexpressed recombinant CrtE protein i.e. its ability to catalyse the condensation addition reaction of C₁₅ (FPP) and C₅ (IPP) isoprenoid units into a C₂₀ compound (GGPP). CrtE enzyme activity was tested *in-vivo* during cultivation of recombinant strain i.e. *E. coli* DH5 α /pCAS30 in shaking flask cultivation (as per section 2.2.1.1). As control, *E. coli* DH5 α /pJF119 Δ N was cultivated. The amount of GGPP produced can be seen in figure 3.8. Cell growth in *E. coli* DH5 α /pCAS30 was affected after induction, when compared to the control strain. As a result, *E. coli* DH5 α /pCAS30 reached lower cell density as compared to that achieved in *E. coli* DH5 α /pJF119 Δ N (OD_{600nm} of 4.02 and 6.20 respectively). Cells were extracted and isoprenoid analysis (GC-MS) was performed by Mr. Tobias Vallon and Dr. Karin Lemuth (Universität Stuttgart, Institute of Biochemical Engineering) as described in 2.2.4.6. A small amount of GGPP (7 ± 5 nM) was detected in *E. coli* DH5 α / pCAS30 before induction. Constant increase in GGPP production was observed between 9 h, 16 h and 28 h samples, with the cultures reaching a maximum of 188 ± 14 nM (i.e. 84.4 µg/l) of GGPP after 52 h. No GGPP was detected in any of *E. coli*

DH5 α /pJF119 Δ N samples. To the contrary, no quantifiable GGPP was detected during GC-MS as described as Vallon et. al. 2008 in wild type *E. coli* LJ110. During the same GC-MS analysis of the above samples *E. coli* DH5 α /pJF119 Δ N strain produced 32 ± 4 nM (12.2 μ g/l) of FPP during 52 h. No FPP was detected in *E. coli* DH5 α /pCAS30 culture samples. These results for FPP and GGPP production may indicate that the produced FPP was successfully converted by the CrtE overexpressed in *E. coli* DH5 α /pCAS30. Hence it could be concluded that the 188 ± 14 nM of GGPP produced in *E. coli* DH5 α /pCAS30, compared to the *E. coli* DH5 α /pJF119 Δ N (control strain) was due to the active CrtE overexpressed, which was not the case in *E. coli* DH5 α /pJF119 Δ N.

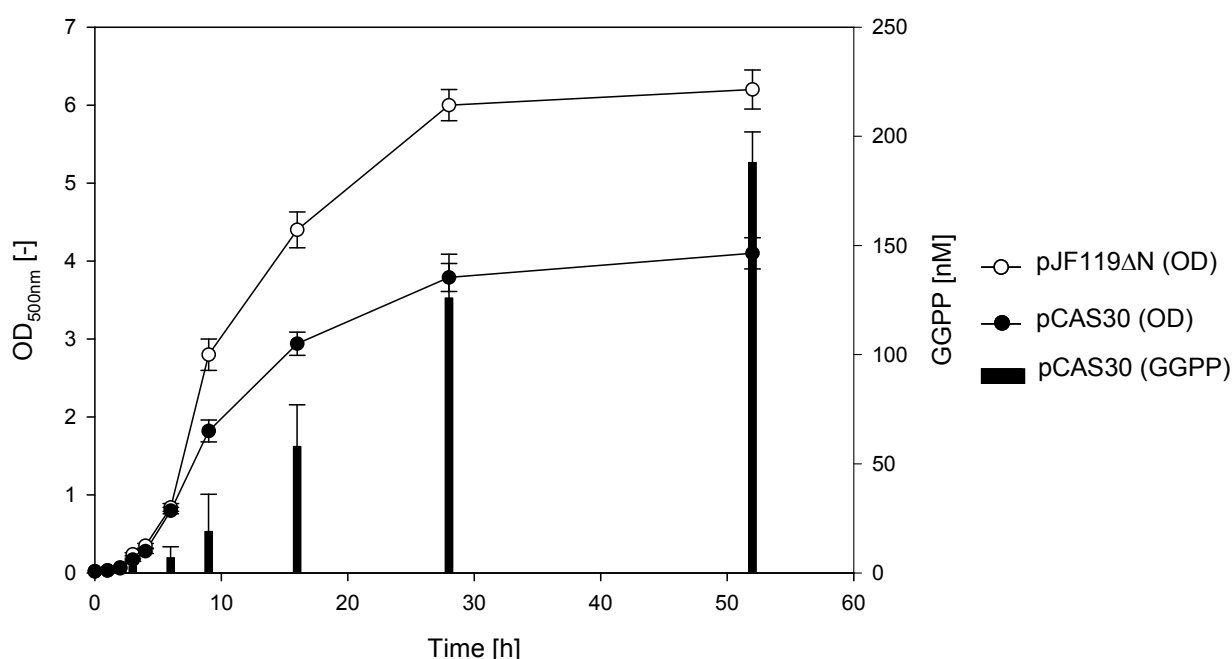


Figure 3.8: GGPP production in shaking flask. *E. coli* DH5 α /pCAS30 and its control *E. coli* DH5 α /pJF119 Δ N were cultivated in shaking flask at 30 °C in LB-Glycerol-Amp100 medium. Cultures were induced at approx. OD_{500nm} of 0.8 with 1 mM IPTG (final conc.). Cell density on left hand Y-axis (OD_{500nm}) w.r.t. time (h) shown as line chart. GGPP production in *E. coli* DH5 α /pCAS30 (in nM) is represented on Y-axis on the right hand side (shown as bar chart). No GGPP was detected in *E. coli* DH5 α /pJF119 Δ N and hence cannot be seen in this figure. The standard deviation is based on the data from two independent experiments.

After it was confirmed that CrtE expressed in *E. coli* DH5 α /pCAS30 was able to produce GGPP, transformation of *E. coli* LJ110 cells with plasmid pCAS30 was performed to obtain *E. coli* LJ110/pCAS30 strain. Here, *E. coli* LJ110 was used as host strain for GGPP production in bioreactor cultivation using glucose as sole carbon and energy source. The reason for this has been described in section 2.2.1.1.

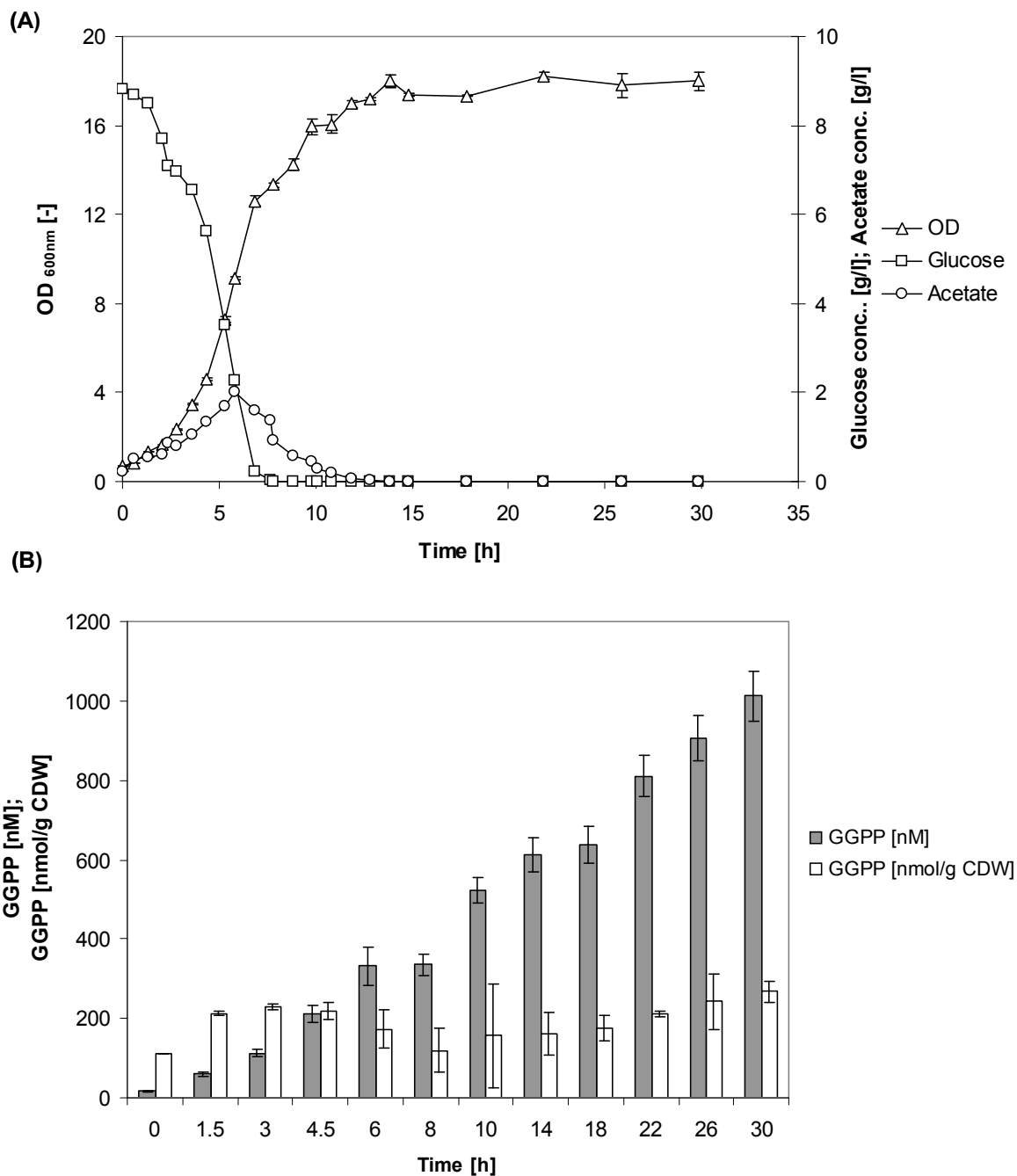


Figure 3.9: Cell growth and GGPP production in *E. coli* LJ110 / pCAS30 in bioreactor. Results have been partly published in Vallon et. al. 2008. Cultivation was carried out in 3.7 L bioreactor KLF2000 (Bioengineering AG, Switzerland) with a working volume of 1.8 L (minimal/mineral medium with 8 g/l glucose as carbon source and 100 μ g/l ampicillin). Cultivation was in batch mode, at 37 °C, at pH of 7.0, with dissolved oxygen concentration > 50 % saturation. Cultures were induced with 0.1 mM IPTG (final concentration) at 5.83 h. Standard deviation was calculated based on two independent samples (i.e. cell pellet used for extraction of isoprenoid compounds)

(A) Cell density represented as OD_{600nm}

(B) GGPP produced shown in bar charts.

E. coli LJ110/pCAS30 strain was cultivated in bioreactor in a minimal medium-2 (section 2.1.3) with glucose as sole carbon and energy source (cultivation conditions in section 2.2.1.2.b). As mentioned in section 3.1.1 it was planned to use *E. coli* LJ110 strain for production in bioreactor and *E. coli* BW25113 strain for recombination experiments.

Batch cultivation of *E. coli* LJ110/pCAS30 strain in minimal medium with glucose as sole carbon source was carried out to study the GGPP production. Cultivation was carried out by Tobias Vallon and Dr. Karin Lemuth (Universität Stuttgart, Institute of Biochemical Engineering) and isoprenoid analysis by Mr. Tobias Vallon. These results have been partly published in Vallon et. al. 2008. Cultures were induced with 0.1 mM IPTG at 5.83 h. Growth rate calculated during exponential phase reached a maximum of 0.53 h^{-1} (3.83 h), which constantly dropped down till 13.83 h at $\text{OD}_{600\text{nm}}$ of 18.0 (i.e. start of stationary phase). Starting glucose concentration of 8.8 g/l in the minimal medium-2 was consumed in 7.83 h. During this period 2 g/l of acetic acid was formed. Between 7.83 h and 14.83 h the accumulated acetic acid presumably was utilized as carbon source for growth.

Isoprenoid analyzed by GC-MS method detected $17 \pm 1 \text{ nM}$ of intracellular GGPP at 0 h (see figure 3.9), which suggested that the pre-culture had produced GGPP, without induction. GGPP levels doubled from $111 \pm 1 \text{ nmol}$ of GGPP per gram cell dry weight i.e. $\text{nmol} / \text{g CDW}$ to $229 \pm 8 \text{ nmol/g CDW}$ in the first 3 hours of cultivation. During the exponential growth phase (3 h to 8 h), the GGPP level in terms of almost nanomolar i.e. nM, tripled ($112 \pm 8 \text{ nM}$ to $335 \pm 48 \text{ nM}$).

FPP was not detected before induction with IPTG (i.e. before 5.83 h). No FPP was detected in any of the samples during GC-MS analysis after 10 h, but GGPP levels tripled between 8 h and 30 h from, $335 \pm 48 \text{ nM}$ to $1012 \pm 62 \text{ nM}$, with GGPP yield increased more than twice from $120 \pm 16 \text{ nmol/g CDW}$ to $268 \pm 7 \text{ nmol/g CDW}$. This may suggest that after induction whatever FPP was produced, was converted into GGPP as a result of overexpressed CrtE proteins.

Table 3.5: Calculated properties of *Ggh-Syn* recombinant proteins

Protein Name (Source)	Molecular size - M_w [kDa]	Isoelectric point - pI
Ggh-Syn (<i>Synechocystis</i> PCC6803)	44.80	8.08

M_w and pI values were calculated using the ExPASy proteomic server

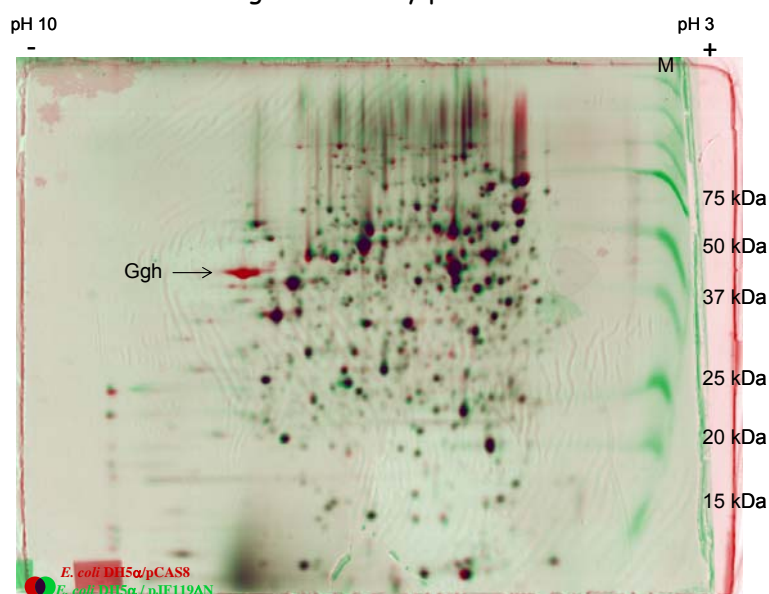


Figure 3.11: 2D-Gel Electrophoresis for the overexpression of *Ggh-Syn*. *E. coli* DH5 α / pCAS8 was cultivated in LB medium at 37°C in shaking flask. As control *E. coli* DH5 α / pJF119 Δ N was cultivated under same conditions. Cultures were induced with 1 mM IPTG at approx. OD_{600nm} of 0.8. Sample taken 6 h after induction were treated according to section 2.2.3.8 to obtain two SDS gels which were overlapped using Delta 2D software. Green colour spots represent the control i.e. *E. coli* DH5 α / pJF119 Δ N and red colour spots represents *E. coli* DH5 α / pCAS8. An additional red spot in *E. coli* DH5 α / pCAS8 was seen at approx. 42.3 kDa and pI value of 8.0 (shown by an arrow) This additional spot closely corresponded to the predicted mass and pI value of *Ggh* protein from *Synechocystis* PCC6803 is shown in table 3.5.

When the two 2D-gels (*E. coli* DH5 α / pCAS8 and *E. coli* DH5 α / pJF119 Δ N) were superimposed (using Delta 2D software), most of the expressed proteins (i.e. seen here as spots) on one gel overlapped the corresponding spots from another gel, except for one strong spot seen in red colour (shown by an arrow). This meant that the additional spot most likely represented the overexpressed protein in *E. coli* DH5 α / pCAS8 sample which was absent in *E. coli* DH5 α / pJF119 Δ N. The calculated molecular mass of *Ggh* protein is 44.8 kDa and an isoelectric point (pI) of 8.08 (using ExPASy program). The approx. molecular size and pI value of the red spot was calculated based on the R_f (distance migrated divided by total gel length) method (see details in section 2.2.5.8). Based on R_f calculation the molecular size of overexpressed protein was 42.3 kDa and pI of 8.0, which closely corresponds to that of the predicted properties of *Ggh-Syn* protein (less than 5 % of the

standard deviation to the expected values). From the intensity of the apparent Ggh-Syn protein spot, it can be qualitatively concluded that moderate level of Ggh-Syn protein overexpression was achieved.

3.3.2. Shaking flask cultivation of *E. coli* DH5 α / pCAS11 and Phytyl pyrophosphate (PPP) analysis using GC-MS

Plasmid pCAS11 was provided by Dr. Albermann, which consisted of *crtE* and *ggh-Syn* genes from *P. ananatis* and *Synechocystis PCC6803*, respectively, in pJF119 Δ N. Expression of CrtE and Ggh-Syn proteins in *E. coli* DH5 α / pCAS11 was tested on 2D gel electrophoresis before using this plasmid for PPP production. As control *E. coli* DH5 α /pCAS8 and *E. coli* DH5 α /pJF119 Δ N strains were cultivated at same conditions. The calculated molecular mass and pI value for CrtE and Ggh-Syn proteins are shown in table 3.6.

When two gels (i.e. *E. coli* DH5 α /pCAS11 and *E. coli* DH5 α /pCAS8) were over-lapped (using 2D Delta software) an extra strong protein spot was seen in red color (pCAS11) (shown by arrow in Figure 3.12) at approx. 32 kDa and pI of 6.0 (calculated based on R_f method). This size closely corresponded to the estimated Molecular mass (M_w) and pI of CrtE protein shown in table 3.6. At approx. M_w of 42 kDa and pI of approx. 8.0 (both calculated based on R_f method), a dark black spot (i.e. when green and red spot overlap each other) was seen. This closely corresponded to the estimated M_w and pI of Ggh-Syn shown in table 3.6. This meant that, Ggh-Syn and CrtE were overexpressed in *E. coli* DH5 α /pCAS11 and Ggh-Syn was overexpressed in *E. coli* DH5 α /pCAS8. Additionally, 3 strong protein spots (marked with circles) at approximately the same molecular size that of CrtE protein were observed. These spots could not be identified. 2D gel for *E. coli* DH5 α /pCAS11 was overlapped with the 2 D gel for *E. coli* DH5 α /pJF119 Δ N (another control), and has already been shown in Figure 3.11.

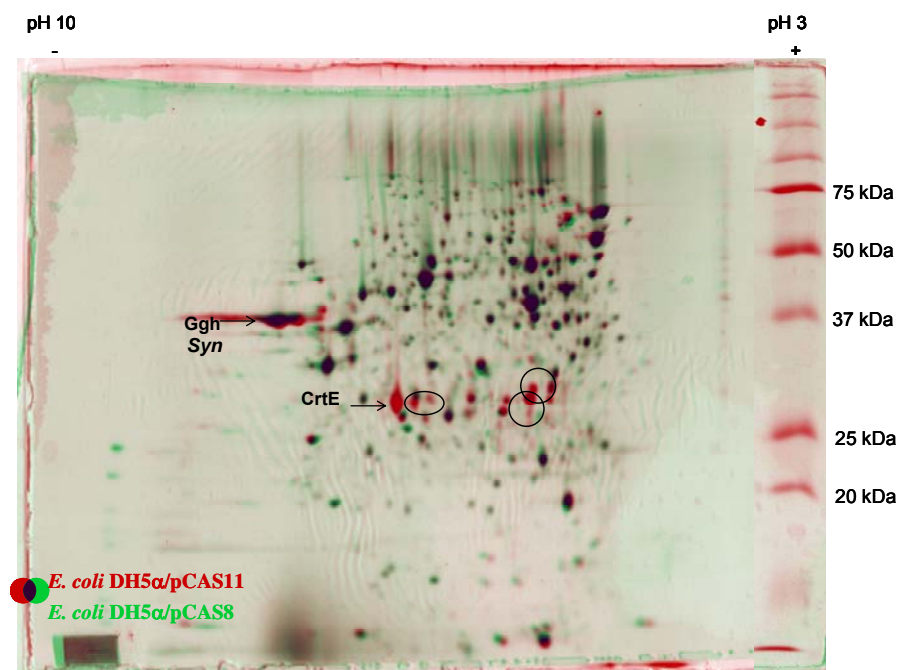


Figure 3.12: 2 D Gel electrophoresis showing expression of CrtE and Ggh-Syn in *E. coli* DH5 α /pCAS11. *E. coli* DH5 α / pCAS11 and its control, *E. coli* DH5 α / pCAS8, were cultivated in shaking flask in LB-Amp100 medium at 30 °C. Cultures were induced with 1 mM IPTG (final conc.) at OD_{600nm} of 0.8. Shown are 2 gels representing the 2 cultures (each, 6 h sample after induction) overlapped using Delta 2D software. *E. coli* DH5 α /pCAS8 is shown in green, and *E. coli* DH5 α /pCAS11 is shown in red. Ggh-Syn is expressed in both constructs, shown by arrow at approx. 42 kDa. 4 strong additional red spots were seen in *E. coli* DH5 α /pCAS11. One red spot at approx. 32 kDa was identified as CrtE protein (marked by arrow). But the other 3 red spots shown with circles could not be identified.

Table 3.6: Calculated properties of recombinant proteins

Protein Name (Source)	Molecular size - M _w [kDa]	Isoelectric point - pI
CrtE (<i>Pantoea ananatis</i>)	32.58	6.04
Ggh-Syn (<i>Synechocystis</i> PCC6803)	44.80	8.08

M_w and pI values were calculated using the ExpASY proteomic server

E. coli DH5 α is able to produce the precursors for GGPP (i.e. FPP and IPP) production. Production of PPP in *E. coli* DH5 α / pCAS11 should be possible when the expressed CrtE and Ggh-Syn (in plasmid pCAS11) are active. CrtE overexpression in recombinant *E. coli* DH5 α / pCAS30 had produced GGPP (section 3.1.2). Hence, it was important to test whether the overexpressed Ggh-Syn protein (in pCAS11) is able to catalyze the 3 step reduction of GGPP to PPP. This was tested via *in-vivo* cultivation experiment of *E. coli* DH5 α / pCAS11 in shaking flask in LB-Glycerol-Amp100. As control, *E. coli* DH5 α / pCAS30

was cultivated under same conditions. Both cultures were induced with 1 mM IPTG (final conc.) at OD_{600nm} of 0.8. Samples taken (cell pellet obtained after centrifugation) were extracted for isoprenoid and quantified using the GC-MS method (section 2.2.4.6. & 3.2.2). This analysis was performed by Tobias Vallon and Dr. Karin Lemuth (Universität Stuttgart, IBVT). GC-MS results detected no PPP in any of *E. coli* DH5 α /pCAS11 samples, nor in any of the control *E. coli* DH5 α /pCAS30 samples. The GC-MS method used here was previously tested for analysis of PPP (hydrolysis of phytol standard). Instead of PPP, the GC-MS analysis detected GGPP in both cultures i.e. *E. coli* DH5 α /pCAS11 and *E. coli* DH5 α /pCAS30 (Albermann et. al. 2008). Hence, it was concluded that, even though the Ggh-Syn was present, the *in-vivo* enzyme activity of Ggh-Syn expressed in *E. coli* DH5 α /pCAS11 was not sufficient to carry out the 3 step reduction reaction of GGPP into PPP. It could not be confirmed from literature whether there are other enzymatic reactions of PPP in *E. coli* K-12 strains. Keller et. al 1998, had successfully shown overexpression of recombinant Ggh from *Arabidopsis thaliana* (Ggh-At) in *E. coli* JM109 strain. The activity of expressed Ggh-At was successfully shown in an *in-vitro* assay using radioactive GGPP and enzyme homogenate (Ggh-At). Stability of PPP in *E. coli* K-12 could not be confirmed from the available literature. More details regarding the possible reasons for the lack of PPP production in recombinant *E. coli* K-12 are discussed in section 4.3.5

3.4. *In-vivo* biosynthesis of δ -Tocochromanol precursors (MGGBQ and / or MPBQ) in recombinant *E. coli*

3.4.1. Overexpression of Homogentisate Phytyl transferase (*hpt*) from *Synechocystis PCC6803* in *E. coli* DH5 α /pCAS7

Hpt from *Synechocystis sp. PCC6803* (Hpt-Syn) can catalyze the production of δ -tocochromanol precursors (MGGBQ and/or MPBQ) by decarboxylation and prenylation of HGA (derived from shikimate pathway) (Collakova et.al. 2001). HGA being the common substrate, the second precursor could either be GGPP and / or PPP. In case of the second substrate being GGPP, MGGBQ is produced and in case if it's PPP, MPBQ is produced (DellaPenna et.al 2006). Hpt-Syn from *Synechocystis PCC6803* can take GGPP as well as PPP as substrates, with strong preference towards PPP over GGPP (Collakova et. al. 2001).

slr1736 gene, alias *hpt-Syn* from *Synechocystis PCC6803* was cloned in pJF119 Δ N to obtain plasmid pCAS7 (refer to chapter 2, table 2.2). Plasmid pCAS7 was obtained from Dr. Albermann. Overexpression of Hpt-Syn in *E. coli* DH5 α /pCAS7 was studied on SDS-PAGE. As control *E. coli* DH5 α / pJF119 Δ N was cultivated under similar conditions (section 2.2.3.1). SDS-PAGE results can be seen in figure 3.14). An additional strongly stained protein band was seen in lane 4 (*E. coli* DH5 α / pCAS7, 4 h after induction, shown by an arrow) compared

to its control strain in lane 3 (*E. coli* DH5 α / pJF119 Δ N, 4 h after induction). A strong protein band was also seen in *E. coli* DH5 α /pCAS7 before IPTG induction (lane 2).

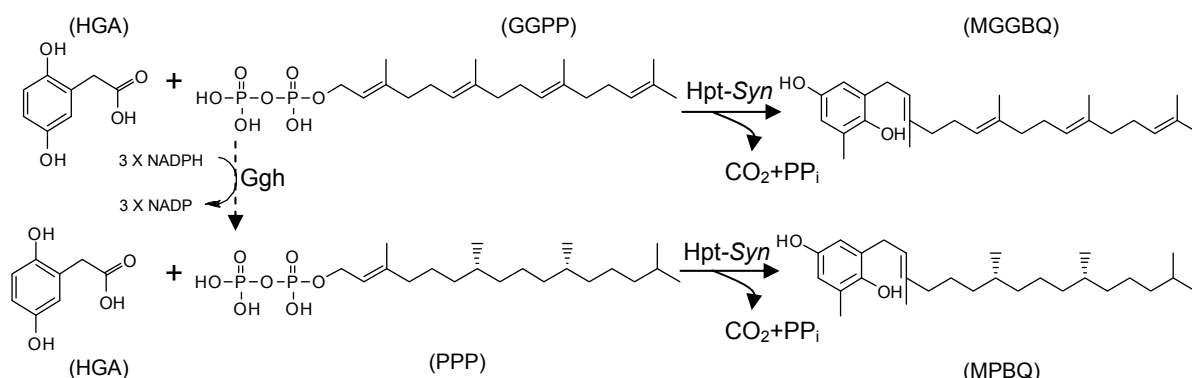


Figure 3.13: Scheme showing the prenylation of HGA with GGPP and/or PPP to produce MGGBQ and/or MPBQ respectively. Both reactions are catalysed by Hpt-Syn (*Synechocystis* PCC6803) releasing carbon dioxide (CO₂) and pyrophosphates (PP_i) as by-products.

The apparent molecular mass of the additional band in lane 4, calculated based on R_f method showed a 33.1 kDa protein in size which closely corresponded to the calculated molecular mass of Hpt-Syn protein of 34.4 kDa (table 3.7). No protein band at this size was present in the control samples with pJF119 Δ N i.e. (lanes 1 and 3). Hpt-Syn being a hydrophobic protein migrates faster than the protein marker. That is the reason why it has a smaller protein size (on gel) than the calculated size shown in table 3.7.

Table 3.7: Calculated properties of recombinant protein Hpt-Syn

Protein Name (Source)	Molecular size - M _w [kDa]	Isoelectric point - pI
Hpt-Syn (<i>Synechocystis</i> PCC6803)	34.4	9.02

M_w and pI values were calculated using the ExpASY proteomic server.

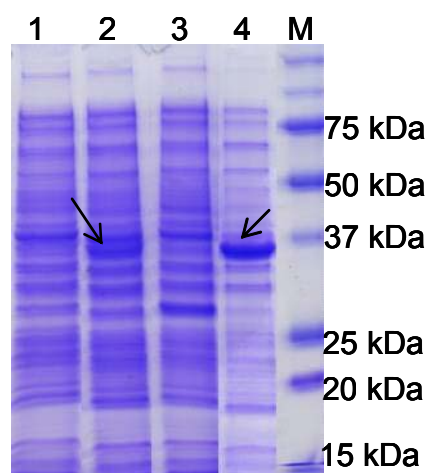


Figure 3.14: SDS-PAGE showing over expression of Hpt-Syn protein. Cultures were induced with 1 mM IPTG. Approx. 10 μ g of protein was loaded in each lane. Expected molecular size of Hpt-Syn protein is 34.4 kDa. Additional band in lane 2 & 4 (shown by arrow) representing the over expressed Hpt-Syn protein at 32.8 kDa.

Lane 1: *E. coli* DH5 α / pJF119 Δ N (before IPTG)

Lane 2: *E. coli* DH5 α / pCAS7 (before IPTG)

Lane 3: *E. coli* DH5 α / pJF119 Δ N (4 h after IPTG)

Lane 4: *E. coli* DH5 α / pCAS7 (4 h after IPTG)

M: Protein marker

For MPBQ biosynthesis, *hpd*, *crtE*, *ggh-Syn* and *hpt-Syn* encoding Hpd, CrtE, Ggh-Syn and Hpt-Syn proteins has to be co-expressed together in recombinant *E. coli*. For MGGBQ biosynthesis, *hpd*, *crtE*, and *hpt-Syn* encoding Hpd, CrtE and Hpt-Syn proteins respectively, has to be co-expressed together in recombinant *E. coli*. Since, these 4 genes were not taken from a single Vitamin E producing organism, an artificial gene cluster was constructed that consisted of a gene cassette containing the 4 genes under the control of a single tac promoter. Plasmid pCAS29 ($P_{tac} \rightarrow ggh-Syn \rightarrow crtE \rightarrow hpd \rightarrow hpt-Syn$) was provided by Dr. Albermann for further studies (refer chapter 2, table 2.2) (Albermann et.al. 2008).

2D Gel Electrophoresis of *E. coli* DH5 α / pCAS29 samples.

By use of 2D gel electrophoresis it was studied whether all the 4 proteins (Hpd, CrtE, Ggh-Syn and Hpt-Syn) are overexpressed in *E. coli* DH5 α /pCAS29. Hence, *E. coli* DH5 α /pCAS29 was cultivated in LB-Amp100 in shaking flask and as control *E. coli* DH5 α /pJF119 Δ N was cultivated. The 2D gel electrophoresis results can be seen in figure 3.15. Three additional protein spots (in green) marked by arrow at 36 kDa, 31.5 kDa and 42.4 kDa (calculated based on R_f method) closely corresponded to the calculated Mw of Hpd, CrtE and Ggh-Syn respectively as shown in table 3.8. Overexpression of Hpd and CrtE was stronger as compared to Ggh-Syn. Ggh-Syn expression in *E. coli* DH5 α /pCAS29 was much weaker when compared to the Ggh-Syn expression in *E. coli* DH5 α /pCAS8 (figure 3.11) and *E. coli* DH5 α /pCAS11 (figure 3.12). The reason for the low expression of Ggh-Syn in *E. coli* DH5 α /pCAS29 was unknown at this point. The fourth protein expected in *E. coli* DH5 α /pCAS29 was Hpt-Syn. Predicted pI and Mw values for this Hpt-Syn protein are 9.02 and 34 kDa respectively (using ExPASy proteomic server).

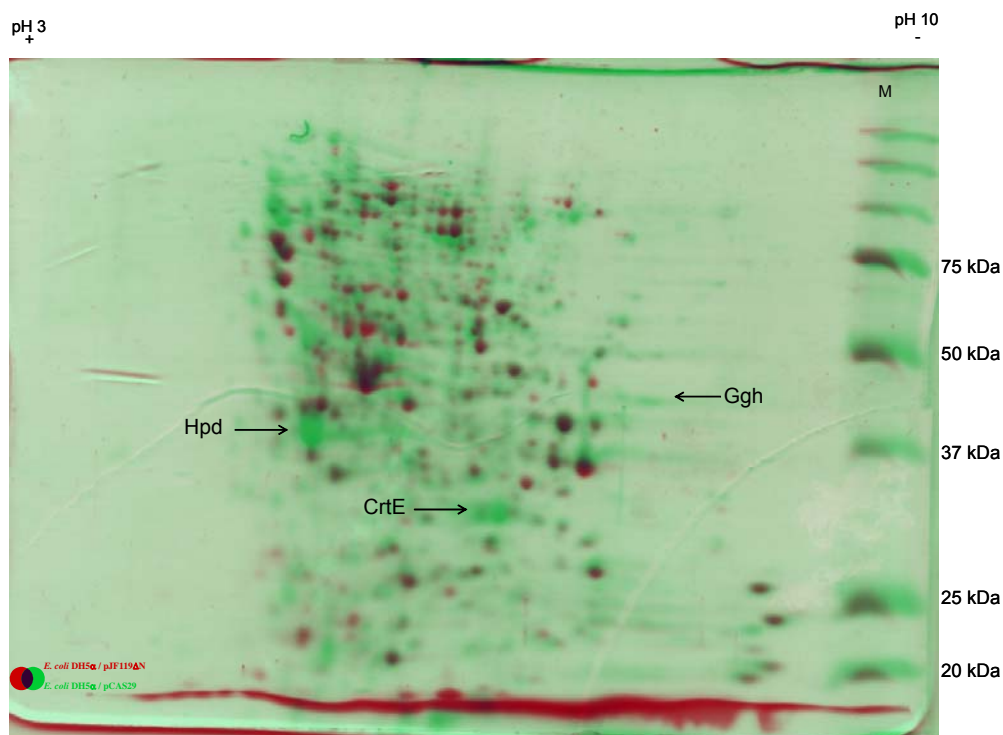


Figure 3.15: 2D Gel electrophoresis showing the overlapped gels for *E. coli* DH5 α /pCAS29 (in green) and its control *E. coli* DH5 α /pJF119 Δ N (in red). *E. coli* DH5 α /pCAS29 and its control *E. coli* DH5 α /pJF119 Δ N were cultivated in LB-Amp100 in shaking flask at 30°C. Cultures were induced with 1 mM IPTG at approx. OD_{600nm} of 0.8. Sample taken 6 h after induction was used for the 2D analysis. The two gels were overlapped and are shown here. Additional protein spots were seen on *E. coli* DH5 α /pCAS29 gel (in green) marked with arrows and named HpD, CrE and Ggh-Syn. Hpt-Syn being membrane bound protein cannot be seen in this 2 D gel electrophoresis analysis. 7 cm long pI stripes with pH ranging between 3 and 10 were used.

Table 3.8: Calculated properties of recombinant proteins

Protein Name (Source)	Molecular size - M _w [kDa]	Isoelectric point - pI
HpD (<i>Pseudomonas putida</i> KT2440)	40.04	5.07
CrE (<i>Pantoea ananatis</i>)	32.58	6.04
Ggh-Syn (<i>Synechocystis</i> PCC6803)	44.80	8.08
Hpt-Syn (<i>Synechocystis</i> PCC6803)	34.41	9.02

M_w and pI values were calculated using the ExpASY proteomic server

Based on the Kyte-Doolittle hydrophathy plot, it was predicted that *slr1736* gene from *Synechocystis* sp. PCC 6803 encodes hydrophobic proteins (Hpt-Syn) with more than one transmembrane domain resulting the protein to be membrane bound (Savidge et. al. 2002). 2D gel electrophoresis is capable of separating and visualizing hundreds of unknown

proteins simultaneously (Delta 2 decodon software). But a disadvantage of this technique is that it can fail to detect hydrophobic proteins or with pI values of 10 or very small (< 10 kDa) or very large (> 120 kDa) (Fountoulakis and Takács 2000). During the 1st dimension (i.e. IEF) these hydrophobic proteins may precipitate during application or may not bind to the IPG stripes during re-hydration step (details of 2D gel electrophoresis can be seen in section 2.5.3.7). Hpt-Syn being hydrophobic and pI value of 9.02 fits into the category where it cannot be detected easily during 2D gel electrophoresis. It may be the reason why no additional band (at pI of 9.0 and Mw of approx. 34 kD was observed) in *E. coli* DH5 α /pCAS29 gel was seen, compared to *E. coli* DH5 α /pJF119 Δ N. Hpt-Syn protein was not detected during any of the other 2D gel electrophoresis performed during this study (wherever *hpt-Syn* gene was overexpressed along with other genes). Overexpression of Hpd, CrtE, Hpt-Syn and GGh-Syn in *E. coli* DH5 α /pCAS29 was also studied on SDS-PAGE. As the expected Mw for CrtE and Hpt-Syn were relatively close i.e. 32.58 kDa and 34.41 kDa, it was not possible to clearly identify the protein bands (results not shown here).

3.4.2. HPLC Analysis and Liquid-Chromatography Mass Spectroscopy (LC-MS) characterization of δ -tocochromanol precursor compounds, produced in *E. coli* DH5 α / pCAS29

E. coli DH5 α / pCAS29 was cultivated in LB-Gly-Amp100 in shaking flask at 30 °C for MPBQ/MGGBQ production. As control, *E. coli* DH5 α / pCAS18 was cultivated under same conditions. Plasmid pCAS18 carried the following genes under the tac promoter i.e. $P_{tac} \rightarrow ggh-Syn \rightarrow crtE \rightarrow hpd \rightarrow hpt-Syn$ in pJF119 Δ N. Culture supernatant was analysed for HGA accumulation and cell pellet was analysed for lipophilic δ -tocochromanol precursors (MGGBQ and MPBQ) by HPLC analysis (HPLC conditions and set-up in section 2.2.4.1). Extraction of lipophilic compounds from cells was obtained according to method described in section 2.2.5.1.

HPLC chromatograms of *E. coli* DH5 α / pCAS18 and *E. coli* DH5 α / pCAS29 are shown in figure 3.16-A & B respectively. *E. coli* DH5 α / pCAS29 sample showed 2 additional peaks, (peak 1 at retention time of 15.4 min and peak 2 at 23.9 min) which were absent in *E. coli* DH5 α / pCAS18. The maximum UV absorption for peak 1 and 2 were 292 nm and 253 nm respectively (shown in the insets of the figure 3.16A and 3.16B). Since no MPBQ and MGGBQ standards were available, these two peaks (peak 1 & 2) still were unidentified products. These yet unidentified products were characterized for molecular mass by LC-MS analysis (detailed method refer 2.2.4.4).

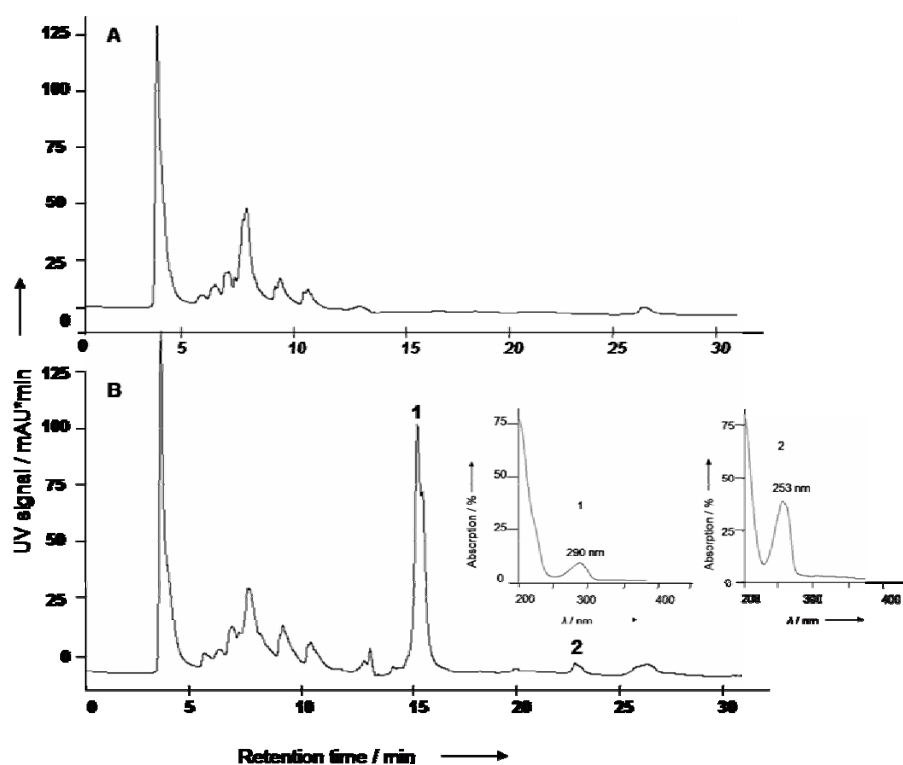


Figure 3.16: HPLC chromatogram showing the cell extract of *E. coli* DH5 α /pCAS29 sample. In the insets are shown the maximum UV absorption spectrum for peak 1 (at 292 nm) and peak 2 (at 253 nm) (A) HPLC Chromatogram for *E. coli* DH5 α /pCAS18 sample (B) HPLC Chromatogram for *E. coli* DH5 α /pCAS29 sample.

The theoretical masses of the expected compounds i.e. MGGBQ and MPBQ in its reduced and oxidized forms are listed in table 3.9.

Table 3.9: Theoretical mass of MGGBQ and MPBQ in its reduced and oxidized forms. From here onwards, the above nomenclatures would be used throughout the study.

Expected Compound	Chemical Formula	Theoretical Mass [Da]
Reduced MGGBQ [MGGBQ _(reduced)]	C ₂₇ H ₄₀ O ₂	396.2
Oxidized MGGBQ [MGGBQ _(oxidized)]	C ₂₇ H ₃₈ O ₂	394.2
Reduced MPBQ [MPBQ _(reduced)]	C ₂₇ H ₄₆ O ₂	402.2
Oxidized MPBQ [MPBQ _(oxidized)]	C ₂₇ H ₄₄ O ₂	400.2

Extraction of the above *E. coli* DH5 α / pCAS29 sample was analysed by LC-MS and the mass spectrum (in positive ion mode) is shown in figure 3.17. The mass for peak 1 from LC chromatogram which is equivalent to HPLC peak 1 in fig. 3.16B, showed the experimental mass of 397.2 Da ($[M+H]^+$) & 414.2 Da ($[M+NH_4]^+$) (shown in part A of figure 3.17). M is the mass of the sample analysed and H⁺ is the hydrogen ion (1 Da), NH₄⁺ is the ammonium ion (18 Da). This gives the mass of the sample analysed i.e. M = 396.2 Da, which corresponds to the expected mass of MGGBQ (reduced form) (as shown in table 3.9). Similarly, peak 2 from LC chromatogram (equivalent to HPLC peak 2 in fig. 3.16B) resulted a mass of 395.2 Da ($[M+H]^+$) & 412.2 Da ($[M+NH_4]^+$) (figure 3.17B). This gives mass of M = 394.2 Da, which corresponds to the expected mass of MGGBQ oxidized form (as shown in table 3.9).

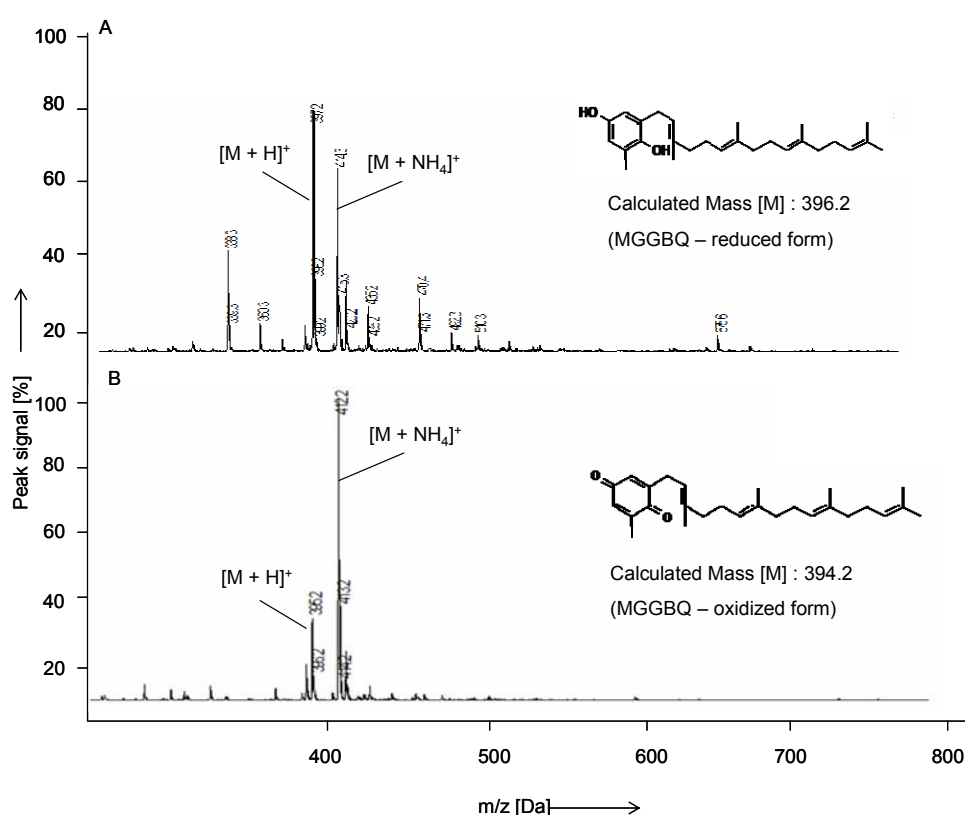


Figure 3.17: Mass Spectroscopy (MS) analysis of sample extracted from *E. coli* DH5 α / pCAS29. (A) Represents the MS spectra for HPLC peak 1 (B) Represents the MS spectra for HPLC peak 2. In the inserts of (A) and (B) shown are the chemical structures of reduced and oxidized form of MGGBQ respectively.

Based on the LC-MS results, no signal corresponding to a mass [M] of 400.2 Da or 402.2 Da was obtained in the MS spectra in positive ion mode neither the equivalent in negative ion mode. Hence, it was concluded that no MPBQ was formed in *E. coli* DH5 α / pCAS29. It is known from section 3.1.3 that PPP was not detected in *E. coli* DH5 α /pCAS11 despite overexpression of Ggh-Syn (2D gel electrophoresis Figure 3.12). One possible reason from several could be that no PPP was available for Hpt-Syn to produce MPBQ, as the Ggh-Syn

expressed in *E. coli* DH5 α / pCAS29 was unable to produce PPP. Before plasmid pCAS29 was used for any study, it was confirmed that, the nucleotide base pair (bp) sequence was correct (personal communication with Dr. Albermann). Transcript analysis of plasmid pCAS29 detected mRNA transcript for *hpd*, *crtE*, *hpt* and most importantly for *ggh* too (Albermann et. al. 2008). To conclude, the LC - MS results gave a mass that corresponded to what appears to be MGGBQ, and hence no MPBQ was produced in *E. coli* DH5 α / pCAS29. The reason why MPBQ was not synthesized was studied further and discussed in detail in section 3.17 & 4.4 respectively.

3.4.3. Quantification of MGGBQ produced in recombinant *E. coli* carrying pCAS29.

The quantification of MGGBQ_(reduced) and MGGBQ_(oxidized) was not possible, since the respective standards for calibration were not commercially available or not accessible by any other sources. No absorption coefficient for MGGBQ molecule has been reported in literature so far. Hence, MGGBQ concentration was calculated based on the correlation obtained during an *in-vitro* reaction of MGGBQ and Tocopherol cyclase (for details please refer section 2.2.3.7 in materials and method and section 3.5.2 *in-vitro* assay to produce δ -tocotrienol). The HPLC peak area (area under peak 1 in fig. 3.16) for MGGBQ_{reduced} is calculated by the HPLC program in mAU*min which is x . y is MGGBQ_{reduced} in μg . The correlation obtained was: $y = x / 7.8708$ (Albermann et. al. 2008).

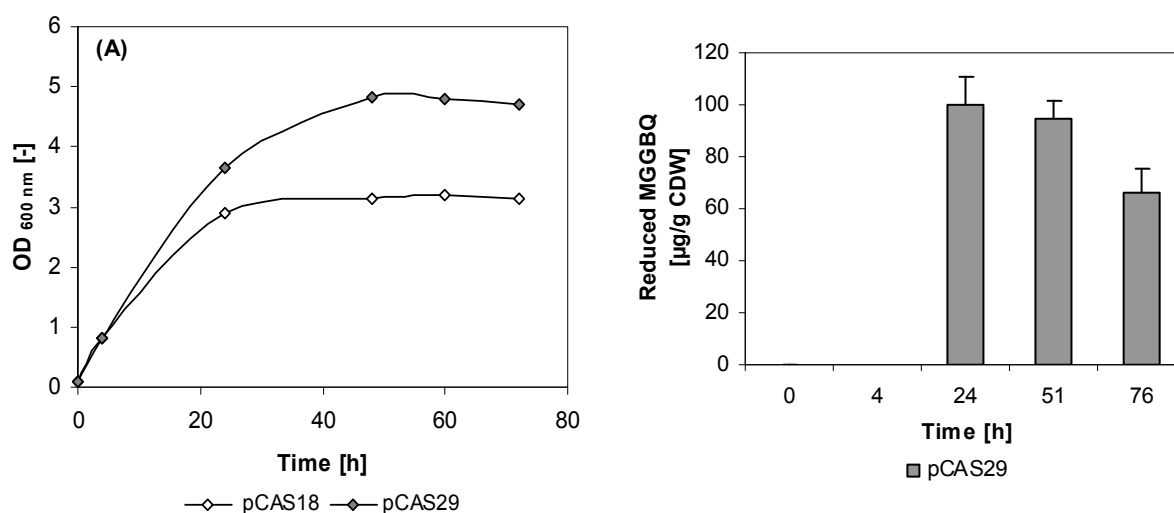


Figure 3.18: Cell density and MGGBQ production in *E. coli* DH5 α /pCAS29. *E. coli* DH5 α /pCAS29 and its control *E. coli* DH5 α /pCAS18 were cultivated in shaking flask in LB-Gly-Amp100 medium at 30 °C. Cultures were induced with 1mM IPTG at approx. OD_{600nm} of 0.8. (A) Growth curve shown as OD_{600nm} w.r.t time. (B) MGGBQ_{reduced} was produced in *E. coli* DH5 α / pCAS29 cultures. No MGGBQ_{reduced} was detected during HPLC analysis of *E. coli* DH5 α / pCAS18 samples. MGGBQ analysed by HPLC was quantified using the correlation mentioned in the text.

It was not clear at this point when and where the oxidation of MGGBQ takes place in *E. coli* DH5 α /pCAS29 cells. Hence, as no correlation between MGGBQ_(reduced) and MGGBQ_(oxidized) existed the amount of MGGBQ_(oxidized) was not taken into account. Using the above mentioned correlation MGGBQ_(reduced) was quantified in μg per litre of culture i.e. $\mu\text{g/l}$ and μg per gram of cellular dry weight (CDW) i.e. $\mu\text{g/g}$ CDW. The results can be seen in figure 3.18. *E. coli* DH5 α / pCAS18 cells did not grow above OD_{600 nm} of 3.0 while, *E. coli* DH5 α /pCAS29 reached an OD_{600 nm} of 5.1. Estimated concentration of MGGBQ_(reduced) was 96 $\mu\text{g/g}$ CDW with no MGGBQ formed in control strain. The MGGBQ_(reduced) concentration decreased after 51 h which meant that MGGBQ_(reduced) started oxidizing. *E. coli* DH5 α /pCAS29 culture supernatant had turned slightly brown at 51 h and at 76 h they turned further dark brown. The cell pellets of the samples (51h and 76 h) after harvesting were slightly brownish compared to the cell pellet of the control strain which didn't produce MGGBQ. This effect was different compared to HGA producing strains, where the cell pellet was pale/white. The cell pellet colour of the control which didn't produce any MGGBQ remained pale/white. Another observation was that the amount of MGGBQ_(oxidized) increased steadily between 24 h and 76 h (based on the HPLC peak area, results not shown here). This may be due to the oxidation of MGGBQ_(reduced) to MGGBQ_(oxidized) by molecular oxygen during prolonged cultivation. It was discussed in section 3.6 (figure 3.6) that HGA tends to oxidize and subsequently polymerise into a brown ochronotic pigment. Similarly, the head group of MGGBQ_(oxidized), (an analogue of HGA) is also presumed to further polymerise which may offer the brown colour to the cell pellets (Albermann et.al. 2008). Both these reasons may be responsible for the decrease in MGGBQ_(reduced). The loss in MGGBQ_(reduced) into MGGBQ_(oxidized) and subsequently into brown colour could not be taken into account for the estimation of MGGBQ concentration.

3.4.4. MGGBQ production in Infors bioreactor

In section 3.4, it was shown that the Hpd, CrtE and Hpt-Syn expressed in *E. coli* DH5 α / pCAS29 strain were active as it resulted in MGGBQ production in LB-Glycerol-Amp100 medium in shaking flask. It was shown that HGA and GGPP was produced using MM-Glucose-Amp100 and MM-Glycerol-Amp100 in *E. coli* BW25113/pCAS2JF (shaking flasks) and in *E. coli* LJ110/pCAS30 (bioreactor) respectively, where either glucose or glycerol was supplemented as the sole carbon and energy source. To study the MGGBQ production and to study the robustness of *E. coli* BW25113 carrying a plasmid pCAS29 (a multi-copy vector), *E. coli* BW25113/pCAS29 was cultivated in bioreactor in MM-Glucose-Amp100 and MM-Glycerol-Amp100.

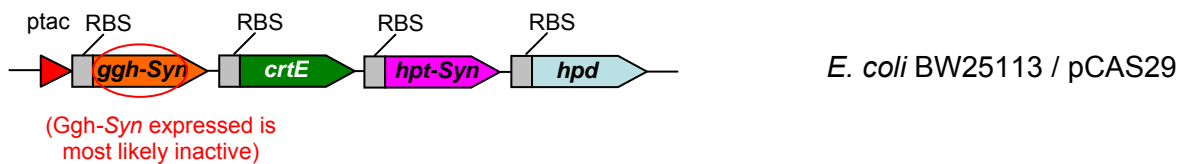


Figure 3.19: Scheme representing strain *E. coli* BW25113 / pCAS29. *Ggh-Syn* protein encoded by the *ggh-Syn* gene in plasmid pCAS29 has been shown in section 3.4.1 to be apparently inactive *in-vivo* (here marked with orange circle).

E. coli BW25113 / pCAS29 (shown in figure 3.19) was cultivated in a 3.6 L Infors bioreactor (Wald, Switzerland) in MM-Glucose-Amp100 and MM-Glycerol-Amp100. All fermentations carried out with *E. coli* BW25113/pCAS29 in bioreactor were operated initially in batch mode and later in fed batch mode (i.e. batch-fedbatch). During the fed-batch mode, glucose (in case of MM-Glucose-Amp100) or Glycerol (in case of MM-Glycerol-Amp100) was fed continuously using a feeding pump. Cultivation was done at 30 °C, at constant pH of 7.0 (maintained by addition of 5 N KOH) and pO₂ concentration of 30 % oxygen saturation. Each fermentation was repeated, in order to assess the reproducibility of the results. Results can be seen in Figure 3.20 to 3.22.

Cultures were induced with 0.25 mM IPTG (final conc.) at OD_{600nm} of approx. 2.0 in MM-Glucose-Amp100 (i.e. at 8 h) and in MM-Glycerol-Amp100 (i.e. at 18 h). At the end of batch process the cell density of 1.7 g/l CDW (MM-Glucose-Amp100) and 2.3 g/l CDW (MM-Glycerol-Amp100) was reached. Fed-batch cultivation was started by feeding glucose/glycerol at feed rates (g/h) shown in figure 3.21 such that there was no overflow of glucose or glycerol in the culture medium. Cultures in glycerol medium has a long lag phase compared to that in glucose medium. In glucose medium the cultures grew exponentially during batch process with maximum growth rate of 0.32 h⁻¹ compared to 0.15 h⁻¹ in glycerol medium. Cultures in glucose medium entered stationary phase at 46 h (final OD_{600nm} of 21.5 ± 0.2) compared to 58 h in glycerol medium (final OD_{600nm} of 26.7 ± 0.3).

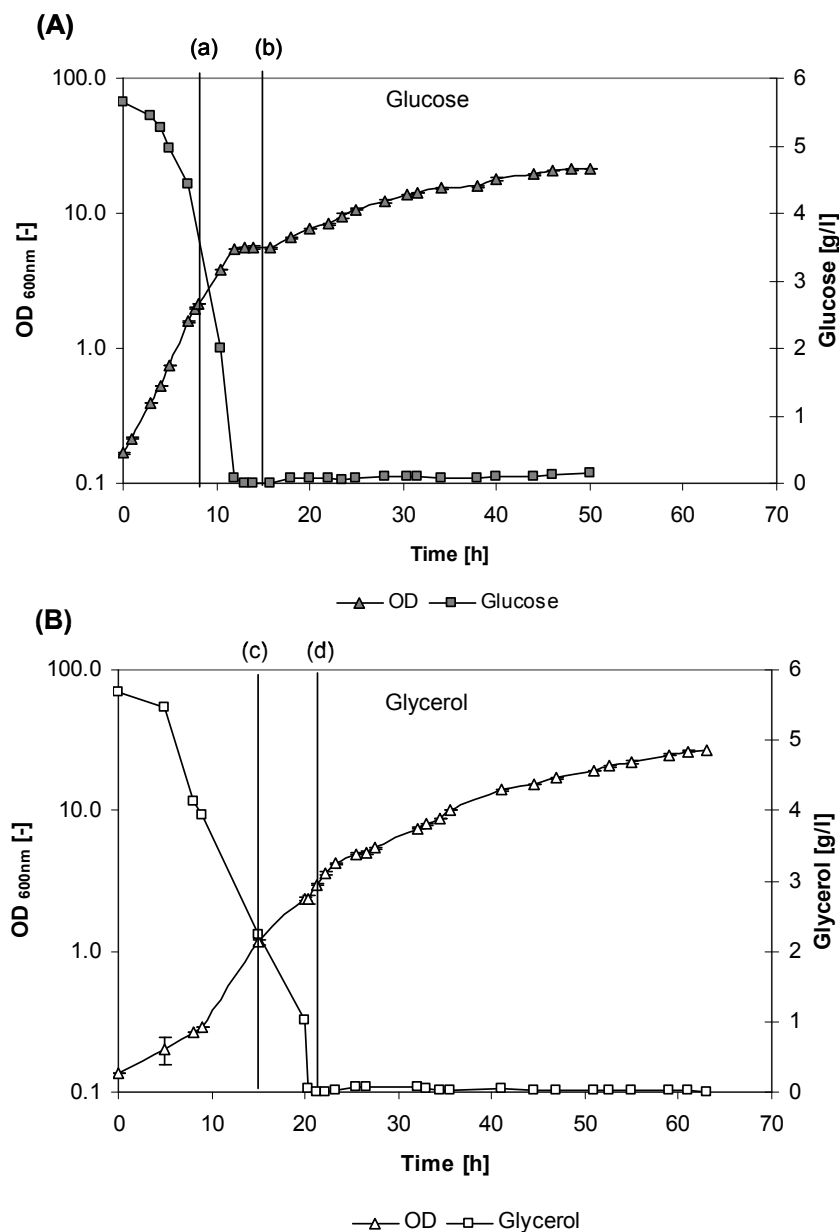


Figure 3.20: Batch-Fed batch fermentation of *E. coli* BW25113/pCAS29 in Infors bioreactor for MGGBQ production. Fermentation carried out at 30 °C, at constant pH of 7.0 and pO₂ concentration of 30 % of saturation. (A) Cell growth curve and glucose concentration in bioreactor during fermentation in MM-Glucose-Amp100. (B) Cell growth curve and glycerol concentration in bioreactor during fermentation in MM-Glycerol-Amp100.

Cell density represented as OD_{600nm} w.r.t time (scale on left hand side) and glucose or glycerol concentration in gram per liter of culture (scale on right hand side). Vertical lines (a) and (c) show the time of induction 0.25 mM IPTG (final conc.). Vertical lines (b) and (d) show the start of fed-batch process (glucose and glycerol feeding resp.).

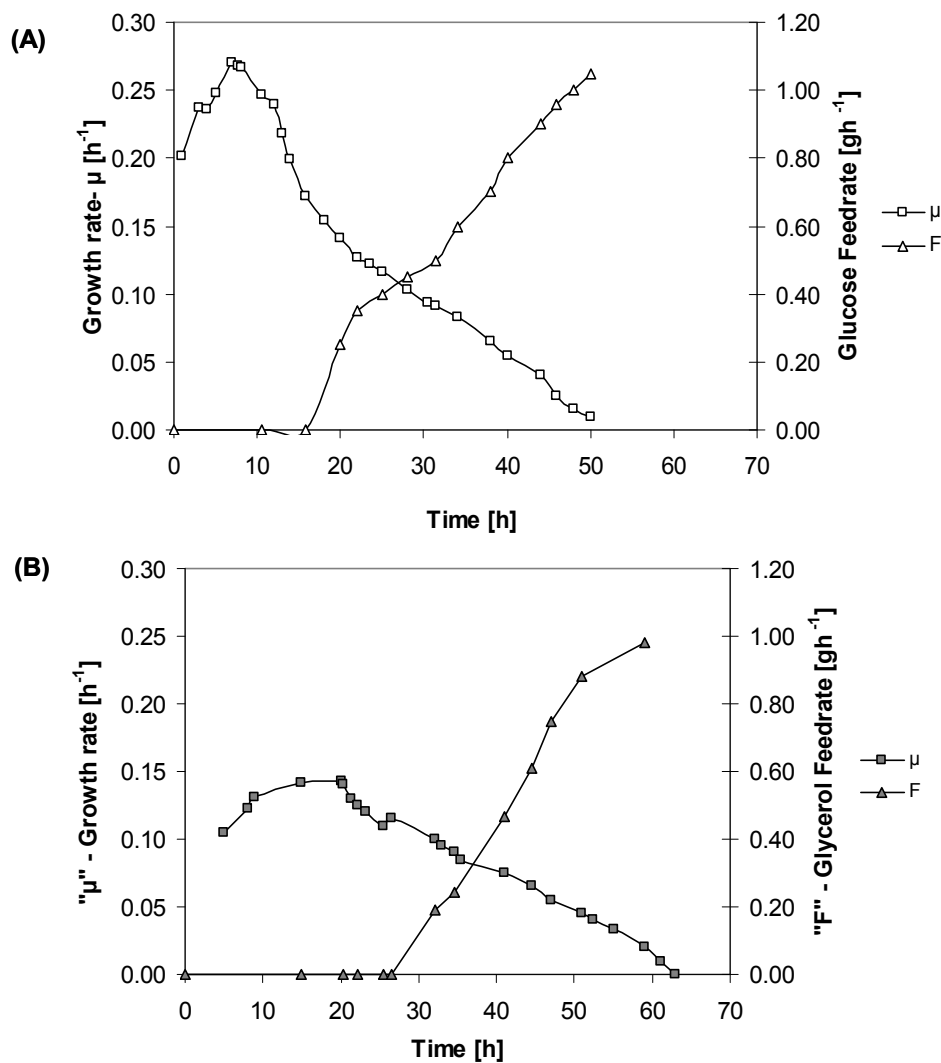


Figure 3.21: Cell growth rate (μ) and Glucose/Glycerol Feed rate (F) during fed batch fermentation of *E. coli* BW25113/pCAS29. (A) Fermentation carried out in MM-Glucose-Amp100 (B) Fermentation carried out in MM-Glycerol-Amp100. Fermentation temperature of 30 °C, pH of 7.0, and pO₂ concentration of 30 % saturation were maintained constant throughout the fermentation.

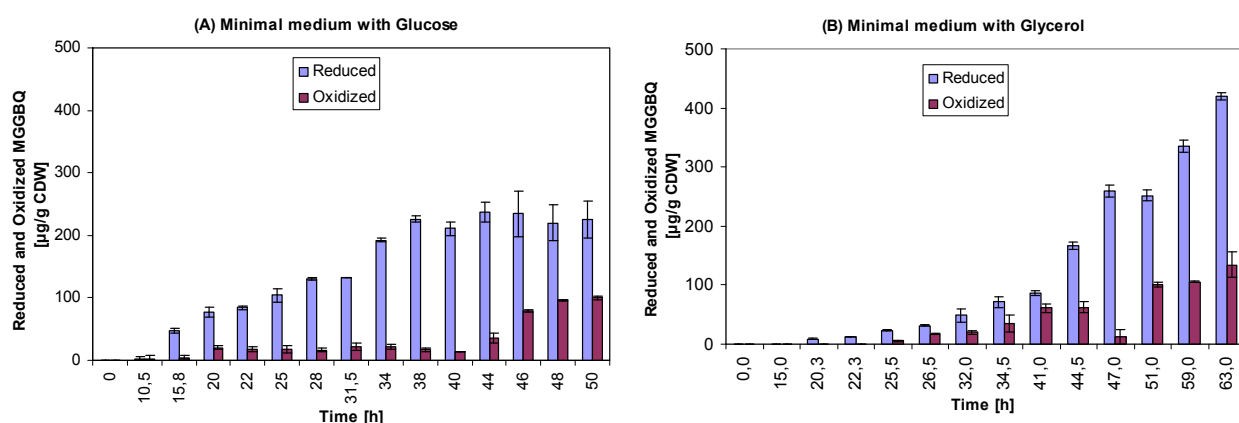


Figure 3.22: MGGBQ production in *E. coli* BW25113 / pCAS29 in bioreactor in minimal medium in (A) glucose and (B) glycerol, as sole carbon and energy source. S.D values are calculated from the average values of 2 independent samples, which were separately extracted and analyzed by HPLC. In appendix, a graph showing MGGBQ concentration vs. time graph is shown as figure A.3-10.

The MGGBQ production shown here is the total MGGBQ. This is calculated as follows:

Total MGGBQ = [MGGBQ]_{reduced} + [MGGBQ]_{oxidized in terms of reduced}. [MGGBQ]_{oxidized in terms of reduced} is calculated by conversion of oxidized form of MGGBQ into reduced form, in presence of ascorbic acid. The following correlation was established and used to calculate the [MGGBQ]_{oxidized in terms of reduced}. [MGGBQ]_{oxidized in terms of reduced} = $x/5.107$, where [MGGBQ]_{oxidized in terms of reduced} is in µg, and x is peak area of oxidized MGGBQ (at 253 nm) in mAU*min.

No MGGBQ was detected in any samples, before induction, in cells grown in MM-Glucose-Amp100 and MM-Glycerol-Amp100. This showed that the P_{tac} promoter is tightly control in minimal medium. Induction with 0.25 mM IPTG (final conc.) led to MGGBQ production reaching a level of 52 µg / g CDW and 49 µg / g CDW resp. (total MGGBQ) at the end of batch process (90 % of the total MGGBQ was in reduced form i.e. MGGBQ_(Reduced)). Start of fed batch process resulted in linear increase in MGGBQ_(Reduced) (MGGBQ_(Oxidized) being constant) with time both in terms of product yield per gram dry biomass (µg/g CDW) or concentration (µg/l of culture) in case of MM-Glucose-Amp100 while in case of MM-Glycerol-Amp100 the increase in total MGGBQ was gradual till the end. Wherever the MGGBQ_(Reduced) product yield remained constant, the reduced MGGBQ concentration increased (can be seen for 28 and 31.5 h samples). The MGGBQ_(Reduced) concentration increased continuously till 46 h, while the yield of product per gram dry biomass was constant since 38 h. After 40 h, the share of MGGBQ_(Oxidized) started increasing and at the end of cultivation, MGGBQ_(Oxidized) was approx. 40 % of the total MGGBQ. Oxygen concentration (pO₂) in fermenter was always maintained constant at 30 % during fed-batch process.

At the end of cultivation, acetic acid accumulated in MM-Glucose was 3.75 mM and in MM-Glycerol it was 2.45 mM. No HGA was detected in any of the samples before 34 h. Oxygen supply to the cells was maintained constant at 30 % of that saturated concentration. HGA

concentration in medium increased after 36 h and reached 1.62 mM (glucose medium) and 1.87 mM (glycerol medium) at the end of fermentation. During the end phase of cultivation where cell growth dropped down to below 0.05 h^{-1} , the oxygen uptake dropped down and as a result the excess oxygen concentration may have influenced the oxidation of HGA and MGGBQ. Supernatant samples at the end of fermentations were brown in colour.

A test for plasmid segregational stability (described in section 2.2.1.4) was performed to find out how many recombinant *E. coli* cells lost the plasmid pCAS29, during bioreactor cultivation (MM-Glucose-Amp100 and MM-Glycerol-Amp100), over a period of 48 h. Results of the plasmid segregational stability test are shown in figure 3.23. In case of MM-Glucose-Amp100, after 40 h, approx. 50 % cells were plasmid carriers (based on ampicillin resistance). During the batch process (15 h in MM-Glucose-Amp100 and 21 h in MM.Glycerol-Amp100) approx. 85-90 % of the recombinant *E. coli* cells possessed the plasmid pCAS29. Most of the plasmid loss occurred during the fed-batch process. 40 h after induction approx. 50 % of *E. coli* cells still carried the plasmid (in glucose medium) compared to 60 % (in glycerol medium).

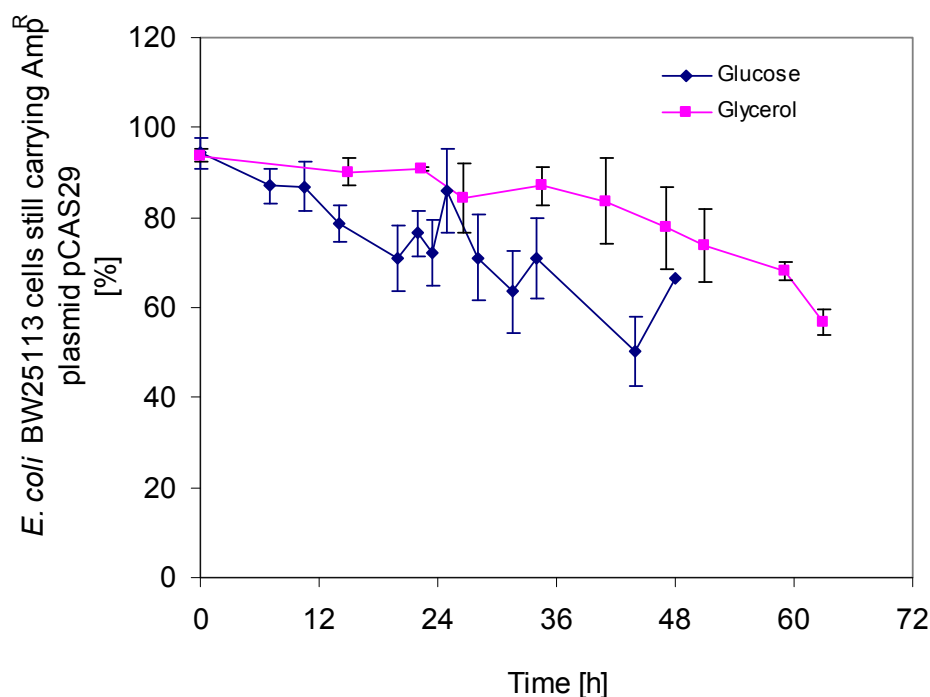


Figure 3.23: Plasmid stability test for plasmid pCAS29 during fermentation of *E. coli* BW25113/pCAS29 strain in bioreactor. Blue colour indicates fermentation in MM-Glucose-Amp100 and pink colour indicates fermentation in MM-Glycerol-Amp100. S.D is calculated based on the average of two independent measurements.

MGGBQ yield was also calculated in terms of μg of total MGGBQ produced per gram of carbon source consumed. A comparison of MGGBQ yield achieved during cultivation of *E. coli* BW25113/pCAS29 in MM-Glucose-Amp100 or MM-Glycerol-Amp100 can be seen in

figure 3.24. The MGGBQ yield in terms of μg total MGGBQ produced per g of carbon source cannot be compared directly w.r.t time, as the glycerol cultures had long lag phase and hence was continued till 58 h (i.e. both cultures were cultivated for sample number of hours after induction with IPTG i.e. approx. 40 h). For most of the fermentation time, the MGGBQ yield (carbon) in glucose was higher, compared to that in glycerol.

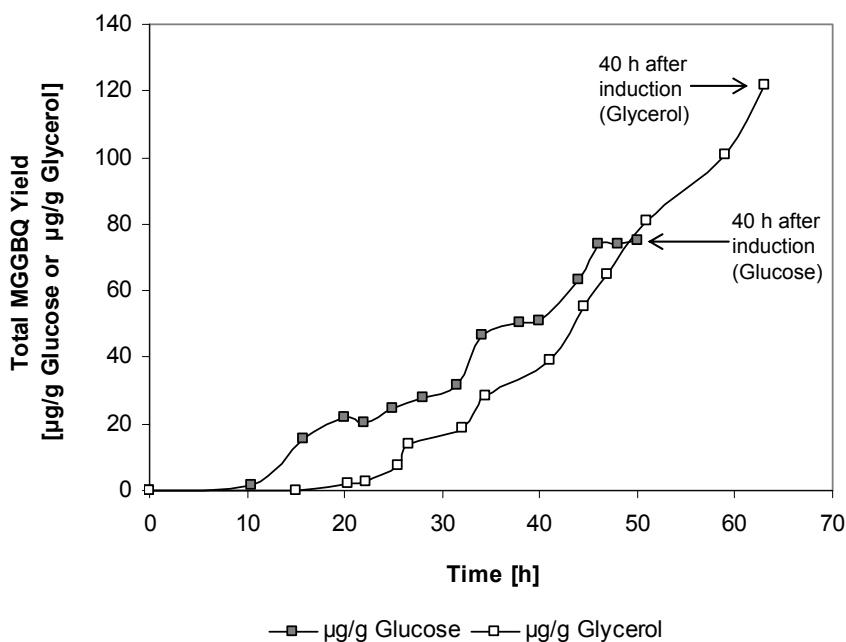


Figure 3.24: Total MGGBQ yield shown in terms of μg product per g of glucose or per g of glycerol consumed during bioreactor cultivation of *E. coli* BW25113/pCAS29 in minimal medium with glucose/glycerol and Amp100; cultivated at 30 °C at constant pH 7.0.

Table 3.10: Overview showing the highest $\text{MGGBQ}_{\text{total}}$ produced in *E. coli* BW25113/pCAS29 strain in Infors fermenter

	Glucose			Glycerol		
	Total MGGBQ			Total MGGBQ		
	$\mu\text{g/l}$	$\mu\text{g/g CDW}$	$\mu\text{g/g Glucose}$	$\mu\text{g/l}$	$\mu\text{g/g CDW}$	$\mu\text{g/g Glycerol}$
<i>E. coli</i> BW25113/pCAS29	2164 ± 199	325 ± 33	78 ± 5	4591 ± 236	554 ± 29	128 ± 11

In this section, it was shown that except Ggh-Syn, all the other enzymatic reactions in the MGGBQ biosynthesis pathway were functional. Overall, fermentation in MM-glycerol was better with respect to MGGBQ concentrations, yields (MGGBQ per gram CDW), and yields (MGGBQ per g of sugar source if compared with identical hours after induction). Segregational stability of plasmid pCAS29 was also better in medium with glycerol compared to glucose.

3.5. Enzymatic *In-vitro* Synthesis of δ -Tocotrienol

3.5.1. Overexpression and His-Tag purification of tocopherol cyclase (Cyc-At) from *Arabidopsis thaliana* in pQE31-*vte1* in recombinant *E. coli*

Tocopherol cyclase (Cyc) catalyzes the ring cyclization of MPBQ, MGGBQ, DMPBQ and DMGGBQ to produce δ -tocopherol, γ -tocopherol, δ -tocotrienol and γ -tocotrienol, respectively, (as shown in figure 3.25). This is the last enzymatic step for δ and β tocochromanol synthesis. Hence, to achieve δ -tocochromanol in recombinant *E. coli*, the final step would be to clone tocopherol cyclase in a strain which forms MGGBQ or MPBQ.

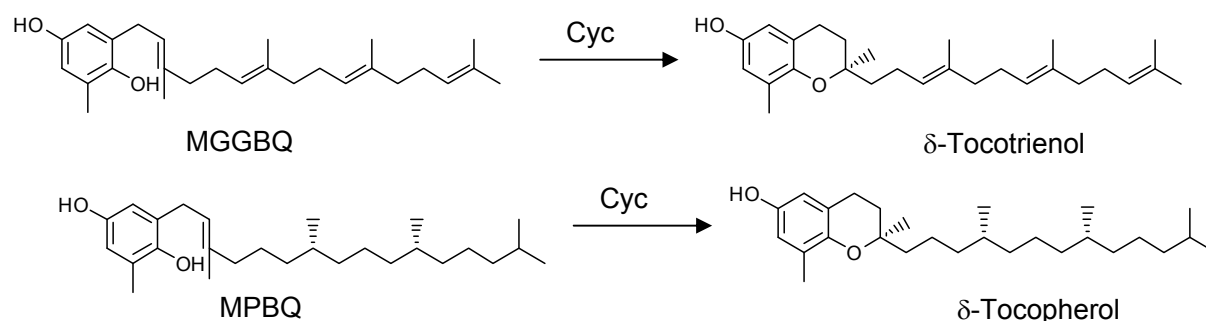


Figure 3.25: Scheme showing Cyc catalyzing the cyclization reaction of MGGBQ and MPBQ to δ -tocotrienol and δ -tocopherol respectively.

Tocopherol cyclase from *Arabidopsis thaliana*, (*At4g32770* / *vte1* alias *cyc-At*) had been cloned in pQE31 vector (N-terminal His-Tag), and had been successfully expressed in *E. coli* (Porfirova and Dörmann 2002). Qiagen vector pQE31 carrying *cyc* encoding Cyc-At was called pQE31-*Vte1*. *E. coli* M15 strain carrying plasmid pQE31-*Vte1* and pREP4 (repression vector) was a generous gift from Dr. Peter Dörmann (MPI, Golm). Here, the tocopherol cyclase protein (*Arabidopsis thaliana*) expressed in *E. coli* M15 / pQE31-*vte1* + pREP4 would be termed as Cyc-At in this study to differentiate between Cyc proteins from other organisms, which would be discussed in later section. To verify, whether the plasmid (pQE31-*vte1*) is intact, and to check the overexpression level of Cyc-At proteins in plasmid pQE31-*Vte1*, *E. coli* M15 was used as host strain (as it was delivered by Dr. Dörmann).

Cyclase protein from *Arabidopsis thaliana* expressed in *Arabidopsis thaliana* has a size of 54 kDa. It contains a functional transit peptide which is used in transporting the protein to the chloroplasts. Here this Cyclase protein from *Arabidopsis thaliana* consisting of the functional transit peptide (+FTP) is abbreviated as (Cyc_{+FTP}-At). Once (Cyc_{+FTP}-At) proteins are transported to the chloroplast of *Arabidopsis thaliana* the transit / signal peptide is cleaved. This Cyclase protein is abbreviated as (Cyc-At) in this study. The Cyc-At proteins without functional transit peptide gives a molecular size of 47 kDa (Porfirova et.al 2002). Similarly,

tocopherol cyclase from *maize* also has a signal peptide (Provencher et. al. 2001). The Cyc-*At* protein overexpressed in pQE31-*vte1* was cloned without the transit signal peptide.

E. coli M15 / pQE31-*vte1* + pREP4 was cultivated in LB-Amp100-Km25 (kanamycin 25 µg/ml) in shaking flask (details in section 2.2.3.5). *E. coli* M15 / pQE31 + pREP4 was cultivated as control. Both cultures were induced with 1 mM IPTG (final conc.) at approx. OD_{600nm} of 0.8 and cultivated for total 12 h at room temperature (22 °C). Samples tested for Cyc-*At* expression on SDS-PAGE can be seen in figure 3.26.



Fig. 3.26: SDS-PAGE analysis of His-Cyc-*At* fusion protein after Ni-NTA enrichment. Arrow marked at 47 kDa represents the enriched Cyc-*At* protein.

A strong band at 46.5 kDa (calculated according to R_f method) was seen in cell free extract sample (clear lysate) of *E. coli* M15 + pQE31-*Vte1* + pREP4 (lane 1). This molecular mass of expressed protein corresponded to the predicted mass of Cyc-*At* protein without transit peptide i.e. 47 kDa (according to ExpASY). This was absent in the control (lane 2). Cyc-*At* was purified using a Nickel-NTA column using Qiagen kit (for details please refer section 2.2.3.5 & Protocol 9 from Qiagen Expressionist 5th Edition). Portion of the unbound Cyc-*At* proteins was found in washed fraction after 1st and 2nd washing (lane 3 and 5). Compared to wash 1 & wash 2 (lane 3 & 5 resp.), relatively very small amount of *At*-Cyc proteins were seen after 3rd wash (lane 7). Hence, the Ni-NTA column was eluted and enriched Cyc-*At* protein band at 47 kDa was seen (lane 8 & 9). Extra protein bands at approx. 28 kDa & approx 60 kDa were also seen in the eluted fraction (lane 8 & 9). The reason for this contamination during elution is unknown. The smaller proteins (i.e. approx 28 kDa) proteins could be some form of degraded proteins of Cyc-*At* and the one at approx. 60 kDa could be some unrelated bacterial proteins which bound to the Ni-NTA column. Their molecular masses correspond to those of bacterial chaperonins, those involved in the proper folding of nascent proteins in *E. coli* (Hendrickson et. al 2000). Approx. 800 µg of protein (0.25 mg/ml) was obtained to perform *in-vitro* reaction with MGGBQ. Purity of the Cyc-*At* protein in lane 8 and 9 was estimated to be is approx. more than 80 % of the total protein

3.5.2. *In-vitro* assay of His-Cyc-*At* fusion proteins and purified MGGBQ

His-Cyc-*At* fusion proteins (> 80 % purity) were obtained as shown in the previous section. Purified and concentrated MGGBQ was obtained as described in section 2.2.3.5. The *in-vitro* enzymatic reaction was carried out in aqueous phase i.e. phosphate buffer (pH 7.0). But the substrate MGGBQ being hydrophobic in nature, has a very low solubility in aqueous phase. Hence to increase the solubility of MGGBQ in aqueous phase, the lipophilic tail of MGGBQ was covered with methyl- β -cyclodextrin, leaving the soluble chromanol head group exposed to aqueous phase for cyclization reaction to occur. This resulted in a substrate-cyclodextrin complex (MGGBQ-cyclodextrin complex) which was used for the *in-vitro* assay as described by Kumar et.al. 2005. Details of the preparation method of this complex can be found in section 2.2.5.4. The following reactions were carried out with varying amount of Cyc-*At* protein ranging from 0 (control, reaction 1) to 50 μ g (reaction 5) as shown in the table 3.10 below.

Reaction component / Reaction Nr.	End. Conc. in reaction mixture	Reaction	Reaction	Reaction	Reaction	Reaction
		1	2	3	4	5
		0.0 μ g Protein	0.1 μ g Protein	1.0 μ g Protein	10.0 μ g Protein	50.0 μ g Protein
0.25 μ l/ μ g Cyc- <i>At</i> Protein	variable (μ l)	0.0 μ l	0.4 μ l	4 μ l	40 μ l	200 μ l
1 M Ascorbic acid	75 mM	75 μ l	75 μ l	75 μ l	75 μ l	75 μ l
1 M DTT	4 mM	4 μ l	4 μ l	4 μ l	4 μ l	4 μ l
1 M Potassium phosphate (7.3 pH)	200 mM	200 μ l	200 μ l	200 μ l	200 μ l	200 μ l
MGGBQ Substrate- cyclodextrin complex	Approx. 9.5 μ M	100 μ l	100 μ l	100 μ l	100 μ l	100 μ l
Water (balance)	Variable	621.0 μ l	620.6 μ l	617.0 μ l	581.0 μ l	421.0 μ l
Volume	TOTAL	1000 μ l	1000 μ l	1000 μ l	1000 μ l	1000 μ l

Table 3.10: Reaction conditions during *in-vitro* reaction assay with His-tag Cyc-*At* proteins. Five reactions, with varying Cyc-*At* protein concentrations, ranging from 0 to 50 μ g / ml were carried out at 30 °C, in a closed 1.5 ml reaction cup, with 1.0 ml reaction volume. 200 μ l of sample was taken at different time point and extracted in 200 μ l hexane to analyse δ -tocotrienol produced and un-reacted MGGBQ substrate. Extract in hexane was analyzed by HPLC.

In reaction 1 (without *Cyc-At* proteins), δ -tocotrienol was not detected in any of the samples, when analyzed by HPLC. In the control sample (i.e. without *Cyc-At* proteins) approx. 80 % of MGGBQ was detected after 35 h of reaction. No δ -tocotrienol was produced in control. This 20 % decrease in MGGBQ in control sample, was likely due to loss via oxidation of MGGBQ and apparent polymerisation. Reaction with 0.1 μ g *Cyc-At* protein (reaction 2) also resulted in no detection of δ -tocotrienol in any of the samples. Reaction with 1.0 μ g *Cyc-At* proteins (i.e. reaction 3) produced 0.177 ± 0.05 μ M of δ -tocotrienol after 35 h with 80 % of the initial MGGBQ being converted. With 50 μ g *Cyc-At* proteins (reaction 5), 80 % of MGGBQ was utilized after 11 h to produce 1.46 ± 0.27 μ M δ -tocotrienol before reaching 1.69 ± 0.40 μ g δ -tocotrienol after 35 h with all MGGBQ converted. 10 μ g of *At-Cyc* proteins (reaction 4) resulted in highest level of δ -tocotrienol after 35 h i.e. 5.17 ± 0.54 μ M. HPLC chromatograms for control (reaction 1) in Figure 3.27 a) and for reaction 3 can be seen in Figure 3.27 b) c) d). Best conversion was achieved with 10 μ g/ml reaction. The cyclization reaction was slow, since after 11 h of incubation approx. 50 % (5 μ M) of MGGBQ was utilized while only 1.0 μ M of δ -tocotrienol was formed (i.e. 20 % of the total δ -Tocotrienol produced at the end of the reaction). After 35 h almost 90 % of the starting MGGBQ amount was consumed and approx. 5.05 μ M was produced (can be seen from fig. D). Injection of standard δ -Tocotrienol resulted in a single peak at 18.2 minutes, which had the same retention time as that of the product peak. Co-injection of a sample (11 h) with standard δ -Tocotrienol also resulted in a single peak (i.e. product and standard). This *in-vitro* reaction was performed for another to times independently, and resulted in similar δ -tocotrienol concentrations with standard deviation between 10 - 20 %. This experiment confirmed that *At-Cyc* proteins accept MGGBQ as substrate during *in-vitro* reactions. Hence, sub-cloning of *vte1* i.e. *cyc-At* was started in pCAS29. No kinetic parameters were determined for *Cyc-At* enzyme with MGGBQ as substrate. Apparent K_m value of 90 μ M was measured with DMPBQ by Kumar 2008. Based on the *in-vitro* assay, the calculated activity of *Cyc-At* was 14.7 nmol/ mg protein/ h.

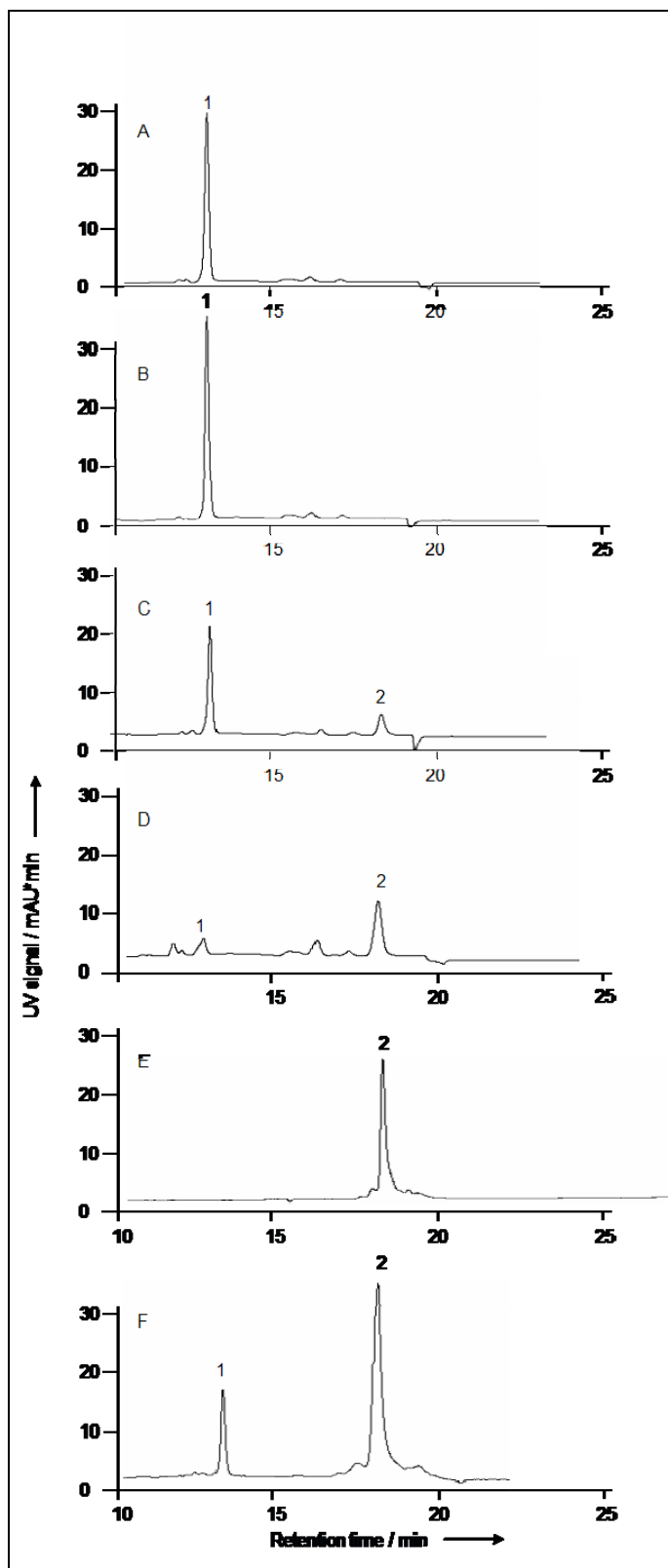


Figure 3.27: HPLC chromatogram of *in-vitro* enzymatic reaction between enriched *Cyc-At* protein and purified MGGGBQ.

HPLC chromatograms of samples from *in-vitro* δ -Tocotrienol assay. MGGGBQ in the form of MGGGBQ-cyclodextrin complex was used as the substrate in this activity assay (a-d).

a) Control reaction carried out without protein. MGGGBQ (un-reacted after 35 h) represented by peak 1.

b) Reaction carried out with purified His-Cyc-At fusion proteins (10 μ g; see the Experimental Section for details). MGGGBQ represented by peak 1 at start of incubation.

c) Reaction products after 11 h of incubation showing un-reacted MGGGBQ (4.5 μ M) and a new peak nr. 2 representing δ -Tocotrienol (1 μ M).

d) Reaction products after 35 h of incubation: 90% of the MGGGBQ had been consumed, and 5.05 μ M of δ -Tocotrienol, represented by peak 2, had been produced.

e) δ -Tocotrienol HPLC standard (75 μ M).

f) Reaction product after 11 h of incubation (i.e., c), co-injected with 0.6 μ g of δ -Tocotrienol standard (in hexane)

3.6. *In-vivo* biosynthesis of δ -Tocotrienol in Recombinant *E. coli*

3.6.1. Overexpression of tocopherol cyclase (*Cyc-A1*) from *Arabidopsis thaliana* in *E. coli* DH5 α / pCAS50

Vte1 (*At4g32770*) from plasmid pQE31-*vte1* was amplified by PCR and cloned into pJF119 Δ N to obtain plasmid pCAS50. Plasmid pCAS50 was provided by Dr. Albermann for further studies.

E. coli DH5 α / pCAS50 was cultivated in LB-Amp100 medium in shaking flask at 30 °C. As control *E. coli* DH5 α carrying empty vector pJF119 Δ N was cultivated. Cultures were induced with 1 mM IPTG (final conc.) and samples were checked for *Cyc-A1* expression on SDS-PAGE. An additional protein band at approx. 47 kDa (calculated by R_f method, see figure 3.28) was seen in *E. coli* DH5 α /pCAS50 sample, 4 h after IPTG induction (lane 3, shown by an arrow). This protein size corresponded to the predicted size of *Cyc-A1* protein of 47 kDa. No additional band at this size was observed in the control strain, after induction (lane 4). No *Cyc-A1* protein expression was seen in any sample before induction.

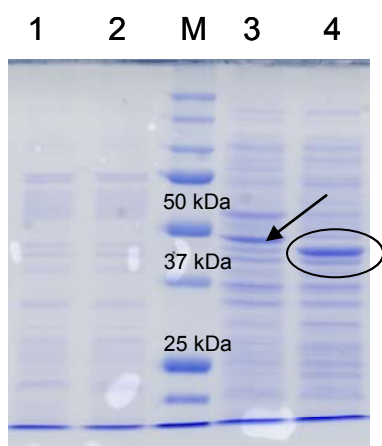


Figure 3.28: SDS-PAGE showing over expression of *Cyc-A1* protein in plasmid pCAS50. Expected size of His-*Cyc-A1* fusion protein is 47 kDa. A strong additional stained band seen in lane 3 at approx. 47 kDa (marked with an arrow) corresponds to the expected *Cyc-A1* protein size. An unidentified strong protein band at approx. 42 kD was also seen in lane 4 (control strain 4 h after IPTG). Due to low protein concentration in samples before induction, max. 2.5 μ g of protein could be loaded in lanes 1 & 2. In lane 3 & 4, 10 μ g of protein was loaded. A strong protein band at approx. 40 kDa was seen, which could not be identified.

Lane 1: *E. coli* DH5 α / p CAS50 (before IPTG)

Lane 2: *E. coli* DH5 α / p JF119 Δ N (before IPTG)

Lane 3: *E. coli* DH5 α / pCAS50 (4 h after IPTG)

Lane 4: *E. coli* DH5 α / pJF119 Δ N (4 h after IPTG)

3.6.2. HPLC and LC-MS analysis of δ -Tocotrienol produced *in-vivo* in *E. coli* DH5 α / pCAS47

cyc-A1 was cloned in the artificial cluster constructed in pCAS29 to obtain a new construct pCAS47 (scheme shown in figure 3.29). This plasmid was provided by Dr. Albermann to study the *in-vivo* biosynthesis of δ -tocotrienol.

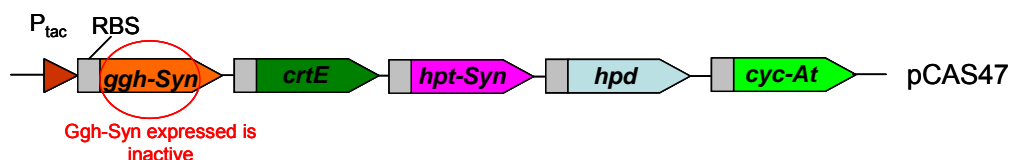


Figure 3.29: Scheme showing plasmid pCAS47. *cyc-At* was cloned into plasmid pCAS29 to obtain pCAS47. *Ggh-Syn* expressed in pCAS29 was most likely inactive (section 3.4.5). Hence, it is expected that *Ggh-Syn* would be most likely inactive in pCAS47 (same cultivation conditions in *E. coli* DH5 α /pCAS29 and *E. coli* DH5 α /pCAS47).

E. coli DH5 α / pCAS47 was cultivated in shaking flask in LB-Glycerol-Amp100 medium and as control *E. coli* DH5 α / pCAS29 was cultivated. *E. coli* DH5 α / pCAS47 culture consistently showed a long lag phase compared to the *E. coli* DH5 α / pCAS29 before induction. Cultures were induced with 1 mM IPTG (final conc.) at OD_{600nm} of 0.8 (i.e. *E. coli* DH5 α / pCAS29 after 4 h and *E. coli* DH5 α / pCAS47 after 7 h). 1 mM of IPTG was used for all over-expression experiments which were performed before studying the *in-vivo* and *in-vitro* activity. Later in this study, expression experiments with varying inducer concentrations were performed (refer section 3.18.1). After induction, the cell growth of *E. coli* DH5 α / pCAS47 was affected while it reached an OD_{600nm} of 0.95 at 12 h, from 0.79 at 7 h. On the contrary cell growth in the control (without cyclase) i.e. *E. coli* DH5 α / pCAS29 cultures after induction, grew exponential till 19 h before slowing down. It attained a stationary phase at 55 h and at the end of cultivation reached an OD_{600nm} of 5.2. *E. coli* DH5 α / pCAS47 cultures after 12 h, grew slow to reach the highest OD_{600nm} of 2.4 at 36 h. The probable reason for the poor cell growth in *E. coli* DH5 α / pCAS47 cells is unknown. One of the possible reasons could be either the toxicity of expressed *Cyc-At* proteins or the toxicity of δ -tocotrienol compound itself for *E. coli* cell growth. Two independent experiments to study the cell growth and protein expression for *E. coli* DH5 α /pCAS29 and *E. coli* DH5 α /pCAS47 cultures were performed. The standard deviation for growth curves was within $\pm 10\%$ (OD_{600nm}) and similar pattern for protein expression (2D-gel electrophoresis) was seen in respective cultures. Samples were extracted for MGGBQ and δ -Tocotrienol production and analyzed with HPLC. HPLC chromatogram is shown in figure 3.30.

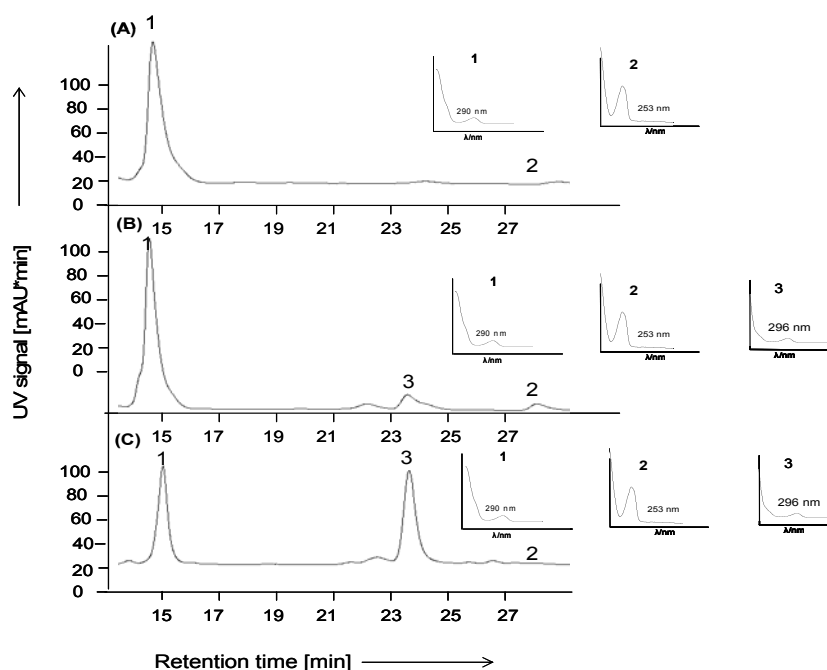


Figure 3.30: HPLC chromatogram for MGGBQ and δ -tocotrienol production. **(A)** Chromatogram representing the extract of *E. coli* DH5 α /pCAS29 sample at 290 nm. **(B)** Chromatogram representing the extract of *E. coli* DH5 α /pCAS47 sample at 290 nm. **(C)** Chromatogram showing the above sample **B** i.e. *E. coli* DH5 α /pCAS47 co-injected with δ -tocotrienol standard at 290 nm. Peak 1 at retention time (R.T) of 15.4 minutes in all samples represents reduced MGGBQ with maximum UV absorbance at 290 nm (shown in inset on right hand side). Peak 2 at R.T of approx. 23.8 minutes in (B) and (C) samples represents δ -tocotrienol with maximum UV absorbance at 296 nm (shown in subset on right hand side). Peak 3 at R.T of 28.5 minutes in all samples represents oxidized MGGBQ with maximum UV absorbance at 253 nm (shown in subset on right hand side).

At the time of induction less than 25 $\mu\text{g/g}$ CDW of MGGBQ was produced in *E. coli* DH5 α / pCAS29 while 5 $\mu\text{g/g}$ CDW in *E. coli* DH5 α / pCAS47. After induction, MGGBQ levels in *E. coli* DH5 α / pCAS29 increased to reach a maximum of 571 $\mu\text{g/l}$ after 31 h. MGGBQ production was maintained almost constant till 51 h, after that it started dropping down, presumably as a result of oxidation.

In case of *E. coli* BW25113/pCAS47, after induction with IPTG, MGGBQ yield and concentration increased till 31 h, where it reached the maximum of 372 ± 23 $\mu\text{g/g}$ CDW, before it started to decrease slowly. δ -Tocotrienol production started at 19 h (i.e. 12 h (after induction), with 3.33 ± 0.26 $\mu\text{g/g}$ CDW accumulated at 31 h. After 31 h, the δ -tocotrienol concentration started increasing steadily to reach a maximum of 15.0 ± 0.48 $\mu\text{g/g}$ CDW after 74 h. There was a sudden decrease in MGGBQ_{total} yield after 44 h, with a gradual increase in δ -Tocotrienol. Most of the MGGBQ_{reduced} was presumably oxidized, resulting in loss of MGGBQ. This may be due to prolonged incubation of the cultures. This lost MGGBQ was therefore not available as substrate for *Cyc-At*.

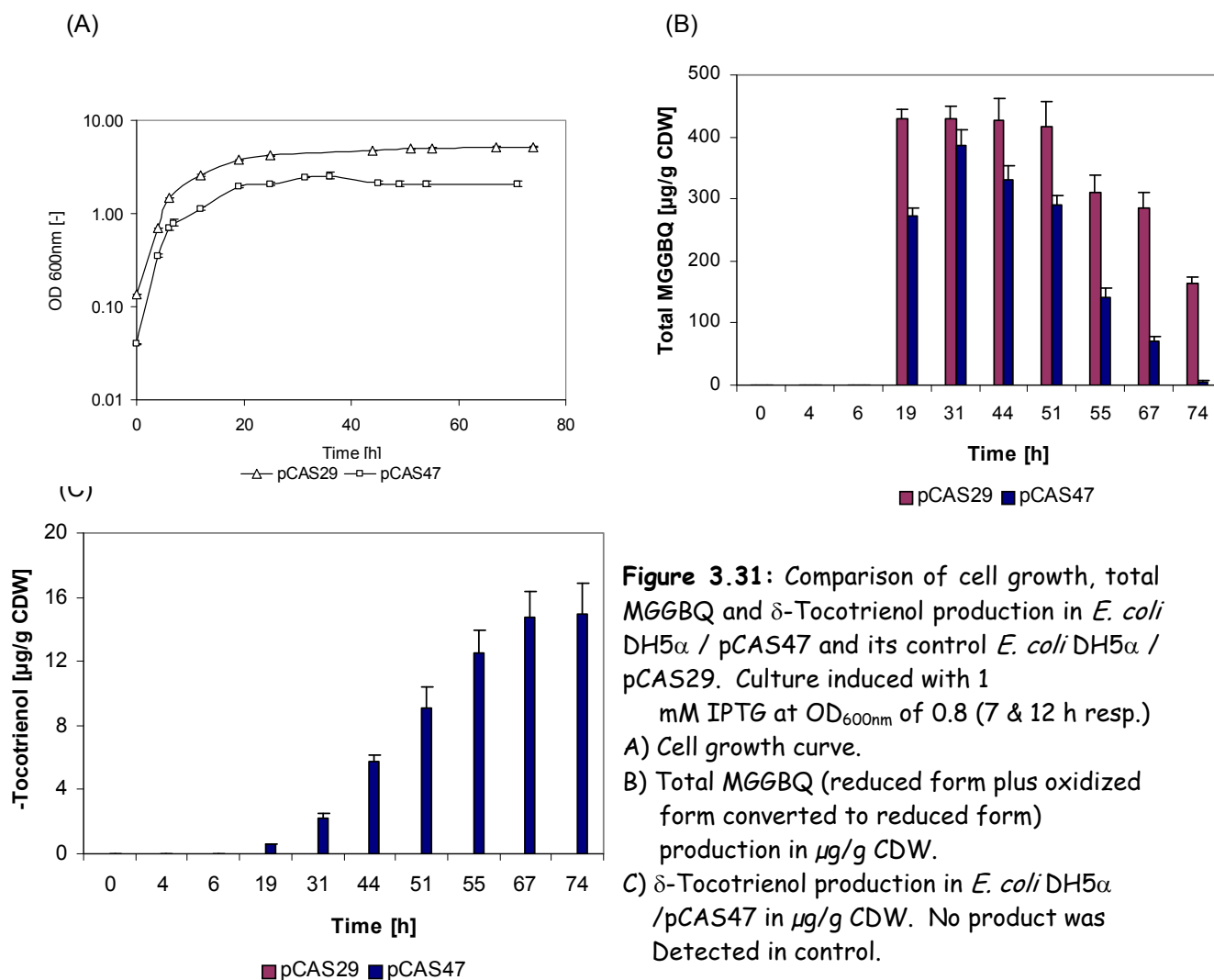


Figure 3.31: Comparison of cell growth, total MGGBQ and δ -Tocotrienol production in *E. coli* DH5 α / pCAS47 and its control *E. coli* DH5 α / pCAS29. Culture induced with 1 mM IPTG at OD_{600nm} of 0.8 (7 & 12 h resp.)
 A) Cell growth curve.
 B) Total MGGBQ (reduced form plus oxidized form converted to reduced form) production in $\mu\text{g/g}$ CDW.
 C) δ -Tocotrienol production in *E. coli* DH5 α / pCAS47 in $\mu\text{g/g}$ CDW. No product was Detected in control.

3.6.3. Characterization of extracted product from *E. coli* DH5 α /pCAS47 by LC-MS:

The extracted sample from *E. coli* DH5 α / pCAS47 was analyzed by LC-MS. Liquid Chromatography resulted in 3 major peaks peaks 1, 2, and 3 (LC chromatogram not shown here). These 3 peaks corresponded to peak 1, 2 and 3 (based on retention time) obtained during HPLC analysis (figure 3.30). The mass spectrum in positive ion mode $[\text{M}+\text{H}]^+$ for these peaks resulted in the m/z of 397 Da, 395 Da and 397 Da and $[\text{M}+\text{NH}_4]^+$ of 414 Da, 412 Da and 414 Da, respectively. This corresponded to the theoretical masses of MGGBQ_{reduced}, MGGBQ_{oxidized} and δ -Tocotrienol, respectively. MS chromatogram is shown in Figure 3.32.

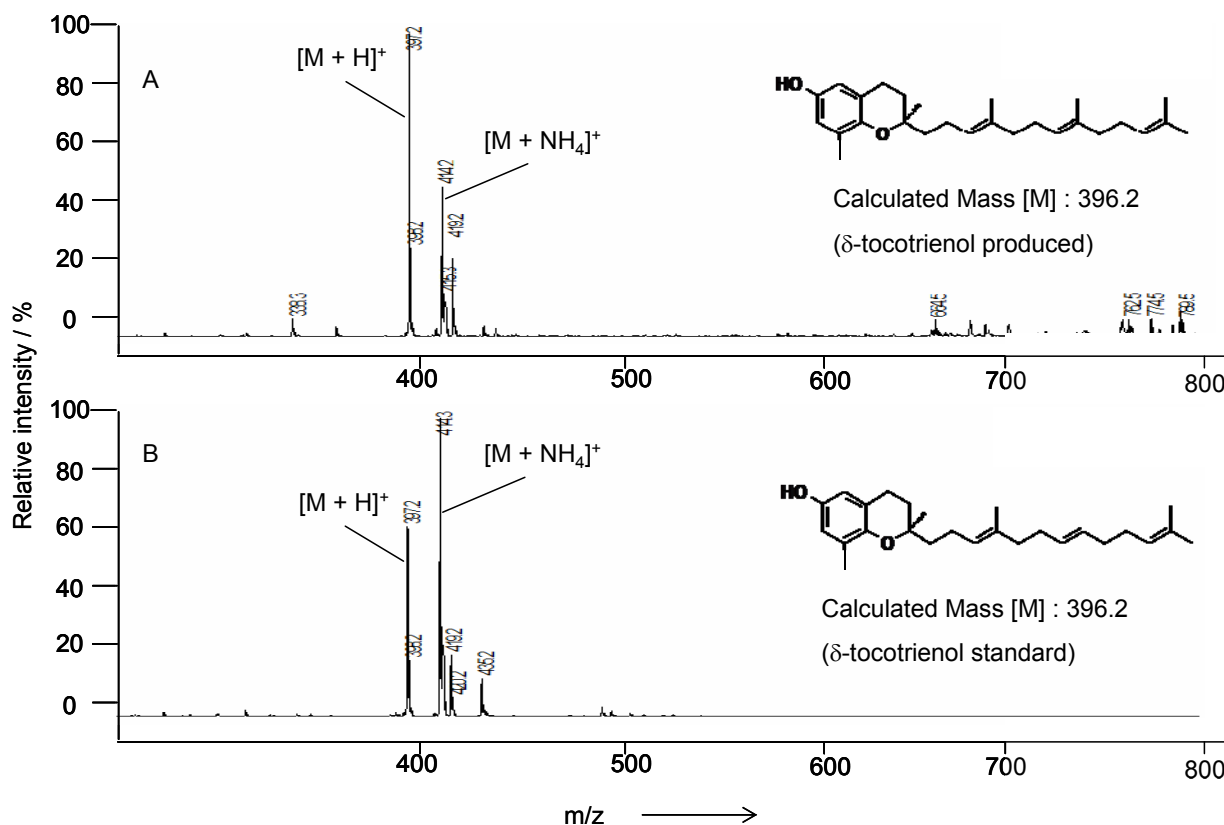


Figure 3.32: LC-MS result showing δ -tocotrienol produced in *E. coli* DH5 α /pCAS47 shown in (A) compared to the standard δ -tocotrienol MS spectrum in (B). The spectrum shown here has been obtained in a positive ion mode. Additionally, some unidentified weak signals at m/z between 600 and 800 nm were seen in the extract of *E. coli* DH5 α /pCAS47 sample.

δ -Tocotrienol biosynthesis in Infors Bioreactor with *E. coli* BW25113 / pCAS47

E. coli BW25113/pCAS47 strain was cultivated in MM-Glucose-Amp100 and in MM-Glycerol-Amp100, where glucose and glycerol respectively, were used as sole carbon and energy source. Fermentation was carried out at 30 °C, using batch-fed batch strategy. The results from these 2 cultivations are shown in figure 3.33. *E. coli* BW25113 / pCAS47 cells grew relatively slower in MM-Glycerol as compared to that in MM-Glucose, which can also be seen from the growth rate (μ) i.e. 0.18 h⁻¹ vs. 0.22 h⁻¹ respectively (refer figure 3.33 B). Cultures in MM-Glucose-Amp100 and MM-Glycerol were induced at OD_{600nm} of 2.0 (i.e. 13 h and 16.5 h respectively), with 0.25 mM IPTG (final conc.). During the batch process, cell growth in MM-glucose reached an OD_{600nm} of 4.4 (19 h) as compared to OD_{600nm} of 7.6 (26 h). Acetic acid produced in MM-Glucose was 1.91 g/l and in MM-Glycerol was 0.82 g/l during the respective period (i.e. batch process). After the start of fed-batch process, i.e. 19 h (MM-Glucose) and 26 h (MM-Glycerol), the growth rate in MM-Glycerol was higher as compared to that in MM-Glucose. The total acetic acid produced in MM-Glucose at the end of cultivation was 3.42 g/l as compared to 1.97 g/l in MM-Glycerol. As a result, cell density reached in MM-Glucose

was approx. 30 % lower (OD_{600nm} of 17.8) than, that reached in MM-Glycerol (OD_{600nm} of 26.1). During the fed-batch process, the concentration of glucose or glycerol in bioreactor was maintained such that the carbon source (glucose or glycerol) at anytime during the cultivation is limited. Hence, the concentration of glucose or glycerol at any point of time didn't exceed 0.15 g/l.

Even though, cultures in MM-Glycerol grew at lower growth rates than in MM-Glucose, MGGBQ_{Reduced} production started at 13 h. MGGBQ_{reduced} and MGGBQ_{oxidized} yields are shown in figure 3.34. No MGGBQ_{oxidized} was detected in MM-Glycerol or MM-Glucose at 13 h. In MM-Glucose, the MGGBQ_{reduced} yield ($\mu\text{g/g CDW}$) increased sharply between 13 and 21.5 h before starting to decrease. In contrast, in the rise in MGGBQ_{reduced} yield ($\mu\text{g/g CDW}$) in MM-Glycerol was low between 13 and 33 h compared to that in MM-Glucose. The MGGBQ_{reduced} yield in MM-Glucose after 21.5 h, started dropping steeply i.e. from 925 $\mu\text{g/g CDW}$ to 59 $\mu\text{g/g CDW}$ at 42 h. In both cultures at any time during cultivation, the MGGBQ_{oxidized} yield was below 15 $\mu\text{g/g CDW}$. At 42 h the colour of broth in MM-Glucose had already turned brown. The culture supernatant colour at 42 h (MM-Glucose) was light brown but the cell pellet was much darker. The highest HGA concentration in culture supernatant analysed were 0.95 mM (in MM-Glucose at 48 h) and 1.23 mM (in MM-Glycerol at 58 h). This may perhaps be due to the oxidation of MGGBQ with apparent polymerization. This also may explain that the MGGBQ_{oxidized} yields were low. Another reason for the decrease in MGGBQ_{reduced} yield was the formation of δ -tocotrienol between 25.25 h and 48 h. In contrast, MGGBQ_{oxidised} yields were constant between 26 h and 33 h and increased slightly between 33 h and 43.5 h. The decrease in MGGBQ_{reduced} after 25.25 h was also gradual, as the increase with low level of MGGBQ_{oxidised} formed. The culture supernatant at 43.5 h was slightly brown, and cell pellet colour pale/white. MGGBQ productivity in terms of MGGBQ_{total} produced per gram of carbon (glucose or glycerol) consumed in case of MM-Glucose (199 $\mu\text{g/g glucose}$) was 1.68 times higher than achieved in MM-Glycerol (118 $\mu\text{g/g glycerol}$), at different times during cultivation. Possible polymerisation product(s) of MGGBQ_{oxidised} could not be identified and quantified in this study.

δ -Tocotrienol concentration and yield in MM-Glucose increased gradually from 25.25 h to 48 h to reach the maximum of 50.6 $\mu\text{g/l}$ and 9.4 $\mu\text{g/g CDW}$ respectively after 48 h. δ -Tocotrienol concentration and yield in MM-Glycerol production started before 29.25 h and increased gradually to reach a maximum of 43.1 $\mu\text{g/l}$ and 5.3 $\mu\text{g/g CDW}$ at 55.5 h. Cultivation in MM-Glucose and MM-Glycerol produced approximately similar amounts of δ -tocotrienol in terms of $\mu\text{g/l}$ and in terms of carbon flux into δ -tocotrienol (see figure 3.35 and 3.36 resp.). The δ -tocotrienol yields in terms of ($\mu\text{g/g CDW}$) are different in numbers due to the fact that the cell

dry weight reached in MM-Glucose was lower than that achieved in case of MM-Glycerol-Amp100.

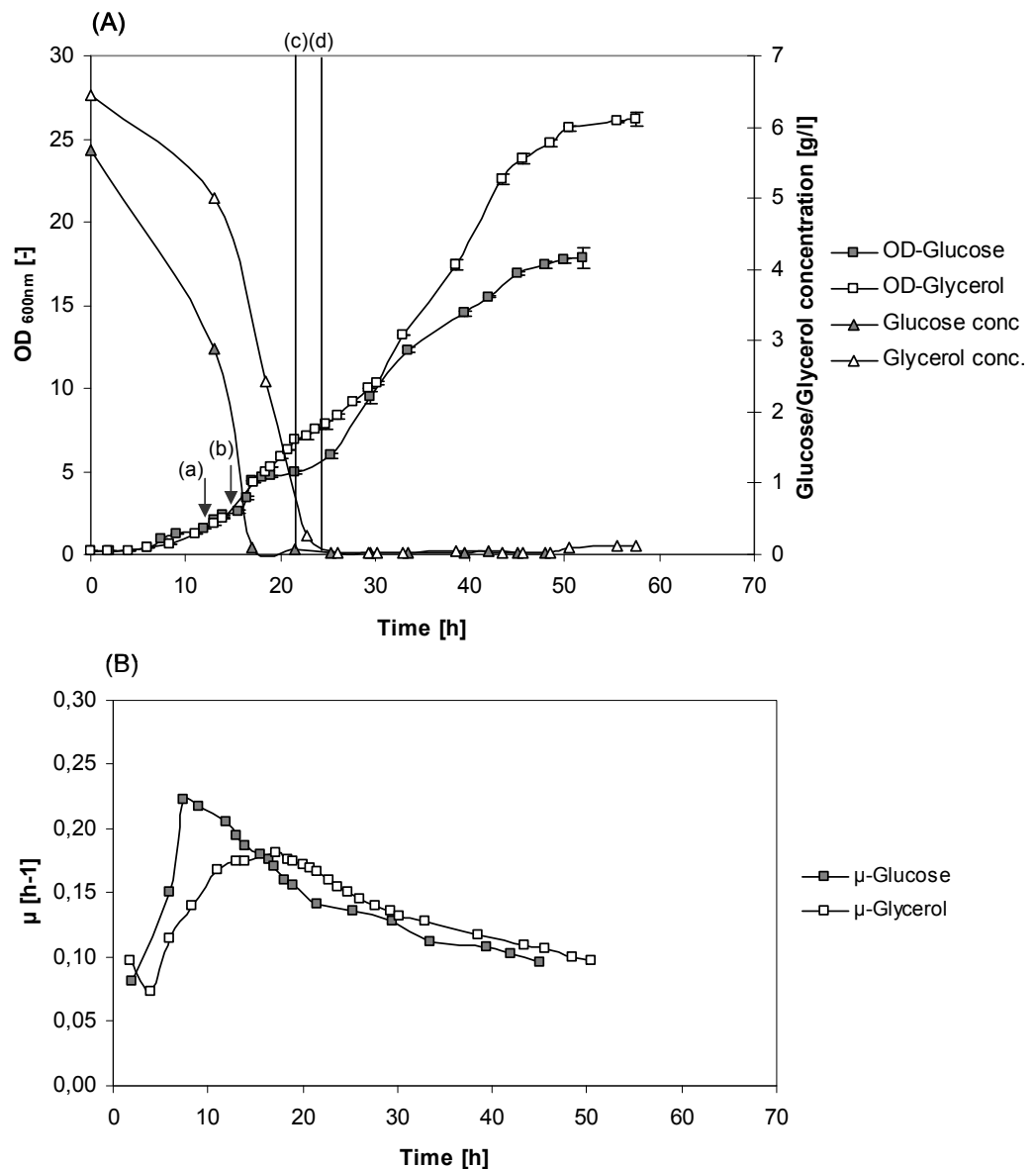


Figure 3.33: Cultivation results of *E. coli* BW25113 / pCAS47 in 3.6 L Infors HT bioreactor in minimal medium using glucose and glycerol as carbon, energy source (30°C). Cultures induced with 0.25 mM IPTG (shown by arrows). **(A)** Cell growth curve (represented by OD_{600nm} scale on left hand side). (a) and (b) shows the time of induction with 0.25 mM IPTG in glucose and glycerol resp. (c) and (d) shows the time of start of glucose and glycerol feeding resp. Filled squares represents OD_{600nm} in glucose as carbon source and empty squares represents glycerol as carbon source. Glucose (filled triangles) and Glycerol (empty triangles) concentration in bioreactor during cultivation (scale on right hand side) **(B)** Growth rate (μ) in h⁻¹ calculated during cultivation. Cultivation was done according to conditions mentioned in section 2.2.3. In total two cultivations were carried out in MM-Glucose-Amp100 and two cultivations in MM-Glycerol-Amp100 medium. The standard deviation between the two cultivations was below ± 20 % w.r.t total MGGBQ and below ± 10 % w.r.t. δ -tocotrienol.

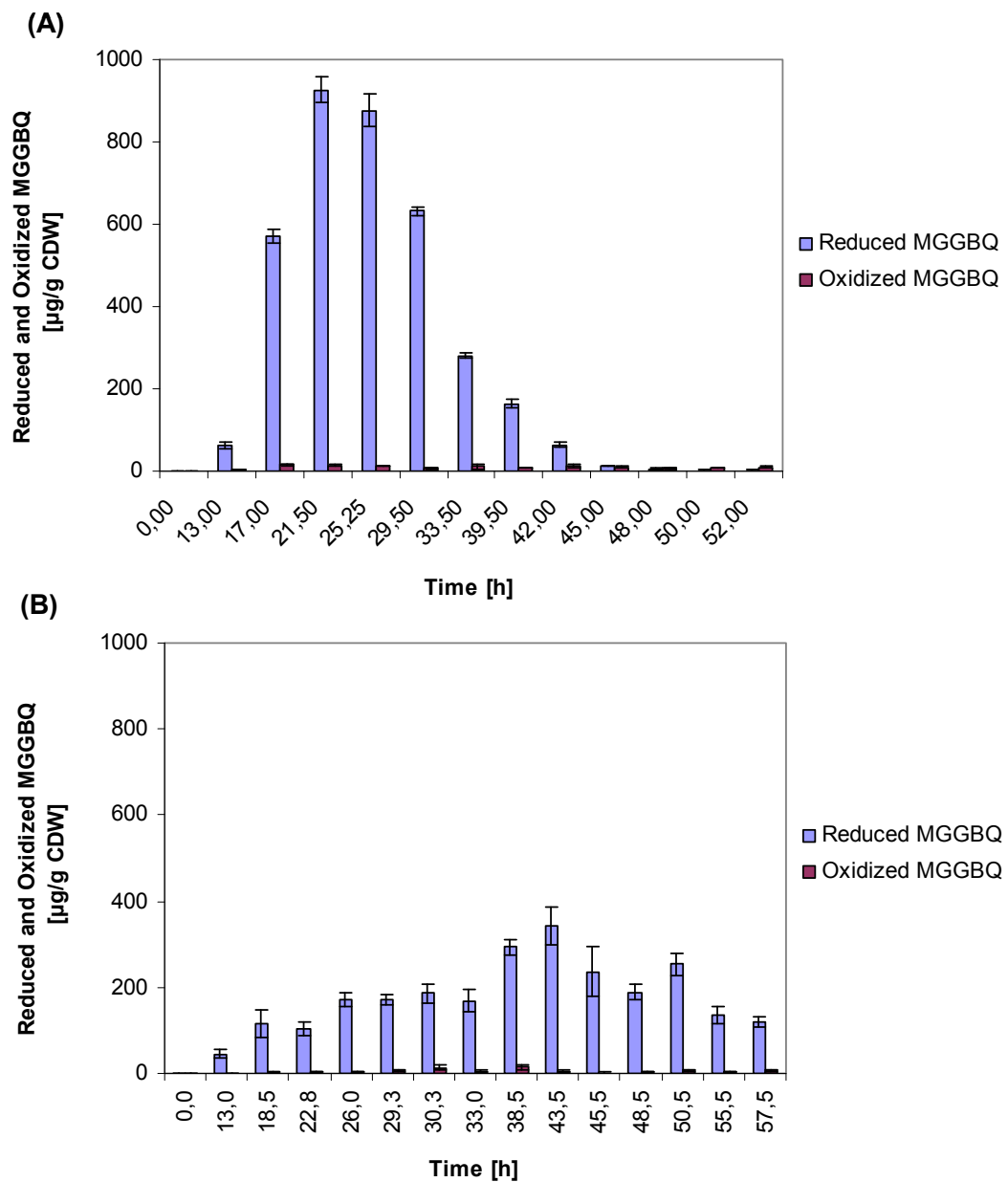


Figure 3.34: Yields of $MGGQBQ_{reduced}$ and $MGGQBQ_{oxidized}$ reached during cultivation of *E. coli* BW25113/pCAS47 in bioreactor at 30°C in minimal medium using different carbon sources.

(A) in Glucose

(B) in Glycerol

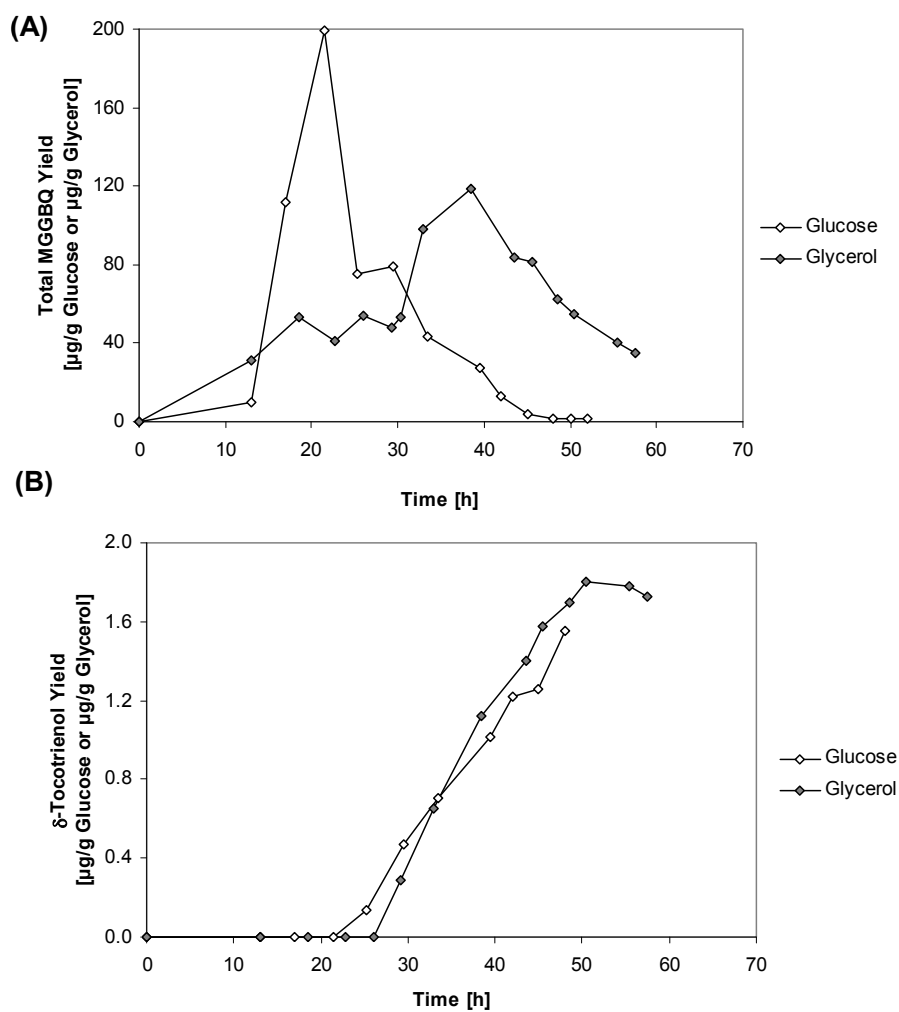


Figure 3.35: Total MGGBQ and δ -Tocotrienol product yields during cultivation of *E. coli* BW25113/pCAS47 in bioreactor at 30°C in minimal medium using different carbon sources. (A) Glucose (B) Glycerol

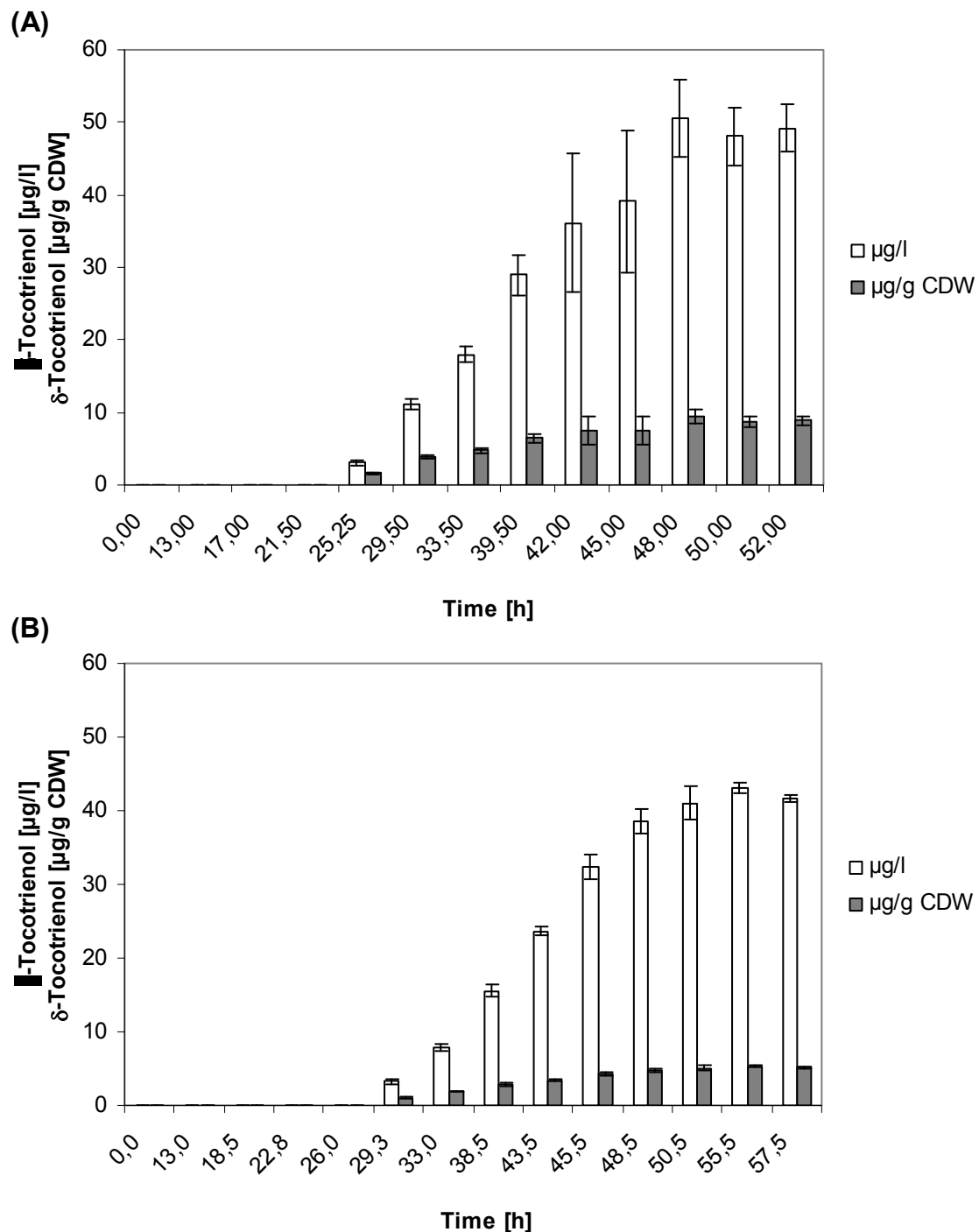


Figure 3.36: MGGBQ_{total} and δ -tocotrienol yield (μg per gram of carbon source consumed) during cultivation of *E. coli* BW25113/pCAS47 in bioreactor at 30°C in minimal medium using different carbon sources. (A) MGGBQ_{total} yield (B) δ -Tocotrienol yield

δ -tocotrienol concentration and yield w.r.t time, during the entire cultivation didn't decrease. No evidence for any decay or oxidation of δ -tocotrienol was observed as seen with MGGBQ_{reduced}. In this section, it was successfully shown that δ -tocotrienol can be produced in recombinant *Escherichia coli* strain carrying a multi-copy plasmid using either glucose or glycerol as the sole carbon and energy source.

B) Microbial Synthesis of δ -Tocotrienol using *E. coli* strain carrying chromosomal inserted heterologous genes

All the five vitamin E biosynthesis genes (i.e. for δ -tocochromanol biosynthesis) cloned individually in vector pJF119 Δ N (i.e. pCAS2JF, pCAS30, pCAS7, pCAS8 and pCAS50) and all combined in vector pJF119 Δ N (i.e. pCAS47) were shown to over-express recombinant proteins in *E. coli* (except that of Ggh-Syn in pCAS29 and pCAS47, explained in section 3.16 and 3.17). It was also shown that the use of multi-copy plasmids pCAS29 and pCAS47 for production of pathway products MGGBQ and δ -tocotrienol resp. was not desired due to there segregational instability in holding the plasmids in host strain during cultivation in bioreactor.

To overcome these disadvantages, a stable recombinant *E. coli* strain was to be constructed by inserting heterologous genes in the chromosome of *E. coli* using the homologous recombination technique, similar to described in Datsenko and Wanner 2000. Some of the rare sugar degradation gene loci on the *E. coli* chromosome were chosen as target region for insertion of the expression cassettes (Albermann et.al.2010). Use of sugar degradation genes offers an advantage in accurate screening of the newly constructed strains (by homologous recombination). Screening was carried out on MacConkey agar plates supplemented with corresponding sugar(s) at 1 % (final conc.). Specifically, L-fucose, maltose, lactose, D-xylose and D-ribose degradation operon were selected to insert *hpd*, *crtE*, *hpt-Syn*, *cyc-At* and *idi* expression cassettes respectively. These sugars listed, are not essential for any laboratory application in this study (e.g. cultivation in complex or minimal medium experiments). Results showing, how these chromosomally integrated strains were constructed, and its respective product yield in shaking flask and bioreactor cultivation are mentioned in detail in section 3.2.1 onwards. As an example, detailed procedure and results are shown for insertion of *hpd* expression cassette in fucose operon, and, insertion of further expression cassettes was performed in a similar way. Apart from these results, the details of the construction of the chromosomally integrated strains (using homologous recombination methods) are mentioned in section 2.2.1.6, 2.2.1.7.

3.7. *In-vivo* biosynthesis of HGA in recombinant *E. coli*

3.7.1. Construction of *E. coli* CS1 strain

Chromosomal Integration of *hpd* expression cassette in fucose operon of *E. coli* BW25113 *lacZ*⁺ and *E. coli* LJ110

Plasmid pCAS2JF used previously for HGA production was modified by ligation (section 2.2.4) of HindIII digested 1.1 kB FRT-*cat*-FRT fragment in 6.2 kB HindIII digested pCAS2JF fragment. Ligation mixture was incubated overnight at 16°C. Chemical transformation (section 2.1.5) of overnight ligation mixture in chemical competent (section 2.2.1.5) *E. coli*

DH5 α cells resulted in 12 transformants after overnight incubation on LB-Amp100-Cm25 agar plates at 37°C. Plasmid isolated from these transformants, was named as pCAS2JF-cat-FRT and was further tested by digesting (2.2.2.4) the plasmid with restriction enzymes. Digestion with HindIII resulted in approx. 1.1 & 6.2 kB fragments and digestion with NdeI resulted in approx. 1.1, 2.9 and 3.4 kB fragments (approx. sizes calculated based on R_f method). Clone manager 7.0 was used to calculate the expected fragment sizes after digestion with restriction enzymes. The sizes of DNA fragments predicted after digestion were, 1085 and 6394 bps kB with HindIII, and 1145 bp, 2909 bps and 3425 bps with NdeI (calculated using clone manager program). The experimental results obtained closely corresponded with the expected fragment sizes calculated by Clone manager 7.0. Out of 12 plasmids isolated from 12 transformants, only 4 plasmids had the correct sizes, based on the above results of digestion with restriction enzymes.

The correct pCAS2JF-FRT-cat-FRT plasmid (isolated from positive clone nr. 1) was used as template for PCR amplification (2.2.2.2). Primers “*fucI* - integr”, and “*fucP* - integr” (table 2.1.2.5) were used for amplification of the DNA fragment *Ptac-hpd*-FRT-*cat*-FRT from plasmid pCAS2JF-FRT-*cat*-FRT. The resulting PCR fragment i.e. *Ptac-hpd*-FRT-*cat*-FRT has a region homologous to specific base pairs (50-70 nt) in *fucI* and *fucP* loci. *E. coli* BW25113 strain carrying plasmid pKD46 (ampicillin resistant plasmid expressing λ -recombinase induced by arabinose) was transformed by electroporation (2.2.1.5) with the PCR amplified fragment *Ptac-hpd*-FRT-*cat*-FRT, spread on LB+Cm25 agar plates, and incubated overnight at 30°C.

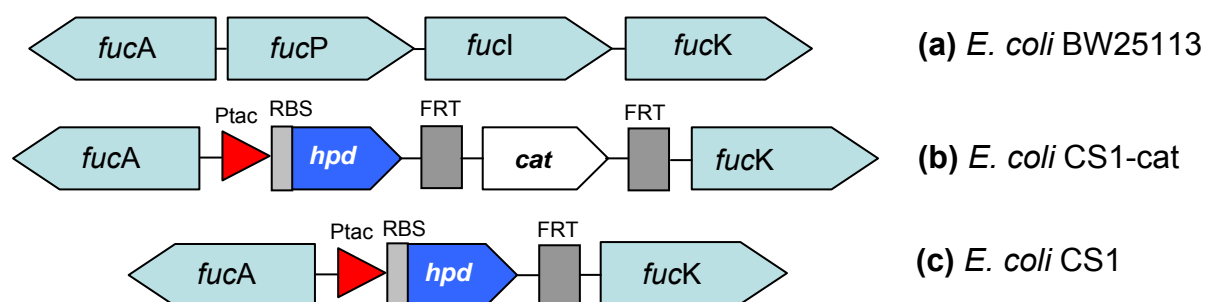


Figure 3.37: Scheme showing chromosomal integration of *hpd* gene in fucose locus. (a) Showing wild type *E. coli* BW25113 (*lacZ*⁺) strain with *fucA*, *fucP*, *fucI* & *fucK* loci all in place before integration. (b) The site of fucose locus after integration of *Ptac-hpd*-FRT-*cat*-FRT in *fucP* & *fucI* region of *E. coli* BW25113 (*lacZ*⁺) chromosome. (c) The final strain after removal of chloramphenicol residual cassette (*cat*) with *Ptac-hpd* integrated at the site of *fucI* and *fucP* i.e. *fucIP::P_{tac}-hpd*. The gene sizes in this figure are not drawn to the scale.

4 clones obtained on LB-Cm25 agar plates were tested on MacConkey agar plates supplemented with L-fucose (1 % w/v final concentration). Wild type *E. coli* BW25113 where the fucose operon is still intact is able to utilize L-fucose hence producing acid. This reduces

the pH below 6.8 hence turning the colourless neutral red dye (one of the ingredients of MacConkey agar) into pink/red colour, which in turn gives the colonies pink/red colour. Clones tested on MacConkey agar plates with fucose which remained pale/white in colour after incubation, were termed as positive clones. Out of the 4 clones tested on MacConkey agar plates with L-fucose, only one was positive, and other 3 were negative (i.e. those which turned red). The positive clone obtained was *E. coli* BW25113 *fucIP::Ptac -hpd-FRT-cat-FRT* and named as *E. coli* CS1-*cat* for convenience. *E. coli* CS1-*cat* was tested further with colony PCR using primers 9, 10 and 11, 12 (table 2.4). Primer position is shown in figure 3.38. PCR with primers 9 and 10 resulted in 1.1 kB and with 11 and 12 resulted in 1.4 kB DNA fragments which correspond to the expected sizes.

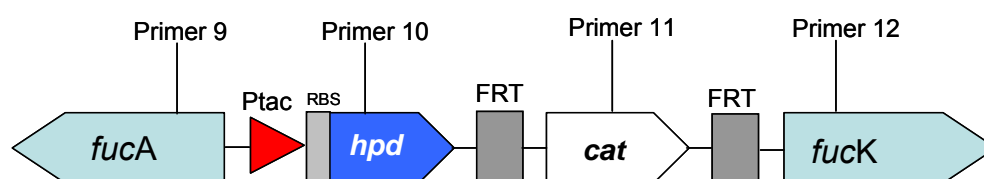


Figure 3.38: *E. coli* CS1-*cat* strain showing the location of PCR control primers. These control primers were used for colony PCR, to verify the correct position of insertion of *hpd* expression cassette in fucose operon. For primers 9, 10, 11 and 12, refer to table 2.4.

E. coli CS1-*cat* was transformed with plasmid pCP20 (Cherepanov and Wackernagel 1995) that carries a FLP recombinase which recognises the FRT site for the removal of chloramphenicol resistance cassette (*cat*). This resulted in a chloramphenicol resistance (Cm) free strain called *E. coli* CS1. Hence, *E. coli* CS1 now has a single copy of *hpd* gene integrated in place of the *fucI* and *fucP* locus (see Figure 3.3)

Wild type *E. coli* W3110 (also known as LJ110, Zeppenfeld et. al. 2000) is widely used as production strain (*E. coli* W3110 were used for, homoacetate production by Causey et.al. 2003; for the production of L-phenylalanine and other aromatic amino acids by Oldiges et.al. 2004; lactic acid production by Zhou et. al. 2003 etc.). In this study, it was decided to use *E. coli* LJ110 as host strain in shaking flask and bioreactor cultivations as production strain, for synthesis of δ -tocochromanol pathway intermediates and products. Hence, transduction was used to transfer the *hpd* expression cassette in the chromosome of *E. coli* LJ110. *E. coli* CS1-*cat* (a derivative of *E. coli* MG1655, *E. coli* BW25113) was infected with P1 lysate (see 2.2.1.8.) to obtain phage lysate carrying (among others) *fucIP::Ptac -hpd-FRT-cat-FRT* gene fragment. Transduction (see 2.2.1.8) of *E. coli* LJ110 with the above phage lysate resulted in 25 transductants, selected on LB plates with chloramphenicol. Transductants obtained were tested on MacConkey agar supplemented with L-fucose. All transductants had the pale/white phenotype, meaning that all transductants were positive i.e. *hpd* expression

cassette was successfully inserted in host *E. coli* LJ110. Removal of phage particles adhering on transductant colonies was carried out by colony purification (3 times) on LB-Cm25 agar plates. If no cell lysis is observed (visual test for ragged or smooth colony shape) after overnight incubation at 37 °C, the transductants were considered to be free of phage particles. After the colony purification, based on the above visual test, it was considered that all the transductants were free of phage particles. Hence, the new strain obtained i.e. *E. coli* LJ110 *fucIP::Ptac-hpd-cat* was named as *E. coli* CS1.1-cat. Control PCR tests with primers 9, 10 and 11, 12 resulted in bands of approx. 1.1 kB and approx. 1.4 kB respectively, as expected. Removal of *cat* resistance cassette yielded *E. coli* CS1.1 strain. *E. coli* CS1.1 was tested with control PCR with primer 9, 10 to result in 1.1 kb fragment which was expected. Due to the elimination of chloramphenicol resistance cassette PCR with control primers 11 and 12 was not performed. *E. coli* CS1.1 and wild type *E. coli* LJ110 strains were spread on MacConkey agar plate supplemented with 1 % (w/v) L-fucose and incubated overnight at 37°C. Such an agar plate is shown in figure 3.39.



Figure 3.39: MacConkey agar plate with 1 % (w/v) L-fucose.

- (a) *E. coli* LJ110 *fucIP::Ptac-hpd* (*E. coli* CS1.1)
 (b) *E. coli* LJ110 (wild type)

3.7.2. HGA Biosynthesis in *E. coli* CS1 in Shaking Flask Cultivation

After successful integration of the *fucPI::Ptac-hpd* expression cassette into *E. coli* BW25113 *lacZ⁺* strain, it was important to verify the activity of Hpd. This was tested *in-vivo*, in a shaking flask cultivation experiment. *E. coli* CS1 was cultivated in shaking flask in minimal medium using glucose or glycerol as sole carbon and energy source at 30 °C. As control, parent strain *E. coli* BW25113 *lacZ⁺* was cultivated under same conditions. Cultures were induced with 0.25 mM IPTG (final conc.) at OD_{600nm} of 0.8. *E. coli* CS1 and its parent strain, reached similar cell densities (OD_{600nm} of 5.7 and 6.2 resp., see fig. 3.40), in glucose as carbon source. While in case of glycerol, cell growth of *E. coli* CS1 ceased after 27 h (OD_{600nm} of 5.3), while the parent strain grew further and reached higher cell density of OD_{600nm} of 6.8 after 42.5 h. Both strains in glycerol as carbon source grew slower, than those in glucose, before and after induction.

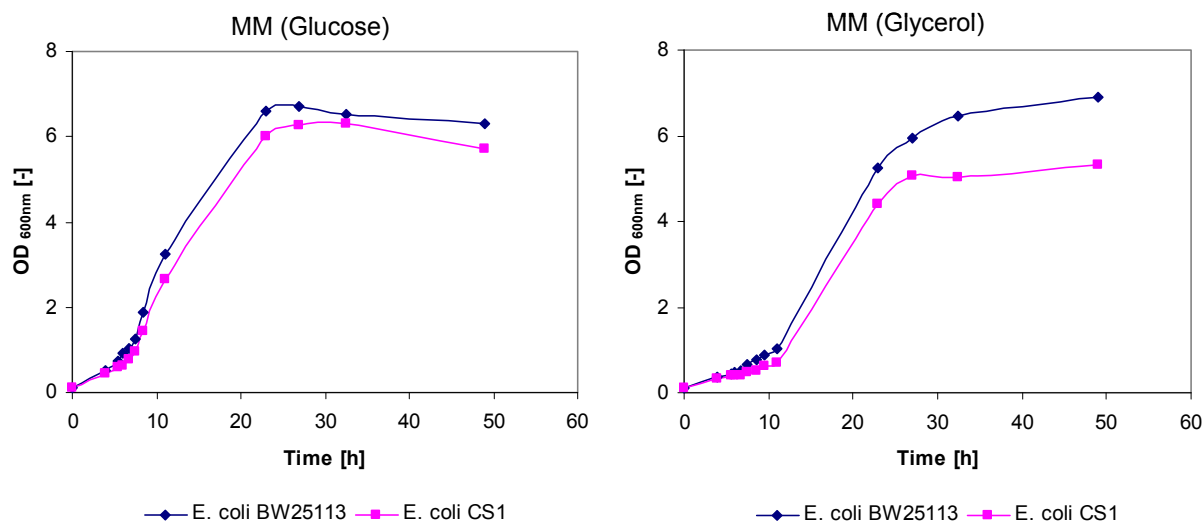


Figure 3.40: Comparison of cell growth curve in chromosomal integrated strain *E. coli* CS1. *E. coli* CS1 (in pink) and its host *E. coli* strain *E. coli* BW25113 *lacZ* (in blue) cultivated in shaking flask in minimal medium with different glucose sources. (A) Glucose (B) Glycerol. Cultures induced with 0.25 mM IPTG, at OD_{600nm} of 0.8.

HGA analysed by HPLC in supernatant samples of *E. coli* CS1 showed that the HGA production (shown in figure 3.41) in glucose started early (at 11 h) and increased 5 times at 23 h, before reaching the maximum level of 749 µg/l after 32.5 h. HGA production in *E. coli* CS1 in glycerol, started between 11 and 23 h, before it reached the highest level of 869 µg/l after 32.5 h. Supernatant from *E. coli* CS1 in glucose and in glycerol started turning brown after 32.5 h and at the end cultivation (42.5 h), the cultures turned dark brown (similar to as observed in section 3.1, figure 3.5B). HGA concentration started decreasing, as a result of HGA oxidation and further polymerization to form brown ochronotic pigments. No *p*-HPP was detected in any of the *E. coli* CS1 supernatant samples. In the parent strain neither *p*-HPP nor HGA was detected in any of the supernatant samples. To conclude, single copy of *hpd* gene in *E. coli* CS1 was sufficient to expression Hpd protein which successfully produced the aromatic precursor HGA for δ-tocochromanol synthesis.

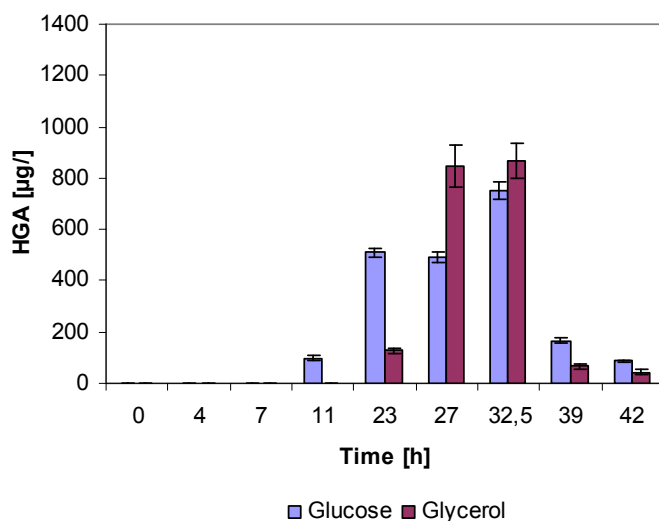


Figure 3.41: HGA production in chromosomally integrated strain *E. coli* CS1. Shaking flask cultivation in minimal medium with glucose or glycerol as sole carbon and energy source. Cultures were induced with 0.25 mM IPTG at $OD_{600\text{nm}}$ of 0.8. HGA shown in terms of concentration in μg per liter of medium. No HGA detected in the parent strain *E. coli* BW25113 *lacZ*⁻ and hence not shown in this figure.

3.8. *In-vivo* biosynthesis of GGPP in recombinant *E. coli*

3.8.1. Construction of *E. coli* CS2 strain

Chromosomal Integration of *crtE* Expression Cassette in *E. coli* BW25113 and *E. coli* LJ110

Plasmid pCAS30 was modified by ligation of HindIII / HindIII digested 1.1 kB FRT-*cat*-FRT fragment in 6.2 kB HindIII / HindIII digested pCAS30 fragment. Ligation and chemical transformation in *E. coli* BW25113 *lacZ*⁺ strain resulted in more than 50 transformants. Plasmid isolated from 4 transformants was digested with HindIII and NdeI/BamHI resulted in 1.1 & 6.2 kB and 0.9 kB and 6.4 kB fragments respectively. This new plasmid construct was pCAS30-FRT-*cat*-FRT.

Plasmid pCAS30-FRT-*cat*-FRT was used as template for PCR. Primers *malE*-integr and *malG*-integr (i.e. primer nr. 3 & 4 from table 2.1.2.5) were used for amplification of a fragment of expression cassette, i.e. *P*_{tac}-*crtE*-FRT-*cat*-FRT. This resulting amplified fragment of the expression cassette has a region homologous to 22 base pairs in *malE* and *malG* loci. *E. coli* BW25113 *lacZ*⁺ strain carrying a plasmid pKD46 (expressing λ -recombinase induced by arabinose) was transformed by electroporation with the fragment *P*_{tac}-*crtE*-FRT-*cat*-FRT.

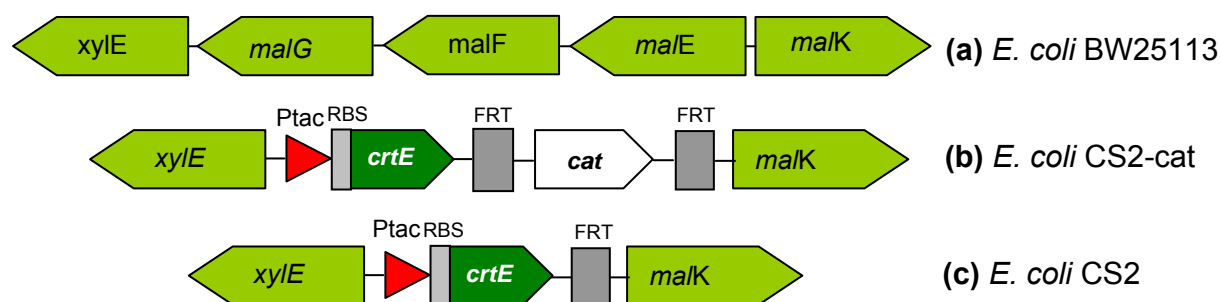


Figure 3.42: Chromosomal integration of *crtE* in *malEFG* locus of *E. coli* BW25113 strain. (a) Representing the intact maltose operons in wild type *E. coli* BW25113 strain (*lacZ*⁺). (b) *malEFG* locus being knocked out and knocked in by *P*_{tac}-*crtE*-FRT-*cat*-FRT fragment to obtain new strain *E. coli* CS2-*cat*. (c) Strain *E. coli* CS2-*cat* after getting rid of one FRT site along with the chloramphenicol resistance cassette to obtain *E. coli* CS2 strain. The sizes of each gene are not drawn to its respective scale.

11 clones obtained on LB-Cm25 agar plates were tested on MacConkey agar plates supplemented with maltose (1 % w/v final concentration). 6 clones remained white/pale i.e. were positive. These positive clones of new strain obtained was *E. coli* BW25113 *malEFG*::*P*_{tac}-*crtE*-FRT-*cat*-FRT, and named as *E. coli* CS2-*cat* for convenience. *E. coli* CS2-*cat* was tested further with colony PCR using primers 13, 14 and 15, 16 (table 2.1.2.5). Primer position is shown in figure 3.43. PCR with primers 13 and 14 resulted in 1.0 kB and with 15 and 16 resulted in 1.4 kB fragments which correspond to the expected size.

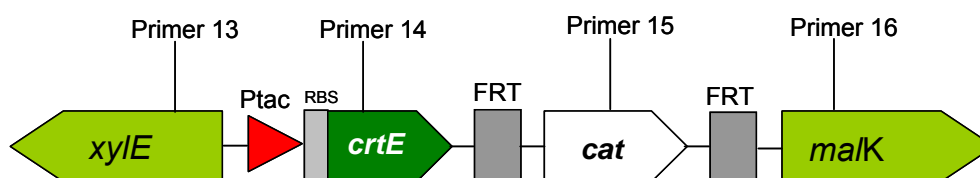


Figure 3.43: Showing the *E. coli* CS2-*cat* strain and the location of PCR control primers used for colony PCR to verify the correct position of insertion of *crtE* expression cassette in maltose operon. For primers 13, 14, 15 and 16 refer table 2.1.2.5.

Removal of chloramphenicol resistance cassette (*cat*) from *E. coli* CS2-*cat* was performed using same method as described previously to obtain *E. coli* CS2. MacConkey agar test and control PCR performed. The same transduction method was used to transduce *E. coli* LJ110 with phage lysate prepared from *E. coli* CS2-*cat* to chloramphenicol resistance. Single colony purification yielded a new strain *E. coli* LJ110 *malEFG::Ptac-crtE-FRT-cat-FRT* named as *E. coli* CS2.1-*cat*. Removal of *cat* cassette yielded a new strain, which was named as *E. coli* CS2.1.

3.8.2. GGPP Production in Bioreactor in *E. coli* CS2.1

E. coli CS2.1 and *E. coli* LJ110 (as control) were cultivated in a 3.7 l KLF2000 bioreactor (Bioengineering AG, Switzerland) at the Institute of Biochemical Engineering. Cultivation was carried out in 1.8 l minimal medium 2 (see 2.1.3) using glucose as sole carbon and energy source. Comparison of cell growth curve, FPP and GGPP production is shown in figure 3.44 (A, B and C). Both cultures were induced with 0.1 mM IPTG in exponential phase (approx. OD_{500nm} of 2.0). (the IPTG conc. was based on the best results from shaking flask cultivation w.r.t. cell growth, glucose consumption and acetate; results not shown here; personal communication with Mr. Vallon) 5.83 h after inoculation, the cell density represented in OD_{500nm} in both cultures were identical. (Note: standard wavelength for OD measurement at the Institute of Bioprocess Engineering, IBVT), during fermentation of *E. coli* strains was 500 nm. Hence the OD measurement for GGPP experiments which were carried out at IBVT were performed at 500 nm, compared to 600 nm for HGA, MGGBQ and δ -tocotrienol experiments carried out at Institute of Microbiology). *E. coli* CS2.1 reached stationary phase at OD_{500nm} of 14.4 (7 h) and *E. coli* LJ110 at OD_{500nm} of 17.9 (7.3 h). At this point, the initial 8.8 g/l glucose used as sole carbon and energy source was utilized for biomass, energy, product, and for by-product formation. The cell density in both cultures decreased, before the respective cells started using the by-product acetic acid as carbon source to reach higher cell densities. Stationary phase ended at 12.3 h in both cultures, and fermentation was stopped after 30 h. Isoprenoid analysis (isolation and GC-MS method described in 2.2.4.6) showed formation of FPP in *E. coli* LJ110, while, no FPP was detected in *E. coli* CS2.1.

Main product detected in *E. coli* CS2.1 was GGPP. At the time when initial glucose was exhausted, maximum GGPP level (668 nM) was reached. GGPP concentrations remained more or less constant till the end of fermentation. Surprisingly, weak signals for GGPP during MS analysis of *E. coli* LJ110 were detected. A small amount of GGPP (10 ± 5 nM) in *E. coli* LJ110 was quantified.

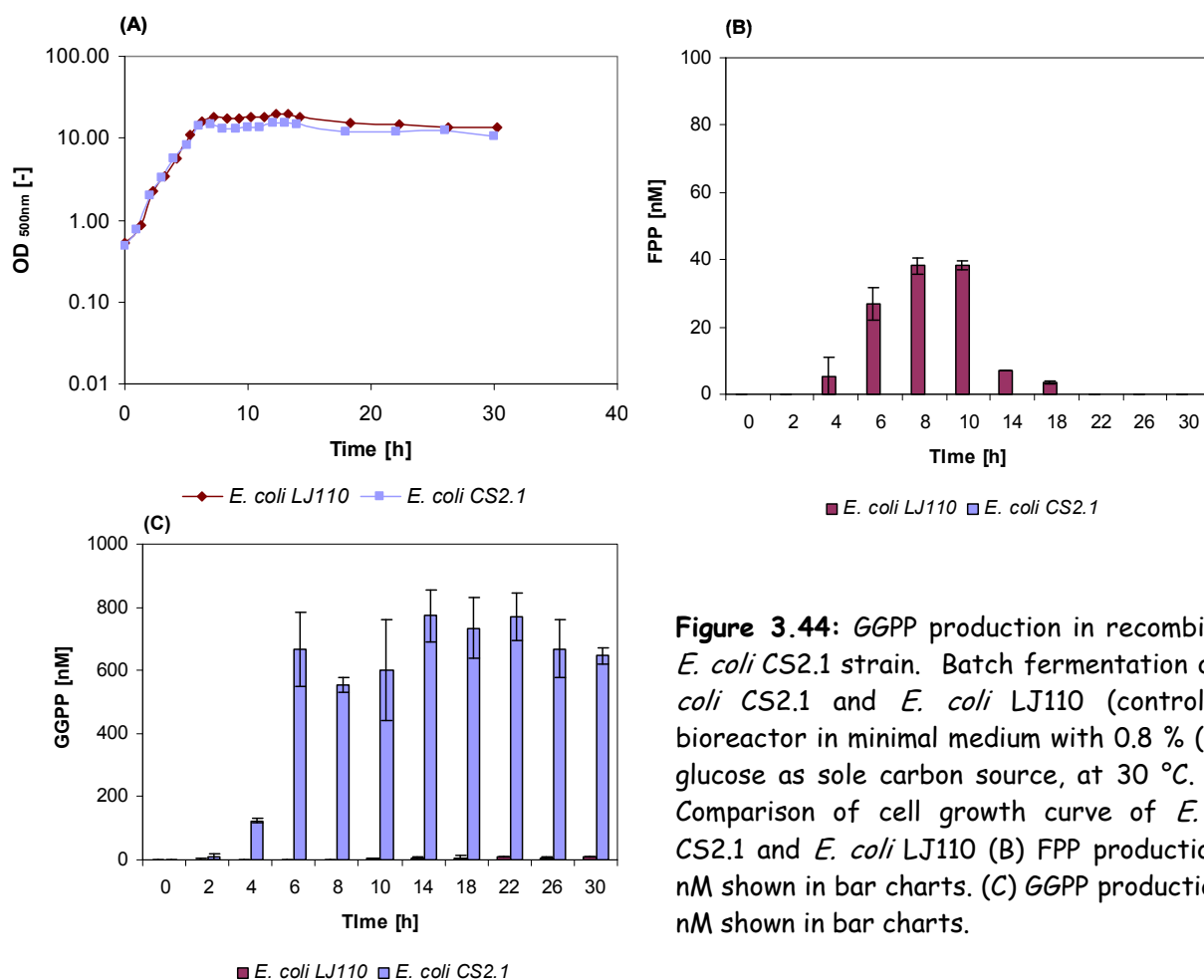


Figure 3.44: GGPP production in recombinant *E. coli* CS2.1 strain. Batch fermentation of *E. coli* CS2.1 and *E. coli* LJ110 (control) in bioreactor in minimal medium with 0.8 % (w/v) glucose as sole carbon source, at 30 °C. (A) Comparison of cell growth curve of *E. coli* CS2.1 and *E. coli* LJ110 (B) FPP production in nM shown in bar charts. (C) GGPP production in nM shown in bar charts.

Table 3.11: Acetic acid accumulated during GGPP production.

Time [h]	Acetic acid [g/l]	
	<i>E. coli</i> LJ110	<i>E. coli</i> CS2.1
0	0.34 ± 0.05	0.24 ± 0.03
2.27	0.52 ± 0.08	1.95 ± 0.12
5.27	0.71 ± 0.11	1.61 ± 0.21
6.27	0.89 ± 0.09	2.02 ± 0.20
10.27	0.00 ± 0.00	1.78 ± 0.17
14.27	0.00 ± 0.00	0.00 ± 0.00

Acetic acid determination was performed by enzymatic kit (see 2.2.4.2). The standard deviation was calculated based on 2 independent samples (supernatant) taken during bioreactor cultivation.

Acetic acid concentrations result of samples taken at 1.27, 3.27, 4.27, 7.27, 8.27, 9.27, 11.27, 12.27 hours are not shown in this table.

3.9. Biosynthesis of MGGBQ in recombinant *E. coli*

3.9.1. Construction of *E. coli* CS3, *E. coli* CS4, *E. coli* CS5 & *E. coli* CS6 strains

Chromosomal Integration of *hpt* expression cassette in *E. coli* BW25113 *lacZ*⁺

Plasmid pCAS7 was modified to obtain pCAS7-FRT-*cat*-FRT. This was done by ligating SphI digested 1.1 kB fragment of FRT-*cat*-FRT with SphI digested 6.2 kB pCAS7 fragment. Digestion of plasmid pCAS7-FRT-*cat*-FRT with SspI resulted in 3 fragments of approx. 800 bp, 2 kb and 4.5 kb which corresponded to the expected size obtained by restriction mapping (757 bp, 1932 bp and 4643 bp).

P_{tac}-*hpt*-FRT-*cat*-FRT fragment was amplified using primers Δ *lacZYA* 2 and Δ *lacZYA* 3 (primer nr. 5 and 6 in table 2.1.2.5) using pCAS7-FRT-*cat*-FRT as template. Δ *lacZYA* 2 and Δ *lacZYA* 3 primers have the 50 nucleotides sequence homologous to specific region in *lacZ* and *lacA* respectively. *E. coli* BW25113 / pKD46 was transformed by electroporation with the PCR purified P_{tac}-*hpt*-FRT-*cat*-FRT fragment. Same procedure was used to verify the 5 positive transformants which were carrying the *hpt* gene in lactose locus. The new strain obtained was *E. coli* BW25113 *lacZYA*::P_{tac}-*hpt*-FRT-*cat*-FRT. This was named as *E. coli* CS3-*cat*.

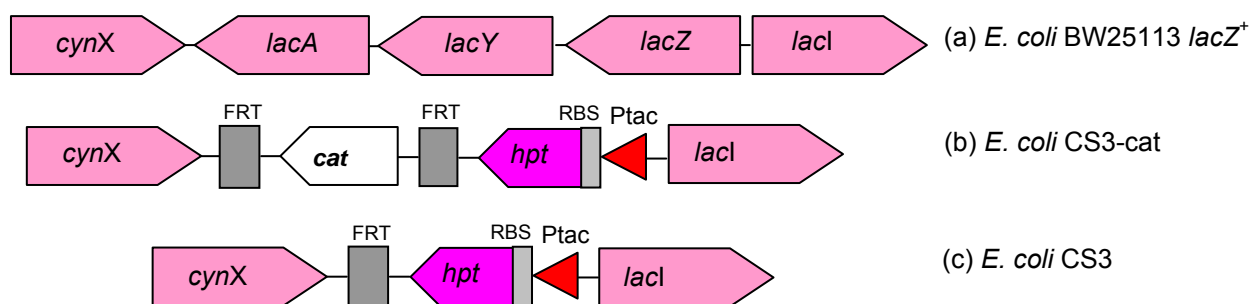


Figure 3.45: Scheme showing the exact location of homologous recombination of *hpt* gene in the lactose operon of *E. coli* BW25113 *lacZ*⁺ strain. (a) Parent strain *E. coli* BW25113 *lacZ*⁺ showing the intact lactose operon. (b) After homologous recombination of P_{tac}-*hpt*-FRT-*cat*-FRT fragment in *lacZYA* locus of *E. coli* BW25113 *lacZ*⁺ to obtain *E. coli* CS3-*cat*. (c) After removal of chloramphenicol resistance cassette from *E. coli* CS3-*cat* to obtain *E. coli* CS3.

Chromosomal Integration of *hpt*, *hpd* and *crtE* Expression Cassettes in *E. coli* BW25113 *lacZ*⁺ to obtain *E. coli* CS6

Phage lysate carrying *lacZYA::P_{tac}-hpt-FRT-cat-FRT* was obtained by infecting *E. coli* CS3-cat with P1 lysate (method previously discussed see section 3.2.1). Several efforts to transduce *E. coli* CS2.2 with the phage lysate carrying *lacZYA::P_{tac}-hpt-FRT-cat-FRT* failed. The reason, why P1-phage transduction of *E. coli* CS2.2 strain failed, is not understood. In order to study the tocochromanol biosynthetic pathway in recombinant *E. coli*, it was decided to use *E. coli* BW25113 *lacZ*⁺ as host strain for production of δ -tocochromanol. Hence *E. coli* CS3 was taken as host strain for further integration. *hpd* expression cassette was integrated in fucose operon by transduction (P1 lysate carrying *fuclP::P_{tac}-hpd-FRT-cat-FRT*). Single colony purification and test with MacConkey agar supplemented with fucose and lactose, and control PCR test verified in new strain *E. coli* BW25113 *lacZYA::P_{tac}-hpt-fuclP::P_{tac}-hpd-cat*. This was named as *E. coli* CS4-cat. Removal of *cat* cassette yielded *E. coli* CS4 which can be seen in figure 3.46.

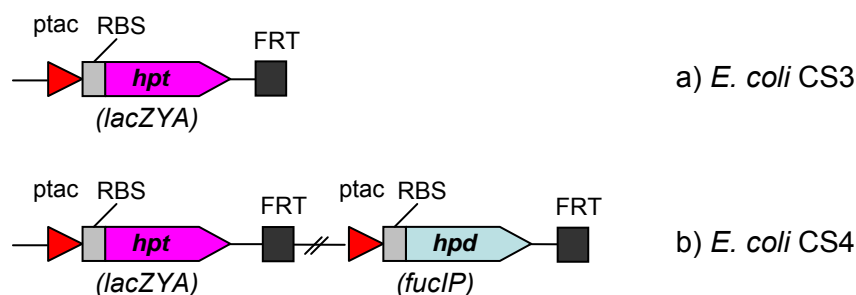


Figure 3.46: Scheme showing chromosomally integrated strains, *E. coli* CS3 & *E. coli* CS4. As the two loci (*lacZYA* and *fuclP*) are not adjacent, it has been shown with an interrupted line a) *E. coli* CS3 which consists of *hpt* expression cassette in lactose operon b) *E. coli* CS4 which consists of *hpt-Syn* and *hpd* expression cassettes in lactose and fucose operon resp.

E. coli CS3 was taken as host strain for further integration. *CrtE* expression cassette was integrated in maltose operon by transduction (P1 lysate carrying *malEFG::P_{tac}-crtE-FRT-cat-FRT*). After single colony purification, test with MacConkey agar supplemented with lactose and maltose, and control PCR test resulted in positive strain *E. coli* BW25113 *lacZYA::P_{tac}-hpt-malEFG::P_{tac}-crtE-cat*. This was named as *E. coli* CS5-cat. Removal of *cat* cassette yielded *E. coli* CS5 which can be seen in figure 3.47.

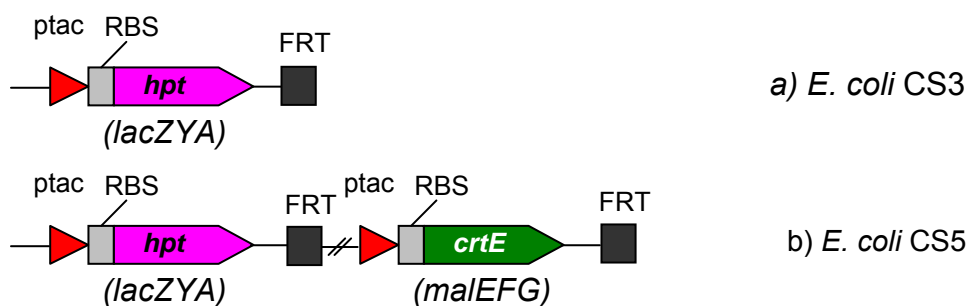


Figure 3.47: Scheme showing chromosomally integrated strains, *E. coli* CS3 & *E. coli* CS5. a) *E. coli* CS3 which consists of *hpt* expression cassette in lactose operon b) *E. coli* CS5 which consists of *hpt-Syn* and *crtE* expression cassettes in lactose and maltose operons resp.

E. coli CS5 was taken as host strain for further integration. *Hpd* expression cassette was integrated in fucose operon by transduction ($P_{lac}::P_{tac}hpd$ -FRT-*cat*-FRT). Single colony purification, test with MacConkey agar with lactose, maltose and fucose, and control PCR test were positive resulting in a new strain, *E. coli* BW25113 *lacZYA::P_{tac}-hpt_{Syn}-malEFG::P_{tac}-crtE-fucIP::P_{tac}-hpd-cat*. This was named as *E. coli* CS6-*cat*. Removal of *cat* cassette yielded *E. coli* CS6 which can be seen in figure 3.48.

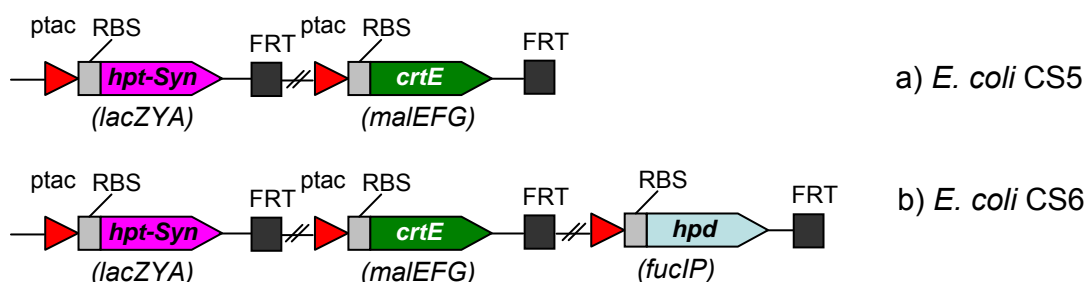


Figure 3.48: Scheme showing chromosomally integrated strains, *E. coli* CS5 and *E. coli* CS6. a) *E. coli* CS5 which consists of *hpt-Syn* and *hpd* expression cassettes in lactose and fucose operon resp. b) *E. coli* CS6 which consists of *hpt-Syn*, *hpd* and *crtE* expression cassettes in lactose, fucose and maltose operons resp.

MGGBQ biosynthesis in shaking flask in *E. coli* CS6, and analysis of recombinant gene expression using 2D-Gel electrophoresis.

To test the expression of Hpt-Syn, Hpd and CrtE proteins, *E. coli* CS6 strain was cultivated in LB medium in shaking flask (see 2.2.3.1 for details), at 30 °C. As control, the parent strain, *E. coli* BW25113 *lacZ⁺* was cultivated under similar conditions. Cultures were induced with 0.25 mM IPTG at OD_{600nm} of 0.8. Cell samples from both cultures i.e. 4 h after induction was tested on 2D gel electrophoresis (see figure 3.24 b). Calculated molecular size and pI value of expected proteins is shown in table 3.12.

Table 3.12: Calculated properties of recombinant proteins (Hpt-Syn, Hpd and CrtE)

Protein Name	Molecular size - M_w [kDa]	Isoelectric point - pI
Hpt-Syn	34.41	9.02
Hpd	40.04	5.07
CrtE	32.58	6.04

M_w and pI values were calculated by using the ExPASy proteomic server.

Samples from *E. coli* BW25113 *lacZ*⁺ and *E. coli* CS6 were tested on SDS-PAGE for protein overexpression. No single separate additional bands in SDS-PAGE, in *E. coli* CS6 samples were seen when compared to *E. coli* BW25113 *lacZ*⁺ samples. SDS-PAGE showing these samples can be seen in appendix Figure A3. Hence, samples to test protein overexpression were tested on 2D gel electrophoresis. When the two gels representing *E. coli* BW25113 *lacZ*⁺ (in green) and *E. coli* CS6 (in red) were overlaid (Delta 2D), three additional protein spots were detected (seen in red spots also marked by arrows). The M_w of these unidentified spots (with R_f method) yielded 39.4 kDa, 31.5 kDa and 73.5 kDa, with pI values of 5.02, 6.1 and 6.15 respectively. Hpt-Syn being membrane associated and highly hydrophobic (based on Kyte & Doolittle Hydrophathy) cannot be seen on 2D gel. The spots at 39.4 kDa and pI of 5.02 closely corresponded to Hpd protein and the spot at 31.5 kDa and pI of 6.1 corresponded to CrtE protein. The extra protein at 73.5 kDa and pI of 6.15 remained unknown.

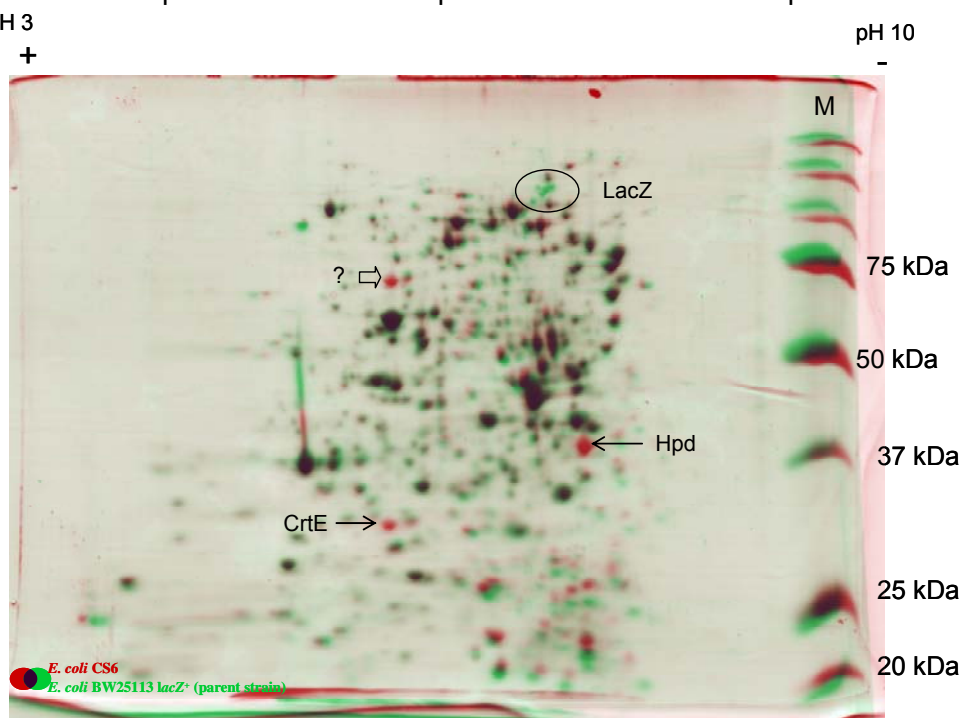


Figure 3.49: 2 D Gel electrophoresis. In green is *E. coli* BW25113 *lacZ*⁺ (parent strain) and in red is *E. coli* CS6. Hpd, and CrtE protein over expressed in *E. coli* CS6 can be seen as red spots

at approx. 40 kDa and approx. 32 kDa resp. (marked by arrows). Hpt being a membrane bound couldn't be detected on 2D gel (discussed previously in section 3.4.1 & 3.4.2. A strong unidentified protein spot (marked with block arrow) can also be seen. Some additional unidentified protein spots in green and red could be seen, approx. between 20 and 30 kDa (pI between 5.0 and 6.0). These were not properly overlaid and hence seen in their respective colours. An additional protein spot (in green, circled) in parent strain *E. coli* BW25113 lacZ⁺ was seen at approx. 82 kDa, pI of 4.76. This corresponded with the lacZ⁺ protein.

E. coli strains carrying chromosomal integrated *hpd* (*E. coli* CS1) or *crtE* (*E. coli* CS2.1) expression cassette yielded HGA or GGPP respectively. To test whether Hpt-Syn expressed in *E. coli* CS3 is functionally active, it had to be combined with Hpd and CrtE expressing system. Hence, *E. coli* CS6 which consisted of single copies of *hpt-Syn*, *hpd* and *crtE* on chromosome was cultivated in LB medium supplemented with 2 % (w/v) glycerol along with *E. coli* CS4 and *E. coli* CS5 strains were cultivated as controls. Cultures were induced with 0.25 mM IPTG (final conc.) at OD_{600nm} of 0.8. Cell densities and MGGBQ produced during these experiments are shown in figure 3.50.

The cell growth before induction, and 6 to 7 h after induction was identical in all three strains. *E. coli* CS4 (*hpt-Syn* and *hpd* expression cassette) strain achieved lower cell densities than *E. coli* CS5 and *E. coli* CS6. Cell pellets were extracted and analyzed by HPLC. MGGBQ_{reduced} and MGGBQ_{oxidised} were detected in *E. coli* CS6. Neither MGGBQ_{reduced}, nor MGGBQ_{oxidised} were detected in strains *E. coli* CS4 and *E. coli* CS5. MGGBQ_{Total} yield (µg/g CDW) remained constant between 12 h and 23 h at 193 µg/g CDW, and 196 µg/g CDW respectively, but the increase in MGGBQ concentration during this time was minimal (227 to 268 µg/l). The *E. coli* CS6 culture at 23 h entered the stationary phase where the MGGBQ_{total} yield increased from 196 to 232 µg/g CDW (maximum MGGBQ_{Total} in MGGBQ_{Reduced} form) at 27 h. *E. coli* CS6 cultures at 48 h turned brown with decreased MGGBQ levels. This was likely due to the oxidation of MGGBQ and possible polymerization which was seen from the decreasing concentration of MGGBQ_{Reduced} and increased MGGBQ_{Oxidised}. As a result it can be concluded that Hpt-Syn was apparently active.

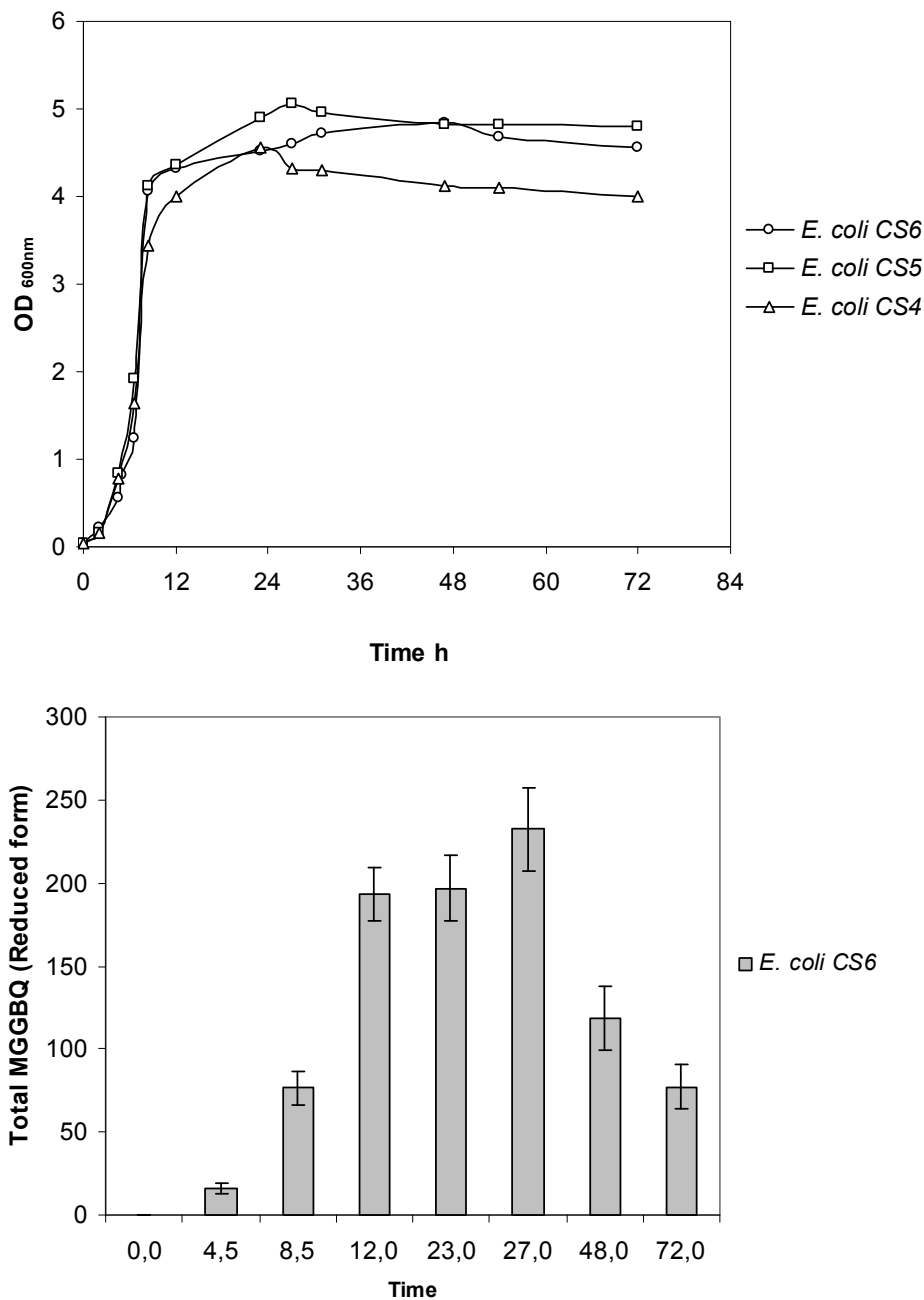


Figure 3.50: Cell growth curve and MGGBQ production in recombinant *E. coli* CS6 cells in shaking flask. Cultivation was carried out in LB-Glycerol medium at 30°C, at 100 RPM. Cultures were induced with 0.25 mM IPTG at approx. OD_{600nm} of 0.8. (A) Cell density shown in OD_{600nm}. (B) Total MGGBQ (in terms of reduced form) productivity shown in bar charts for *E. coli* CS6 strain. No MGGBQ was detected in control strains *E. coli* CS5 and *E. coli* CS4 in any samples. Standard deviations calculated based on 2 independent extractions of 2 independent samples and two independent HPLC analysis. The cultivations were repeated once more, with results having below 10 % S.D.

3.9.2. MGGBQ biosynthesis in Infors bioreactor in *E. coli* CS6

E. coli CS6 strain was shown to produce MGGBQ_{reduced} in LB-Glycerol medium in shaking flask in section 3.21.1. In section 3.4.5 it was shown that both forms of MGGBQ (reduced and oxidised) were produced in *E. coli* BW25113 strain carrying a multi-copy plasmid pCAS29 in minimal medium using glucose as well as glycerol as sole carbon and energy source in bioreactor. Due to the problem faced regarding the stability of the plasmid in *E. coli* BW25113 *lacZ*⁺ during the cultivation, a chromosomal integrated strain *E. coli* CS6 was constructed. It is expected, that the chromosomal integrated strains (also called as plasmid-free in this study) are robust i.e. it genetically stable, and are more productive in MGGBQ compared to plasmid encoded biosynthesis gene. To study and compare the effect of single copy of *hpt-Syn*, *hpd* and *crtE* genes on MGGBQ and the robustness, *E. coli* CS6 strain was cultivated in bioreactor (conditions refer 2.2.1.2.a) in minimal medium using glucose or glycerol as sole carbon, energy source and without any antibiotics. The cell growth curve and glucose/glycerol concentration during cultivation of *E. coli* CS6 in MM-Glucose and MM-Glycerol is shown in Figure 3.51. The starting OD_{600nm} of 0.12 in both cultivations was identical. The cultures were induced with 0.25 mM IPTG at OD_{600nm} of 2.0. Growth rates in the batch process in MM-Glucose medium were relatively higher than that in MM-Glycerol which can be seen from the bacterial growth rate (μ) shown in figure 3.52. During the fed-batch process the feed rate of glucose or glycerol (500 g/l stock) seen from figure 3.52 had approximately similar trend. The glucose or glycerol concentration in medium in bioreactor during this fed batch process never exceeded 0.4 g/l. After 37 h and 38 h the maximum OD_{600 nm} of 28.6 and 27.5 in MM-Glucose and MM-Glycerol respectively were achieved.

MGGBQ concentrations ($\mu\text{g/l}$), and MGGBQ yields ($\mu\text{g/g CDW}$), achieved in *E. coli* CS6 in MM-Glucose and MM-Glycerol can be seen in figure 3.53. Here the MGGBQ_{total} i.e. sum of MGGBQ_{reduced} plus the MGGBQ_{oxidized} forms (converted into MGGBQ_{reduced} form by chemical reduction during analysis is shown). In batch process, higher MGGBQ_{total} yields were reached in MM-Glycerol, as compared to MM-Glucose. During the fed-batch process in MM-Glucose (from 17 h to 50 h), MGGBQ yields increased 18 times from $34 \pm 3 \mu\text{g/g CDW}$ to $604 \pm 51 \mu\text{g/g CDW}$ and concentration increased 64 times, from $83 \pm 7 \mu\text{g/l}$ to $5317 \pm 232 \mu\text{g/l}$. In MM-Glycerol during the fed-batch process MGGBQ_{total} yield doubled from $388 \pm 22 \mu\text{g/g CDW}$ after 21.75 h to $669 \pm 59 \mu\text{g/g CDW}$ after 58 h, while the MGGBQ_{total} conc. during the same period increased 5 times from $1190 \pm 159 \mu\text{g/l}$ to $5559 \pm 492 \mu\text{g/l}$. This difference between the MGGBQ conc. and yields in glucose and glycerol as carbon source was mainly due to the high level of MGGBQ produced in presence of glycerol as compared to glucose. During the last 10-12 hours of respective fermentation, the colour of the cultures turned

brown. The culture sample after centrifugation was brown, while the cell pellet was pale/white. The cell pellet samples started turning brown in the last 6 to 8 hours of fermentation. During the batch phase, HGA production in MM-Glycerol was below 1 mg/l at 26.75 h, and increased at a very high rate to reach 420 ± 28 mg/l (approx. 2.5 mM) after 58 h. Extracellular accumulation of HGA in MM-Glucose was low until 38 h and started to increase thereafter to reach the 231 ± 10 mg/l (approx. 1.37mM) after 48 h.

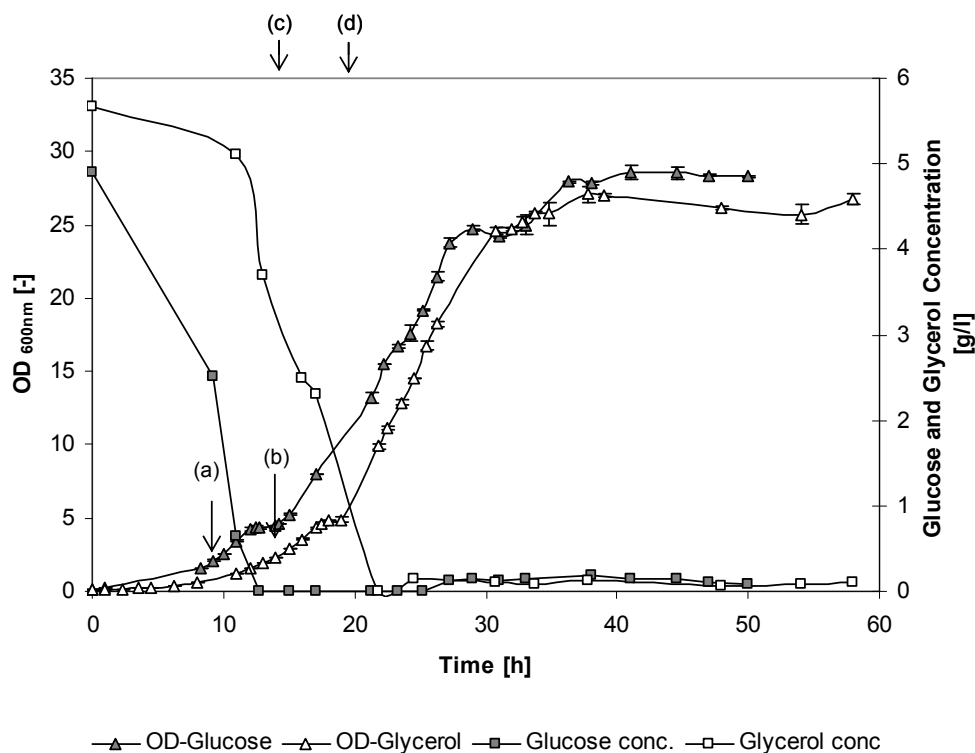


Figure 3.51: Bioreactor cultivation results of *E. coli* CS6 strain in minimal medium with glucose or glycerol as sole carbon and energy source. Cell density represented by OD_{600nm} on left hand side y-axis vs. cultivation time in hours on x-axis. Glucose and Glycerol concentration in bioreactor in g/l is shown on y-axis (right hand side) with respect to cultivation time (x-axis) in hours. (a) and (b) indicates the time of induction with 0.25 mM IPTG in MM-Glucose and MM-Glycerol respectively. (c) and (d) indicates the start of fed batch process i.e. feeding of glucose and glycerol respectively.

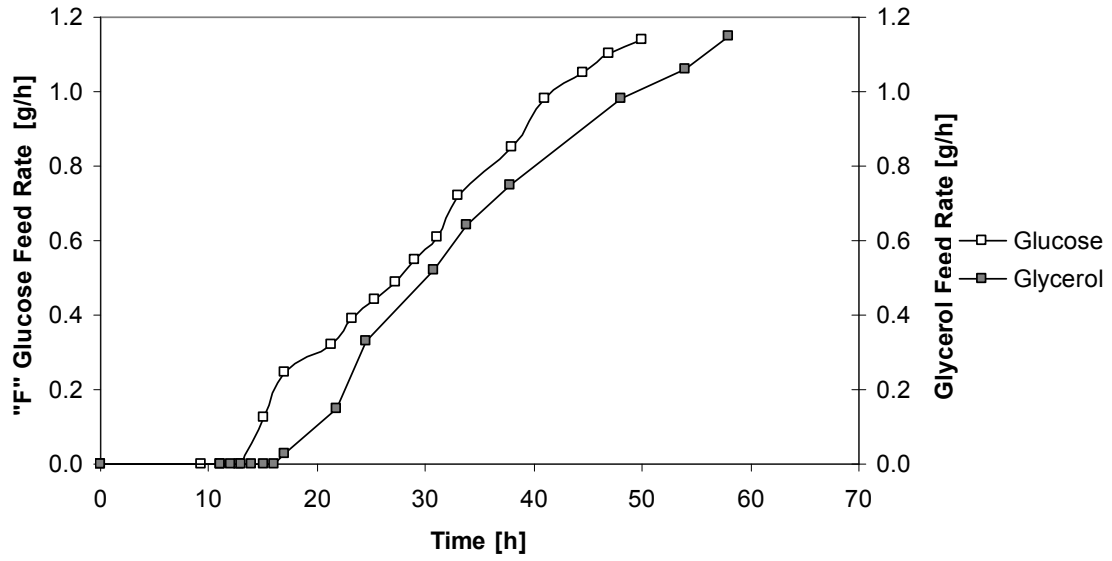


Figure 3.52: Glucose and Glycerol Feed Rates calculated in terms of gram of glucose/glycerol fed per hour i.e. gh^{-1} during cultivation of *E. coli* CS6 in minimal medium once using glucose and another using glycerol as carbon and energy source.

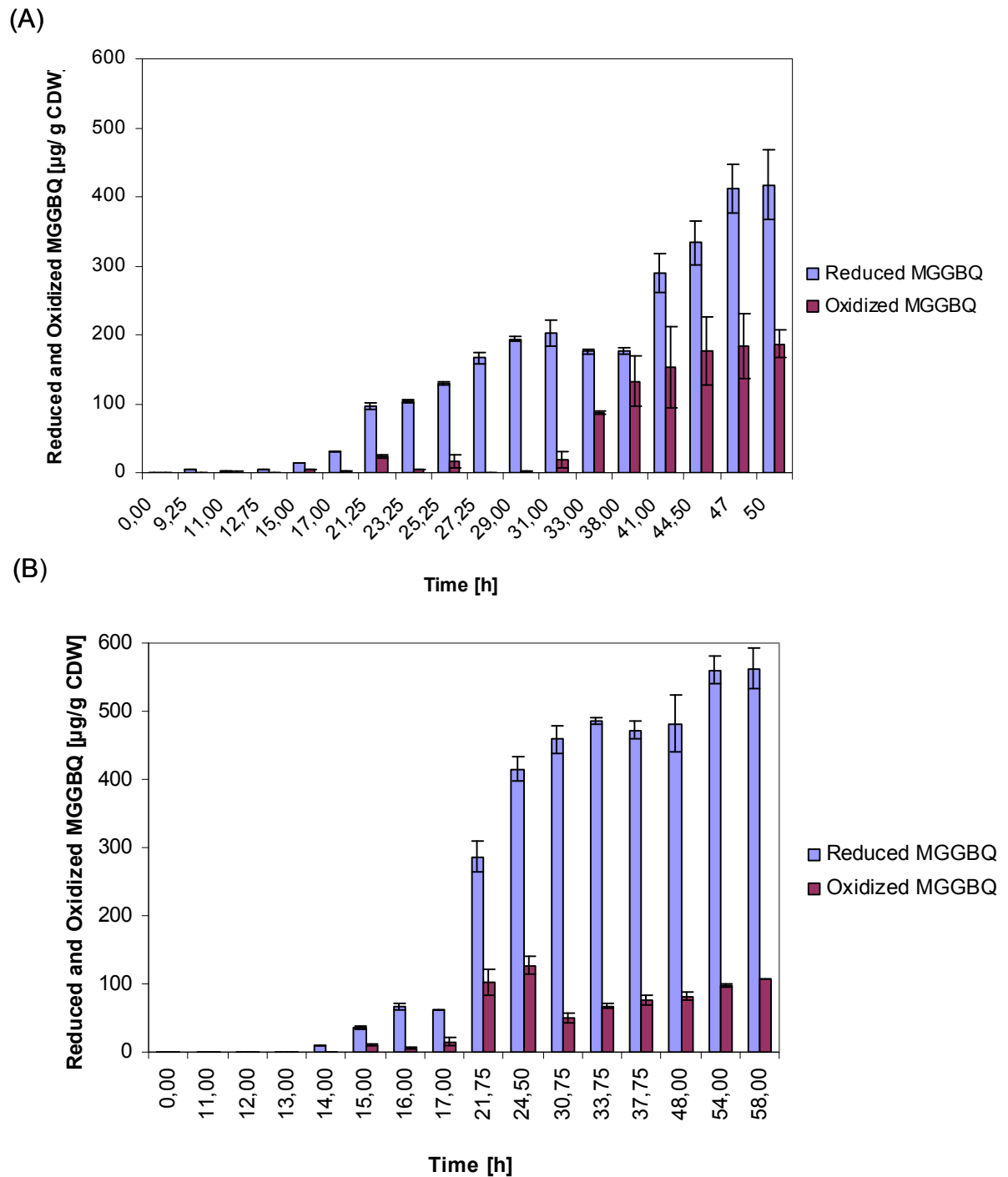


Figure 3.53: MGGQB (reduced and oxidized) yields shown in terms of μg MGGQB per g of cell dry weight i.e. $\mu\text{g/g}$ CDW in *E. coli* CS6 in minimal medium supplemented with either glucose or glycerol as carbon and energy source in bioreactor. (A) in MM-glucose medium (B) in MM-glycerol medium.

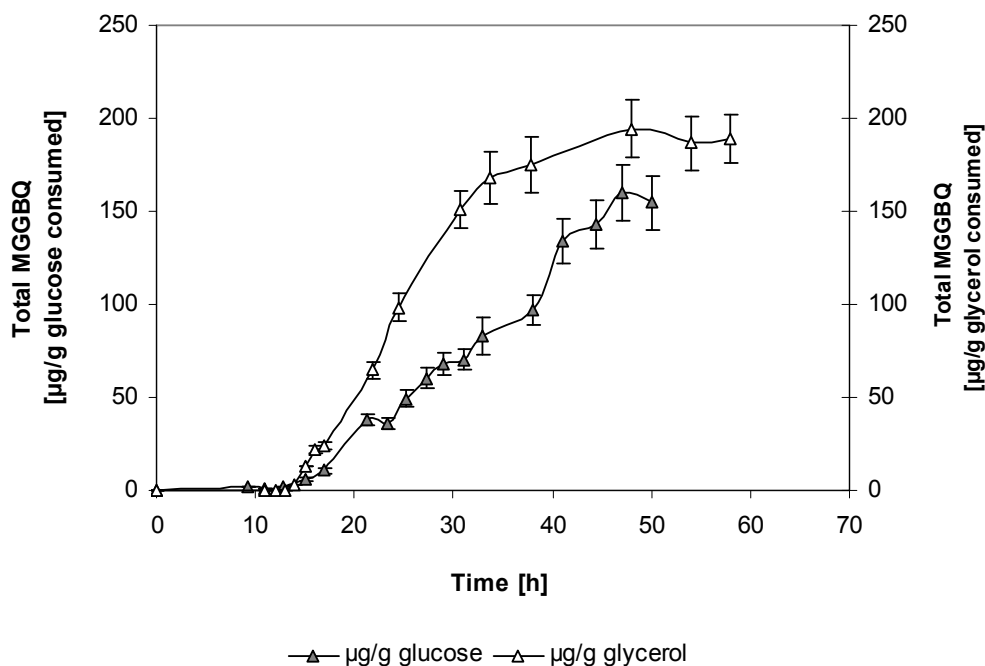


Figure 3.54: Total MGGGBQ product yield per gram of resp. carbon source consumed. Cultivation of *E. coli* CS6 strain in bioreactor in minimal medium once using glucose and another using glycerol as sole carbon and energy source.

Table 3.13: Overview showing the highest $MGGGBQ_{total}$ produced in *E. coli* CS6 strain during bioreactor cultivation

	MM-Glucose			MM-Glycerol		
	Total MGGGBQ			Total MGGGBQ		
	µg/l	µg/g CDW	µg/g Glucose	µg/l	µg/g CDW	µg/g Glycerol
<i>E. coli</i> CS6	5317 ± 232	604 ± 51	160 ± 10	5560 ± 492	669 ± 159	194 ± 15

$MGGGBQ_{total} = MGGGBQ_{reduced} + MGGGBQ_{oxidized}$; represented in terms of $MGGGBQ_{reduced}$.

Glycerol resulted in slightly better carbon source than glucose, when the MGGGBQ yields (in terms of µg of MGGGBQ produced, per g of carbon source consumed) were compared.

But if the carbon flux (in %) (Figure A3-2 in appendix) towards MGGGBQ was compared in terms of carbon mole MGGGBQ produced / carbon mole consumed, glycerol was more efficient than glucose as carbon source. Concentration of MGGGBQ produced during bioreactor cultivation was in submilligram level which resulted in such lower carbon fluxes and hence is not discussed in detail further.

3.9.3. Characterisation of MGGBQ using LC-MS

HPLC analysis of *E. coli* CS6 samples resulted in identical retention time and identical UV maximum absorption for peak 1 and 2, as that obtained for in *E. coli* DH5 α /pCAS29 and *E. coli* BW25113/pCAS29 samples. Peak 1 and peak 2 in *E. coli* DH5 α /pCAS29 samples were characterized with LC-MS (shown in figure 3.17). To confirm whether the HPLC peak 1 and peak 2, detected in *E. coli* CS6 corresponded to MGGBQ_{reduced} and MGGBQ_{oxidised} respectively, the extract sample (bioreactor cultivation MM-Glucose) was characterized by LC-MS using the same method described in section 2.2.4.4. These analyses were performed by Dr. W. Armbruster, Universität Hohenheim, Stuttgart. The results of LC-MS can be seen in appendix Figure A3-3. Strong signals in Fig. A3-3 (B) at 397.2 Da and 414.2 Da in positive mode corresponded to the mass of MGGBQ_{reduced} i.e. [M+H⁺] and [M+NH₄⁺]. Where M is the mass of sample in Da when calculated resulted in 396 Da. Similarly, in figure A3 (C), the signals at 395.2 Da and 412.2 Da shown in positive mode corresponded to MGGBQ_{oxidised} i.e. [M+H⁺] and [M+NH₄⁺]. After calculation, M resulted in 394 Da which corresponded to the expected mass of oxidized MGGBQ. Hence, from the LC-MS results it was confirmed that both MGGBQ_{reduced} and MGGBQ_{oxidized} were produced during cultivation of *E. coli* CS6 in MM-Glucose and MM-Glycerol in bioreactor.

3.9.4. Elucidation of the chemical structure of MGGBQ by NMR

To confirm, whether the MGGBQ_{reduced} produced in *E. coli* CS6 during bioreactor cultivation in minimal medium (3.14.2) has the correct chemical configuration i.e. 2-methyl-6-geranylgeranylbenzoquinol and not 2-methyl-5-geranylgeranylbenzoquinol. Since all the configurations would have identical chromatographic properties and mass it cannot be confirmed only from LC-MS results that the product obtained from convergence of two pathways i.e. HGA and GGPP is really 2-methyl-6-geranylgeranylbenzoquinol and not another compound. Hence, it was important to fully characterise the product by NMR analysis. Sample preparation for NMR analysis required pure MGGBQ (preferably in one form i.e. reduced form) and in amount more than 10 mg.

Purification of MGGBQ produced in *E. coli* CS6 in MM-Glucose in bioreactor (experimental results shown in section 3.14.2) was harvested after 50 h. Cultivation of *E. coli* CS6 was repeated in MM-Glucose to check the reproducibility of the above results. The S.D for cell density was below 5 % and the MGGBQ concentration and yield were below 12 %. Culture of *E. coli* CS6 in MM-Glucose from the repeat cultivation was also harvested at the end of experiment. Approximately, 50-52 g of wet cell biomass (from each MM-Glucose bioreactor cultivation) i.e. approx. 100 g cell biomass was processed for extraction and isolation of MGGBQ (method described in section 2.2.5.1 and 2.2.5.2). Purification of MGGBQ was

carried out according to the method described in (section 2.2.5.3). Estimated MGGBQ_{reduced} obtained after purification was 11.6 mg and was analyzed by NMR for elucidation of the chemical structure. NMR analysis and its interpretation was performed at Universität Hohenheim, Stuttgart at Institute of Bioorganic Chemistry by Dr. Jürgen Conrad. ¹H and ¹³C NMR spectrum and data are included in appendix A3-4 to A3-6.

Heteronuclear adiabatic HSQC and HMBC correlations along with ROESY correlations allowed the unambiguous assignment of the substitution patterns of the aromatic ring and the side chain (figure A3-5 in appendix). Evaluation of the ROESY spectrum revealed an *all*-(E) configuration in the side chain. Band selective HSQC and HMBC experiments were applied to clearly assign closely resonating ¹³C NMR signals e.g. δ values of 40.52, 40.43, and 40.39 ppm in crowded regions of the NMR spectra, thus enabling both, a complete NMR assignment and the verification of the proposed structure. All hydrogen atoms and carbon atoms on isoprenoid chain from 1' to 15' (shown in figure A3-6) were detected from ¹H and ¹³C NMR analysis. Magnified ¹H & ¹³C NMR spectrum for small range of δ values can be seen in appendix. Clear signals indicating the 3 methyl groups on side chain were also obtained. Signals representing the 3 *trans* double bonds on the side chain were also detected (seen from ROESY spectrum in appendix). Signals representing hydrogen and carbon atoms forming the aromatic ring, the methyl group at carbon 6 position on aromatic ring, were obtained. Signals showing the 2 hydroxyl groups on carbon 1 and 4 positions were also obtained. 2D NMR analysis results (shown in appendix) for these sample resulted in data confirming the characteristic properties of the proposed MGGBQ structure.

3.10. Biosynthesis of δ -tocotrienol in a chromosomal integrated *E. coli* strain

3.10.1. Construction of *E. coli* CS7 strain

Chromosomal Integration of *cyc*_{At} expression cassette in *E. coli* CS6 and analysis of protein expression by 2D-Gel electrophoresis

Plasmid pCAS50 was modified by ligation of HindIII digested 1.1 kB, FRT-*cat*-FRT fragment in 6.4 kB HindIII digested pCAS50 fragment. Plasmids were isolated from different transformants obtained after transforming ligation mixture in *E. coli* DH5 α . Digestion of these plasmids from different clones with restriction enzyme HindIII resulted in 1.1 kB & 6.4 kB and digestion with NdeI/BamHI resulted in 1.3 kB and 6.2 kB. This corresponded to the expected sizes calculated using Clone Manager program. This new plasmid was named pCAS50-FRT-*cat*-FRT.

pCAS50-FRT-*cat*-FRT was used as template for PCR amplification. Primers *xy*/A-integr and *xy*/B-integr (i.e. primer nr. 21 & 22 from table 2.1.2.5) were used for amplification of a fragment P_{tac}-*cyc*_{At}-FRT-*cat*-FRT. On each side of this fragment 50 nucleotides are homologous to a region in *xy*/A and *xy*/B locus. *E. coli* CS6 strain carrying a plasmid pKD46 (expressing λ -recombinase induced by arabinose) was transformed by electroporation with the fragment P_{tac}-*cyc*_{At}-FRT-*cat*-FRT. 21 transformants obtained were tested on MacConkey agar plates with xylose, with their respective control strain. These transformants were screened on MacConkey agar plate each supplemented with 4 different sugars (fucose, maltose, lactose and xylose). Two transformants were found to be positive as they didn't turn red on any of the MacConkey agar plates with xylose, or maltose, or lactose or fucose. The new strain was named as *E. coli* CS7-*cat*. PCR control test with primers P27 and P11 and P28 and P11 yielded PCR product of 1.05 kb and 1.30 kb sizes which corresponds with the expected sizes calculated using Clone manager 7.0. Elimination of *cat* resistance gene was carried out by using temperature sensitive recombinase (pCP20) (method 2.2.2.5) yielded *E. coli* CS7 which can be seen in figure 3.25.

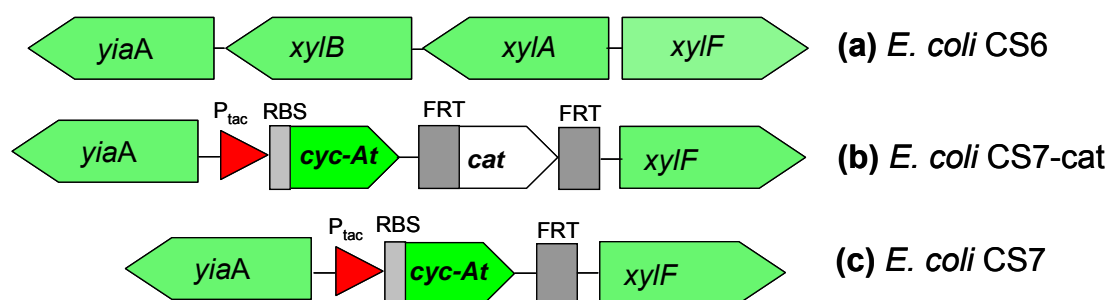


Figure 3.55: Scheme showing chromosomal integration of *cycAt* gene in xylose locus. (a) Showing the intact loci *yiaA*, *xylB*, *xylA* and *xylF* in *E. coli* CS6 strain before integration. This *E. coli* CS6 strain already has *hpt_{Syn}*, *crtE* and *hpd* expression cassettes integrated in lactose, maltose and fucose operon resp. (b) The site of xylose locus after integration of *P_{tac}-cycAt-FRT-cat-FRT* in *xylA* & *xylB* region of *E. coli* CS6 chromosome. (c) The final strain obtained i.e. *E. coli* CS7 after removal of chloramphenicol residual cassette (*cat*) with *P_{tac}-cycAt* integrated at the site of *xylA* and *xylB* i.e. *xylAB::P_{tac}-cycAt*.

The newly obtained strain *E. coli* CS7, is shown schematically with comparison to the *E. coli* CS6 strain in figure 3.56A.

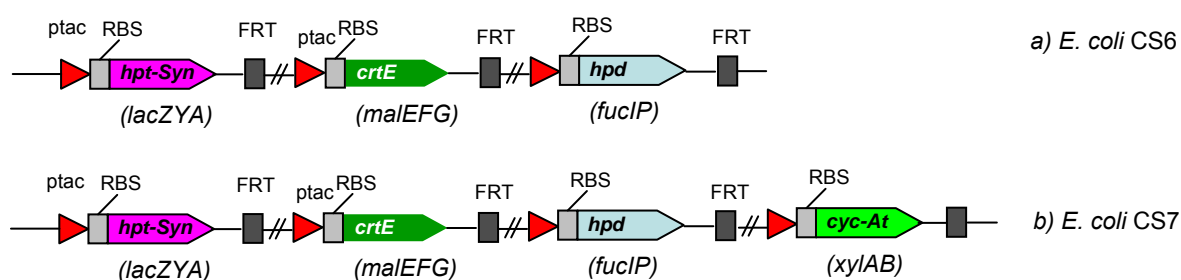


Figure 3.56A: Scheme showing chromosomally integrated strains *E. coli* CS6 & *E. coli* CS7. a) *E. coli* CS6 which consists of *hpt-Syn*, *hpd* and *crtE* expression cassettes in lactose, fucose and maltose operons resp. b) *E. coli* CS7 which consists of an additional *cyc-At* expression cassette in xylose operon in *E. coli* CS6.

After confirming that *cycAt* expression cassette was correctly integrated in xylose operon in the desired location of the newly constructed strain *E. coli* CS7, expression of Hpd, CrtE, Hpt-Syn and Cyc-At was tested on 2D gel electrophoresis. *E. coli* CS7 was cultivated in LB medium in shaking flask (2.2.3.1) and as control *E. coli* CS6 was cultivated. Cultures were induced with 0.25 mM IPTG at OD_{600nm} of 0.8. Sample 6 h after induction was tested for protein expression on 2D gel electrophoresis shown in figure 3.56. The Hpd and CrtE protein at 39.6 kDa and 31.4 kDa resp. seen in both strains perfectly overlapped each other (marked as Hpd and CrtE resp. in figure 3.56B). Hpt-Syn being hydrophobic protein could not be detected in any of the 2 samples (calculated values of 34.4 kDa and pI of 9.02). An additional protein spot in red colour was visible in *E. coli* CS7 sample which was absent in *E. coli* CS6. This red spot had a mass of 46.2 kDa and pI of 5.88 (based on R_f method) which closely corresponded to the calculated properties (ExpASY) of Cyc-At protein.

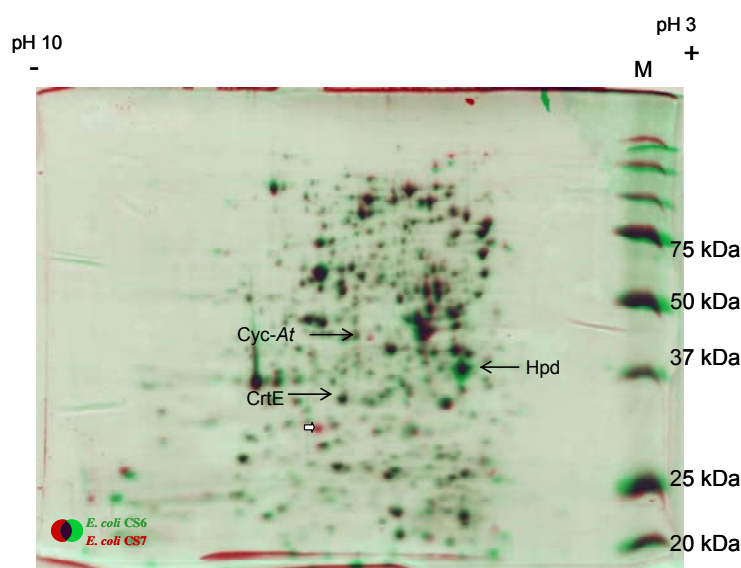


Figure 3.56B: 2 D gel electrophoresis for *E. coli* CS6 and *E. coli* CS7 samples. Gels were overlaid i.e. *E. coli* CS6 (in green) and *E. coli* CS7 (in red). Hpd and CrtE protein seen in both samples are marked with arrow. Additional protein band (red spot) in *E. coli* CS7 sample at approx. 46.2 kDa was seen. Cyc-At has calculated size of 47 kDa and pI of 5.95. An unidentified protein was observed on the 2 D gel in *E. coli* CS7 strain shown by block arrow.

δ -Tocotrienol Biosynthesis in *E. coli* CS7 in Shaking Flask

After confirming the Cyc-At expression in *E. coli* CS7, it was important to check the activity of the cyclase level expressed. This was done *in-vivo* in *E. coli* CS7 strain by cultivation in shaking flask in LB – Glycerol, at 30 °C. As control *E. coli* CS6 strain was cultivated under identical conditions. If Cyc-At expressed in *E. coli* CS7 is active, *E. coli* CS7 cells would produce MGGBQ along with δ -tocotrienol. The control strain *E. coli* CS6 which do not carry *cyc-At* gene would not produce δ -tocotrienol. This difference should be visible during the HPLC analysis of samples extracted.

Both strains reached almost identical cell densities till the time of induction. Cultures were induced with 0.25 mM IPTG at approx. OD_{600nm} of 0.8 (4.5 h). Results are shown in figure 3.57. 4 h after induction, cell growth in *E. coli* CS7 cultures had already started to retard when compared to that in *E. coli* CS6 cultures. After 72 h, *E. coli* CS7 cells reached a final OD_{600nm} of 4.01 while *E. coli* CS6 reached a final OD_{600nm} of 4.45. Cell pellet samples extracted and analyzed by HPLC showed MGGBQ (in reduced and oxidized form) in both strains. *E. coli* CS7 produced 1.6 times more total MGGBQ in terms of $\mu\text{g/g}$ CDW as compared to *E. coli* CS6 after 24 h. Perhaps the maximum MGGBQ level attained in *E. coli* CS6 was within the first 24 h of cultivation. This could not be confirmed as no sample for MGGBQ/ δ -tocotrienol extraction was taken between 4 h and 24 h. Lower cell dry weight achieved in *E. coli* CS7 as compared to *E. coli* CS6 after 24 h also automatically contributed to higher MGGBQ yields. The 48 h sample showed that the total MGGBQ productivity and

yield in both cultures decreased by approx. 30-35 % to what it was after 24 h. Decrease in total MGGBQ in *E. coli* CS6 of 40 % continued between 48 h and 72 h while the decrease in total MGGBQ in *E. coli* CS7 during this period was 14 %. HPLC analysis of the same samples was able to detect δ -tocotrienol in *E. coli* CS7 cells while no δ -tocotrienol was detected in any of the cell samples of *E. coli* CS6. Small amount ($0.13 \pm 0.02 \mu\text{g/g}$ CDW or $0.17 \pm 0.03 \mu\text{g/l}$) of δ -tocotrienol was produced in *E. coli* CS7 cells after 24 h. δ -tocotrienol productivity and yield doubled from 24 h to 48 h, and increased marginally from $0.39 \pm 0.05 \mu\text{g/g}$ CDW ($0.52 \pm 0.06 \mu\text{g/l}$) to $0.45 \pm 0.05 \mu\text{g/g}$ CDW ($0.58 \pm 0.07 \mu\text{g/l}$) between 48 and 72 h. There was only a small increase in δ -tocotrienol and small decrease in total MGGBQ despite of approx. $200 \mu\text{g/g}$ CDW MGGBQ was still available for cyclization reaction between 48 and 72 h in *E. coli* CS7. This indicates that the tocopherol cyclase activity was rate limiting.

Results in figure 3.57 showed that *Cyc-At* expressed from the single copy of *cyc-At* gene integrated in the chromosome of *E. coli* CS7 strain was able to catalyze the cyclization reaction by converting MGGBQ into small amount of δ -Tocotrienol in complex medium using glycerol as additional carbon source.

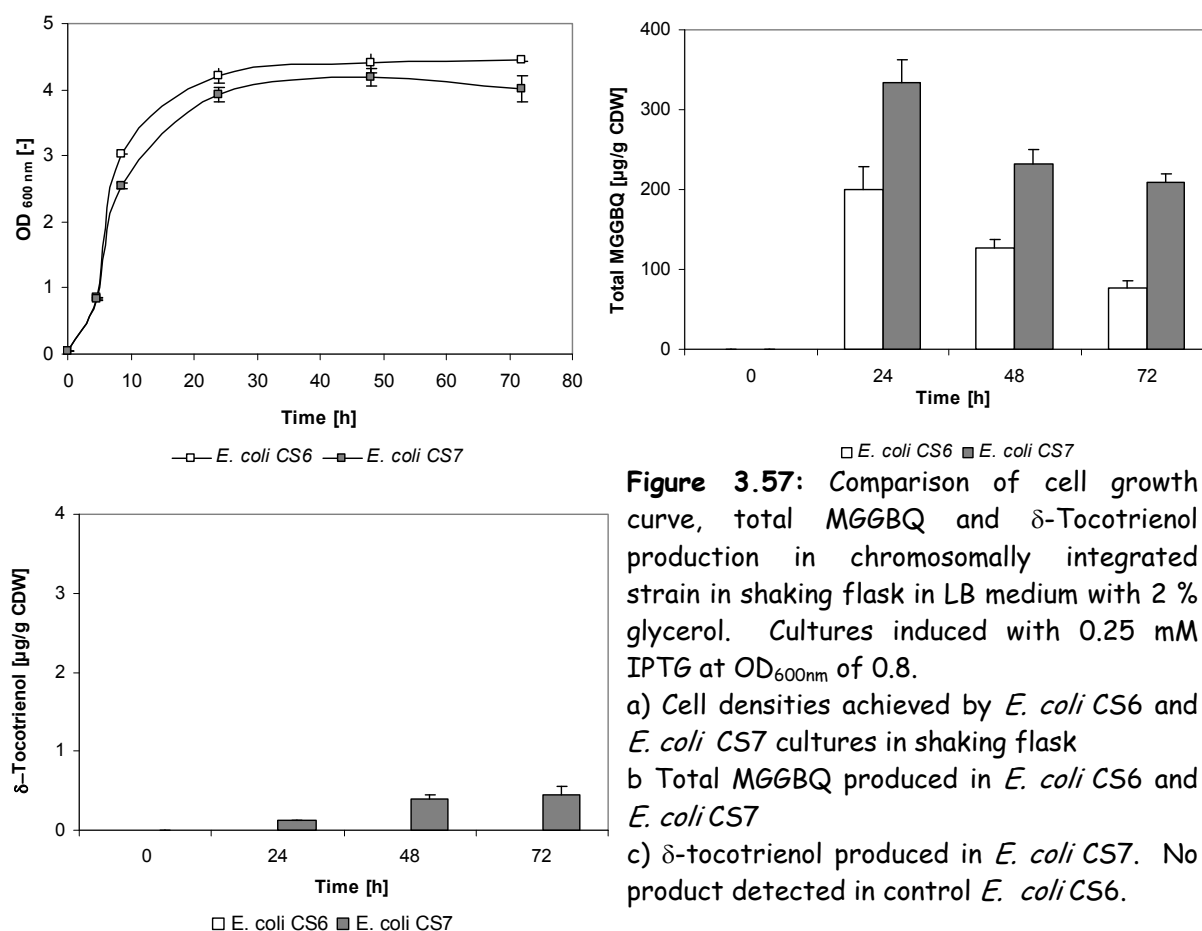


Figure 3.57: Comparison of cell growth curve, total MGGBQ and δ -Tocotrienol production in chromosomally integrated strain in shaking flask in LB medium with 2 % glycerol. Cultures induced with 0.25 mM IPTG at OD_{600nm} of 0.8.

a) Cell densities achieved by *E. coli* CS6 and *E. coli* CS7 cultures in shaking flask

b) Total MGGBQ produced in *E. coli* CS6 and *E. coli* CS7

c) δ -tocotrienol produced in *E. coli* CS7. No product detected in control *E. coli* CS6.

3.10.2. δ -Tocotrienol Biosynthesis in Bioreactor in *E. coli* CS7

To study if *E. coli* CS7 was able to produce δ -tocotrienol in minimal medium using glucose or glycerol as sole carbon and energy source, it was cultivated in bioreactor. Cultivation results of *E. coli* CS7 in bioreactor in MM-Glucose and MM-Glycerol are shown in figure 3.58 to 3.61.

E. coli CS7 cultures in MM-Glucose was induced with 0.25 mM at 13.5 h and glucose feeding was started after 18.5 h when the initial glucose in MM was completely consumed. During the fed batch cultivation (16.5 h to 27 h) the growth rate (μ) was approx. constant (0.17 to 0.18 h⁻¹). The cultures reached stationary phase at 45 h and cultivation was stopped after 48 h. *E. coli* CS7 cultures in MM-Glycerol grew slower than those in MM-Glucose (maximum μ of 0.19 h⁻¹ and 0.26 h⁻¹ resp.). Glycerol feeding was started at 27 h when all the initial glycerol in MM-Glycerol was consumed. *E. coli* CS7 in MM-Glucose and MM-Glycerol reached approximately identical cell densities OD_{600nm} of 22 to 23 at the end of cultivation (48 h and 62 h respectively). Refer to figure 3.58.

MGGBQ production pattern in MM-Glucose and MM-Glycerol differed from each other. MGGBQ production started only after induction with IPTG in both cases. 25 % of the final amount of reduced MGGBQ produced in MM-Glucose was already produced after 16h. After starting of fed batch cultivation, the MGGBQ_{reduced} yield (in $\mu\text{g/g CDW}$), quadrupled between 16 and 22 h. The MGGBQ_{reduced} yield decreased further with MGGBQ_{oxidized} yield remaining constant. One reason for the decrease in reduced MGGBQ was due to the conversion of it into δ -tocotrienol ($0.45 \pm 0.05 \mu\text{g/l}$ or $0.15 \pm 0.02 \mu\text{g/g CDW}$) which could be seen in 27 h sample in figure 3.60. The MGGBQ_{reduced} yield gradually decreased from 27 h to 43.75 h before it was almost exhausted at 48 h. During this time MGGBQ_{oxidized} and δ -tocotrienol also increased gradually to reach 586 $\mu\text{g/g CDW}$ and 3.3 $\mu\text{g/g CDW}$ respectively. MGGBQ_{reduced} production in *E. coli* CS7 in MM-Glycerol started at 16 h and increased at slow rate from 67.5 $\mu\text{g/g CDW}$ to 182.5 $\mu\text{g/g CDW}$ at 23.5 h. MGGBQ_{oxidized} was produced between 23.5 h and 27 h which resulted in decrease in MGGBQ_{reduced} yield. After 27 h the yield of MGGBQ_{reduced}, increased more than 8 times, i.e. from 114 $\mu\text{g/g CDW}$ to 907 $\mu\text{g/g CDW}$ at 47 h. Further it decreased to approx. half with increase in δ -tocotrienol concentration. The difference to that in MM-Glucose was that the oxidized MGGBQ yield didn't increase above 165 $\mu\text{g/g CDW}$. The δ -tocotrienol production increased from $4.8 \pm 0.4 \mu\text{g/l}$ to $26.6 \pm 1.8 \mu\text{g/l}$ from 30.25 h to 54 h and didn't increase further till 60 h despite the presence of approx. 400 $\mu\text{g/g CDW}$ of MGGBQ_{reduced} (Refer figure 3.61). Once again it showed that cyclase activity was limiting at least in case of MM-Glycerol where reduced MGGBQ was available and δ -

tocotrienol production almost stagnated after 62 h. At this point it was not clear why the *E. coli* CS7 cultures didn't carry out the cyclization reaction. When *E. coli* CS7 cultivation in MM-Glucose and MM-Glycerol were compared produced approximately the same amounts of reduced MGGBQ and δ -tocotrienol.

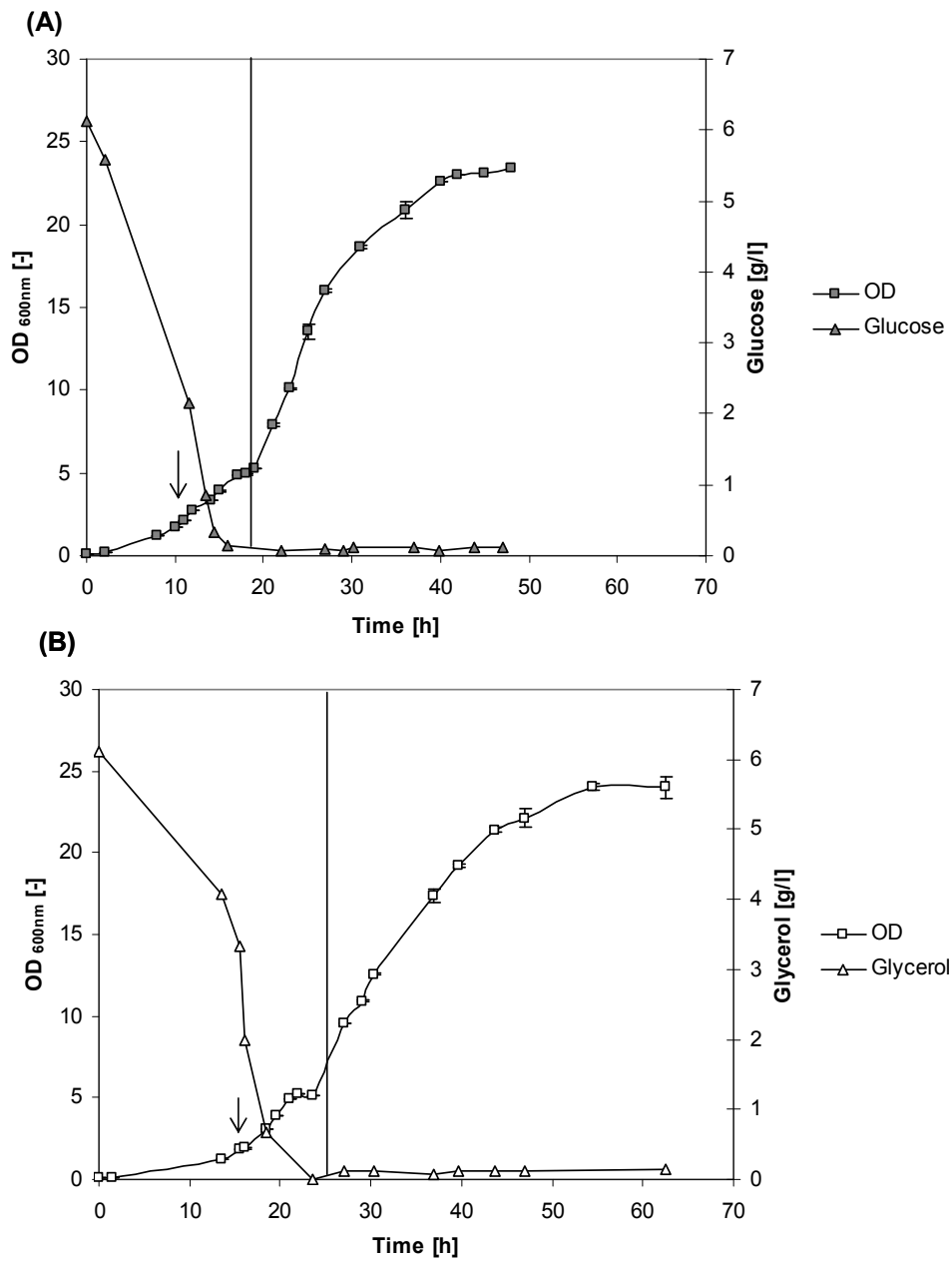


Figure 3.58: Cell growth and glucose/glycerol concentration curve during bioreactor cultivation of *E. coli* CS7 in minimal medium at 30°C. (A) Glucose. (B) Glycerol. Arrows in (A) and (B) represents the time of induction with 0.25 mM IPTG. Vertical lines show the time at which fed batch process was started with feeding of carbon source glucose or glycerol.

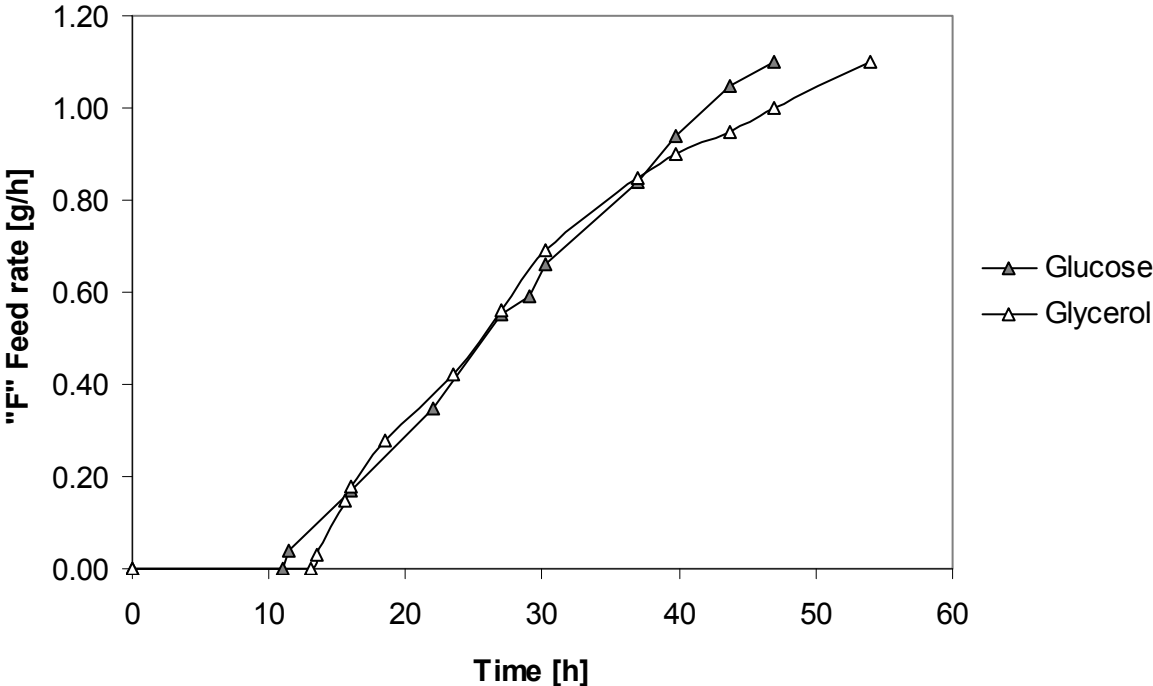


Figure 3.59: Glucose/Glycerol Feed Rate (F) during bioreactor cultivation of *E. coli* CS7 in minimal medium at 30°C

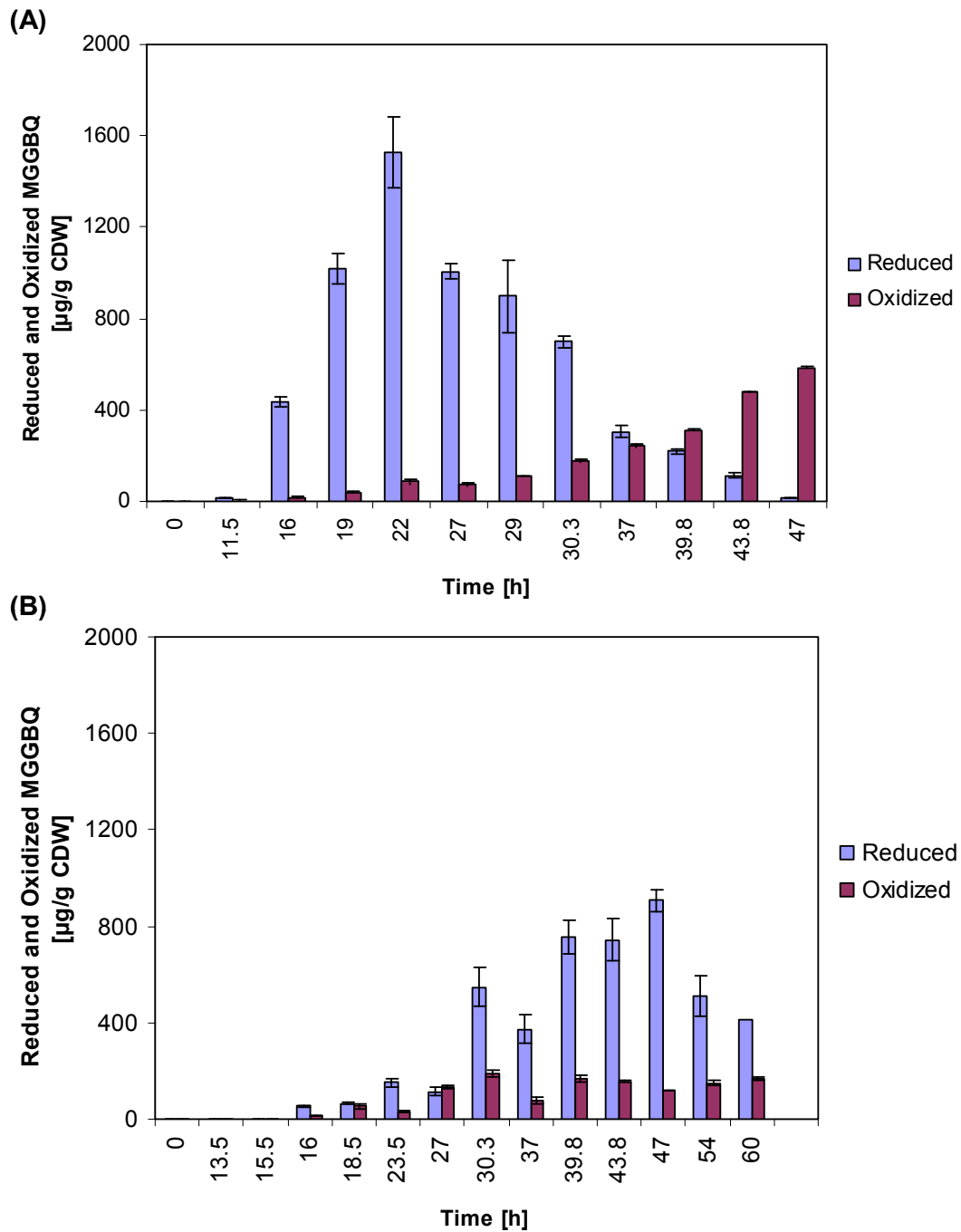


Figure 3.60: Reduced and Oxidized MGG BQ yields achieved in *E. coli* CS7 during bioreactor cultivation in minimal medium at 30 °C. (A) Glucose as sole carbon and energy source (B) Glycerol as sole carbon and energy source.

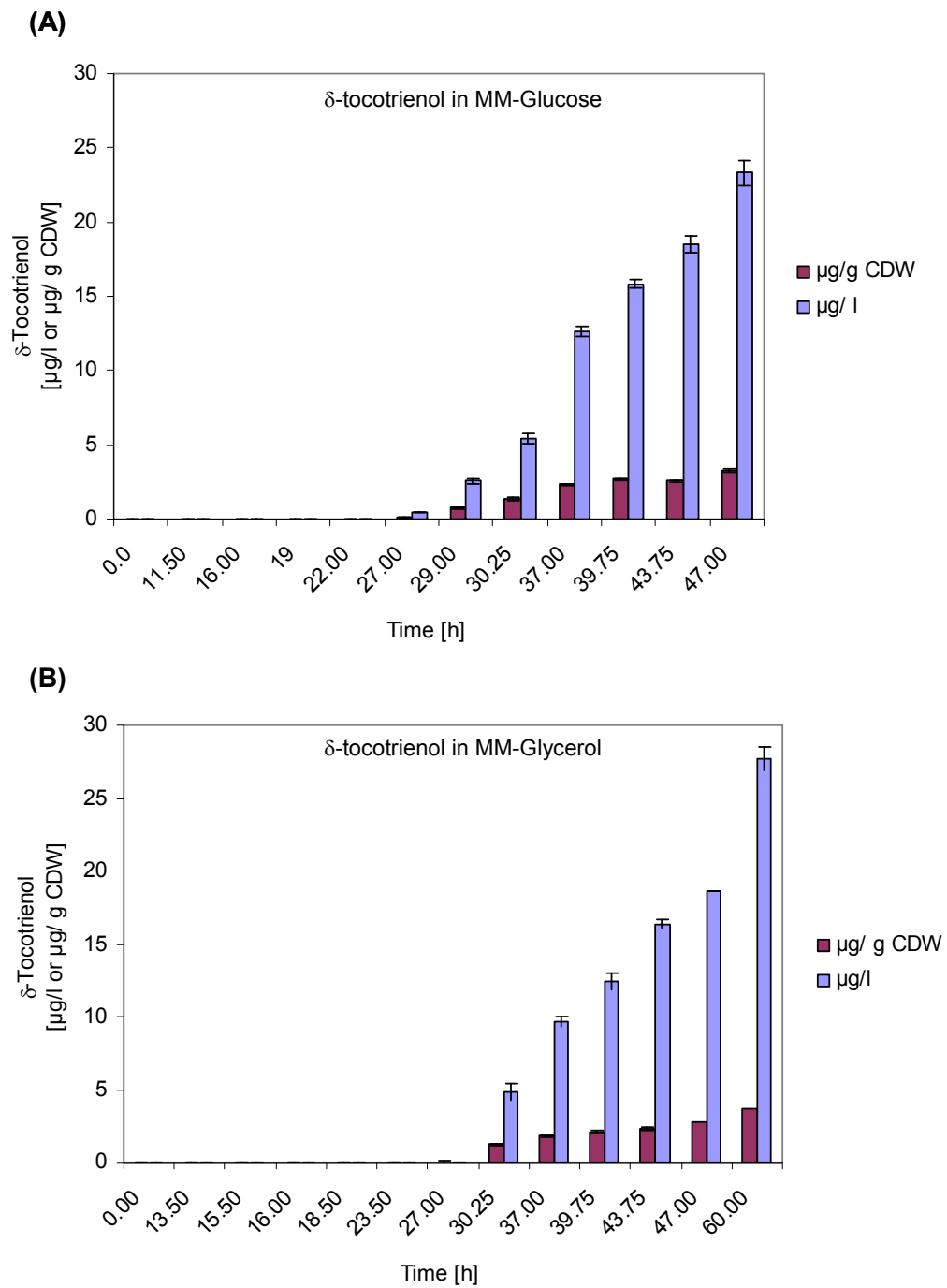


Figure 3.61: δ -Tocotrienol production in *E. coli* CS7 strain during cultivation in bioreactor at 30 °C in minimal medium (A) Glucose as carbon, energy source (B) Glycerol as carbon, energy source.

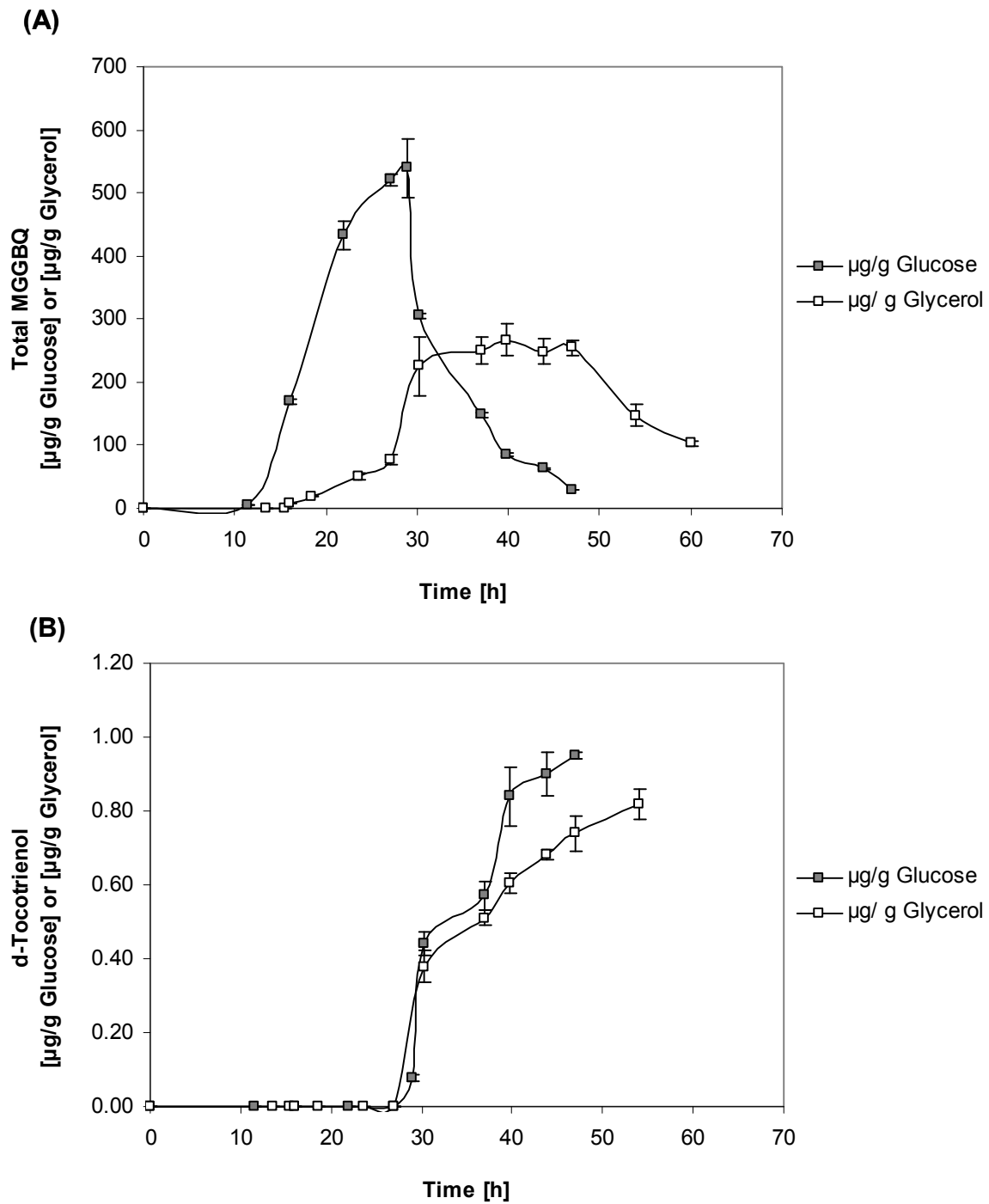


Figure 3.62A: Product yield calculated per gram of carbon source utilized during bioreactor cultivation of *E. coli* CS7 in minimal medium using either glucose or glycerol at 30 °C.

(A) Total MGGBQ yield in µg/g Glucose or g Glycerol consumed

(B) δ-Tocotrienol yield in µg/g Glucose or g Glycerol consumed

3.11. Increased MGGBQ in Recombinant *E. coli* Strains

Increased MGGBQ in Recombinant *E. coli* Strains by Co-expression of 1-Deoxy-D-Xylulose-5-Phosphate Synthase (Dxs) and Isopentenyl Pyrophosphate Isomerase (Idi) from DXP Pathway

DXP or non-mevalonate pathway exists in bacteria and plants that leads to synthesis of IPP and DMAPP which are the important building blocks for isoprenoid production. It was shown that carotenoid production could be increased by co-expression of either IPP isomerase (Idi) or FPP synthase (*IspA*) or by co-expression of deoxy-xylulose phosphate synthase (*Dxs*) (Lemuth et al. 2011). It was also shown that the co-expression of deoxy-xylulose phosphate reductoisomerase (*Dxr*), *Idi* and *IspA* combined in metabolically engineered *E. coli* improved the isoprenoids yields by increasing the carbon flux via DXP pathway (Lee et al. 2004 and Jones et al. 2000). In theory based on the above studies MGGBQ levels could also be increased by co-expression of *Dxs*, *Idi* and *IspA* in *E. coli* CS6 strain. Since the isoprenoid precursor for MGGBQ biosynthesis i.e. FPP and IPP is derived from DXP pathway increasing carbon flux might increase the precursor for GGPP production i.e. FPP and IPP. Plasmid pJOE5559.1 was obtained from Dr. Josef Altenbuchner, Institute of Industrial Genetics, Universität Stuttgart, Germany, that consisted of *dxs*, *idi* and *ispA* genes from *E. coli* K12 encoding 1-deoxy-D-xylulose-5-phosphate synthase, Isopentenyl pyrophosphate isomerase and FPP isomerase respectively. This plasmid had a kanamycin resistance cassette and all the 3 genes were under the control of a rhamnose inducible promoter (details table 2.1.2.2).

Increasing MGGBQ levels in *E. coli* CS6 by using additional plasmid pJOE5559.1

E. coli CS6 was transformed with pJOE5559.1, and cultivated in shaking flask at 30 °C in LB-Glycerol supplemented with 25 µg/l of chloramphenicol. As control *E. coli* CS6 was transformed with control vector pHWG640 (see section 2.1.2.) under similar conditions. Both cultures were induced with 0.25 mM IPTG and 0.2 % (w/v) rhamnose at approx. OD_{600nm} of 0.8. Cell densities and total MGGBQ productivities achieved in this experiment are shown in figure 3.62B. Control strain reached an OD_{600nm} of 5.0 while *E. coli* CS6 / pJOE5559.1 reached slightly lower OD_{600nm} of 4.6. Total MGGBQ produced in *E. coli* CS6 / pJOE5559.1 was approx. 7 times higher MGGBQ (in terms of µg per g CDW) and 9.3 times higher (in terms of µg per liter of culture) than in the control *E. coli* CS6 / pHWG640. The over expression of the 3 genes in DXP pathway had a positive influence on the total MGGBQ production. It was not clear what is the effect of each individual enzyme on MGGBQ

production, or if this positive effect is seen only when all necessary proteins are expressed together. Hence, contribution of each single gene to this MGGBQ increase was unknown. Hence, it was planned to co-express single enzyme i.e. Idi, Dxs and LspA on plasmid using *E. coli* CS6 as host strain and study its effect on MGGBQ production.

MGGBQ production in *E. coli* CS6/pHWG640 compared to that in *E. coli* CS6 was lower by approx. 20 % i.e. 219 $\mu\text{g/l}$ compared to 268 $\mu\text{g/l}$ after 24 h of cultivation time.

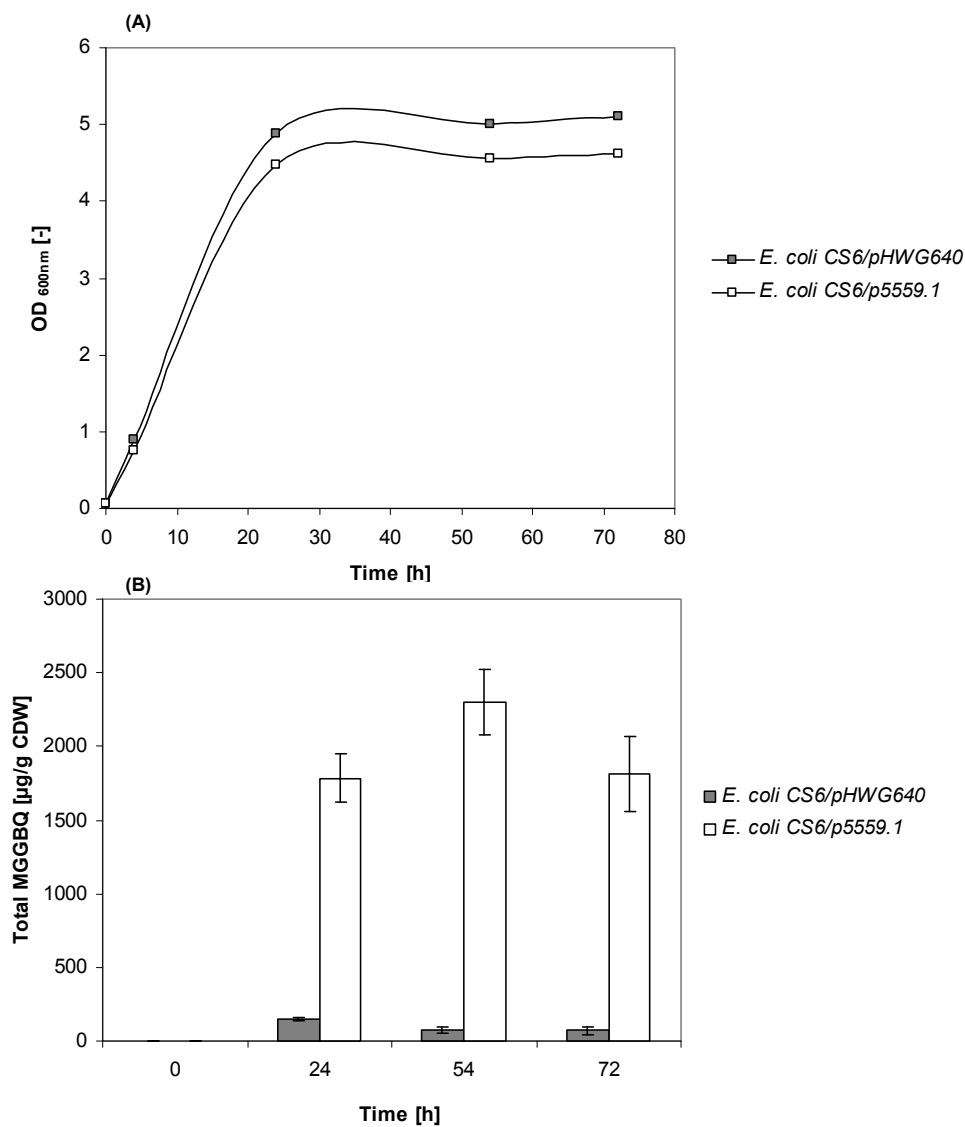


Figure 3.62B: Cell density and MGGBQ produced in shaking flask experiment in LB-Glycerol-Cm25. *E. coli* CS6/pHWG640 and *E. coli* CS6/p5559.1 were induced with 0.25 mM IPTG and 0.2 % (w/v) rhamnose. (A) Cell density in terms of OD_{600nm}. (B) Total MGGBQ productivity in $\mu\text{g/g CDW}$.

Influence of co-expression of Isopentenyl pyrophosphate isomerase (*idi*) in *E. coli* CS6 strain on MGGBQ production level

Idi gene from *Escherichia coli* K12 was cloned in pJF119 Δ N vector to obtain plasmid pCAS10 (pJF119-*idi* in Lemuth et.al. 2011). Plasmid pCAS10 was kindly provided by Dr. Albermann for further study. *E. coli* CS6 was transformed with plasmid pCAS10 and cultivated in shaking flask in LB-Glycerol-Amp100 at 30 °C for MGGBQ production. As control *E. coli* carrying empty vector pJF119 Δ N was cultivated. Cultures were induced with 0.25 mM IPTG at approx. OD_{600nm} of 0.8. Samples taken after induction with IPTG were extracted and analysed by HPLC. Results can be seen in figure 3.63. Both cultures grew identically till OD_{600nm} of 3.8. After that the *E. coli* CS6 / pJF119 Δ N growth slowed down to reach a final OD_{600 nm} of 5.1 \pm 0.2, while *E. coli* CS6 / pCAS10 continued to grow further till OD_{600 nm} of 6.2 \pm 0.2. MGGBQ_{total} production at 8 h in *E. coli* CS6 / pJF119 Δ N was slightly higher than *E. coli* CS6 / pCAS10. Host strain *E. coli* CS6, was cultivated without any plasmid/vector.

8 h sample in *E. coli* CS6/pCAS10 and its control *E. coli* CS6/pJF119 Δ N produced similar amounts of MGGBQ_{total} i.e. approx. 9.0 and 12.5 μ g /g CDW respectively. MGGBQ_{total} production in *E. coli* CS6/pCAS10 between 8 h and 24 h was twice compared to its control. At 48 h and 72 h, eventhough the MGGBQ_{total} dropped down in both cases due to oxidation and polymerisation of MGGBQ, *E. coli* CS6/pCAS10 had produced almost 9 to 10 times higher MGGBQ_{total} compared to its control (Refer to Figure 3.63, section B). Increased MGGBQ yield in *E. coli* CS6 / pCAS10 strain indicates that the co-expression of *Idi* along with MGGBQ biosynthetic genes has a strong positive effect on MGGBQ production. Based on these results, it was planned to integrate *idi* gene in chromosome of *E. coli* CS6. To do this, ribose operon was selected.

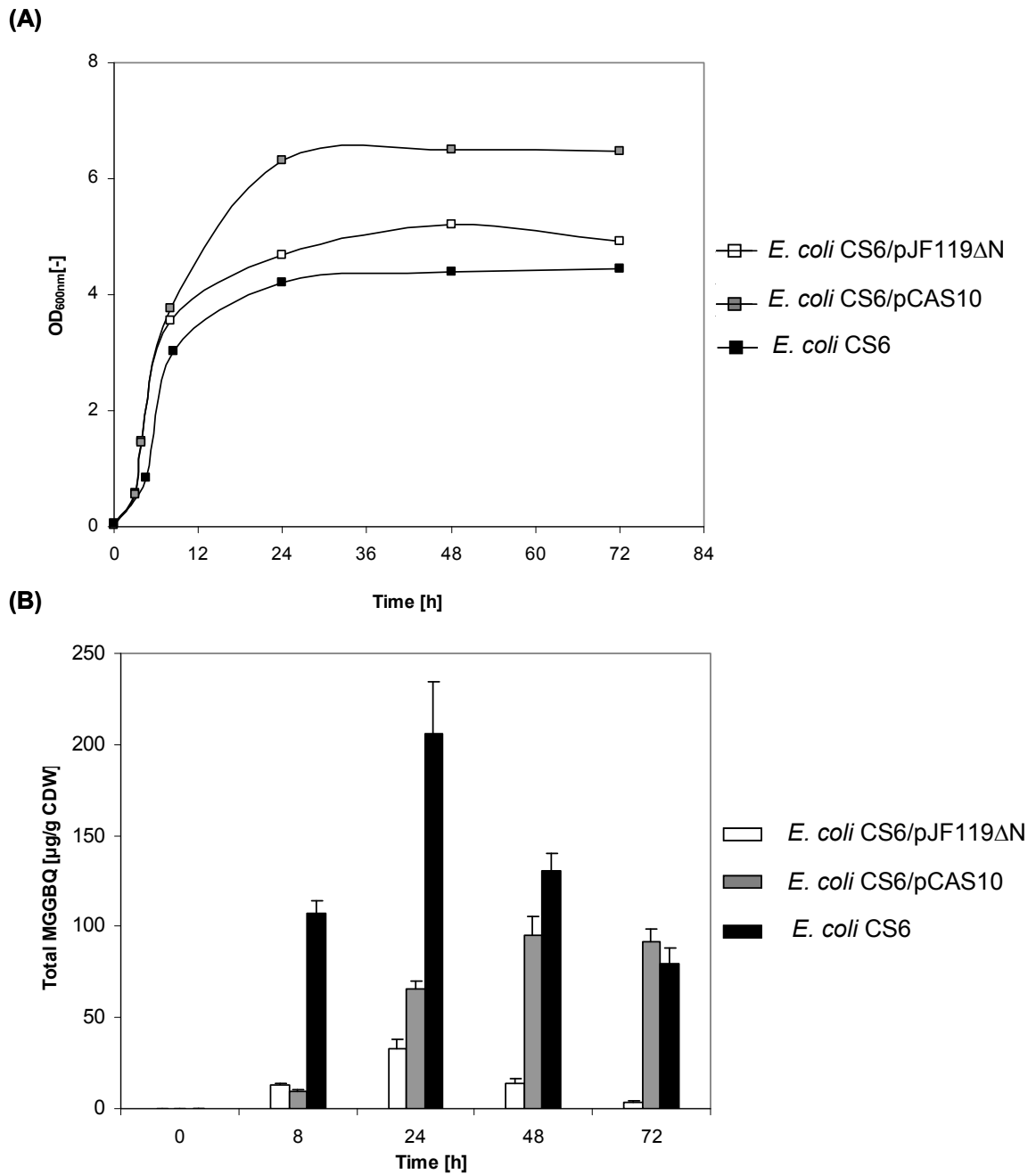


Figure 3.63: Cell density and MGGBQ production when *Idi* is co-expressed in *E. coli* CS6 in shaking flask in LB-Glycerol. 100 $\mu\text{g/ml}$ of ampicillin was added to *E. coli* CS6/pJF119 Δ N and *E. coli* CS6/pCAS10 cultures. Cultures induced with 0.25 mM IPTG. *E. coli* CS6 is shown in this figure as a reference so that the total MGGBQ production of the other two strains can be compared with it. (A) Cell density in terms of OD_{600nm}. (B) Total MGGBQ productivity in $\mu\text{g/g CDW}$.

3.11.1. Construction of *E. coli* CS8 and biosynthesis of MGGBQ in bioreactor

Chromosomal Integration of *idi* expression cassette in *E. coli* CS6 and analysis of protein expression on 2D Gel Electrophoresis

Plasmid pCAS10 was modified by ligation of HindIII / HindIII digested 1.1 kB FRT-*cat*-FRT fragment into 5.4 kB HindIII / HindIII digested pCAS10 fragment. Successful ligation produced a new plasmid pCAS10-FRT-*cat*-FRT. Clones obtained after transformation with ligation mixture were tested by digesting the plasmid with restriction enzyme HindIII which resulted in 1.1 & 5.4 kB. This corresponded to the expected size from restriction mapping.

pCAS10-FRT-*cat*-FRT was used as template for PCR amplification. Primers *rbsD*-integr and *rbsK*-integr (i.e. primer nr. 7 & 8 from table 6) were used for amplification of a fragment P_{tac}-*idi*-FRT-*cat*-FRT. This resulting fragment has a region homologous to some base pairs in *rbsD* and *rbsK* loci. *E. coli* CS6 strain carrying a plasmid pKD46 (expressing λ -recombinase induced by arabinose) was transformed by electroporation with the fragment P_{tac}-*idi*-FRT-*cat*-FRT. As a result, 6 transformants were obtained and were tested on MacConkey agar plate each supplemented with 4 different sugars (fucose, maltose, lactose and ribose). Each of these MacConkey agar plate were streaked with there respective control strain. All the 6 transformants were regarded as positive as none of them turned red on MacConkey agar plates with sugars. These 6 transformants were further tested with PCR using primers P1-Control-*idi*-*rbs* and P2-Control-*idi*-*rbs* yielded PCR product of 1.8 kB size which corresponds with the expected size. The new strain was named as *E. coli* CS8-*cat*. Using plasmid pCP20, the *cat*^r cassette was removed from *E. coli* CS8-*cat* to obtain a new strain named *E. coli* CS8 (shown in figure 3.64).

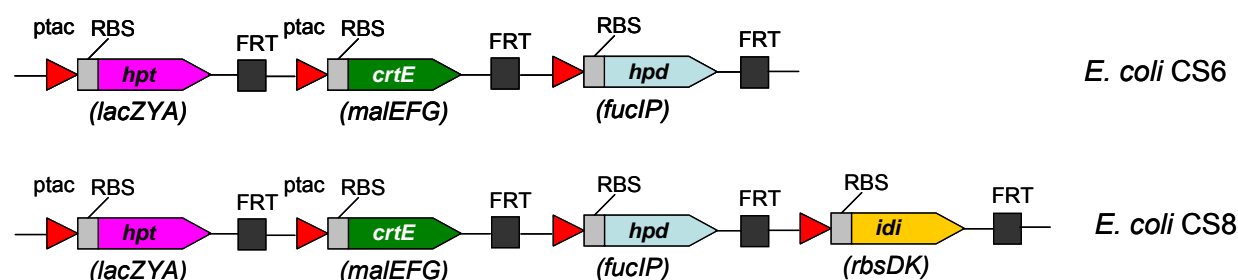


Figure 3.64: Scheme showing chromosomal integrated strains *E. coli* CS6 and *E. coli* CS8. The difference between the two is 4th expression cassette (*idi*) in ribose operon i.e. rbsDK locus in case of *E. coli* CS8 strain.

Overexpression level of Idi in the newly constructed *E. coli* CS8 strain was studied. *E. coli* CS6 and *E. coli* CS8 were cultivated in LB medium at 30 °C. Cultures were induced with 0.25 mM IPTG at OD_{600nm} of 0.8. Cell samples from both cultures i.e. 6 h after induction was

tested on 2D gel electrophoresis (see figure 3.65). Hpd and CrtE proteins were detected in both samples (overlapped and hence seen as dark spots marked at 40 kDa and 32 kDa respectively). Hpt-Syn being membrane associated was not detected on 2D gel. Idi protein has a calculated size of 20.5 kDa (ExpASy). An extra red spot at approx. 21.2 kDa was observed in *E. coli* CS8 (seen in red spots also marked by arrows).

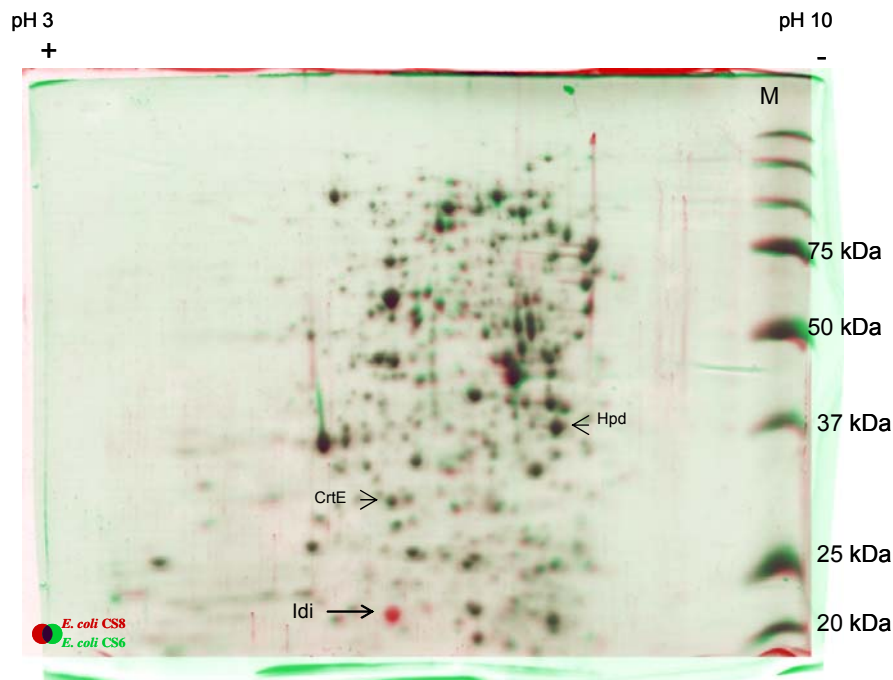


Figure 3.65: 2 D Gel electrophoresis. In green is *E. coli* CS6 and in red is *E. coli* CS8. Hpd, and CrtE protein overlapped (both dark red coloured spots, shown by arrows) at approx. 40 and 32 kDa respectively. An additional red spot at approx. 20 kDa was seen in *E. coli* CS8 sample which corresponds to the expected size of Idi protein from *E. coli*.

To study the effect of *idi* expression cassette in the newly constructed strain *E. coli* CS8 on the MGGBQ (total) productivity it was cultivated in shaking flask in LB-Glycerol at 30 °C. As control *E. coli* CS6 was cultivated under same conditions. Cultures were induced with 0.25 mM IPTG at OD_{600nm} of 0.8. Results of this experiment can be seen in figure 3.66. Till 8.5 h both cultures had almost reached identical cell density (approx. OD_{600nm} of 2.95). Between 8.5 and 24 h the cell growth in *E. coli* CS8 was affected and reached stationary phase at 36 h while the control *E. coli* CS6 grew further to reach a final OD_{600nm} of 4.1. The total MGGBQ produced in *E. coli* CS8 after 24 h was more than 2.5 times higher (in terms of µg/g CDW) when compared to its control *E. coli* CS6 without *idi* expression cassette. Total MGGBQ yield after 48 h and 72 h in both cultures decreased but the decrease in *E. coli* CS8 was slower than in *E. coli* CS6 which suggests that MGGBQ was produced in *E. coli* CS8 but

simultaneously oxidized and polymerized. After confirming the positive impact of expression of *Idi* in *E. coli* CS8 over *E. coli* CS6, *E. coli* CS8 was cultivated in bioreactor in minimal medium using glucose and/or glycerol as sole carbon and energy source to compare the respective carbon flux into total MGGBQ production.

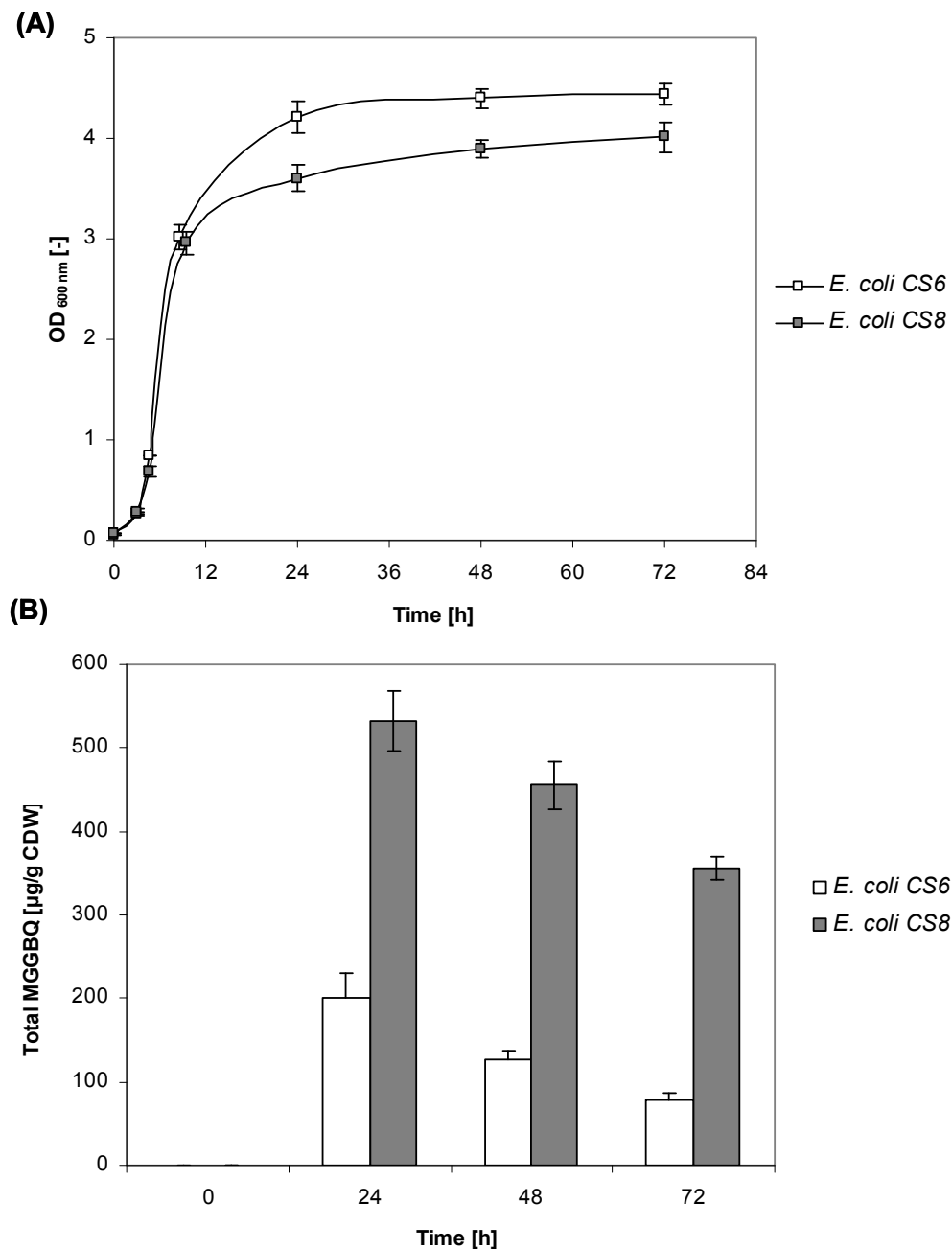


Figure 3.66: Effect of chromosomally integrated *idi* expression cassette in *E. coli* CS8 on MGGBQ production. Shaking flask cultivation carried out at 30 °C in LB-Glycerol medium, induction with 0.25 mM at OD_{600nm} of 0.8. *E. coli* CS6 is used as a control for *E. coli* CS8. (A) Shows cell density in OD_{600nm} as a function of time. (B) Shows the total MGGBQ production in µg/g CDW as a function of time. S.D calculated from 2 different samples taken during cultivation which were extracted and analyzed (HPLC) separately. Shaking flask cultivation of both strains were carried out thrice independently under identical conditions and medium. The S.D in all the three experiments w.r.t to the total MGGBQ production was less than 10 % (µg/l as well as µg/g CDW).

Increased MGGBQ Production using *E. coli* CS8 Strain in Minimal Medium in Infors Bioreactor

E. coli CS8 was cultivated twice in minimal medium using glucose and twice in minimal medium using glycerol as sole carbon and energy source in bioreactor. Cultivation were carried out at 30 °C at constant pH of 7.0.

E. coli CS8 cultures in MM-Glucose and MM-Glycerol were induced with 0.25 mM IPTG at approx. OD_{600nm} of 2.1 ± 0.1 at 13.75 h and 16.0 h respectively (shown by (a) and (b) arrows in figure 3.67 A). *E. coli* CS8 in MM-Glucose medium (μ_{\max} of 0.24 h^{-1}) grew better than in MM-Glycerol medium (μ_{\max} of 0.16 h^{-1}). Cell growth in MM-Glucose after 30 h slowed down where the growth rates in both medium was almost identical (μ of $0.08 \pm 0.02 \text{ h}^{-1}$). *E. coli* CS8 cultures in glycerol reached higher cell density (OD_{600nm} of approx. 28.0) as compared to that achieved in *E. coli* CS8 in glucose.

No MGGBQ was produced before induction with IPTG either in MM-Glucose or in MM-Glycerol (see figure 3.68). During batch process, the total MGGBQ produced in both medium was below 200 $\mu\text{g/g}$ CDW. Fed batch process produced higher total MGGBQ levels in MM-Glycerol as compared to MM-Glucose. Acetic acid produced during the entire fed batch process in MM-Glycerol was relatively low (approx. 1.2 g/l) as compared to that produced in MM-glucose (approx. 2.1 g/l). This may be a possible reason for the slow growth in MM-Glucose after 30 h. As a result at the end of respective cultivations, total MGGBQ produced in *E. coli* CS8 in MM-Glycerol was at least 20 % higher ($1285 \pm 117 \mu\text{g/g}$ CDW) than as that produced in *E. coli* CS8 in glucose ($1076 \pm 105 \mu\text{g/g}$ CDW). Even though the difference in total MGGBQ was not significant, MM-Glucose produced almost 38 % of oxidized MGGBQ as compared to only 21 % in MM-Glycerol (figure 3.68).

MGGBQ_{total} yield based on sugar, showed that since the start of MGGBQ production in MM-Glycerol (i.e. 16.5 h) the MGGBQ_{total} resulted in higher yields as compared to that in MM-Glucose (figure 3.69). Highest MGGBQ_{total} in MM-Glycerol reached $224 \pm 6 \mu\text{g/g}$ glycerol and that in MM-Glucose reached $187 \pm 4 \mu\text{g/g}$ glucose.

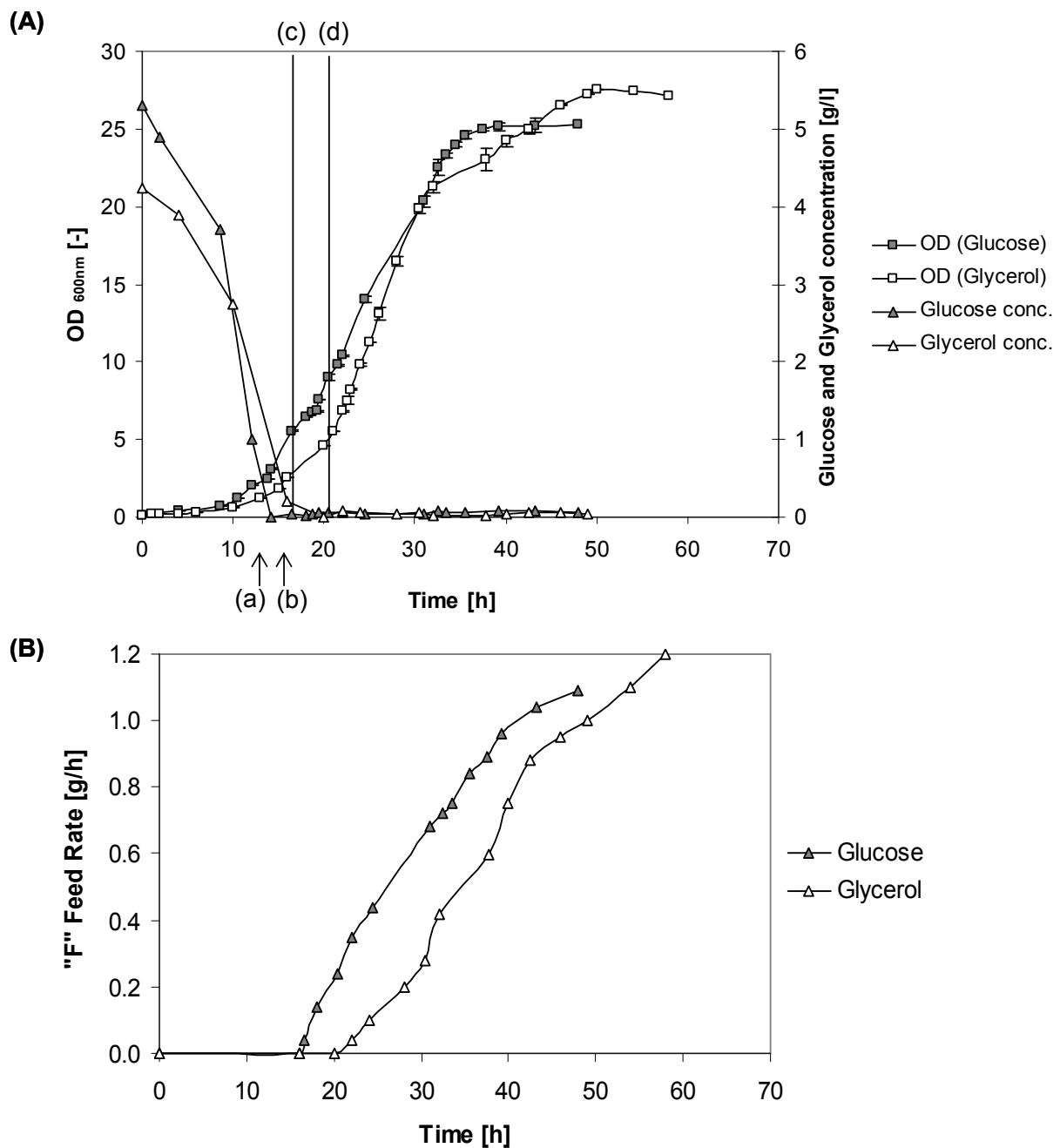
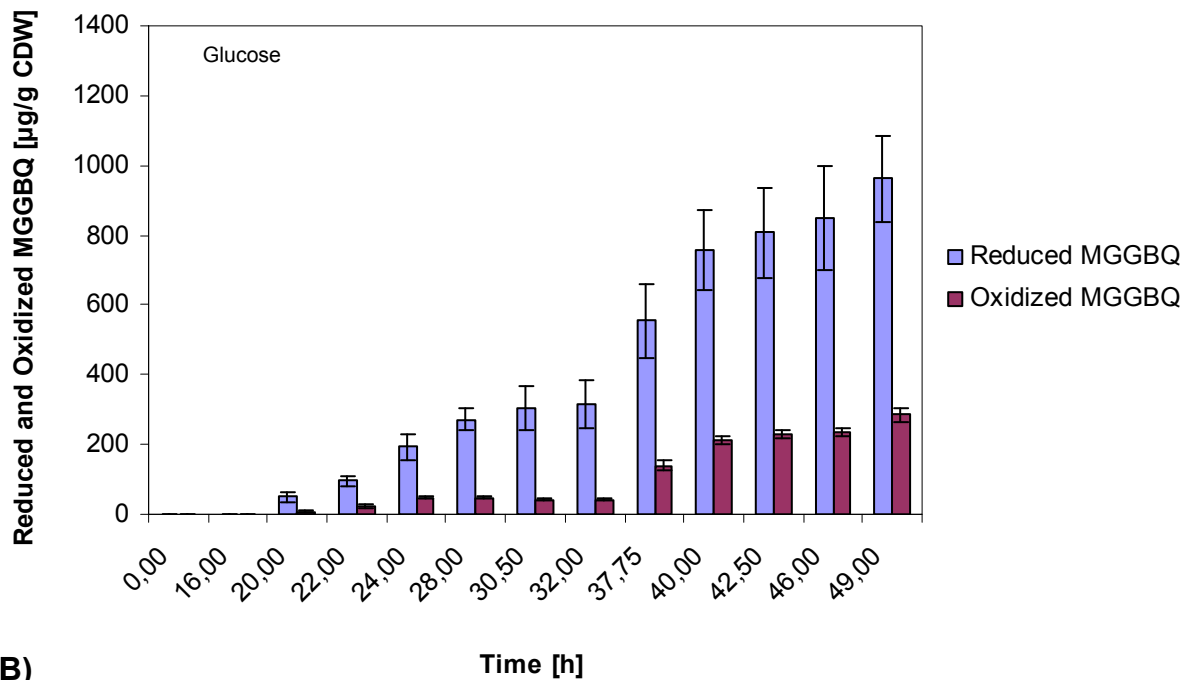


Figure 3.67: Cultivation results of *E. coli* CS8 strain in Infors bioreactor in minimal medium using glucose and glycerol as carbon and energy source.

(A) Cell growth curve shown in OD_{600nm} on left hand side y-axis, Glucose and Glycerol concentration in bioreactor vs. time shown on right hand side Y-axis. Vertical lines (a) and (b) indicate the time of induction with 0.25 mM IPTG in glucose and glycerol as carbon source respectively. Vertical lines (c) and (d), indicates the start of fed-batch cultivation by feeding glucose or glycerol stock solution respectively. (B) Feed rates of glucose and glycerol calculated used as sole carbon and energy source.

(A)



(B)

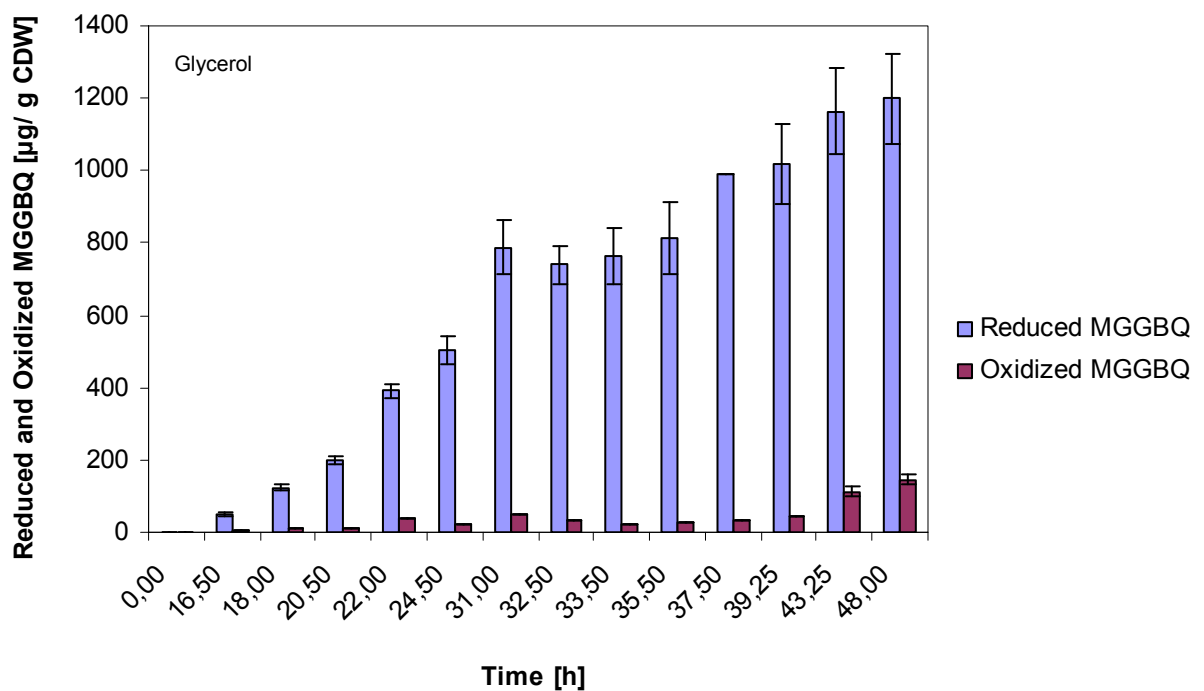


Figure 3.68: Reduced and Oxidized MGGBQ production in *E. coli* CS8 strain in bioreactor. Cultivation was carried out in minimal medium with glucose/glycerol as sole carbon and energy source at 30°C using batch-fed batch cultivation strategy. Cultures induced with 0.25 mM IPTG. (A) MGGBQ yield using glucose as carbon and energy source (B) MGGBQ yield using glycerol as carbon and energy source

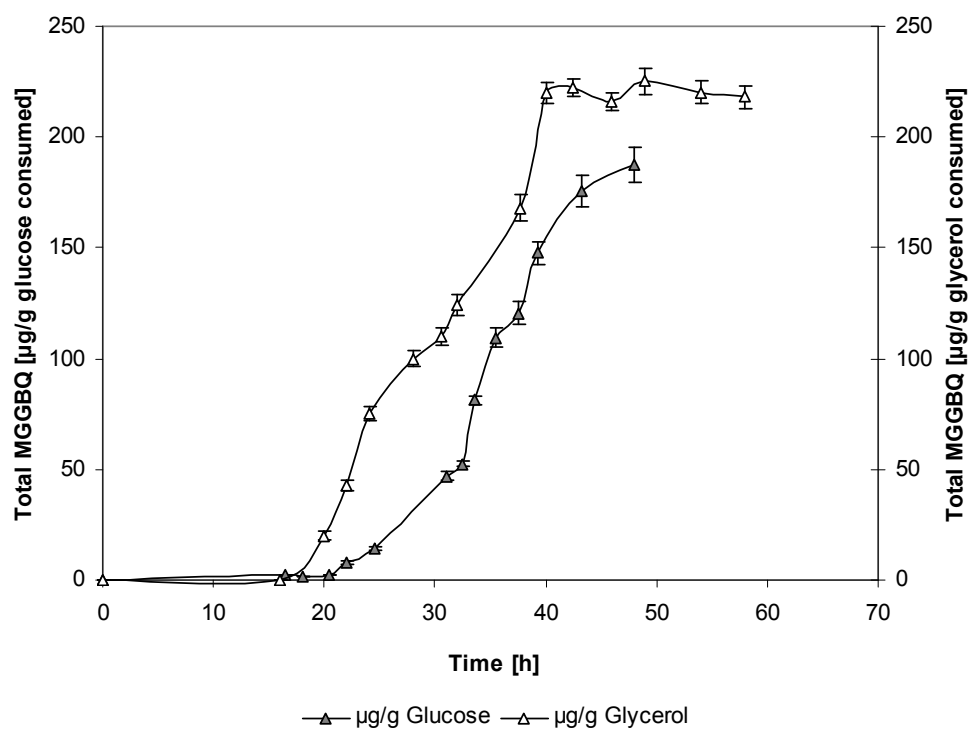


Figure 3.69: Total MGGBQ yield calculated per gram of carbon source (glucose/glycerol) consumed during cultivation of *E. coli* CS8 strain in bioreactor in minimal medium at 30 °C.

Influence of co-expression of Dxs in *E. coli* CS6 and *E. coli* CS8 strains on MGGBQ production

After studying the positive effect of Idi co-expression in *E. coli* CS6 on the yield of MGGBQ_{total}, the influence of Dxs co-expression on total MGGBQ in *E. coli* CS6 and *E. coli* CS8 as host strains was tested.

dxs gene from *Corynebacterium glutamicum* was already cloned into pJF119HE (modified pJF119 Δ N) vector to obtain a new plasmid pJF119HE-dxs-C.glut (personal communication from Dr. Natalie Trachtmann), and was kindly provided for further expression and cultivation experiments. Protein over-expression was in *E. coli* was shown and enzyme was shown to be active during *in-vitro* tests (personal communication with Dr. N. Trachtmann). Before using the plasmid, protein over-expression was confirmed. SDS-PAGE and can be seen in figure 3.70. *E. coli* BW25113 / pJF119HE-dxs-C.glut was cultivated in LB-Amp100. As control *E. coli* BW25113 /pJF119HE was cultivated. Cultures were induced with 1 mM IPTG at approx. OD_{600nm} of 0.8. Additional protein bands at approx. 68 kDa (R_f method) in lane 2 and 4 were observed after de-staining the acrylamide gel. These were absent in control strains (lane 1 and 3). Dxs has a calculated protein size of 69 kDa (ExpASy) which closely corresponded with the protein size obtained experimentally. This suggests that the Dxs from *C. glutamicum* was overexpressed in *E. coli* BW25113 strain with and without IPTG induction. Activity of the expressed Dxs protein was tested during *in-vivo* experiment, where the plasmid pJF119HE-dxs-C.glut was used for cultivation experiment for MGGBQ production, using *E. coli* CS6 and *E. coli* CS8 as host strains. Host strains with control vector (pJF119HE) were used as control strain.

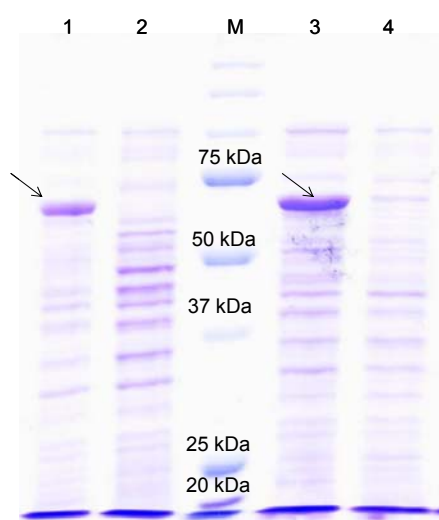


Figure 3.70: SDS-PAGE for Dxs over-expression. 10 μ g of protein sample (cell free crude extract) was loaded in each lane.

1: *E. coli* BW25113// pJF119HE-dxs-C.glut (3h) i.e. before IPTG

2: *E. coli* BW25113/pJF119HE (3h) i.e. before IPTG

M: molecular marker

3: *E. coli* BW25113/ pJF119HE-dxs-C.glut (8h) i.e. 5 h after IPTG

4: *E. coli* BW25113/pJF119HE (8h) i.e. 5 h after IPTG

Thick stained bands in lane 1 and 3 are marked with arrow representing the over-expressed Dxs protein (approx. 68 kDa) which are absent in control (lane 2 and 4 resp.)

Shaking flask cultivation of *E. coli* CS6/ pJF119HE-dxs-C.glut and *E. coli* CS8/ pJF119HE-dxs-C.glut was carried out in LB-Glycerol-Amp100 at 30 °C to produce MGGBQ. As control, *E. coli* CS6/pJF119ΔN and *E. coli* CS8/ pJF119ΔN strains were cultivated under identical conditions. Cultures were induced with 0.25 mM IPTG at approx. OD_{600nm} of 0.8. Till the time of induction all strains grew equally well. After induction *E. coli* CS6 and *E. coli* CS8 carrying pJF119HE-dxs-C.glut plasmid grew better than the strains carrying empty vector and reached two times higher cell mass after 72 h (see figure 3.71, graph A). *E. coli* CS8/pJF119HE-dxs-C.glut strain reached higher cell density than *E. coli* CS6/ pJF119HE-dxs-C.glut.

Total MGGBQ production (figure 3.71, graph B) in strains carrying plasmid pJF119HE-dxs-C.glut was higher than strains carrying the empty vector. The increase in total MGGBQ in *E. coli* CS6 /pJF119HE-dxs-C.glut (was 8.5 times as compared to *E. coli* CS6/ pJF119HE. The increase in MGGBQ in *E. coli* CS8 /pJF119HE-dxs-C.glut was 20 times as compared to *E. coli* CS8/ pJF119HE. Over-expression of Dxs in *E. coli* CS6 and *E. coli* CS8 had a strong effect on total MGGBQ production without negatively affecting the cell growth. This experiment was repeated under same conditions to reproduce identical MGGBQ yields with standard deviations less than 10 % (in terms of μg/l and μg/g CDW). The reason for the increased total MGGBQ level in strains carrying pJF119HE-dxs-C.glut plasmid can be explained as the Dxs over-expressed increases the carbon flux via DXP pathway*. The difference in total MGGBQ produced in *E. coli* CS6/ pJF119HE-dxs-C.glut and *E. coli* CS8 pJF119HE-dxs-C.glut may be due to the *Idi* expressed in *E. coli* CS8 strain which perhaps increases the pool of FPP and IPP. Hence, it was decided to overexpress Dxs protein in *E. coli* CS8 strain to increase the MGGBQ production level. Instead of using an extra copy of foreign *dxs* gene for chromosomal integration into another sugar operon a new chromosomal integration technique was used. (Albermann et. al. 2010). The native promoter of *dxs* in *E. coli* CS8 strain was replaced by P_{T5} promoter to obtain a new construct. This is discussed in detail in next section.

* Independent attempts to study the effect of Dxs overexpression (using plasmid pJF119EH-dxs-C.glut) in another host strain and production system were unable to see any significant increase in product yield (Personal communication, Prof. Georg Sprenger), as seen in this study.

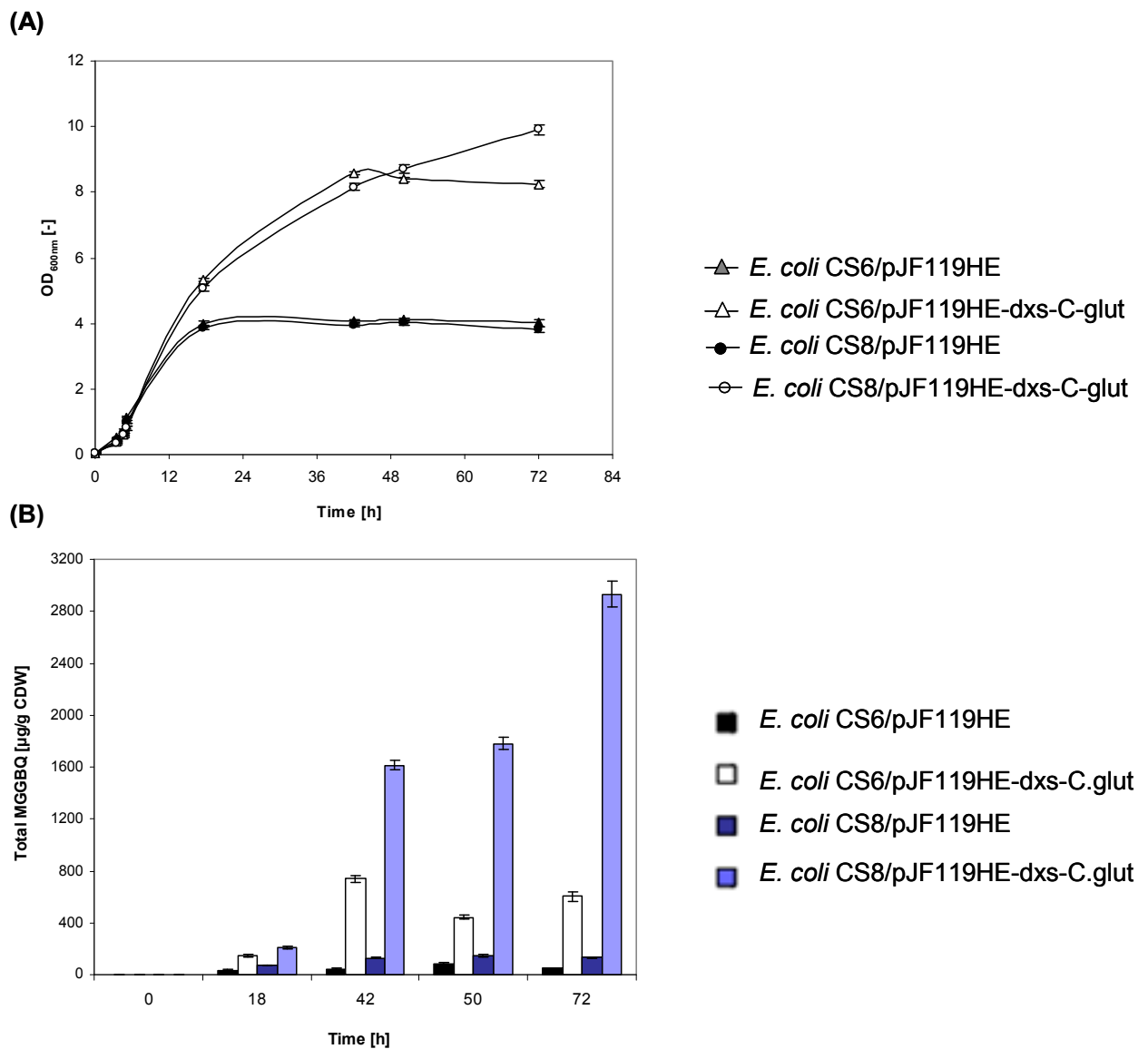


Figure 3.71: Effect of co-expression of Dxs (in plasmid) in *E. coli* CS6 and *E. coli* CS8 on total MGGBQ production. Cultivations were carried out in shaking flask at 30 °C in LB-Glycerol-Amp100 medium. Cultures induced with 0.25 mM IPTG at approx. OD_{600nm} of 0.8. (A) Line chart shows the cell density (OD_{600nm}) calculated during cultivation. (B) Bar chart represents the total MGGBQ yield calculated in $\mu\text{g/g}$ CDW. This experiment was repeated to confirm the results obtained. The S.D for OD and total MGGBQ yield was below 10 %.

3.11.2. Construction of *E. coli* CS10 and biosynthesis of MGGBQ in Infors bioreactor

Exchange of the native *dxs* promoter by an IPTG inducible P_{T5} - promoter and analysis of protein expression on 2D Gel Electrophoresis

pQE31 vector from Qiagen was modified by inserting FRT-cat-FRT fragment to obtain pQE31-FRT-cat-FRT vector (Lemuth et.al. 2011). The resulting vector was kindly provided by Dr. Albermann for further study. P_{T5}-*dxs*-FRT-cat-FRT fragment from pQE31-FRT-cat-FRT vector was amplified by PCR using primers P_{T5}-*dxs*-P1 and P_{T5}-*dxs*-P2 (nr. 23 and 24 in table 6). The purified fragment was transformed in *E. coli* CS8/pKD46 by electroporation. 14 Transformants obtained were tested by control PCR using primers Control-*dxs*-1 and Control-*dxs*-2 (nr. 25 and 26 in table 6). 3 transformants resulted in a PCR product of approx. 2 kb was obtained which corresponded to the expected size. The new strain obtained was named as *E. coli* CS10-*cat*. Removal of *cat* resistance cassette using temperature sensitive recombinase (pCP20) resulted in *E. coli* CS10 strain shown in figure 3.72.

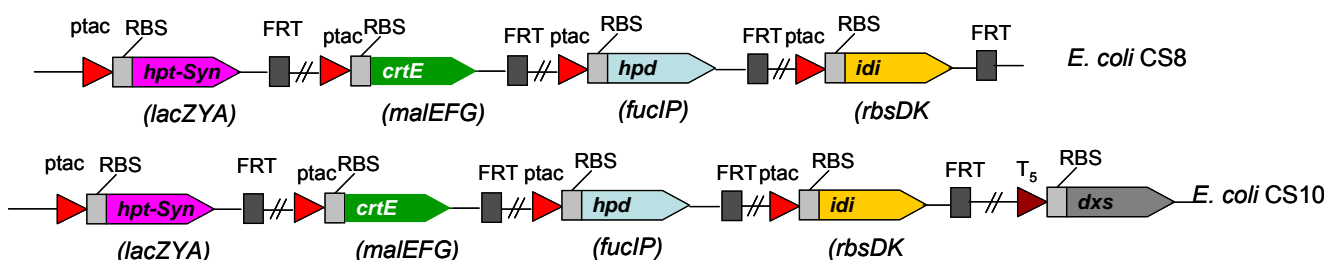


Figure 3.72: Scheme showing chromosomal integrated strains *E. coli* CS8 and *E. coli* CS10. *E. coli* CS10 was obtained by replacing the native *dxs* promoter with P_{T5} promoter (IPTG inducible promoter) in *E. coli* CS8 to obtain new strain *E. coli* CS10.

Over expression of Dxs protein in *E. coli* CS10 was studied by 2D gel electrophoresis. As control *E. coli* BW25113 (*lacZ*⁺) strain was used in this study. Results are shown in figure 3.73. Hpt-Syn being a membrane bound protein was not detected in both strains on the gel. Moderate expression of CrtE as compared to strong expression of Hpd and Idi proteins in both strains was observed. An additional spot at 67.4 kDa and pI of 6.15 (R_f method) was seen in red. Both the values closely corresponded to the calculated properties of Dxs protein (*E. coli* K12) calculated from ExPASy i.e. molecular mass of 69 kDa and pI value of 6.08.

To study the effect of Dxs with P_{T5} promoter instead of its native promoter on the MGGBQ production level, *E. coli* CS10 was cultivated in shaking flask in LB-Glycerol at 30 °C and as control *E. coli* CS8 was used. The cultivation experiment results can be seen in figure 3.74.

Cultures were induced with 0.25 mM IPTG at approx. OD_{600nm} of 0.8. Till induction cell growth in both strains was almost identical. After 72 h cell density reached in *E. coli* CS10 strain was slightly higher than in *E. coli* CS8. This indicated that Dxs expression in *E. coli* CS10 did not negatively affect the cell growth at least during the conditions used in this study. Total MGGBQ produced in *E. coli* CS10 ($749 \pm 43 \mu\text{g/g CDW}$) was approx. 50 % higher than that produced in *E. coli* CS8 ($510 \pm 35 \mu\text{g/g CDW}$) after 24 h (figure 3.74B).

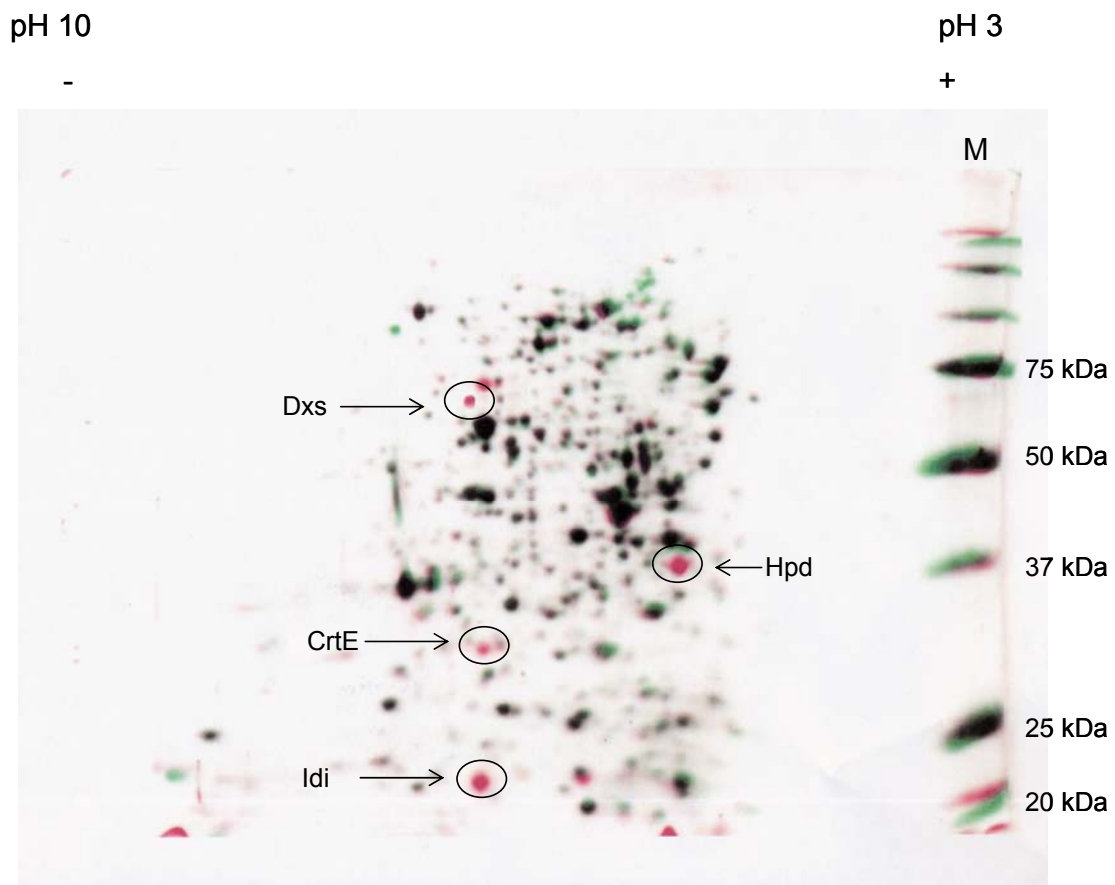


Figure 3.73: Comparison of 2D gel electrophoresis of *E. coli* CS10 sample with *E. coli* BW25113 *lacZ*⁺ sample. Red colour represents *E. coli* CS10 sample and green colour *E. coli* BW25113 (*lacZ*⁺) sample. Hpt-Syn was not detected in *E. coli* CS10 sample since it's a membrane bound protein. Other 4 proteins expected in *E. coli* CS10 were found during 2D gel electrophoresis and are marked in circles.

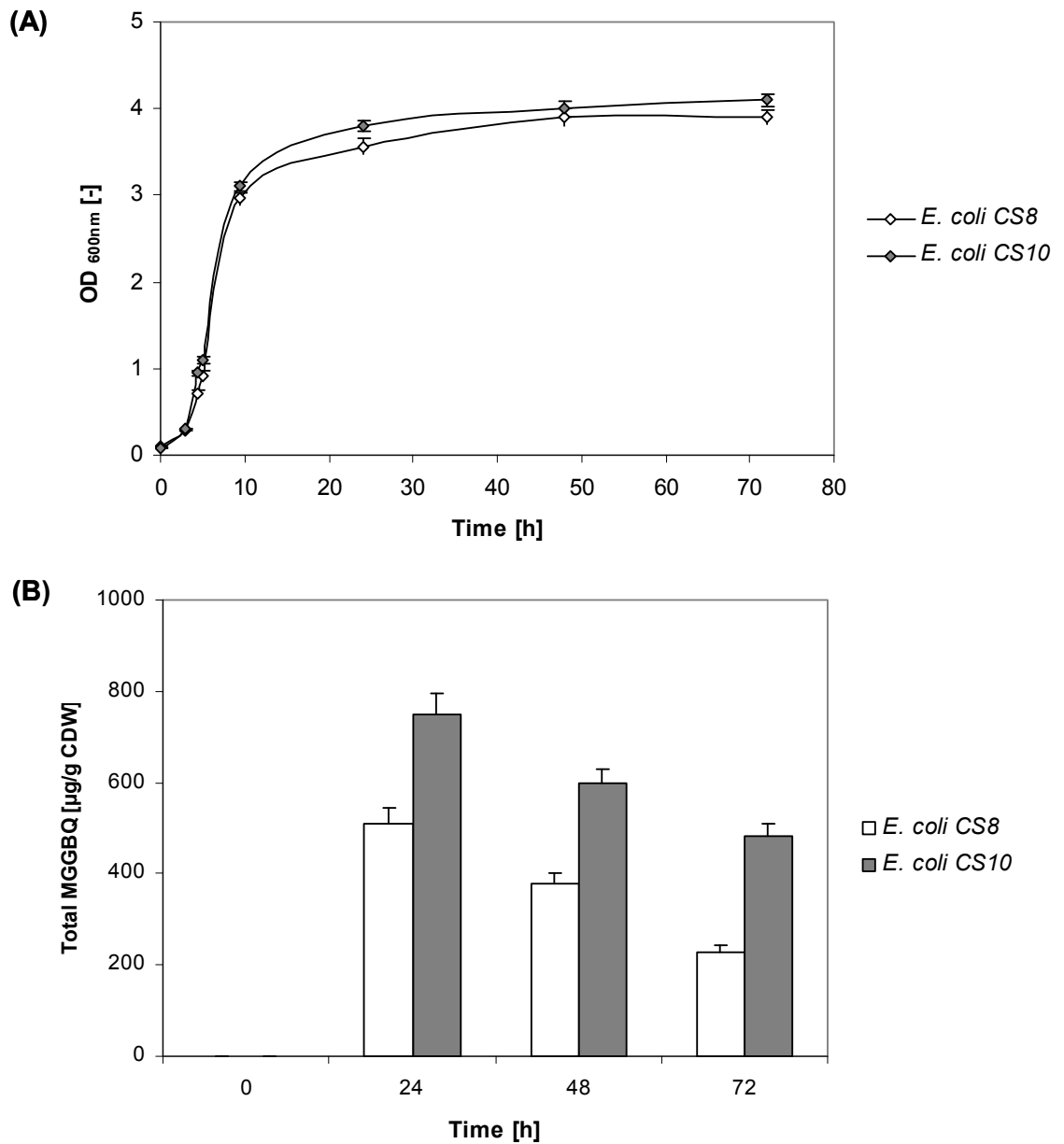


Figure 3.74: Effect of P_{T5} -dxs over expression in *E. coli* CS10 strain during MGGBQ production. *E. coli* CS10 and *E. coli* CS8 were cultivated in LB-Glycerol medium in shaking flask at 30 °C. Cultures were induced at OD_{600nm} of 0.8. (A) Cell growth curve represented as OD_{600nm} vs. time. (B) Total MGGBQ produced represented in µg/g CDW vs. time.

Comparison of Glucose and Glycerol as C-source for MGGBQ production in *E. coli* CS10 in Infors HT bioreactor

After it was confirmed that *E. coli* CS10 produced higher MGGBQ levels than *E. coli* CS8 strain because of the presence of P_{T5} promoter instead of the native promoter for *dxs* gene, it was decided to cultivate *E. coli* CS10 strain in bioreactor in minimal medium using glucose or glycerol as sole carbon and energy source. Similar cultivation conditions were used as that used during cultivation of *E. coli* CS6 and *E. coli* CS8 strains.

E. coli CS10 cultures in MM-Glucose and MM-Glycerol were induced with 0.25 mM IPTG at approx. OD_{600nm} of 2.0. Cultures in MM-Glucose reached a maximum growth rate of 0.40 h^{-1} as compared to 0.30 h^{-1} in MM-Glycerol during exponential phase. During the fed batch process the cell growth in MM-Glucose was better than in MM-Glycerol and as a result reached an OD_{600nm} of 30.3 and 27.5 respectively at the end of respective cultivation (see figure 3.75).

MGGBQ production started after IPTG induction in MM-Glucose and MM-Glycerol. Small quantities of MGGBQ (reduced and oxidized) were produced during batch process in both medium. Total maximum MGGBQ production levels in MM-Glycerol ($1882 \pm 79\text{ }\mu\text{g/g CDW}$) were higher than in MM-Glucose ($1576 \pm 58\text{ }\mu\text{g/g CDW}$) (figure 3.76). Most of this total MGGBQ was produced during early hours of fed batch process i.e. 25 h and 36 h in MM-Glucose and MM-Glycerol respectively, and after that till end of cultivation the increase in total MGGBQ level was not substantial. Culture colour in both medium at the end of cultivation was light brown. HGA accumulation in supernatant in MM-Glucose and MM-Glycerol started after 40 h and 47 h with final concentration in both medium below 20 mg/l. Acetic acid produced during cultivation of *E. coli* CS10 was the lowest when compared to *E. coli* CS6 and *E. coli* CS8 with 1.3 g/l and 0.9 g/l accumulated in MM-Glucose and MM-Glycerol at the end of cultivation. Total MGGBQ yield based on per gram of carbon source consumed resulted in glycerol reaching the highest carbon flux with $454\text{ }\mu\text{g/g}$ glycerol and glucose with $347\text{ }\mu\text{g/g}$ glucose.

The results of *E. coli* CS6 and *E. coli* BW25113/pCAS29 are compared and discussed along with *E. coli* CS7 and *E. coli* BW25113/pCAS47 in chapter 4. The MGGBQ production in all the 3 chromosomally integrated strains (*E. coli* CS6, *E. coli* CS8 and *E. coli* CS10) are also compared and discussed.

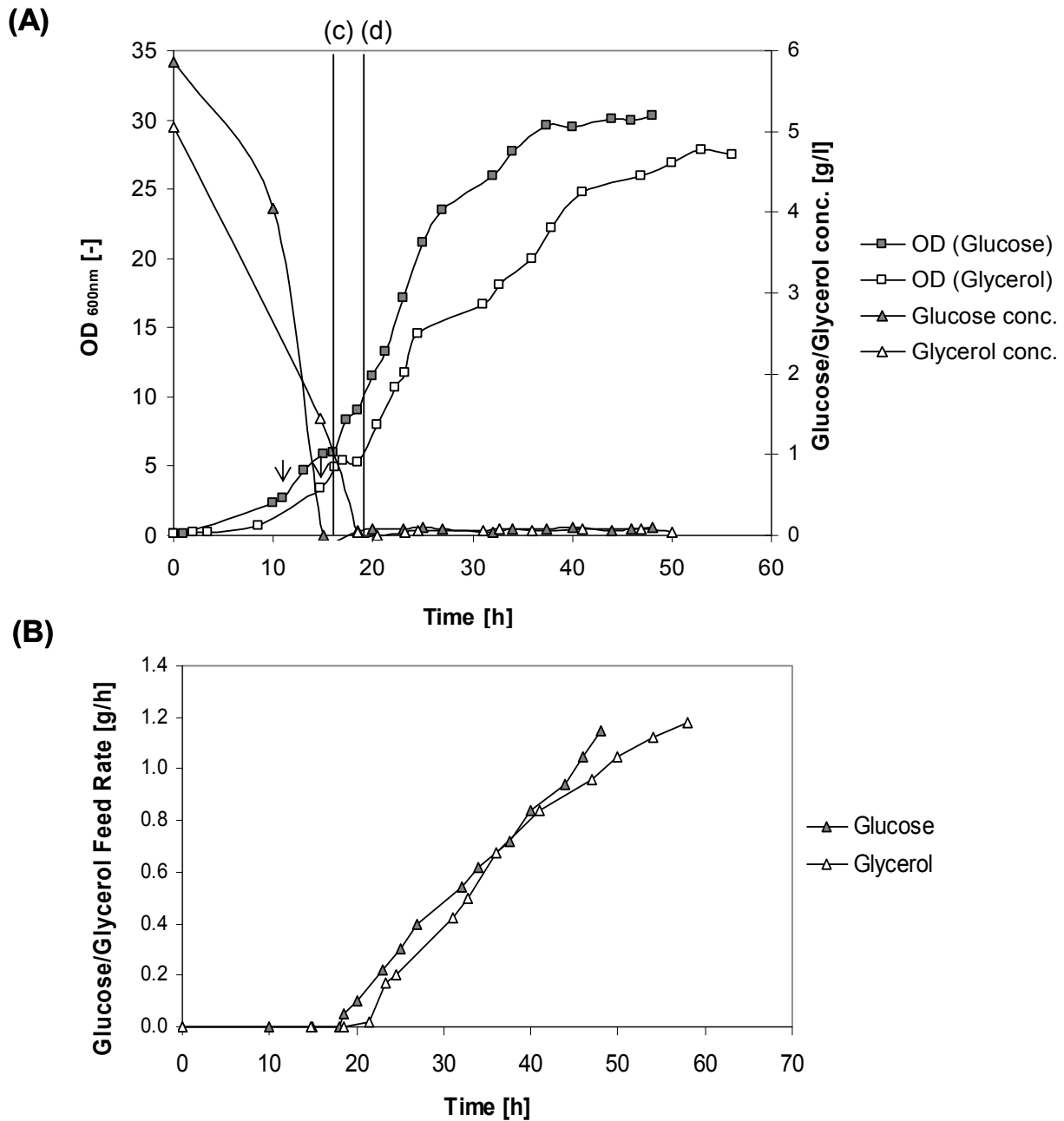


Figure 3.75: Fed-batch cultivation of *E. coli* CS10 strain at 30 °C in MM-Glucose and MM-Glycerol, in Infors Bioreactor. (A) Cell growth calculated as cell density (OD_{600nm}) w.r.t time and glucose/glycerol concentration curve in bioreactor. Arrows represents the time of induction with 0.25 mM IPTG. Vertical lines indicate the time of fed batch process i.e. (c) glucose feeding (d) glycerol feeding. (B) Feed rates of glucose or glycerol fed during the fed-batch phase of cultivation.

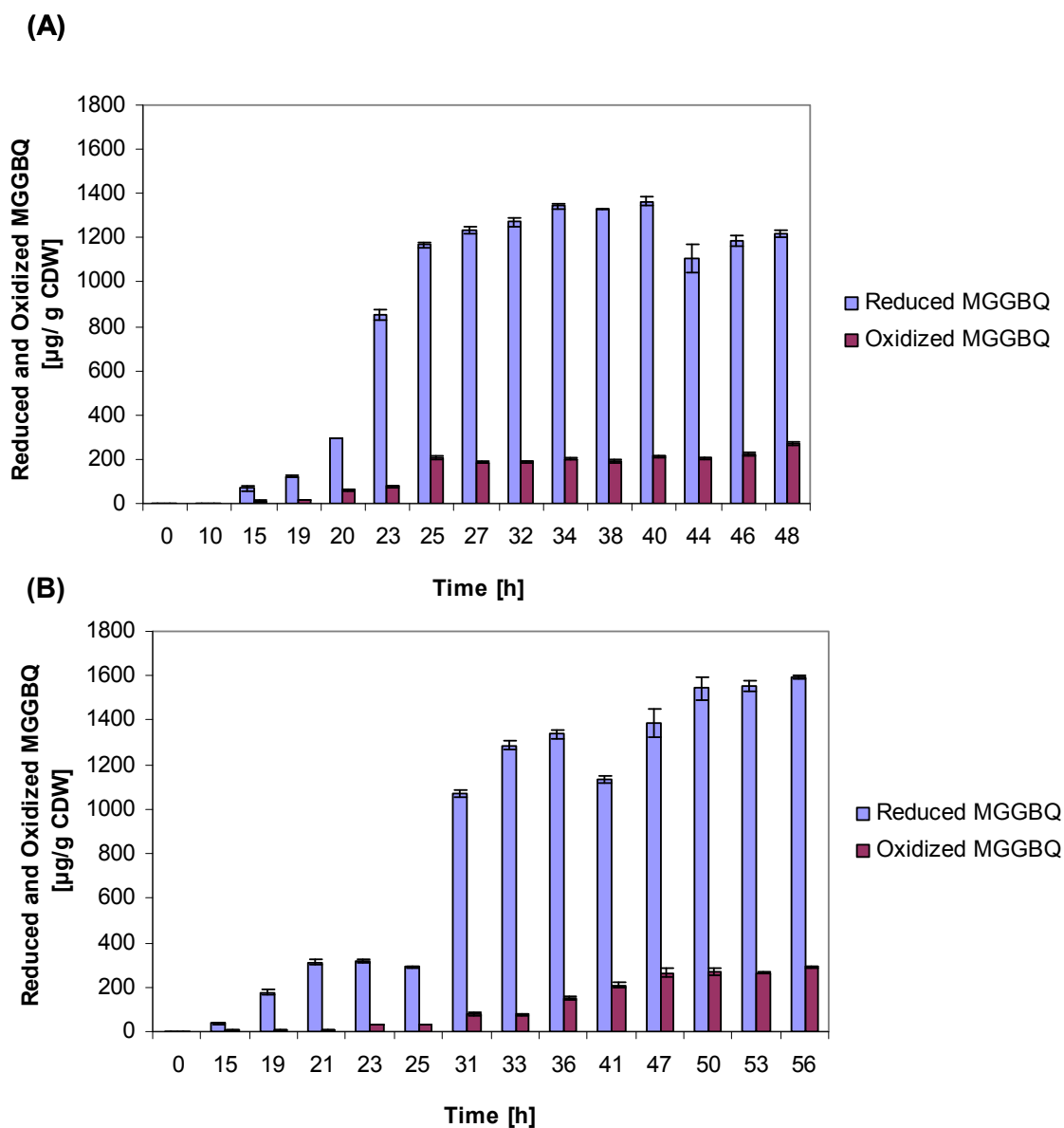


Figure 3.76: Bar charts showing the MGG BQ production levels achieved, during cultivation of *E. coli* CS10 in Infors bioreactor at 30 °C in minimal medium using (A) Glucose (B) Glycerol

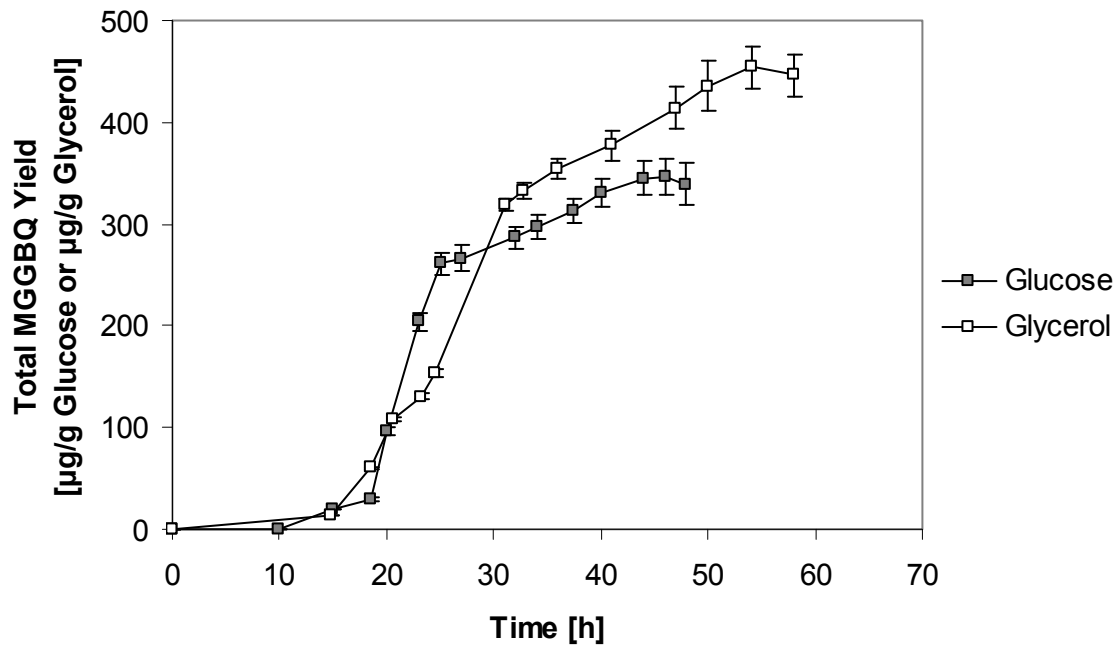


Figure 3.76C: Carbon flux into MGG BQ (total) during bioreactor cultivation of *E. coli* CS10 in minimal medium using glucose or glycerol as sole carbon and energy source. Carbon flux calculated in μg of total MGG BQ produced per gram of carbon source consumed.

3.12. Increased δ -Tocotrienol production in recombinant chromosomal integrated strain *E. coli* CS9 strain

3.12.1. Construction of *E. coli* CS9 strain

After confirming that *E. coli* CS8 produced higher MGGBQ concentrations and yields in MM-Glucose and MM-Glycerol compared to *E. coli* CS6 (as a result of additional overexpression of FPP isomerase), chromosomal integration of *cyc-At* gene in *xylAB* loci was started. A similar procedure was followed as used for construction of *E. coli* CS7 strain. Instead of *E. coli* CS6, here *E. coli* CS8 was used as host strain. *E. coli* CS8 strain carrying a plasmid pKD46 (expressing λ -recombinase induced by arabinose) was transformed by electroporation with the fragment P_{tac} -*cycAt*-FRT-*cat*-FRT. 6 transformants obtained were tested on MacConkey agar plates, with respective control strain. These transformants were screened on MacConkey agar plate, each supplemented with 4 different sugars (fucose, maltose, lactose ribose and xylose). Three transformants were found to be positive as they didn't turn red on any of the McConkey agar plates with xylose, or ribose or maltose, or lactose or fucose. The new strain was named as *E. coli* CS9-*cat*. PCR control test with primers P27 and P11 and P28 and P11 yielded PCR product of approx. 1.1 kb and 1.3 kb sizes which corresponds with the expected sizes calculated using Clone manager 7.0. Elimination of *cat* resistance gene was carried out by using temperature sensitive recombinase (pCP20) (method 2.2.2.5) yielded strain *E. coli* CS9 which can be seen in figure 3.77A.

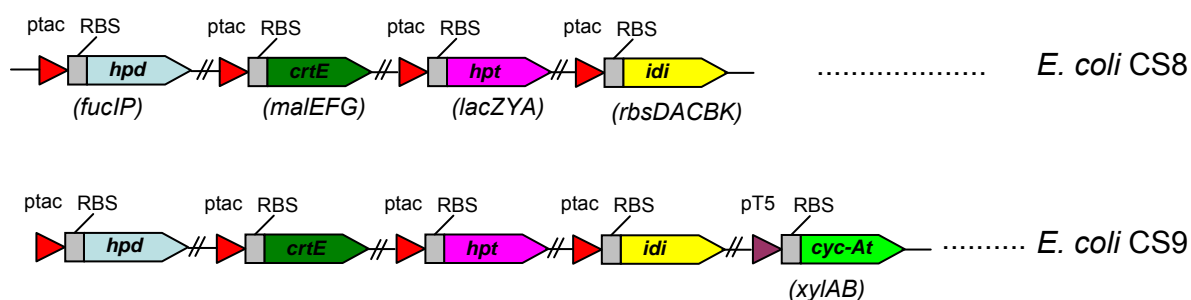


Figure 3.77A: Scheme representing chromosomal integrated strains *E. coli* CS8 and *E. coli* CS9. *cyc-At* gene was integrated in the *xylAB* loci of *E. coli* CS8 strain to obtain *E. coli* CS9-*cat* (not shown here). *E. coli* CS9 was obtained after removal of *cat* resistance cassette from *E. coli* CS9-*cat*.

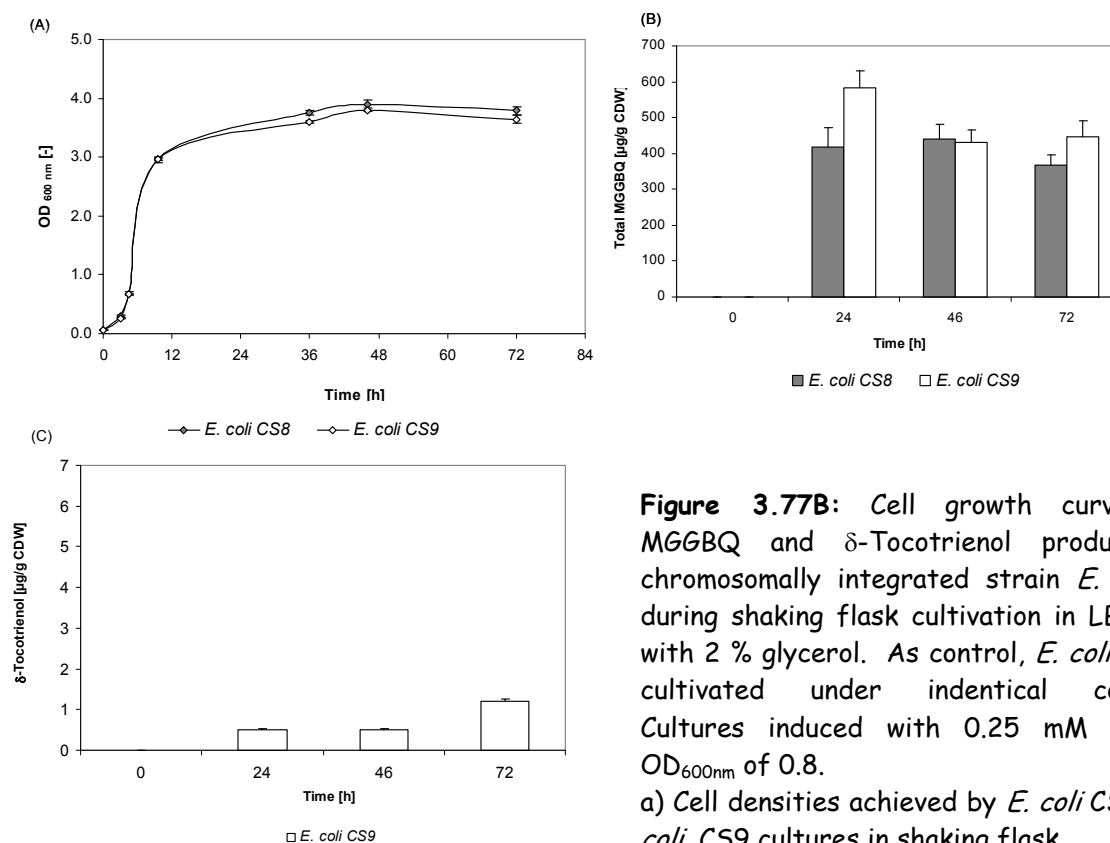


Figure 3.77B: Cell growth curve, total MGGBQ and δ -Tocotrienol production in chromosomally integrated strain *E. coli* CS9 during shaking flask cultivation in LB medium with 2 % glycerol. As control, *E. coli* CS8 was cultivated under identical conditions. Cultures induced with 0.25 mM IPTG at OD_{600nm} of 0.8.

a) Cell densities achieved by *E. coli* CS8 and *E. coli* CS9 cultures in shaking flask
 b Total MGGBQ produced in *E. coli* CS8 and *E. coli* CS9
 c) δ -tocotrienol produced in *E. coli* CS9. No δ -tocotrienol was detected in control strain, *E. coli* CS8.

During the shaking flask cultivation in LB+Glycerol, *E. coli* CS8 & *E. coli* CS9 grew equally well to reach a final OD_{600nm} of approx. 3.8 after 72 h. *E. coli* CS9 produced high amounts of MGGBQ compared to that in *E. coli* CS8. Similar behaviour was observed when results of *E. coli* CS6 and *E. coli* CS7 were compared. Additionally δ -tocotrienol was detected in *E. coli* CS9 cells when the extract was analysed by HPLC. Results can be seen in figure 3.77B. Hence, it was confirmed that the *Cyc-At* was expressed and was active. MGGBQ_{total} yield in *E. coli* CS9 was approx. 1.8 times higher when compared to that in *E. coli* CS7. δ -tocotrienol yield in *E. coli* CS9 was approx. 2 times higher when compared to *E. coli* CS7 in shaking flask (LB+Glycerol). To conclude, in complex medium (LB+Glycerol), it was observed that higher the produced MGGBQ_{total}, higher is the conversion into δ -tocotrienol. It was to be further studied during the bioreactor cultivation in minimal medium using glucose/glycerol as sole carbon and energy source, whether the same effect could be seen as seen in LB + Glycerol medium.

3.12.2 δ -Tocotrienol Biosynthesis in *E. coli* CS9 in Bioreactor

Key to study would be the increase in δ -tocotrienol production of *E. coli* CS9 when cultivated in bioreactor in MM+Glucose and MM+Glycerol. This was performed and the results can be seen in figure 3.78

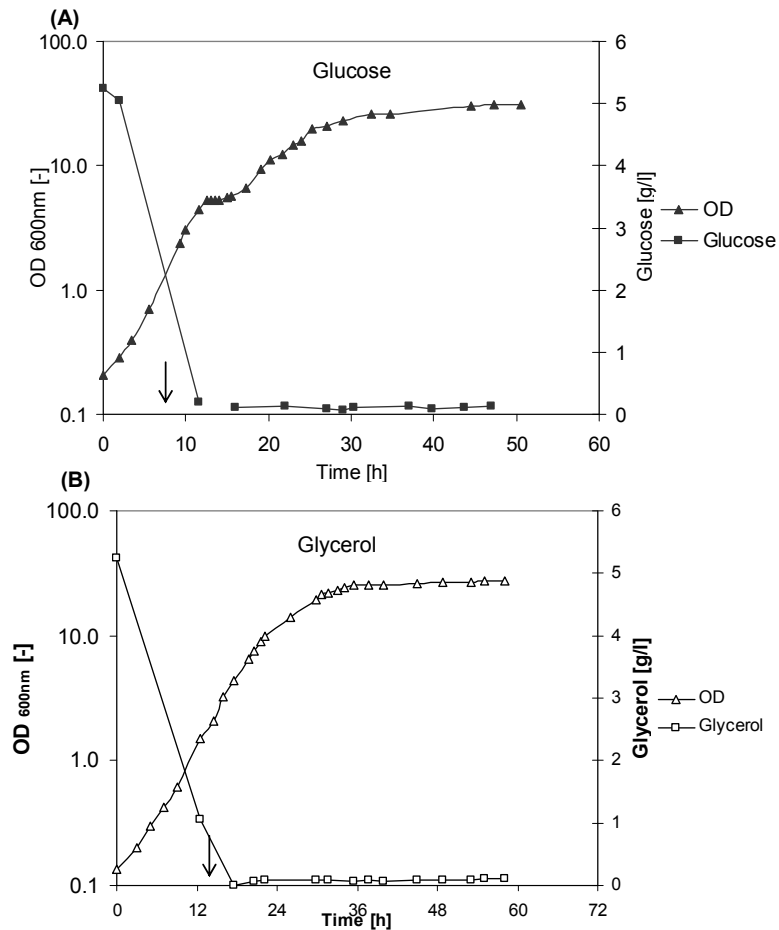


Figure 3.78: Graph showing cell growth and the glucose/glycerol concentration during cultivation of *E. coli* CS9 in Infors bioreactor. (A) Show results in MM + Glucose medium. (B) Show results in MM + Glycerol medium. Arrows shows the time of induction with 0.25 mM IPTG (end conc.).

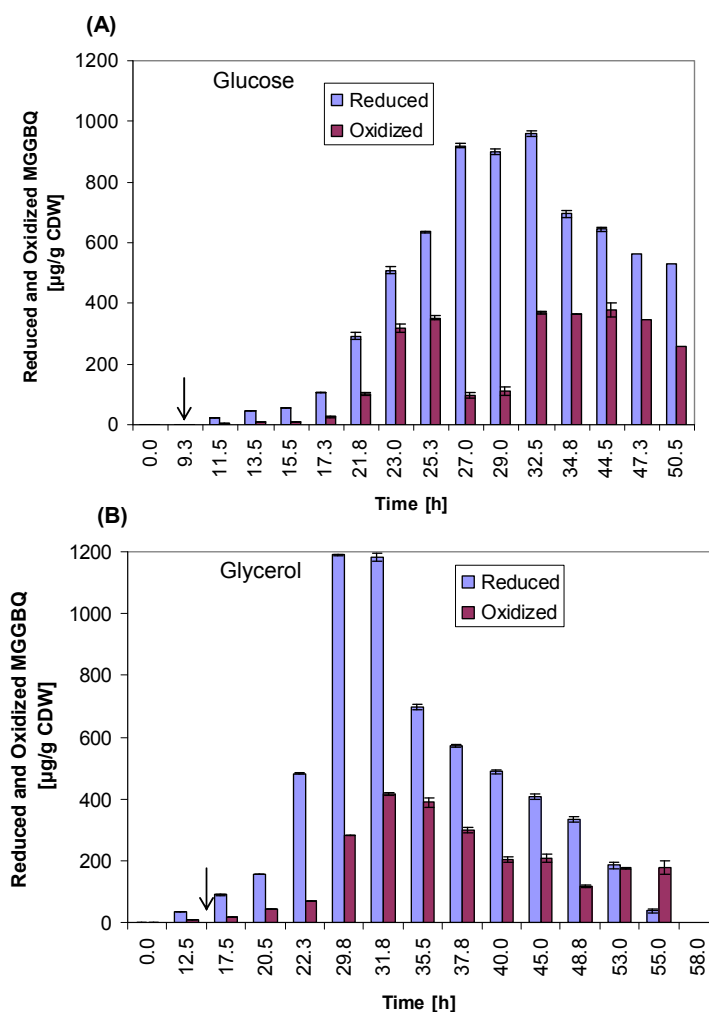


Figure 3.79: Bar chart showing MGGGBQ yields in *E. coli* CS9 strain during cultivation in Infors bioreactor. (A) Shows MGGGBQ yields in MM+Glucose medium. (B) Shows MGGGBQ yields in MM+Glycerol medium. Arrow indicates the time of induction with 0.25 mM IPTG (end concentration).

It is clearly seen from the figure 3.79 that MGGGBQ biosynthesis begins before induction with IPTG in case of MM-Glycerol, which is not the case in MM-Glucose medium. As a result of that, maximum MGGGBQ production was also observed in MM+Glycerol medium ($1190 \pm 23 \mu\text{g/g CDW}$ of MGGGBQ_{reduced} & $416 \pm 31 \mu\text{g/g CDW}$ of MGGGBQ_{oxidised} at 31.75 h) This suggests that the P_{tac} promoter is not tightly regulated in case of medium consisting of glycerol. Cultures in MM-Glucose and MM-Glycerol started turning brown after 34.75 h and 45 h respectively. The final HGA concentrations in medium at the end of respective fermentation were approx. 0.55 mM and 0.42 mM HGA respectively. Based on this result, it was observed that δ -tocotrienol producing recombinant *E. coli* strains (in this study) i.e. (*E. coli* CS7, *E. coli* CS9, and *E. coli* BW25113/pCAS47) produced less HGA compared to the MGGGBQ producing strains (*E. coli* CS6, *E. coli* CS8, *E. coli* CS10, and *E. coli* BW25113/pCAS29). Even though, MGGGBQ production in MM-Glycerol started earlier

compared to that in MM-Glucose, the δ -tocotrienol production in both medium started approx. at same time i.e. 15.5 h after induction in respective cultivations (figure 3.80). Interestingly, the cyclisation reaction into δ -tocotrienol in glycerol medium was comparatively faster than in glucose medium, but it failed to increase further at higher rate. δ -tocotrienol production in glucose medium increased steadily over the fermentation period of 48 h. Even though, *E. coli* CS9 produced higher amounts of δ -tocotrienol compared to *E. coli* CS7 (i.e. 4.20 $\mu\text{g/g}$ CDW & 3.95 $\mu\text{g/g}$ CDW vs. 3.2 $\mu\text{g/g}$ CDW & 3.69 $\mu\text{g/g}$ CDW in glucose and glycerol resp.) Cyc-At was found to be limiting in both strains and both carbon sources, as MGGBQ reduced in excess of 500 $\mu\text{g/g}$ CDW was available within the cell.

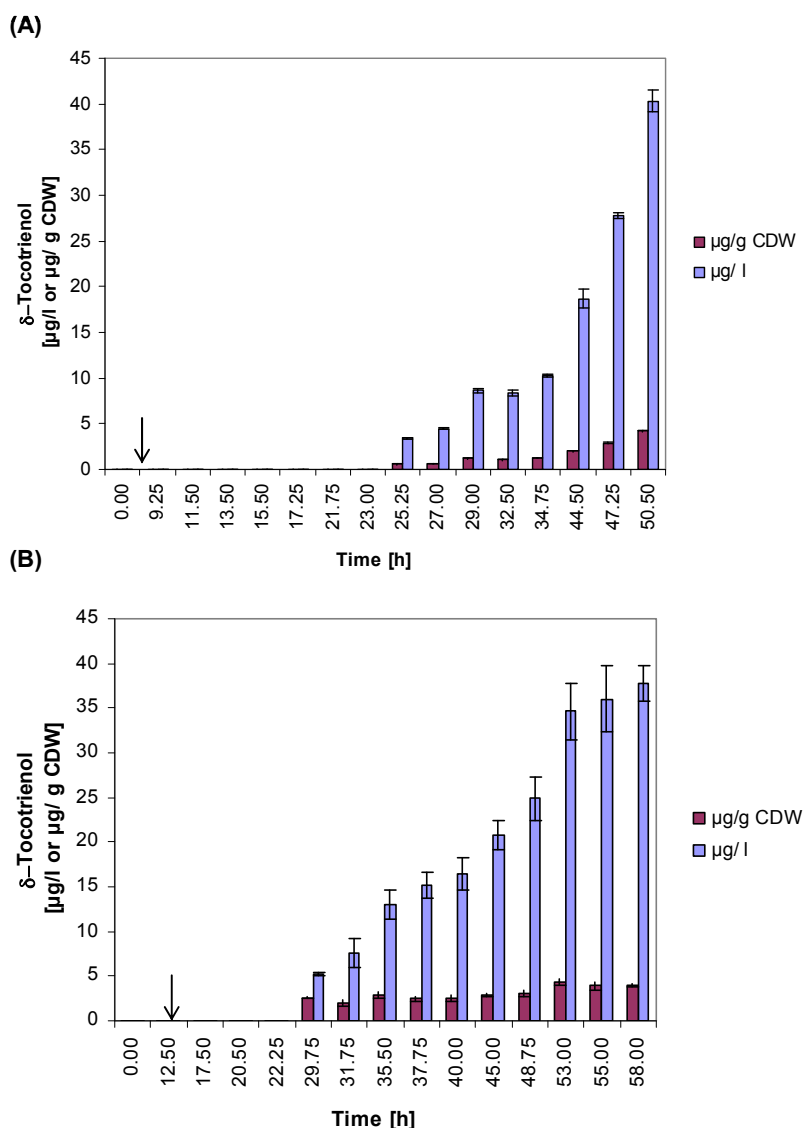


Figure 3.80: δ -tocotrienol yields and concentration in *E. coli* CS9 during cultivation in Infors bioreactor. (A) Fermentation in MM+Glucose medium. (B) Fermentation in MM+Glycerol medium. Arrow indicates the time of induction with 0.25 mM IPTG (end concentration).

3.13. Study to increase the conversion of MGGBQ to δ -tocotrienol in *E. coli* strains

3.13.1. Effect of inducer concentration on δ -tocotrienol and protein expression level

To study the effect of cyclase expression level on δ -tocotrienol production *E. coli* BW25113/pCAS47 strain during shaking flask cultivation in LB-Glycerol-Amp100 medium at 30 °C was induced with different IPTG concentrations. As control *E. coli* BW25113/pCAS29 was used under identical conditions. Cell growth in *E. coli* BW25113/pCAS47 was slightly inhibited in all IPTG concentrations when compared to its respective control (*E. coli* BW25113/pCAS29) (figure 3.81 A & B). Substantial difference was seen in *E. coli* BW25113/pCAS47 cultures when induced with 0.1, 0.25 and 1 mM IPTG which was not the case in *E. coli* BW25113/pCAS29. Whether the level of cyclase expressed or the amount of δ -tocotrienol produced negatively affects the cell growth is not clear at this point.

Total MGGBQ produced in *E. coli* BW25113/pCAS47 cultures (all IPTG concentrations) were almost identical (between 200 and 300 $\mu\text{g/g}$ CDW). But the δ -tocotrienol produced in *E. coli* BW25113/pCAS47 when induced with 0.25 mM IPTG was the highest (4 $\mu\text{g/g}$ CDW) i.e. 2.4 times more than without induction. On the other hand total MGGBQ production in *E. coli* BW25113/pCAS29 was the highest without induction (i.e. 0 mM IPTG). This might be due to the fact that the P_{tac} promoter is not tightly regulated in complex medium. On the contrary, *E. coli* BW25113/pCAS47 cultures without induction produced the lowest δ -Tocotrienol amounts. The cultures with 0.1 mM and 1.0 mM IPTG produced almost same amounts of δ -tocotrienol. The high IPTG concentration of 1 mM used for induction of *E. coli* BW25113/pCAS47 culture might have been detrimental to cell growth, which indirectly would have affected the MGGBQ and δ -tocotrienol yields. All this implies that, some other unknown factors also contribute towards lower MGGBQ conversion to δ -tocotrienol, apart from *Cyc-At* expression level and activity.

4 $\mu\text{g/g}$ CDW of δ -tocotrienol concentration was the highest level achieved by using *E. coli* BW25113 (lacZ^+) strain (plasmid or chromosomally integrated strains). Refer figure 3.81-C, D, E. Hence, further cultivations were carried out where *Cyc-At* was co-expressed in chromosomally integrated strain as host strains to produce more than 4 $\mu\text{g/g}$ CDW or higher levels of δ -tocotrienol.

After confirming that induction with 0.25 mM IPTG in *E. coli* BW25113/pCAS47 cells yielded in highest δ -tocotrienol (4 $\mu\text{g/g}$ CDW i.e. 4.4 $\mu\text{g/l}$) it was important to check the protein expression level in these cells with different IPTG concentrations. Hence, *E. coli*

BW25113/pCAS47 cells induced with 0, 0.1, 0.25 and 1.0 mM IPTG were analyzed by 2D gel electrophoresis for protein expression. Cyclase activity and expression level being the rate limiting was of more interest. 12 h after induction samples were loaded on 2D gel electrophoresis and the gels can be seen in figure 3.82.

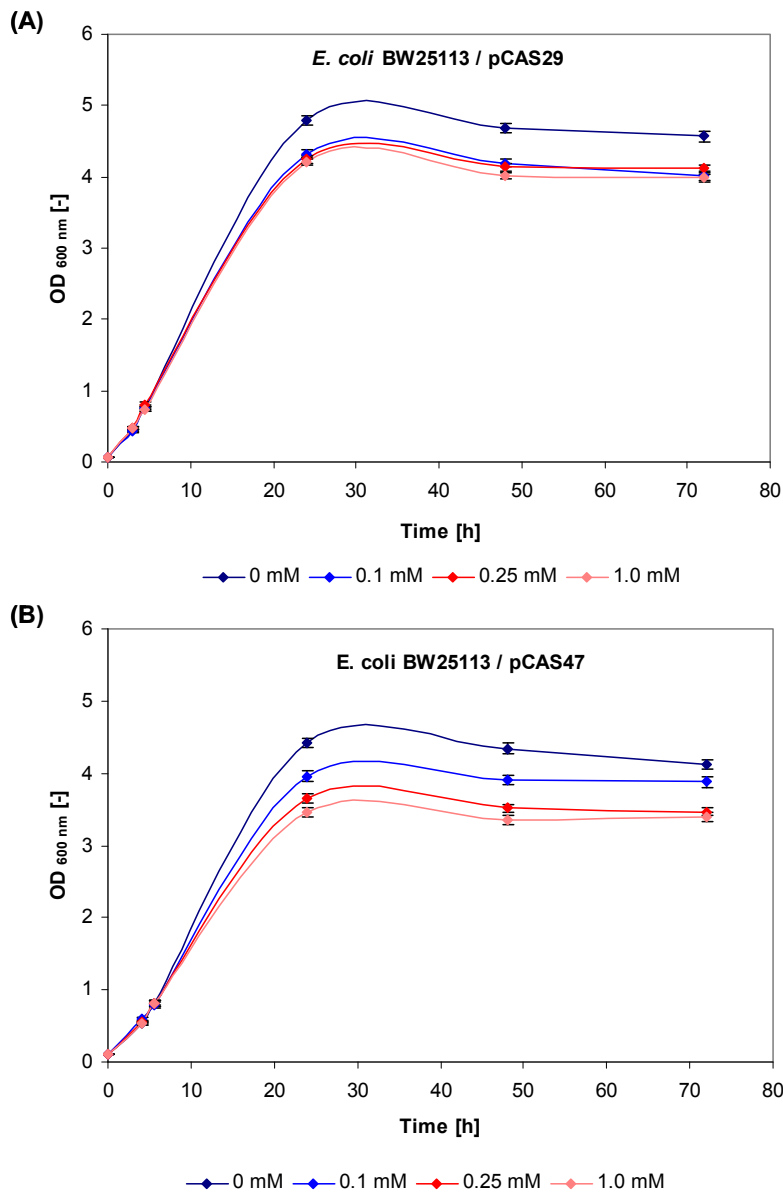


Figure 3.81 A & B: Cell densities achieved under different IPTG induction concentrations. Cultivation was carried out in shaking flask at 30 °C in LB + Glycerol + Amp100. Cell density represented as OD_{600nm} on y-axis with respect to time. **(A)** *E. coli* BW25113/pCAS29 **(B)** *E. coli* BW25113/pCAS47

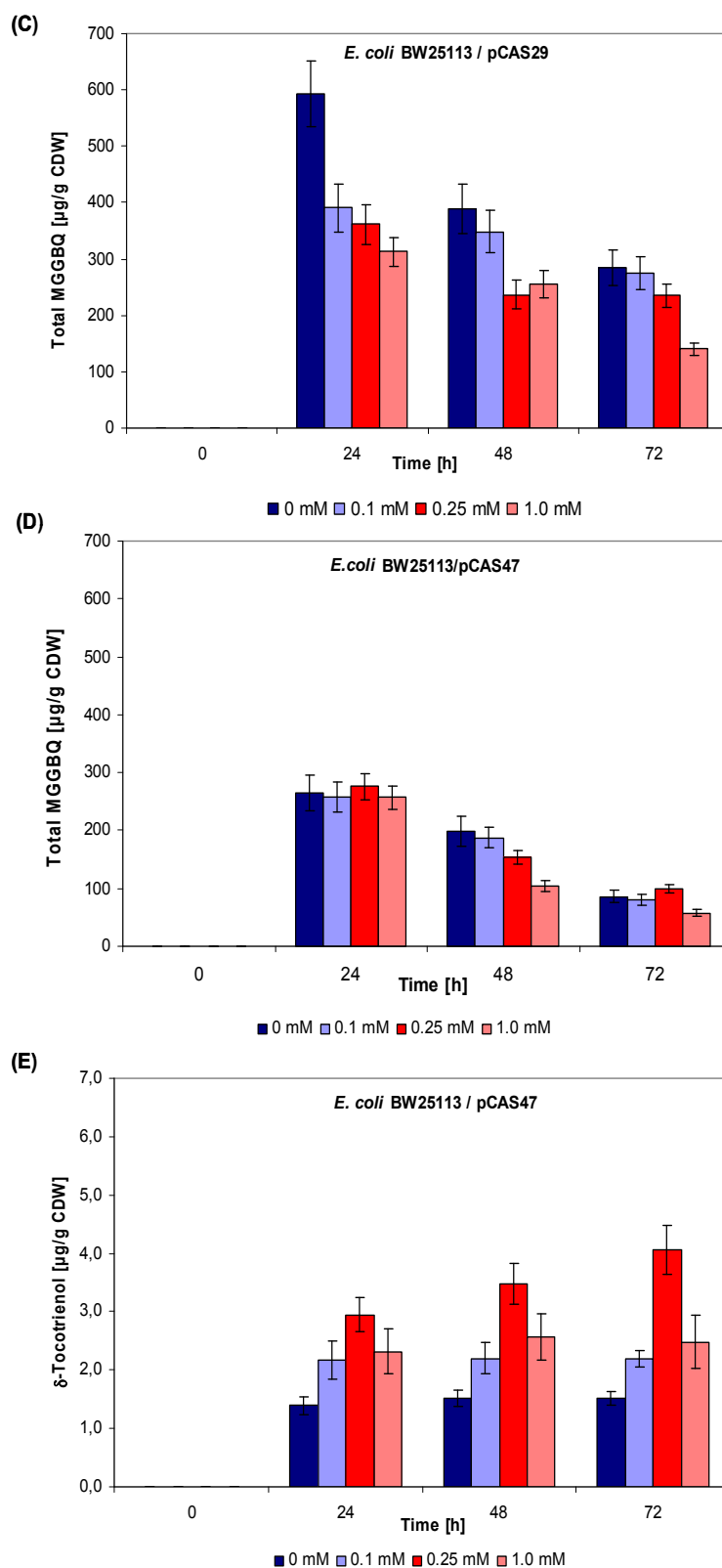


Figure 3.81 C, D & E: (C) Total MGGBQ production in *E. coli* BW25113/pCAS29 (D) Total MGGBQ production in *E. coli* BW25113 / pCAS47 (E) δ -tocotrienol production in *E. coli* BW25113 / pCAS47. No δ -tocotrienol was detected in *E. coli* BW25113 / pCAS29 during HPLC analysis. This experiment was repeated under identical conditions to compare the MGGBQ and δ -tocotrienol yields. The scale of δ -tocotrienol (y-axis) shown is 100 times smaller than that of total MGGBQ scale.

In figure 3.82, 2 D gel electrophoresis for *E. coli* BW25113/pCAS29 and *E. coli* BW25113/pCAS47 (induced with 0 mM IPTG) samples were overlapped. Hpd protein (40 kDa), CrtE (32 kDa), Ggh-Syn (37 kDa) were detected in both samples. An extra protein band at approx. 46.2 kDa was spotted on *E. coli* BW25113/pCAS47 gel which corresponds to the molecular size of Cyc-At. In the Fig. 3.82, *E. coli* BW25113 / pCAS47 with 0 mM IPTG is compared with 1 mM IPTG. The increase in amount of protein over-expressed in case of Hpd, CrtE can be easily seen. Ggh-Syn was seen on 2D gel when induced with 1 mM IPTG which was expressed and seen on qualitative level in 0 mM sample. Small increase in Cyc-At protein level was seen when induced with 1 mM IPTG as compared to 0 mM. This may be one of the possible reasons, why not all of the MGGBQ was converted into δ -Tocotrienol during the different shaking flask and bioreactor cultivation experiments. Ggh-Syn at 0 mM was not expressed (at least not visible on gel) but at 1 mM IPTG was expressed (visible on gel). Expression was not strong when compared to Hpd and CrtE or when compared to Ggh protein itself expressed as single protein using plasmid pCAS8 (see fig. 3.11). This might be one of the reasons why no MPBQ was formed and hence no δ -tocopherol was formed. Possible reasons why no MPBQ was produced has been discussed in detail in section 4.4.

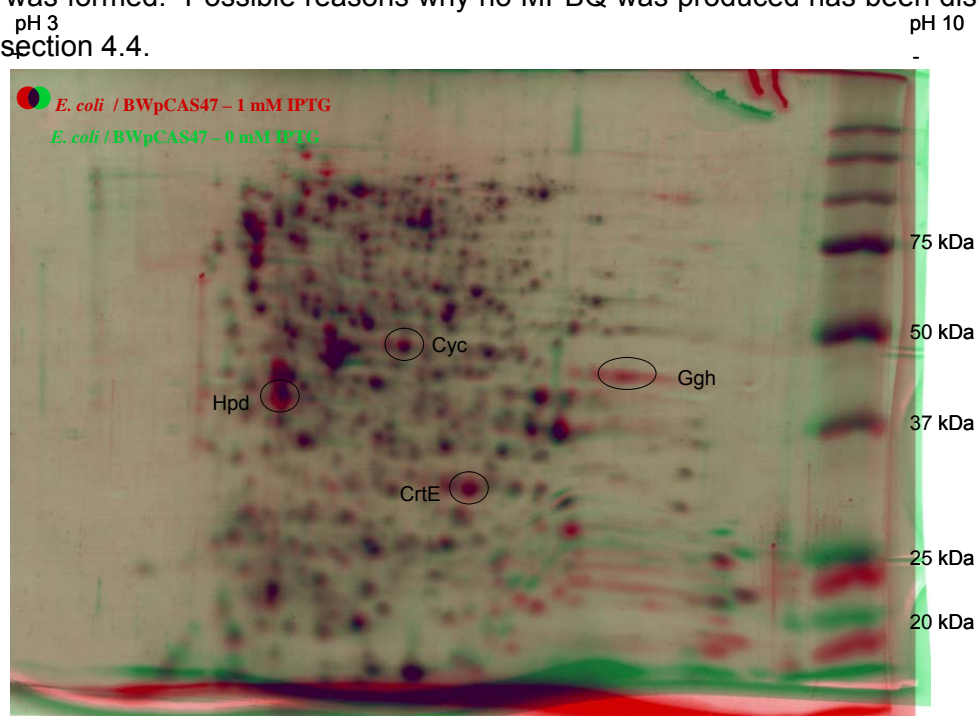


Figure 3.82: Comparison of 2D Gel Electrophoresis for *E. coli* BW25113 / pCAS47 induced with 1 mM with 0 mM IPTG. Cultures with 0 mM is shown in green colour and cultures induced with 1 mM shown in red colour. The spots marked with circles are the proteins overlapping each other. No Hpt could be seen in 2D gel electrophoresis since it's a membrane protein. Protein marker is shown in kDa on right hand side. The IPG stripes used for IEF had a pH gradient from 3 to 10 which can be seen on top of gel from left to right i.e. from (+) to (-).

3.13.2. New plasmid constructs carrying *cyc-At* gene in multi-copy vectors and co-expression in *E. coli* CS6 and / or *E. coli* CS8 strains

It was seen in section 3.11.2. during the bioreactor cultivation of *E. coli* CS7 in MM-Glucose and MM-Glycerol, that the MGGBQ_{reduced} was partially converted into δ -tocotrienol, partially oxidised to form MGGBQ_{oxidised} and the rest remained utilised (especially in the last 8-10 hours of respective cultivation in Fig. 3.60). Till date, no study showing utilisation of MGGBQ_{oxidised} as substrate for *Cyc-At* for cyclisation reaction has been published. As a result, δ -tocotrienol produced in *E. coli* CS7 was low. δ -tocotrienol production can be either be increased by one or more following factors,

- a) Increasing the production of MGGBQ_{reduced}
- b) Increasing the conversion of MGGBQ_{reduced} into δ -tocotrienol
- c) Minimising the oxidation of MGGBQ

In order to study, how to increase the conversion of MGGBQ_{reduced} into δ -tocotrienol, experiments to increase the *Cyc-At* expression level in *E. coli* CS6 and *E. coli* CS8 (both strains able to produce MGGBQ) were performed i.e. using *E. coli* CS6 and *E. coli* CS8 as host strains (MGGBQ_{reduced} producing strains), for co-expression of *Cyc-At* using a single plasmid.. This may probably increase the conversion of MGGBQ into δ -tocotrienol.

Hence, *cyc-At* was cloned into different expression vectors (multi-copy) to enhance the cyclase expression level. This *Cyc-At* (plasmid) was co-expressed in *E. coli* CS6 and *E. coli* CS8 and then the MGGBQ_{total} and δ -tocotrienol production were compared with *E. coli* CS7 strain which has a single copy of *Cyc-At*.

Cultivation of *E. coli* CS6 / pQE31-*Vte1* in shaking flask

E. coli CS6 was shown to produce MGGBQ (see section 3.4). To produce δ -tocotrienol plasmid pQE31-*Vte1* was transformed into *E. coli* CS6. pQE31-*Vte1* plasmid carries *cyc-At* in pQE31 vector. Plasmid pQE31-*Vte1* was kindly provided by Dr. Peter Dörmann for studying the cyclase activity. pQE31-*Vte1* has an IPTG inducible *tac* promoter. *Vte1* is the tocopherol cyclase gene (*Cyc*) from *Arabidopsis thaliana*.

Plasmid pQE31-*Vte1* was shown in section 3.1.5 to express *Cyc-At* protein and was shown in figure 3.26 that purified *Cyc-At* protein can catalyse the cyclization reaction of MGGBQ into δ -tocotrienol. Shaking flask cultivation result showed that cell density reached in *E. coli* CS6/pQE31-*Vte1* reached in was slightly lower than in *E. coli* CS6/pQE31 (Figure 3.83). Cultures were induced with 0.25 mM IPTG at approx. OD_{600nm} of 0.8. Both strains produced approximately 220 μ g/g CDW of MGGBQ (total) after 24 h. MGGBQ production increase continued in *E. coli* CS6/pQE31 between 24 and 54 h before it reached 457 + 39 μ g/g CDW

after 74 h. On the other hand, MGGBQ production in *E. coli* CS6/pQE31-Vte1 strain also increased continuously from 24 h to 54 h and 74 h, but the difference in the increase was lower than that in *E. coli* CS6/pQE31. δ -tocotrienol was produced between 24 h and 54 h in *E. coli* CS6/pQE31-Vte1 and reached a concentration of $0.88 \pm 0.15 \mu\text{g/l}$ of δ -tocotrienol (i.e. $0.83 \pm 0.11 \mu\text{g/g CDW}$). No δ -tocotrienol was detected in the control *E. coli* CS6/pQE31 in any of the samples analyzed.

In this case it was seen that the strain i.e. *E. coli* CS6/pQE31-Vte1 in which *Cyc-At* was expressed and δ -tocotrienol was produced, the cell growth was less than the control strain. But the effect of both (δ -tocotrienol and *Cyc-At* proteins) on cell growth was not that significant as that seen in *E. coli* DH5 α /pCAS29 and *E. coli* DH5 α /pCAS47 (Fig. 3.31). *E. coli* DH5 α /pCAS47 produced $15 \mu\text{g/g CDW}$ of δ -tocotrienol, compared to $0.88 \mu\text{g/g CDW}$ produced in *E. coli* CS6/pQE31-Vte1. *E. coli* CS6/pQE31-Vte1 strain had *hpd*, *crtE* and *hpt-Syn* genes (single copy) under IPTG inducible *tac* promoter along with the *cyc-At* gene in plasmid pQE31-Vte1 also under IPTG inducible *tac* promoter. Perhaps this may have limited the cyclase activity and perhaps be the reason for low conversion of MGGBQ to δ -tocotrienol. Hence, *cyc-At* was cloned in a new pHWG640 vector (modified pAW229, rhamnose inducible) to construct a new plasmid pCAS59 (details in section 2.2.2). This plasmid was provided by Dr. Albermann for further experiments producing δ -tocotrienol.

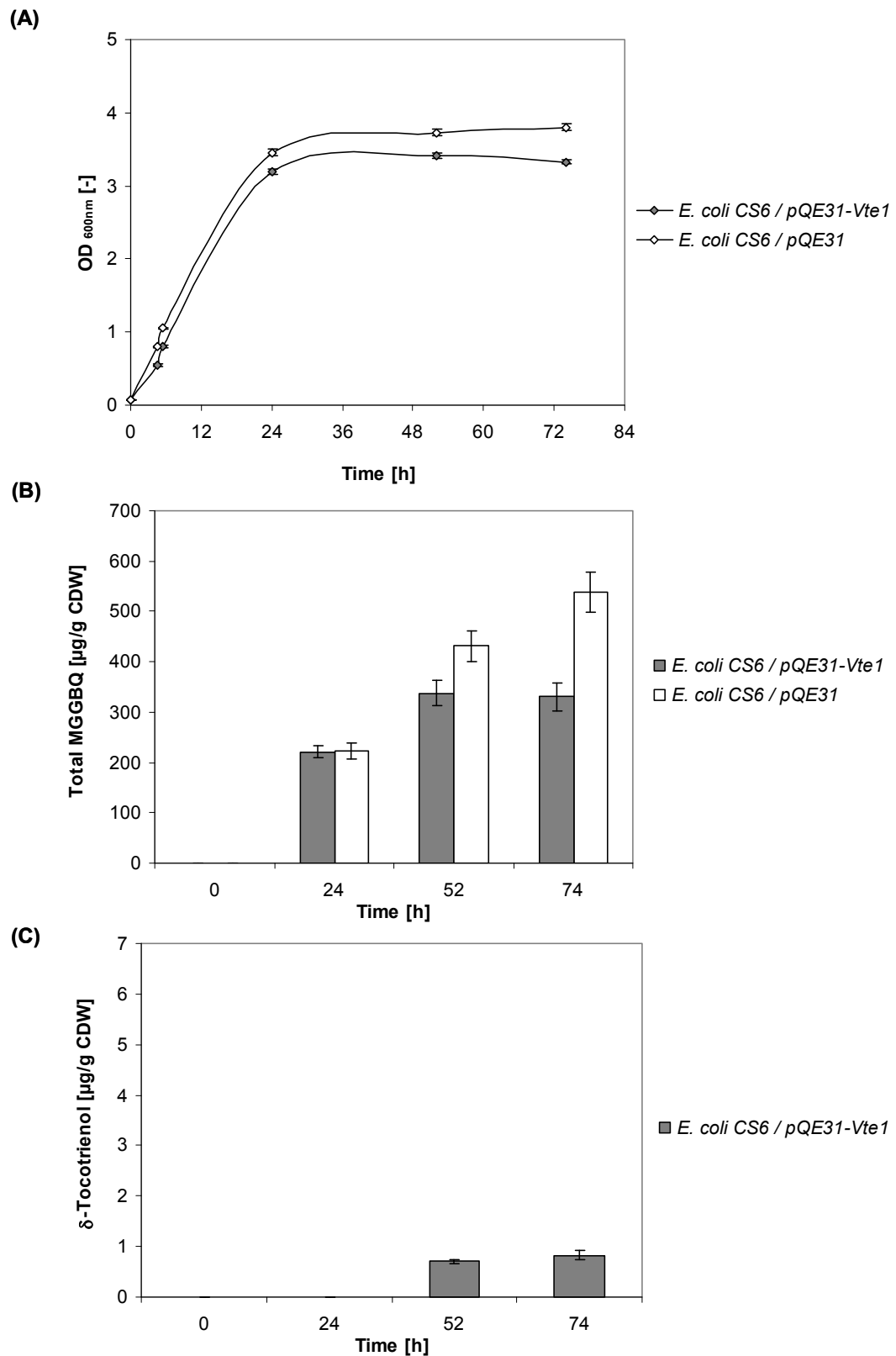


Figure 3.83: Shaking flask cultivation results of *E. coli CS6/pQE31-Vte1* and *E. coli CS6 / pQE31*. Cultivation carried out in LB - Glycerol - Amp100 at 30 °C. Cultures were induced with 0.25 mM IPTG at OD_{600nm} of 0.8. (A) Cell growth curve represented as OD_{600nm} vs. time (B) Total MGGBQ production shown in µg/g CDW (C) δ-Tocotrienol production shown in µg/g CDW.

Cultivation of *E. coli* CS6 / pCAS59 in shaking flask

To study, if the rhamnose promoter can enhance the *in-vivo* cyclase activity, plasmid pCAS59 was used to coexpress *Cyc-At* in *E. coli* CS6 strains. Plasmid pCAS59 was kindly provided by Dr. Albermann for further study. As control, *E. coli* CS6 / pHWG640 was cultivated. Cultivation was carried out in LB-Glycerol-Cm50 medium in shaking flask at 30 °C. Cultures were induced with 0.25 mM IPTG and 0.2 % (w/v) rhamnose at OD_{600nm} of 0.8. *E. coli* CS6/pCAS59 reached lower cell densities than that of its control *E. coli* CS6 / pHWG640 after 72 h. Total MGGBQ produced in both strains after 24 h exceeded 400 µg / g CDW (Refer figure 3.84). Between 24 h and 54 h, the MGGBQ level in the control dropped down to 350 ± 18 µg/g CDW while that in *E. coli* CS6/pCAS59 increased to 541 ± 21 µg/g CDW. It was observed that the *E. coli* CS6/pHWG640 cultures had turned brown at 54 h. This perhaps may be the reason why the MGGBQ level decreased between 24 and 54 h. The MGGBQ level in control *E. coli* CS6/pHWG640 decreased further to 320 ± 11 µg/g CDW after 74 h while it also decreased to 202 µg/g CDW in *E. coli* CS6 / pCAS59. 0.69 ± 0.09 µg/g CDW of δ-Tocotrienol was detected during HPLC analysis in *E. coli* CS6/pCAS59 in 24 h sample. Linear increase of 60-66 % in δ-tocotrienol was observed between 24 and 54 h and 54 and 72 h. Final δ-tocotrienol level reached was 1.88 µg / g CDW. It is possible that the control *E. coli* CS6/pHWG640 cultures may have attained the maximum MGGBQ production (µg/g CDW) before 24 h. Since no sample was taken before 24 h for MGGBQ extraction, it could not be confirmed. It seems that the MGGBQ production in *E. coli* CS6/pCAS59 reached the maximum level between 24 and 72 h. The conversion of MGGBQ_{reduced} into δ-tocotrienol was very slow. One reason may be either the low cyclase activity due to incorrect protein folding or inaccessibility of substrate MGGBQ to the *Cyc-At* enzyme *in-vivo*. It is seen from the result that at 72 h, the substrate MGGBQ_{reduced} was still available (approx. 200 µg/g CDW) in *E. coli* CS6/pCAS59.

It is well studied that expression of recombinant proteins (esp. eukaryotic) in *E. coli* may not be able to carry out the post translational modifications that is usually required for the eukaryotic protein function (Hannig and Makrides 1998). No report on *Cyc-At* mis-folding in recombinant *E. coli* was available till date. Hence, *Cyc-At* mis-folding in this study as a possible reason for low conversion of MGGBQ_{reduced} to δ-tocotrienol could not be confirmed. Additionally, overexpression of plasmid encoded genes initiate transcription of heat shock genes and several stress responses, and can often result in aggregation of encoded protein in form of inclusion bodies (Lesley et.al. 2002; Sørensen and Mortensen 2005).

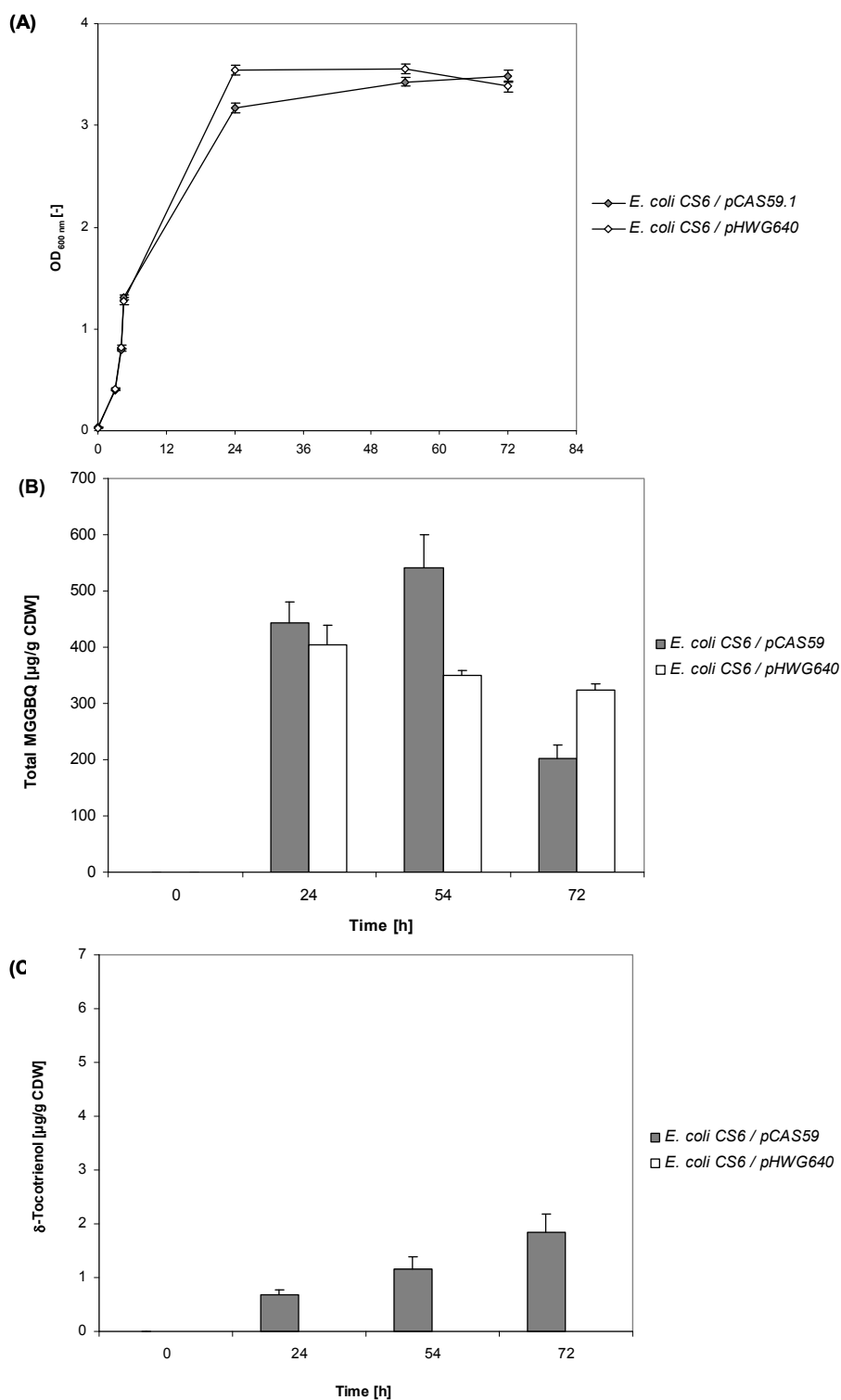


Figure 3.84: Conversion of MGGBCQ to δ -tocotrienol during cultivation of *E. coli* CS6/pCAS59 and *E. coli* CS6/pHWG640 in shaking flask in LB - Glycerol - Cm50 at 30°C. (A) Cell growth curve shown in OD_{600nm} vs. time. (B) Bar chart showing total MGGBCQ production in µg/g CDW (C) Bar chart showing δ -tocotrienol produced in *E. coli* CS6/pCAS59 in µg/g CDW. No δ -tocotrienol was detected in control *E. coli* CS6/pHWG640. This experiment was repeated under identical conditions. The S.D in MGGBCQ results was less than 10 % and S.D for δ -tocotrienol was less than 20 %.

Cultivation of *E. coli* CS6 / pGEX-Cyc-At and *E. coli* CS8/ pGEX-Cyc-At in shaking flask

To address the issue of a possible protein misfolding or formation of inclusion bodies, it was decided to express the Cyc-At protein as GST fusion protein. This may improve the yield of active cyclase by producing correctly folded recombinant proteins. This was done by genetically linking the target protein i.e. Cyc-At with a fusion partner which is expressed with a high yield in soluble form. Glutathione-S-transferase (GST) is some of the most common fusion partners used to express high amount of soluble protein (Hansen and Eriksen 2007). GST-fusion system being an affinity protein purification, the Cyc-At can be induced as GST-Cyc-At fusion proteins and can be purified in its native form by binding GST to the chromatography resin. Cyc-At gene was cloned into pGEX vector (see table 2.1.2.3) which carries ampicillin resistance and has a P_{tac} promoter. 1.3 kb NdeI/BamHI digested cyc-At fragment was ligated with 6.4 kb NdeI/BamHI digested pGEX fragment. Resulting plasmid was named as pGEX-Cyc-At. Digestion with XhoI / Scal resulted in 2 fragments with approx. size of 6.9 kb and 0.8 kb. Clone Manager Software 7.0 after restriction with above enzymes showed expected product size of 6994 bp and 813 kb. These sizes corresponded with the results obtained after XhoI / Scal digestion. Nucleotide sequence of vte1 insert in pGEX-Cyc-At plasmid showed 100 % identity with the At4g32770 gene from *Arabidopsis thaliana*. Samples before and after IPTG induction were tested on SDS-PAGE (shown in fig.3. 85) for protein expression.

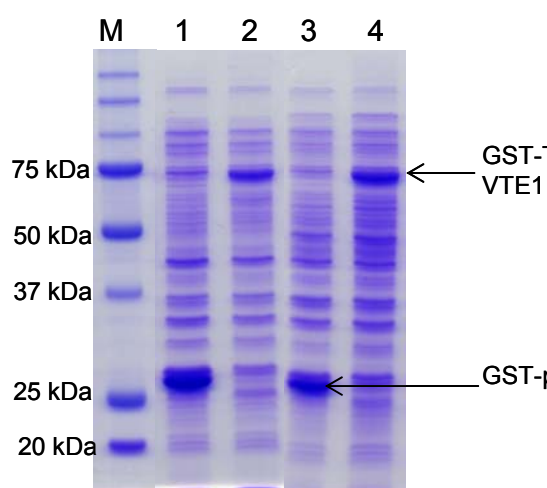


Figure 3.85: SDS-PAGE showing GST-Cyc_{At} fusion protein. *E. coli* BW25113 strain carrying pGEX-Cyc-At was cultivated in LB-Amp100 medium, at 37°C. As control *E. coli* BW25113/pGEX was cultivated. Cultures were induced with 1 mM IPTG at OD_{600nm} of 0.8. Sample description in different lanes:
 M : Protein marker
 1: *E. coli* BW25113/pGEX (before IPTG)
 2: *E. coli* BW25113/pGEX-Cyc-At (before IPTG)
 3: *E. coli* BW25113/pGEX (4 h @ IPTG)
 4: *E. coli* BW25113/pGEX- Cyc-At (4 h @ IPTG)

A strong protein band at approx. 75 kDa was seen in *E. coli* BW25113 / pGEX-Cyc-At before and after induction. This shows that the the lac repressor has no tight control on the expression of genes encoding the Cyc-At proteins. In the control strain, a strong protein band was seen at approx. 25 kDa. Cyc-At protein has a predicted mass of 47 kDa and GST protein alone 26 kDa (EXPASY). Hence, the GST-Cyc-At fusion protein has a calculated

mass of 73 kDa. This mass corresponds to the strong over expression seen in pGEX-Cyc-*At* samples. The strong band in the control corresponds to GST protein alone.

E. coli CS6 and *E. coli* CS8 each were transformed with plasmid pGEX-Cyc-*At*. As control each strain was transformed with empty vector pGEX. These strains were cultivated in shaking flask in LB-Glycerol-Amp100 at 30 °C for the production of MGGBQ and δ -tocotrienol. Cultures were induced with 0.25 mM IPTG at OD_{600nm} 0.8. Control strains as compared to the strains carrying pGEX-Cyc-*At* plasmid grew slightly better till the time of induction. After induction with 0.25 mM IPTG at OD_{600nm} of 0.8, cell growth in control strains was strongly inhibited, reaching maximum cell density OD_{600nm} between 1.5 and 2.0. Reason for the poor growth was not known immediately. On the contrary, the strain carrying pGEX-Cyc-*At* grew much better reaching a cell density of OD_{600nm} between 5.8 and 6.4. (Refer to figure 3.86). *E. coli* CS6 /pGEX-Cyc-*At* cell growth compared to that of *E. coli* CS6/pCAS59 was also better. MGGBQ production in case of both controls was below 5 μ g /g CDW. In case of *E. coli* CS6/ pGEX-Cyc-*At* also MGGBQ level produced was comparatively low (approx. 30 μ g/g CDW) as compared to that in *E. coli* CS8 / pGEX-Cyc-*At* producing slightly more than 300 μ g/g CDW (36 h). This MGGBQ level decreased with time. *E. coli* CS6 / pGEX-Cyc-*At* started producing δ -Tocotrienol between 36 and 50 h (0.8 μ g/g CDW) and reaching the maximum of 1.7 μ g/g CDW in 96 h. On the other hand, *E. coli* CS8 / pGEX-Cyc-*At* started producing δ -Tocotrienol before 36 h (1.5 μ g/ g CDW) and finally reaching 6.4 μ g/ g CDW. This was the highest δ -tocotrienol produced in *E. coli* BW25113 strain till now. Similar experiment was performed without IPTG induction which resulted in slightly lower yields compared to 0.25 mM IPTG. Looking at the results, one can draw a correlation i.e. low MGGBQ corresponds to higher δ -tocotrienol (in case of *E. coli* CS8/pGEX-Cyc-*At*) and higher MGGBQ levels corresponds to lower δ -tocotrienol (in case of *E. coli* CS6/pGEX-Cyc-*At*). This has been discussed in detail in chapter 4 (section 4.5.5).

This experiment was repeated, where the standard deviation (S.D) for cell growth (between first and second experiment) was within \pm 5 %. Similar behaviour in cell growth was observed during the second cultivation experiment as that observed during the first experiment. The S.D for MGGBQ and δ -tocotrienol yields was within \pm 20 %. One reason for the poor cell growth in control strain may be the overproduction of GST protein, before and after IPTG induction. After seeing these experimental results, it was concluded that neither Cyc-*At* proteins nor δ -tocotrienol is toxic or detrimental to the *E. coli* cell growth. GST –tagged proteins provide higher degree of purification along with increased solubility of recombinant proteins. But it also has a few disadvantages that since the tagged proteins are of larger sizes it may be degraded by proteases (Smith & Corcoran 2001). A few reports on

toxic behaviour of GST proteins in the host strain have been reported, but not clearly understood (Saluta & Bell 1998).

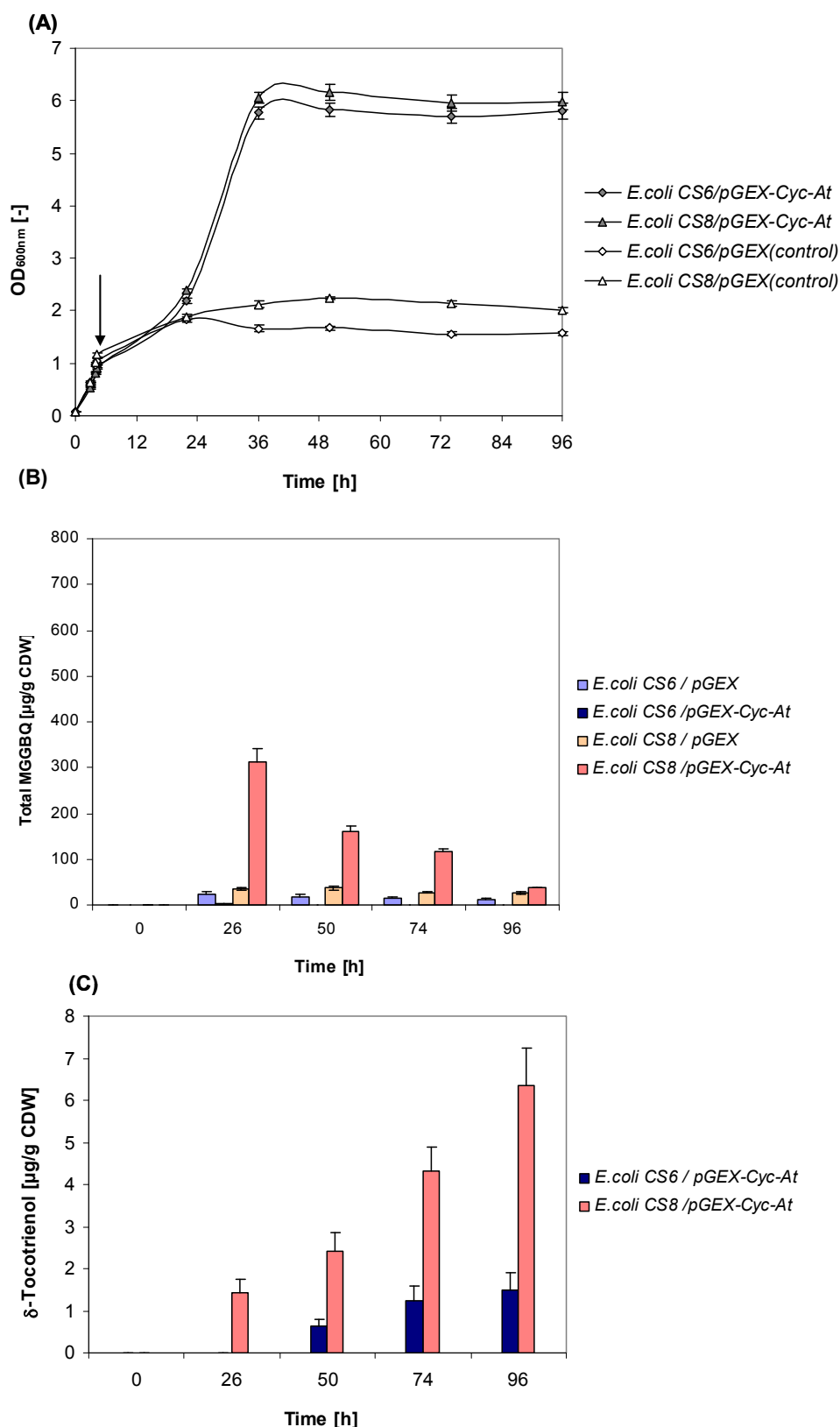


Figure 3.86: Conversion of MGGBQ to δ -tocotrienol during cultivation of *E. coli* CS6/pGEX-Cyc-At and *E. coli* CS8/pGEX-Cyc-At in shaking flask in LB - Glycerol - Amp100 at 30°C. (A) Cell growth curve shown in OD_{600nm} vs. time. (B) Bar chart showing total MGGBQ production in $\mu\text{g/g}$ CDW (C) Bar chart showing δ -tocotrienol produced in *E. coli* CS6/pGEX-Cyc-At and *E. coli* CS8/pGEX-Cyc-At in $\mu\text{g/g}$ CDW. No δ -tocotrienol was detected in respective controls *E. coli* CS6/pGEX and *E. coli* CS8/pGEX and hence not shown in bar charts.

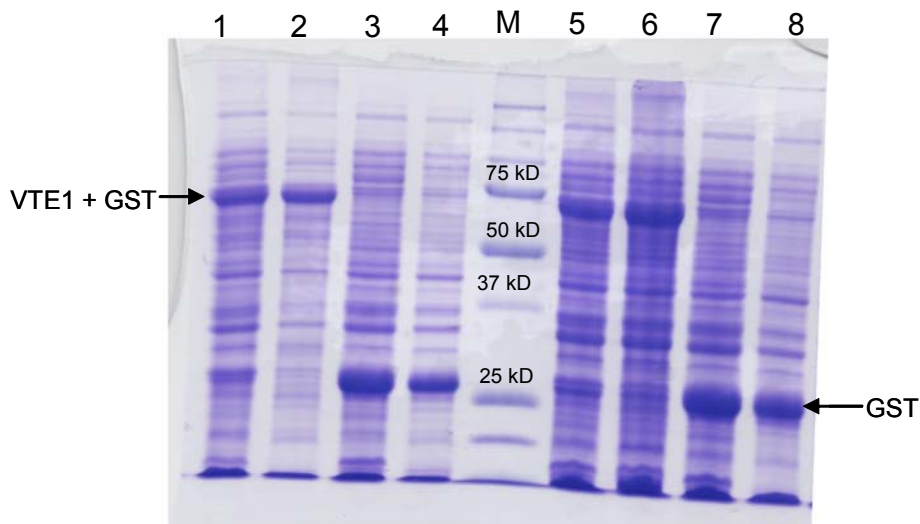


Figure 3.87: SDS-PAGE showing *GST-Cyc-At* fusion protein expressed in *E. coli* CS6 / pGEX-*Cyc-At*. As control, samples from *E. coli* CS6 / pGEX cultures were loaded. M stands for protein marker. *GST* protein has a theoretical mass of 26 kD (shown by an arrow) and *Cyc-At* alone 47 kD. Hence *GST-Cyc_{At}* protein has a combined mass of 73 kD (shown by an arrow). 10 μ g of cell free crude extract was loaded to each lane.

1: <i>E. coli</i> CS6 / pGEX- <i>Cyc-At</i> - 26 h (0 mM)	5: <i>E. coli</i> CS6 / pGEX- <i>Cyc-At</i> - 50 h (0 mM)
2: <i>E. coli</i> CS6 / pGEX- <i>Cyc-At</i> - 26 h (0.25 mM)	6: <i>E. coli</i> CS6 / pGEX- <i>Cyc-At</i> - 50 h (0.25 mM)
3: <i>E. coli</i> CS6 / pGEX - 26 h (0 mM)	7: <i>E. coli</i> CS6 / pGEX - 50 h (0 mM)
4: <i>E. coli</i> CS6 / pGEX - 26 h (0.25 mM)	8: <i>E. coli</i> CS6 / pGEX - 50 h (0.25 mM)

3.13.3. Purification of *GST-Cyc_{At}* fusion protein

E. coli BW25113 / pGEX-*Cyc-At* was cultivated in 200 ml LB-Amp100 medium in 1 L shaking flask at 30 °C. Cultures were induced with 1 mM IPTG at OD_{600nm} of 0.8. Cultures after 16 h of incubation were harvested at 3000 g at 4 °C for 15 minutes and stored at -20 °C. These cells were used for purification of *GST-Cyc_{At}* fusion proteins using protocol 2.2.3.6.

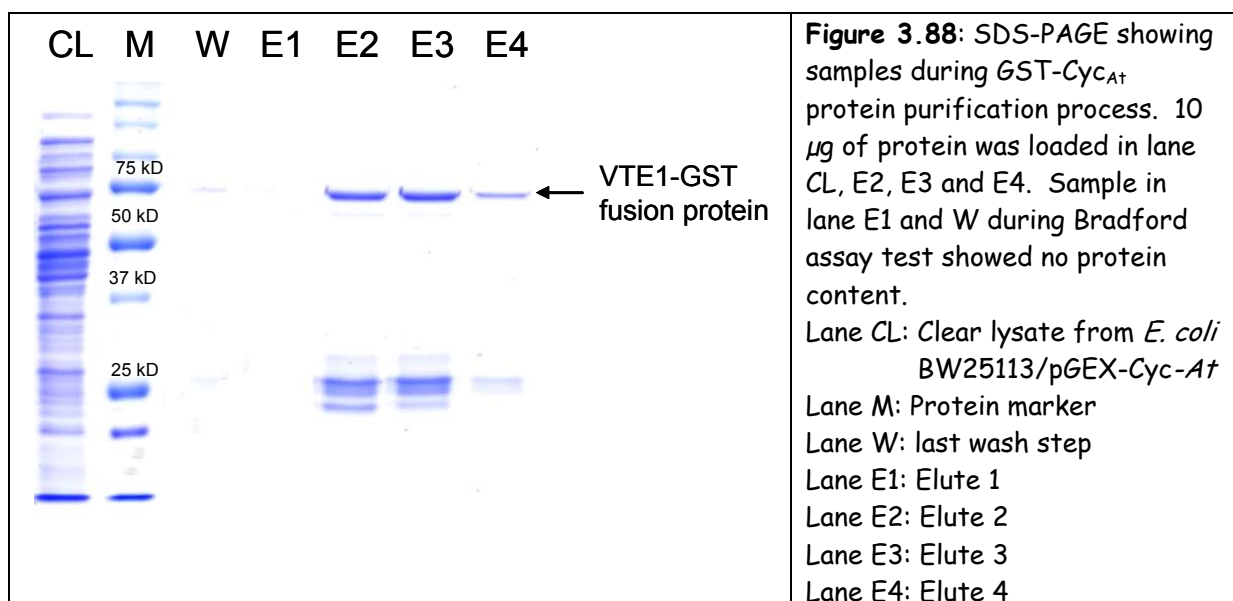


Figure 3.88: SDS-PAGE showing samples during *GST-Cyc_{At}* protein purification process. 10 μ g of protein was loaded in lane CL, E2, E3 and E4. Sample in lane E1 and W during Bradford assay test showed no protein content.

Lane CL: Clear lysate from *E. coli* BW25113/pGEX-*Cyc-At*

Lane M: Protein marker

Lane W: last wash step

Lane E1: Elute 1

Lane E2: Elute 2

Lane E3: Elute 3

Lane E4: Elute 4

In the wash fraction no GST-Cyc-*At* was lost (figure 3.88). Enriched GST-Cyc-*At* protein at approx. 73 kDa was seen in the elute fractions E2 E3 and E4. In the same lanes protein bands ranging from approx. 20 to 30 kDa were also seen. Some of the protein may be the GST alone and rest unknown proteins/impurities. The grade of purity of GST-Cyc-*At* proteins was approx. 60-70 % of the total protein in lane E2, E3 and E4. To compare both fusion proteins i.e His-Cyc_{At} and GST-Cyc_{At} an *in-vitro* enzymatic reaction was carried out and discussed in details in next section. The *in-vitro* reaction with both purified enzymes was performed as shown in the table 3.14 below,

Table 3.14: Comparison of His- and GST- Cyc-*At* proteins during *in-vitro* enzymatic reaction for δ -tocotrienol biosynthesis

Reaction component / Reaction Nr.	End. Conc.	1 His-Cyc- <i>At</i>	2 Control for 1	3 GST-Cyc- <i>At</i>	4 Control for 3
Cyc- <i>At</i> fusion Protein	μg	10.0	0	10.0	0
Cyc- <i>At</i> fusion Protein	Variable	40 μl	0	40 μl	0
1 mM Ascorbic acid	75 mM	75 μl	75 μl	75 μl	75 μl
1 mM DTT	4 mM	4 μl	4 μl	4 μl	4 μl
Potassium phosphate (7.3 pH)	200 mM	200 μl	200 μl	200 μl	200 μl
Substrate-cyclodextrin complex	Approx. 9.5 mM	100 μl	100 μl	100 μl	100 μl
Water (balance)	Variable	Rest	Rest	Rest	Rest
Buffer		-	40 μl ⁽¹⁾	-	40 μl ⁽²⁾
Volume	TOTAL	1000 μl	1000 μl	1000 μl	1000 μl

⁽¹⁾ His-Tag elution buffer

⁽²⁾ GST-Tag elution buffer

3.13.4. Comparison of His- and GST- fusion protein i.e. His-Cyc_{At} and GST-Cyc_{At} in *in-vitro* enzymatic reaction with MGGBQ

During *in-vivo* biosynthesis experiments (section 3.3.2.c), the GST-Cyc_{At} protein produced higher δ -tocotrienol amounts (approx. 6.5 $\mu\text{g/g}$ CDW), it was decided to compare the enzyme activities of His- and GST- tagged Cyc-*At* enzymes during an *in-vitro* enzymatic reaction. Hence, *in-vitro* enzymatic reaction was carried out as described in section 2.2.3.7. Results can be seen in figure 3.89. 10 μg of enriched enzyme (His-Cyc-*At* & GST-Cyc-*At*) was used for *in-vitro* reaction. GST-Cyc_{At} fusion protein produced 50 % more δ -tocotrienol yield after 42 h when compared to His-Cyc_{At} fusion protein.

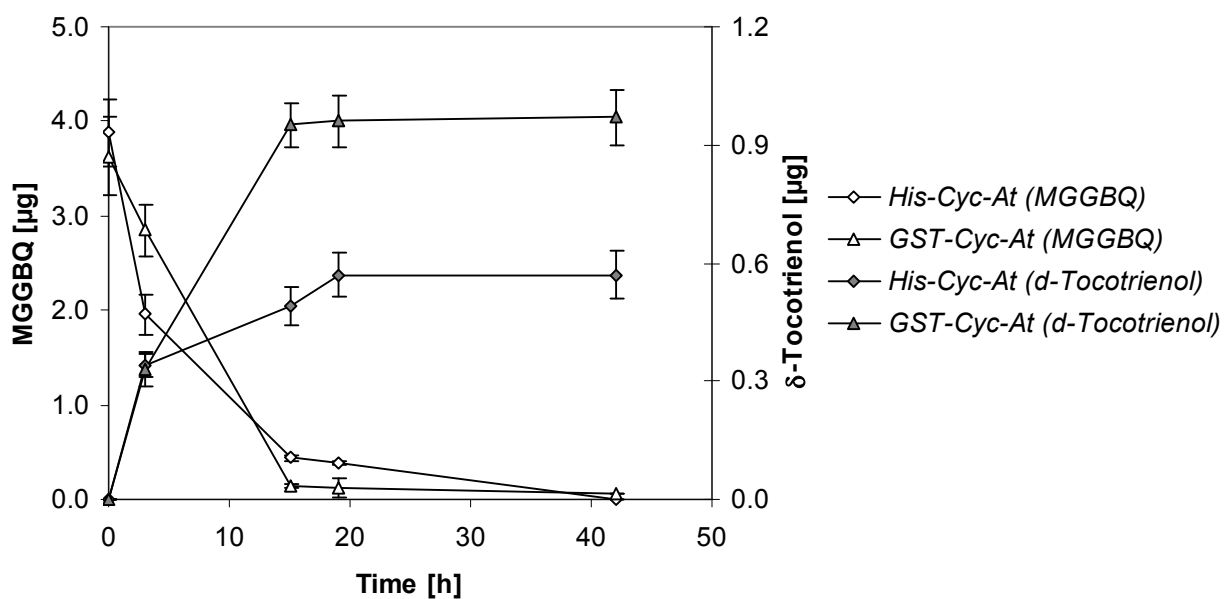


Figure 3.89: Comparison of *in-vitro* enzymatic reaction carried out with different *Cyc_{At}* fusion proteins (*His-Cyc-At* & *GST-Cyc-At*) and *MGGBQ_{reduced}* for δ -tocotrienol production. 10 μ g of each fusion protein was used for the resp. reaction. The control reactions with respective elution buffers (i.e. without proteins) instead of fusion *Cyc_{At}* proteins didn't produce any δ -tocotrienol and didn't consume any *MGGBQ* and hence has not been shown in the figure.

The enzyme activity calculated based on the *in-vitro* reaction for *His-Cyc-At* was 39.4 nmol/mg protein/h and 60.2 nmol/mg protein/h for *GST-Cyc-At*. Clearly, *GST-Cyc-At* resulted in higher δ -tocotrienol yield during *in-vivo* and *in-vitro* biosynthesis compared to any strain which was capable of producing δ -tocotrienol in this study.

3.14. Attempts to produce MPBQ using new reductase and transferase enzymes

No MPBQ was produced in *E. coli* DH5 α /pCAS29 (section 3.1.4). To try and produce MPBQ, the important step is the reduction of GGPP to PPP, which is catalyzed by geranylgeranyl reductase (Ggh) (Keller et.al. 1998). Ggh from *Synechocystis PCC6803* (Ggh-Syn) was expressed in *E. coli* DH5 α /pCAS29 (shown on 2D gel electrophoresis, figure 3.15). The DNA sequence of Ggh-Syn in plasmid pCAS29 showed 100 % identity when compared to the gene ChIP (ORF sll1091) i.e. *ggh-Syn* gene sequence (Personal communication Dr. Albermann). Based on the RT real time PCR, it was also confirmed that *ggh-Syn* in pCAS29 had been transcribed (Albermann 2008). In a second experiment, PPP was not detected in *E. coli* DH5 α /pCAS11 (section 3.8) where Ggh-Syn was shown to be overexpressed on 2D gel electrophoresis. These two results indicated that the Ggh-Syn was apparently inactive during the *in-vivo* biosynthesis of PPP and MPBQ. Hence, it was decided to clone *ggh* gene from *Arabidopsis thaliana* i.e. *ggh-At*. Ggh-At protein sequence has 76 % identity with that of Ggh-Syn (ExpASY). Ggh from *Arabidopsis thaliana* (Ggh-At) expressed in *E. coli* has been shown to catalyze the 3 step reduction of GGPP during an *in-vitro* enzymatic reaction (Keller et. al. 1998). This assay was carried out using the cell lysate from *E. coli* which had expressed the Ggh-At proteins. No assay with Ggh-Syn has been reported till date. Hence in this section, experiments would be performed to carry out biosynthesis of MPBQ using new plasmid constructs (*ggh-At* and/or *hpt-At* in pJF119 Δ N or pHWG640 vector) along with combination of different chromosomally integrated strains and plasmid constructs.

ggh-Syn gene was cloned in pJF119 Δ N vector to obtain plasmid pCAS8. *chIP* from *Arabidopsis thaliana* (called *ggh-At*) or geranylgeranyl reductase from plants, contains N-terminal plastid transit sequences. Hence *ggh-At* was cloned into pJF119 Δ N to obtain a new plasmid construct pCAS33 (personal communication Dr. Albermann). Since it was planned to express Ggh-At in *E. coli* as host system and not in plants/eukaryotic system a truncated version of *ggh-At* i.e. without the transit signal peptide was also cloned in pJF119 Δ N to obtain plasmid pCAS53 (personal communication Dr. Albermann). Both plasmids were provided by Dr. Albermann for further studies regarding MPBQ biosynthesis. It was confirmed that the DNA sequence for *ggh-At* with and without transit signal peptide in plasmid pCAS33 and pCAS53 respectively, was 100 % identical to that in databank (NCBI) (Personal communication with Dr. Albermann). Before using the plasmids pCAS33 and pCAS53, it was confirmed that the Ggh-At (including transit signal peptide and truncated resp.) were expressed in *E. coli* DH5 α /pCAS33 and *E. coli* DH5 α /pCAS53 strains respectively. *E. coli* CS6 strain was transformed with pCAS8, pCAS33 and pCAS53 each and cultivated in shaking flask at 30°C in LB-Glycerol-Amp100. As control strain *E. coli*

CS6/pJF119 Δ N was cultivated. Cell growth of all 3 strains (expressing Ggh) after induction with 0.25 mM IPTG was strongly inhibited when compared to the control strain *E. coli* CS6/pJF119 Δ N (figure 3.87A). Cells extracted for MPBQ/MGGBQ were analyzed by HPLC. As expected, MGGBQ_{reduced} and MGGBQ_{oxidized} were detected in control strain *E. coli* CS6/pJF119 Δ N. This was concluded based on the identical retention times of 15.4 and 23.9 minutes observed in case of *E. coli* DH5 α /pCAS29 (figure 3.16). *E. coli* CS6/pCAS8, *E. coli* CS6/pCAS33 and *E. coli* CS6/pCAS53 samples also detected MGGBQ_{reduced} and MGGBQ_{oxidized}, but failed to detect an additional peak, when compared to the control strain *E. coli* CS6/pJF119 Δ N. The total MGGBQ produced in the control *E. coli* CS6/pJF119 Δ N was higher than the other strains. Hence it was concluded, that the Ggh-At, with and without signal peptide, failed to produce MPBQ during the experiments performed in shaking flask experiments.

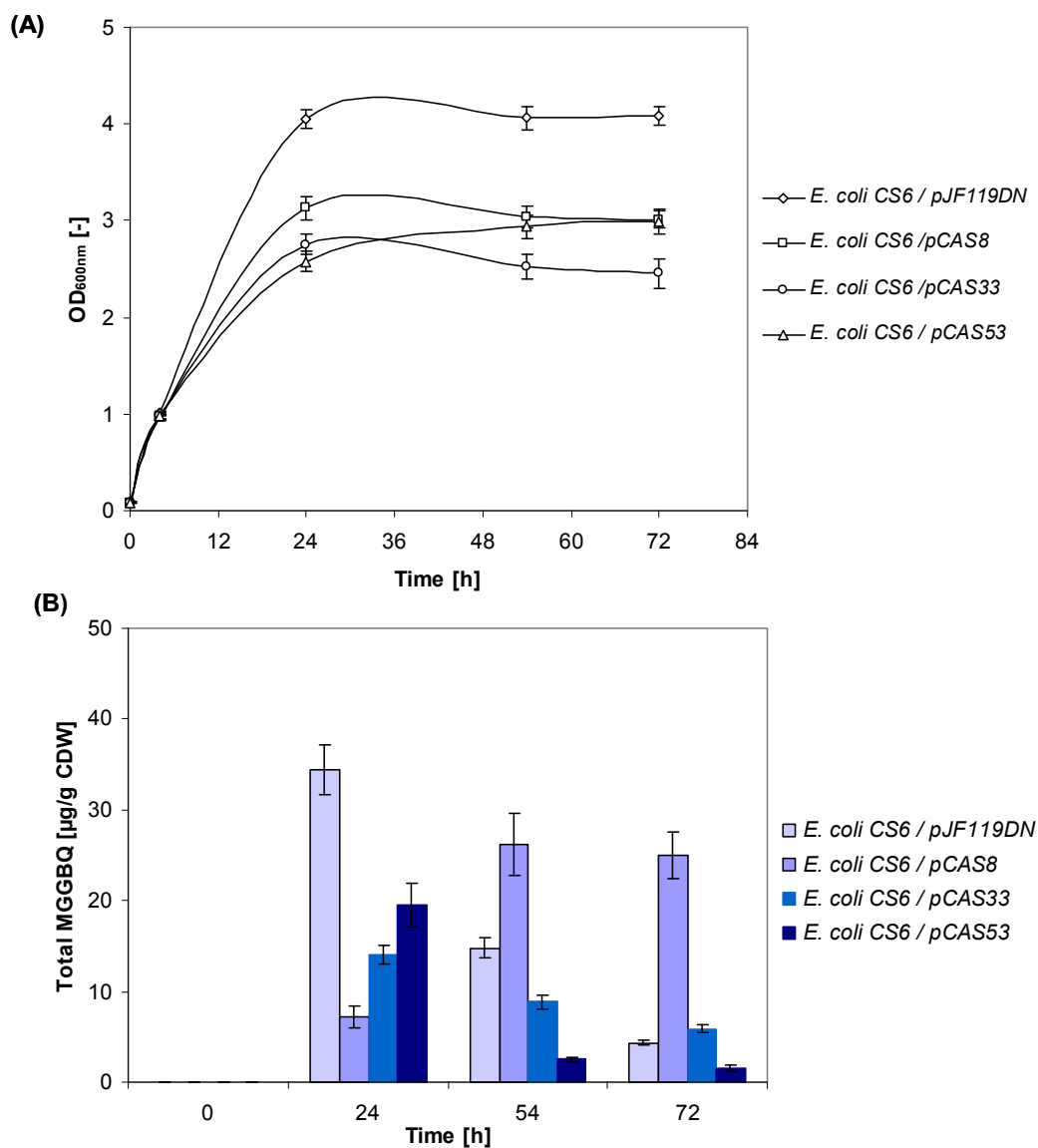


Figure 3.90: Experimental results showing efforts to produce MGGBQ and MPBQ in *E. coli* CS6 carrying different geranylgeranyl reductase (*Ggh*). Cultivation carried out in shaking flask cultivation at 30°C in LB-Glycerol-Amp100. Cultures were induced with 0.25 mM IPTG at approx. OD_{600nm} of 0.8. (A) Cell density measured during cultivation shown in OD_{600nm} vs. time. (B) Total estimated MGGBQ amounts produced by different cultures analysed by HPLC. Additional peak representing MPBQ (reduced and/or oxidized) were expected apart from peak(s) detected (reduced and oxidized MGGBQ peaks). Since no additional peaks were detected, only MGGBQ yields are shown in this figure.

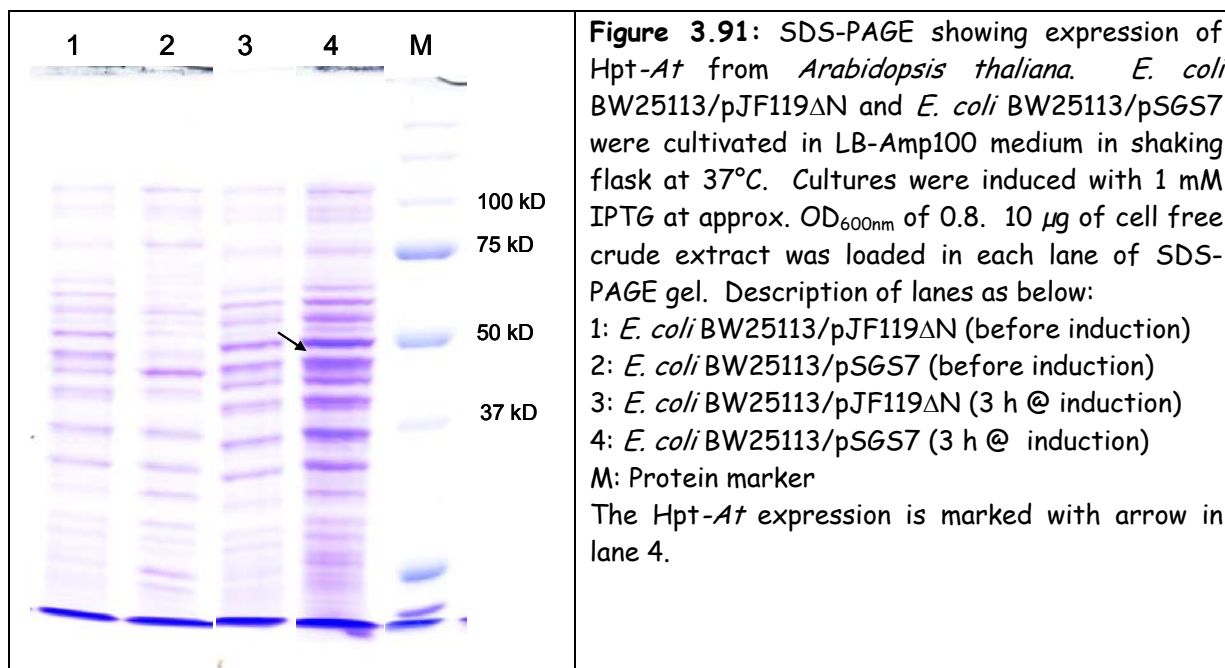
Co-expression of Hpt from *Arabidopsis thaliana* (Hpt-At) in *E. coli* CS6

Hpt from *Arabidopsis thaliana* shows substrate specificity towards PPP and HGA (Collakova et. al.2001). In order to make use of this characteristic, *hpt* gene from *Arabidopsis thaliana* (*hpt-At*) was cloned in pJF119ΔN vector to obtain a new plasmid pSGS7. This plasmid was used in different *E. coli* constructs in attempts to produce MPBQ.

Hpt from *Synechocystis PCC 6803* (Hpt-Syn) is able to accept GGPP and PPP as substrate. On the other hand Hpt from *Arabidopsis thaliana* (Hpt-At) has a specificity to PPP and does not accept GGPP as its substrate. Hence *hpt-At* gene encoding Hpt-At was cloned into pJF119ΔN.

1.23 kb EcoRI / XbaI digested *hpt-At* gene fragment (from pUni51+cDNA *hpt-At*, T3 promoter) was ligated with 5.4 kb EcoRI / XbaI digested pJF119ΔN fragment. Successful ligation and transformation in *E. coli* BW25113 strain resulted in 11 clones. Plasmids were isolated from these 11 clones and tested by digestion with restriction enzyme. Digestion with BglI resulted in two fragments of approximate sizes of 2.4 kb and 3 kb. Digestion with Aval resulted in two fragments of approx. size 3.7 kb and 3 kb. These results corresponded with the fragment size digested with BglI and Aval each of 2317 bp, 4507 bp and 3753 and 3071 bp respectively (calculated by Clone Manager 7.0). Out of 11 clones 2 were positive and the plasmid was named as pSGS7. A weak expression of Hpt-At in *E. coli* BW25113 / pSGS7, 3 h after induction (end conc. of 1 mM IPTG), was seen on SDS-PAGE (in lane 4 in figure 3.91). The calculated size (R_f method) of this weak band was approx. 43.2 kDa, which corresponded with the actual size of Hpt-At protein of 44.1 kDa (ExpASY). This expressed Hpt-At band is shown by an arrow in figure 3.91. No additional band was seen in *E. coli* BW25113 / pSGS7 before induction (lane 2) and in any of the control samples (lane 1 & 3).

E. coli CS2.2 cells (*E. coli* LJ110 *fucIP::P_{tac}-hpd-malEFG::P_{tac}-crtE*) carrying above described plasmid pSGS7 and pCAS39 (*ggh-At* in pHWG640 vector) was cultivated for MPBQ production. Two controls were used, first one *E. coli* CS2.2 carrying pSGS7 and pHWG640, and second one *E. coli* CS2.2 carrying pJF119ΔN and pCAS39. As MGGBQ producing strain *E. coli* CS2.2 along with plasmid pCAS19 (*hpt-Syn* in pHWG640) vector) was Iso cultivated. Induction with 0.25 mM IPTG and 0.2 % (w / v) rhamnose resulted in neither MPBQ nor MGGBQ in any of the culture samples extracted and analysed by HPLC. Cultures turned brown after 48 h, which may indicate that HGA was produced. MGGBQ was detected in *E. coli* CS2.2/pCAS19 strain, which suggested that either *Ggh-At* in pCAS39 was inactive, or *Hpt-At* in pSGS7 was inactive or both were inactive under the cultivation conditions used in this study.



To test Hpt-At, it was and is important to use a strain which can produce PPP and HGA as it is only accept PPP as substrate along with HGA (Collakova 2001). To produce PPP in *E. coli* (*in-vivo*) an active Ggh (along with CrtE) is required. Without active Ggh, Hpt-At activity cannot be shown. Since PPP was inaccessible (not commercially available). it was not possible to test the *in-vitro* activity of this Hpt-At.

Addition of external HGA to *E. coli* BW25113 cells carrying plasmid pCAS12 (*crtE*, *ggh-Syn* and *hpt-Syn*)

In this section attempts for biosynthesis of MPBQ were made based on the hypothesis that, no MPBQ could be produced when GGPP and HGA are readily available for Hpt-Syn enzyme i.e. there is a competition between Ggh-Syn and Hpt-Syn enzymes for the substrate GGPP. In order to produce MPBQ, GGPP has to be reduced by Ggh-Syn enzyme to produce PPP and only then Hpt-Syn can catalyze the condensation reaction between PPP and HGA to produce MPBQ. Hence, the shaking flask experiment was designed in such a way that it allows enough time for the reduction reaction of GGPP into PPP and simultaneously expresses Hpt-Syn *in vivo* recombinant *E. coli* DH5α / pCAS12. As control, *E. coli* DH5α / pCAS11 (*crtE* and *ggh-Syn*) was cultivated at 30°C in shaking flask in minimal medium with 10 g/l glucose + Amp100 medium. Before using these plasmids, expression of *crtE*, *ggh-Syn* proteins was confirmed (see figure 3.92). Hpt-Syn in *E. coli* DH5α/pCAS12 couldn't be verified on 2D-gel electrophoresis, as Hpt-Syn is a membrane bound protein. Due to the close proximity of molecular sizes of CrtE (32.58 kDa) and Hpt-Syn (34.41 kDa), it couldn't be identified as single band in SDS-PAGE gel (not shown). All cultures were induced with with 0.25 mM IPTG at OD_{600nm} of 0.8. 2 hours after induction,

Flask F1 with *E.coli* DH5 α /pCAS12 & Flask F2 *E. coli* DH5 α /pCAS11 was not supplemented with HGA, flask F3 with with *E.coli* DH5 α /pCAS12 strain and flask F4 with *E. coli* DH5 α /pCAS11 were supplemented with 5 mM HGA each. 10h after induction flask F5 with *E.coli* DH5 α /pCAS12 strain and flask F6 with *E.coli* DH5 α /pCAS11 were supplemented with 5 mM HGA each. Samples were taken for MGGBQ and MPBQ analysis and the results are shown in figure 3.93C. *E. coli* BW25113/pCAS12 and its control *E. coli* BW25113/pCAS11 in which no HGA was added grew better as compared to there respective strains with addition of HGA (see figure 3.93 A and B).

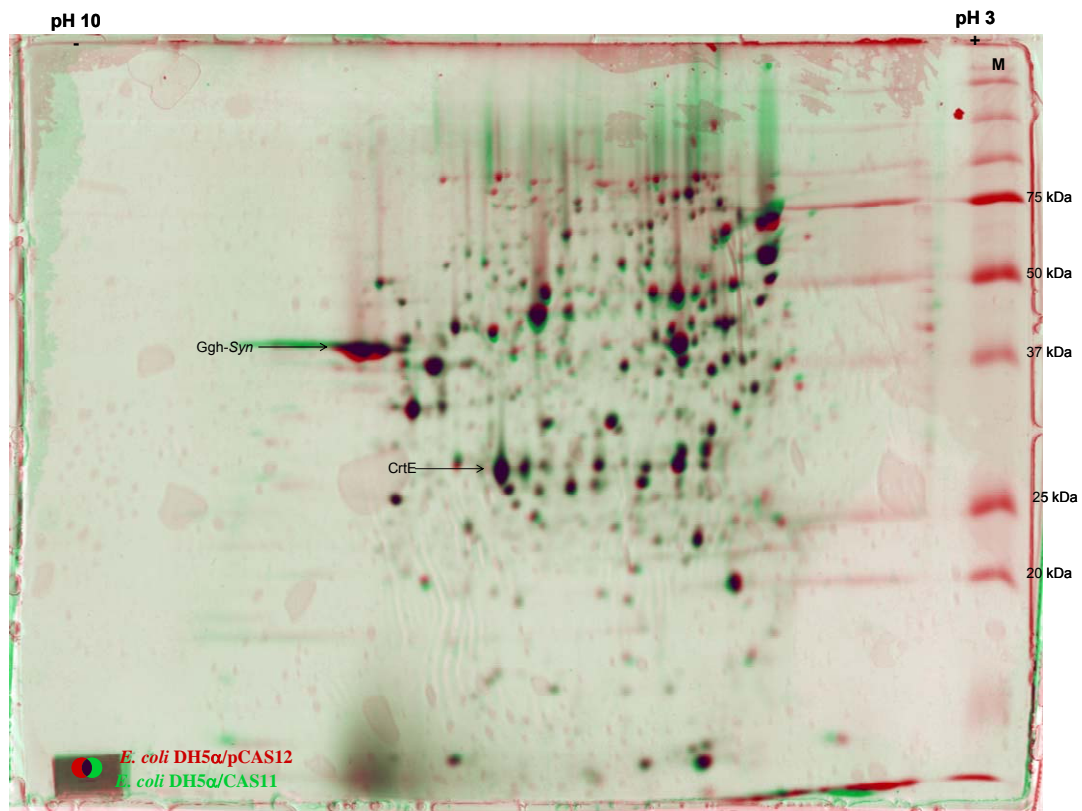


Figure 3.92: 2D gel electrophoresis showing *E. coli* DH5 α /pCAS11 and *E. coli* DH5 α /pCAS12 samples. In green is *E. coli* DH5 α /pCAS11 and in red colour is *E. coli* DH5 α /pCAS12. Cultures were cultivated in shaking flask in LB-Amp100 medium, at 30 °C. Cultures were induced at approx. OD600nm of 0.8 with 1.0 mM IPTG (end concentration). Samples collected, 6 h after induction, were used for 2 D gel electrophoresis. *Ggh-Syn* protein band and *CrtE* were seen in both samples (shown by arrow, at approx. 45 kDa and 33 kDa resp.). Additional *Hpt-Syn* band was expected incase of *E. coli* DH5 α /pCAS12 sample. *Hpt-Syn* being a membrane bound protein was not seen during this analysis.

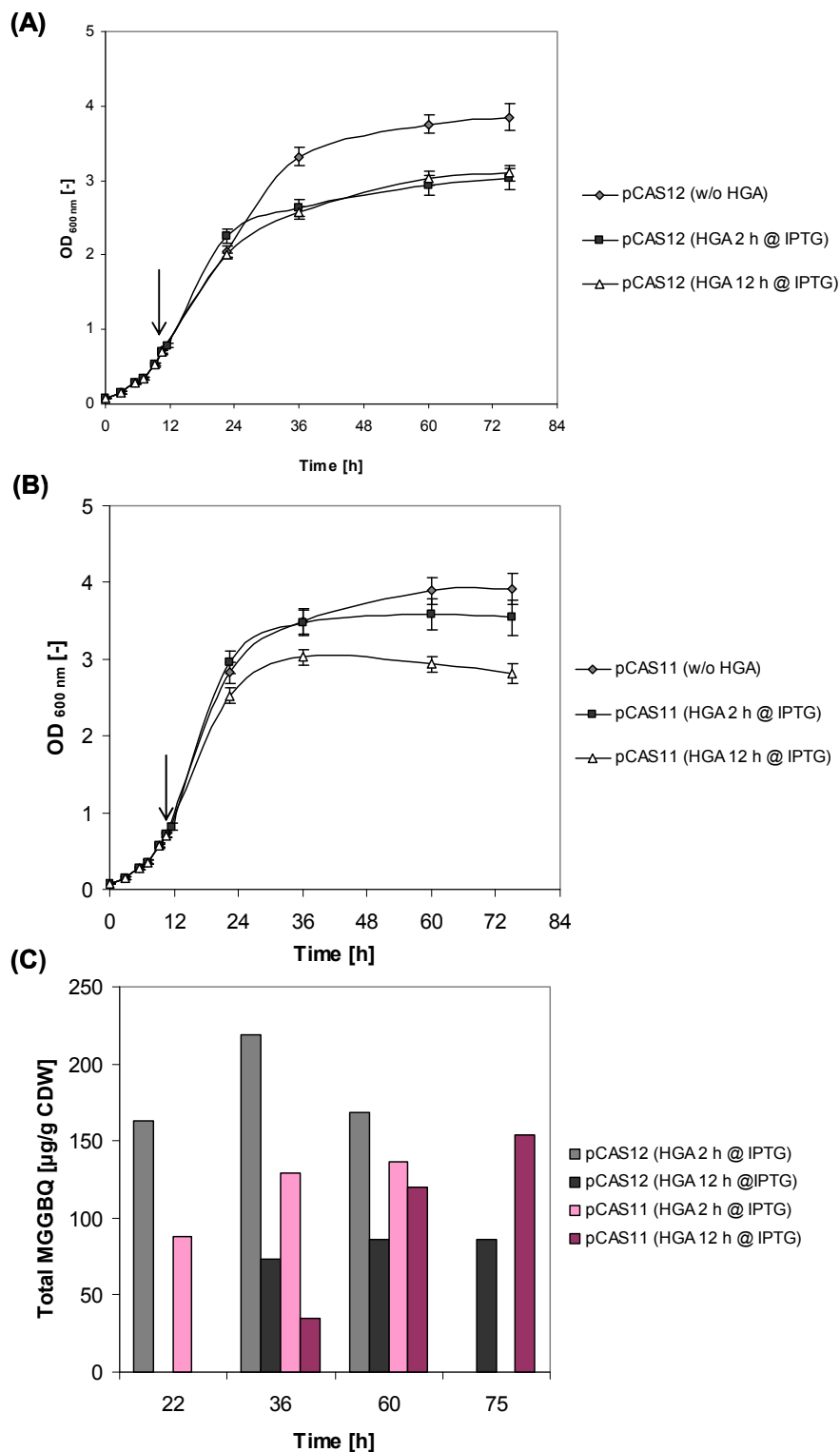


Figure 3.93: Experiment results for MPBQ production using external addition of HGA. (A) Cell density achieved in *E. coli* BW25113/pCAS12 in different conditions (B) Cell density achieved in control *E. coli* BW25113/pCAS11 in different conditions. (C) Total estimated MGG BQ produced by different cultures shown in $\mu\text{g/g}$ CDW shown in bar charts. No MGG BQ was detected in cultures where no HGA was added externally during cultivation. The time points 12 h, 24 h and 48 h represents the time after HGA addition. MPBQ was expected in *E. coli* BW25113/pCAS12 cultures with addition of HGA. No additional peak other than MGG BQ peak with the standard method used in this study) was detected in any of the samples. This meant that no MPBQ was produced in any cultures.

All cultures were induced with 0.25 mM IPTG at approx. OD_{600nm} of 0.8. As expected, neither MGGBQ nor MPBQ was detected in HPLC analysis in *E. coli* BW25113/pCAS12 and its control *E. coli* BW25113/pCAS11 cultures, where no HGA was added. In the other strains, with HGA addition (i.e. 2 h and 12 h after induction), only MGGBQ was detected. *E. coli* BW25113/pCAS12 (with HGA addition at 2 h and 10 h) after induction was expected to produce MPBQ, but failed to do so (HPLC didn't detect any additional major peak apart from MGGBQ peak). Instead, it produced MGGBQ. In *E. coli* BW25113/pCAS12 where HGA was added 2 h after IPTG induction, produced $163 \pm 11 \mu\text{g/g CDW}$ of MGGBQ_(Total) was produced as compared to $73 \pm 6 \mu\text{g/g CDW}$ in the same strain where HGA was added 12 h after induction (see figure 3.93C). There was marginal increase in the total MGGBQ produced in both cultures in 24 h after HGA addition. In the case of the control *E. coli* BW25113/pCAS11 (i.e. pCAS11 with *crtE* and *ggh-Syn* only) total MGGBQ produced in both cases (HGA added 2 h or 12 h after induction) was not very different (i.e. approx. $120 \pm 13 \mu\text{g/g CDW}$) but was lower than in *E. coli* BW25113/pCAS12 cultures. These results suggest that, either the hypothesis was wrong, or perhaps more experiments are required with optimized cultivation conditions (e.g. with respect to the time of HGA addition).

CHAPTER 4 – Discussion

4.1. Hpd Over-expression and HGA biosynthesis

Molecular cloning of gene, encoding *p*-hydroxyphenylpyruvate dioxygenase (*hpd*) from various organisms, overexpression and purification of the Hpd enzyme were reported in 1999 (Denoya 1994, Garcia et. al. 1999). Crystal structure of Hpd protein from *Pseudomonas fluorescens* (Serre et. al 1999), *Streptomyces avermitilis* (Brownlee et. al. 2004), *Zea mays* and *Arabidopsis thaliana* (Fritze et. al. 2004) has been solved. In this study, recombinant Hpd protein from *Pseudomonas putida* was strongly over-expressed in *E. coli* DH5 α / pCAS2JF (figure 3.2). On the contrary, Hpd overexpression in *E. coli* CS1 tested on SDS-PAGE did not yield a clear single additional band when compared to the control (wild type *E. coli* BW25113) (figure appendix A3-8). Hence Hpd overexpression in multi-copy plasmid i.e. multi-copy genes and a single copy gene could not be compared directly. But it was successfully demonstrated that Hpd protein encoded by the *hpd* gene from *Pseudomonas putida* KT2440 is a functional dioxygenase based on the HGA produced in *E. coli* CS1 strain and *E. coli* DH5 α / pCAS2JF during shaking flask cultivation experiments (figures 3.41A and 3.5 respectively). HGA production in *E. coli* DH5 α / pCAS2JF (Figure 3.5) strain was approx. 1.5 times higher than in *E. coli* CS1 strain (Figure 3.41A), both in MM-Glucose as well as in MM-Glycerol. The fact that, HGA was produced in *E. coli* CS1 strain and not in control strain (*E. coli* BW25113) is one indication that the expression of recombinant Hpd protein occurred perhaps at a low level, which was not visible on SDS-PAGE gel as mentioned above. *p*-HPP is a water soluble compound and after production during cultivation, accumulated in the medium. No *p*-HPP was detected in the supernatant samples (*E. coli* CS1 and *E. coli* BW25113/pCAS2JF) analysed by HPLC, is another indication that sufficient levels of Hpd being expressed. One of possible reasons for low cell density achieved in *E. coli* BW25113/pCAS2JF cultures, may be the accumulation of HGA (above a certain unknown level in the medium), which may have been toxic to the cells. Since, HGA toxicity towards *E. coli* cells had not been reported till date, HGA toxicity towards *E. coli* cells could not be confirmed. Another possible reason for poor cell growth may be toxicity of the strong over expression of Hpd proteins.

On the contrary, *E. coli* CS1 cells expressed low Hpd protein produced moderate amount of HGA grew relatively better than *E. coli* BW25113/pCAS2JF. No quantitative data regarding the level of HGA production in recombinant *E. coli* is available (except reported by Albermann et.al 2008). Small amounts of *p*-HPP (varied during the cultivations) were found in control strains.

Overexpression of high level of Hpd proteins or accumulation of high levels of HGA in medium maybe the reason for poor cell growth in *E. coli* BW25113/pCAS2JF. Since the aim of this study was to produce δ -tocotrienols and not high levels of intermediates use of high copy number of *hpd* genes i.e. multi-copy plasmid was not recommended even though it produces slightly high levels of HGA.

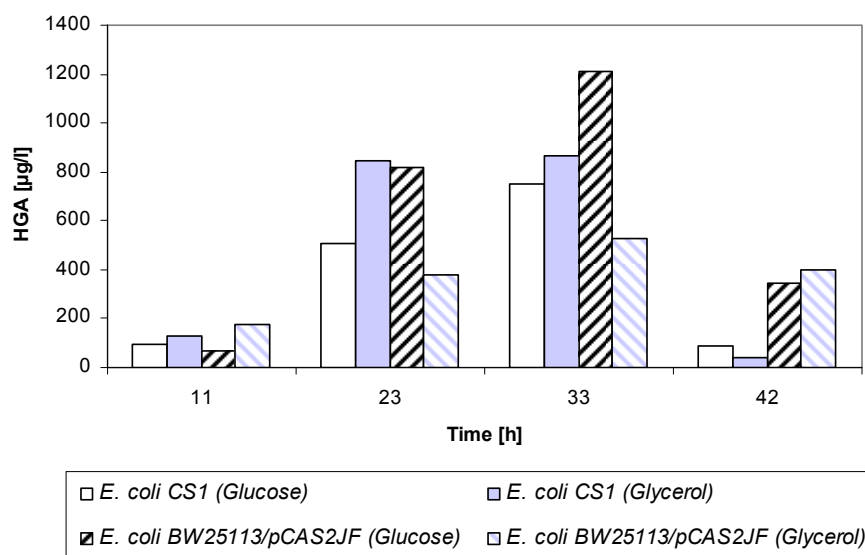


Figure 4.1: Graphical comparison of HGA production in different strains. Maximum HGA amounts achieved in respective cultivations are shown in this bar chart. Refer to section 3.4 and 3.41 for details of shaking flask cultivation experiments.

Effect of high HGA accumulation or higher Hpd over-expression (over-expression of Hpd in plasmid pCAS2JF in *E. coli* CS6 as host, refer section 3.18, Fig. 3.90) confirmed that it had no significant effect on MGGBQ levels i.e. the precursor of δ -tocotrienol. Hence, it seems that the HGA produced in *E. coli* CS1 strain even though approx. 50 % lower than in *E. coli* BW25113/pCAS2JF is sufficient and not rate limiting for MGGBQ production. Addition of tyrosine (0.25 g/l) to the minimal medium increased the HGA level to 7.5 mg/l and 5.6 mg/l in plasmid and chromosomally integrated strain respectively (results not shown). This increase might be due to the fact that *E. coli* carries 3 different aminotransferases which can convert tyrosine to HPP which is precursor for HGA (Sprenger 2007). In case, if Hpd is the rate limiting enzyme or the shikimate pathway is critical in the tocopherol biosynthesis pathway HGA levels could be increased by overexpression of *aroF*, *aroB*, *aroL* in the shikimate pathway (chapter 1, figure 1.6).

Oxidation of HGA

E. coli BW25113 / pCAS2JF and *E. coli* CS1 culture supernatant samples (in MM-Glucose and MM-Glycerol) started turning brown after 27 h and 33 h respectively. At the end of shaking flask cultivation the supernatant samples from both the cultures had turned dark

brown. The cell pellet obtained was pale/white in colour. HGA is similar to catecholamines and other melanin precursors in structure (Hegedus 2000). HGA after produced by recombinant cells undergoes non-enzymatic oxidation and polymerization into brown ochronotic pigments (Gunsior et. al. 2000), shown in figure 4.2. At higher HGA concentrations of approx. above 600 $\mu\text{g/l}$ especially, when HGA is not further utilised as substrate in biosynthesis pathway, the oxidation is spontaneous.

No direct correlation between the amount of HGA and the intensity of brown pigment was available or could be established. Based on this it was concluded that, HGA accumulation above a certain concentration (above 600 $\mu\text{g/l}$) was unstable, and hence it was difficult to calculate the highest concentration of HGA produced in each recombinant *E. coli* strain used in this study.

Hpd is the responsible enzyme for the conversion of HPP to HGA. *E. coli* BW25113 strain carrying plasmid pCAS2JF resulted in 1210 $\mu\text{g/l}$ and the chromosomally integrated strain (*E. coli* CS1) in MM-Glucose resulted in 796 $\mu\text{g/l}$ of HGA. These HGA concentration values are the highest quantifiable HGA concentration. Even higher HGA levels could have been reached if HGA oxidation was avoided.

Oxidation of HGA may increase during aerobic cultivations, especially during prolonged incubations. This was observed during the *in-vivo* production of HGA in *E. coli* BW25113/pCAS2JF and *E. coli* CS1 in Erlenmeyer flask which also resulted in brown pigment after prolonged incubation (after 24 h). This phenomenon was clearly seen in figure 3.5B where the control strain after prolonged incubation didn't turn brown while the *E. coli* BW25113/pCAS2JF culture supernatant had turned dark brown after 39 h (refer to section 3.1.2) as a result of HGA oxidation.

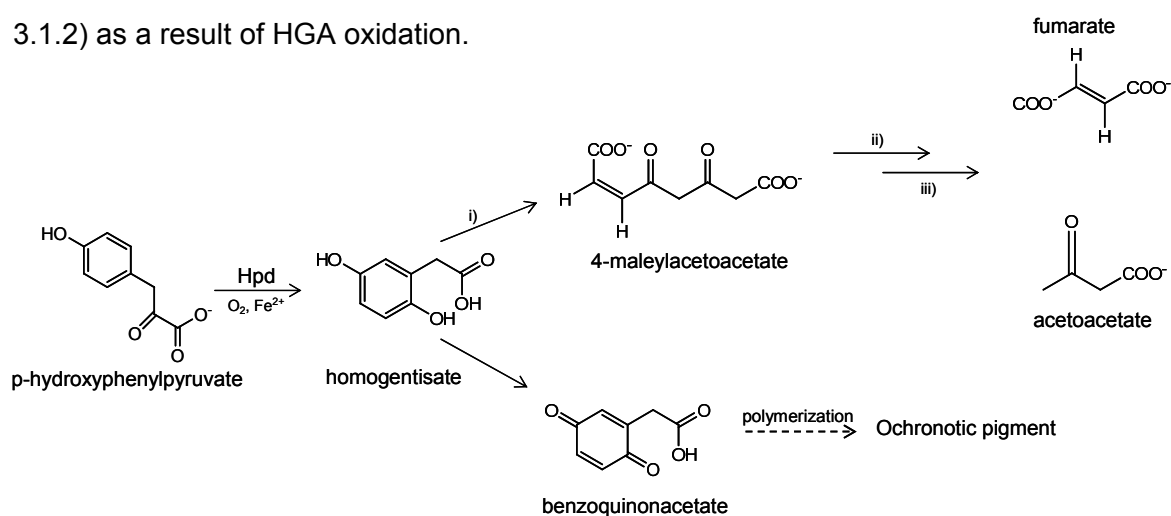


Figure 4.2: Scheme showing oxidation of HGA into brown ochronotic pigments. Oxidation of homogentisate (HGA) into benzoquinonacetate and further polymerisation (in many enzymatic steps) into ochronotic pigment (Gunsior et. al 2004). HGA can also be converted into maleylacetoacetate (MAA). i) reaction is catalysed by homogentisate 1,2 dioxygenase.

One possible reason for HGA accumulation in medium may be due to excessive production of HGA in recombinant *E. coli* strains (in this study). During *E. coli* CS6 and *E. coli* CS8 and *E. coli* CS10 bioreactor cultivation, no HGA was found in culture supernatant till approx. 30 h of fermentation time. HGA may have started accumulating in medium, due to the limitation of the other pathway enzymes to utilise it as substrate.

4.2. CrtE over-expression and GGPP biosynthesis

Most of the analytical methods to quantify the isoprenoid compounds used radioactive labelled compounds (Song 2003; Saisho et. al. 1997). One of the very few non-radioactive methods used till recently, is the use of recombinant Farnesyl and Geranylgeranyl protein transferase I for conjugation of FPP and GGPP respectively (Tong et. al. 2005). But this method needed a specific protein transferase for the each single respective isoprenoid compounds to be analysed, which was one of the limitation and which made the quantification an expensive method. Methods for isoprenoid analysis are not simple and very tedious to perform. Hence a new method for quantification of GGPP was developed based on GC-MS and described in chapter 2 and 3. This method was relatively simple, non-radioactive and precise as compared to the other methods reported in literature (Vallon et. al. 2008). This method could also be used for quantification of other isoprenoid compounds like FPP, GPP, and PPP along with GGPP. In the novel method developed at Universität Stuttgart the detection of isoprenoid diphosphates in recombinant *E. coli* cells involved its extraction from cells, conversion of FPP and GGPP into the corresponding alcohols by alkaline phosphatase and finally determination of farnesol and geranylgeraniol by GC-MS. Isoprenoid extraction was carried out as described in Tong et. al 2005.

GGPP synthase (CrtE) from *Pantoea ananatis* (formerly known as *Erwinia uredovora*) had been overexpressed in *E. coli* and purified in the early 1990's (Wiedemann et. al. 1993). In the present study, CrtE was strongly over expressed in plasmid pCAS30 in *E. coli* as host strain (figure 3.7, SDS-PAGE gel). Over expression of CrtE in *E. coli* CS2 was not visible on SDS-PAGE when compared to its control i.e. wild type *E. coli* BW25113 strain (appendix A3-8).

Over expression of CrtE in *E. coli* BW25113/pCAS30 and *E. coli* CS2 was not compared directly on 2D gel electrophoresis. It could be indirectly concluded based on the CrtE over expression seen in a chromosomally integrated strain *E. coli* CS6 on 2D gel electrophoresis (figure 3.49) that CrtE should have been expressed in *E. coli* CS2 strain as it was shown that large amounts (668 mM) of GGPP was produced in *E. coli* CS2.1 compared to the wild type *E. coli* strain.

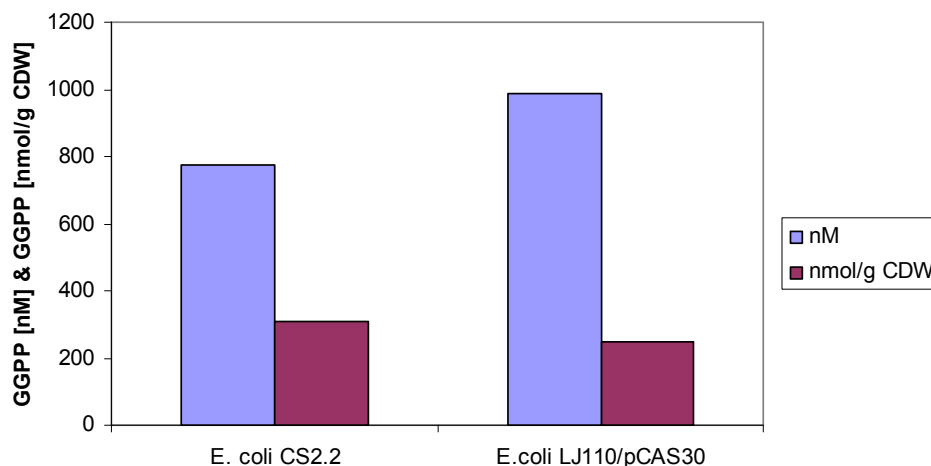


Figure 4.3: Graphical comparison of GGPP production in a Bioengineering fermenter in different strains. Maximum GGPP amounts achieved in respective fermentation are shown in this bar chart. For details of cultivation conditions refer to section 3.2.2 and 3.8.2).

Lipophilic isoprenoid side chain, GGPP is the second precursor for MGGBQ production which is the central precursor for all tocotrienol compounds. It is well studied that the wild type *E. coli* K12 strain is able to produce the two common building blocks IPP and DMAPP via DXP pathway (Rohmer et.al. 1996, Rohdich et. al.2003). Wild type *E. coli* K12 strain possesses a gene that encodes FPP synthetase. FPP synthetase catalyses the condensation of C5 compound IPP with DMAPP and geranyl diphosphate to yield FPP (Fujisaki et. al. 1986). A gene encoding GGPP synthase (CrtE) is not found in *E. coli* K12 and thus the organism should be unable to convert FPP into GGPP. But during the bioreactor cultivation of *E. coli* LJ110 in MM-Glucose, along with 38.4 ± 7.3 nM of FPP, surprisingly, a small amount of GGPP (approx. 9.1 ± 4.5 nM) was detected. Quantification of GGPP concentration had to be extrapolated as the peak area was below detection limit of $0.2 \mu\text{M}$ of the novel method developed. One study had shown that, *E. coli* K12 strain produces long chain compounds like undecaprenyl pyrophosphate, octaprenyl pyrophosphates via sequential condensation of FPP and IPP catalysed by different prenyl synthase enzymes (Baba et. al. 1985, Kainou et.al. 2001). Hence it was predicted that wild type *E. coli* K12 may produce small quantities of GGPP. The fact that *E. coli* K-12 strain possesses all the genes encoding the enzymes of DXP pathway, made it suitable for isoprenoid production (Rohdich et. al. 2003). In this study, GGPP production in multi-copy number plasmid pCAS30 in *E. coli* LJ110 strain (*E. coli* LJ110 / pCAS30) was compared with a single copy number *crtE* gene integrated in a chromosome of *E. coli* BW25113 (*E. coli* CS2.1). In both cases no FPP at anytime was detected which might imply that enough CrtE was expressed to convert all FPP to GGPP. *E. coli* CS2.1 strain showed robust or equally good production of GGPP compared to *E. coli* LJ110 / pCAS30 strain. It has been previously shown that low copy number plasmid perform well or better than

high copy number plasmid when a metabolite is produced (Jones et.al 2000). The metabolic burden exerted on cells carrying low-copy number plasmid, is comparatively higher than in cells, carrying a single copy of gene(s) on chromosome (Jones et.al. 2000). This metabolic burden is significantly higher after induction during bioreactor cultivation. One major factor of it being the load exerted while keeping the high level of protein production in plasmid (high copy) as compared to the low or minimal level using low or single copy chromosomally integrated strain. GGPP concentration (nmol/l) and GGPP yield (nmol/g CDW) in *E. coli* LJ110 /pCAS30 strain at the time of respective induction time was approx. twice as that in *E. coli* CS2.1 strain (214.3 ± 11.0 nM & 219.4 ± 22.5 nmol/g CDW vs. 121.2 ± 5.4 nM & 105.6 ± 4.2 nmol/g CDW respectively). Induction of *E. coli* LJ110/pCAS30 cells had no impact on GGPP concentration (nmol/l) as it increased continuously till end of 30 h fermentation, while induction of *E. coli* CS2.1 cells observed sudden increase in GGPP production in the first 4-6 hours after induction.

After induction with IPTG, the *E. coli* LJ110/pCAS30 strain (which carried multi-copy plasmid pCAS30) grew slower compared to the cells *E. coli* CS2.1 (which carried a single copy of *crtE* gene). On the other hand, IPTG induction had no negative effect on the cell growth in *E. coli* CS2.1, perhaps due to the presence of only single copy of *crtE* gene resulting in low levels or sufficient level of CrtE over-expression and hence balancing the cell growth and GGPP yield.

4.3. MGGBQ Biosynthesis

In section 3.1.4 it was shown that *E. coli* BW25113/pCAS29 was able to produce MGGBQ. *E. coli* DH5 α / pCAS29 grew better than the control strain *E. coli* DH5 α / pCAS18 (figure 3.18). Absence of *hpt-Syn* gene, and the apparently inactive over-expressed Ggh-Syn in *E. coli* DH5 α /pCAS18, resulted in accumulation of the aromatic precursor, HGA, and the isoprenoid precursor GGPP as end products. In this study, accumulation of GGPP did not inhibit cell growth, but accumulation of HGA or its follow-up products (i.e. above 600 μ g/l HGA) had inhibited cell growth. A similar effect was seen, when HGA and GGPP were produced using multi-copy plasmids in *E. coli* BW25113/pCAS2JF and *E. coli* LJ110 /pCAS30 respectively in different experiments (Figure 3.4A & 3.8 respectively). The over-expression of Hpd, CrtE (protein spots on 2D gel electrophoresis) occurred in both strains and hence cannot be the reason for lower cell density in *E. coli* DH5 α /pCAS18 as compared to *E. coli* DH5 α / pCAS29. *E. coli* DH5 α /pCAS18 cultures had turned brown after 24 h which was not the case in *E. coli* DH5 α / pCAS29 cultures. Supernatant samples of *E. coli* DH5 α /pCAS18 cultures were brown in colour (cell pellet was pale/white in colour), which may indicate that HGA was produced and accumulated. Prolonged incubation (> 24 h) without further use as substrate might have oxidised the HGA and further polymerised into ochronotic pigment. Supernatant samples of

E. coli DH5 α /pCAS29 cultures didn't turn brown till 48 h. No GGPP was analysed in any of the cultures samples. Culture samples were harvested and lipophilic MGGBQ was extracted from cells using acetone. The extracted MGGBQ in acetone was concentrated using rotary vacuum before redissolving the sample in 1 ml of acetonitrile. MGGBQ extract in acetonitrile was analysed by HPLC. *E. coli* DH5 α /pCAS29 resulted in 2 peaks each and based on LC-MS they represented MGGBQ, one in reduced form and another in oxidized form. As the cultures grew older i.e. 24 h, 48 h and 72 h the cell pellet colour changed from white to light brown to brown. As HGA oxidises and polymerises to brown pigment, similarly the aromatic head of MGGBQ_{reduced} form may also oxidise to MGGBQ_{oxidised} form and may further polymerise (refer figure 4.2) (Albermann et.al. 2008).

Induction with different IPTG concentrations resulted in an unexpected result (Figure 3.78 C). Cultures without induction produced the highest MGGBQ_{total} concentration i.e. 591 μ g/g CDW after 24 h. The amount of MGGBQ_{total} in all *E. coli* DH5 α /pCAS29 cultures decreased to 235 - 285 μ g/g CDW as a result of oxidation. The MGGBQ level in culture with 1 mM IPTG dropped even low reaching 139 μ g / g CDW. Cultures induced with 1 mM IPTG also grew slower and reached a lower final OD_{600nm} of 3.99 as compared to other cultures induced with (0, 0.1 and 0.25 mM IPTG) reaching between 4.15 – 4.57. High level of protein expression (Hpd, CrtE and Ggh) was seen in *E. coli* BW25113/pCAS29 cultures induced with 1 mM IPTG as compared to cultures induced with 0, 0.1 and 0.25 mM IPTG (2D gel electrophoresis, refer figure 3.79). More than one copy of each gene, combined with the use of high inducer concentration, may have resulted in high levels of recombinant protein expression. This high level of protein expression may have exerted a metabolic burden attributed by plasmid replication and gene expression can decrease the cell growth rate and productivity (Kim 1991; Yazdani 2002). This may be one of the possible reasons why *E. coli* BW25113/pCAS29 induced with 1mM IPTG performed poorer, than cultures induced with 0.1 mM, 0.25 mM and un-induced cultures. Production of MGGBQ in un-induced cultures may be the result of the leakiness of the *tac* promoter.

In this work, heterologous genes (*hpd-P.putida*, *crtE-P.ananatis* and *hpt-Synechocystis PCC6803*) were inserted in the chromosome (fucose, maltose and lactose loci resp.) of *E. coli* BW25113 (*lacZ+*) to construct a robust MGGBQ producing strain named *E. coli* CS6. No significant physiological effect was observed in *E. coli* CS6 strain when growth was compared to the wild type *E. coli* BW25113 (*lacZ+*). Insertion of heterologous genes into the different sugar degradation genes assisted in the screening of correct transformant on MacConkey agar plates supplemented with respective sugar(s). *E. coli* CS4 (*hpt-Syn*; *hpd*) and *E. coli* CS2.2 (*hpd*; *crtE*) (not shown) resulted in lower cell growth compared to *E. coli* CS5 (*crtE*; *hpt-Syn*) & *E. coli* CS6 (please refer to figure 3.50A). The 2D gel electrophoresis showed proteins

spots for Hpd and CrtE in *E. coli* CS6. Hpt-Syn being a membrane associated protein, could not be detected on 2D gel electrophoresis (Collakova and DellaPenna 2003). Similarly Hpd protein was detected in *E. coli* CS4, Hpd and CrtE spots detected in *E. coli* CS2.2 and CrtE spot in *E. coli* CS5 (results not shown). Based on the molecular masses obtained from mass spectroscopy study for each peak during LC, it was shown that both forms of MGGBQ were produced in *E. coli* CS6 (section 3.4.2) via biosynthesis pathway shown in figure 1.2.

Integration of an additional copy of *idi* gene in ribose locus and a T₅ promoter replacement for the native *dxs*, in *E. coli* CS6 strain, increased the MGGBQ_{total} by approx. 2.4 times compared to *E. coli* CS6. Additional over-expression of Idi and Dxs in *E. coli* CS6 enhanced the carbon flux via DXP pathway, resulting in higher accumulation of DMAPP and IPP, hence increasing the pool of precursor for FPP production.

Segregational Plasmid Stability

Segregational plasmid stability of plasmid pCAS29 during bioreactor cultivation of *E. coli* BW25113/pCAS29 was analysed by conventional technique of parallel plating of culture samples. A series of dilution of culture samples in respective medium with Amp100 were plated once on selective and once non-selective plates i.e. in this case on LB-Agar-Amp100 and LB Agar respectively. The problem of recombinant *E. coli* cells losing plasmid started with the preculture. The 12 h overnight incubated shaking flask pre-culture (*E. coli* BW25113/pCAS29) in exponential phase used for the inoculation of fresh MM-Glucose-Amp100 in bioreactor showed that approx. 97 ± 2 % of the recombinant *E. coli* cells were carrying plasmid. Population of recombinant *E. coli* cells carrying the ampicillin resistance plasmid pCAS29 during the batch fermentation (15 h) was approx. 79 ± 4 %. As the glucose feeding was started, the number of recombinant *E. coli* cells possessing the plasmid started dropping significantly. At the end of fermentation (46 h) only 63 ± 7 % of recombinant *E. coli* cells possessed the plasmid pCAS29. This drop in recombinant cells losing Amp^r plasmid may be due to several reasons. Plasmid stability is also dependent on the type of feeding strategy. Here linear and intermittent glucose/glycerol feeding strategy was used which to a certain extend would have helped to reduce the cells losing there plasmid. Exponential feeding strategy has the results in more then 50 % plasmid stability (Friehs 2004).

Plasmid pCAS29 used in this study, has an ampicillin resistance gene encoding for enzyme β -lactamase. Due to the presence of ampicillin (end conc. of 100 μ g/l) in MM-Glucose from start of fermentation, the *E. coli* BW25113/pCAS29 grew well.

Induction with IPTG induces the recombinant proteins along with proteins which can degrade antibiotics e.g. β -lactamase produced during cultivation is secreted in periplasm. Hence, use

of ampicillin in the medium for selection pressure, might end up the cells losing the plasmid which in turn could result in decreased productivity.

Ampicillin is perhaps not the best choice for antibiotics (preferred is Kanamycin) when it comes to cultivation for production of metabolites. But it is a widely used antibiotic since many of the cloning vectors are constructed with ampicillin resistance gene. Methicillin also has a *bla* but is almost 10 times expensive than ampicillin. For industrial processes, it can be one of the expensive media component and a greater problem (in some processes like vaccine production, therapeutics etc.) while downstream processing of culture supernatant. Leakiness of promoter systems in plasmids often allows growth of cell population that is plasmid free and or that has reduced capacity for high level expression of protein (Weickert et. al. 1996). It was seen from shaking flask results that the *tac* promoter in pCAS29 and pCAS47 plasmids is not tightly regulated, especially in shaking flask conditions (used in this study) when LB+Glycerol+Amp100 medium is used for cultivation. Induction with 1mM IPTG, in *E. coli* BW25113/pCAS29 and *E. coli* BW25113/pCAS47 cultures can have negative effect the physiology of the host. Hence both conditions were avoided in this study and induction with 0.25 mM IPTG was performed and in case of GGPP it was done with 0.1 mM IPTG. Loss of plasmid leads to decrease in productivity of recombinant product. In this case the MGGBQ productivity in *E. coli* BW25113/pCAS29 decreased with time. Plasmid stability is usually higher in minimal medium with glucose compared to complex media with glucose (Friebs et.al 2004).

Glycerol as carbon source proved more valuable in both cases i.e. *E. coli* CS6 and *E. coli* BW25113 / pCAS29 in fermenter, since they produced 1.25 and 1.9 times higher MGGBQ than that produced using glucose. The reason for the plasmid strain to perform so well in glycerol might be due to the low acetate production. This resulted in the plasmid strain to reach higher cell densities in glycerol as compared to glucose. In general, when the MGGBQ produced calculated per carbon mole consumed, glycerol as carbon source would result in even higher numbers as compared to that in glucose.

4.3.1. Purification of MGGBQ and analysis of its chemical structure by NMR

MGGBQ produced during two bioreactor cultivation of *E. coli* CS6 in MM-Glucose was extracted, purified and the chemical structure of MGGBQ was elucidated by NMR studies.

MPBQ and MGGBQ standards were not commercially available. MPBQ and / or MGGBQ were the expected product of *E. coli* DH5a/pCAS29. LC-MS analysis results showed that only MGGBQ was produced in *E. coli* DH5a/pCAS29 based on the molecular mass of 2-methyl-6-geranylgeranylbenzoquinol. 3 different isomers of MPBQ had been isolated from the lipids of

algae *Scenedesmus obliquus* (Henry et. al. 1987). Those three isomers 2-methyl-6-phytyl benzoquinone, 2-methyl-3-phytyl benzoquinone, and 2-methyl-5-phytyl benzoquinone were formed in the ratio of 65 %, 8 % and 27 % respectively. Hence, to know the exact chemical structure of MGGBQ produced in large quantities and purified for NMR analysis.

Previous attempts comprised of shaking flask cultivations of MGGBQ producing *E. coli* strains (plasmid-encoded) in LB-Glycerol medium. MGGBQ was extracted from cells and treated with sodium borohydrate to convert all the oxidized MGGBQ into reduced form of MGGBQ. This mixture was purified using HPLC method (explained in materials and method section 2.2.5.2). Samples which included MGGBQ_{reduced} were collected, and loads from 8 such sample injections were pooled together. Concentrated, washed with acetone twice, and concentrated again. NMR analysis of this sample in deuterated acetone was carried out. NMR analysis did give some δ values which corresponded to the expected values. But the ^1H NMR spectrum was with lot of disturbing signals representing fatty acids between 1.0 and 2.5 ppm. Leftover glycerol from cultivation also could be seen at δ values between 3.5 and 3.8 ppm (results not shown in this report). Another problem was the stability of reduced MGGBQ. The probability of the purified MGGBQ to oxidize during the NMR analysis existed. Hence, to stabilize the reduced MGGBQ form experiments for derivatization were carried out. Initially, methylation of the hydroxyl group on the benzene ring at carbon 4 position of MGGBQ was performed with diazomethane. No methylated form of MGGBQ was detected during HPLC analysis. Same method was successfully used for methylation of hydroquinone and methyl hydroquinone. A further attempt to acetylate the MGGBQ at the carbon 4 position was carried out with acetyl chloride. HPLC analysis of sample after Acetylation did not detect any additional peak other than MGGBQ (data not shown). After observing that the *E. coli* CS6 strain was able to produce large quantities of MGGBQ in fermenter in minimal medium with glucose the cells at the end of fermentation were extracted and MGGBQ (section 2.2.5.1) was purified (section 2.2.5.2). Use of ascorbic acid during the entire extraction and purification time helped in avoiding the oxidation of MGGBQ. Use of minimal medium with glucose perhaps helped in avoiding the high contents of fatty acids. Signals representing all the methyl groups (refer Appendix A3-6).

4.3.2. Improved MGGBQ yield as a result of increased precursor

MGGBQ is produced as a result of convergence of two different pathways i.e. two precursors from two different pathways (HGA from shikimate pathway and GGPP from DXP pathway). Since glucose or glycerol was used as the sole carbon and energy sources for MGGBQ production the carbon flux in these two pathways had to be increased. Hence, methods for increasing the pool of precursor *p*-HPP for HGA production and/or increasing the pool of IPP, FPP precursor for GGPP production were started. High Hpd over expression levels in

different constructs and excess HGA amounts leading to toxic brown pigments. Hence increasing the HGA production was not an optimal solution, rather increasing carbon flux through DXP pathway was seen as the limiting factor. Experiments during GGPP synthesis showed that sufficient level of CrtE was expressed to convert the entire FPP precursor to GGPP (since no or negligible amounts of FPP was found in cell pellets of *E. coli* LJ110/pCAS30 and *E. coli* CS2). Hence increasing the existing CrtE expression level would not enhance the MGGBQ production. Experiments in section 3.4 where *E. coli* CS6 combined with pJF119 Δ N, pCAS30 showed no increase in MGGBQ.

dxs and *idi* genes in the isoprenoid pathway being the rate controlling enzymes in isoprenoid pathway (Harker et. al 1999) these two were over expressed in *E. coli* CS6. Experiments with *E. coli* CS6 carrying pJF119 Δ N and pCAS10 each increased MGGBQ yields by at least 3 times. Experiments with *E. coli* CS6 carrying pJF119 Δ N and pJF119HE-*dxs*-C.glut (*Dxs* from *Corynebacterium glutamicum*) each increased MGGBQ yields by at least 8 times. This might be due to the increased expression levels of *Idi* and *Dxs* proteins which could increase the precursor concentration of IPP and FPP. The same CrtE expression level is capable of converting the excess pool of FPP and IPP to GGPP and the same Hpt expression level is capable of converting the excess GGPP into MGGBQ with the excess HGA being produced (which would get spontaneously oxidized if not utilized). Over expression of *Dxs* in recombinant *E. coli* expressing *DdsA* (decaprenyl diphosphate synthase) produced 2 times higher CoQ10 production levels as compared to that without over expression of *Dxs* (Kim et. al. 2006). In another case, overexpression of *Dxs* in recombinant *E. coli* (with leaky promoter) without induction increased lycopene production by 8 times (Rodríguez-Villalón et. al. 2008). Single copy of *idi* gene produced 64 % more MGGBQ ($\mu\text{g/g}$ CDW) in *E. coli* CS8 strain as compared to *E. coli* CS6. Over-expression of existing copy of *dxs* resulted in 21 % more MGGBQ ($\mu\text{g/g}$ CDW) in *E. coli* CS10 as compared to *E. coli* CS8 and almost 105 % increase as compared to *E. coli* CS6. *Dxs* is a critical enzyme in DXP pathway since it catalyses the 1st reaction in DXP pathway (Sprenger et. al. 1997). Higher expression of *Dxs* would lead to higher carbon flux in this pathway which would increase the pool of isoprenoid precursors IPP and DMAPP for FPP and hence for GGPP production. Hence, chromosomal integration of *idi* gene in *E. coli* CS6 was carried out which resulted in *E. coli* CS8. The *E. coli* CS8 produced approx. 1.8 times more MGGBQ with additional *Idi* overexpression as compared to that without *Idi* overexpression in *E. coli* CS6.

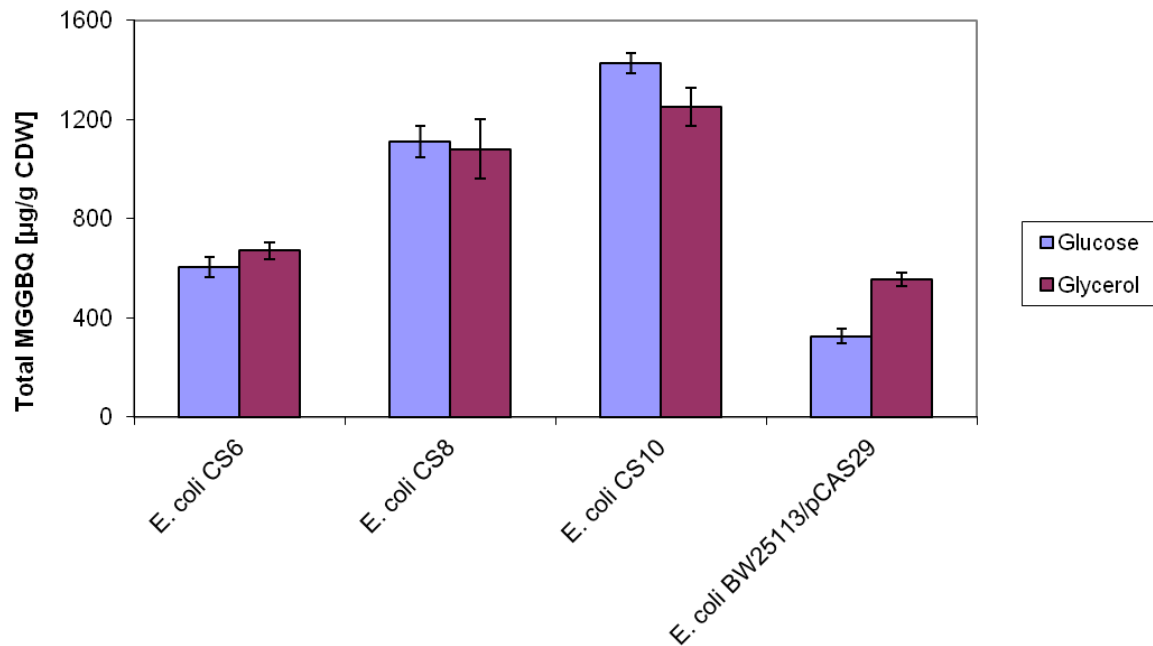


Figure 4.4: Graphical comparison of MGGBQ production in Infors fermenter in different strains. Maximum MGGBQ amounts achieved in respective fermentations are shown in this bar chart. Refer to sections 3.4.4, 3.9.2, 3.11.1, 3.11.2 for experimental details.

Overexpression of *Idi* and *Dxs* combine i.e. *E. coli* CS8 with pJF119HE-dxs-C.glut produced even higher MGGBQ i.e. 20 times as compared to the control *E. coli* CS8 / pJF119ΔN. Hence, co-expression of *Dxs* in MGGBQ producing strain was further pursued. Instead of using an extra copy of *dxs* gene from another microorganism, a chromosomal T_5 promoter replacement for *dxs* gene of the host strain *E. coli* itself, was carried out in *E. coli* CS8 that lead to new strain *E. coli* CS10. Similar chromosomal modifications i.e. P_{T_5} -*idi*, P_{T_5} -*ispC*, P_{T_5} -*ispB* each in *E. coli* MC1061 / pPCB15 resulted in 1.4, 0.8 and 1.3 times higher β -carotene yields respectively (Yuan et. al 2006). Hence only chromosomal integration of promoter P_{T_5} exchange was carried out. *E. coli* CS10 produced approx. 1.5 times more MGGBQ as compared to *E. coli* CS8. Over expression of *Dxs* and *Idi* simultaneously resulted in a greater impact on MGGBQ production. When *Dxs* was co-expressed in β -carotene producing recombinant *E. coli* strains, the β -carotene production increased multiple times (Yuan et. al. 2006). *E. coli* CS10 when cultivated in fermenter in minimal medium with glucose, ended up producing 1.35 times more MGGBQ then produced in *E. coli* CS8, and approx. 2.4 times more MGGBQ when compared to *E. coli* CS6 strain.

4.3.3. Instability of MGGBQ_{reduced}

MGGBQ produced in the first 15 – 18 h of bioreactor cultivation (*E. coli* DH5a/pCAS29 and *E. coli* CS6) is MGGBQ_{reduced}. Slowly, as the fermentation progresses, amount of MGGBQ_{reduced}

and MGGBQ_{oxidised} increases. It is thought that, once MGGBQ_{reduced} is produced in recombinant *E. coli* cells, its lipophilic tail sticks to the cell membrane, exposing the chromanol ring to oxidation and further polymerisation (Albermann et. al. 2008). Especially during cultivation in bioreactor the saturated concentration of oxygen in medium is relatively higher ($\geq 30\%$) than in shaking flask. *E. coli* CS6 cultures from fermenter after 30 h of cultivation started turning brown. Cell pellet was washed twice in 0.9 % (w/v) NaCl solution and centrifuged. The resulting cell pellet retained the brown colour while the supernatant was clear. Culture supernatants after 40-42 h of cultivation started turning brown and this was due to the HGA oxidation.

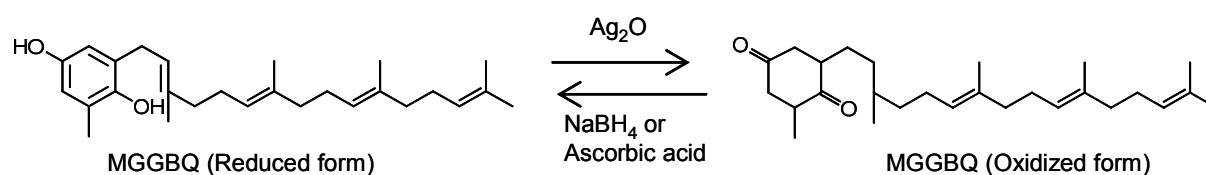


Figure 4.5: Scheme for oxidation of MGGBQ (Peddibhothla 2003).

4.4. Ggh activity and its influence on PPP, MPBQ and δ -Tocopherol Biosynthesis in this study

4.4.1. Over-expression of Ggh-Syn protein in recombinant *E. coli*

Strong over-expression of Ggh-Syn was observed when it was expressed as a single recombinant protein (Figure 3.11), or co-expressed with CrtE (Figure 3.12). When Ggh-Syn was co-expressed with Hpd, CrtE, Hpt-Syn, relatively weak expression was observed compared to strong Hpd and CrtE expression (Figure 3.15). Induction with 0.1 mM, 0.25 mM 1.0 mM, and uninduced cultures resulted in same observation.

In plasmid pCAS29, *ggh* gene is the first gene in the artificial gene cluster. May be the positioning of each gene order in the biosynthetic gene cluster (for e.g. in pCAS29) has a effect on the mRNA. Eventhough the mRNA transcript were detected (Albermann et.al. 2008), no reductase activity was found in any of the *in-vivo* biosynthesis experiments involving Ggh-Syn i.e. PPP, MPBQ and δ -tocotrienol biosynthesis. The DNA sequence identity of *ggh-Syn* in plasmid pCAS29 and gene *chIP* (ORF *sll1019*) from *Synechocystis* PCC6803 was 100 % (Personal communication with Dr. Albermann).

4.4.2. Possible reasons for failure of conversion of GGPP to PPP

PPP was not detected during any experiment carried out in this study with recombinant *E. coli* strain. GGPP was synthesized *in-vivo* in *E. coli* DH5 α /pCAS11. CrtE and Ggh-Syn proteins were detected on 2D gel electrophoresis.

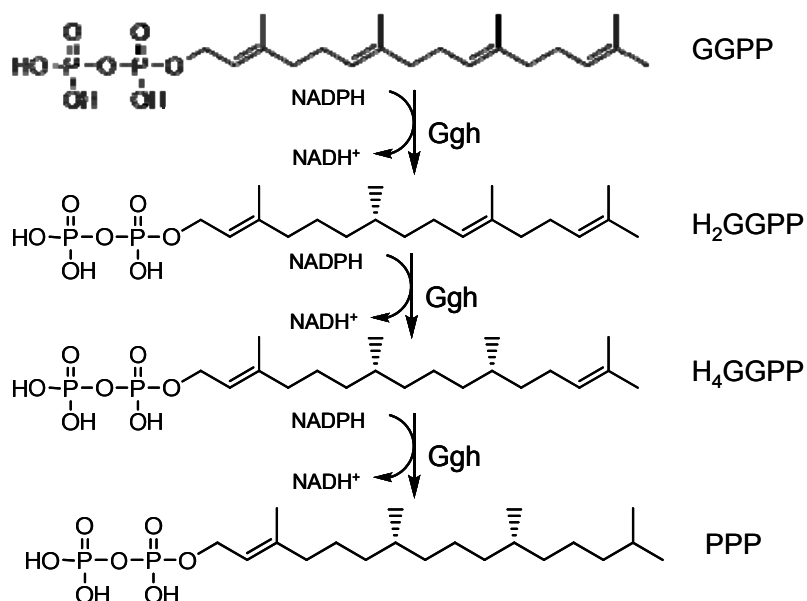


Figure 4.6: Three step reduction of GGPP to PPP catalysed by Ggh. Each single reduction step requires 1 mole of NADPH which results in reduction of a *trans* double bond on isoprenoid chain. (Keller et. al. 1998)

Perhaps the expressed Ggh-Syn protein was apparently inactive, and hence could not catalyze the reduction of GGPP to PPP. Another possible reason may be sufficient availability of 3 moles of co-factor NADPH to reduce 1 mole of GGPP to PPP. PPP can only be formed if the reduction reaction occurs at all the 3 positions in the isoprenoid side chain of GGPP (as shown in figure 4.6). Reduction at one or two positions can result in dihydrogeranylgeranyl pyrophosphate (H₂GGPP) and tetrahydrogeranylgeranyl pyrophosphate (H₄GGPP) respectively (Keller et. al. 1998). The structure of those can be seen in figure 4.6.

No standards for H₂GGPP and H₄GGPP compounds were available to test whether this newly developed method was able to detect such compounds. Hence, it is not known whether the GC-MS method developed (Vallon et.al. 2008) can detect H₂GGPP and H₄GGPP. GGPP was seen to be stable after being produced in recombinant *E. coli* cells. Stability of PPP (if produced) in recombinant *E. coli* is not known. There are other enzymes reported which can utilize PPP (if produced) for phyloquinone synthesis. Apart from the two unknown facts, IspB (Kim et. al. 2006) present in wild type *E. coli* is an enzyme which would take away the produced GGPP and IPP to produce ubiquinone 8 hence leaving no or low amounts of GGPP for PPP production. Hence, the activity of Syn-Ggh was not sufficient for conversion of GGPP to PPP under the conditions used in this study. It was shown that Hpt-Syn expressed in *E. coli* DH5 α /pCAS29 was active as it produced MGGBQ (LC-MS results) but failed to produce MPBQ (LC-MS results). This showed GGPP was the preferred substrate to Hpt-Syn over PPP. Hpt-Syn can accept GGPP and PPP as substrate with the higher substrate specificity

towards PPP (Collakova and DellaPenna 2003). Since, PPP was not detected *Syn*-Hpt may perhaps had only GGPP as substrate and hence catalysed the reaction between HGA and GGPP to produce MGGBQ. Recombinant protein expression in *E. coli* BW25113 / pCAS29 cells, on 2D gel electrophoresis with different IPTG concentrations, show that Hpd and CrtE protein expression level increased with increased IPTG concentration. Very small difference in Ggh-*Syn* expression (based on the dark red colour intensity of the spot) was seen between cultures induced with 1 mM IPTG and the one without induction. All 4 genes (*hpd*, *crtE*, *ggh-Syn*, *hpt-Syn*) are clustered and are under the control of common *tac* promoter, to ensure the simultaneous expression of each recombinant protein. If compared to the Ggh-*Syn* expression profile in pCAS8 where *ggh-Syn* is the only foreign gene cloned or in case of pCAS11 where *crtE* and *ggh-Syn* are the foreign genes cloned in pJF119ΔN vector (see section 3.3.1 and 3.2.3). This low expression of Ggh-*Syn* in *E. coli* DH5α/pCAS29 may be one of the problems in further production of all saturated tocochromanols. If H₂GGPP and / or H₄GGPP were produced instead of PPP, it's not known whether Hpt-*Syn* in plasmid pCAS29 can take those as substrates instead of PPP. *E. coli* CS6 / pCAS8 cells also resulted in no MPBQ. Although it produced MGGBQ the amount was lower than that produced in the control *E. coli* CS6 / pJF119ΔN.

Ggh-At was cloned to obtain pCAS33. *Ggh-At* was expressed in *E. coli* as recombinant protein and shown functionally active during *in-vitro* reaction with radioactive labelled GGPP as substrate and *E. coli* cell lysate (*Ggh-At*) to produce PPP (Keller et. al. 1998). *In-vivo* shaking flask experiments with *E. coli* CS6 / pCAS33 (shaking flask) didn't result in any additional peak representing the expected MPBQ (refer section 3.5.1). Here again the MGGBQ levels were lower than in the control *E. coli* CS6 / pJF119ΔN. In another cultivation experiment in fermenter, *E. coli* CS2.2 / pCAS19 + pCAS33 resulted in only MGGBQ. The control strain *E. coli* CS2.2 / pCAS19 + pJF119ΔN produced higher levels of MGGBQ. The *chlP* / (*ggh-At*) gene from *Arabidopsis thaliana* or from plants contains N-terminal plastid transit sequences. The cloned *At-ggh* gene cloned in pCAS33 included the transit peptide signal. Since, the *Ggh-At* would be expressed in *E. coli*, a truncated *ggh-At* without the signal peptide was cloned to obtain plasmid pCAS53 (personal communication Dr. Albermann). *E. coli* CS6 / pCAS53 when cultivated in shaking flask resulted in no MPBQ. The amount of MGGBQ level was far lower than that produced in the control *E. coli* CS6 / pJF119ΔN. Shaking flask experiments with *E. coli* CS6 carrying *ggh-At* or *ggh-Syn* in plasmid form produced low levels of MGGBQ than in the control *E. coli* CS6 / pJF119ΔN. The *E. coli* strains in which Ggh (*Syn/At*) were expressed didn't grew well, compared to their respective controls. Ggh protein expressed may have inhibited cell growth. Partial reduction of GGPP is taking place with no PPP produced and less GGPP available for Hpt-*Syn* to

produce MGGBQ. Few suggestions regarding, how to find the solution to this problem has been mentioned in outlook section (4.7).

hpt-Syn was used during attempts to produce all MPBQ. This Hpt-Syn could take GGPP as well as PPP as substrates with approx. 20 % preference to GGPP (Collakova and DellaPenna 2001). First hypothesis, why MPBQ is not formed during cultivation of *E. coli* strains carrying plasmid pCAS29 could be, the condensation reaction between GGPP and HGA to produce MGGBQ is faster and hence no GGPP is available for reduction to PPP. Since HGA and GGPP are already present in cell along with *Syn-Hpt* enzyme, this reaction can be easily catalyzed with no GGPP remaining for the reduction in presence of Ggh (even if expressed in its active form). Experiments performed in section 3.5.3 resulted in only MGGBQ production with no MPBQ detected during HPLC analysis. On the other hand *hpt* from *Arabidopsis thaliana* i.e. *At-hpt* recognizes only PPP as its substrate (not GGPP) (Collakova and DellaPenna 2001). Hence, *hpt (vte2)* from *Arabidopsis thaliana* was cloned into pJF119ΔN vector to obtain pSGS7.

Strong overexpression of Hpt-Syn was shown in *E. coli* DH5α/pCAS8 (figure 3.11). A weak expression of Hpt-*At* was also shown in *E. coli* BW25113/pSGS7 (figure 91). Eukaryotic proteins (Hpt from *Arabidopsis thaliana*) are expressed at low levels in *E. coli* membranes as compared to cyanobacterium (Hpt from *Synechocystis* PCC6803) (Sadre et.al. 2006). It was also shown by Sadre et. al 2006 that the Hpt-*At* expressed as GST-fusion protein was accumulated 10 times lower than the GST-tagged fusion Hpt protein from *Chlamydomonas reinhardtii* (*C. reinhardtii*) (Sadre at. al. 2006). Collakova and co-workers (2001) also reported unsuccessful expression of Hpt-*At* protein on the SDS-Gel stained by coomassie blue. Hpt-Syn was shown to be functional in which it catalysed the transferase reaction between HGA and GGPP to produce MGGBQ (Albermann et.al. 2008).

Syn-Hpt expressed in *E. coli* had at least 30 times higher specific activity as compared to Hpt-*At* expressed in *E. coli* (Collakova et. al 2001). This specific activity was with respect to PPP as substrate. Hpt-*At* expressed in *E. coli* DH5α/pCAS39+pSGS7 during shaking flask cultivation, failed to produce MPBQ (results not shown). This could be due to poor expression level of Hpt-*At* proteins in *E. coli* (as reported by Sadre et. al. 2006) and seen in this study too. The Hpt-*At* activity cannot be tested until PPP is produced in-vivo. Hpt-*At* has a low specific activity when compared to *Syn-Hpt* (Collakova 2001). This has been explained by poor stability of the Hpt-*At* proteins in *E. coli* (Collakova 2001) and the low level of these proteins (as is the case in the experiments in this study).

In literature the enzyme activity experiments with Hpt-*At*, Hpt-*Syn*, Ggh-*At* and Ggh-*Syn* were carried out either with purified enzymes, or with membrane proteins or using mutants (i.e. the respective gene was knocked out). Wherever *in-vitro* experiments were carried out, targeted substrate/s were used. In this study all the experiments were carried out in *in-vivo* recombinant *E. coli* cells.

4.4.3. δ -Tocopherol biosynthesis

All attempts to produce the saturated phytyl chain compound, PPP had failed. Lack of substrate to Hpt-*Syn* resulted in no production of MPBQ. Despite of an active Cyc-*At*, no δ -tocopherol could be produced. The reason for this may be apparently the lack of substrate availability (MPBQ) for the cyclisation reaction.

4.5. δ -Tocotrienol Biosynthesis

4.5.1. Over-expression of Cyc-*At* in recombinant *E. coli*

Genes specific for Vitamin E biosynthesis i.e. *ggh*, *hpt* and *cyc* genes from *Synechocystis* PCC 6803 (i.e. *ggh-Syn*, *hpt-Syn* & *cyc-At* resp.) were cloned and expressed in *E. coli*. Genes encoding *p*-hydroxyphenylpyruvate and geranylgeranyl pyrophosphate synthase are necessary for Vitamin E production but they are not pathway specific for e.g. CrtE converting FPP and IPP into GGPP could be channelized towards carotenoid production (β -carotene, lycopene, astaxanthin, canthaxanthin etc.) (Lemuth et.al. 2011). Ggh-*Syn* was apparently inactive and with Hpt-*Syn* yielding MGGBQ. Cyc-*Syn* was cloned in plasmid pCAS27 (pAW229 vector). It was provided by Dr. Albermann for further study. Weak Cyc-*Syn* expression (43 kDa, theoretical mass calculated by EXPASY is 43.05 kDa) was seen on SDS-PAGE gel (not shown here). *E. coli* DH5 α /pCAS29 + pCAS27 were cultivated in LB+Glycerol+Amp100+Cm50 medium in shaking flask. Cultures were induced with 0.25 mM IPTG and 0.2 % (w/v) rhamnose (final concentrations) at OD_{600nm} of 0.8. As control, *E. coli* DH5 α /pCAS29 + pHWG640 was cultivated under identical conditions. Both strains produced MGGBQ. No δ -tocotrienol was detected in any of the extracted samples of *E. coli* DH5 α /pCAS29 + pCAS27. Possible reason for this would be either an inactive Cyc-*Syn* or low expression level of Cyc-*Syn* or the possibility that Cyc-*Syn* enzyme does not accept MGGBQ as its substrate. His-Tagged Cyc-*Syn* was strongly expressed on western blot by Kumar et.al. 2005. But this high level of expression failed to show the catalytic active when DMPBQ was used as substrate. The authors thought it might be due to the different pI value (rather high value of 8.3) for Cyc-*Syn* as compared to Cyc from other organisms. Since the other cyclases from plants and other photosynthetically organisms are hydrophobic proteins

with low pI (between 5 and 6.5) values with a relatively higher share of number of conserved Trp residues (Provencher et al., 2001). Since the activity test was done *in-vitro*, the reaction conditions might have not been suitable for Cyc-Syn proteins. Similarly, Sattler et. al (2003) successfully cloned and expressed *slr1737* gene (*cyc*) from *Synechocystis PCC6803* and found no activity.

In general, cyanobacterial orthologs of *slr1737* has an amino acid sequence identity, ranging between 41 – 97 %, and plant orthologs having higher identity ranging between 61 to 79 % (Kumar 2005). Cyc-Syn has 41 % amino acid sequence identity with Cyc-*At* based on BLAST result. Vte1-*At* cloned in pCAS50 showed lower expression level on SDS-PAGE gel as compared to *pvte1* (in pQE31 vector) for unknown reasons.

4.5.2. Heterologous biosynthesis of δ -Tocotrienol in recombinant *E. coli*

***In-vivo* biosynthesis of δ -Tocotrienol in different *E. coli* strains**

E. coli DH5 α / pCAS47 cultures produced MGGBQ and δ -tocotrienol, which was confirmed by the molecular mass calculated by LC-MS. This culture produced 15 μ g/g CDW of δ -tocotrienol and as a result grew poorly, reaching a final OD_{600nm} of 2.4 after 72 h. Other experiments with *E. coli* DH5 α / pCAS47 induced with 0 mM, 0.25 and 0.5 mM grew better than the one which was induced with 1 mM IPTG. But these cultures produced low δ -tocotrienol amounts (results not shown) as compared to cultures induced with 1 mM IPTG. Thus it appears that high concentration of inducer results in high expression levels of Cyc-*At* proteins and relatively high levels of δ -tocotrienol compared to those cultures un-induced and induced with 0.1 & 0.25 mM Cyc-*At* expression above a certain level may be detrimental to cell growth or higher δ -tocotrienol levels be toxic for the cells. *E. coli* DH5 α / pCAS29 induced with 1 mM, grew till OD_{600nm} of 5.5. *E. coli* DH5 α cells expressing Cyc-*At* and producing δ -tocotrienol grew poor. This poor growth could also be influenced by the type of host strain. Hence, plasmid pCAS47 and as control pCAS29 each were transformed in each of the following host strains *E. coli* DH5 α , *E. coli* BW25113 and *E. coli* LJ110. *E. coli* DH5 α / pCAS47 produced the highest amounts of δ -tocotrienol with *E. coli* LJ110 producing the lowest. On the contrary, *E. coli* DH5 α as host strain grew badly as had been observed previously. *E. coli* BW25113 as host strain reached the highest cell density amongst the 3 host strains (results not shown in this study).

Plasmid free strains *E. coli* CS7 & *E. coli* CS9

Integration of *cyc-At* into the xylose loci of *E. coli* CS6 strain resulted in *E. coli* CS7 strain. *E. coli* CS7 produced MGGBQ and δ -tocotrienol. The MGGBQ produced in *E. coli* CS7 was higher compared to that produced in control *E. coli* CS6 (330 μ g/g CDW and 200 μ g/g CDW

resp.). That means the MGGBQ produced using single copy and multiple copies (i.e. in *E. coli* CS7 and *E. coli* BW25113/pCAS47 resp.) is comparable, but the conversion to δ -tocotrienol is 4 times higher in multi-copies gene i.e. 0.8 $\mu\text{g/g}$ CDW in *E. coli* CS7 (refer to figure 3.57) and 4.0 $\mu\text{g/g}$ CDW in *E. coli* BW25113 / pCAS47 (refer to figure 3.31). One explanation would be the comparatively higher level of Cyc-At proteins expressed in plasmid pCAS47 as compared to that in *E. coli* CS7. One possible reason might be the rate limiting Cyc-At enzyme in δ -tocotrienol biosynthesis in recombinant *E. coli*. The *E. coli* CS9 strain produced 575 $\mu\text{g/g}$ CDW MGGBQ but conversion into δ -tocotrienol was only 1.6 $\mu\text{g/g}$ CDW. This shows the correlation of higher MGGBQ amounts resulting lower tocotrienol amounts. Eventhough, *E. coli* CS9 produced more MGGBQ compared to *E. coli* BW25113 / pCAS47, the δ -tocotrienol amount is higher in the latter. This again indicates to the same correlation of higher MGGBQ amounts resulting lower tocotrienol amounts.

δ -Tocotrienol production in Infors fermenter using multi-copy plasmid vs. single copy genes

During all bioreactor cultivations of *E. coli* CS7 and *E. coli* BW25113/pCAS47 strains, small quantities of MGGBQ were detected before IPTG induction. This confirmed that the *tac* promoter was tightly regulated in minimal medium. Immediately, after IPTG induction, irrespective of multi-copy or single copy genes, both strains started producing MGGBQ. In both strains the cyclisation reaction was slow which can be seen from the result that no tocotrienol was formed in the first 8 to 10 hours after induction, even though the MGGBQ levels reached at its highest level. Interestingly, as the MGGBQ levels started decreasing (partly due to oxidation of MGGBQ) δ -tocotrienol production started. At one stage at 35 h both strains had produced approx. between 2 and 3 $\mu\text{g/g}$ CDW of δ -tocotrienol. By the end of fermentation, *E. coli* BW25113 / pCAS47 produced thrice the amount of δ -tocotrienol (9 $\mu\text{g/g}$ CDW) that was produced by *E. coli* CS7 (2.8 $\mu\text{g/g}$ CDW). This may be due to the stronger expression of Cyc-At proteins in *E. coli* BW25113 / pCAS47 strain (multiple copies of *cyc-At* genes per cell) compared to that in *E. coli* CS7 (single copy of *cyc-At* gene per cell). When glycerol was used as sole carbon and energy source, the difference between the δ -tocotrienol produced in *E. coli* CS7, *E. coli* CS9 and *E. coli* BW25113/pCAS47 was not significantly large compared (3.4, 4.2 and 4.8 $\mu\text{g/g}$ CDW) to that seen in glucose.

Chromosomal integrated strain producing MGGBQ harbouring different plasmids carrying *cyc-At* genes

δ -Tocotrienol produced in *E. coli* CS6 along with 3 plasmids pCAS59, pQE31-Vte1 and pGEX-Cyc-At each, didn't increase significantly the δ -tocotrienol yields i.e. 1.4 $\mu\text{g/g}$ CDW,

0.39 $\mu\text{g/g}$ CDW and 1.2 $\mu\text{g/g}$ CDW respectively. The protein expression on SDS-PAGE gel in case of pCAS59 was very low compared to that in pQE31-Vte1 and pGEX-Cyc-At.

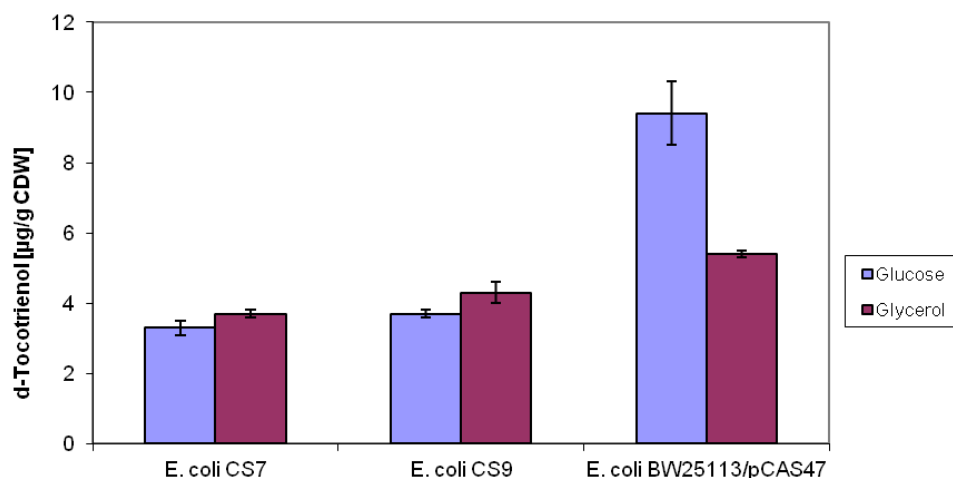


Figure 4.7: Comparison of δ -Tocotrienol production in Infors fermenter in different strains. Maximum δ -tocotrienol amounts achieved in respective fermentations have been shown in the bar charts. Refer to section 3.10.2, 3.12.2, 3.6.3 for experimental details.

In-vitro enzymatic reaction with Cyc-At purified from pQE31-Vte1 and pGEX-Cyc-At had shown complete conversion of MGGBQ into δ -tocotrienol and hence the reason for lower δ -tocotrienol production in *in-vivo* production using pQE31-Vte1 and pGEX-Cyc-At plasmids could not be explained. On the other hand *E. coli* CS8 / pGEX-Vte1 produced 6.4 $\mu\text{g/g}$ CDW of δ -tocotrienol as well as the protein expression level seen on SDS-PAGE was high and cells grew to an $\text{OD}_{600\text{ nm}}$ of 6.0. MGGBQ produced was about 300 $\mu\text{g/g}$ CDW. These experiments were repeated twice resulting in standard deviation of $\pm 20\%$ in MGGBQ and δ -tocotrienol amounts. Based on these experiments, it can be concluded that neither Cyc-At is toxic to the cells, nor δ -tocotrienol accumulation in recombinant *E. coli* cells is a problem for cell growth. Toxicity of the enzyme tocopherol cyclase is out of question since they grow and produce tocotrienol expressing high cyclase levels. As the GST-Cyc-At resulted in higher δ -tocotrienol yield during *in-vivo* and *in-vitro* biosynthesis it is clear that the Cyc-At produced in *E. coli* BW25113/pCAS47 and *E. coli* CS7 is highly active and hence further study regarding the protein structure is necessary to understand the problem of low δ -tocotrienol yield resulting from cyclization reaction. It can be concluded that correct folding of Cyc-At proteins in recombinant *E. coli* is crucial if higher levels of δ -tocotrienol is to be produced.

4.5.3. Cyclization reaction in recombinant *E. coli* - a bottleneck?

Activity of tocopherol cyclase

From all the experiments for δ -tocotrienol production it seems that the first reason for low conversion is the low level of tocopherol cyclase expressed in recombinant *E. coli*. If one compares the over expression of these single genes in vector pJF119 Δ N i.e. SDS or 2D-Gel Electrophoresis figures 3.2, 3.7, 3.11, 3.14 and 3.28, one can see that Cyc expression level was the lowest. This could be the reason for it to be rate limiting. When Cyc-At was expressed as GST protein, the expression level increased increasing the conversion of MGBBQ to δ -tocotrienol.

High MGBBQ low tocotrienol, a paradox?

In all the δ -tocotrienol biosynthesis experiments performed in this study, a common correlation was seen between the amount of MGBBQ_{total} produced to the amount of δ -tocotrienol produced. If any two strains were compared, always the strain producing higher MGBBQ_{reduced} produced lower δ -Tocotrienol, and vice-versa. One explanation for this correlation may be that the MGBBQ_{reduced} and tocotrienol inside the *E. coli* cells may be competing for the membrane insertion i.e. the polar aromatic head group. Despite, high amounts of MGBBQ_{reduced} is produced; the conversion to δ -tocotrienol is still low. The excess MGBBQ_{reduced} compared to the low amounts of δ -tocotrienol accumulates in the membrane fraction, hence converted to MGBBQ_{oxidised}. In the opposite case, low amounts of MGBBQ_{reduced} are produced; the conversion is still low. But there is no excess MGBBQ_{reduced} to be converted to MGBBQ_{oxidised}. This way, more MGBBQ_{reduced} is available for conversion to δ -tocotrienol compared to, if it is converted into MGBBQ_{oxidised}.

MGBBQ_{oxidized} as inhibitor for cyclisation reaction

MGBBQ_{oxidized} yield (μ g/g CDW) increases in the last 12 h of bioreactor cultivation. This increased MGBBQ_{oxidized} apparently gets polymerised (similar to HGA) producing brown pigments. These unidentified compounds may hinder the accessibility of MGBBQ_{reduced} and hence inhibit or slow the tocotrienol biosynthesis apparently the cyclisation reaction. Since, no evidence supporting this theory was available in this study, it remains a speculation.

4.6. CONCLUSION

For the first time, it has been shown that the precursor for all tocotrienols i.e. MGBBQ and the Vitamin E derivative δ -tocotrienol could be produced using a multi-copy plasmid in a non-photosynthetic bacteria using metabolic engineering (published in Albermann et. al. 2008). In this

study, it was shown that complex natural compounds like δ -tocotrienols can be produced from a simple and relatively inexpensive sugar source as sole carbon and energy source. In this work, it was shown that a plasmid-free recombinant *E. coli* strain that carried the biosynthetic genes for the *in-vivo* biosynthesis of δ -tocotrienol. The homologous recombination method used in this study also allowed the deletion of the resistance marker. MGGBQ and δ -Tocotrienol producing plasmid free strains can be cultivated in fermenters without any antibiotics. This engineering strategy also offers the plasmid free strains the robustness during fermentation. This approach also allows the plasmid free strains to control individual gene expression levels by using different promoters, or by use of different expression plasmids. This approach also allows one expression cassette to be inserted in two or more loci of the host strain.

Plasmid free strain produced almost similar amounts of GGPP and 1.8 times higher MGGBQ_{total} than strain encoded with plasmids. HGA produced in plasmid encoded strains was approx. 20 % higher than in plasmid free strain. This advantage in plasmid encoded strain came at a cost of extremely poor cell growth. In case of δ -tocotrienol, plasmid encoded strain produced approx. 2.5-3.0 times higher δ -tocotrienol than produced in plasmid free strains. Again, the higher δ -tocotrienol in plasmid encoded strains was achieved at a cost of lower cell densities.

The results obtained in this study partly or wholly support that; the use of single copy gene can lead to a stable biosynthesis of a natural complex compound.

Based on the above comparison it can be concluded that use of a single copy of individual gene, in the δ -tocotrienol biosynthesis pathway, was sufficient to show that the biosynthesis pathway was completely functional. These plasmid free strains with single copy of individual genes are analogous to the natural vitamin E producers.

Homogentisate Phytol transferase activity was rate limiting step in MGGBQ biosynthesis. While for δ -tocotrienol biosynthesis activity and level of tocopherol cyclase was very critical. Glycerol resulted in a better carbon and energy source as compared to glucose during fermentation in fermenter in minimal medium. HGA and GGPP produced in chromosomal integrated strains were comparable to that produced using multi-copy plasmid.

By introducing extrachromosomal copy of *idi* and promoter exchange of the native *dxs* gene, it significantly increased the carbon flux towards the DXP pathway. This resulted in 2.4 times increase in MGGBQ amounts.

4.7. OUTLOOK

Reductase Activity

Purification of recombinant Ggh-*At* and /or Ggh-*Syn* proteins has to be carried out. This will enable to perform the *in-vitro* reaction with GGPP in presence of the purified recombinant Ggh-*At* and / or Ggh-*Syn* proteins. Once the activity of Ggh-*At* and/or Ggh-*Syn* is shown successfully, then *in-vivo* biosynthesis of PPP in recombinant *E. coli* can be performed. The results of this *in-vivo* biosynthesis would find out the real problem and confirm one of the possible hypothesis/explanations given in this study.

Transferase Activity (Hpt)

Hpt-*At* enzyme which shows substrate specificity towards PPP only, has to be expressed, verified in recombinant *E. coli*. Expression levels of Hpt-*At* into recombinant *E. coli* is relatively low (Sadre 2006). In order to increase the expression level, use of either a GST or MAL or STREP Tagged fusion protein is recommended. Once, reductase activity is shown, only then it would be possible to show the transferase activity (*in-vivo*) for Hpt-*At* enzyme. Study on *in-vivo* biosynthesis of MPBQ is only possible with an active reductase and an active transferase especially Hpt-*At*.

Transferase Activity (HggT)

In order to increase tocotrienol yields one important factor would be to increase the pool of MGGBQ available for the cyclase (Cyc) and / or the two different methyltransferases (MPBQ-MT and γ -TMT). Experiments in section 3.4 showed that Hpt is the rate limiting step in MGGBQ production. Hence, a transferase should be used which is specific to GGPP instead of PPP and GGPP both (same as in the existing plasmid pCAS29, *hpt* from *Synechocystis PCC6803*). Homogentisic acid geranylgeranyl transferase (*hggT*) gene from Barley or Wheat or Rice seeds must be cloned and used for MGGBQ production. HggT from Barley (HggT-Barley) when overexpressed in *Arabidopsis thaliana* resulted in production of tocotrienol with 10 fold increase in total vitamin E contents. Overexpression of barley HggT-barley in corn seeds resulted in tocopherol and tocotrienol content by 6 fold (Cahoon et. al. 2003).

Cyclase Activity

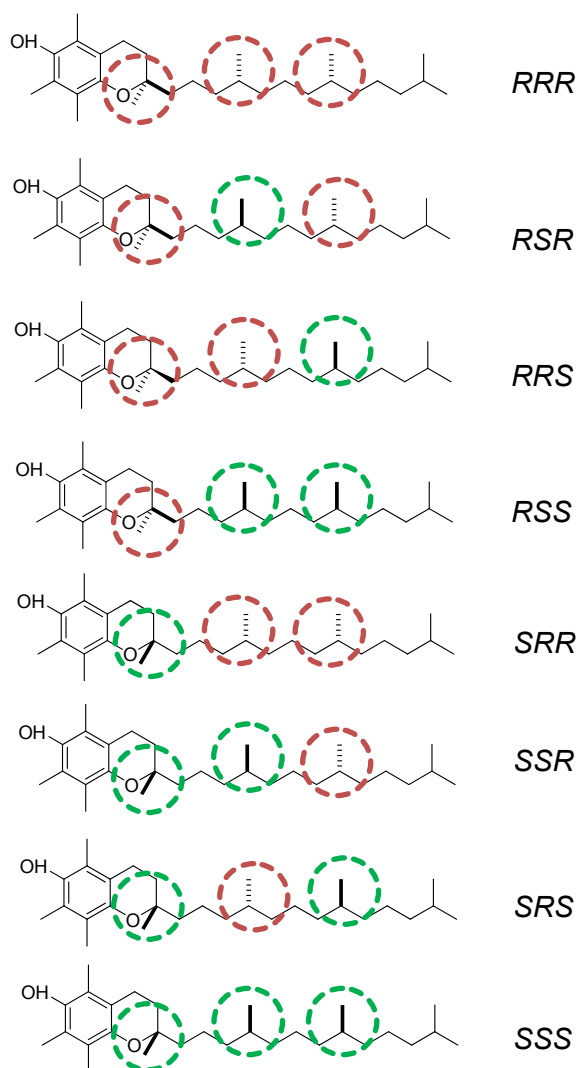
Instead of increasing the pool of available MGGBQ to increase tocotrienol formation, one method would be to study the cyclase activity itself. New cyclase genes from palm fruits or wheat seeds should be cloned and studied for its cyclase activity since these natural food sources exclusively produces tocotrienol in large quantities.

Purification of the His-Tag Vte1 and / or GST-Tag Vte1 protein should be performed to solve the crystal structure. This structure would help in understanding the enzymatic reaction mechanism and the active site of cyclase enzyme.

Heterologous biosynthesis of different Vitamin E derivatives

To obtain all the 4 forms of tocotrienols and 4 forms of tocopherols in recombinant *E. coli* strain, cloning of further vitamin E biosynthesis genes is suggested. The 2 methyltransferases, i.e. gene *slf0418* encoding MPBQ-MT enzyme and gene *slr0089* encoding γ -TMT has to be cloned. After over-expression in recombinant *E. coli* is tested, enzyme activity can be tested easily by using plasmid-free strain *E. coli* CS6 or *E. coli* CS7 (as host strains) along with the newly constructed plasmids.

APPENDIX

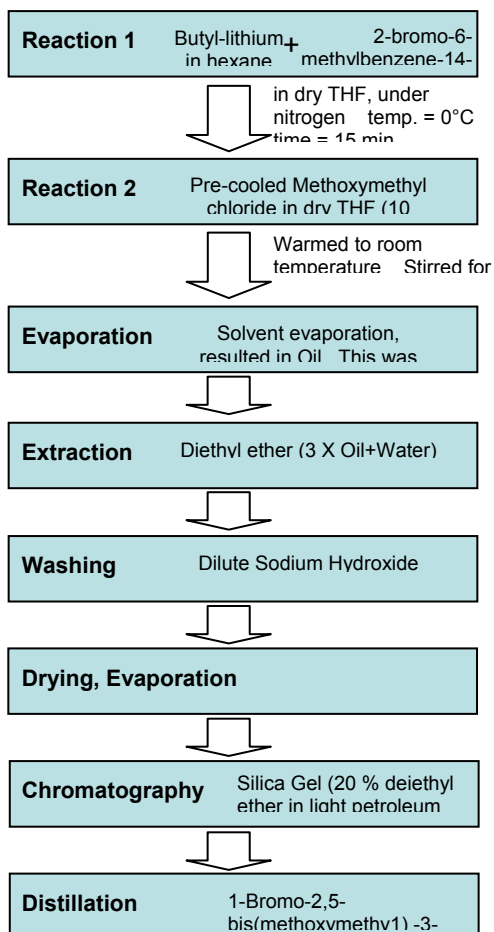


Appendix A 1-1: Chemical structure of 8 different stereoisomers obtained during chemical synthesis of α -tocopherol resulting in a racemic mixture (Source: BASF).

Appendix A1-2 (a) & (b): Chemical Synthesis of MGGBQ (reduced) MGGBQ (oxidized) (Begley et.al. 1990).

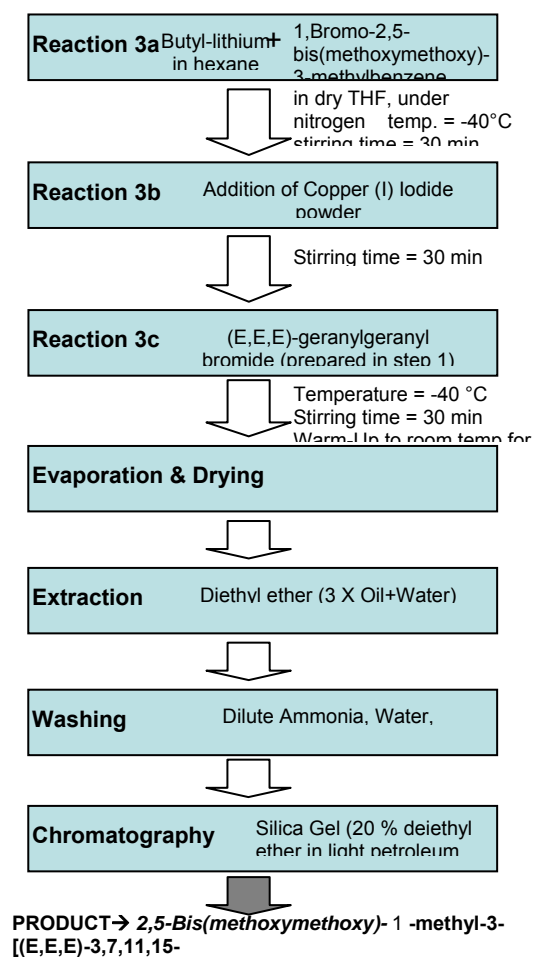
(a)

Step 2: 81 % Yield



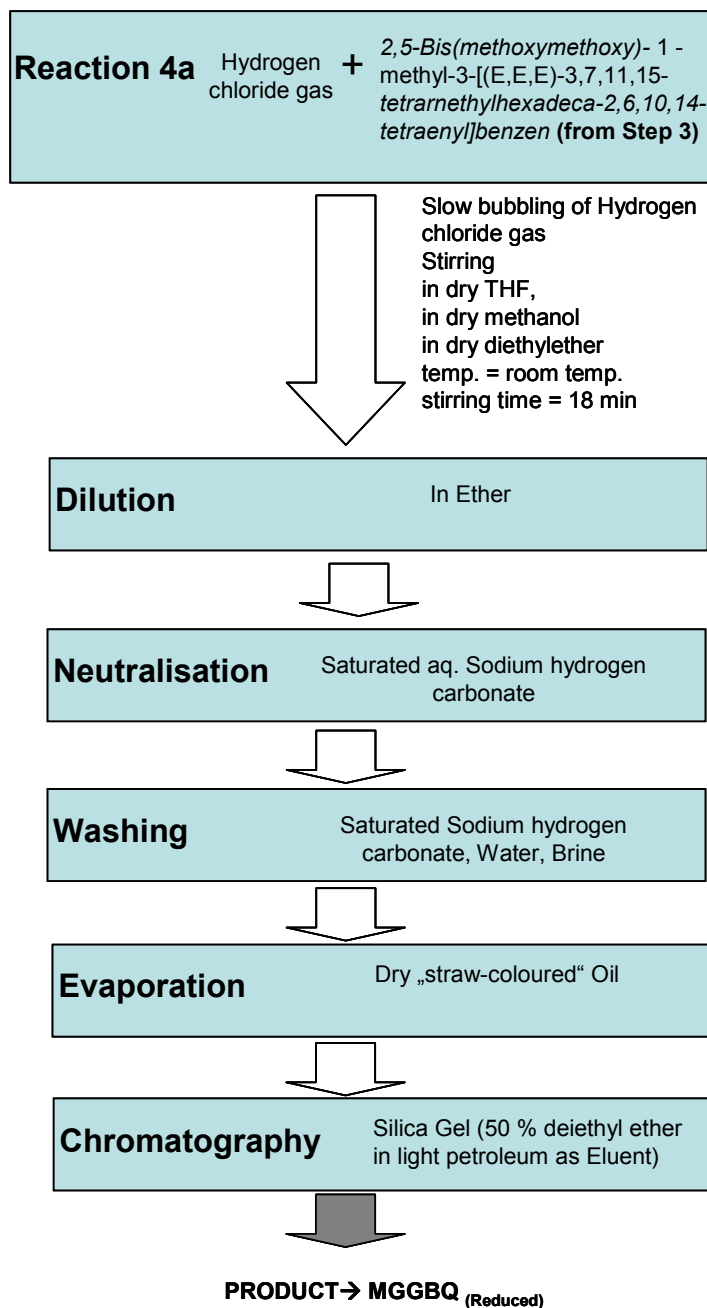
(b)

Step 3: 58 % Yield



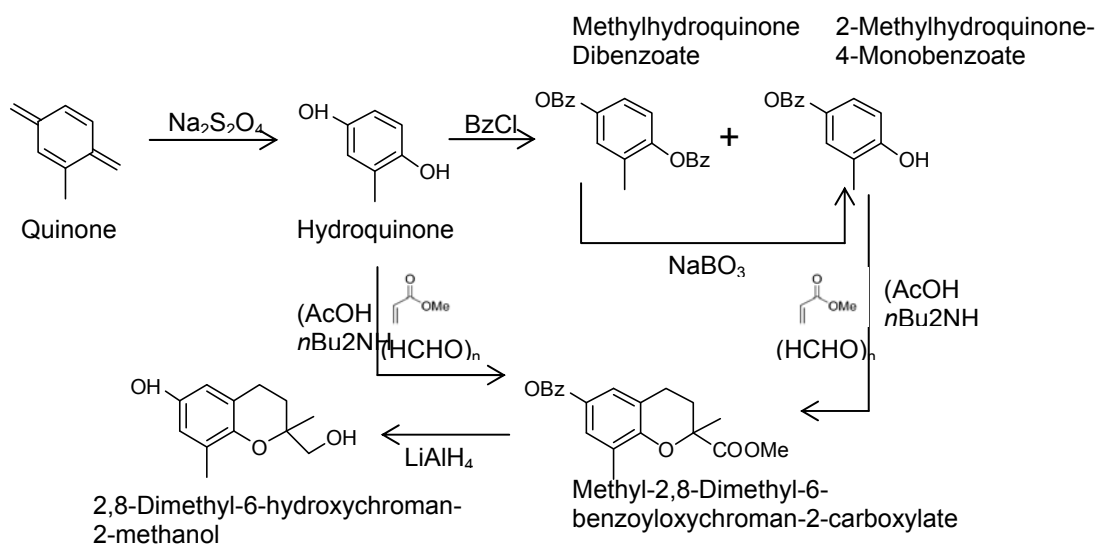
Appendix A1-2 (c): Chemical Synthesis of MGGBQ (reduced) MGGBQ (oxidized)

Step 4:



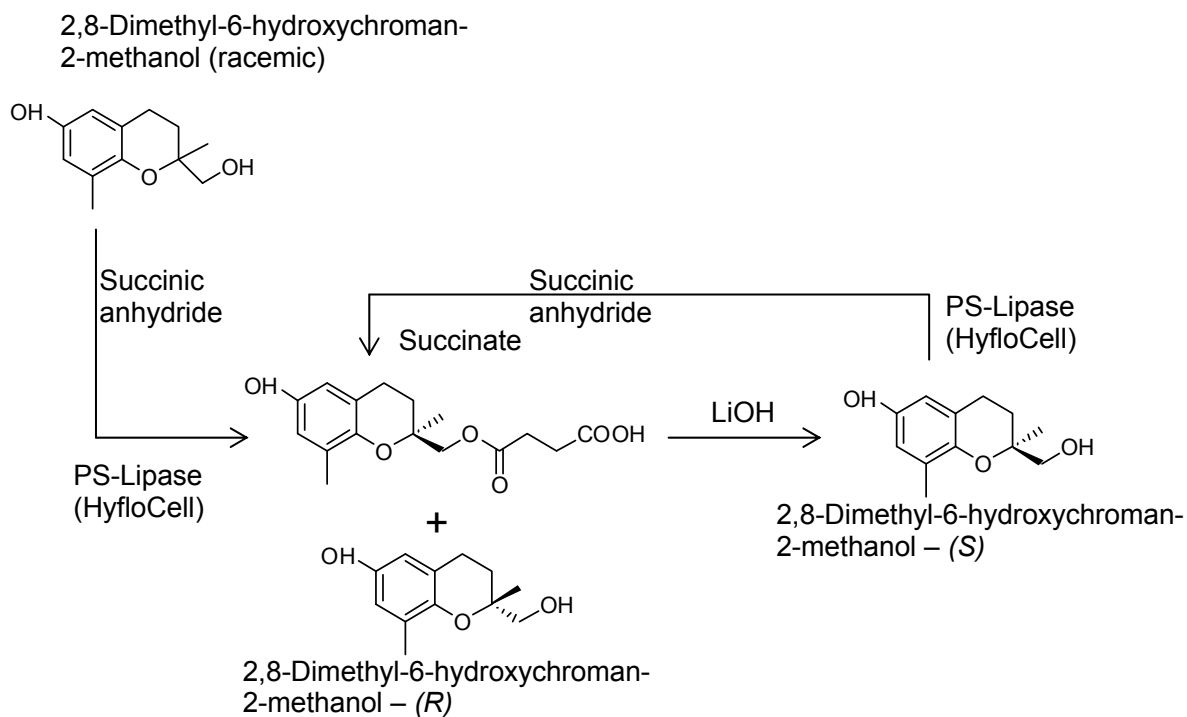
Appendix A1-3 (a) - (c)

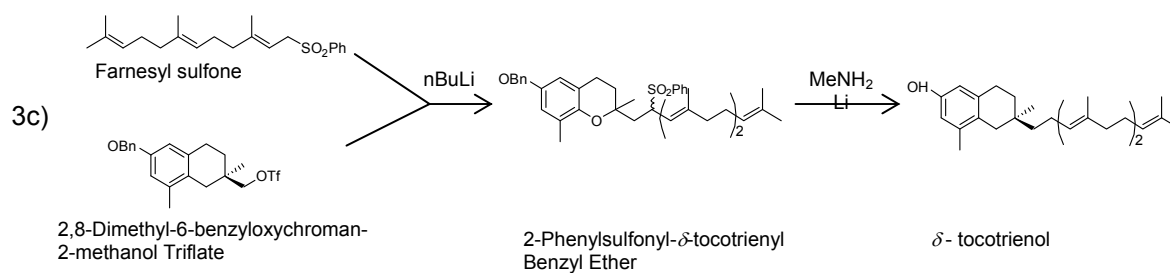
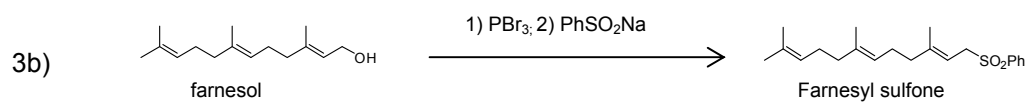
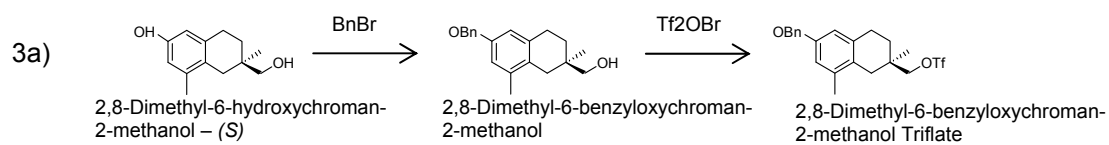
(a) Step 1: Synthesis of building block „Chromanmethanol“



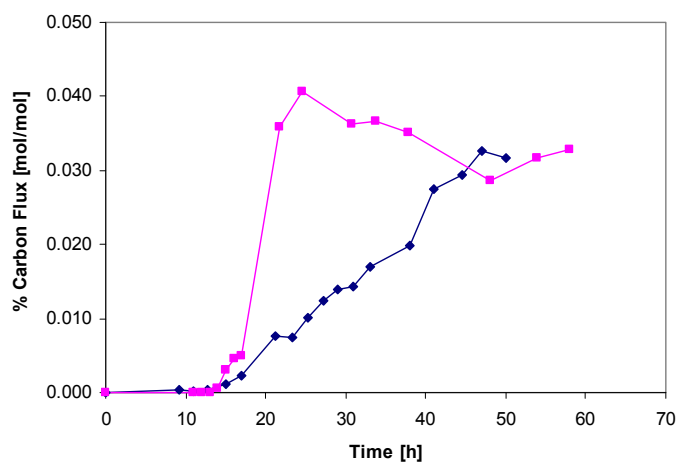
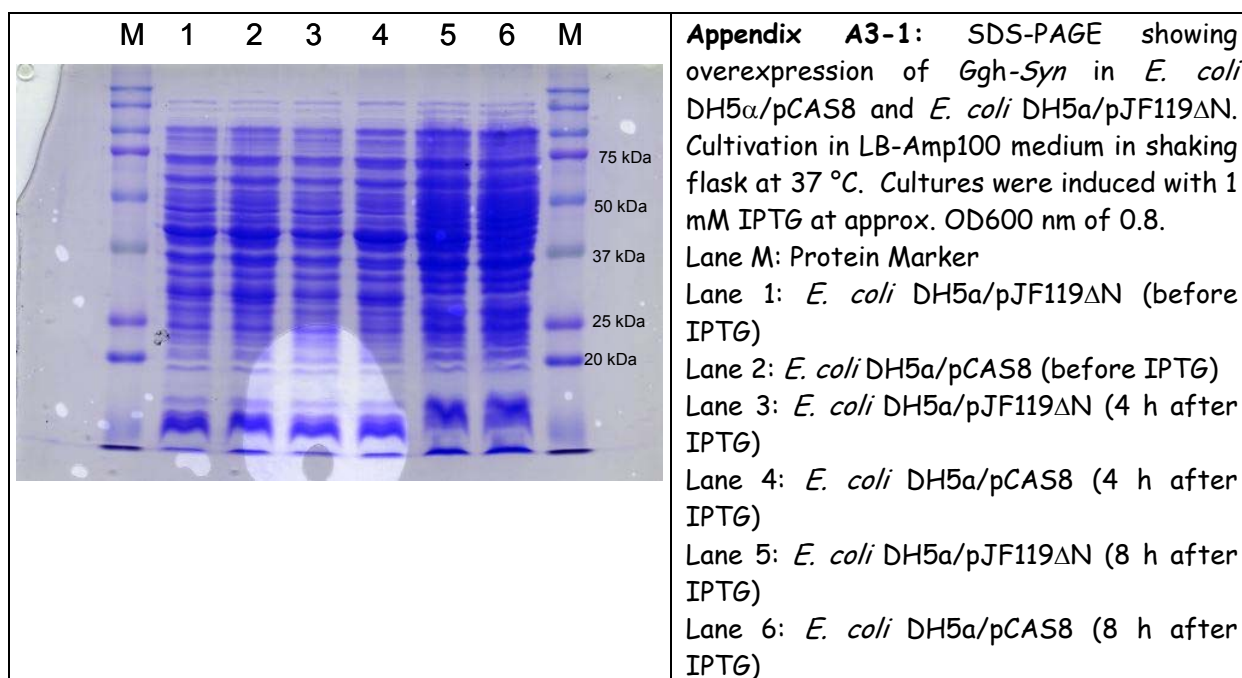
BzCl: benzoyl chloride

(b) Step 2: Resolution of Chromanmethanols



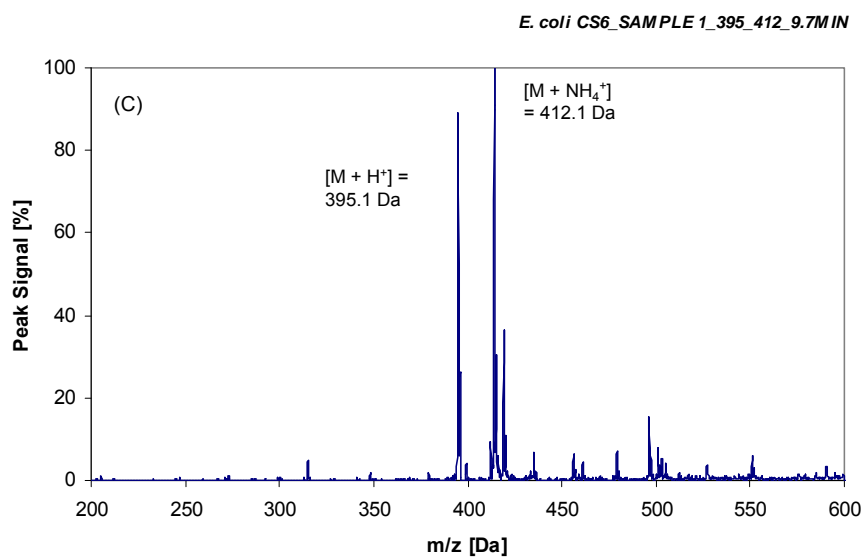
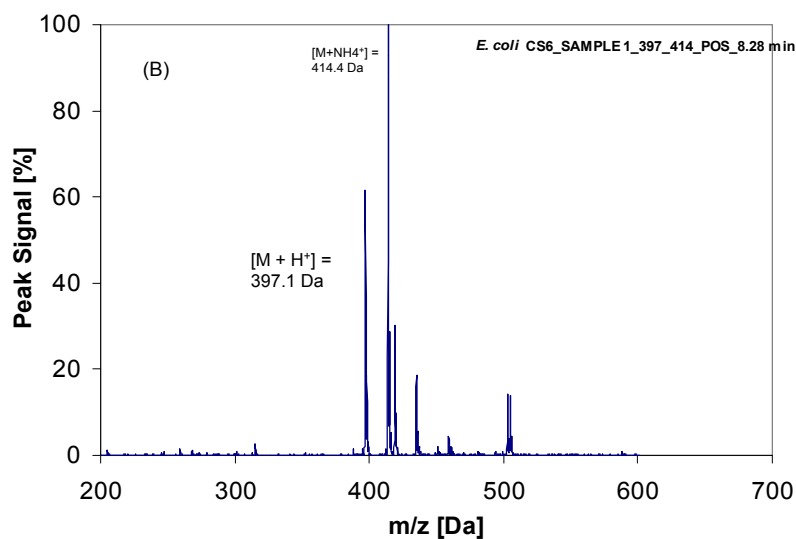
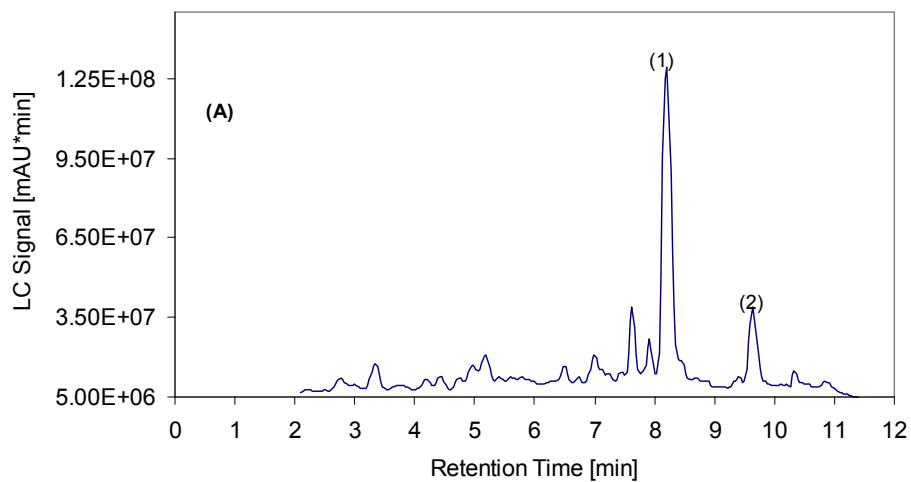
(c) Step 3: Synthesis of δ -tocotrienol

Appendix for Chapter 3



Appendix A3-2: Carbon flux (carbon mole in MGGQBQ per carbon mole fed) calculated in %, during bioreactor cultivation of *E. coli* CS6 strain in MM-Glucose and MM-Glycerol at 30 °C.

Appendix A3-3: LC-MS chromatogram. LC-MS chromatogram of *E. coli* CS6 (MM-Glucose) produced in Bioreactor cultivation.



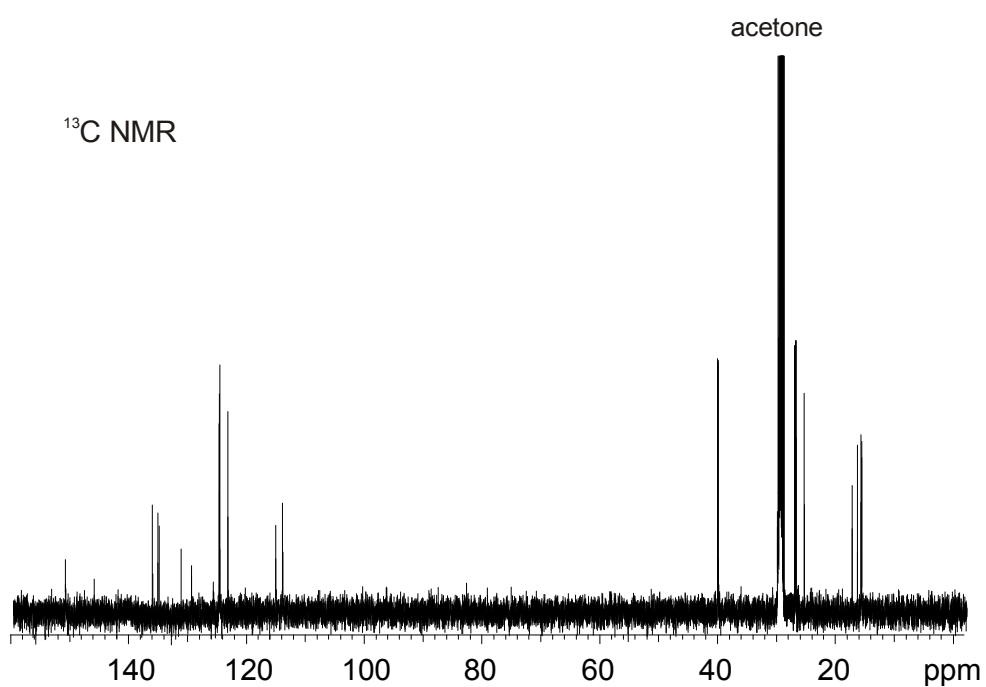
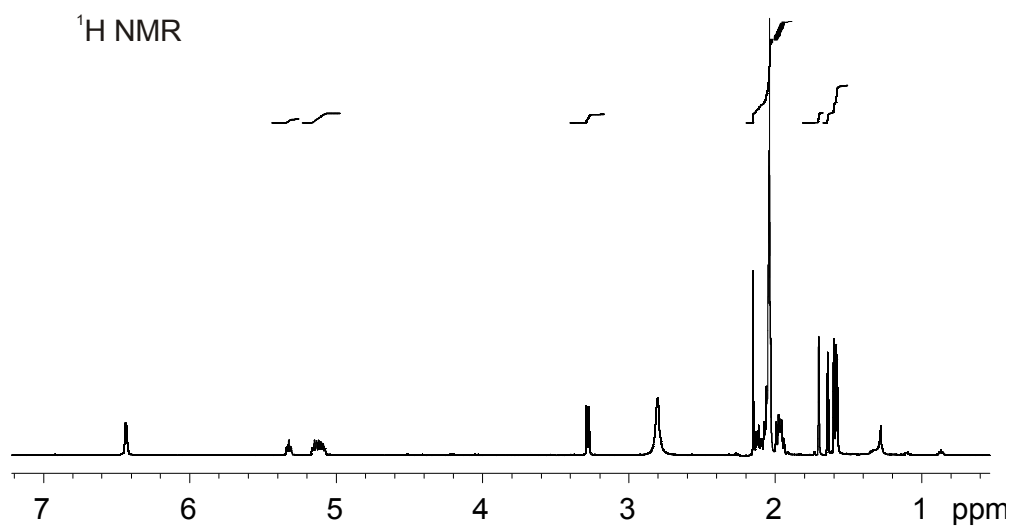
Appendix A3-4: NMR Results

^1H NMR performed on purified sample (in presence of ascorbic acid) resulted in the following chemical shifts (δ):

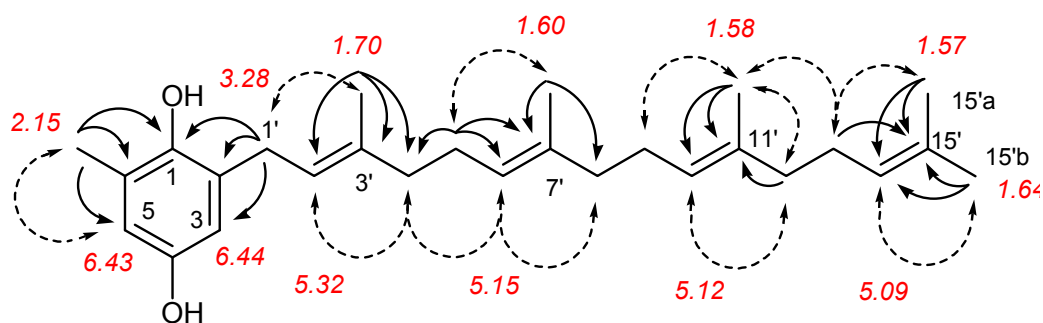
^1H NMR (500 MHz, δ in ppm): δ 6.44 (bd, $J = 2.9$ Hz, 1H, H-3), 6.43 (bd, $J = 2.8$ Hz, 1H, H-5), 5.32 (bd, $J = 7.3$ Hz, 1H, H-2'), 5.15 (bt, $J = 7.3$ Hz, 1H, H-6'), 5.12 (bt, $J = 7.8$ Hz, 1H, H-10'), 5.09 (bt, $J = 7.8$ Hz, 1H, H-14'), 3.28 (d, $J = 7.3$ Hz, 2H, H-1'), 2.15 (s, 3H, CH₃-6), 2.12 (ov, 2H, H-5'), 2.07 (ov, 2H, H-9'), 2.05 (ov, 2H, H-13'), 2.04 (ov, 2H, H-4'), 1.98 (ov, 2H, H-8'), 1.96 (ov, 2H, H-12'), 1.70 (s, 3H, CH₃-3'), 1.64 (s, 3H, CH₃-15b'), 1.60 (s, 3H, CH₃-7'), 1.58 (s, 3H, CH₃-11'), 1.57 (s, 3H, CH₃-15a'); ov = signals partially overlapped.

^{13}C NMR performed on purified sample resulted in the following chemical shifts (δ):

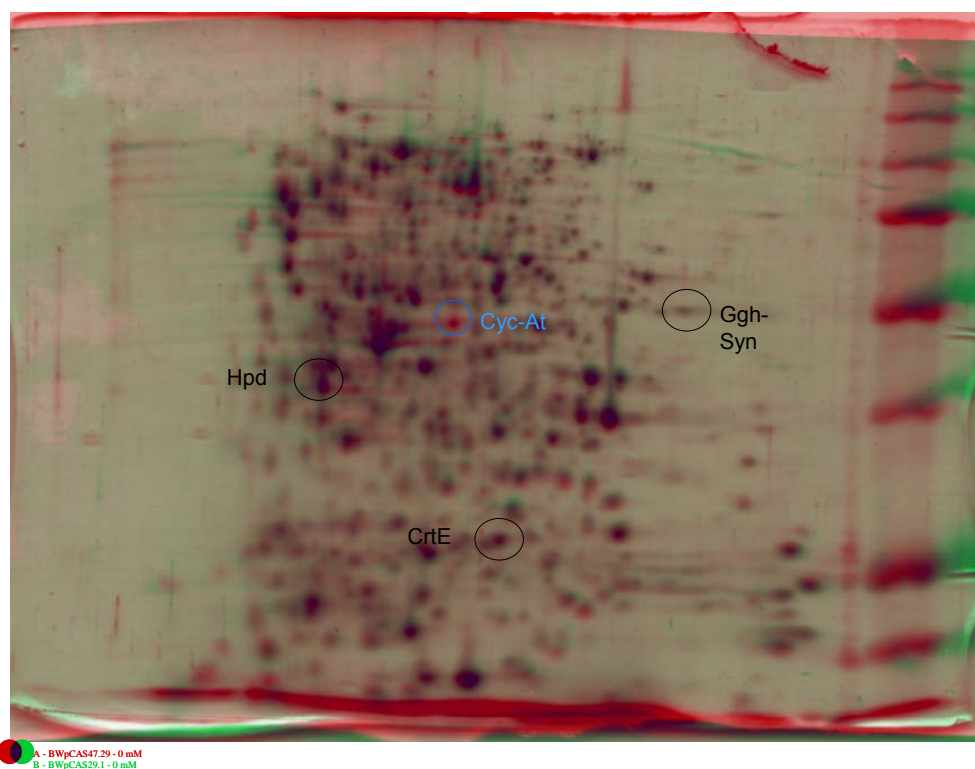
^{13}C NMR (125 MHz, δ in ppm): δ 151.29 (C-4), 146.50 (C-1), 136.41 (C-3'), 135.58 (C-7'), 135.38 (C-11'), 131.58 (C-15'), 129.86 (C-2), 126.15 (C-6), 125.16 (C-14'), 125.10 (C-10'), 125.03 (C-6'), 123.64 (C-2'), 115.45 (C-5), 114.36 (C-3), 40.52 (C-4'), 40.43 (C-12'), 40.39 (C-8'), 29.32 (C-1'), 27.44 (C-13'), 27.35 (C-5'), 27.25 (C-9'), 25.80 (CH₃-15b'), 17.68 (CH₃-15a'), 16.79 (CH₃-6), 16.19 (CH₃-3'), 16.06 (CH₃-7'), 16.03 (CH₃-11').



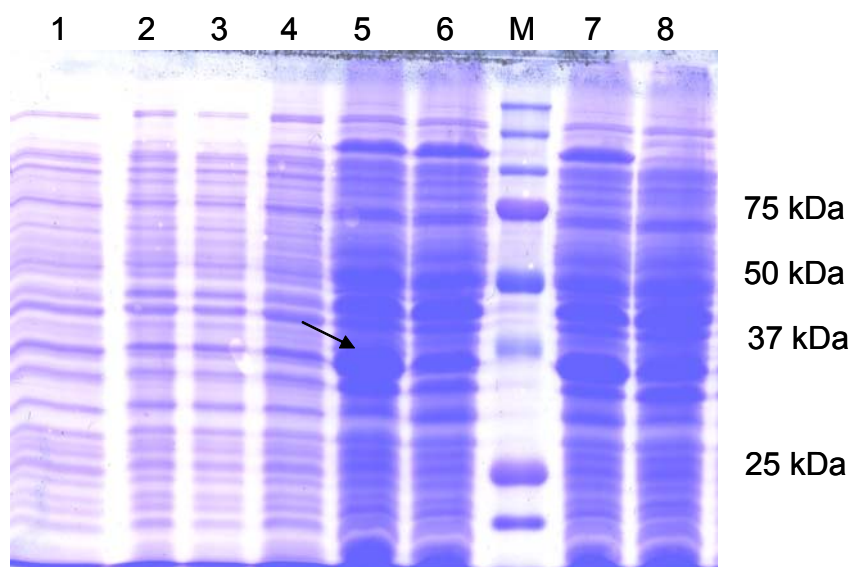
Appendix A3-5: NMR Spectrum of proposed MGGBQ structure in acetone- d_6 (500 and 125 MHz). A) ^1H NMR spectrum and B) ^{13}C NMR spectrum



Appendix A3-6:ROESY (←---→) and HMBC correlations (—→) of the proposed MGGGBQ structure. Selected ¹H chemical shifts are given in red.

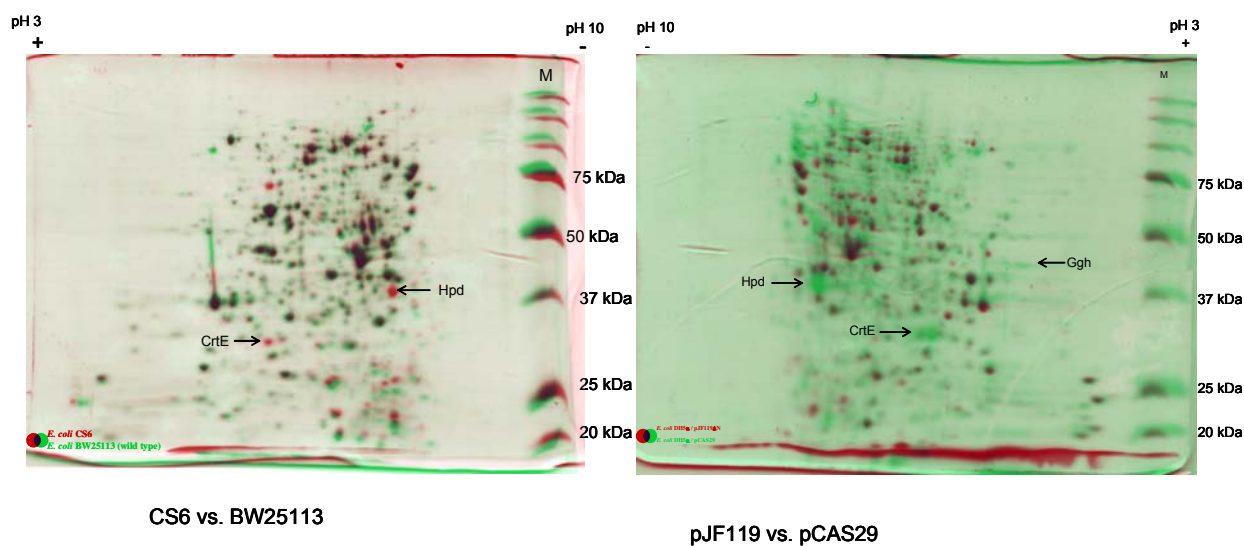


Appendix A3-7: 2 D gel electrophoresis. In green is the *E. coli* BW25113/pCAS29 sample and in red is the *E. coli* BW25113/pCAS47 sample. Both cultures are uninduced. Samples used for loading the gels were taken 8 h after inoculation. Cultivation was carried out in shaking flask, LB+Glycerol+Amp100 at 30 °C. The picture below shows the two overlapped gels.

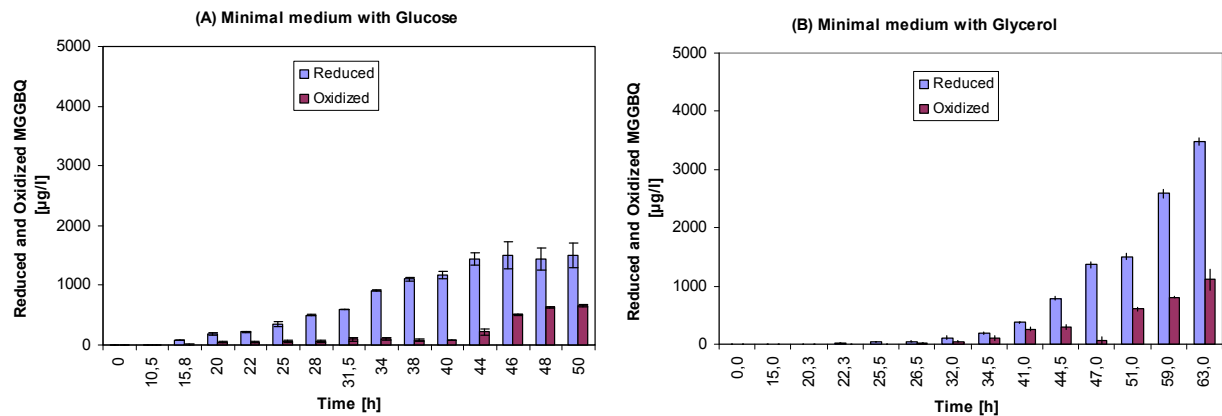


Appendix A3-8: SDS-PAGE showing over-expression of Hpd and CrtE in chromosomally integrated strains.

1 - <i>E. coli</i> LJ110 (CS1) w/o IPTG induction	5 - <i>E. coli</i> LJ110 (CS1) after IPTG induction
2 - <i>E. coli</i> LJ110 (CS2.1) w/o IPTG induction	6 - <i>E. coli</i> LJ110 (CS2.1) after IPTG induction
3 - <i>E. coli</i> LJ110 (CS2.2) w/o IPTG induction	7 - <i>E. coli</i> LJ110 (CS2.2) after IPTG induction
4 - <i>E. coli</i> LJ110 (WT) w/o IPTG induction	8 - <i>E. coli</i> LJ110 (WT) after IPTG induction

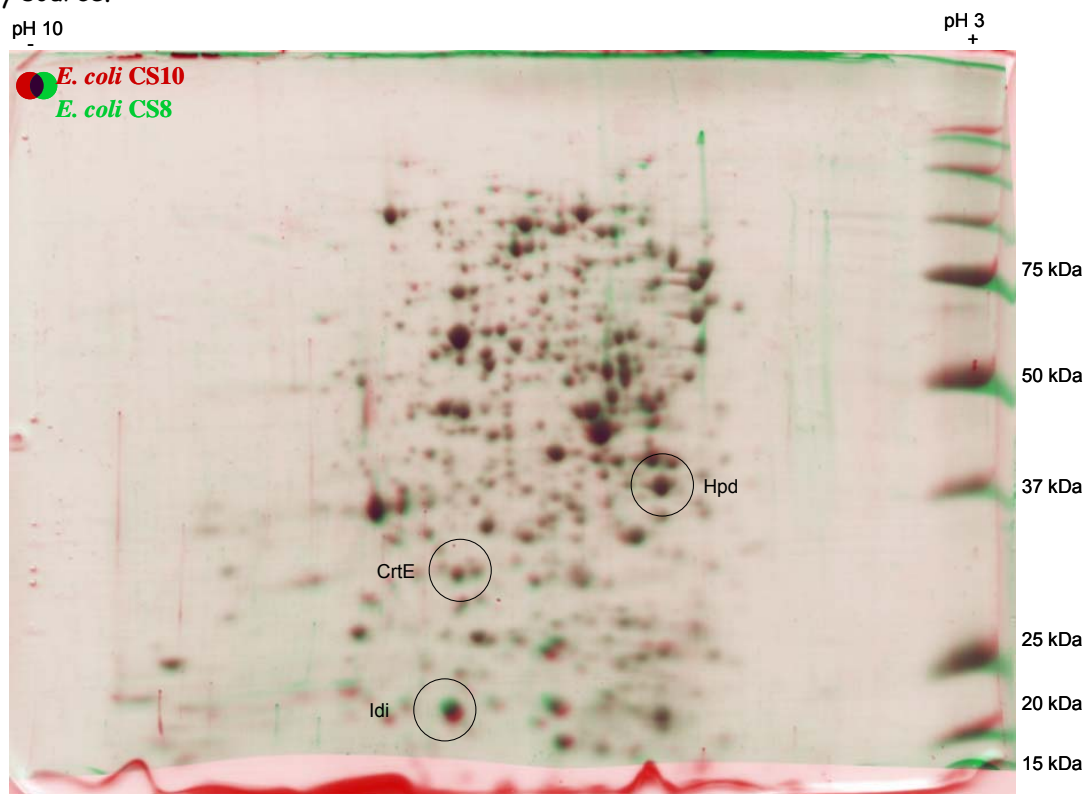


Appendix A3-9: Comparison of 2D-gel electrophoresis results of *E. coli* CS6 (on left side) and *E. coli* BW25113/pCAS29 (on right side). The gel representing *E. coli* CS6 is compared with wild type *E. coli* BW25113 and the one representing *E. coli* BW25113/pCAS29 is compared with *E. coli* BW25113/pJF119 Δ N.



Appendix A3-10: Concentration of MGGBQ (reduced and oxidized) in *E. coli* BW25113/pCAS29 in fermenter.

Concentration of MGGBQ (reduced and oxidized) produced during cultivation of *E. coli* BW25113/pCAS29 in fermenter using glucose (fig. A) and glycerol (fig. B) as sole carbon and energy source.



Appendix A3-11: 2D gel electrophoresis of *E. coli* CS10 and *E. coli* CS8 overlapped. *E. coli* CS8 and *E. coli* CS10 were cultivated in LB medium in shaking flask at 30 °C. Cultures were induced with 0.25 mM IPTG at OD_{600nm} of 0.8. 12 h after induction of each sample was analysed by 2D gel electrophoresis. The difference between the two strains is the *E. coli* CS10 carrying an additional T₅-promoter instead of native promoter for *dxs* gene. Three proteins Hpd, CrE and Idi marked with black rings were expressed and detected in both strains. Hpd being a membrane bound protein was not detected in both samples. Hpd has an expected molecular mass of Hpd 34.4 kDa and pI of 9.02. Dxs protein was expected in *E. coli* CS10 strain and absent in *E. coli* CS8 strain. No additional protein spot in red colour (i.e. *E. coli* CS10) was detected at the expected size of 69.2 kDa and pI value of 6.09. Neither any additional spot in this area was seen in *E. coli* CS8 strain.

Acknowledgements

I would like to express my deepest regards to my supervisor Prof. Dr. Georg A. Sprenger, for giving me the opportunity to work on this scientific problem for my doctoral thesis. First of all, I want to sincerely thank him for his patience and faith he has shown in me throughout these years. I thank him for his guidance and new ideas he provided me during the experimental work. I appreciate his time (especially the holiday times) and efforts he invested in reading this thesis and manuscript.

I would like to thank Prof. Vlada Urlacher, for be willing to write the second review of my thesis.

My biggest acknowledgement goes to Dr. Christoph Albermann. Without him, I would have not been writing this acknowledgment. He introduced me to the world of molecular biology and inspired me to work on Recombinant *Escherichia coli*. He taught me the different techniques used in a molecular biology laboratory. Whenever I had a question or an unsolved problem, his doors were always open for discussion. I always went back from his office with thought provoking ideas, which started the ball rolling again. He provided me with many plasmids which I used in this study.

I wish to thank the DFG for sponsoring the SFB706 –B3 project and the other cooperation partners. I would specially thank Dr. Karin Lemuth, Dipl. Ing. Tobias Vallon & Dipl. Ing. Alexander Müller, from the Institute for Bioprocess Engineering, for performing fermentation for GGPP production and for developing a novel GC-MS method for GGPP analysis.

I deeply thank Dr. Wolfgang Armbruster from Universität Hohenheim for performing the LC-MS analysis on the MGGBQ and δ -tocotrienol samples. I thank Dr. Jürgen Conrad from Universität Hohenheim for giving us important suggestions in preparing the MGGBQ sample for NMR analysis. I thank you for doing the NMR test and elucidation of the chemical structure of MGGBQ.

I would like to thank my Lab. 3 colleagues Dr. Anne Samland and Dr. Sarah Schneider for there cooperation in laboratory duties. Special thank goes to Dr. Natalie Trachtmann for providing me lots of primers, and showing me the preparation of 2D Gel Electrophoresis. I would like to thank my other colleagues, at the institute for there support throughtout my stay.

I would like to thank my parents and my sister who always send blessings from India so that I finish my work sometime soon. Last, but not least I thank my dear wife Aisha for the

tremendous contribution in terms of time, patience and for bearing with me when I was annoyed. She sacrificed a lot during these years and made sure that I have enough time for my experiments and work. It is because of her and our son Aman that I am seeing the end to the tunnel. I should also acknowledge Aman, who was a great source of motivation to finish this thesis, as he missed his papa every evening.

References

- Albermann, C., Ghanegaonkar, S., Lemuth, K., Vallon, T., Reuss, M., Armbruster, W., Sprenger, G.A.** (2008). Biosynthesis of the Vitamin E Compound δ -Tocotrienol in Recombinant *Escherichia coli* Cells. *Chem. Bio. Chem.* 9, 2524-2533.
- Albermann, C., Trachtmann, N., Sprenger, G.A.** (2010). A simple and reliable method to conduct and monitor expression cassette integration into the *Escherichia coli* chromosome. *Biotechnology Journal* 5, 32-38.
- Aggrawal, B.B., Sundaram, C., Prasad, S., Kannappan, R.** (2010). Tocotrienols, the vitamin E of the 21st century: Its potential against cancer and other chronic diseases. *Biochemical Pharmacology* 80, 1613 – 1631.
- Arias-Barrau, E., Olivera, E. R., Luengo, J. M., Fernández, C., Galán, B., García, J. L., Díaz, E., Minámbres, B.** (2004). The Homogentisate Pathway: a Central Catabolic Pathway Involved in the Degradation of L-Phenylalanine, L-Tyrosine, and 3-Hydroxyphenylacetate in *Pseudomonas putida*, *Journal of Bacteriology* 186 (15), 5062–5077
- Awata, H., Endo, F., Mastuda, I.** (1994). Structure of the Human 4-Hydroxyphenylpyruvic Acid Dioxygenase Gene (HPD), *Genomics*, 23, 534-539.
- Arora, K., Pedersen, P.L.** (1995). Glucokinase of *Escherichia coli*: Induction in Response to the stress of Overexpressing Foreign Proteins. *Archives of Biochemistry and Biophysics* 319 (2), 574-578.
- Austin, J.R.II., Frost, E., Vidi, P., Kessler, F., Staehelin, L.A.** (2006). Plastoglobules are lipoprotein subcompartments of the chloroplast that are permanently coupled to thylakoid membranes and contain biosynthetic enzymes. *Plant Cell* 18, 1693–1703.
- Azzi, A., Stocker, A.** (2000). Vitamin E: non-antioxidant roles. *Progress in Lipid Research* 39, 231-255.
- Azzi, A.** (2007). Molecular mechanism of alpha-tocopherol action. *Free Radical Biology and Medicine* 43, 16-21.

Bachmann, B.J. (1972). Pedigrees of some mutant strains of *Escherichia coli* K-12. *Microbiology and Molecular Biology Reviews* 36, 525-557.

Baba, T., Muth, J., Allen, C.M. (1985). Photoaffinity labeling of undecaprenyl pyrophosphate synthetase with a farnesyl pyrophosphate analogue. *Journal of Biological Chemistry* 260, 10467–10473.

Baba, T., Ara, T., Hasegawa, M., Takai, Y., Okumura, Y., Baba, M., Datsenko, K.A., Tomita, M., Wanner, B.L., Mori, H. (2006). Construction of *Escherichia coli* K-12 in frame, single-gene knockout mutants: the Keio collection. *Molecular Systems Biology* 2006 doi:10.1038/msb4100050

Blattner, F.R., Plunkett, III. G., Bloch, C.A., Perna, N.T., Burland, V., Riley, M., Collado-Vides, J., Glasner, J.D., Rode, C.K., Mayhew, G. F., Gregor, J., Davis, N. W., Kirkpatrick, H.A., Goeden, M.A., Rose, D. J., Mau, B., Shao, Y. (1997). The Complete Genome Sequence of *Escherichia coli* K-12. *Science* 277 (5331), 1453-1462.

Begley, M. J., Fish, P. V., Pattenden G., (1990). Synthesis of Marine Toxins. A Biomimetic Approach to the Novel Spirobenzoquinonefuran Stypoldione. *Journal of the Chemical Society, Perkin Transactions 1*, 2263-2271.

Bongaerts, J., Krämer, M., Müller, U., Raeven, L., Wubbolts, M. (2001). Metabolic Engineering for Microbial Production of Aromatic Amino Acids and Derived Compounds. *Metabolic Engineering* 3, 289-300.

Bradley, F. C., Lindstedtj, S., Lipscombq, J. D., Que, L. Jr., Roe, A. L., Rundgrenj, M. (1986). 4-Hydroxyphenylpyruvate Dioxygenase Is an Iron-Tyrosinate Protein. *The Journal of Biological Chemistry* 261 (25), 11693-11696.

Bradford, M.M. (1976). Rapid and Sensitive Method for Quantitation of Microgram Quantities of Protein Utilizing Principle of Protein-Dye Binding. *Analytical Biochemistry* 72, 248-254.

Brownlee, J., He, P., Moran, G. R., Harrison, D. H. T. (2008) Two Roads Diverged: The Structure of Hydroxymandelate Synthase from *Amycolatopsis orientalis* in Complex with 4-Hydroxymandelate. *Biochemistry* 47 (7), 2002-2013.

Brigelius-Flohé, R. Traber, M.G. (1999). Vitamin E: function and metabolism. *The Journal of the Federation of American Societies for Experimental Biology (FASEB)* 13, 1145-1155.

Brigelius-Flohé, R., Kelly, F.J., Salonen, J.T., Neuzil, J., Zingg, J.M., Azzi, A. (2002). The European perspective on vitamin E: current knowledge and future research. *The American Journal of Clinical Nutrition* 76; 703-716.

Brigelius-Flohé, R. (2006). The Bioactivity of vitamin E: Research Reviews. *Nutrition* 19, 174–186.

Brownlee, J.M., Johnson-Winters, K., Harrison, D.H., Moran, M.R. (2004). Structure of the ferrous form of (4-hydroxyphenyl) pyruvate dioxygenase from *Streptomyces avermitilis* in complex with the therapeutic herbicide. *Biochemistry* 43, 6370–6377.

Cahoon, E.B., Hall, S.E., Ripp, K.G., Ganzke, T.S., Hitz, W.D., Coughlan, S. J. (2003). Metabolic redesign of vitamin E biosynthesis in plants for tocotrienol production and increased antioxidant content. *Nature Biotechnology* 21 (9), 1082-1087.

Cahoon, E.B., Shockley, J.M., Dietrich, C.R., Gidda, S.K., Mullen, R.T., Dyer, J.M. (2007). Engineering oilseeds for sustainable production of industrial and nutritional feedstocks: solving bottlenecks in fatty acid flux. *Current Opinion in Biotechnology* 10, 236–244.

Caretto, S., Speth, E.B., Fachechi, C., Rala, R., Zacheo, G, Giovianazzo, G. (2004). Enhancement of vitamin E production in sunflower cell cultures. *Plant Cell Rep.* 23, 174-179.

Causey, T. B., Zhou, S., Shanmugam, K. T., Ingram, L. O. (2003). Engineering the metabolism of *Escherichia coli* W3110 for the conversion of sugar to redox-neutral and oxidized products: Homoacetate production. *Proceedings of the National Academy of Sciences of the United States of America* 100 (3), 825-832.

Chen, S., Li, H., Liu, G. (2006). Progress of vitamin E metabolic engineering in plants. *Transgenic Research* 15, 655-665.

Cheng, Z., Sattler, S., Maeda, H., Sakuragi, Y., Bryant, D.A., DellaPenna, D. (2003). Highly divergent methyltransferases catalyze a conserved reaction in tocopherol and plastoquinone synthesis in cyanobacteria and photosynthetic eukaryotes, *Plant Cell* 15, 2343–2356.

Cherepanov, P.P., Wackernagel, W. (1995). Gene disruption in *Escherichia coli*: TcR and Km^R cassettes with the option of Flp-catalyzed excision of the antibiotic-resistance determinant. *Gene*, 158, 9-14.

Chênevert, R., Courchesne, G., Pelchat, N. (2006). Chemoenzymatic synthesis of both enantiomers of α -tocotrienol. *Bioorganic & Medicinal Chemistry*, 14, 5389-5396.

Ching, L.S., Mohamed, S. (2001). Alpha-Tocopherol Content in 62 Edible Tropical Plants. *Journal of Agricultural and Food Chemistry* 49, 3101-3105.

Collakova, E., DellaPenna, D. (2001). Isolation and Functional Analysis of Homogentisate Phytoltransferase from *Synechocystis* sp. PCC 6803 and *Arabidopsis*. *Plant Physiology* 127, 1113–1124.

Collakova, E., DellaPenna, D. (2003). Homogentisate phytoltransferase activity is limiting for tocopherol biosynthesis in *Arabidopsis*. *Plant Physiology* 131 (2), 632-642.

Couladouros, E.A., Pápas, A.M., Moutsos, V.I., Lampropoulou, M. (2004). Chemical synthesis of δ -tocotrienol from 2-vinylchromane compound. *Patent US7038067 B2*, 1-14.

Comitato, R., Nesaretnam, K., Leoni, G., Ambra, R., Canali, R., Bolli, A., Marino, M., Virgili, F. (2009). A novel mechanism of natural vitamin E tocotrienol activity: involvement of Er β signal transduction. *American Journal of Physiology – Endocrinology and Metabolism* 297, 427-437.

Couladouros, E.A., Moutsos, V.I., Lampropoulou, M. Little, J.L., Hyatt, J.A. (2007). A short and convenient chemical route to optically pure 2-methyl Chromanmethanols. Total Asymmetric Synthesis of β -, γ -, and δ - Tocotrienols. (2007). *Journal of Organic Chemistry*, 72. 6735-6741.

Chun, J., Lee, J., Ye, L., Exler, J., Eitenmiller, R.R. (2006). Tocopherol and tocotrienol contents of raw and processed fruits and vegetables in the United States diet. *Journal of Food Composition and Analysis* 19, 196-204.

Chung, C.T., Niemela, S.L., Miller, R.H. (1989). One-step preparation of competent *Escherichia coli*: transformation and storage of bacterial cells in the same solution.

Proceedings of National Academy of Sciences of the United States of America 86 (7), 2172-2175.

Culioli, G., Ortalo-Magne', i.A, Valls, R., Hedio, C., Clare, A.S., Piovetti, L. (2008). Antifouling Activity of Meroditerpenoids from the Marine Brown Alga *Halidrys siliquosa*. *Journal of Natural Products* 71 (7), 1121 – 1126.

Das, S., Nesaretnam, K., Das, D. K. (2007). Tocotrienols in cardioprotection. *Vitamins and Hormones* 76, 419–433.

Das, S., Mukherjee, S., Lekli, I., Gurusamy, N., Bardhan, J., Raychoudhury, U., Chakravarty, R., Banerji, S., Knowlton, A.A., Das, D.K. (2012). Tocotrienols confer resistance to ischemia in hypercholesterolemic hearts: insight with genomics. *Molecular Cell Biochemistry* 360(1-2), 35-45.

Datsenko, K.A., and Wanner, B.L. (2000). One-step inactivation of chromosomal genes in *Escherichia coli* K-12 using PCR products. *Proceedings of the National Academy of Sciences of the United States of America* 97, 6640-6645.

Dähnhardt, D., Falk, J., Appel, J., van der Kooij, T.A.W., Schultz-Friedrich, R., Krupinska, K., (2002). The hydroxyphenylpyruvate dioxygenase from *Synechocystis* sp. PCC 6803 is not required for plastoquinone biosynthesis. *Federation of European Biochemical Societies Letters* 523, 177-181.

Darmon, N., Darmon, M., Ferguson, E. (2006). Identification of nutritionally adequate mixtures of vegetable oils by linear programming. *Journal of Human Nutrition and Dietetics* 19 (1), 59-69.

Dell, K.A., Frost, J.W. (1993). Frost, Identification and removal of impediments to biocatalytic synthesis of aromatics from D-glucose: rate-limiting enzymes in the common pathway of aromatic amino acid biosynthesis. *Journal of American Chemical Society* 115, 11581–11589.

DellaPenna, D. (2005). Progress in dissection of and manipulation of vitamin E synthesis. *Trends in Plant Science* 10 (12), 574-579.

- DellaPenna, D., Pogson, B.J.** (2006). Vitamin synthesis in plants: Tocopherols and Carotenoids. *Annual Review of Plant Biology. Annual Review on Plant and Biology* 57, 711–738.
- Denoya, C. D., Skinner, D. D., Morgenstern, M. R.** (1994). A *Streptomyces avermitilis* Gene Encoding a 4-Hydroxyphenylpyruvic Acid Dioxygenase-Like Protein That Directs the Production of Homogentisic Acid and an Ochronotic Pigment in *Escherichia coli*. *Journal of Bacteriology* 176 (17), 5312-5319.
- Drotleff, A., Ternes, W.** (1999). Cis/Trans isomers of Tocotrienols - occurrence and bioavailability. *European Food Research and Technology* 210, 1-8.
- Durfee, T., Nelson, R., Baldwin, S., Plunkett, III, G., Burland, V., Mau, B., Petrosino, J. F., Qin, X., Muzny, D.M., Ayele, M., Gibbs, R.A., Csörgő, B., Pósfai, G., Weinstock, G.M., Blattner, F.R.,** (2008) The Complete Genome Sequence of *Escherichia coli* DH10B: Insights into the Biology of a Laboratory Workhorse. *Journal of Bacteriology* 90(7), 2597-2606.
- Eisenreich, W., Schwarz, M., Cartayrade, A., Arigoni, D., Zenk, M.H., Bacher, A.** (1998). The deoxyxylulose phosphate pathway of terpenoid biosynthesis in plants and microorganisms. *Chemistry and Biology* 5(9), R221-233.
- Eitenmiller, R.R., Lee, J.** (2004). Vitamin E: Food Chemistry, Composition and Analysis. ISBN: 0-8247-0688-9, Marcel Dekker, New York.
- Falk, F., Brosch, M., Schafer, A., Braun, S., Krupinska, K.** (2005). Characterization of transplastomic tobacco plants with a plastid localized barley 4-hydroxyphenylpyruvate dioxygenase. *Journal of Plant Physiology* 162, 738-742.
- Fritze, I.M. Linden, L., Freigang, J., Auerbach, G., Huber, R., Steinbacher, S.** (2004). The Crystal Structures of *Zea mays* and *Arabidopsis* 4-Hydroxyphenylpyruvate Dioxygenase *Plant Physiology* 134, 1388–1400.
- Friehs, K.** (2004). Plasmid copy number and plasmid stability. *Advances in Biochemical Engineering and Biotechnology* 86, 47-82.
- Fountoulakis, M., Takacs, B.** (2000). Enrichment and Proteomic Analysis of Low-Abundance Bacterial Proteins. *Methods in Enzymology* 358, 288 – 306.

- Fujisaki, S., Nishino, T., Katsuki, H.** (1986) Isoprenoid synthesis in *Escherichia coli*. Separation and partial purification of four enzymes involved in the synthesis. *Journal of Biochemistry* 99, 1327–1337.
- Fürste, J.P., Pansegrau, W., Frank, R., Blöcker, H., Scholz, P., Bagdasarian, M., Lanka, E.** (1986). Molecular-Cloning of the Plasmid Rp4 Primase Region in a Multi-Host-Range Tacp Expression Vector. *Gene* 48, 119-131.
- Garcia, I., Rodgers, M., Pepin, R., Hsieh, T.F., Matringe, M.** (1999) Characterization and subcellular compartmentation of recombinant 4 hydroxyphenylpyruvate dioxygenase from *Arabidopsis* in transgenic tobacco. *Plant Physiology* 119, 1507-1516.
- Gerwick, W., Fenical, W.** (1981). Ichthyotoxic and Cytotoxic metabolites of the Tropical Brown Alga *Stypodium zonale* (Lamouroux) Papenfuss. *Journal of Organic Chemistry* 46 (1), 22-27.
- Gibson, M.I., Gibson, F.** (1964). Preliminary studies on the isolation and metabolism of an intermediate in aromatic biosynthesis: Chorismic acid. *Biochemistry Journal* 90, 248–256.
- Götz, A., Goebel, W.,** (2010). Glucose and glucose 6-phosphate as carbon sources in extra- and intracellular growth of enteroinvasive *Escherichia coli* and *Salmonella enterica*. *Microbiology* 156 (4), 1176-1187.
- Gömöry, J., Králik, M., Kaszonyi, A.** (2011). Towards the synthesis of (all-*rac*)- α -tocopherol from trimethylhydroquinone and isophytol at reduced pressure. *Acta Chimica Slovaca*, 4(1), 3-14.
- Gunsior, M., Ravel, J., Challis, G.L., Townsend, C.A.** (2004). Engineering phydroxyphenylpyruvate dioxygenase to a *p*-hydroxymandelate synthase and evidence for the proposed benzene oxide intermediate in homogentisate formation. *Biochemistry* 43 (3), 663-674.
- Hanahan, D.** (1983). Studies on transformation of *Escherichia coli* with plasmids. *Journal of Molecular Biology* 166, 557-580.
- Hansen, R., Eriksen, N.T.** (2007). Activity of recombinant GST in *Escherichia coli* grown on

glucose and glycerol. *Protein Biochemistry* 42, 1259-1263.

Hannig, G., Makrides, S.C. (1998). Strategies for optimizing heterologous protein expression in *Escherichia coli*. *Trends in Biotechnology (TIBTECH)* 16, 54-60.

Harker, M., Bramley, P.M. (1999). Expression of prokaryotic 1-deoxy-D-xylulose-5-phosphatases in *Escherichia coli* increases carotenoid and ubiquinone biosynthesis. *Federation of European Biochemical Society Letters* 448 (1), 115-119.

Hegedus, Z.L. (2000). The probable involvement of soluble and deposited melanins, their intermediates and the reactive oxygen side-products in human diseases and aging. *Toxicology* 145, 85–101.

Heller, K.B., Lin, E.C.C., Wilson, T.H. (1980). Substrate-Specificity and Transport-Properties of the Glycerol Facilitator of *Escherichia-coli*. *Journal of Bacteriology* 144, 274-278.

Hendrickson, W.A., Gottesman, M.E. (2000). Protein Folding and Unfolding by *E. coli* Chaperones and Chaperonins. *Current Opinion in Microbiology* 3, 197-202.

Hoppe, P.P. Krennrich, G. (2000). Bioavailability and potency of natural source and allracemic α -tocopherol in the human: a dispute. *European Journal of Nutrition* 39, 183-193.

Horvath, G., Wessjohann, L., Bigirimana, J., Jansen, M., Guisez, Y., Caubergs, R., Horemans, N. (2006). Differential distribution of tocopherols and tocotrienols in photosynthetic and non-photosynthetic tissues. *Phytochemistry* 1185–1195.

Hunter, W. (2007). The Non-Mevalonate Pathway of Isoprenoid Precursor Biosynthesis. *The Journal of Biological Chemistry* 28 (30), 21573-21577.

Johnson-Winters, K., Purpero, V.P., Kavana, M., Nelson, T., Moran, G.R. (2003). 4-Hydroxyphenyl pyruvate Dioxygenase from *Streptomyces avermitilis*: The Basis for Ordered Substrate Addition. *Biochemistry* 42, 2072-2080.

Jones, K.L., Kim, S.W., Keasling, J.D. (2000). Low-Copy Plasmids can Perform as Well as or Better Than High-Copy Plasmids for Metabolic Engineering of Bacteria. *Metabolic Engineering* 2, 328-338.

Kaback, H.R., Stadtman, E.R. (1966). Proline uptake by an isolated cytoplasmic membrane preparation of *Escherichia coli*. *Proceedings of the National Academy of Sciences of the United States of America* 55 (4), 920-927.

Kainou, T., Okada, K., Suzuki, K., Nakagawa, T., Matsuda, H., Kawamukai, M. (2001) Dimer formation of octaprenyl-diphosphate synthase (IspB) is essential for chain length determination of ubiquinone. *The Journal of Biological Chemistry* 276, 7876–7883.

Kabbe., H.J., Heitzer, H., (1978). Eine neue Synthese von 3,4-Dehydro- α -tocotrienol und Vitamin-E. *Synthesis* 12, 888-889..

Karrer, P., Fritzsche, H., Ringier, B., Salomon, H. (1938). Synthesis of α -Tocopherol (Vitamin E). *Nature* 141 (3580), 1057.

Karrer, P., Rentschler, H., (1944). Ein Tocol mit bicyclischer Seitenkette. *Helvetica Chimica Acta* 27, 1297-1300.

Karunanandaa, B., Qi, Q., Haoa, M., Baszis, S. R., Jensen, P. K., Wong, Y. H., Jiang, J., Venkatramesh, M., Gruys, K. J., Moshiri, F., Post-Beittenmiller, D., Weiss, J. D., Valentin H. E. (2005). Metabolically engineered oilseed crops with enhanced seed tocopherol. *Metabolic Engineering* 7, 384–400.

Kamal-Eldin, A., Appelqvist, L. (1996). The chemistry and antioxidant properties of tocopherols and tocotrienols. *Lipids* 31, 671–701.

Kayoko, Y., Lim, J., Dale, J.M., Chen, H., Shinn, P., Palm, C.J., Southwick, A.M., Wu, H.C., Kim, C., Nguyen, M., Pham, P., Cheuk, R., Karlin-Newmann, G., Liu, S.X., Lam, B., Sakano, H., Wu, T., Yu, G., Miranda, M., Quach, H.L., Tripp, M., Chang, C.H., Lee, J.M., Toriumi M, Chan, M.M.H., Tang, C.C., Onodera, C.S., Deng, J.M., Akiyama. K., Ansari, Y., Arakawa, T, Banh, J, Banno F, Bowser L, Brooks S, Carninci P, Chao Q, Choy N, Enju, A, Goldsmith, A.D., Gurjal, M., Hansen, N.F., Hayashizaki Y, Johnson-Hopson C, Hsuan, V.W., Iida, K., Karnes, M., Khan, S., Koesema, E., Ishida J., Jiang P.X., Jones T., Kawai J., Kamiya A., Meyers C., Nakajima M., Narusaka M., Seki M., Sakurai, T., Satou M., Tamse R., Vaysberg M., Wallender E.K., Wong C., Yamamura Y., Yuan S., Shinozaki, K., Davis, R.W., Theologis A., Ecker, J.R. (2003). Empirical Analysis of Transcriptional Activity in the *Arabidopsis* Genome. *Science* 302, 842-846.

- Keith, K. E., Killip, L., He, P., Moran, G. R., Valvano M. A.** (2007). *Burkholderia cenocepacia* C5424 Produces a Pigment with Antioxidant Properties Using a Homogentisate Intermediate, *Journal of Bacteriology* 189 (24), 9057–9065.
- Keller, Y., Bouvier, F., D'harlingue A., Camara B.** (1998). Metabolic compartmentation of plastid prenylipid biosynthesis - Evidence for the involvement of a multifunctional geranylgeranyl reductase. *European Journal of Biochemistry* 251, 413-417.
- Kim, J.Y. and Ryu, D.D.Y.** (1991). The effects of plasmid content, transcription efficiency, and translation efficiency on the productivity of a cloned gene in *Escherichia coli*. *Biotechnology and Bioengineering* 38, 1271-1279.
- Kim, S.J., Kim, M.D., Choi, J.H., Kim, S.Y., Ryu, Y.W., Seo, J.H.** (2006). Amplification of 1-deoxy-D-xylulose 5-phosphate (DXP) synthase level increases coenzyme Q10 production in recombinant *Escherichia coli*. *Applied Microbiology and Biotechnology* 72, 982-985.
- Klein, E.A, Thompson, I.M, Lippman, S.M.** (2001). SELECT: The next prostate cancer prevention trial—Selenium and Vitamin E Cancer Prevention Trial. *The Journal of Urology* 166, 1311-1315.
- Klein, E.A.** (2004). Selenium and vitamin E cancer prevention trial. *Annual New York Academy of Science* 1032, 234-241.
- Khanna, S., Roy, S., Slivka, A., Tara, K.S., Craft, M.A., Soma, C., Rink, C., Notestine, M. A., DeVires, C., Parinandi, N.L., Sen, C.K.** (2005). Neuroprotective properties of the natural vitamin E alpha-tocotrienol. *Stroke: A Journal of Cerebral Circulation* 26 (10), 2258-2264.
- Khanna, S., Roy, S., Park, H.A., Sen, C.K.** (2007). Regulation of c-Src activity in glutamate-induced neurodegeneration. *Journal of Biological Chemistry* 282(32), 23482-23490.
- Krämer, M., Bongaerts, J., Bovenberg, R., Kremer, S., Müller, U., Orf, S., Wubbolts, M., Raeven, L.** (2003). Metabolic engineering for microbial production of shikimic acid. *Metabolic Engineering* 5, 277-283.
- Kumar, R., Raclaru, M., Schusseler, T., Gruber, J.** (2005). Characterisation of plant tocopherol cyclases and their overexpression in transgenic *Brassica napus* seeds. *Federation of European Biochemical Society Letters* 579, 1357-1364.

(a) **Kuzuyama, T., Takagi, M., Takahashi, S., Seto, H.** (2000). Cloning and characterization of 1-deoxy-D-xylulose 5-phosphate synthase from *Streptomyces* sp. strain CL190, which uses both the mevalonate and nonmevalonate pathways for isopentenyl diphosphate biosynthesis. *Journal of Bacteriology* 182, 891-897.

Kuzuyama, T., Takahashi, S., Watanabe, H., and Seto, H., (1998). Direct formation of 2-C-methyl-D-erythritol 4-phosphate from 1-deoxy-D-xylulose 5-phosphate by 1-deoxy-D-xylulose 5-phosphate reductoisomerase, a new enzyme in the non-mevalonate pathway to isopentenyl diphosphate. *Tetrahedron Letters* 39, 4509-4512.

(c) **Kuzuyama, T., Takagi, M., Kaneda, K., Dairi, T., Seto, H.** (2000). Formation of 4-(cytidine 5'-diphospho)-2-C-methyl-D-erythritol from 2-C-methyl-D-erythritol 4-phosphate by 2-C-methyl-D-erythritol 4-phosphate cytidyltransferase, a new enzyme in the nonmevalonate pathway. *Tetrahedron Letters* 41, 703-706.

Kuzuyama, T. (2002). Mevalonate and Non-Mevalonate Pathways for Biosynthesis of Isoprene units. *Bioscience Biotechnology and Biochemicals*. 66(8), 1619-1627.

Lange, B.M., Rujan, T., Martin, W., Croteau, R. (2000). Isoprenoid biosynthesis: The evolution of two ancient and distinct pathways across genomes. *Proceedings of the National Academy of Sciences of the United States of America* 97(24), 13172-13177.

Lee, K.P., Kim, C., Landgraf, F., Apel, K. (2007). EXECUTER1- and EXECUTER2-dependent transfer of stress-related signals from the plastid to the nucleus of *Arabidopsis thaliana*. *Proceedings of the National Academy of Sciences of the United States of America* 104, 10270-10275.

Lee, P.C., Petri, R., Mitjs, B.N., Watts, K.T., Schmidt-Dannert, C. (2005). Directed evolution of *Escherichia coli* farnesyl diphosphate synthase (IspA) reveals novel structural determinants of chain length specificity. *Metabolic Engineering* 7(1), 18-26.

Lemuth, K., Steuer, K., Albermann, C. (2011). Engineering of a plasmid-free *Escherichia coli* strain for improved *in vivo* biosynthesis of astaxanthin. *Microbial Cell Factories* 10 (29), 1-12.

Lesley, S.A., Graziano, J, Cho, C.Y., Knuth, M.W., Klock, H.E. (2002). Overexpression of plasmid encoded genes initiate transcription of heat shock genes and several stress

responses, and can often result in aggregation of encoded protein in form of inclusion bodies. *Protein Engineering*, 15 (2), 153-160.

Liang, P.H., Ko, T.P., Wang, A.H.J. (2002). Structure, mechanism and function of prenyltransferases. *European Journal of Biochemistry* 269, 3339–3354.

Lichtenthaler, H.K. (1999). The 1-Deoxy-D-Xylulose-5-Phosphate Pathway of Isoprenoid Biosynthesis in Plants. *Annual Review of Plant Physiology and Plant Molecular Biology* 50, 47-65.

Lippman, S.M., Klein, E.A., Goodman, P.J., Lucia, M.S., Thompson, I.M., Ford, L.G. (2009). Effect of selenium and vitamin E on risk of prostate cancer and other cancers: the Selenium and Vitamin E Cancer Prevention Trial (SELECT). *Journal of American Medical Association* 301, 39-51.

Lin, E.C.C. (1976). Glycerol Dissimilation and its Regulation in Bacteria. *Annual Review of Microbiology* 30, 535-578.

Lois, L. M., Campos, N., Putra, S. R., Danielson, K., Rohmer, M., Boronat, A. (1998). *Proceedings of the National Academy of Sciences of the United States of America* 95, 2105-2110.

Lonn, E., Bosch, J., Yusuf, S. (2005). HOPE and HOPE-TOO Trial Investigators. Effects of long-term vitamin E supplementation on cardiovascular events and cancer: a randomized controlled trial. *Journal of American Medical Association* 293(11), 1338-1347.

Liu, K., Chougnat, A., Woggon, W.D. (2008). Short Route to α -Tocopherol. *Angewandte Chemie International Edition* 47, 5827-5829.

Maeda H, DellaPenna D. (2007). Tocopherol functions in photosynthetic organisms. *Current Opinion in Plant Biology* 10 (3), 260-265.

Math, S.K., Hearst, J.E., Poulter, C.D. (1992). The *crtE* gene in *Erwinia herbicola* encodes geranylgeranyl diphosphate synthase. *Proceedings of the National Academy of Sciences of the United States of America* 89, 6761-6764.

Manetsch, R., Krasinski, A., Radic, Z., Raushel, J., Taylor, P., Sharpless, K.B., Kolb,

H.C. (2004). In situ click chemistry: enzyme inhibitors made to their own specifications. *Journal of American Chemical Society* 126(40), 12809–12818.

Mayer, H., Schudel, P., Rüegg, R., Isler, O. (1963). Über die chemie des vitamins. Die total synthese von (2R, 4'R, 8R)- und (2S, 4'R, 8'R)- α -tocopherol. *Helvetica Chimica Acta* 46, 650-671.

Mayer, H., Metzger J., Isler, O. (1967). Die Stereochemie von natürlichem γ -Tocotrienol (Plastochromanol-3) Plastochromanol-8 und Plastochromenol-8). *Helvetica Chimica Acta* 50, 1376-1393.

Miller, J.H. (1972). Experiments in Molecular Genetics. Cold Spring Harbor Laboratory Press, Cold Spring Harbor.

Miller, E.R., Pastor-Barruso, R., Dalal, D., Riemersma, R.A., Appel, L.J., Guallar, E. (2005). Meta-Analysis: High Dosage Vitamin E Supplementation May Increase All-Cause Mortality. *Annals of Internal Medicine* 142, 37- 46.

Misawa, N., Nakagawa, M., Kobayashi, K., Yamano, S., Izawa, Y., Nakamura, K., Harashima, K. (1990). Elucidation of the *Erwinia uredovora* carotenoid biosynthetic pathway by functional analysis of gene products expressed in *Escherichia coli*. *Journal of Bacteriology* 172, 6704-6712.

Moran G. R. (2004). Minireview: 4-Hydroxyphenylpyruvate dioxygenase. *Archives of Biochemistry and Biophysics* 433, 117–128.

Meyer, D., Schneider-Fresenius, C., Horlacher, R., Peist, R., Boos, W. (1997). Molecular Characterization of Glucokinase from *Escherichia coli* K-12. *Journal of Bacteriology* 179 (4), 1298–1306.

Munne-Bosch, S., Alegre, L. (2002). The functions of tocopherols and tocotrienols in plants. *Critical Reviews in Plant Science* 21, 31–57.

Mustacich, D.J., Bruno, R.S., Traber, M.G. (2007). Vitamin E. *Vitamins and Hormones* 76, 1-21.

Nelson, K. E., Weinel, C., Paulsen, I. T., Dodson, R. J., Hilbert, H., Martins dos Santos,

V. A. P., Fouts, D. E., Gill, S. R., Pop, M., Holmes, M., Brinkac, L., Beanan, M., DeBoy, R. T., Daugherty, S., Kolonay, J., Madupu, R., Nelson, W., White, O., Peterson, J., Khouri, H., Hance, I., Lee, P. C., Holtzapple, E., Scanlan, D., Tran, K., Moazzez, A., Utterback, T., Rizzo, M., Lee, K., Kosack, D., Moestl, D., Wedler, H., Lauber, J., Stjepandic, D., Hoheisel, J., Straetz, M., Heim, S., Kiewitz, C., Eisen, J., N. Timmis, K., Düsterhöft, A., Tümmler B., Fraser C. M. (2002). Complete genome sequence and comparative analysis of the metabolically versatile *Pseudomonas putida* KT2440. *Environmental Microbiology* 4(12), 799–808.

Nesaretnam, K., Meganathan, P. (2011). Tocotrienols: inflammation and cancer. *Annals of the New York Academy of Sciences, Issue: Nutrition and Physical Activity in Aging, Obesity, and Cancer* 1229, 18-22.

Netscher, T., Malaisé G., Bonrath, W., Breuninger, M. (2007). A new route to Vitamin E key-intermediates by olefin cross-metathesis. *Catalysis Today* 121 (1-2), 71-75.

Netscher, T. (1996). Stereoisomers of Tocopherols-Syntheses and Analytics. *Chimia* 50 (11), 563-569.

Norris, S.R., Shen, X., DellaPenna, D. (1998). Complementation of the *Arabidopsis* pds1 mutation with the gene encoding *p*-hydroxyphenylpyruvate dioxygenase. *Plant Physiology* 117, 1317-1323.

Nutraingredients Magazine: www.nutraingredients.com

Mar. 2001

Jun. 2004

Nov. 2010

Jun. 2011

O'Farrell, P.H. (1975). High resolution two-dimensional electrophoresis of proteins. *Journal of Biological Chemistry* 250, 4007-4021.

Ogino, T., Garner, C., Markley, J.L., Herrmann, K.M. (1982). Biosynthesis of aromatic compounds: ¹³C NMR spectroscopy of whole *Escherichia coli* cells. *Proceedings of the National Academy of Sciences of the United States of America* 79, 5828–5832.

Ogbonna, J. C. (2009). Microbiological production of tocopherols: current state and

prospects. *Applied Microbiology and Biotechnology* 84, 217–225.

Oldiges, M., Kunze, M., Degenring, D., Sprenger, G.A., Takors, R. (2004). Stimulation, monitoring, and analysis of pathway dynamics by metabolic profiling in the aromatic amino acid pathway. *Biotechnology Progress* 20, 1623-1633.

Oh, S.K., Kim, I.J., Shin, D.H., Yang, J., Kang, H., Han, K.H. (2000). Cloning, characterization and heterologous expression of a functional geranylgeranyl pyrophosphate synthase from sunflower (*Helianthus annuus* L.). *Journal of Plant Physiology* 157, 535-542.

Parker, R.S. (1989). Dietary and Biochemical Aspects of Vitamin E. *Advances in Food and Nutrition Research* 33, 157-232.

Pan, J.G., Rhee, J.S., Lebeault, J.M. (1987). Physiological constraints in increasing biomass concentration of *E. coli* B in fed-batch culture. *Biotechnology Letters* 9, 89-94.

Patel, V., Rink, C., Khanna, S., Sen, C.K. (2011). Tocotrienols: The lesser known form of natural Vitamin E. *Indian Journal of Experimental Biology* 49, 732-738.

Patent (2004) Method of Vitamin E production. (EP1095001).

Pearce, B. C., Parker, R. A., Deason, M. E., Qureshi, A. A. & Wright J. J. K. (1992). Hypocholesterolemic activity of synthetic and natural tocotrienols. *Journal of Medicinal Chemistry* 35, 3595-3606.

Pearce, B.C., Parker, R.A., Deason, M.E., Dischino, D.D., Gillespie, E., Qureshi, A.A., Volk, K., Wright, J.J. (1994). Inhibitors of cholesterol biosynthesis. 2. Hypocholesterolemic and antioxidant activities of benzopyran and tetrahydronaphthalene analogues of the tocotrienols. *Journal of Medicinal Chemistry* 37 (4), 526–541.

Peddibhotla, S., Cheng, Z., DellaPenna, D., Tepe, J.J. (2003). Efficient two-step synthesis of methylphytylbenzoquinones: precursor intermediates in the biosynthesis of vitamin E. *Tetrahedron Letters*, 44, 237-239.

Pittard, A.J., Neidhardt, F.C., Curtiss III, R., Ingraham, J.L., Lin, E.C.C., Low, K.B., Magasanik, B., Reznikoff, W.S., Riley, M., Schaechter, M., Umbarger, H.E. (1996). Biosynthesis of aromatic amino acids: *Escherichia coli* and *Salmonella*, *Cellular and*

Molecular Biology, American Society of Microbiology, 458–484.

PN Newswire (May 2011). Production, Market and Benchmarking of Synthetic Vitamin E in China (www.pnwires.org)

Porfirova, S., Bergmüller, E., Tropf, S., Lemke, R., Dörmann, P. (2002). Isolation of an *Arabidopsis* mutant lacking vitamin E and identification of a cyclase essential for all tocopherol biosynthesis. *Plant Biology* 99 (19), 12495–12500.

Postma, P.W., Lengeler, J.W., Jacobson, G.R. (1993). Phosphoenolpyruvate: carbohydrate phosphotransferase systems of bacteria. *Microbiology and Molecular Biology Reviews* 57, 543-594.

Provencher, L. M., Miao, L., Sinha, N., Lucas, W. J. (2001). Sucrose Export Defective Encodes a Novel Protein Implicated in Chloroplast-to-Nucleus Signaling. *The Plant Cell* 13, 1127–1141.

Qi, Q., Hao, M., Ng, W-on., Slater, S.C., Baszis, S.R., Weiss, J.D., Valentin, H.E., (2005). Application of the *Synechococcus nirA* Promoter To Establish an Inducible Expression System for Engineering the *Synechocystis* Tocopherol Pathway. *Applied and Environmental Microbiology* 71(10), 5678-5684.

Quinn, P.J. (2004). Review-Antioxidants and Prophylactics: Is the Distribution of α -Tocopherol in Membranes Consistent with Its Putative Functions? *Biochemistry (Moscow)*, 69 (1), 58-66. Translated from *Biokhimiya*, (2004), 69 (1), 74-84.

Qureshi, A.A., Pearce, C., Nor, R.M., (1996). Dietary δ -tocopherol attenuates the impact of δ -tocotrienol on hepatic 3-hydroxy-3-methylglutaryl coenzyme A reductase activity in chickens. *Journal of Nutrition* 126, 389–394.

Raclaru, M., Gruber, J., Kumar, R., Sadre, R., Lühs, W., Zarhluol, M.K., Friedt, W., Frentzen, M., Weier, D. (2006). Increase of the tocopherol content in transgenic *Brassica napus* seeds by overexpression of key enzymes involved in prenylquinone biosynthesis. *Molecular Breeding* 18, 93-107.

Rippert, P., Scimemi, C., Dubald, M., Matringe, M. (2004). Engineering Plant Shikimate Pathway for Production of Tocotrienol and Improving Herbicide Resistance. *Plant Physiology*

134, 92-100.

Rodwell, V.W., Beach, M.J., Bischoff, K.M., Bochar, D.A., Darnay, B.G., Friesen., J.A., Gill, J.F., Hedl, M., Starck, J. T., Kenelly, P.J., Kim, D.Y., Wang., Y. (2003). 3-Hydroxy-3-methylglutaryl-Co-A reductase. *Methods in Enzymology* 324, 259-280.

Rohmer, M., Knani, M., Simonin, P., Sutter, B., Sahm, H. (1993). Isoprenoid biosynthesis in bacteria: a novel pathway for the early steps leading to isopentenyl diphosphate. *Biochemistry Journal* 295(2), 517–524.

Rohmer, M. (1999). The discovery of a mevalonate independent pathway for isoprenoid biosynthesis in bacteria, algae and higher plants. *Natural Product Report* 16, 565-574.

Rohmer, M., Seemann, M., Horbach, S., Bringer-Meyer, S., Sahm, H. (1996). Glyceraldehyde 3-phosphate and pyruvate as precursors of isoprenic units in an alternative non-mevalonate pathway for terpenoid biosynthesis. *Journal of American Chemical Society* 118, 2564–2566.

Rosen, B.P., Tsuchiya, T. (1979). Preparation of Everted Vesicles from *Escherichia coli* for the Measurement of Calcium Transport. *Methods in Enzymology* 56, 233-241.

Rodríguez-Villalón, A., Pérez-Gil, J., Rodríguez-Concepción, M. (2008). Carotenoid accumulation in bacteria with enhanced supply of isoprenoid precursors by up-regulation of exogenous or endogenous pathways. *Journal of Biotechnology* 135 (1), 78-84.

Rohdich, F., Hecht, S., Bacher, A., Eisenreich, W. (2003). The deoxyxylulose phosphate pathway of isoprenoid biosynthesis. Discovery and function of the ispDEFGH genes and their cognate enzymes. *Pure Applied Chemistry* 75, 393–405.

Rüetschi, U., Odelhög, B., Linstedt, S., Barros-Söderling, J., Persson, B., Jörnvall, H. (1992). Characterization of 4-hydroxyphenylpyruvate dioxygenase – primary structure of Pseudomonas enzyme. *European Journal of Biochemistry* 205, 459-466.

Sadre, R., Gruber, J., Frentzen, M. (2006). Characterization of homogentisate prenyltransferases involved in plastoquinone-9 and tocochromanol biosynthesis. *Federation of European Biochemical Society Letters* 580, 5357-5362.

- Saluta, M., Bell, P.A.**, (1998). Troubleshooting GST fusion protein expression in *E. coli*. *Life Science News* 1, 1-3.
- Sambrook, J., Fritsch, E.F., Maniatis, T.** (1989). *Molecular Cloning: a Laboratory Manual*. Cold Spring Harbor Laboratory Press.
- Sattler, S.E., Gililand, L.U., Magallanes-Lundback, M., Pollard, M., DellaPenna, D.** (2004). Vitamin E Is Essential for Seed Longevity and for Preventing Lipid Peroxidation during Germination. *The Plant Cell* 16, 1419-1432.
- Sattler, S. E., Cahoon, E. B., Coughlan, S. J., DellaPenna D.** (2003). Characterization of Tocopherol Cyclases from Higher Plants and Cyanobacteria. Evolutionary Implications for Tocopherol Synthesis and Function. *Plant Physiology* 132, 2184–2195.
- Saiki, R.K., Scharf, S., Faloona, F., Mullis, K.B., Horn, G.T., Erlich, H.A., Arnheim, N.** (1985). Enzymatic Amplification of Beta-Globin Genomic Sequences and Restriction Site Analysis for Diagnosis of Sickle-Cell Anemia. *Science* 230, 1350-1354.
- Saisho, Y., Morimoto, A., Umeda, T.** (1997). Determination of Farnesyl pyrophosphate in dog and human plasma by high-performance liquid chromatography with fluorescence detection. *Analytical Biochemistry* 252, 89–95.
- Sano, M., Ernesto, C., Thomas, R.G.** (1997). A controlled trial of selegiline, α -tocopherol, or both as treatment for Alzheimer's disease. *New England Journal of Medicine* 336, 1216–1222.
- Savidge, B., Weiss, J.D., Wong, Y.H., Lassner, M.W., Mitsky, T.A., Shewmaker, C.K., Post-Beittenmiller, D., Valentin, H.E.** (2002). Isolation and characterization of homogentisate phytyltransferase genes from *Synechocystis* sp. PCC 6803 and *Arabidopsis*. *Plant Physiology* 129(1), 321-332.
- Scheldz, M., Seidler, A., Beyer, P., Neuhaus, G.** (2001). A novel phytyltransferase from *Synechocystis* sp. PCC 6803 involved in tocopherol biosynthesis. *Federation of European Biochemical Society Letters* 499 (1-2), 15-20.
- Schneider, C.** (2005). Chemistry and Biology of Vitamin E, *Molecular Nutrition and Food Research* 49 (1), 7-30.

- Schneider, S., Sandalova, T., Schneider, T., Sprenger, G.A., Samland, A.K.** (2008). Replacement of a Phenylalanine by a Tyrosine in the Active Site Confers Fructose-6-phosphate Aldolase Activity to the Transaldolase of *Escherichia coli* and Human Origin. *The Journal of Biological Chemistry* 283 (44), 30064-30072.
- Schryvers, A., Weiners, J.H.** (1981). The Anaerobic sn-Glycerol-3-phosphate Dehydrogenase of *Escherichia coli*. Purification and Characterisation. *The Journal of Biological Chemistry* 256 (19), 9959-9965.
- Schwender, J., Seemann, M., Lichtenthaler, H.K., Rohmer, M.** (1996). Biosynthesis of isoprenoids (carotenoids, sterols, prenyl side-chains of chlorophylls and plastoquinone) via a novel pyruvate/glyceraldehyde 3-phosphate non-mevalonate pathway in the green alga *Scenedesmus obliquus*. *Biochemistry Journal* 316(2), 73-80.
- Schudel, P., Mayer, H., Metzger, J., Ruegg, R., Isler, O.** (1963). Die Synthese von *rac.* all-trans $-\zeta$ und $-\epsilon$ -Tocopherol. *Helvetica Chimica Acta* 46(4), 2517-2526.
- Scott, J.W., Bizzarro, F.T., Parrish, D.R., Saucy, G.,** (1976). Syntheses of (2*R*, 4'*R*, 8'*R*)- α -Tocopherol and (2*R*, 3'*E*, 7'*E*)- α -Tocotrienol. *Helvetica Chimica Acta* 59, 290-306.
- Serbinova, E., Kagan, V., Han, D., Packer, L.** (1991). Free radical recycling and intramembrane mobility in the antioxidant properties of alpha-tocopherol and alphanatocotrienol. *Free Radical Biology & Medicine* 10 (5), 263–275.
- Sen, C.K., Khanna, S., Roy, S.** (2007). Tocotrienols in health and disease: The other half of the natural vitamin E family. *Molecular Aspects of Medicine* 28, 692-728.
- Sen, C.K., Rink, C., Khanna, S.** (2010). Palm Oil–Derived Natural Vitamin E α -Tocotrienol in Brain Health and Disease. *Journal of American College Nutrition* 29 (3), 314-323.
- Serre, L., Sailland, A., Sy, D., Boudec, P., Rolland, A., Pebay-Peyroula, E., Cohen-Addad, C.** (1999). Crystal structure of *Pseudomonas fluorescens* 4-hydroxyphenylpyruvate dioxygenase: an enzyme involved in the tyrosine degradation pathway. *Structure* 7 (8), 977-988.

Shirai, A. (2008). Global Analysis of Gel Mobility of Proteins and Its Use in Target Identification. *Journal of Biological Chemistry* 283 (16), 10745-10752.

Shpilyov, A.V., Zinchenko, V.V., Shestakov, S.V., Grimm, B., Lokstein, H. (2005). Inactivation of the geranylgeranyl reductase (ChIP) gene in the cyanobacterium *Synechocystis* sp. PCC 6803. *Biochimica et Biophysica Acta (BBA) - Bioenergetics* 1706 (3), 195-203.

Shintani, D., DellaPenna, D. (1998). Elevating the vitamin E content of plants through metabolic engineering. *Science* 282, 2098–2100.

Shintani, D.K., Cheng, Z., DellaPenna, D. (2002). The role of 2-methyl-6-phytylbenzoquinone methyltransferase in determining tocopherol composition in *Synechocystis* sp. PCC6803. *Federation of European Biochemical Society Letters* 511 (1), 1-5.

Shrivastava, R., Pisareva, T., Norling, B. (2005). Proteomic studies of the thylakoid membrane of *Synechocystis* sp. PCC 6803. *Proteomics* 5 (18), 4905-4916.

Slover, H.T. (1971). Tocopherols in foods and fats. *Lipid* 6, 291-296.

Smith, D.B., Corcoran, L.M. (2001). Expression and Purification of Glutathione-S-Transferase Fusion Proteins. *Current Protocols in Molecular Biology*, Chapter 16, Unit 16.7.

Soll, J., Schultz, G. (1979). Comparison of geranylgeranyl and phytyl substituted methylquinols in the tocopherol synthesis of spinach chloroplasts. *Biochemical and Biophysical Research Communications* 91, 715-720.

Soll, J., Kemmerling, M., Schultz, G. (1980). Tocopherol and plastoquinone synthesis in spinach chloroplasts and subfractions. *Archives of Biochemistry and Biophysics* 204 (2), 544-550.

Soll, J., Schultz, G. (1981). Phytol synthesis from geranylgeraniol in spinach chloroplasts. *Biochemical and Biophysical Research Communications* 99, 907-912.

Soll, J. (1987). α -Tocopherol and plastoquinone synthesis in chloroplast membranes. *Methods in Enzymology* 148, 383-392.

- Song, L.** (2003). Detection of farnesyl diphosphate accumulation in yeast ERG9 mutants. *Analytical Biochemistry* 317, 180–185.
- Sørensen, H.P, Mortensen, K.K.** (2005). Soluble expression of recombinant proteins in the cytoplasm of *Escherichia coli*. *Microbial Cell Factories*, 4, 1-8.
- Souci, S.W., Fachmann, W., Kraut, H.** (1989). Food Composition and Nutrition Tables 1989/90. *Wissenschaftliche Verlagsgesellschaft mbH*, Stuttgart, Germany.
- Sprenger, G.** (2006). Aromatic Amino Acids. *Microbiology Monographs* DOI 10.1007/7171_2006_067, 5, 93-127.
- Sprenger, G.A.** (2007). From scratch to value: engineering *Escherichia coli* wild type cells to the production of L-phenylalanine and other fine chemicals derived from chorismate. *Applied Microbiology Biotechnology* 75, 739–749.
- Sprenger, G., Schörken, U., Wiegert, T., Grolle, S., de Graaf, A.A., Taylor, S.V., Begley, T.P., Bringer-Meyer, S., Sahm, H.** (1997). Identification of thiamine-dependent synthase in *Escherichia coli* required for the formation of 1-deoxy-D-xylulose 5-phosphate precursors to isoprenoids, thiamine and pyridoxol. *Proceedings of the National Academy of Sciences of the United States of America* 94 (24), 12857-12862.
- Srivastava, R., Pisareva, T., Norling, B.** (2005). Proteomic studies of the thylakoid membrane of *Synechocystis* sp. PCC6803. *Proteomics* 5, 4905-4916.
- Stocker, A., Rüttiman, A., Woggon, W.D.** (1993). Identification of the tocopherol cyclase in the blue-green algae *anabaena variabilis* Kutzing (cyanobacteria). *Helvetica Chimica Acta* 76, 1729-738.
- Stocker, A., Netscher, T., Ruttimann, A., Muller, R.K., Schneider, H., Todaro, L.J., Derungs, G., Woggon, W.D.** (1994). The reaction mechanism of chromanol ring formation catalyzed by tocopherol cyclase from *Anabaena variabilis* Kutzing (cyanobacteria). *Helvetica Chimica Acta* 77, 1721-1737.
- Stocker, A., Fretz, H., Frick, H., Rüttimann, A. Woggon, W. D.** (1996). The substrate specificity of tocopherol cyclase. *Bioorganic and Medicinal Chemistry* 4 (7), 1129-1134.

- Suzuki, Y.J., Tsuchiya, M., Wassall, S.R., Choo, Y.M., Govil, G., Kagan, V.E., Packer, L.** (1993). Structural and dynamic membrane properties of alpha-tocopherol and alphanatocotrienol: implication to the molecular mechanism of their antioxidant potency. *Biochemistry* 32 (40), 10692–10699.
- Sundram, K., Gapor, M., Top, A.** (1992). Vitamin E from palm oil: Its extraction and nutritional properties. *Lipid Technology* 4, 137–141.
- Sussmann, R.A., Angeli, C.B., Peres, V.J., Kimura, E.A., Katzin, A.M.** (2011). Intraerythrocytic stages of *Plasmodium falciparum* biosynthesize Vitamin E. *Federation of European Biochemical Society Letters* 585, 3985-3991.
- Tan, B.** (2005). Appropriate Spectrum Vitamin E and New Perspectives on Desmethyl Tocopherols and Tocotrienols. *The Journal of the American Nutraceutical Association* 8 (1), 35-42.
- Tappel, A., Zalkin, H.** (1960). Inhibition of lipid peroxidation in microsomes by vitamin E. *Nature* 185, 35.
- Takaya, A., Zhang, Y.W., Asawatreratanakul, K., Wititsuwannakul, D., Wititsuwannakul, R., Takahashi, S., Koyama, T.** (2003). Cloning, expression and characterization of a functional cDNA clone encoding geranylgeranyldisphosphate synthase of *Hevea brasiliensis*. *Biochimica et Biophysica Acta* 1625, 214-220.
- Tong, H., Holstein, S. A., Hohl, R. J.** (2005). Simultaneous determination of farnesyl and geranylgeranyl pyrophosphate levels in cultured cells. *Analytical Biochemistry* 336, 51–59.
- Traber, M.G.** (2006). How much vitamin E? just enough! *American Journal of Clinical Nutrition* 84(5), 959-960.
- Traber, M.J., Atkinson, J.** (2007). Vitamin E, antioxidant and nothing more. *Free Radicals in Biology and Medicine* 43, 4-15.
- Tribe, D.E., Pittard, J.** (1979). Hyperproduction of tryptophan by *Escherichia coli* genetic manipulation of the pathways leading to tryptophan formation. *Applied and Environmental Microbiology* 38, 181-190.

- Threlfall, D.R., Whistance, G.R.** (1971). Biosynthesis of isoprenoid quinones and chromanols. *Aspects of Terpenoid Chemistry and Biochemistry*, 357–404.
- Van-Eenennaam, A.L., Lincoln, K., Durrett, T.P., Valentin, H.E., Shewmaker, C.K., Thorne, G.M., Jiang, J., Baszis, S.R., Levering, C.K., Aasen, E.D., Hao, M., Stein, J.C., Norris, S.R., Last, R.L.** (2003). Engineering Vitamin E Content: From *Arabidopsis* Mutant to Soy Oil. *The Plant Cell* 15, 3007-3019.
- Vallon, T., Ghanegaonkar, S., Vielhauer, O., Müller, A., Albermann, C., Sprenger, G.A., Reuss, M., Lemuth, K.** (2008). Quantitative analysis of isoprenoid diphosphate intermediates in recombinant and wild-type *Escherichia coli* strains. *Applied Microbiology and Biotechnology* 81, 175-182.
- Voegele, R.T., Sweet, G.D., Boos, W.** (1993). Glycerol kinase of *Escherichia coli* is activated by interaction with the glycerol facilitator. *Journal of Bacteriology* 175, 1087–1094.
- Wang, X., Quinn, P.J.** (1999). Vitamin E and its function in membranes. *Progress in Lipid Research* 38 (4), 309-336.
- Wang, C.H., Stern, I., Gilmour, C.M., Klungsoyr, S., Reed, D.J., Bialy, J.J., Christensen, B.E., Cheldelin, V.H.** (1958). Comparative study of glucose catabolism by the radiorespirometric method. *Journal of Bacteriology* 76, 207-216.
- Watts, K.T., Mijts, B.N., Schmidt-Dannert, C.** (2005). Current and Emerging Approaches for Natural Product Biosynthesis in Microbial Cells. *Advances in Synthetic Catalysis* 347, 927–94
- Wiese, A., Wilms, B., Syldatk, C., Mattes, R., Altenbuchner, J.** (2001). Cloning, nucleotide sequence and expression of a hydantoinase and carbamoylase gene from *Arthrobacter aurescens* DSM 3745 in *Escherichia coli* and comparison with the corresponding genes from *Arthrobacter aurescens* DSM 3747. *Applied Microbiology and Biotechnology* 55, 750-757.
- Wiedemann, M., Misawa, N., Sandmann, G.** (1993). Purification and Enzymatic Characterization of the Geranylgeranyl Pyrophosphate Synthase from *Erwinia uredovora* after Expression in *Escherichia coli*. *Archives of Biochemistry and Biophysics* 306 (1), 152-157.

- Weikert, M.J., Doherty, D.H, Best, E., Olins, P.O.** (1996). Optimization of heterologous protein production in *Escherichia coli*. *Current Opinion in Biotechnology* 7, 494-499.
- Weiner, J.H.** (1974). The Localization of Glycerol-3-Phosphate Dehydrogenase in *Escherichia coli*. *Journal of Membrane Biology* 15, 1-14.
- Wilke, D.** (1999). Chemicals from Biotechnology: molecular plant genetics will challenge the chemical and the fermentation industry. *Applied Microbiology and Biotechnology* 52, 135-145.
- Whittle, K.J., Dunphy, P.J., Pennock, J.F.** (1966). The isolation and properties of delta-tocotrienol from *Hevea latex*. *Biochemistry Journal* 100 (1), 138-145.
- Wu, K., Zhao, Y., Liu, B.H., Li, Y., Liu, F., Guo, J., Yu, W.P.** (2002). RRR-alpha-tocopheryl succinate inhibits human gastric cancer SGC-7901 cell growth by inducing apoptosis and DNA synthesis arrest. *World Journal of Gastroenterology* 8, 26– 30.
- Yang, C., Pflugrath, J.W., Camper, D.L., Foster, M.L., Pernich, D.J., Walsh, T.A.** (2004). Structural basis for herbicidal inhibitor selectivity revealed by comparison of crystal structures of plant and mammalian 4-hydroxyphenylpyruvate dioxygenases. *Biochemistry* 43, 10414 – 10423.
- Yazdani, S. S. and Mukherjee, K. J.** (2002). Continuous-culture studies on the stability and expression of recombinant streptokinase in *Escherichia coli*. *Bioprocess Biosystems Engineering* 24, 341–346.
- Yuan, L.Z., Rouvie`re, P.E., LaRossa, R.A., Suh, W.** (2006). Chromosomal promoter replacement of the isoprenoid pathway for enhancing carotenoid production in *E. coli* *Metabolic Engineering* 8, 79–90.
- Yu, W., Simmons-Menchaca, M., Gapor, A., Sanders, B.G., Kline, K.** (1999). Induction of apoptosis in human breast cancer cells by tocopherols and tocotrienols. *Nutrition and Cancer* 33, 26–32.
- Zhou, S., Causey, T. B. Hasona, A., Shanmugam, K. T., Ingram, L. O.** (2003). Production of Optically Pure D-Lactic Acid in Mineral Salts Medium by Metabolically Engineered *Escherichia coli* W3110. *Applied and Environmental Microbiology* 69 (1), 399-407.

Zhou, C., Tabb, M.M., Sadatrafiei, A., Grün, F., Blumberg, B. (2004). Tocotrienols activate the steroid and xenobiotic receptor, SXR, and selectively regulate expression of its target genes. *Drug Metabolism and Disposition* 32 (10), 1075-1082.

Zeppenfeld, T., Larisch, C., Lengeler, J.W., Jahreis, K. (2000). Glucose transporter mutants of *Escherichia coli* K-12 with changes in substrate recognition of IICB(Glc) and induction behavior of the ptsG gene. *Journal of Bacteriology* 182, 4443–4452.

Zingg, J.M., Azzi, A. (2004). Non-antioxidant activities of vitamin E. *Current Medicinal Chemistry* 11, 1113–1133.